

AD _____

Award Number: DAMD17-98-1-8254

TITLE: Targeted Chemotherapy of Tumors and Metastases with
Hyaluronic Acid-Anti-Tumor Bioconjugates

PRINCIPAL INVESTIGATOR: Glenn D. Prestwich, Ph.D.

CONTRACTING ORGANIZATION: University of Utah
Salt Lake City, Utah 84102

REPORT DATE: August 2001

TYPE OF REPORT: Final

PREPARED FOR: U.S. Army Medical Research and Materiel Command
Fort Detrick, Maryland 21702-5012

DISTRIBUTION STATEMENT: Approved for Public Release;
Distribution Unlimited

The views, opinions and/or findings contained in this report are those of the author(s) and should not be construed as an official Department of the Army position, policy or decision unless so designated by other documentation.

20020124 238

REPORT DOCUMENTATION PAGE

Form Approved
OMB No. 074-0188

Public reporting burden for this collection of information is estimated to average 1 hour per response, including the time for reviewing instructions, searching existing data sources, gathering and maintaining the data needed, and completing and reviewing this collection of information. Send comments regarding this burden estimate or any other aspect of this collection of information, including suggestions for reducing this burden to Washington Headquarters Services, Directorate for Information Operations and Reports, 1215 Jefferson Davis Highway, Suite 1204, Arlington, VA 22202-4302, and to the Office of Management and Budget, Paperwork Reduction Project (0704-0188), Washington, DC 20503

1. AGENCY USE ONLY (Leave blank)		2. REPORT DATE August 2001	3. REPORT TYPE AND DATES COVERED Final (15 Jul 98 - 14 Jul 01)	
4. TITLE AND SUBTITLE Targeted Chemotherapy of Tumors and Metastases with Hyaluronic Acid-Anti-Tumor Bioconjugates			5. FUNDING NUMBERS DAMD17-98-1-8254	
6. AUTHOR(S) Glenn D. Prestwich, Ph.D.				
7. PERFORMING ORGANIZATION NAME(S) AND ADDRESS(ES) University of Utah Salt Lake City, Utah 84102 E-Mail: GPRESTWICH@DEANS.PHARM.UTAH.EDU			8. PERFORMING ORGANIZATION REPORT NUMBER	
9. SPONSORING / MONITORING AGENCY NAME(S) AND ADDRESS(ES) U.S. Army Medical Research and Materiel Command Fort Detrick, Maryland 21702-5012			10. SPONSORING / MONITORING AGENCY REPORT NUMBER	
11. SUPPLEMENTARY NOTES				
12a. DISTRIBUTION / AVAILABILITY STATEMENT Approved for Public Release; Distribution Unlimited				12b. DISTRIBUTION CODE
13. ABSTRACT (Maximum 200 Words) Metastatic cancer cells over-express characteristic variants of the hyaluronic acid (HA) receptors CD44 and RHAMM, which mediate cell adhesion, cell motility, and cell proliferation. Rapid uptake and catabolism of HA is common in several breast cancer cell-lines. We developed a targeted delivery system for controlled release of chemotherapeutic drugs, and we prepared HA-Taxol to test our hypothesis that HA-anti-tumor prodrugs will be more effective therapeutic agents than the unconjugated drugs. FITC-labeled HA and FITC-HA-Taxol showed selective uptake, and both FITC-HA-Taxol and HA-Taxol showed selective cytotoxicity to breast, colon, and ovarian cancer cells in culture. Release of free drug from the HA-prodrug form was demonstrated by HPLC. Evaluation of the HA-Taxol in nude mice bearing xenografted human tumors, with or without co-treatment with chondroitin sulfate to saturate HA uptake by non-target tissues, demonstrated <i>in vivo</i> efficacy. A macromolecular prodrug, HMPA-DOX-HA, in which a biocompatible polymer serves as the carrier and HA serves as a targeting moiety, was impressive in improving efficacy and targeting of HMPA-DOX. A second line of research revealed the molecular basis of the RHAMM-HA interaction, and has provided peptide leads for disrupting the oncogenic transformation of RHAMM-overexpressing cells.				
14. SUBJECT TERMS breast cancer, Taxol, receptor-mediated uptake, selective toxicity, peptide library			15. NUMBER OF PAGES 321	
			16. PRICE CODE	
17. SECURITY CLASSIFICATION OF REPORT Unclassified	18. SECURITY CLASSIFICATION OF THIS PAGE Unclassified	19. SECURITY CLASSIFICATION OF ABSTRACT Unclassified	20. LIMITATION OF ABSTRACT Unlimited	

NSN 7540-01-280-5500

Standard Form 298 (Rev. 2-89)
Prescribed by ANSI Std. Z39-18
298-102

Table of Contents

Cover page	1
Report documentation page	2
Table of Contents	3, 4
A. Introduction	5
B. Body	5, 6
C. Key Research Accomplishments	7, 8
D. Reportable Outcomes	9-12
E. Conclusions	12
F. References	13-14
G. Appendix Materials	15

Biosketches

G.D. Prestwich	16,17
K.P. Vercruysse	18,19
Y. Luo	20,21
M.R. Ziebell	22
N.J. Bernshaw	23,24

Publications

Y. Luo and G.D. Prestwich, "Synthesis and Cytotoxicity of Hyaluronan-Taxol Antitumor Bioconjugates," <i>Bioconjugate Chem.</i> , 10 , 755-763 (1999).	25-34
G.D. Prestwich, Y. Luo, M.R. Ziebell, K.P. Vercruysse, K.R. Kirker, and J.S. MacMaster, "Chemically-Modified Hyaluronan: New Biomaterials and Probes for Cell Biology," in <i>New Frontiers in Medical Sciences: Redefining Hyaluronan</i> Padua, Italy (G. Abatangelo and P.H. Weigel, eds.) Elsevier Science, pp. 181-194 (2000).	35-48
Y. Luo, M.R. Ziebell, and G.D. Prestwich, "A Hyaluronic Acid -Taxol Anti-tumor Bioconjugate Targeted to Cancer Cells," <i>Biomacromolecules</i> , 1 , 208-218 (2000).	49-60

Y. Luo, K.R. Kirker, and G.D. Prestwich, "Modification of Natural Polymers: Hyaluronic Acid," <i>Methods of Tissue Engineering</i> (A. Atala and R. Lanza, eds.), Academic Press, Orlando, Florida, in press (2001).	61-75
G.D. Prestwich, Y. Luo, K.R. Kirker, M.R. Ziebell, and J. Shelby, "Hyaluronan Biomaterials for Targeted Drug Delivery and Wound Healing," <i>HA 2000</i> , Woodhead Publishing Ltd., Abington, UK, in press (2000).	76-83
M.R. Ziebell, Z.-G. Zhao, B. Luo, Y. Luo, E.A. Turley, and G.D. Prestwich, "Peptides that Mimic Carbohydrates: High Affinity Ligands for A Hyaluronic Acid Binding Domain," <i>Chem. & Biol.</i> , in press (2001).	84-126
Y. Luo and G.D. Prestwich, "Novel Biomaterials for Drug Delivery," <i>Exp. Opin. Ther. Patents</i> , in press (2001).	127-142
Y. Luo and G.D. Prestwich, "Cancer-Targeted Macromolecular Chemotherapeutics," <i>Current Cancer Drug Targets</i> , submitted (2001)	143-204
Y. Luo, N.J. Bernshaw, Z.-R. Lu, J. Kopecek, And G.D. Prestwich, "HPMA - Hyaluronic Acid - Adriamycin Bioconjugates: Targeted Delivery of Adriamycin to Cancer Cells," in preparation (2001).	205-245
S. Zhang, W.F. Cheung, J. Lu, M.R. Ziebell, S.A. Turley, R. Harrison, D. Zylka, N. Ahn, D. Litchfield, G.D. Prestwich, T. Cruz, and E.A. Turley, "Intracellular RHAMM Isoforms Bind Directly to erk1 and These Interactions are Required for Transformation and for Podosome Formation via the erk Kinase Pathway," <i>Molec. Cell. Biol.</i> , in revision (2001).	246-286
G.D. Prestwich, "Biomaterials from Chemically- Modified Hyaluronan," <i>Glycoforum</i> http://glycoforum.gr.jp/science/hyaluronan/HA18/HA18E.html (2001).	287-303
A.J. Day and G.D. Prestwich, "Hyaluronan Binding Proteins: Tying Up the Giant," <i>J. Biol. Chem.</i> , in press (2000).	304-321

A. Introduction

In this project, we developed an innovative approach for utilizing a natural polysaccharide biopolymer, hyaluronic acid (HA), to solubilize, stabilize, and achieve targeted intracellular delivery of anti-cancer agents to tumors and metastases. The coupling of an anti-tumor agent to HA gives a soluble, tumor-targeted drug conjugate. HA receptors are over-expressed on a variety of aggressively growing cancers, and in many cell-types, correlate with increased metastatic potential and with rate of HA uptake and degradation. Alternatively, HA oligosaccharides could be appended to other biocompatible polymeric prodrugs to improve targeting to cancer cells. The use of HA receptor-mediated uptake of a cytotoxic agent to cancerous and invasive cells represents a significant advance in cell-specific drug targeting, as all commonly-used anti-cancer drugs (e.g., anti-metabolites and DNA-targeted agents) and adjuvant techniques (e.g., radiation therapy) have inadequate specificity for cancerous lesions.

Our efforts in the final year have continued towards the development of new prodrug strategies in cell-based assays and in vivo xenografts with the derivatives of the hydrophobic anti-tumor drug Taxol. Our HA-Taxol adduct is water-soluble, shows enhanced target specificity for transformed and metastatic cells; and shows increased uptake and liberation of drug in the target tumor cells. Two papers describing the selective cytotoxicity and selective uptake of HA-Taxol and HA-FITC-Taxol were published. Overall, our efforts included four collaborations: (i) effects in diabetes using PDGF stimulated NIH-3T3 L1 cells (with E.A. Turley, Hospital for Sick Children, Toronto, Canada), (ii) specific cellular effects on CD44 clustering of HA-Taxol (with L. Bourguignon, University of Miami Medical Center, Florida), (iii) *in vivo* human tumor xenograft studies with nude mice (with L. Zhang and C. Underhill, Georgetown University, Washington), and (iv) examination of the ability of HA-Taxol to overcome *p*-glycoprotein-mediated resistance in breast cancer cell lines (with S. Horwitz, Albert Einstein Medical Center, New York). In addition, we have developed a novel use of HA fragments to improve the targeting and selective toxicity of HPMa-ADR, a polymer-bound derivative of adriamycin (with J. Kopecek, Department of Pharmaceutics and Pharmaceutical Chemistry, UUtah).

B. Body

This section describes research accomplishments associated with the specific tasks outlined in the original IDEA award application. Publications in Reportable Outcomes are cited withfor each of the tasks and/or research accomplishments.

Task 1. Synthesize HA-anti-tumor drug bioconjugates with four anti-cancer drugs (Brefeldin A, Taxol, geldanamycin, and camptothecin)

We synthesized and chemically characterized hemisuccinate active-ester forms of brefeldin A and Taxol. HA-adipic dihydrazide (HA-ADH) conjugates of Taxol hemisuccinate were prepared and evaluated in cell-based toxicity assays (D.1.a.). The purity and molecular size of drug bioconjugates was established by GPC and drug loading was evaluated by UV. In addition, we synthesized and purified fluorescently-labeled HA with three fluorophores at each of three molecular sizes (12, 200, and 1,200 kDa), as well as a doubly-labeled HA-Taxol-FITC molecule for simultaneous monitoring of selective cellular uptake and toxicity (D.1.c.). Preparation of other HA-drug bioconjugates was deferred to focus on full assessment of HA-Taxol as the model system. The chemistry of the HA modifications for drug attachment was described in several review articles (D.1.b., d., g., j., k.) and a website (D.1.i)

In addition, we developed a novel use of HA fragments to improve the targeting and selective toxicity of HPMA-DOX, a polymer-bound derivative of doxorubicin with Professor Kopecek). This has led to exciting publishable results (D.1.l.), an invited review (D.1.k.), and an application to the DOD Prostate Cancer program.

Task 2. Establish analytical methods to monitor enzymatic release of drugs from bioconjugates and quantify metabolites in cell cultures

We conducted *in vitro* tests with commercial esterase and hyaluronidase (Hase) and developed a robust HPLC assay for the quantification of Taxol release. No other Taxol-containing materials (except free Taxol drug) were released from the HA-Taxol bioconjugates. We also investigated the release rates of Taxol from the optimal HA-Taxol preparation using cell culture media (with and without cells) and human serum. This has now been published (D.1.c.).

Task 3. Determine efficacy of HA-AT (vs. free AT drugs) in cultured breast cancer and other cell-lines *in vitro*

We obtained and cultured a number of cell-lines: MDA-MB-231, MCF-7, and HBL-100 human breast epithelial cells; HL-60 human leukemia cells; SK-OV-3 human ovarian cancer cells; HCT-116 human colon cancer cells, and NIH 3T3 mouse fibroblast cells. Optimal HA modification levels and drug loading were established. Extensive studies of dose-response and selective cytotoxicity were completed with HA-Taxol, and uptake studies were performed with HA-BODIPY. The uptake of HA-Taxol or HA-BODIPY into cells was blocked by pre-incubation of cells with HA, but not with chondroitin sulfate. A similar result was obtained by flow cytometry using HA-Taxol-FITC. These data were published (D.1.a., c.).

Task 4. Measure efficacy of bioconjugates (vs. free drugs) using human breast cancer epithelial cell tumor xenografts in nude mice

Protocols to accomplish this task using our optimized HA-Taxol preparation have been implemented in experiments underway in two laboratories: UUtah and with collaborators Drs. Zhang and Underhill. We have established dosing protocols and levels, and we have established which tumor cell-lines will be optimal for observing efficacy of the new models.

Task 5. Initiate planning for Phase I safety testing of one or two optimal HA bioconjugates in terminal diagnosis human patients with drug- and radiation-refractory metastasis

We are working with Dr. Richard Wheeler, Director of Clinical Trials of the Huntsman Cancer Institute (UUtah) to develop protocols for Phase I safety tests of HA-ADH and HA-Taxol. Scale-up sterile synthesis of selected HA bioconjugates for larger scale preclinical animal studies and for human trials will be necessary to accomplish these post-award safety trials. Mechanisms for funding the GLP synthesis and preclinical evaluation are being explored.

C. Key Research Accomplishments

This section provides a bulleted list of key accomplishments, both those within the initial objectives and tasks and those that arose as promising leads during the pursuit of the originally outlined tasks.

1. Accomplishments based on original tasks

- HA-Taxol preparations were evaluated for selective cytotoxicity in six cell-lines (D.1.a., c.)
- Fluorescently-labeled HA and fluorescently-labeled HA-Taxol were prepared and characterized (D.1.a., c.)
- Cell binding and uptake of fluorescent HA and HA-Taxol was measured by confocal microscopy and flow cytometry (D.1.a., c.)
- Release of Taxol from HA-Taxol in cell cultures was determined by HPLC (D.1.c.)
- *In vivo* testing of HA-Taxol in nude mice with xenografted human tumors was initiated (internal results plus collaboration)
- Brefeldin A was chemically modified as a prodrug for chemical attachment to HA
- Geldanamycin was chemically modified with hydrazides
- Toxicity of HA-Taxol to wild-type and MDR breast cancer cell-lines was evaluated (collaboration)
- Use of HA for targeting of HPMA-DOX was successful in cell cultures (collaboration) (D.1.k.) and a patent application was filed (D.2.c.)
- Cell biology of HA-FITC-Taxol in CD44 wild-type and mutant cell lines was measured (collaboration) (D.1.m.)

2. Accomplishments ancillary to original tasks but leading to a greater understanding of the mechanism of uptake and to novel drug leads

- The transforming HA receptor RHAMM was expressed in recombinant form and with ^{13}C , ^{15}N labels for structural biological studies whose solution structure was determined using high resolution 2-D and 3-D NMR methods (M.R. Ziebell Ph.D. dissertation)
- Rapid and novel HA-binding assays were established (D.1.e.)
- Peptide libraries (phage-display and beads) were screened and peptides were identified that bind to RHAMM and are taken up by cells (D.1.e., D.1.f.). A patent application (D.2.b.) was filed and a potential licensee was contacted.

- Peptide leads were synthesized, fluorescently-tagged or biotinylated, and biophysical and functional studies of these peptides were initiated (D.1.e.).
- Review articles, a web site (D.1.j.), and book chapters were prepared in the areas of the use of HA for biochemical studies and drug delivery (D.1.b.), for tissue engineering (D.1.d.), for drug delivery (D.1.j.) targeted cancer chemotherapy (D.1.k.), for drug delivery and bioengineering (D.1.g., j.), and the interactions of proteins with HA (D.1.h.)

D. Reportable Outcomes

1. Publications

- a. Y. Luo and G.D. Prestwich, "Synthesis and Cytotoxicity of Hyaluronan-Taxol Antitumor Bioconjugates," *Bioconjugate Chem.*, **10**, 755-763 (1999).
- b. G.D. Prestwich, Y. Luo, M.R. Ziebell, K.P. Vercruysse, K.R. Kirker, and J.S. MacMaster, "Chemically-Modified Hyaluronan: New Biomaterials and Probes for Cell Biology," in *New Frontiers in Medical Sciences: Redefining Hyaluronan* Padua, Italy (G. Abatangelo and P.H. Weigel, eds.) Elsevier Science, pp. 181-194 (2000).
- c. Y. Luo, M.R. Ziebell, and G.D. Prestwich, "A Hyaluronic Acid -Taxol Anti-tumor Bioconjugate Targeted to Cancer Cells," *Biomacromolecules*, **1**, 208-218 (2000).
- d. Y. Luo, K.R. Kirker, and G.D. Prestwich, "Modification of Natural Polymers: Hyaluronic Acid," *Methods of Tissue Engineering* (A. Atala and R. Lanza, eds.), Academic Press, Orlando, Florida, in press (2001).
- e. M.R. Ziebell, Z.G. Zhao, B. Luo, Y. Luo, E.A. Turley, and G.D. Prestwich, "Peptides that Mimic Carbohydrates: High Affinity Ligands for A Hyaluronic Acid Binding Domain," *Chemistry and Biology* in press (2001).
- f. S. Zhang, W.F. Cheung, J. Lu, M.R. Ziebell, S.A. Turley, R. Harrison, D. Zylka, N. Ahn, D. Litchfield, G.D. Prestwich, T. Cruz, and E.A. Turley, "Intracellular RHAMM Isoforms Bind Directly to erk1 and These Interactions are Required for Transformation and for Podosome Formation via the erk Kinase Pathway," *Molec. Cell. Biol.*, in revision (2001).
- g. G.D. Prestwich, Y. Luo, K.R. Kirker, M.R. Ziebell, and J. Shelby "Hyaluronan Biomaterials for Targeted Drug Delivery and Wound Healing," *HA 2000*, Woodhead Publishing Ltd., Abington, UK, in press (2000).
- h. A.J. Day and G.D. Prestwich, "Hyaluronan Binding Proteins: Tying Up the Giant," *J. Biol. Chem.*, in press (2000).
- i. G.D. Prestwich, "Biomaterials from Chemically-Modified Hyaluronan," *Glycoforum* <http://glycoforum.gr.jp/science/hyaluronan/HA18/HA18E.html> (2001).
- j. Y. Luo and G.D. Prestwich, "Novel Biomaterials for Drug Delivery," *Exp. Opin. Ther. Patents*, in press (2001).
- k. Y. Luo and G.D. Prestwich, "Cancer-Targeted Macromolecular Chemotherapeutics," *Current Cancer Drug Targets*, submitted (2001)
- l. Y. Luo, N.J. Bernshaw, Z.-R. Lu, J. Kopecek, and G.D. Prestwich, "HPMA - Hyaluronic Acid - Adriamycin Bioconjugates: Targeted Delivery of Adriamycin to Cancer Cells," submitted (2001).
- m. L.Y.W. Bourguignon, W. Nieves-Neira, Y.-W. Chen, H. Zhu, Y. Luo, and G.D. Prestwich, "A Novel Anti-Tumor Agent, Hyaluronic Acid (HA)-Taxol Conjugates, Causes CD44-Mediated Cytotoxic Killing of Human Ovarian Carcinoma Cells," in preparation (2001).

2. Patents, licenses and disclosures

- a. G.D. Prestwich, Y. Luo, K.P. Vercruysse, "Method for Preparing and Isolating High-Purity Bioconjugates of Hyaluronic Acid," UUtah disclosure filed March 10, 1998.
- b. G.D. Prestwich, "Discovery of Peptides That Mimic Hyaluronic Acid," US Provisional Patent Application No. 60/091,758 filed July 6, 1998. Full filing, July 3, 1999. Full patent filed July 3, 2000.
- c. Y. Luo, G.D. Prestwich, J. Kopecek, and Z.-R. Lu, "Hyaluronic Acid Containing Bioconjugates: Targeted Delivery of Anti-Cancer Drugs to Cancer Cells," U.S. Provisional Application, Filed May 2, 2001.

3. Degrees

Michael R. Ziebell, Physiology & Biophysics, The University at Stony Brook, Stony Brook, New York, PhD, January 2000.

4. Leveraged funding

The chemical modification technology developed was employed in several on-campus applications which were funded internally. These include preparation of HA hydrogel films for drug release and wound healing and the development of HA-modified particles for binding cancer cells. A manuscript was published describing the new hydrogel films, and two manuscripts on wound healing in mice and in pigs are in preparation. An NIH grant application has been submitted by Dr. Y. Luo (Research Assistant Professor with Dr. Prestwich) to the NIH to support development of this material for wound healing.

Hyaluronic Acid Hydrogel Films For Wound Healing
Yi Luo, Principal Investigator
NIH, Glenn D. Prestwich, Co-Investigator
Bioengineering Research Project on Wound Healing

On-campus support was obtained to search for inhibitors of Hase, and to examine other glycosaminoglycan-based films for growth factor release and for improving the mechanical stability by copolymerization with elastin-like peptides.

Attachment of Hyaluronic Acid and Growth of Cells at Metal Interfaces
Center for Biopolymers at Interfaces
2/1/1999 - 1/31/2000

Growth of Cells of Bioactive Peptides on Hyaluronic Acid at Metal Interfaces
Center for Biopolymers at Interfaces
5/01/MM - 4/30/2001

Polysaccharide Hydrogel Membrane for Wound Healing
Center for Biopolymers at Interfaces
11/1/2000 - 10/31/2001

Discovery of New Hyaluronan-Binding Proteins Important in
Development and Metastasis
Technology Innovation Grant
7/1/1999 - 6/30/2001

Development of New, Selective Inhibitors of Hyaluronidase
UUtah Research Foundation, Funding Incentive Seed Grant Program
9/15/1998 - 9/14/1999

Polymerizable Glycosaminoglycans
Center for Biopolymers at Interfaces
4/15/1998 - 4/14/1999

Attachment of Hyaluronate to Surfaces and to PolyHPMA
Center for Biopolymers at Interfaces
11/15/1996 - 11/14/1998

Targeting Anti-cancer Drugs to Metastatic Cells via Hyaluroinc Acid Receptors
Huntsman Cancer
7/1/1996 - 6/30/1998

Our chemically-modified HA was a prominent part of an application for an NIH consortium project to prepare tissue for developing HA substitutes to treat vocal insufficiency. This project was recently funded (Steven Gray, MD, Principal Investigator, UUtah) and we are developing HA materials for prosthetic HA replacement uses, anti-scarring applications, and for preparing tissue scaffolds for tissue regeneration.

Engineering the Vocal Fold Extracellular Matrix
NIH 1 R01 DC04336-01
Steven D. Gray, PI, PI, Glenn D. Prestwich, Project Leader for Scaffold Chemistry

DOD grant applications for breast, ovarian, and prostate cancer were submitted during 2001 by Dr. Prestwich and two of his research faculty members (Drs. J. C. Hinshaw and Y. Luo) in response to RFAs. Dr. Prestwich submitted a Breast Cancer Innovator Award application in June 2001.

Prostate-Targeted Macromolecular Antitumor Agents
Yi Luo, PI, Glenn D. Prestwich, Co-Investigator
Department of Defense
Submitted March 2001

Synthesis of Targeted Drugs for Treating Breast Cancer
Jerald C. Hinshaw, PI, Glenn D. Prestwich, Co-Investigator
Department of Defense
Submitted June 2001

Integrating Molecular Diagnostics and Treatment in Breast Cancer
Glenn D. Prestwich
Department of Defense
Submitted June 2001

Synthesis of Targeted Drugs for Treating Melanoma
Jerald C. Hinshaw, PI, Glenn D. Prestwich, Co-Investigator
UUtah Research Foundation
Submitted July 2001

5. Invited and public presentations

14 invited seminars or contributed posters have been presented at universities or companies by Dr. Prestwich or the research scientists affiliated with this project.

a. Invited

1999

Redefining Hyaluronan, Padua, Italy, 17-19 June

2000

Genzyme Advanced Biomaterials, Cambridge, Massachusetts, 22 April

Department of Defense Breast Cancer Symposium, Atlanta, Georgia, 8-12 June

Gordon Research Conference on Signal Transduction by Engineered Extracellular Matrices, 26 June

Gordon Research Conference on Proteoglycans, 9-14 July

Hyaluronan 2000, North East Wales Institute, United Kingdom, 4-8 September

2001

UUtah School of Medicine, Department of Surgery Retreat, 23 March

NIH BECON Symposium, Invited Panelist, 26, 27 June

Enzyme Regulation in Cancer, Indiana University, 23-25 September

2002

Gordon Research Conference, Signal Transduction

b. Contributed

DOD Era of Hope Atlanta 2000

International Drug Delivery Symposium Salt Lake City, 1999

International Drug Delivery Symposium Salt Lake City 2001

International Hyaluronan 2000, Wrexham, Wales, UK, September 4 - September 9, 2000

Yi Luo, HA containing bioconjugates: Targeted delivery of anti-cancer drug doxorubicin to cancer cells, American Association of Pharmaceutical Scientists, Denver, Colorado October 21-25, 2001

E. Conclusions:

Our results to-date provide an exciting and promising method for the development of a new drug delivery system, and in basic research to identify new drug targets and mechanisms. First, we have successfully demonstrated that HA-Taxol prodrugs are selective and soluble cytotoxic agents against cancer cells, and that their mode of action requires HA receptor-mediated uptake by target cells. We expect that *in vivo* experiments in the next year will demonstrate safety and selective toxicity. Second, we discovered that attachment of HA fragments to the macromolecular prodrug HPMA-DOX increased its targeting to cancer cells and increased cytotoxicity to cancer cells 10- to 20-fold for breast and prostate cancer cell lines. Third, we have obtained important new knowledge about the structure of RHAMM-HA complexes, and we have identified two kinds of polypeptides that selectively interfere with HA-RHAMM interactions and also affect the ability of RHAMM to cause cell transformation.

F. References

Literature references may be found in the preprints included as appendix materials.

G. Appendices

Biosketches of PI and research scientists

Glenn D. Prestwich

Koen P. Vercruysse

Yi Luo

Michael R. Ziebell

Nicole J. Bernshaw

Publications

1. Y. Luo and G.D. Prestwich, "Synthesis and Cytotoxicity of Hyaluronan-Taxol Antitumor Bioconjugates," *Bioconjugate Chem.*, **10**, 755-763 (1999).
2. G.D. Prestwich, Y. Luo, M.R. Ziebell, K.P. Vercruysse, K.R. Kirker, and J.S. MacMaster, "Chemically-Modified Hyaluronan: New Biomaterials and Probes for Cell Biology," in *New Frontiers in Medical Sciences: Redefining Hyaluronan* Padua, Italy (G. Abatangelo and P.H. Weigel, eds.) Elsevier Science, pp. 181-194 (2000).
3. Y. Luo, M.R. Ziebell, and G.D. Prestwich, "A Hyaluronic Acid -Taxol Anti-tumor Bioconjugate Targeted to Cancer Cells," *Biomacromolecules*, **1**, 208-218 (2000).
4. Y. Luo, K.R. Kirker, and G.D. Prestwich, "Chemical Modification of Hyaluronic Acid," *Methods of Tissue Engineering* (A. Atala and R. Lanza, eds.), Academic Press, Orlando, Florida, in press (2001).
5. M.R. Ziebell, Z.G. Zhao, B. Luo, Y. Luo, E.A. Turley, and G.D. Prestwich, "Peptides that Mimic Carbohydrates: High Affinity Ligands for A Hyaluronic Acid Binding Domain," *Chemistry and Biology* in press (2001).
6. S. Zhang, W.F. Cheung, J. Lu, M.R. Ziebell, S.A. Turley, R. Harrison, D. Zylka, N. Ahn, D. Litchfield, G.D. Prestwich, T. Cruz, and E.A. Turley, "Intracellular RHAMM Isoforms Bind Directly to erk1 and These Interactions are Required for Transformation and for Podosome Formation via the erk Kinase Pathway," *Molec. Cell. Biol.*, in press (2001).
7. G.D. Prestwich, Y. Luo, K.R. Kirker, M.R. Ziebell, and J. Shelby Hyaluronan Biomaterials for Targeted Drug Delivery and Wound Healing *HA 2000*, Woodhead Publishing Ltd., Abington, UK, in press (2000).
8. A.J. Day and G.D. Prestwich, "Hyaluronan Binding Proteins: Tying Up the Giant," *J. Biol. Chem.*, in press (2000).
9. G.D. Prestwich, "Biomaterials from Chemically-Modified Hyaluronan ," *Glycoforum* <http://glycoforum.gr.jp/science/hyaluronan/HA18/HA18E.html> (2001).

10. Y. Luo and G.D. Prestwich, "Novel Biomaterials for Drug Delivery," *Exp. Opin. Ther. Patents*, submitted (2001).
11. Y. Luo and G.D. Prestwich, "Cancer-Targeted Macromolecular Chemotherapeutics," *Current Cancer Drug*, submitted (2001)
12. Y. Luo, N.J. Bernshaw, Z.-R. Lu, J. Kopecek, and G.D. Prestwich, "HPMA - Hyaluronic Acid - Adriamycin Bioconjugates: Targeted Delivery of Adriamycin to Cancer Cells," submitted (2001).

Appendix

BIOGRAPHICAL SKETCH

NAME	POSITION TITLE		
PRESTWICH, GLENN D.	Presidential Professor and Chair of Medicinal Chemistry		
EDUCATION/TRAINING <i>(Begin with baccalaureate or other initial professional education, such as nursing, and include postdoctoral training.)</i>			
INSTITUTION AND LOCATION	DEGREE	YEAR(s)	FIELD OF STUDY
California Institute of Technology, Pasadena, California	1970	1970 (Honors)	Chemistry
Stanford University, Palo Alto, California	Ph.D.	1974	Organic Chemistry

Research and Professional Experience

1974, 1977: Cornell University, NIH postdoctoral fellowship, Department of Chemistry (Prof. J. Meinwald)
1974 - 1976: ICIPE, P.O. Box 30772, Nairobi, Kenya; Research Scientist in Chemistry Unit
1977 - 1982: Assistant Professor of Chemistry, SUNY, Stony Brook, New York
1982 - 1984: Associate Professor of Chemistry, SUNY, Stony Brook, New York
1984 - 1996: Professor of Chemistry, SUNY, Stony Brook, New York
1991 - 1992: Visiting Professor, Departments of Chemistry at Harvard University and The University of Utah
1992 - 1996: Professor of Biochemistry and Cellular Biology, SUNY, Stony Brook, New York
1992 - 1996: Director, Center for Biotechnology, SUNY, Stony Brook, New York
1996 - current: Presidential Professor and Chair, Medicinal Chemistry, The University of Utah
1996 - current: Research Professor of Biochemistry; Adjunct Professor of Chemistry and of Bioengineering; Program Leader, Molecular Pharmacology Program, Huntsman Cancer Institute; Director, Center for Cell Signaling, The University of Utah

Research interests: Structures of protein-ligand complexes; phosphoinositide affinity probes; cell signaling; isoprenoid chemical biology; hyaluronic acid biomaterials; molecular olfaction.

Honors: NIH Postdoctoral Fellow, January 1976-June 1977; Fellow of the Alfred P. Sloan Foundation, 1981-1985; Camille and Henry Dreyfus Teacher-Scholar, 1981-1986; Distinguished Research Fellow, Bodega Marine Laboratory, 1989; H.C. Brown Lecturer, Purdue University, 1990; National Institutes of Health Senior Fellowship, 1992; Paul Dawson Biotechnology Award, American Association of Colleges of Pharmacy, 1998; 1999 Tibbetts Award for Utah [to Echelon Research Laboratories, Inc.]; *ChemTracts* (Organic Chemistry), Invited Expert Analyst (1989-current); *Bioconjugate Chemistry* (1992-current); *Current Opinion in Chemical Biology* (1997-current); *Journal of Biological Chemistry* (2000-current); M.D. Anderson Cancer Center Advisory Board, University of Texas (2001-current)

Publications: G.D. Prestwich is author of over 380 journal research articles and book chapters since 1974. Selected relevant publications on HA and other topics from the last six years are included.

- T. Pouyani and G.D. Prestwich, "Functionalized Derivative of Hyaluronic Acid as Drug Carriers and as Novel Biomaterials," *Bioconjugate Chem.*, **5**, 339-347 (1994).
- T. Pouyani, G.S. Harbison, and G.D. Prestwich, "Novel Hydrogels of Hyaluronic Acid: Synthesis, Surface Structure and Solid-State NMR," *J. Am. Chem. Soc.*, **116**, 7515-7522 (1994).
- G.D. Prestwich, G. Dormán, J.T. Elliott, D.M. Marecak, and A. Chaudhary, "Benzophenone Photoprobes for Phosphoinositides, Peptides, and Drugs," *Photochem. Photobiol.*, **65**, 222-234 (1997).
- G.D. Prestwich "Touching all the Bases: Inositol Polyphosphate and Phosphoinositide Affinity Probes from Glucose," *Acc. Chem. Res.*, **29**, 503-513 (1996).
- T. Pouyani and G.D. Prestwich, "Functionalized Derivatives of Hyaluronic Acid," U.S. Patent No. 5,616,568 (April, 1, 1997).
- B. Mehrotra, J.T. Elliott, J. Chen, J.D. Olszewski, A.A. Profit, A. Chaudhary, M. Fukuda, K. Mikoshiba, and G.D. Prestwich, "Selective Photoaffinity Labeling of the Inositol Polyphosphate Binding C2B Domains of Synaptotagmins," *J. Biol. Chem.*, **272**, 4237-4244 (1997).
- G.D. Prestwich, D.M. Marecak, J.F. Marecek, K.P. Vercruysse, and M.R. Ziebell, "Controlled Chemical Modification of Hyaluronic Acid: Synthesis, Applications, and Biodegradation of Hydrazide Derivatives," *J. Controlled Rel.* **53**, 93-103 (1998).
- A. Chaudhary and G.D. Prestwich, "Photoaffinity Analogue for the Anti-inflammatory Drug α -Trinositol: Synthesis and Identification of Putative Molecular Targets," *Bioconjugate Chem.* **8**, 680-685 (1997).
- G.D. Prestwich, D.M. Marecak, J.F. Marecek, K.P. Vercruysse, and M.R. Ziebell, "Chemical Modification of Hyaluronic Acid for Drug Delivery, Biomaterials, and Biochemical Probes," in *The Chemistry, Biology, and Medical Applications of Hyaluronan and its Derivatives* (T. C. Laurent, ed.), pp. 43-65 (1998).
- K.P. Vercruysse, D.M. Marecak, J.F. Marecek, and G.D. Prestwich, "Synthesis and *In vitro* Degradation of New Polyvalent Hydrazide Cross-Linked Hydrogels of Hyaluronic Acid," *Bioconjugate Chem.*, **8**, 686-694 (1997).

- J.T. Elliott, R.A. Jurenka, G.D. Prestwich, and W.L. Roelofs, "Identification of Soluble Binding Proteins for an Insect Neuropeptide," *Biochem. Biophys. Res. Commun.*, **238**, 925-930 (1997).
- I. Abe, T. Dang, Y.F. Zheng, B.A. Madden, C. Feil, K. Poralla, and G. D. Prestwich, "Cyclization of (3S)29-Methylidene-2,3-oxidosqualene by Bacterial Squalene:Hopene Cyclase: Irreversible Enzyme Inactivation and Isolation of an Unnatural Dammarenoid," *J. Am. Chem. Soc.*, **119**, 11333-11334 (1997).
- A. Chaudhary, J. Chen, Q.-M. Gu, W. Witke, D.J. Kwiatkowski, and G.D. Prestwich, "Probing the Phosphoinositide 4,5-bisphosphate Binding Site of Human Profilin I," *Chem. & Biol.* **5**, 273-281 (1998).
- A. Chaudhary, Q.-M. Gu, O. Thum, A.A. Profit, Y. Qing, L. Jeyakumar, S. Fleischer, and G.D. Prestwich, "Specific Interaction of Golgi Coatmer α -COP with Phosphatidylinositol 3,4,5-Trisphosphate," *J. Biol. Chem.*, **273**, 8344-8350 (1998).
- Y.F. Zheng, I. Abe, and G.D. Prestwich, "Inhibition Kinetics and Affinity Labeling of Bacterial Squalene:Hopene Cyclase by Thia-Substituted Analogs of 2,3-Oxidosqualene," *Biochemistry*, **37**, 5981-5987 (1998).
- K.P. Vercruysse and G.D. Prestwich, "Hyaluronate Derivatives in Drug Delivery," *Crit.Rev. Ther. Drug Carrier Syst.* **15**, 513-555 (1998).
- I. Abe, Y.F. Zheng, and G. D. Prestwich, "Photoaffinity Labeling of Oxidosqualene Cyclase and Squalene Cyclase by a Benzophenone-Containing Inhibitor," *Biochemistry*, **37**, 5779-5784 (1998).
- G.D. Prestwich and K.P. Vercruysse, "Therapeutic Applications of Hyaluronic Acid and Hyaluronan Derivatives," *Pharmaceut. Sci. & Technol. Today*, **1**, 42-43 (1998).
- L. Collis, C. Hall, L. Lange, M.R. Ziebell, G.D. Prestwich, and E.A. Turley, "Rapid Hyaluronan Uptake is Associated with Enhanced Motility: Implications for an Intracellular Mode of Action," *FEBS Lett.*, **440**, 444-449 (1998).
- M. Mason, K.P. Vercruysse, K.R. Kirker, R. Frisch, D.M. Marecak, G.D. Prestwich, and W. Pitt, "Hyaluronic Acid-Modified Polypropylene, Polystyrene, and Polytetrafluoroethylene," *Biomaterials*, in press (1999).
- K.P. Vercruysse, M.R. Ziebell, and G.D. Prestwich, "Control of Enzymatic Degradation of Hyaluronan by Divalent Cations," *Carbohydr. Res.*, **318**, 26-37 (1999).
- Y. Luo and G.D. Prestwich, "Synthesis and Cytotoxicity of a Hyaluronic Antitumor Bioconjugate," *Bioconjugate Chem.*, **10**, 755-763 (1999).
- G.D. Prestwich, Y. Luo, M.R. Ziebell, K.P. Vercruysse, K.R. Kirker, and J.S. MacMaster, "Chemically-Modified Hyaluronan: New Biomaterials and Probes for Cell Biology," in *New Frontiers in Medical Sciences: Redefining Hyaluronan* Padua, Italy (G. Abatangelo and P.H. Weigel, ed.) Elsevier, pp 181-194 (2000).
- J.T. Elliott, W.J. Hoekstra, B.E. Maryanoff, and G.D. Prestwich, "Photoactivatable Peptides Based on BMS-197525, A Potent Antagonist of the Human Thrombin Receptor (PAR-1)," *Bioorg. Med. Chem. Lett.*, **9**, 279-284 (1999).
- Q. Yan, G.D. Prestwich, and W.J. Lennarz, "The Ost1p Subunit of Yeast Oligosaccharyl Transferase Recognizes the Peptide Glycosylation Site Sequence, -Asn-X-Ser/Thr-," *J. Biol. Chem.* **274**, 5021-5025 (1999).
- S.M. Jones, R. Klinghoffer, G.D. Prestwich, A. Toker, and A. Kazlauskas, "PDGF Induces an Early and a Late Wave of PI 3-Kinase Activity, and Only the Late Wave is Required for Progression Through G1," *Curr. Biol.*, **9**, 512-521 (1999).
- S. Zhang, W.F. Cheung, J. Lu, M.R. Ziebell, S.A. Turley, R. Harrison, D. Zylka, N. Ahn, D. Litchfield, G.D. Prestwich, T. Cruz, and E.A. Turley, "Intracellular RHAMM Isoforms Bind Directly to erk1 and These Interactions are Required for Transformation and for Podosome Formation via the erk Kinase Pathway," *Molec. Cell. Biol.*, in press (2000).
- M. Mason, K.P. Vercruysse, K.R. Kirker, R. Frisch, D.M. Marecak, G.D. Prestwich, and W.G. Pitt, "Hyaluronic Acid-Modified Polypropylene, Polystyrene, and Polytetrafluoroethylene," *Biomaterials*, **21**, 31-36 (2000).
- Y. Luo, M.R. Ziebell, and G.D. Prestwich, "A Hyaluronic Acid - Taxol® Anti-tumor Bioconjugate Targeted to Cancer Cells," *Biomacromolecules*, **1**, 208-218 (2000).
- Y. Luo, K.R. Kirker, and G.D. Prestwich, "Cross-Linked Hyaluronic Acid Hydrogel Films: New Biomaterials for Drug Delivery," *J. Controlled Rel.*, **69**, 169-184 (2000).
- G.D. Prestwich, "Biomaterials from Chemically-Modified Hyaluronan," *Glycoforum*, in press (2001).
- Y. Luo, K.R. Kirker, and G.D. Prestwich, "Chemical Modification of Hyaluronic Acid," *Methods of Tissue Engineering* (A. Atala and R. Lanza, eds.), Academic Press, Orlando, Florida, in press (2000).
- G.D. Prestwich, Y. Luo, K.R. Kirker, M.R. Ziebell, and J. Shelby Hyaluronan Biomaterials for Targeted Drug Delivery and Wound Healing *HA 2000*, Woodhead Publishing Ltd., Abington, UK, in press (2000).
- Y. Luo, K.R. Kirker, and G.D. Prestwich, "Hyaluronic Acid Hydrogel Film: A New Biomaterial for Drug Delivery and Wound Healing," *HA 2000*, Woodhead Publishing Ltd., Abington, UK, in press (2000).
- A.J. Day and G.D. Prestwich, "Hyaluronan Binding Proteins: Tying Up the Giant," *J. Biol. Chem.*, in press (2000).
- M.R. Ziebell, Z.-G. Zhao, B. Luo, Y. Luo, E.A. Turley, and G.D. Prestwich, "Peptides that Mimic Carbohydrates: High Affinity Ligands for A Hyaluronic Acid Binding Domain," *J. Biol. Chem.*, submitted (2000).
- S. Ozaki, D.B. DeWald, J.C. Shope, J. Chen, and G.D. Prestwich, "Intracellular Delivery of Phosphoinositides and Inositol Phosphates using Polyamine Carriers," *Proc. Natl. Acad. Sci., USA*, **27**, 11286-11291 (2000).

BIOGRAPHICAL SKETCH

NAME		POSITION TITLE	
KOEN P. VERCRUYSE		Research Assistant Professor	
EDUCATION/TRAINING			
INSTITUTION AND LOCATION	DEGREE (if applicable)	YEAR(s)	FIELD OF STUDY
University of Ghent, Belgium	B.Sc.	1990	Pharmaceutical Sciences
University of Ghent, Belgium	Ph.D.	1995	Pharmaceutical Sciences

Research and Professional Experience

1991 Lab of Galenic Development, Lilly Services S.A., Mont-Saint-Guibert, Belgium
1991 - 1995 Lab of General Biochemistry and Physical Pharmacy, University of Ghent, Belgium
1995 - 1996 Postdoctoral Research Associate, Department of Chemistry, SUNY at Stony Brook, NY
1996 - 1998 Postdoctoral Research Associate, Department of Medicinal Chemistry, University of Utah, Salt Lake City, Utah.
1998 - 2000 Research Assistant Professor, Department of Medicinal Chemistry, University of Utah
2000 - current Assistant Professor, Tennessee State University, Nashville, Tennessee

Publications

Dekeyser, P.M; De Smedt, S.; Vercruysse, K.; Demeester, J.; Lauwers, A. "High-performance size-exclusion chromatography of proteoglycans extracted from bovine articular cartilage" *Anal. Chim. Acta*, 1993, 279, 123-127.
 Vercruysse, K.P.; Lauwers, A.R.; Demeester, J.M. "Kinetic investigation of the degradation of hyaluronan by hyaluronidase using gel permeation chromatography" *J. Chrom. B: Biomed. Appl.*, 1994, 656, 179-190.
 Vercruysse, K.P.; Lauwers, A.R.; Demeester, J.M. "Absolute and empirical determination of the enzymatic activity and kinetic investigation of the action of hyaluronidase on hyaluronan using viscosimetry" *Biochem. J.*, 1995, 306, 153-160.
 Vercruysse, K.P.; Lauwers, A.R.; Demeester, J.M. "Kinetic investigation of the action of hyaluronidase on hyaluronan using the Morgan-Elson and neocuproine assay" *Biochem. J.*, 1995, 310, 55-59.
 Demeester, J.; Vercruysse, K.P.; "Hyaluronidase" in "Pharmaceutical Enzymes" (Lauwers, A.; Scharpe, S.; editors), 1997, pp 155-186, Marcel Dekker, Inc., New York.
 Vercruysse, K.P.; Marecak, D.M.; Marecek, J.F.; Prestwich, G.D. "Synthesis and in vitro degradation of new polyvalent hydrazide cross-linked hydrogels of hyaluronic acid" *Bioconjugate Chem.*, 1997, 8, 686-694.
 Van Eeckhout, N., Vercruysse, K., Lauwers, A., and Demeester, "Investigation of the activation of hyaluronidase by CaCl_2 using viscosimetry and gel-permeation chromatography", *Archives of Physiology and Biochemistry*, 1997, 105, p133.
 Prestwich, G.D.; Marecak, D.M.; Marecek, J.F.; Vercruysse, K.P.; Ziebell, M.R. "Chemical modification of hyaluronic acid for drug delivery, biomaterials, and biochemical probes" *Wenner-Gren Foundation International Symposium : The chemistry, biology, and medical applications of hyaluronan and its derivatives*, 1998, 72, pp 43-65.
 Prestwich, G.D.; Marecak, D.M.; Marecek, J.F.; Vercruysse, K.P.; Ziebell, M.R. "Controlled chemical modification of hyaluronic acid: synthesis, applications, and biodegradation of hydrazide derivatives" *J. Controlled Rel.*, 1998, 53, 93-103.
 Prestwich, G.D. and Vercruysse, K.P. "Therapeutic applications of hyaluronic acid and hyaluronan derivatives", *Pharm. Sci. & Tech. Today*, 1998, 1, 42-43.
 Vercruysse, K.P. and Prestwich, G.D.; "Hyaluronate derivatives in drug delivery"; *Crit. Rev. Therap. Drug Car. Syst.*; 1998, 15, pp.513-555.
 Mitchell, M.; Vercruysse, K.; Kirker, K.; Frish, R.; Marecak, D.; Prestwich, G.; Pitt, W. "Hyaluronic acid-modified polypropylene, polystyrene, and polytetrafluoroethylene"; *Biomaterials*, 1999 (in press).
 K.P. Vercruysse, M.R. Ziebell, and G.D. Prestwich, "Control of Enzymatic Degradation of Hyaluronan by Divalent Cations," *Carbohydr. Res.*, **318**, 26-37 (1999).

G.D. Prestwich, Y. Luo, M.R. Ziebell, K.P. Vercruysse, K.R. Kirker, and J.S. MacMaster,
"Chemically-Modified Hyaluronan: New Biomaterials and Probes for Cell Biology," in *New Frontiers
in Medical Sciences: Redefining Hyaluronan* Padua, Italy (G. Abatangelo and P.H. Weigel, eds.)
Elsevier Science, pp. 181-194 (2000).

Grants awarded

May 1998 University of Utah Faculty Research and Creative Grant for "Hyaluronan-fluorescent
probe conjugate with quenched fluorescence as substrate for hyaluronidase"
September 1998 University of Utah Research Foundation Funding Incentive Seed Grant Program for
"Development of New, Selective Inhibitors of Hyaluronidase" with Glenn D. Prestwich

*** * * As of separation August 2000 * * * ***

Presently Dr. Vercrussye is an assistant professor at Tennessee State University, Nashville

BIOGRAPHICAL SKETCH

Provide the following information for the key personnel in the order listed on Form Page 2.

NAME LUO, YI	POSITION TITLE Research Assistant Professor		
EDUCATION/TRAINING (<i>Begin with baccalaureate or other initial professional education, such as nursing, and include postdoctoral training.</i>)			
INSTITUTION AND LOCATION	DEGREE (if applicable)	YEAR(s)	FIELD OF STUDY
Nanjing University, Nanjing, PR China	BSc	1989	Organic Synthesis
Wuhan University, Wuhan, PR China	MSc	1991	Organic Synthesis
Wuhan University, Wuhan, PR China	PhD	1994	Bioactive Polymers

RESEARCH AND PROFESSIONAL EXPERIENCE: Concluding with present position, list, in chronological order, previous employment, experience, and honors. Include present membership on any Federal Government public advisory committee. List, in chronological order, the titles, all authors, and complete references to all publications during the past three years and to representative earlier publications pertinent to this application. If the list of publications in the last three years exceeds two pages, select the most pertinent publications. **DO NOT EXCEED TWO PAGES.**

Research and Professional Experience:

1994 - 1996	Postdoctoral Researcher, Department of Chemistry, Beijing University, Beijing, PR China
1996 - 1997	Researcher, National Institute of Health Sciences, Tokyo, Japan
1997 - 2000	Postdoctoral Research Associate, Medicinal Chemistry, The University of Utah
2000 - current	Research Assistant Professor, Medicinal Chemistry, The University of Utah

Publications

- Y.Luo, "Study on Reaction Mechanism with Basic Principles of Organic Chemistry," *DAXUE HUAXUE (University Chemistry)*, 1991, 6(4), 42.
- Y.Luo, X.J.Wu, Z.P.Chen, Z.X.Jiang, "Synthesis and Structure of Langmuir-Blodgett Films of A Novel Amphiphilic Porphyrin," *Chin. Chem. Lett.*, 1992, 3(5), 377.
- Y.Luo, X.J.Wu, Z.P.Chen, Z.X.Jiang, "Synthesis of A Novel Amphiphilic Porphyrin and Properties of Langmuir-Blodgett Films," *Chem. J. Chin. Universities*, 1992, 13(8), 1092.
- X.J.Wu, Y.Luo, Z.P.Chen, Z.X.Jiang, G.G.Xiong, "Structure of L-B Film of A Novel Amphiphilic Porphyrin," *Thin Film Sci. and Tech.*, 1993, 6(4), 314.
- Y.Luo, R.X.Zhuo, C.L.Fan, "Synthesis and Antitumor Activity of Peptidyl-N¹-hydroxymethyl-5-Fluorouracil," *Chin. Chem. Lett.*, 1993, 4(7), 581.
- Y.Luo, R.X.Zhuo, C.L.Fan, "Synthesis and Antitumor Activity of Peptidyl-N¹-hydroxymethyl-5-Fluorouracil," *Chem. J. Chin. Universities*, 1994, 15(4), 545.
- Y.Luo, R.X.Zhuo, C.L.Fan, "Synthesis and Antitumor Activity of Biodegradable Polyphosphamides Containing 5-Fluorouracil," *Chem. J. Chin. Universities*, 1994, 15(5), 767.
- Y.Luo, R.X.Zhuo, C.L.Fan, "Synthesis and Drug Release Properties of Biodegradable Polyphosphate Esters," *Chem. J. Chin. Universities*, 1994, 15(6), 932.
- Y.Luo, R.X.Zhuo, C.L.Fan, "Biodegradable Polyphosphate Esters and Drug Release," *Chem. J. Pharmaceuticals*, 1994, 25(6), 265.
- Y.Luo, R.X.Zhuo, C.L.Fan, "Synthesis and Antitumor Activity of Polyphosphate Polymeric Drugs Containing Hexestrol," *Chem. J. Chin. Universities*, 1994, 15(7), 1090.
- R.X.Zhuo, Y.Luo, G.L.Tao, "Immobilized Enzymes"(Review), *Ionic Exchange and Absorption*, 1994, (5), 447.
- Y.Luo, R.X.Zhuo, C.L.Fan, "Sustained Release of Levonorgestrel Using Polyphosphate as Drug Carrier," *Chin. Chem. Lett.*, 1995, 6(4), 333.
- Y.Luo, R.X.Zhuo, C.L.Fan, "Studies on The Magnetic Resonance Contrast Agents: Synthesis and Spin-lattice Relaxivity of Amino Acids and Oligopeptidyl Derivatives of Gd-DTPA," *Chin. Chem. Lett.* 1995, 6(5), 377.

- Y.Luo, R.X.Zhuo, C.L.Fan, "Study on Synthesis of Crosslinking Polyphosphate and Sustained Release of Levonorgestrel," *Chin. J. Synth. Chem.*, 1995, 3(3), 271.
- Y.Luo, R.X.Zhuo, C.L.Fan, "Studies on the Synthesis and Relaxivity of Amino Acids and Oligopeptides of Gd-DTPA Derivatives," *Chemical Journal of Chinese Universities*, 1995, 16(9), 1476.
- Y.Luo, R.X.Zhuo, C.L.Fan, "Studies on Water-soluble Metalloporphyrins as Tumor Targeting Magnetic Resonance Imaging Contrast Agents," *Chemical Journal of Chinese Universities*, 1995, 16(10), 1629.
- Y.Luo, R.X.Zhuo, C.L.Fan, "Synthesis of Crosslinked Polyphosphates and Drug Release," *Chemical Journal of Chinese Universities*, 1995, 16(10), 1633.
- Y.Luo, R.X.Zhuo, "Polymeric Drugs"(Review), *YAOXUE JINZHAN (Progress in Pharmaceutical Sciences)*, 1995, 19(3), 135.
- Y.Luo, R.X.Zhuo, "Magnetic Resonance Imaging Contrast Agents"(Review), *GUOWAI YIYAO (World Pharmacy)*, 1995, 16(4), 200.
- A.S. Hoffman (Translated by Y.Luo), "Intelligent Polymers: Synthesis and Applications in Medicine and Biotechnology" (Review), *GAO FEN ZI TONG BAO (Polymer Bulletin)*, 1995, (4), 245.
- Y.Luo, R.X.Zhuo, C.L.Fan, "Synthesis and Drug Release of Crosslinking Polyphosphates," *Chinese Journal of Reactive Polymers*, 1995, 4(1~2), 127-133.
- Y.Luo, R.X.Zhuo, C.L.Fan, "Sustained Release of Methotrexate with Crosslinking Polyphosphate as Drug Carrier," *Chinese Journal of Pharmaceuticals*, 1996, 27(1), 6.
- Y.Luo, "Controlled Release Methods" (Review), *GAO FEN ZI TONG BAO (Polymer Bulletin)*, 1996, (1), 18.
- Y.Luo, S.Yoshioka, Y.Aso, "Swelling Behavior and Drug Release of Amphiphilic N-Isopropylacrylamide Terpolymer Xerogels Depending on Polymerization Methods: γ -Irradiation Polymerization and Redox Initiated Polymerization," *Chem. Pharm. Bull.*, 1999, 47(4), 579-581.
- Y. Luo, G. D. Prestwich, "Synthesis and Selective Cytotoxicity of a Hyaluronic Acid-Antitumor Bioconjugate," *Bioconjugate Chem.*, 1999, 10(5), 755-763.
- G. D. Prestwich, Y. Luo, M.R. Ziebell, K.P. Vercruysse, K.R. Kirker and J.S. MacMaster, "Chemically-Modified Hyaluronan: New Biomaterials and Probes for Cell Biology," *New Frontiers in Medial Sciences: Redefining Hyaluronan (G. Abatangelo and P.H. Weigel, Ed)*, 2000 Elsevier Science, 2000, 181-194.
- Y. Luo, M. R. Ziebell, G. D. Prestwich, "A Hyaluronic Acid-Taxol Antitumor Bioconjugate Targeted to Cancer Cells," *Biomacromolecules*, 2000, 1(2), 208-218.
- Y. Luo, K.R. Kirker, G. D. Prestwich, "A Novel Hyaluronic Acid Hydrogel Film for Drug Delivery," *J. Controlled Rel.*, 2000, 69(1), 169-184.
- Y. Luo, K.R. Kirker, G.D. Prestwich, "Chemical Modification of Hyaluronic Acid," *Methods of Tissue Engineering* (Anthony Atala and Robert Lanza Ed.), Academic Press, in press.
- B.L. Oliver, Y. Luo, J.Liang, G.D. Prestwich, P.W. Noble, "Low Molecular Weight Hyaluronan Fragments Induce Chemokine Expression by An Extracellular Regulated Kinase-Dependent Pathway in Mouse Macrophage," *J. Exp. Medicine*, in press.
- M.R. Ziebell, B. Luo, Z.G. Zhao, Y. Luo, E.A. Turley, G.D. Prestwich, "The Convergence of Peptide Libraries in the Search of Artificial Ligands to the Hyaluronic Acid Binding Domains of RHAMM and TSG-6," *J. Biol. Chem.*, submitted.
- Y. Luo, K.R. Kirker, G.D. Prestwich, "Hyaluronic acid hydrogel film: a new biomaterial for drug delivery and wound healing", Proceedings of the HA2000 Symposium held in Wrexham, UK, 3-8, September, 2000, Elsevier Science B.V., in press.
- G.D. Prestwich, Y. Luo, K.R. Kirker, M.R. Ziebell, J. Shelby, "Hyaluronan biomaterials for targeted drug delivery and wound healing", Proceedings of the HA2000 Symposium held in Wrexham, UK, 3-8, September, 2000, Elsevier Science B.V., in press.
- Y. Luo, G. D. Prestwich, "Novel Biomaterials for Drug Delivery" (Review), Expert Opinion on Therapeutic Patents, in press.

BIOGRAPHICAL SKETCH

Provide the following information for the key personnel in the order listed on Form Page 2.

NAME	POSITION TITLE
ZIEBELL, MICHAEL R.	Graduate Research Assistant The University of Utah

Education

- 1993-2000: Dept. of Physiology, SUNY Stony Brook, Graduate Program in Biophysics, Completed all required coursework and teaching practicum
- 1992-1993: Indiana University, Bloomington, Coursework in Chemistry and Biology
- 1986-1991: Earlham College, Richmond, Indiana, BA, Physics

Publications:

- G.D. Prestwich, D.M. Marecak, J.F. Marecek, K.P. Vercruysse, and M.R. Ziebell, "Controlled Chemical Modification of Hyaluronic Acid: Synthesis, Applications, and Biodegradation of Hydrazide Derivatives," *J. Controlled Release*, **53**, 93-103 (1998).
- G.D. Prestwich, D.M. Marecak, J.F. Marecek, K.P. Vercruysse, and M.R. Ziebell, "Chemical Modification of Hyaluronic Acid for Drug Delivery, Biomaterials, and Biochemical Probes," in *The Chemistry, Biology, and Medical Applications of Hyaluronan and its Derivatives* (T. C. Laurent, ed.), Portland Press, London, pp. 43-65 (1998).

*** As of graduation January 2000 ***

Presently Dr. Ziebell is a postdoctoral associate,
Department of Neurobiology, Harvard Medical School

BIOGRAPHICAL SKETCH

Provide the following information for the key personnel in the order listed on Form Page 2.

NAME		POSITION TITLE	
BERNSHAW, NICOLE J.		Senior Research Specialist	
EDUCATION/TRAINING <i>(Begin with baccalaureate or other initial professional education, such as nursing, and include postdoctoral training.)</i>			
INSTITUTION AND LOCATION	DEGREE <i>(if applicable)</i>	YEAR(s)	FIELD OF STUDY
University of Ottawa, Ontario, Canada	BSc	1974	Biology
Univ. of British Columbia, Vancouver, BC, Canada	MSc	1976	Biochemistry

RESEARCH AND PROFESSIONAL EXPERIENCE: Concluding with present position, list, in chronological order, previous employment, experience, and honors. Include present membership on any Federal Government public advisory committee. List, in chronological order, the titles, all authors, and complete references to all publications during the past three years and to representative earlier publications pertinent to this application. If the list of publications in the last three years exceeds two pages, select the most pertinent publications. **DO NOT EXCEED TWO PAGES.**

Research and Professional Experience

The University of Utah, Salt Lake City, Utah

Laboratory technician:	Jan.-Mar, 1977
Research Assistant:	April 1977 to August 1980
Research Specialist:	August 1984 to February 1992
Principal Investigator:	March 1992 to August 1992 (SBIR, Phase I)
Senior Research Specialist:	October 1992 to December 1996
Editor:	January 1994 to present (part-time, professional journal)
Senior Research Specialist:	June 1997 to January 2000
Senior Research Specialist:	February 2000 to current

Publications

1. Parker CJ, Stone OL, Bernshaw NJ. Characterization of the enhanced susceptibility of paroxysmal nocturnal hemoglobinuria erythrocytes to complement-mediated lysis initiated by cobra venom factor. *J Immunol* 142: 208-216, 1989.
2. Parker CJ, Stone OL, Bernshaw NJ. Vitronectin (S protein) is associated with platelets. *Br J Haematol* 71: 245-252, 1989.
3. Holguin MH, Fredrick LR, Bernshaw NJ, Parker CJ. Isolation and characterization of a protein from normal erythrocytes that inhibits reactive lysis of the erythrocytes of paroxysmal nocturnal hemoglobinuria. *J Clin Invest* 84: 7-17, 1989.
4. Holguin MH, Wilcox LA, Bernshaw NJ, Rosse WF, Parker CJ. Relationship between the membrane inhibitor of reactive lysis and the erythrocyte phenotypes of paroxysmal nocturnal hemoglobinuria. *Clin Invest* 84:1387-1394, 1989.
5. Holguin MH, Wilcox LA, Bernshaw NJ, Rosse WF, Parker CJ. Erythrocyte membrane inhibitor of reactive lysis. Effects of phosphatidylinositol specific phospholipase C on the isolated and membrane associated protein. *Blood* 75:284-289, 1990.
6. Parker CJ, Bernshaw NJ, Wilcox LA. Analysis of the binding of human C3b to glycoproteins on rabbit and sheep erythrocytes. *Comp Inflam* 7:1-17, 1990.
7. Janatova J, Edes K, Bernshaw NJ, Burns GN, Caldwell KD: Coating inhibitory activity in human tears interferes with formation of immune complexes at polymer surfaces. *Proc ACS Div Polymeric Mats: Sci Eng* 69:277-278, 1993.
8. Janatova J, Edes K, Bernshaw NJ, Burns GN, Caldwell KD. Suppression of the coating inhibitory activity in tears and quantification of tear proteins by ELISA. *J Immunol* 150 (8 Part II): 326A, 1993.
9. Janatova J, Edes K, Wu F, Bernshaw NJ, Burns GL, Mohammad SF. Bovine plasma levels of C3, C4, and Fn in response to CPB and blood pump devices. *Mol Immunol* 30 (Suppl 1): 20, 1993.

10. Janatova J, Bernshaw NJ. A novel blood-biomaterials compatibility test evaluates interaction of biomaterials with complement and other plasma proteins. *Surfaces in Biomaterials '94 Symposium Notebook*: 108-113, 1994.
11. Janatova J, Bernshaw NJ. A Novel Approach To Test Blood-Biomaterials Compatibility. *Transactions of the Society for Biomaterials*: XVIII: 190, 1995.
12. Janatova J, Bernshaw NJ. Mechanisms of complement activation during hemodialysis. *Blood Purif.* 13: 31-32, 1995; *Blood Purif.* 14 (Suppl S1): 18, 1996.
13. Janatova J, Bernshaw NJ. A Novel Approach to Test Blood-Biomaterials Compatibility Uses the ECL Protein Detection System. *ECL™ Highlights* No. 7, Amersham LIFE SCIENCE: 4-6, 1995.
14. Janatova J, Bernshaw NJ. Effect of Surface Modification with Heparin on Interaction with Complement Proteins. *Surfaces in Biomaterials '96 Symposium Notebook*: 123-128, 1996.
15. Fowers KD, Callahan J, Janatova J, Bernshaw NJ, McRea JC. Hemocompatibility of a Heparin Removal Device. *Transactions of the Society for Biomaterials*, the 23rd Ann Meeting: 302, 1997.
16. Janatova J, Bernshaw NJ. Biocompatibility of Biomaterials in Human Serum and Plasma: Complement Activating Potential. *Surfaces in Biomaterials '97 Symposium*, 1997.

Synthesis and Selective Cytotoxicity of a Hyaluronic Acid–Antitumor Bioconjugate

Yi Luo and Glenn D. Prestwich

Department of Medicinal Chemistry, The University of Utah, 30 South
2000 East, Room 201, Salt Lake City, Utah 84112-5820

***Bioconjugate
Chemistry[®]***

Reprinted from
Volume 10, Number 5, Pages 755–763

Synthesis and Selective Cytotoxicity of a Hyaluronic Acid–Antitumor Bioconjugate

Yi Luo and Glenn D. Prestwich*

Department of Medicinal Chemistry, The University of Utah, 30 South 2000 East, Room 201, Salt Lake City, Utah 84112-5820. Received March 18, 1999; Revised Manuscript Received May 21, 1999

A cell-targeted prodrug was developed for the anti-cancer drug Taxol, using hyaluronic acid (HA) as the drug carrier. HA–Taxol bioconjugates were synthesized by linking the Taxol 2'-OH via a succinate ester to adipic dihydrazide-modified HA (HA-ADH). The coupling of Taxol-NHS ester and HA-ADH provided several HA bioconjugates with different levels of ADH modification and different Taxol loadings. A fluorescent BODIPY–HA was also synthesized to illustrate cell targeting and uptake of chemically modified HA using confocal microscopy. HA–Taxol conjugates showed selective toxicity toward the human cancer cell lines (breast, colon, and ovarian) that are known to overexpress HA receptors, while no toxicity was observed toward a mouse fibroblast cell line at the same concentrations used with the cancer cells. The drug carrier HA-ADH was completely nontoxic. The selective cytotoxicity is consistent with the results from confocal microscopy, which demonstrated that BODIPY–HA only entered the cancer cell lines.

INTRODUCTION

Hyaluronic acid (HA)¹ (Figure 1), a linear polysaccharide of alternating D-glucuronic acid (GlcUA) and N-acetyl-D-glucosamine (GlcNAc) units, adopts a three-dimensional structure in solution that shows extensive intramolecular hydrogen bonding. This restricts the conformational flexibility of the polymer chains and induces distinctive secondary (helical) and tertiary (coiled coil) interactions (1). HA is one of several glycosaminoglycan components of the extracellular matrix (ECM), the synovial fluid of joints, and the scaffolding comprising cartilage (2). The remarkable viscoelastic properties of HA and commercial cross-linked derivatives (3) account for their usefulness in joint lubrication. HA–protein interactions play crucial roles in cell adhesion, growth, and migration (4–6), and HA acts as a signaling molecule in cell motility, in inflammation, wound healing, and cancer metastasis (7). The immunoneutrality of HA makes it an excellent building block for the development of novel biocompatible and biodegradable biomaterials used in tissue engineering and drug delivery systems (8–10). For example, HA has been employed as both a vehicle and angiostatic agent in cancer therapy (11–13).

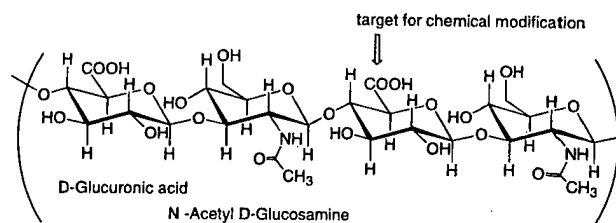


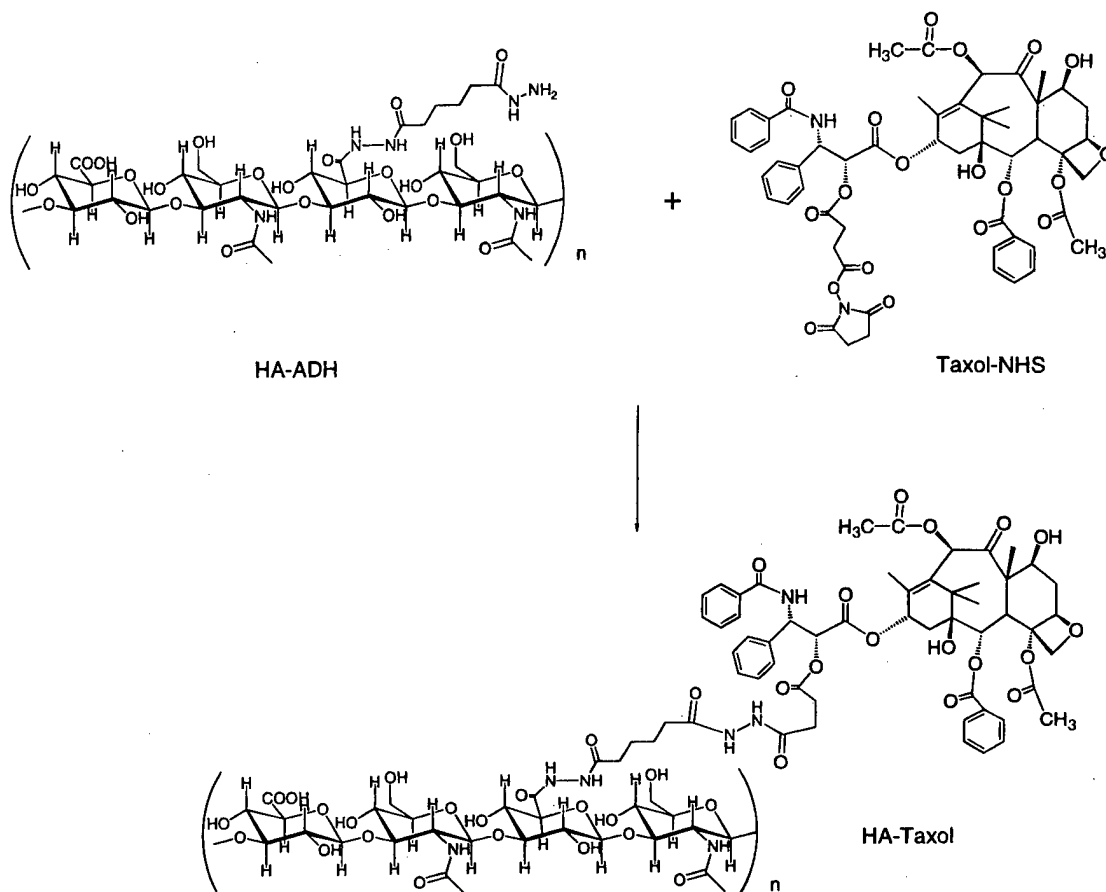
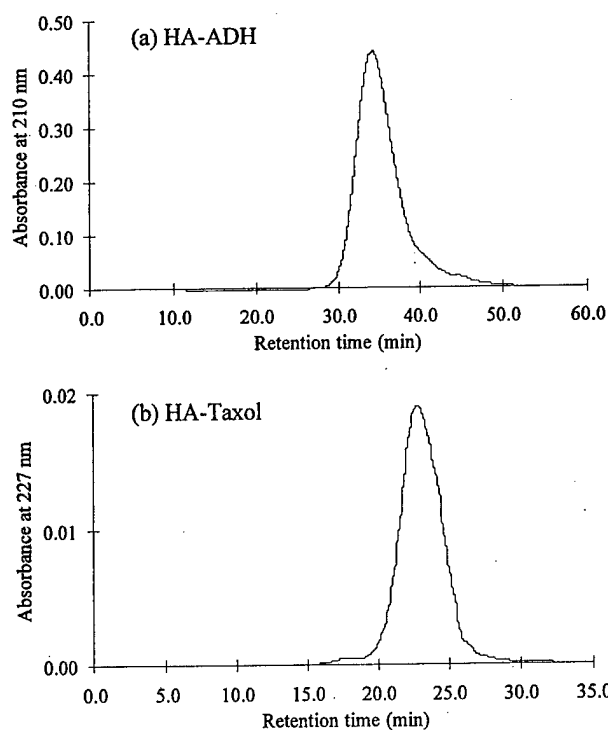
Figure 1. Tetrasaccharide fragment of HA showing the disaccharide repeat units.

The use of biocompatible polymers in the treatment of various ailments has expanded rapidly in the last two decades (14). Moreover, derivatization of such polymers with reporter groups (15) and drugs (16, 17) has emerged as a powerful method for controlling delivery and release of a variety of compounds. Small drug molecules can be linked to the polymer that allows controlled release of the free bioactive group. In general, coupling of antitumor agents to biopolymers provides advantages in drug solubilization, stabilization, localization, and controlled release (18). For example, the linking of a cytotoxic small molecule such as adriamycin to poly(hydroxymethyl)acrylamide (HPMA) gives a new material with improved in vitro tumor retention, a higher therapeutic ratio, avoidance of multidrug resistance (19), and encouraging clinical results. In work with a naturally occurring biocompatible polymer, mitomycin C and epirubicin were coupled to HA by carbodiimide chemistry; the former adduct was selectively taken up by, and toxic to, a lung carcinoma xenograft (20).

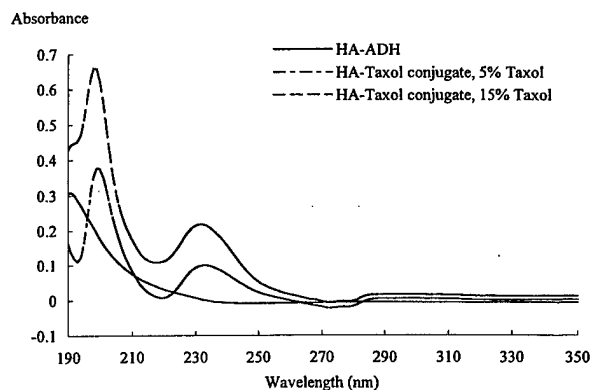
HA is overexpressed at sites of tumor attachment (21) to the mesentery and provides a matrix that facilitates invasion (22). HA is an important signal for activating kinase pathways (23, 24) and regulating angiogenesis in tumors (25). Moreover, several types of cellular HA receptors respond to HA as a signal. These include CD44, a family of glycoproteins originally associated with lymphocyte activation; RHAMM, the receptors for HA-mediated cell motility (26, 27); and HARLEC, responsible

* To whom correspondence should be addressed. Phone: (801) 585-9051. Fax: (801) 585-9053. E-mail: gprestwich@deans.pharm.utah.edu.

¹ Abbreviations: α -MEM, Minimal Essential Medium, Eagle; ADH, adipic dihydrazide; BODIPY-FL, 4,4-difluoro-5,7-dimethyl-4-bora-3a, 4a-diaza-s-indacene-3-propionic acid; D-MEM, Dulbecco's Modified Eagle Medium; DPPC, diphenylphosphoryl chloride; ECM, extracellular matrix; EDCI, 1-ethyl-3-(3-dimethylamino)propylcarbodiimide; FBS, fetal bovine serum; GlcNAc, N-acetyl-D-glucosamine; GlcUA, D-glucuronic acid; GPC, gel permeation chromatography; HA, hyaluronic acid; HA-ADH, adipic dihydrazide-modified HA; HASE, hyaluronidase; HMPA, poly(hydroxymethyl)acrylamide; LMW, low molecular weight; MTT, thiazoyl blue; SDPP, N-hydroxysuccinimido diphenyl phosphate.

**Figure 2.** Synthesis of HA-Taxol.**Figure 3.** GPC profile. (a) Purified HA-ADH detection at $\lambda = 210$ nm. Waters Ultrahydrogel 250, 2000 columns (7.8 mm ID \times 30 cm) were used in the analysis. (b) Purified HA-Taxol conjugate detection at $\lambda = 227$ nm. Only the Ultrahydrogel 250 column was employed. Eluent was 150 mM, pH 6.5, phosphate buffer/MeOH = 80:20 (v/v); the flow rate was 0.5 mL/min.

for receptor-mediated uptake of HA in liver. Using radiolabeled HA analogues and HA-coupled prodrugs, it

**Figure 4.** UV spectra of HA-Taxol conjugates.

was possible to selectively target tumor cells and tumor metastases through the use of chondroitin sulfate to block "housekeeping" receptors in the liver without affecting specific HA receptors of tumor cells (28–31). Targeting of anti-cancer agents to tumor cells and tumor metastases can be accomplished by receptor-mediated uptake of bioconjugates of these agents to HA (20). Since HA receptors (CD44, RHAMM) are overexpressed in transformed human breast epithelial cells and other cancers (32), selectivity for cancerous cells is markedly enhanced and overall dosages may be reduced. Moreover, coupling of antitumor agents to biopolymers can provide advantages in drug solubilization, stabilization, localization, and controlled release (18). Our methodology (33) for coupling antitumor agents to HA adds further value by specifically targeting the bioconjugate to aggressively growing cancers that overexpress HA receptors.

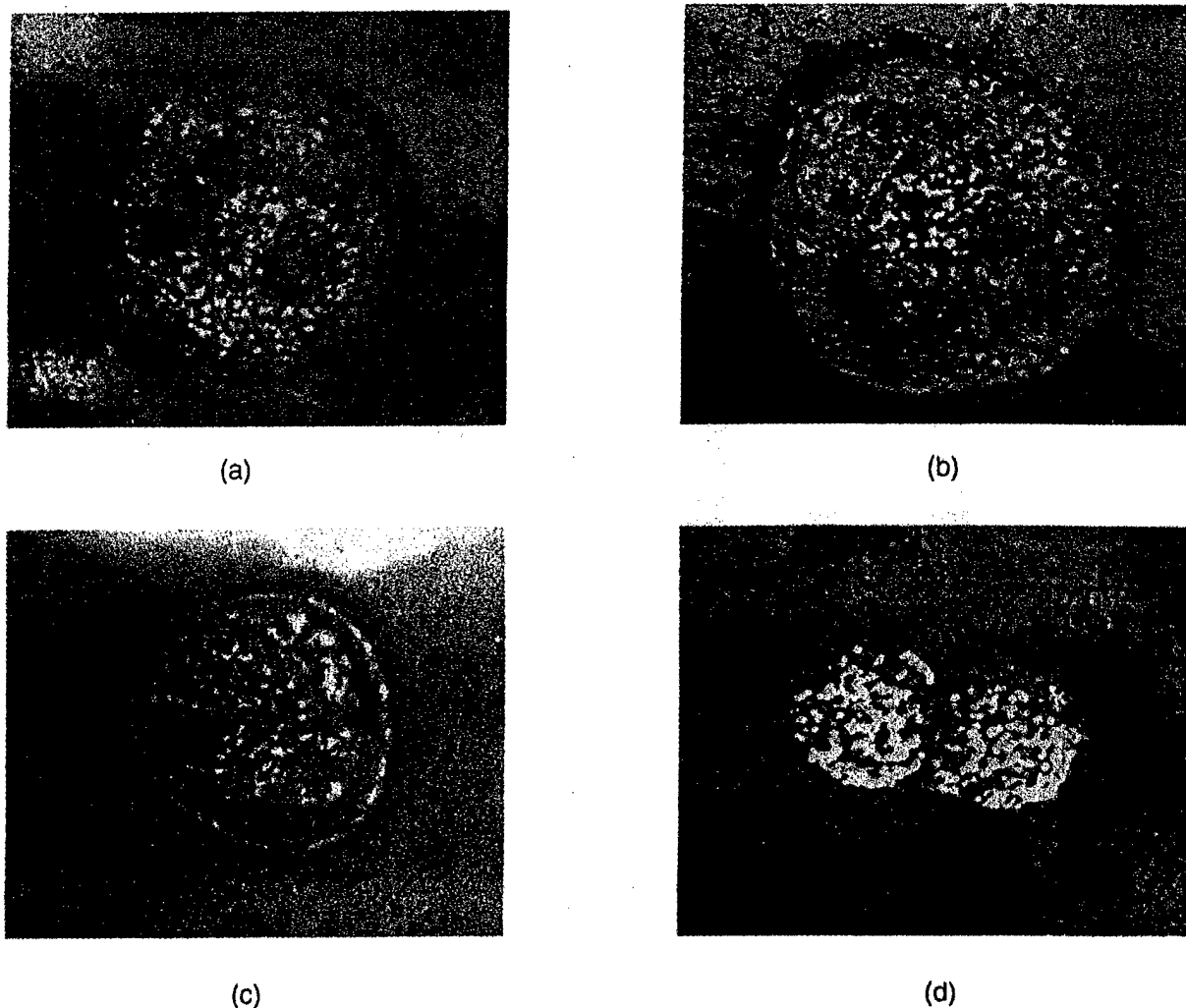


Figure 5. Targeting human breast cancer HBL-100 cells with HA-BODIPY. Panel a fluorescence image shows HA binding to cell surfaces in 3 min. Panels b and c show HA accumulation in the nucleus after 6 and 9 min. In panel d, after 20 min HA, has been completely taken up and fluorescence is dispersed throughout the cells.

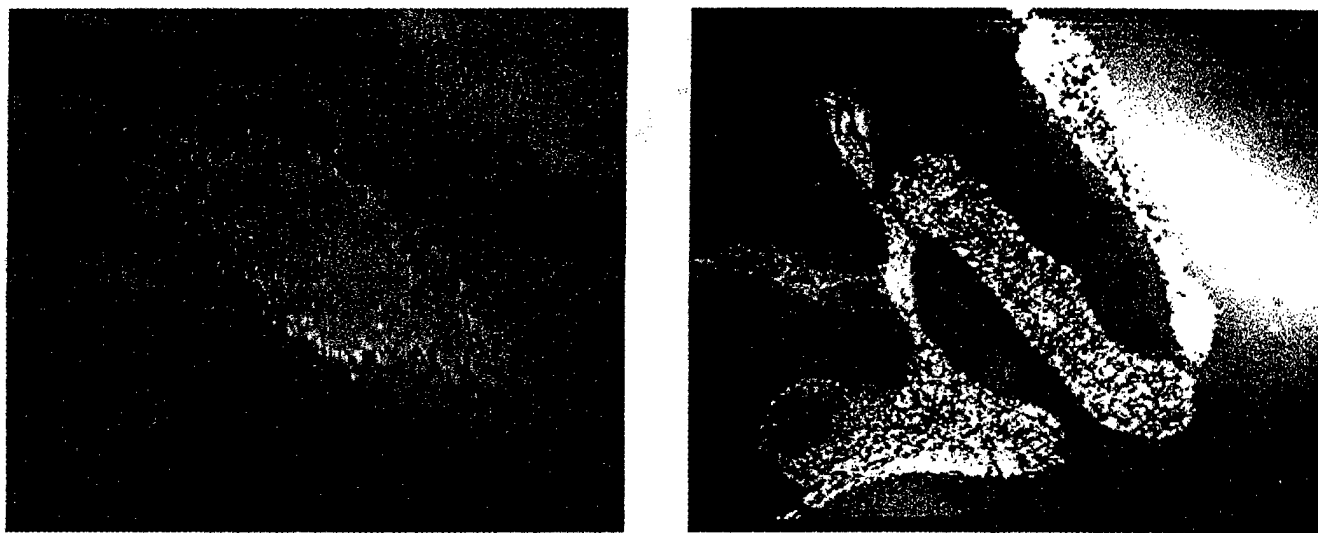


Figure 6. Targeting ovarian cancer SK-OV-3 cells with HA-BODIPY. Panel a shows HA uptake by cells in 15 min. Panel b shows HA uptake by cells in 60 min.

Paclitaxel (Taxol) (34), a diterpenoid originally isolated from the bark of the Pacific yew, *Taxus brevifolia*, is a powerful anti-mitotic agent that acts by promoting tubulin assembly into stable aggregated structures. It binds to microtubules and inhibits their depolymerization into

tubulin. Although Taxol has shown tremendous potential as an anti-cancer compound, its use as an anti-cancer drug is compromised by its poor aqueous solubility. One attempt to address this involved preparation of 2'-OH linked water-soluble poly(ethylene glycol) derivatives

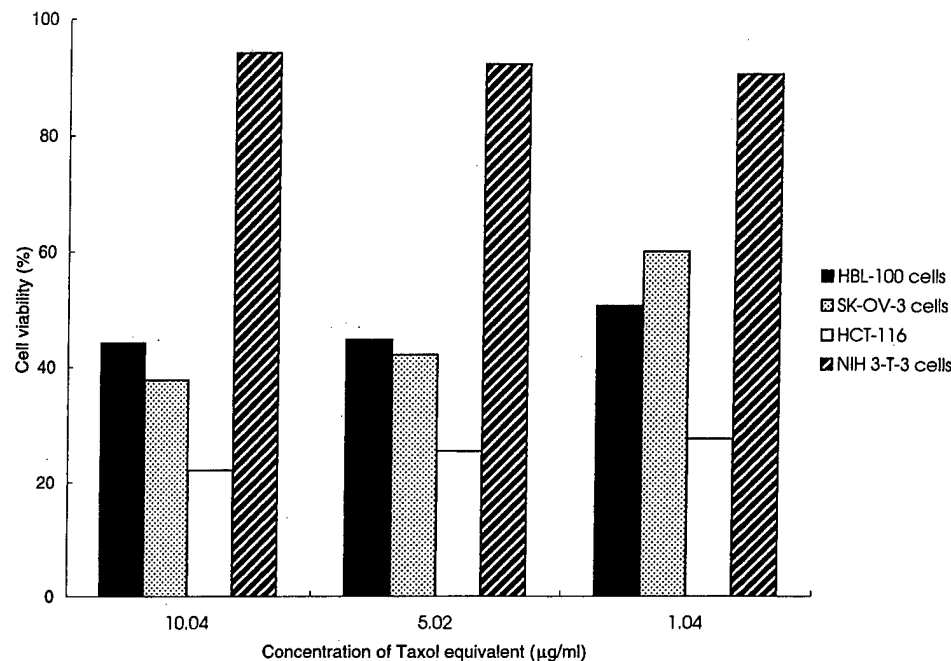


Figure 7. Cytotoxicity of HA-Taxol conjugate with 5% Taxol loading against HBL-100, SK-OV-3, HCT-116, and NIH 3-T-3 cells.

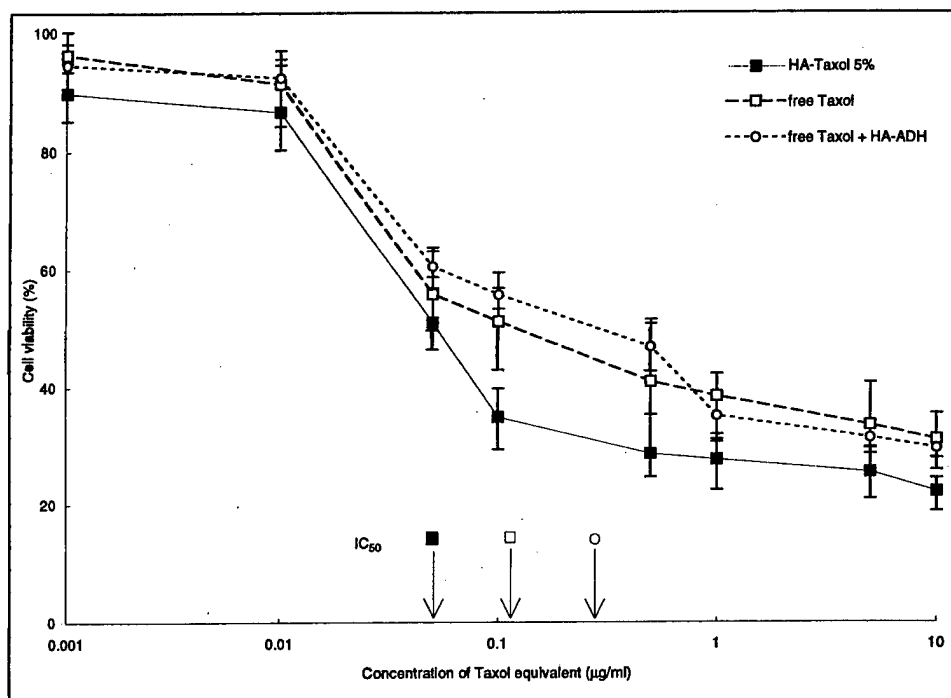


Figure 8. In vitro cytotoxicity of HA-Taxol conjugate with 5% Taxol loading against colon tumor HCT-116 cells.

(35). In this paper, we have taken a different approach that uses a prodrug strategy to both increase water solubility and provide cellular targeting. Thus, we selected Taxol as a model anti-cancer drug for covalent attachment to HA that had been modified with adipic dihydrazide (ADH) (36–38). The coupling of Taxol-2'-hemisuccinate NHS ester to HA-ADH was optimized to give HA-Taxol conjugates with a variety of ADH and Taxol loadings (Figure 2). Selective in vitro cell cytotoxicity was studied with an untransformed mouse fibroblast cell line (NIH 3-T-3) and with three human cell lines: HCT-116 colon tumor cells, HBL-100 breast cancer cells, and SK-OV-3 ovarian cancer cells. In addition, a fluorescent (BODIPY)-labeled HA bioconjugate was prepared

and employed to visualize selective uptake of HA by confocal microscopy.

MATERIALS AND METHODS

General. Fermentation-derived HA (sodium salt, M_w 1.5 MDa) was provided by Clear Solutions Biotechnology, Inc. (Stony Brook, NY). 1-Ethyl-3-[3-(dimethylamino)propyl]carbodiimide (EDCI), ADH, succinic anhydride, diphenylphosphoryl chloride (DPPC), *N*-hydroxysuccinimide, and triethylamine were purchased from Aldrich Chemical Co. (Milwaukee, WI). Bovine testicular hyaluronidase (Hase, 880 units/mg) was obtained from Sigma Chemical Co. (St. Louis, MO). Paclitaxel (Taxol) was purchased from CBI Tech, Inc. (Cambridge, MA). 4,4-

Diffuoro-5,7-dimethyl-4-bora-3a,4a-diaza-s-indacene-3-propionic acid, hydrazide (BODIPY-FL hydrazide) was obtained from Molecular Probes, Inc. (Portland, OR). All solvents were of reagent grade or HPLC grade (Fisher Scientific Co., Santa Clara, CA). CH_2Cl_2 and acetonitrile were distilled from CaH_2 .

Analytical Instrumentation. All ^1H NMR spectral data were obtained using an NR-200 FT-NMR spectrometer at 200 MHz (IBM Instruments Inc.). UV-Vis spectra were recorded on a Hewlett-Packard 8453 UV-Vis diode array spectrophotometer (Palo Alto, CA). Gel permeation chromatography (GPC) analysis was carried out on the following system: Waters 515 HPLC pump, Waters 410 differential refractometer, Waters 486 tunable absorbance detector, Waters Ultrahydrogel 250 and 2000 columns (7.8 mm ID \times 30 cm) (Milford, MA). The GPC eluent was 150 mM phosphate buffer, pH 6.5:MeOH = 80:20 (v/v), and the flow rate was 0.5 mL/min. The system was calibrated with HA standards supplied by Dr. S. Gustafson (University of Uppsala, Sweden), and thus the molecular sizes of each HA oligosaccharide and the corresponding bioconjugates were calculated from the standard samples. Confocal fluorescence images of HA-BODIPY binding and uptake by cells were recorded using a Zeiss Microscope (Carl Zeiss, Inc., Germany). Coulter Counter was from Coulter Electronics, Inc. (Hialeah, FL). Cell viability was determined by thiazoyl blue (MTT) dye uptake protocols at 540 nm, which was recorded on a Bio-Rad M-450 microplate reader (Hercules, CA).

Synthesis of Taxol-NHS Ester. To a stirred solution of 270 mg of Taxol and 38 mg (1.2 equiv) of succinic anhydride in 13 mL of CH_2Cl_2 at room temperature was added 36 μL (10-fold molar excess) of dry pyridine. The reaction mixture was stirred for 3 days at room temperature and then concentrated in vacuo. The residue was dissolved in 5 mL of CH_2Cl_2 , and Taxol-2'-hemisuccinate was purified on silica gel (wash with hexane; elute with ethyl acetate) to give 258 mg of product (86%). FAB-MS calcd for $\text{C}_{51}\text{H}_{55}\text{NO}_{17}$: 953.99. Found: 954.4 (MH^+).

Next, *N*-hydroxysuccinimido diphenyl phosphate (SDPP) was prepared from 10 mmol of diphenylphosphoryl chloride, 10 mmol of *N*-hydroxysuccinimide, and 10 mmol of triethylamine in 6 mL of CH_2Cl_2 as previously described (39). Crude SDPP was triturated with ether, dissolved in ethyl acetate, washed (2×10 mL H_2O), dried (MgSO_4), and concentrated in vacuo to give SDPP with mp 89–90 $^\circ\text{C}$ (85%). To a solution of 150 mg of Taxol-hemisuccinate and 82 mg (1.5 equiv) of SDPP in 5 mL of acetonitrile was added with 88 μL (4 equiv) of triethylamine. The reaction was stirred for 6 h at room temperature, and then concentrated in vacuo. The residue was dissolved in 5 mL of ethyl acetate and 2 mL of hexane and purified on silica gel. SDPP gave superior yields in less time and under milder conditions than did any carbodiimide coupling reagent. The purified Taxol-NHS ester was dried for 24 h in vacuo at room temperature to give 134 mg (80%). FAB-MS calcd for $\text{C}_{55}\text{H}_{58}\text{N}_2\text{O}_{19}$: 1051.07. Found: 1051.5 (MH^+).

Preparation of Low Molecular Weight (LMW) HA. To a solution of 2.0 g of high molecular mass HA (1.5 MDa) in pH 6.5 PBS buffer (4 mg/mL) was added hyaluronidase (HAse) (10 units/mg of HA). The degradation was carried out at 37 $^\circ\text{C}$, 190 rpm stirring for 1 h, then 95 $^\circ\text{C}$ for 20 min. Dialysis tubing (M_w cutoff 3 500 Da) was prepared by soaking the membrane in water at room temperature for 3–4 h and subsequently rinsing it with water. The solution was dialyzed against water for 4 days using this washed membrane tubing. The retained material was filtered through a 0.2 μm cellulose acetate

membrane (Corning) and lyophilized to give 1.12 g of LMW HA (56%).

Adipic Dihydrazido-Functionalized HA (HA-ADH). HA-ADH was prepared as described previously (37, 38, 40). In a representative example, LMW HA (50 mg) was dissolved in water to give a concentration of 4 mg/mL, and then a 5-fold excess of ADH was added into the solution. The pH of the reaction mixture was adjusted to 4.75 by addition of 0.1 N HCl. Next, 1 equiv of EDCI was added in solid form. The pH of the reaction mixture was maintained at 4.75 by addition of 0.1 N HCl. The reaction was quenched by addition of 0.1 N NaOH to adjust the pH of reaction mixture to 7.0. The reaction mixture was then transferred to pretreated dialysis tubing (M_w cutoff 3 500) and dialyzed exhaustively against 100 mM NaCl, then 25% EtOH/ H_2O and finally H_2O . The solution was then filtered through 0.2 μm cellulose acetate membrane, flash frozen, and lyophilized. The purity of HA-ADH was measured by GPC. The substitution degree of ADH was determined by the ratio of methylene hydrogens to acetyl methyl protons as measured by ^1H NMR. In this example, 37 mg of HA-ADH was obtained with an 18% loading based on available carboxylates modified.

HA-Taxol. Several loadings were prepared following a general protocol (Figure 2). In a representative example, HA-ADH with 18% ADH loading (10 mg, 4.4 μmole hydrazide) was dissolved in 3 mM, pH 6.5, phosphate buffer to give a concentration of 1 mg/mL. To this mixture was added Taxol-NHS ester dissolved in sufficient DMF ($\text{DMF}:\text{H}_2\text{O} = 2:1$, v/v) to give a homogeneous solution, and the reaction mixture was stirred at room temperature for 24 h. The reaction mixture was dialyzed successively against 50% acetone/ H_2O and water (membrane tubing, M_w cutoff 3 500). The solution was then filtered through a 0.2 μm membrane and then lyophilized. The purity of HA-Taxol conjugate was measured by GPC analysis. Taxol loading was determined by UV absorbance ($\lambda_{\text{max}} = 227$ nm, $\epsilon = 2.8 \times 10^4$) in 80:20 $\text{CH}_3\text{CN}:\text{H}_2\text{O}$.

BODIPY-FL-Labeled HA. In a representative reaction, 100 mg of LMW HA was dissolved in 10 mL of H_2O , and 10 mL of an acetone solution (0.8 mg/mL) of BODIPY-FL hydrazide was added. The pH was adjusted to 4.75 with 0.1 N HCl, and then 51.5 mg (3 molar equiv) of EDCI was added in solid form into the mixture. The reaction was stirred overnight at room temperature at pH 4.75. The HA-BODIPY was purified by dialysis against H_2O , and its purity was characterized by GPC with detection at 210 nm (HA) and 502 nm (BODIPY).

In Vitro Cell Culture Cytotoxicity. The cytotoxicity of HA-Taxol conjugates was determined using a 96-well plate format in quadruplicate with increasing doses: 0.001, 0.01, 0.1, 0.5, 1, 5, 10, 50, and 100 $\mu\text{g}/\text{mL}$. Each well contained approximately 20 000 cells in 200 μL of cell culture media. Cells were cultured in the following media: HBL-100 cells, high glucose D-MEM (Dulbecco's Modified Eagle Medium) + 10% FBS (fetal bovine serum) + 1% sodium pyruvate; SK-OV-3 cells, D-MEM/F12 + 10% FBS; HCT-116 cells, α -MEM (Minimal Essential Medium, Eagle) + 10% FBS; NIH 3-T-3 cells, high glucose D-MEM + 10% FBS.

HA-Taxol conjugates and HA-ADH control were added as stock solutions in $\text{DMSO}:\text{H}_2\text{O} = 1:1$ (v/v); free Taxol was added as a DMSO stock solution. A 2 μL aliquot of the stock solution was added to each well of the cell culture plate. Cells were incubated at 37 $^\circ\text{C}$ for 3 days with the test material, and cell viability was determined using MTT dye uptake by reading plates at 540 nm.

Table 1. Optimization of ADH Modification of HA and the Reaction Condition

molar ratio of HA:ADH:EDCI	reaction time (min)	ADH loading (%)
1:40:4	5	28.3
	10	31.2
	15	31.4
	30	32.2
	60	38.6
	120	45.7
	240 ^a	44.0
1:5:0.5	15	9.0
1:5:1	15	17.5
1:10:1	15	18.0
1:20:1	15	19.0
1:10:0.2	180	19.3

^a No 0.1 N HCl was used to maintain the pH of the reaction mixture.

Response was graded as percent live cells compared to untreated controls (41).

RESULTS

Degradation and Modification of HA. LMW HA was generated by degradation of high molecular mass HA (1.5 MDa) with testicular Hase. This enzyme degrades HA to generate a series of even-numbered HA oligosaccharides with the *N*-acetylglucosamine moiety at the reducing terminus (42). Thus, incubation of a solution of high molecular mass HA in pH 6.5 PBS buffer with testicular Hase at 37 °C provided partially degraded HA. Small fragments, HA oligosaccharides, and buffer salts were removed by dialysis against H₂O (four changes per day). The final LMW HA product was lyophilized, and an aliquot was analyzed by GPC analysis: $M_n = 3883$, $M_w = 11\,199$, and molecular dispersity (DP) = 2.88. This corresponds to an average of 28 disaccharide repeats/LMW HA molecule. This preparation is quite reproducible as time, temperature, and concentrations of HA and Hase are controlled.

The use of the mild and versatile hydrazide method for preparation of chemically modified HA derivatives (36, 37) allows attachment of reporter molecules, drugs, cross-linkers, and any combination of the above moieties to HA (10, 33, 40). Covalent attachment of ADH to the carboxylic acid groups of HA provides a controlled loading of pendant hydrazide functionalities arrayed along the hyaluronate backbone, used herein for the attachment of an antitumor agent. We selected LMW HA for modification in this study for four main reasons. First, it was possible to perform reproducible chemical modifications and to monitor the extent of modification by simple proton NMR methods. Second, LMW HA can be cleared from the body via ultrafiltration by the kidney. Third, the LMW HA bioconjugates were expected to provide a readily injectable nonviscous solution at concentrations up to 10 mg/mL, and the LMW materials should suffer minimal further degradation in plasma and would be rapidly taken up by cells. Finally, with LMW HA bioconjugates, we were confident that future efforts to cross-link the material into a hydrogel could also be easily controlled.

Thus, LMW HA (4 mg/mL) was mixed with ADH at several concentrations (Table 1). The pH of the reaction mixture was adjusted to 4.75, and then different quantities of solid EDCI were added in solid form to initiate the reaction. An increase in pH was observed immediately corresponding to proton uptake in the coupling reaction. The pH of the reaction mixture was maintained

Table 2. Optimization of Taxol Loading. Both the Total ADH Modification of HA and the Molar Ratio of ADH to Taxol-NHS Ester during the Conjugation Reaction Were Varied

(HA) _x (HA-ADH) _y (HA-ADH-Taxol) _z					
preparation	composition of HA-Taxol conjugates			solubility in H ₂ O	ADH%: Taxol-NHS ^a
	HA (x) (%)	HA-ADH (y) (%)	HA-ADH-Taxol (z) (%)		
A. ADH loading = 9% ^b					
1	91	7.8	1.2	yes	9:5
2	91	7.7	1.3	yes	9:9
3	91	3.8	5.2	yes	9:18
B. ADH loading = 18%					
4	82	16.4	1.6	yes	18:5
5	82	16.1	1.9	yes	18:10
6	82	15.8	2.2	yes	18:15
7	82	3.1	14.9	partially ^c	18:36
C. ADH loading = 45%					
8	55	30	15	no	45:90

^a The molar ratio used in the grafting reaction of HA-ADH and Taxol-NHS that resulted in the composition of the HA-Taxol conjugates. ^b Total ADH loading for modified HA = $y + z$. ^c Limited solubility; only soluble below 0.1 mg/mL due to high loading of Taxol.

at 4.75 by addition of 0.1 N HCl. Preliminary studies had provided guidelines as to ratios of HA:ADH:EDCI suitable to achieve a given percentage modification of the glucuronate functions of HA. The reaction was stopped by addition of 0.1 N NaOH to adjust the pH of reaction mixture to 7.0. The HA-ADH was purified by sequential dialysis against 100 mM NaCl, 25% EtOH/H₂O, and H₂O. The dialyzed solutions were filtered through a 0.2 μ m membrane, and then lyophilized to give HA-ADH in yields ranging 50–70%.

The purity and molecular size distribution of the HA-ADH was measured by GPC. The narrow single-peak GPC profile detected by UV (210 nm) (Figure 3a) and RI indicated that both large and small impurities had been completely removed. It is essential to establish this fact rigorously to ensure that all subsequent molecules added also become covalently attached, rather than remaining noncovalently associated. In addition, the GPC results showed that there was virtually no molecular weight decrease due to further HA degradation or increase due to bifunctional cross-linking during the modification reaction. The loading of ADH on the polymer backbone was determined by ¹H NMR spectroscopy studies with D₂O as a solvent. The degree of substitution could be calculated by integration of the ADH methylene signals using the methyl resonance ($\delta = 1.95$ – 2.00 ppm) of the acetamido moiety of the GlcNAc residues of HA as an internal standard (37). Thus, ¹H NMR integration confirmed that different ADH loadings occurred with different ratios of reactants and for different reaction times. The relationship between the degree of substitution of ADH and the reaction conditions, i.e., molar ratio of HA:ADH:EDCI, and reaction time was optimized. The results are shown in Table 1. Importantly, the degree of ADH substitution on HA was influenced primarily by the HA:EDCI ratio, with the amount of excess ADH varying from 5 to 25-fold having little effect. The carbodiimide quantity is thus the controlling factor for determining ADH loading on HA.

Taxol (paclitaxel) is a taxane natural product that promotes polymerization of tubulin and stabilizes the structure of intracellular microtubules. This process has the effect of inhibiting the normal dynamics reorganization of the microtubules, which is necessary for inter-

Table 3. In Vitro Cytotoxicity of HA-Taxol Conjugates against Different Cell Lines

HA-Taxol preparations	IC ₅₀ (μg/mL) ^d					
	HBL-100 ^e		SK-OV-3 ^e		HCT-116 ^e	
	conjugate ^b	Taxol equivalents ^c	conjugate	Taxol equivalent	conjugate	Taxol equivalent
1	48.0 (118 μM)	1.21 (1.42 nM)	21.5 (53 μM)	0.54 (0.64 nM)	7.20 (17.8 μM)	0.18 (0.21 nM)
3	16.4 (37 μM)	1.65 (1.93 nM)	8.0 (18.2 μM)	0.80 (0.94 nM)	0.52 (1.2 μM)	0.052 (0.061 nM)
7	6.8 (12.4 μM)	1.58 (1.85 nM)	0.37 (0.68 μM)	0.086 (0.10 nM)	0.11 (0.20 μM)	0.026 (0.030 nM)
8 ^a	68.0 (115 μM)	1.48 (17.3 nM)	7.2 (17.3 nM)	1.56 (1.83 nM)	2.15 (3.65 μM)	0.47 (0.55 nM)

^a Dissolved in 3:1 DMSO/H₂O. ^b The data in these columns show the IC₅₀ of HA-Taxol conjugates against the tumor cell line. ^c The data in these columns are calculated as the Taxol equivalents present in the HA-Taxol bioconjugate using the molar ratios in Table 2. This calculation allows comparison of conjugated and free Taxol. ^d The IC₅₀ value is the molarity at which 50% of tumor cell death was observed after 72 h under standard tissue culture conditions. ^e Cell type.

phase and mitotic functions. Because of the problems in administering emulsified forms of this water-insoluble drug, Taxol was selected as the model anti-cancer drug in our study. Taxol was first converted to its 2'-hemisuccinate derivative by standard methods (43), and its structure was confirmed spectroscopically. Second, the activated Taxol-NHS ester was prepared by coupling with SDPP. Taxol-NHS was then coupled to HA-ADH in 3 mM phosphate buffer at pH 6.50 using DMF as a cosolvent to maintain a homogeneous solution. The purification of HA-Taxol bioconjugate was carried out by dialysis of the reaction mixture against 50% acetone/H₂O. The purity of the HA-Taxol conjugate was determined by GPC analysis, monitoring absorbance at 227 nm (Figure 3b) and RI. The single symmetrical GPC peak showed that no free Taxol or other small molecular impurities remained in this preparation. The Taxol was quantified by UV absorbance at 227 nm (Figure 4) in 80% acetonitrile: H₂O. To obtain the optimal modification on HA for anti-cancer ability, HA-Taxol conjugates with different Taxol loading were synthesized. Table 2 shows the optimization of Taxol loading and the molar ratio of HA-ADH to Taxol-NHS during the conjugation reaction. These data demonstrate that the molar ratio of ADH to Taxol-NHS during the grafting reaction is critical in determining the Taxol loading of the bioconjugate.

Fluorescently labeled HA has been prepared with several chemistries and used in other studies of receptor-mediated uptake. Most recently, RHAMM-mediated uptake and trafficking of HA by transformed fibroblasts (44) was observed with Texas Red-HA. Previously, fluorescein-HA was employed to study HA uptake in a variety of systems, e.g., cells expressing CD44 variants (21, 45–48), uptake by tumor cells for correlation with metastatic potential (49, 50), internalization by chondrocytes (51), and as a measure of liver endothelial cell function (52). In this study and in the Texas Red study, hydrazide derivatives of the dyes were used to form covalent bishydrazide linkages to the HA carboxylic acid functions under the mild all-aqueous conditions employed for other hydrazide modifications of HA (33).

To study the binding ability of HA to tumor cells and uptake by cells, a variety of fluorescently labeled HA derivatives were prepared. Of those evaluated for use with cancer cells, we obtained the best results with the BODIPY fluorophore (Y. Luo, M. R. Ziebell, unpublished results). Thus, BODIPY-FL hydrazide was coupled to LMW HA using EDCI as the condensing agent to give HA-BODIPY, which was purified by dialysis against H₂O; the loading of GPC-homogeneous HA-BODIPY was determined spectrophotometrically to be 1.8% (based on available glucuronates).

Cell-Based Assays for Uptake and Toxicity. An aliquot (2 μL) of a 1.5 mg/mL aqueous stock solution HA-BODIPY was added to 100 μL cell culture media with

tumor cells cultured on cover slips. Confocal images of HA-BODIPY uptake by HBL-100 cells can be seen in Figure 5. Initially, the HA-BODIPY can be seen on cell membrane; over the course of several minutes, it is taken up into the cell and then gradually begins to accumulate in the nucleus. After 20 min, cells showed HA-BODIPY in most compartments. Uptake of HA-BODIPY into SK-OV-3 cells occurred with a similar appearance and time course (Figure 6). These data suggest that HA binds readily to tumor cell surface and is rapidly taken up via HA receptor-mediated pathways. This supports the notion that HA should be a good targeting polymer for selective delivery of anti-cancer drugs to tumor cells. Similar results were observed independently with HA-Texas Red uptake by transformed fibroblasts (44). Importantly, nontransformed cells, such as the NIH 3-T-3 fibroblasts, did not show this binding and rapid uptake of HA-BODIPY.

Next, the cytotoxicity of HA-Taxol conjugates was measured using a 96-well plate format in quadruplicate with increasing doses from 0.001 to 100 μg/mL. The cytotoxicity of HA-Taxol conjugates was studied by using the MTT assay to identify cells still active in respiration (41). HA-Taxol conjugates showed effective cytotoxicity against SK-OV-3, HBL-100, and HCT-116 cell lines, while no cytotoxicity against NIH 3-T-3 cells was observed at concentrations up to 10 μg/mL of Taxol equivalents (Figure 7). These results confirm the selective toxicity of HA-Taxol toward different cell lines, and the known overexpression of CD44 by HBL-100 (53) and SK-OV-3 cells (54) suggests that this selective toxicity is due to receptor-mediated binding and uptake of the HA-Taxol bioconjugate.

The HA-BODIPY binding and uptake results support the hypothesis that selective toxicity of HA-Taxol is due to receptor-mediated events. This was further explored by investigating the relative toxicity of polymer-bound and free Taxol, as well as examining the effect of the polymeric carrier itself on the toxicity of the drug. Thus, Figure 8 summarizes the cytotoxicity data for HA-Taxol (5% Taxol loading) with HCT-116 colon cancer cells. The bioconjugate showed increased cytotoxicity, e.g., lower IC₅₀, relative to free Taxol or free Taxol mixed with the HA-ADH carrier. In a further control experiment, we had established that HA-ADH alone elicited no detectable change in cell viability at a concentration 10 times higher than the maximal concentration of HA-Taxol conjugate used. These data support the notion that the increased cytotoxicity of HA-Taxol conjugates requires cellular uptake of the complex followed by hydrolytic release of the active Taxol by cleavage of the labile 2' ester linkage.

The in vitro cytotoxicity results of HA-Taxol conjugates with different modifications against different cell lines are shown in Table 3. For the least-modified HA (9% ADH modification), higher cytotoxicity was observed

as Taxol loading increased. However, the cytotoxicity of highly modified HA actually decreased at the highest Taxol loading. Apparently, high loading of Taxol decreased the solubility of HA-Taxol conjugate, masked the HA receptor recognition elements of HA, caused aggregation of the polymeric conjugate, and thus limited the toxicity of the conjugate relative to that of free drug. Clearly, the cytotoxicity of HA-Taxol conjugates depends on a balance between minimal HA modification and maximal Taxol loading.

ACKNOWLEDGMENT

Financial support for this work was provided by Department of Army (DAMD 17-9A-1-8254) and by the Huntsman Cancer Foundation at The University of Utah. Initial studies of HA modification and degradation were performed with M.R. Ziebell (UUtah) and we thank Drs. D.M. Marecek and C.M. Amann (UUtah) for assistance with Taxol modification. We are grateful to D. Schmehl and Dr. L. R. Barrows (UUtah) for assistance with cell cytotoxicity experiments and Mr. Ziebell and Dr. W. G. Pitt (Brigham Young University, Provo, UT) for assistance with confocal microscopy. We thank Dr. L. Y.-W. Bourguignon (University of Miami Medical School, Miami, FL) for providing HBL-100 and SK-OV-3 cells. We are grateful to Clear Solutions Biotech, Inc. (Stony Brook, NY) for providing HA and the Center for Cell Signaling (UUtah) for equipment and facilities.

LITERATURE CITED

- (1) Scott, J. E., Secondary structures in hyaluronan solutions: chemical and biological implications; In *The Biology of Hyaluronan*; C. Foundation, Ed.; J. Wiley & Sons, Ltd.: Chichester, UK, 1989; pp 6–20.
- (2) Laurent, T. C., Laurent, U. B. G., and Fraser, J. R. E. (1995) Functions of hyaluronan. *Ann. Rheum. Dis.* 54, 429–432.
- (3) Larsen, N. E., Leshchiner, E., and Balazs, E. A. (1995) Biocompatibility of Hyal polymers in various tissue compartments. *Mater. Res. Soc. Symp. Proc.* 394, 149–153.
- (4) Knudson, C. B., and Knudson, W. (1993) Hyaluronan-Binding proteins in development, tissue homeostasis, and disease. *FASEB J.* 7, 1233–1241.
- (5) Turley, E. A., The role of a cell-associated hyaluronan binding protein in fibroblast behavior; In *The Biology of Hyaluronan*; C. Foundation, Ed.; J. Wiley & Sons, Ltd.: Chichester, UK, 1989; pp 121–137.
- (6) Underhill, C. B., The interaction of hyaluronate with the cell surface: the hyaluronate receptor and the core protein; In *The Biology of Hyaluronan*; C. Foundation, Ed.; J. Wiley & Sons, Ltd.: Chichester, UK, 1989; pp 87–106.
- (7) Entwistle, J., Hall, C. L., and Turley, E. A. (1996) Hyaluronan receptors: regulators of signaling to the cytoskeleton. *J. Cell Biochem.* 61, 569–577.
- (8) Vercruysse, K. P., and Prestwich, G. D. (1998) Hyaluronate derivatives in drug delivery. *Crit. Rev. Ther. Drug Carr. Syst.* 15, 513–555.
- (9) Freed, L. E., Vunjak-Novakovic, G., Biron, R. J., Eagles, D. B., Lesnoy, D. C., Barlow, S. K., and Langer, R. (1994) Biodegradable polymer scaffolds for tissue engineering. *Bio/Technology* 12, 689–693.
- (10) Prestwich, G. D., Marecek, D. M., Marecek, J. F., Vercruysse, K. P., and Ziebell, M. R., Chemical modification of hyaluronic acid for drug delivery, biomaterials, and biochemical probes; In *The Chemistry, Biology, and Medical Applications of Hyaluronan and its Derivatives*; T. C. Laurent, Ed.; Portland Press: London, 1998; pp 43–65.
- (11) Alam, C. A. S., Seed, M. P., and Willoughby, D. A. (1995) Angiostasis and vascular regression in chronic granulomatous inflammation induced by diclofenac in combination with hyaluronan in mice. *J. Pharm. Pharmacol.* 47, 407–411.
- (12) Ziegler, J. (1996) Hyaluronan seeps into cancer treatment trials. *J. Nat. Cancer Inst.* 88, 397–399.
- (13) Falk, R. E. In *PCT Int. Appl. WO 9740841*; 1997.
- (14) Duncan, R., Dimitrijevic, S., and Evagorou, E. G. (1996) The role of polymer conjugates in the diagnosis and treatment of cancer. *J. Therap. Polymers Pharmaceut. Sci.* 6, 237–263.
- (15) Brinkley, M. (1992) A brief survey of methods for preparing protein conjugates with dyes, haptens, and cross-linking agents. *Bioconjugate Chem.* 3, 2–13.
- (16) Puttnam, D., and Kopecek, J. (1995) Polymer conjugates with anticancer activity. *Adv. Polym. Sci.* 122, 55–123.
- (17) Krinick, N. L., and Kopecek, J., Soluble polymers as targetable drug carriers; In *Targeted Drug Delivery. Handbook of Experimental Pharmacology*; R. L. Juliano, Ed.; Springer-Verlag: Berlin, 1991; pp 105–179.
- (18) Maeda, H., Seymour, L., and Miyamoto, Y. (1992) Conjugates of anticancer agents and polymers: advantages of macromolecular therapeutics in vivo. *Bioconjugate Chem.* 3, 351–362.
- (19) Minko, T., Kopeckova, P., Pozharov, V., and Kopecek, J. (1998) HEMA copolymer bound adriamycin overcomes MDR1 gene encoded resistance in a human ovarian carcinoma cell line. *J. Controlled Release* 54, 223–233.
- (20) Akima, K., Ito, H., Iwata, Y., Matsuo, K., Watari, N., Yanagi, M., Hagi, H., Oshima, K., Yagita, A., Atomi, Y., and Tatekawa, I. (1996) Evaluation of antitumor activities of hyaluronate binding antitumor drugs: synthesis, characterization and antitumor activity. *J. Drug Targeting* 4, 1.
- (21) Yeo, T. K., Nagy, J. A., Yeo, K. T., Dvorak, H. F., and Toole, B. P. (1996) Increased hyaluronan at sites of attachment to mesentery by CD44-positive mouse ovarian and breast tumor cells. *Am. J. Pathol.* 148, 1733–1740.
- (22) Knudson, W. (1996) Tumor-associated hyaluronan: providing an extracellular matrix that facilitates invasion. *Am. J. Pathol.* 148, 1721–1726.
- (23) Nelson, R. M., Venot, A., Bevilacqua, M. P., Linhardt, R. J., and Stamenkovic, I. (1995) Carbohydrate-protein interactions in vascular biology. *Annu. Rev. Cell Dev. Biol.* 11, 601–631.
- (24) Hall, C. L., Yang, B. H., Yang, X. W., Zhang, S. W., Turley, M., Samuel, S., Lange, L. A., Wang, C., Curpen, G. D., Savani, R. C., Greenberg, A. H., and Turley, E. A. (1995) Overexpression of the hyaluronan receptor RHAMM is transforming and is also required for h-ras transformation. *Cell* 82, 19–28.
- (25) Rooney, P., Kumar, S., Ponting, J., and Wang, M. (1995) The role of hyaluronan in tumour neovascularization (review). *Int. J. Cancer* 60, 632–636.
- (26) Hoare, K., Savani, R. C., Wang, C., Yang, B., and Turley, E. A. (1993) Identification of hyaluronan binding proteins using a biotinylated hyaluronan probe. *Connect. Tissue Res.* 30, 117–126.
- (27) Turley, E. A., Belch, A. J., Poppema, S., and Pilarski, L. M. (1993) Expression and function of a receptor for hyaluronan-mediated motility on normal and malignant lymphocytes. *B. Blood* 81, 446–453.
- (28) Gustafson, S., Bjorkman, T., and Westlin, J. E. (1994) Labeling of high molecular weight hyaluronan with I-125-tyrosine: studies in vitro and in vivo in the rat. *Glycoconjugate J.* 11, 608–613.
- (29) Gustafson, S., Hyaluronan in drug delivery; In *The Chemistry, Biology, and Medical Applications of Hyaluronan and its Derivatives*; T. C. Laurent and E. A. Balazs, Ed.; Portland Press: UK, 1997.
- (30) Gustafson, S., and Bjorkman, T. (1997) Circulating hyaluronan, chondroitin sulphate and dextran sulphate bind to a liver receptor that does not recognize heparin. *Glycoconjugate J.* 14, 561–568.
- (31) Samuelsson, C., and Gustafson, S. (1998) Studies on the interaction between hyaluronan and a rat colon cancer cell line. *Glycoconjugate J.* 15, 169–175.
- (32) Culty, M., Nguyen, H. A., and Underhill, C. B. (1992) The hyaluronan receptor (CD44) participates in the uptake and degradation of hyaluronan. *J. Cell Biol.* 116, 1055–1062.
- (33) Prestwich, G. D., D. M., M., Marecek, J. F., Vercruysse, K. P., and Ziebell, M. R. (1998) Controlled chemical modification of hyaluronic acid: synthesis, applications and biodegradation of hydrazide derivatives. *J. Controlled Release* 93–103.

- (34) Teicher, B. A. *Cancer Therapeutics: Experimental and Clinical Agents*; Humana Press: Totowa, New Jersey, 1997; p 451.
- (35) Greenwald, R. B., Gilbert, C. W., Pendri, A., Conover, C. D., Xia, J., and Martinez, A. (1996) Drug delivery systems: water soluble taxol 2'-poly(ethylene glycol) ester prodrugs -- design and in vivo effectiveness. *J. Med. Chem.* 39, 424-431.
- (36) Pouyani, T., and Prestwich, G. D. In *US Patent 5,616, 568*; Research Foundation of SUNY: USA, 1997.
- (37) Pouyani, T., and Prestwich, G. D. (1994) Functionalized derivatives of hyaluronic acid oligosaccharides - drug carriers and novel biomaterials. *Bioconjugate Chem.* 5, 339-347.
- (38) Pouyani, T., Harbison, G. S., and Prestwich, G. D. (1994) Novel hydrogels of hyaluronic acid: synthesis, surface morphology, and solid-state NMR. *J. Am. Chem. Soc.* 116, 7515-7522.
- (39) Ogura, H., Nagai, S., and Takeda, K. (1980) A novel reagent (N-succinimidyl diphenyl phosphate) for synthesis of active ester and peptide. *Tetrahedron Lett.* 21, 1467-1468.
- (40) Vercruysse, K. P., Marecak, D. M., Marecek, J. F., and Prestwich, G. D. (1997) Synthesis and in vitro degradation of new polyvalent hydrazide cross-linked hydrogels of hyaluronic acid. *Bioconjugate Chem.* 8, 686-694.
- (41) Kokoshka, J. M., Ireland, C. M., and Barrows, L. R. (1996) Cell-based screen for identification of inhibitors of tubulin polymerization. *J. Nat. Prod.* 59, 1179-1182.
- (42) Kreil, G. (1995) Hyaluronidases - a group of neglected enzymes. *Protein Sci.* 4, 1666-1669.
- (43) Nicolaou, K. C., Riemer, C., Kerr, M. A., Rideout, D., and Wrasidlo, W. (1993) Design, synthesis and biological activity of protaxols. *Nature* 364, 464-466.
- (44) Collis, L., Hall, C., Lange, L., Ziebell, M., Prestwich, G., and Turley, E. (1998) Rapid hyaluronan uptake is associated with enhanced motility: implications for an intracellular mode of action. *FEBS Lett.* 440, 444-449.
- (45) Chow, G., Knudson, C. B., Homandberg, G., and Knudson, W. (1995) Increased expression of CD44 in bovine articular chondrocytes by catabolic cellular mediators. *J. Biol. Chem.* 270, 27734-27741.
- (46) Lesley, J., and Hyman, R. (1992) CD44 Can be activated to function as an hyaluronic acid receptor in normal murine T-cells. *Eur. J. Immunol.* 22, 2719-2723.
- (47) Lesley, J., English, N., Perschl, A., Gregoroff, J., and Hyman, R. (1995) Variant cell lines selected for alterations in the function of the hyaluronan receptor CD44 show differences in glycosylation. *J. Exp. Med.* 182, 431-437.
- (48) Perschl, A., Lesley, J., English, N., Trowbridge, I., and Hyman, R. (1995) Role of CD44 cytoplasmic domain in hyaluronan binding. *Eur. J. Immunol.* 25, 495-501.
- (49) Asplund, T., and Heldin, P. (1994) Hyaluronan receptors are expressed on human malignant mesothelioma cells but not on normal mesothelial cells. *Cancer Res.* 54, 4516-4523.
- (50) Culty, M., Shizari, M., Thompson, E. W., and Underhill, C. B. (1994) Binding and degradation of hyaluronan by human breast cancer cell lines expressing different forms of CD44: correlation with invasive potential. *J. Cell. Physiol.* 160, 275-286.
- (51) Hua, Q., Knudson, C. B., and Knudson, W. (1993) Internalization of hyaluronan by chondrocytes occurs via Receptor-Mediated endocytosis. *J. Cell Sci.* 106, 365-375.
- (52) Nakabayashi, H., Tsujii, H., Okamoto, Y., and Nakano, H. (1996) Fluorescence-labeled-hyaluronan loading test as an index of hepatic sinusoidal endothelial cell function in the rat. *Int. Hepatol. Commun.* 5, 345-353.
- (53) Iida, N., and Bourguignon, L. Y. W. (1997) Coexpression of CD44 variant (v10/ex14) and CD44S in human mammary epithelial cells promotes tumorigenesis. *J. Cell. Physiol.* 171, 152-160.
- (54) Bourguignon, L. Y.-W., Zhu, H. B., Chu, A., Iida, N., Zhang, L., and Hung, M. C. (1997) Interaction between the adhesion receptor, CD44, and the oncogene product, p185(HER2), promotes human ovarian tumor cell activation. *J. Biol. Chem.* 272, 27913-27918.

BC9900338

Chemically modified hyaluronan: new biomaterials and probes for cell biology

Glenn D. Prestwich, Yi Luo, Michael R. Ziebell, Koen P. Vercruysse, Kelly R. Kirker and John S. MacMaster

Department of Medicinal Chemistry, The University of Utah, Salt Lake City, Utah, USA

Abstract. A mild, controllable modification of hyaluronic acid (HA) has been developed in which monovalent, divalent, or polyvalent hydrazides can be covalently attached to HA to give functionalized derivatives with a high degree of synthetic versatility. Firstly, HA can be covalently modified to produce drug delivery systems and novel hydrogel biomaterials with a variety of desired physical and chemical properties. Specific applications include localizable hydrogels for release of anti-inflammatory agents, materials for tissue engineering and prevention of postsurgical adhesions, novel grafted copolymers for drug delivery, tumor targeted anticancer drugs, and techniques for coating surfaces of polymeric and metal medical devices. Secondly, basic cell biological research on the changes in the location of HA and HA binding proteins (e.g., CD44 and RHAMM) can be demonstrated using cellular probes. Our laboratories have developed versatile routes to synthesize HA-fluors (fluorescein, Texas Red, BODIPY), HA-nanogold, and HA-biotin with controllable levels of modification on the carboxylate groups. Thirdly, HA can be modified to provide biochemical probes for developing new hyaluronidase (HAse) assays and for the discovery of new HA-binding proteins. Examples of each of these three current research areas are presented.

Keywords: binding proteins, drug delivery, hyaluronidase, hydrazide.

Introduction

We have developed a versatile method for chemical modification of HA in which monovalent, divalent, or polyvalent hydrazides can be covalently attached to HA to give functionalized derivatives with many subsequent uses [1–3]. Covalent modifications can alter the chemical and biomechanical properties of HA in ways that permit production of drug delivery systems and novel hydrogel biomaterials [4]. Specific applications described herein include tumor targeted anticancer drugs, hydrogels for localized release of anti-inflammatory or other therapeutic agents, scaffold materials for tissue engineering and slowly bioresorbable films for prevention of postsurgical adhesions. In addition, HA fragments can be incorporated either pre- or postpolymerization to provide novel receptor targeted grafted copolymers for drug delivery. Several techniques for covalently attaching HA onto the surfaces of polymeric or metal medical devices have also been developed [5,6].

Address for correspondence: Prof. Glenn D. Prestwich, The University of Utah, Department of Medicinal Chemistry, 30 South 2000 East, Room 201, Salt Lake City, UT 84112-5820, USA. Tel.: +1-801-585-9051. Fax: +1-801-585-9053. E-mail: gprestwich@deans.pharm.utah.edu

HA can be modified to provide biochemical probes for developing new hyaluronidase (Hase) assays and for the discovery of new HA-binding proteins (HABPs) [6]. These probes can be used to understand the effects of HA on cell physiology, and the uptake, transport, and signaling functions of HA in cells [7]. For example, changes in the location and abundance of both HA and HABPs such as CD44 and RHAMM can be demonstrated using cellular probes.

Current research areas

Five areas of current research at The University of Utah are summarized in this overview: 1. Tumor targeted drug delivery of Taxol[®]; 2. Swellable HA hydrogel biomaterial for wound healing, adhesion management, and drug delivery; 3. Biophysical and biochemical studies of HA-receptor interactions, including novel binding assays and ligands; 4. Surface modification chemistry; and 5. Assays for Hase that permit screening for new inhibitors.

Tumor targeted drug delivery

The uses of chemically modified HA for drug delivery have been recently reviewed [5,8]. A fluorescent BODIPY-HA was synthesized to illustrate cell targeting and uptake of chemically modified HA using confocal microscopy [9]. Next, a cell targeted prodrug was developed for the anticancer drug Taxol[®], using HA as the drug carrier [9]. HA-Taxol[®] conjugates were synthesized by linking the Taxol[®] 2'-OH via a succinate ester to adipic dihydrazide modified HA (HA-ADH) (Fig. 1A). The coupling of Taxol[®]-NHS ester and HA-ADH provided several HA conjugates with different levels of ADH modification and different Taxol[®] loadings. HA-Taxol[®] conjugates showed selective toxicity towards the human cancer cell lines (breast, colon, and ovarian) that are known to over-express HA receptors, while no toxicity was observed towards a mouse fibroblast cell line at the same concentrations used with the human tumor cells. The drug carrier HA-ADH was completely nontoxic. The selective cytotoxicity is consistent with the results from confocal microscopy, which demonstrated that BODIPY-HA entered only the tumor cells.

Selective HA-BODIPY uptake by tumor cells

HA-BODIPY was used to probe the selectivity of HA targeting to tumor cells [9]. HA-BODIPY binding and uptake by tumor cells such as human breast cancer cells HBL-100, ovarian cancer cells SK-OV-3 and colon tumor cells HCT-116, were studied by laser confocal microscopy. The fluorescence images indicated that HA bound readily to tumor cell surfaces and was rapidly taken up via HA receptor mediated pathways. This supports the notion that HA should be a good targeting polymer for selective delivery of anticancer drugs to tumor cells. Similar results were observed independently with HA-Texas Red uptake by transformed fibroblasts [10]. Importantly, nontransformed cells, such as the NIH 3T3

mouse fibroblasts, did not show this binding and rapid uptake of HA-BODIPY. The HA-BODIPY binding and uptake results support the hypothesis that selective toxicity of HA-Taxol[®] is due to receptor mediated events.

Selective toxicity of HA-Taxol[®]

The in vitro cytotoxicity of HA-Taxol[®] conjugates was studied by using the MTT assay to identify cells still active in respiration [11]. HA-Taxol[®] conjugates showed toxicity to SK-OV-3, HBL-100 and HCT-116 cell lines, while no toxicity was observed towards a mouse fibroblast cell line NIH 3T3 at the same concentrations used with the cancer cells (Fig. 1). The selective cytotoxicity is consistent with the results from confocal microscopy, which demonstrated that BODIPY-HA only entered the cancer cells. In addition, the efficacy of HA-Taxol[®] conjugates could be blocked by preincubation of the cells with a 20-fold excess of HA. Together with the known overexpression of CD44 by HBL-100 [12] and SK-OV-3 cells [13], these data suggest that the selective cytotoxicity is due to receptor mediated binding and uptake of the HA-Taxol[®] conjugate. The conjugate showed higher potency, e.g., lower IC₅₀, relative to free Taxol[®] or free Taxol[®] mixed with the HA-ADH carrier [9]. In a further control experiment we established that the drug carrier HA-ADH alone was completely nontoxic.

Studies on the release of Taxol[®] from HA-Taxol[®] were carried out in cell cul-

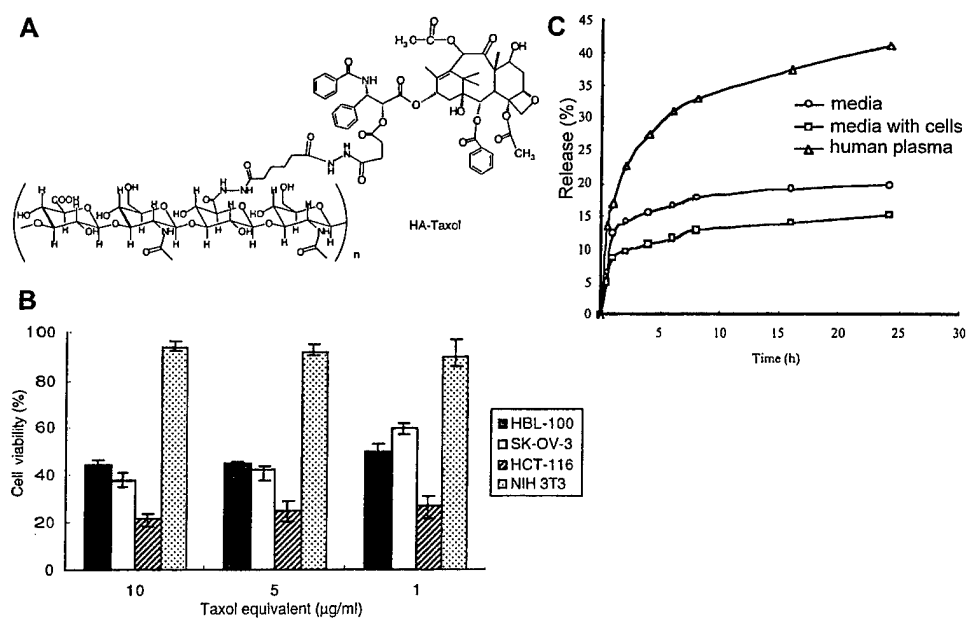


Fig. 1. Tumor-targeting of Taxol[®] with HA. A: structure of HA-Taxol[®]; B: selective toxicity of HA-Taxol[®] to three human cancer cell lines and nontoxicity to mouse fibroblasts; C: time course of Taxol[®] release from HA-Taxol[®].

ture medium with and without cells, and with either Hase, esterase, or human plasma. Figure 1C shows the data for the effects of medium and human plasma. HPLC analysis suggested that only active Taxol[®] was released, corresponding to cleavage of the labile 2' ester linkage; no Taxol[®] hemisuccinate was detected. The conjugate was stable in cell culture media, and the presence of Hase did not affect the Taxol[®] release rate. Taxol[®] release rate is significantly faster in the presence of added esterase. These data support the notion that the increased cytotoxicity of HA-Taxol[®] requires cellular uptake of the complex followed by hydrolytic release of the active Taxol[®] by cleavage of the labile 2' ester linkage.

Fluorescence-activated cell sorting (FACS) with FITC-HA-Taxol[®]

Laser flow cytometry was used to investigate the interaction of the HA-Taxol[®] conjugate with tumor cells using fluorescein-labeled HA-Taxol[®] as the fluorescent probe. It was found that FITC-HA-Taxol[®] bound to the cell surface and was taken up rapidly by tumor cells (HBL-100, SK-OV-3, HCT-116). Binding and uptake of this dual modified HA could be blocked by preincubation with excess of HA, while no binding and uptake was detected in fibroblasts. In addition, the binding and uptake of FITC-HA-Taxol[®] by different cell lines was also evaluated by confocal microscopy, giving results analogous to those obtained with HA-BODIPY. The selective cytotoxicity of HA-Taxol[®] is thus, clearly due to receptor mediated uptake followed by hydrolytic release of the active Taxol[®] via cleavage of the labile 2' ester linkage.

Swellable HA hydrogels

Hydrogels have received significant attention as delivery vehicles. These materials can be engineered to be tissue compatible and to be permeable to different solutes [14]. HA hydrogels can, in principle, be completely bioresorbable materials and have been studied for over two decades [15,16]. Mirroring the new sol gel injectable drug delivery system [17], a novel fast gelling and fast swelling HA hydrogel film was developed as a potential drug delivery system. The new HA film is bio-compatible and biodegradable and is produced from HA-ADH and a bioinert cross-linker. An in vitro drug release device was evaluated and drug release was initially studied by using dyes (i.e., acridine orange, amaranth, and fast green FCF), followed by examination of release rates of several therapeutic agents (i.e., hydrocortisone, dexamethasone, indomethacin, gentamicin, pilocarpine, and diclofenac). It was found that the new HA film could maintain a slow release rate for certain drugs, such as acridine orange, dexamethasone and gentamicin. Differential scanning calorimetric analysis suggested that a polymer-drug interaction exists within the HA hydrogel that could account for the slow release. In particular, prolonged delivery of anti-inflammatory or anti-infective drugs suggested the utility of this novel HA film as a wound dressing material.

The functionalized HA-ADH derivative was cross-linked by a macromolecular cross-linker to give an interpenetrating network hydrogel. The hydrogel could be prepared under extremely mild conditions e.g., in water, phosphate-buffered sa-

line (PBS), or in cell culture medium at room temperature. The gelling process began immediately and was essentially complete in minutes. A solvent casting method was used to obtain HA hydrogel films, which were then dried in air at 37°C for 24 h.

The extent of swelling of HA hydrogel films was investigated using both kinetic and equilibrium swelling studies (Fig. 2). For the kinetic studies HA films were cut into small disks and dyed with acridine orange to facilitate visualization. Next, the diameters of dried disks were measured using a microscope. Then, a buffer solution was added to the film and the diameter was measured at various times. A similar procedure was followed for the equilibrium studies; however, the diameter of the film was measured only after 24 h of equilibration in a buffer solution at 37°C. The swelling ratio, Q , was calculated as indicated below.

$$\left(\frac{\text{Diameter}_{t=x}}{\text{Diameter}_{t=0}} \right)^3 = Q$$

where: $\text{Diameter}_{t=x}$ = Diameter of disk at time interval x

$\text{Diameter}_{t=0}$ = Diameter of dry disk

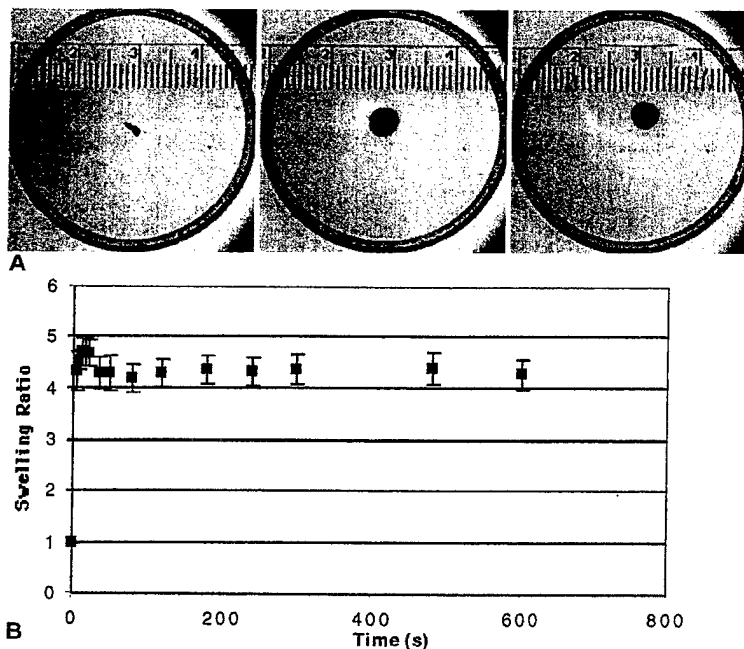


Fig. 2. Swellable HA hydrogel films. A: photographs of an acridine orange stained HA hydrogel film swelling in PBS. From left to right: dry HA film, film after 4 s in PBS, film after 600 s in PBS; B: swelling kinetics of an HA hydrogel film in PBS.

Figure 2B shows the results of kinetic studies; Fig. 2A shows the actual films as seen under the microscope at times 0, 4, and 600 s. These data indicate that the films swell quickly and reach an equilibrium size in less than a minute. The rapid swelling of these proprietary films will be exploited for a variety of in vivo applications in human medicine.

Surface modification chemistry

Plasma etching

Surfaces of polypropylene (PP), polystyrene (PS), and polytetrafluoroethylene (PTFE) were activated with Ar and NH_3 plasmas to aminate the polymer surface [18]. Aminated surfaces were then reacted with HA using three modification conditions. Results showed that ammonia plasma-treated polymers were more reactive toward HA attachment. Of the three chemistries tried, condensation of the aminated surface with succinic anhydride followed by coupling of the newly formed carboxylic acid group with HA-ADH gave the most effective and reproducible HA attachment. HA coatings were evaluated by spectroscopic and physicochemical methods. HA-modified plastic surfaces were quite hydrophilic, as determined by measuring the water contact angle, and should exhibit selectivity in cell attachment and growth.

Controlled chemical modifications of particles

Three types of HA-modified particulate materials (HAMPs) have been produced: 1. affinity resins based on cross-linked agarose; 2. superparamagnetic polystyrene (PS) beads, and 3. controlled pore glass (CPG). In each case, ADH-modified HA was covalently coupled to chemically activated residues on the surface. The affinity resins were prepared by coupling HA-ADH to NHS ester activated Affigel. This affinity matrix has been employed for purification of native and recombinant HABPs. The HA modified magnetic beads and CPG were prepared by oxidative cleavage of glycol modified surfaces to give surface aldehydes. Coupling of HA-ADH to the particle surface resulted in hydrazone linkages, and the extent and location of coupling was monitored in two ways (Fig. 3). Firstly, fluorescence microscopy was employed to detect coupling of fluoresceinylated HA-ADH (rather than nonfluorescent HA-ADH). In addition, the presence of HA on these HAMPs was also checked functionally by testing their ability to bind to the HA-binding domain (HABD) of the receptor for HA mediated motility (RHAMM), described in more detail in Section 4 below. For this detection strategy, Texas Red was conjugated to a GST fusion protein of the 61 amino acid recombinant RHAMM-P1 peptide to give a novel nonimmunological reagent for the detection of HA on surfaces. HAMPs will be employed to isolate HABPs in automated high throughput screens, and in an in vitro process to remove selectively cells expressing high affinity cell surface HABPs.

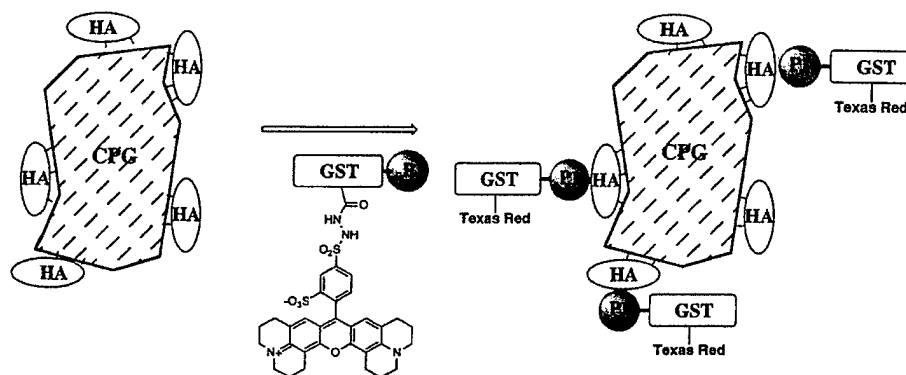


Fig. 3. Surface modification chemistry. The detection of HA covalently coupled through hydrazone linkages to controlled pore glass (CPG) can be accomplished by direct fluorescent detection of the binding of a Texas Red-labeled recombinant GST-RHAMM-P1 polypeptide.

Biophysical and biochemical studies

Biochemical probes and surfaces

Versatile routes to synthesize HA-fluors (including fluorescein, Texas Red, and BODIPY), HA-nanogold, and HA-biotin with controllable levels of modification on the carboxylate groups [10,19] have been developed. In addition, the preparation of HAMPs, such as HA affinity resins on cross-linked dextran ($> 300 \mu\text{m}$), CPG ($100 \mu\text{m}$), and superparamagnetic beads ($4 \mu\text{m}$) was summarized above.

Structural studies of RHAMM

The RHAMM is a cell surface HA receptor, found on fibroblasts and certain tumor cell lines, that modulates cell function through binding extracellular matrix components [20]. Certain isoforms of this receptor have been identified as important in intracellular signaling and extracellular binding [21]. High resolution multidimensional NMR is being used to solve the structure of the HABD of RHAMM; this is the first predominately helical HABD to be studied this way. A solution structure of the mostly beta-sheet containing TGS-6 link module was previously determined by NMR [22,23]. A RHAMM polypeptide that contains the two basic amino acid-rich HABDs was expressed and purified. Based on circular dichroism and NMR experiments, it appeared that the domain was alpha-helical. A complete structure may provide a model for how the two domains selectively bind HA and which amino acid side chains account for the high binding affinity. Based on molecular modeling we hypothesize that a long narrow groove is formed by a helix-loop-helix structure, in which the substrate (e.g., an HA octasaccharide) would be flanked on each side by one of the two HABDs.

Peptide mimics of HA

HABPs control cell function and are implicated in cancer, arthritis, adhesion, and wound healing [7,24]. One medicinal chemistry approach to developing new antagonists and agonists that mimic HA in binding to HABPs involves the use of combinatorial libraries of peptides, either synthetic or from phage display. The first library tested was a random set of 15 amino acid polypeptides encoded in the fUSE-5 phage [25]. The next libraries were eight amino acid, "one-bead, one-peptide" libraries synthesized on 100 μ m PS beads [26]. Each of these libraries was screened against our RHAMM construct expressed as a GST fusion protein (GST-RHAMM-P1). To detect peptides that bound solely to the HABD, we included a competition step in each of our screens, in which HA was first incubated with GST-RHAMM-P1; this preincubation was followed by addition of peptides. In this negative selection step, the peptides that did not bind in this final step were selected as those molecules that exhibited exclusive interaction with the HABD. Phage-displayed peptides are summarized in Table 1, and the affinity of independently synthesized peptides for RHAMM-P1 has been assessed using the assay described below. Interestingly, these peptides interfere with the interaction of RHAMM with erk1 [27]. Although not shown, the bead-derived peptides include an abundance of aromatic and acidic residues. Several recognizable motifs repeat in the twenty peptides sequenced, and the inclusion of unnatural amino acids resulted in novel peptides with nanomolar affinity.

We conclude that a series of hydrophobic amino acids are important in binding, and that the amino acid motif may have quite different characteristics from HA itself. Current efforts focus on identification of peptides that bind uniquely to either RHAMM or to TSG-6 link module.

Rapid binding assays in microtiter plates

In order to verify the binding selectivity and affinity of these above peptides, we developed a series of binding assays that allows us to monitor their binding and determine binding constants to describe their interactions. One such method utilizes a 96 well plate format in which the target protein, GST-RHAMM-P1, is immobilized and biotin-labeled peptides are incubated in the wells. Streptavidin conjugated to horseradish peroxidase is then added followed by a chromogenic substrate. Figure 4A illustrates the basic method, and Fig. 4B shows the determination of a 21 nM binding constant for the binding of the HA2 peptide to

Table 1. Phage-displayed peptides that interact with RHAMM.

HA1	WPVSLTVCSAVWCPL
HA2	GVCNADFCWLPAVVV
HA3	SASPSASKLSLMSTV
HA4	IPFILPAYTLLGHPR
HA5	YSVYLSVAHNFVLPS
HA6	HWCLPLLACDTFARA

RHAMM-P1. Figure 4C illustrates the relative binding affinity and relative ability to displace HA binding for four of the phage-derived peptides.

Fluorescence polarization (FP) assays

To compare the above solid phase assay to solution phase binding we used FP, which measures the degree of anisotropic change of a fluorescent probe [28]. As the binding complex forms, the anisotropy increases, which in turn is a marker for peptide binding. In these experiments, fluorescently labeled peptides were titrated with increasing amounts of the recombinant RHAMM-P1. Preliminary data (not shown) allow estimation of the K_d values, which are consistent with the data obtained from microplate assays.

Hyaluronidase assays

Effects of metals on Hase

The enzymatic degradation of HA by testicular Hase, hyaluronate 4-glucanohydrolase, has an absolute requirement for the inclusion of mono or divalent cations in the reaction mixture. We tested the effects of metal salts on the enzy-

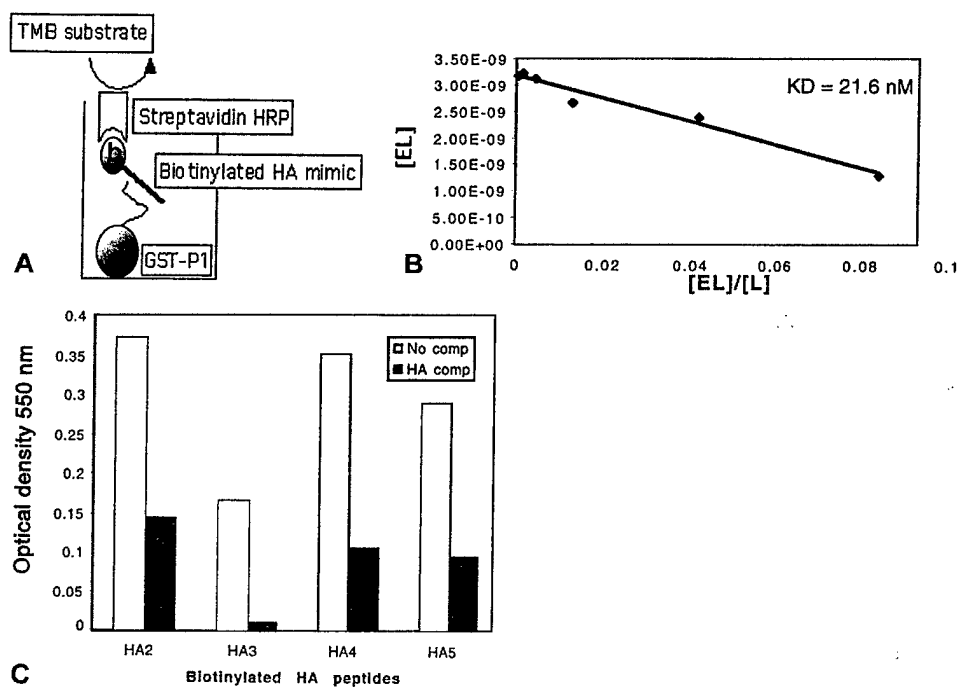


Fig. 4. Binding of HA mimetic peptides to GST-RHAMM-P1-coated microtiter plates. **A**: schematic of assay; **B**: Eadie-Hofstee plot of data for binding of biotinylated HA2, where E is the RHAMM-P1 fusion and L is the HA2 peptide; **C**: relative affinity of binding of four biotinylated phage-derived synthetic peptides showing competition by excess HA. The y-axis is optical density at 550 nm.

matic degradation of HA by Hase by preincubating the metal salts with either HA or with the Hase prior to the enzymatic reaction [29]. The digestion occurred more slowly in the presence of monovalent cations compared to the divalent cations. Most divalent cations activated Hase with equal potency, except for Cu^{2+} . Compared to the digestion in the presence of the other divalent salts, Cu^{2+} suppressed the degradation of HA; however, compared to the digestion in the absence of any salt, Cu^{2+} still activated the digestion of HA by Hase. When HA was preincubated with NaCl or when Hase was incubated with salts like CaCl_2 , CoCl_2 , ZnCl_2 or CuCl_2 , surprisingly no effects on the enzymatic activity could be observed (except for CuCl_2). The combined results suggested that the activating effect of the cations occurs through an activation of HA rather than an activation of Hase. That is, the addition of the cations to HA may change its conformation such that more endoglucanase sites are exposed, thus, facilitating the hydrolysis by the enzyme.

These experiments suggested that any metal-chelating compound might inhibit the degradation of HA by Hase. As predicted, preincubation of EGTA- Na_4 with HA/ CaCl_2 inhibited the degradation of HA by Hase. No inhibition was observed when EGTA- Na_4 was preincubated with Hase prior to the digestion. Thus, judicious selection of Hase assay parameters is critical for the discovery of novel, selective Hase inhibitors and not mere metal-chelating compounds. Total enzymatic digestion of HA in the presence of varying concentrations of Ca^{2+} showed a concentration-dependent regulation of the size of the oligosaccharide end products. These oligosaccharides were fractionated to monodisperse species using anion exchange perfusion chromatography and their size and purity were confirmed using MALDI-TOF analysis.

Fluorescence-based assays for Hase

In most mammals, Hase is found on the acrosomal membrane of spermatozoa and plays a major role in the passage of the spermatozoa towards the oocyte [30]. The enzyme is also present in most animal venoms and several bacterial species produce Hase, enhancing their virulence. Tumors are often enriched in Hase activity compared to normal tissues. This production of Hase can affect the further development of the tumor, e.g., by generating small, angiogenic oligosaccharide fragments from HA polymers present in the extracellular matrix [31]. Thus, inhibitors of the enzyme could have potential as nonhormonal contraceptive agents or as novel anti-angiogenic compounds. In view of the importance of Hase and its inhibitors, there is a need for a simple, rapid, and sensitive assay to evaluate the Hase activity present in any sample or to search for inhibitors of this enzyme.

Methods currently employed often lack the necessary sensitivity, selectivity, or versatility to perform all these tasks. We are developing a fluorescence-dequenching assay using a fluorescently labeled HA conjugate as a substrate for Hase (Fig. 5A). Using the hydrazide methodology, HA was modified with FITC and with Texas Red. This gave a doubly labeled HA substrate in which the fluores-

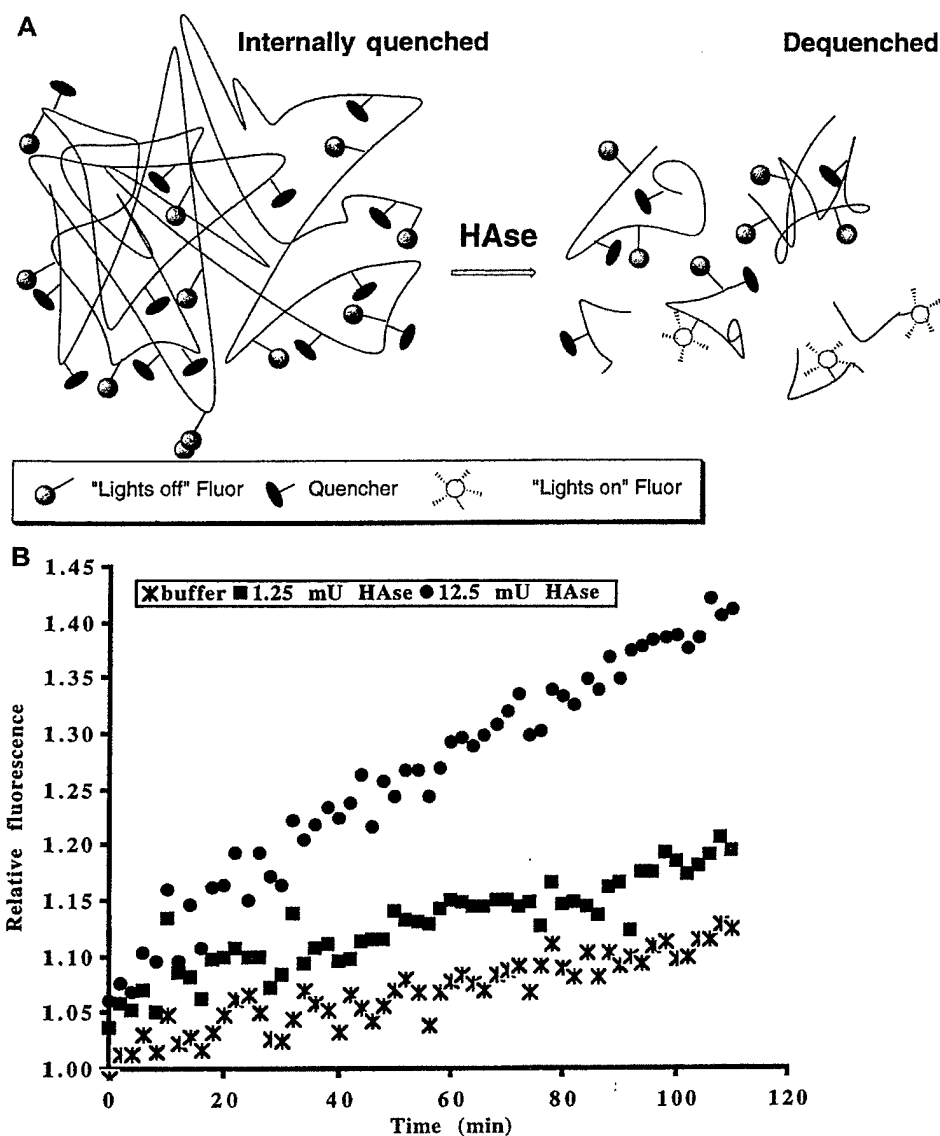


Fig. 5. Fluorescence-dequenching assay for Hase. **A**: schematic of assay; **B**: data from digestion of HA, labeled with FITC and Texas Red, by Hase (0, 1.25 or 12.5 mUnits) in phosphate buffer (pH = 6.4) containing 150 mM NaCl in wells of a 96 well microplate. The fluorescence of FITC (excitation 490 nm, emission 535 nm) was monitored as a function of the reaction time; each data point is the average of three measurements.

cence of FITC was partially quenched by the presence of nearby Texas Red fluorophores. Digestion of this substrate by Hase separates FITC from the Texas Red-containing regions, resulting in an increased fluorescence that can be moni-

tored as a function of the reaction time. Figure 5B illustrates such an increase in FITC fluorescence when HA conjugated with FITC and Texas Red is incubated with two different amounts of Hase compared to the incubation with buffer alone. This proprietary assay can be performed in a 96 well format yielding a high through-put screening assay for Hase activity and/or inhibition.

Conclusions

Modification of HA using adipic dihydrazide (ADH) permits preparation of a wide variety of biomaterials and biochemical probes. In this overview we showed five examples. Firstly, selective toxicity of anticancer drugs coupled to HA to tumor cells illustrated an important method for solubilization and cell targeted intracellular delivery of known antitumor drugs. This method can significantly improve the therapeutic ratio. Secondly, swellable HA hydrogel films with slow release properties for both small molecules and macromolecular drugs allow penetration of a combined wound dressing; drug delivery system that is bio-resorbable. Thirdly, attachment of HA to surfaces provides materials for cell sorting and protein panning to identify new HABPs. Fourthly, interactions of HABPs with HA and HA-mimetic peptides offer insight into cell biology and structural biology of HBP-HA complexes. Finally, doubly labeled HA (using two different covalently attached fluorors) creates a novel assay for detection of Hase activity and thus, for discovery of new Hase inhibitors.

Acknowledgements

We thank the Center for Biopolymers at Interfaces, The University of Utah, the National Institutes of Health Chemical Biology Training Grant, and the US Department of the Army (Breast Cancer IDEA award) for current financial support. We thank Clear Solutions Biotech, Inc. (Stony Brook, NY) for providing HA for these studies and for cooperating in the development of practical uses for the hydrazide technology. New technologies described herein in Sections 1 through 5 may be licensed from The University of Utah and from Clear Solutions.

References

1. Pouyani T, Prestwich GD. Functionalized derivatives of hyaluronic acid oligosaccharides; drug carriers and novel biomaterials. *Bioconjugate Chem* 1994;5(4):339--347.
2. Pouyani T, Prestwich GD. Functionalized derivatives of hyaluronic acid. US Patent No. 5, 616, 568. Research Foundation of SUNY, 1997.
3. Vercruysse KP, Marecak DM, Marecek JF, Prestwich GD. Synthesis and in vitro degradation of new polyvalent hydrazide cross-linked hydrogels of hyaluronic acid. *Bioconjugate Chem* 1997; 8(5):686--694.
4. Pouyani T, Harbison GS, Prestwich GD. Novel hydrogels of hyaluronic acid: synthesis, surface morphology, and solid-state NMR. *J Am Chem Soc* 1994;116(17):7515--7522.
5. Vercruysse KP, Prestwich GD. Hyaluronate derivatives in drug delivery. *Crit Rev Ther Drug*

- Carr Syst 1998;15(5):513–555.
6. Prestwich GD, Marecak DM, Marecek JF, Vercruysse KP, Ziebell MR. Chemical modification of hyaluronic acid for drug delivery, biomaterials, and biochemical probes. In: Laurent TC, Balazs EA (eds) *The Chemistry, Biology, and Medical Applications of HA and its Derivatives*. London: Portland Press, 1998;43–65.
 7. Entwistle J, Hall CL, Turley EA. HA receptors: regulators of signalling to the cytoskeleton. *J Cell Biochem* 1996;61(4):569–577.
 8. Gustafson S. HA in drug delivery. In: Laurent TC, Balazs EA (eds) *The Chemistry, Biology, and Medical Applications of HA and its Derivatives*. UK: Portland Press, 1998;291–304.
 9. Luo Y, Prestwich GD. Synthesis and selective cytotoxicity of a hyaluronic acid-anti-tumor bioconjugate. *Bioconjugate Chem* 1999 (In press).
 10. Collis L, Hall C, Lange L, Ziebell MR, Prestwich GD, Turley EA. Rapid HA uptake is associated with enhanced motility: implications for an intracellular mode of action. *FEBS Lett* 1998;440:444–449.
 11. Kokoshka JM, Ireland CM, Barrows LR. Cell-based screen for identification of inhibitors of tubulin polymerization. *J Nat Prod* 1996;59(12):1179–1182.
 12. Iida N, Bourguignon LY-W. Coexpression of CD44 variant (v10/ex14) and CD44S in human mammary epithelial cells promotes tumorigenesis. *J Cell Physiol* 1997;171:152–160.
 13. Bourguignon LY-W, Zhu HB, Chu A, Iida N, Zhang L, Hung MC. Interaction between the adhesion receptor, CD44, and the oncogene product, p185(HER2), promotes human ovarian tumor cell activation. *J Biol Chem* 1997;272(44):27913–27918.
 14. Kim SW, Bae YH, Okano T. Hydrogel: swelling, drug loading and release. *Pharmacol Res* 1992; 9:283–290.
 15. Tomihata K, Ikada Y. Preparation of cross-linked hyaluronic acid films of low water content. *Biomaterials* 1997;18:189–195.
 16. Yui N, Okano T, Sakurai Y. Inflammation responsive degradation of cross-linked hyaluronic acid gels. *J Contr Rel* 1992;22:105–116.
 17. Jeong B, Bae YH, Lee DS, Kim SW. Biodegradable block copolymers as injectable drug-delivery systems. *Nature* 1997;388:860–862.
 18. Mason M, Vercruysse KP, Kirker KR, Frisch R, Marecak DM, Prestwich GD, Pitt W. Hyaluronic acid modified polypropylene, polystyrene, and polytetrafluoroethylene. *Biomaterials* 1999(In press).
 19. Prestwich GD, Marecak DM, Marecek JF, Vercruysse KP, Ziebell MR. Controlled chemical modification of hyaluronic acid: synthesis, applications, and biodegradation of hydrazide derivatives. *J Contr Rel* 1998(53):93–103.
 20. Wang C, Thor AD, Moore DH II, Zhao Y, Kerschmann R, Stern R, Watson PH, Turley EA. The overexpression of RHAMM, a HA-binding protein that regulates ras signaling, correlates with overexpression of mitogen activated protein kinase and is a significant parameter in breast cancer progression. *Clin Cancer Res* 1998;4(3):567–576.
 21. Zhang S, Chang MC, Zylka D, Turley S, Harrison R, Turley EA. The HA receptor RHAMM regulates extracellular regulated kinase. *J Biol Chem* 1998;273(18):11342–11348.
 22. Kohda D, Morton CJ, Parkar AA, Hatanaka H, Inagaki FM, Campbell ID, Day AJ. Solution structure of the link module: an HA-binding domain involved in extracellular matrix stability and cell migration. *Cell* 1996;86(5):767–775.
 23. Day AJ. The structure and regulation of HA-binding proteins. *Biochem Soc Trans* 1999;27(2): 115–121.
 24. Laurent TC, Laurent UBG, Fraser JRE. Functions of HA. *Ann Rheum Dis* 1995;54(5):429–432.
 25. Smith GP, Patel SU, Windass JD, Thornton JM, Winter G, Griffiths AD. Small binding proteins selected from a combinatorial repertoire of knottins displayed on phage. *J Molec Biol* 1998; 277(2):317–332.
 26. Lam KS, Sroka T, Chen ML, Zhao Y, Lou Q, Wu J, Zhao Z-G. Application of “One-bead One-

- compound" combinatorial library methods in signal transduction research. *Life Sci* 1998;62 (17-18):1577-1583.
27. Zhang S, Cheung W, Lu J, Ziebell MR, Turley SA, Harrison R, Zylka D, Ahn N, Litchfield D, Prestwich GD, Cruz T, Turley EA. Intracellular RHAMM isoforms bind directly to erk1 and these interactions are required for transformation and for podosome formation via the erk kinase pathway. *J Biol Chem* 1999, submitted.
 28. Wu P, Brasseur M, Schindler U. A high through-put STAT binding assay using fluorescence polarization. *Anal Biochem* 1997;249(1):29-36.
 29. Vercruysse KP, Ziebell MR, Prestwich GD. Control of enzymatic degradation of HA by divalent cations. *Carbohydr Res* 1999, In press.
 30. Li M-W, Yudin AI, VandeVoort CA, Sabeur K, Primakoff P, Overstreet JW. Inhibition of monkey sperm hyaluronidase activity and heterologous cumulus penetration by flavanoids. *Biol Reprod* 1997;56:1383-1389.
 31. Lokeshwar VB, Lokeshwar BL, Pham HT, Block NL. Association of elevated levels of hyaluronidase, a matrix-degrading enzyme, with prostate cancer progression. *Cancer Res* 1996;56(3): 651-657.

A Hyaluronic Acid–Taxol Antitumor Bioconjugate Targeted to Cancer Cells

Yi Luo, Michael R. Ziebell, and Glenn D. Prestwich

Department of Medicinal Chemistry, The University of Utah, Salt Lake
City, Utah 84112-5820, and Department of Physiology and
Biophysics, The University at Stony Brook, Stony Brook,
New York 11794-8661

*Bio***MACROMOLECULES**

Reprinted from
Volume 1, Number 2, Pages 208–218

A Hyaluronic Acid–Taxol Antitumor Bioconjugate Targeted to Cancer Cells

Yi Luo,[†] Michael R. Ziebell,^{†,‡} and Glenn D. Prestwich^{*,†}

Department of Medicinal Chemistry, The University of Utah, Salt Lake City, Utah 84112-5820, and
Department of Physiology and Biophysics, The University at Stony Brook,
Stony Brook, New York 11794-8661

Received January 10, 2000

A cell-targeted polymeric prodrug prepared from Taxol and chemically modified hyaluronic acid (HA) was evaluated *in vitro*. Herein we report four results in support of the selective uptake and targeted toxicity of the HA–Taxol prodrug. First, a fluorescently labeled HA–Taxol (FITC–HA–Taxol) was synthesized and used to demonstrate cell-specific binding and uptake using flow cytometry and confocal microscopy. Second, the selective cytotoxicity of FITC–HA–Taxol allowed direct correlation of uptake with selective cytotoxicity. Third, the rapid uptake and selective cytotoxicity of HA–Taxol bioconjugates could be blocked by either excess HA or by an anti-CD44 antibody, but not by chondroitin sulfate (CS). Finally, the release of free Taxol from HA–Taxol in human plasma or in cell culture media revealed that the free drug was hydrolytically released from the bioconjugate by cleavage of the labile 2' ester linkage. Taken together, these data support the notion that the targeted cytotoxicity of HA–Taxol bioconjugates requires receptor-mediated cellular uptake of the bioconjugate followed by hydrolytic release of free Taxol.

Introduction

A major challenge in cancer therapy is to selectively target cytotoxic agents to tumor cells. To decrease undesirable side effects of small molecule anticancer agents, many targeting approaches have been examined. One of the most promising methods involves the combination or covalent attachment of the cytotoxin with a macromolecular carrier.¹ Many kinds of drug carriers, including soluble synthetic and natural polymers,² liposomes,³ microspheres,⁴ and nanospheres^{5,6} have been employed to increase drug concentration in target cells; by altering the pharmacokinetic distribution of drugs, a sustained therapeutic concentration can be maintained at tolerable doses. Soluble polymers seem to offer great potential because they can traverse compartmental barriers in the body⁷ and therefore gain access to a greater number of cell types. A variety of water-soluble polymers, such as human serum albumin (HSA),² dextran,⁸ lectins,⁹ poly(ethylene glycol) (PEG),¹⁰ poly(styrene-*co*-maleic anhydride) (SMA),¹¹ poly(*N*-hydroxylpropylmethacrylamide) (HPMA),¹² and poly(divinyl ether-*co*-maleic anhydride) (DIVEMA)¹³ have been used to prepare polymeric anticancer prodrugs. Such drug–polymer conjugates have demonstrated good solubility in water, increased half-life in the body, and high antitumor effects. For example, the linking of adriamycin to HPMA gives a new prodrug with improved *in vitro* tumor retention, a higher therapeutic ratio, and avoidance of

multidrug resistance.¹² This system is currently in phase II trials against ovarian cancer.

Anticancer polymeric prodrugs can be divided into two targeting modalities: passive and active. The biological activity of the passive targeting drug delivery systems is based on the anatomical characteristics of tumor tissue and allows polymeric prodrugs to more easily permeate tumor tissues and accumulate over time. This is often referred to as the enhanced permeability and retention (EPR) effect. In contrast, active targeting drug delivery systems can be developed using specific interactions between receptors on the cell surface and targeting moieties conjugated to the polymer backbone. In this way, active therapeutic agents conjugated to polymers can be selectively transported to tumor tissues. The active approach therefore takes advantage of the EPR effect but further increases selectivity through receptor-mediated uptake by target cancer cells.

Hyaluronic acid (HA), a linear polysaccharide of alternating D-glucuronic acid (GlcUA) and *N*-acetyl-D-glucosamine (GlcNAc) units, is the only non-sulfated glycosaminoglycan and occurs primarily *in vivo* as sodium hyaluronate. The term hyaluronan refers to both forms. HA is present in the extracellular matrix, the synovial fluid of joints, and the scaffolding that comprises cartilage.¹⁴ It is an immunoneutral building block for preparing biocompatible and biodegradable biomaterials,^{15–18} and has been employed as both a vehicle and an angiostatic agent in cancer therapy.^{19–21} Mitomycin C and epirubicin were coupled to HA by carbodiimide chemistry, and the HA-mitomycin adduct was selectively toxic to a lung carcinoma xenograft.²² Recently, we have described the use of mild hydrazide chemistry to prepare an HA–Taxol bioconjugate,²³ which showed good selectivity

* To whom correspondence may be addressed at The University of Utah, Department of Medicinal Chemistry, 30 South 2000 East, Room 201, Salt Lake City, UT 84112-5820; phone, 801 585-9051; fax, 801 585-9053; e-mail, gprestwich@deans.pharm.utah.edu.

[†] The University of Utah.

[‡] The University at Stony Brook.

in preliminary cell culture studies. In this report, we provide evidence that directly correlates uptake with cytotoxicity using a fluorescently labeled HA—Taxol derivative, and we demonstrate that toxicity is due to hydrolytic release of the parent drug.

HA serves a variety of functions within the extracellular matrix, including direct receptor-mediated effects on cell behavior. These effects occur via intracellular signaling pathways in which HA binds to, and is internalized by, cell surface receptors. Several cell-membrane-localized receptors (HA binding proteins) have been identified including: CD44, RHAMM, IVd4, and the liver endothelial cell clearance receptor.^{24–27} HA—protein interactions play crucial roles in cell adhesion, growth, and migration,^{28–30} and HA acts as a signaling molecule in cell motility, inflammation, wound healing, and cancer metastasis.³¹ The structure and regulation of HA receptors³² are growing areas of structural and cellular biology that are critical to understanding how HA—protein interactions enhance metastasis.

Most malignant solid tumors contain elevated levels of HA,³³ and these high levels of HA production provide a matrix that facilitates invasion.³⁴ Clinically, high HA levels correlate with poor differentiation and decreased survival rate in some human carcinomas. HA is an important signal for activating kinase pathways^{35,36} and regulating angiogenesis in tumors.³⁷ HA internalization is mediated via matrix receptors, including CD44, which is a transmembrane receptor that can communicate cell—matrix interactions into cells and can alter the matrix in response to intracellular signals. The pathological enrichment of HA in tumor tissues suggests that manipulation of the interactions between HA and its receptors could lead to dramatic inhibition of growth or metastasis of several types of tumors. Antibodies to CD44, soluble forms of CD44 or RHAMM, HAse, and oligomers of HA have all been used effectively to inhibit tumor growth or metastasis in animal models.

In addition to elevated HA in the environment surrounding tumors, most malignant cell types overexpress CD44 and RHAMM. As a result, malignant cells with the highest metastatic potential often show enhanced binding and internalization of HA.³⁸ Apparently, such cells can effectively breach the tumor-associated HA barrier by binding, internalizing, and degrading this glycosaminoglycan. Cell culture experiments suggest that CD44-HA interactions occur *in vivo* and are likely to be responsible for retention of HA-enriched matrixes. Thus, HA can bind to the cell surface via interactions with CD44, and a portion subsequently undergoes endocytosis. In addition, internalization of [³H]-labeled HA revealed that intracellular degradation of HA occurs within a low pH environment, such as that of lysosome. Targeting of anticancer agents to tumor cells and tumor metastases can be accomplished by receptor-mediated uptake of bioconjugates of anticancer agents to HA,^{22,23} followed by the release of free drugs through the degradation of HA in cell compartments. Since CD44 and RHAMM isoforms are overexpressed in transformed human breast epithelial cells,³⁹ human ovarian tumor cells,⁴⁰ and other cancers,^{41,42} the selectivity for drug delivery to cancerous cells should be markedly enhanced and overall dosages may be reduced.

Using HA as drug carrier should thus combine the advantages of both the passive and active targeting ability of a polymeric prodrug. Moreover, coupling of antitumor agents to HA can provide advantages in drug solubilization, stabilization, localization, and controlled release.¹¹ Coupling antitumor agents to hydrazide-modified HA^{18,43} adds further selectivity by specifically targeting the polymeric prodrug to aggressively growing cancers that overexpress HA receptors.

Paclitaxel (Taxol) is a powerful antimitotic agent that promotes tubulin assembly into stable aggregated structures.⁴⁴ It binds to microtubules and inhibits their depolymerization into tubulin. Expanding the applications of Taxol in cancer therapy is limited by poor aqueous solubility and by drug-associated neuropathies. Previous attempts to address the solubility issue involved preparation of 2'-OH linked water-soluble PEG derivatives¹⁰ or poly(L-glutamic acid) derivatives.⁴⁵ In our study, Taxol was covalently attached through a labile ester linkage to HA, which had been modified with adipic dihydrazide (ADH).^{46,47} Drug release from the HA—Taxol prodrug was studied *in vitro* in cell culture media with or without cells and also with exogenously added HAse or esterase. Selective *in vitro* cell cytotoxicity was studied with an untransformed mouse fibroblast cell line (NIH 3T3) and with three human cell lines (HCT-116 colon tumor, HBL-100 breast cancer, and SK-OV-3 ovarian cancer). In addition, a fluorescently labeled HA bioconjugate (FITC—HA—Taxol) was prepared (Figure 1) and employed to visualize selective uptake of HA using flow cytometry and confocal microscopy. Both the toxicity and FITC—HA—Taxol uptake by cells were prevented by preincubation with HA or an anti-CD44 antibody, but not by chondroitin sulfate (CS), providing compelling evidence for receptor-mediated uptake of the prodrug.

Materials and Methods

Reagents. Fermentation-derived HA (sodium salt, M_r 1.5 MDa) was provided by Clear Solutions Biotechnology, Inc. (Stony Brook, NY). 1-Ethyl-3-[3-(dimethylamino)propyl]-carbodiimide (EDCI), adipic dihydrazide (ADH), succinic anhydride, diphenylphosphoryl chloride (DPPC), *N*-hydroxysuccinimide, and triethylamine were purchased from Aldrich Chemical Co. (Milwaukee, WI). Bovine testicular HAse (880 U/mg), esterase from porcine liver crude (19 U/mg), and CS type C from shark cartilage, cell culture media, and supplements were obtained from Sigma Chemical Co. (St. Louis, MO). Paclitaxel (Taxol) was purchased from CBI Tech, Inc. (Cambridge, MA). Cephalomannine was purchased from Handetech USA, Inc. (Houston, TX). FITC "isomer I" was obtained from Molecular Probes, Inc. (Portland, OR). All chemicals were reagent grade or HPLC grade (Fisher Scientific Co., Santa Clara, CA). CH₂Cl₂ and acetonitrile were distilled from CaH₂. Anti-human CD44 monoclonal antibody (anti-CD mAb) was purchased from Calbiochem-Novabiochem Corp. (La Jolla, CA).

Cell Culture. HBL-100, a human breast cancer cell line, was maintained in culture in high-glucose D-MEM (Dulbecco's Modified Eagle Medium), which was supplemented with 10% γ -irradiated fetal bovine serum (FBS) and 1%

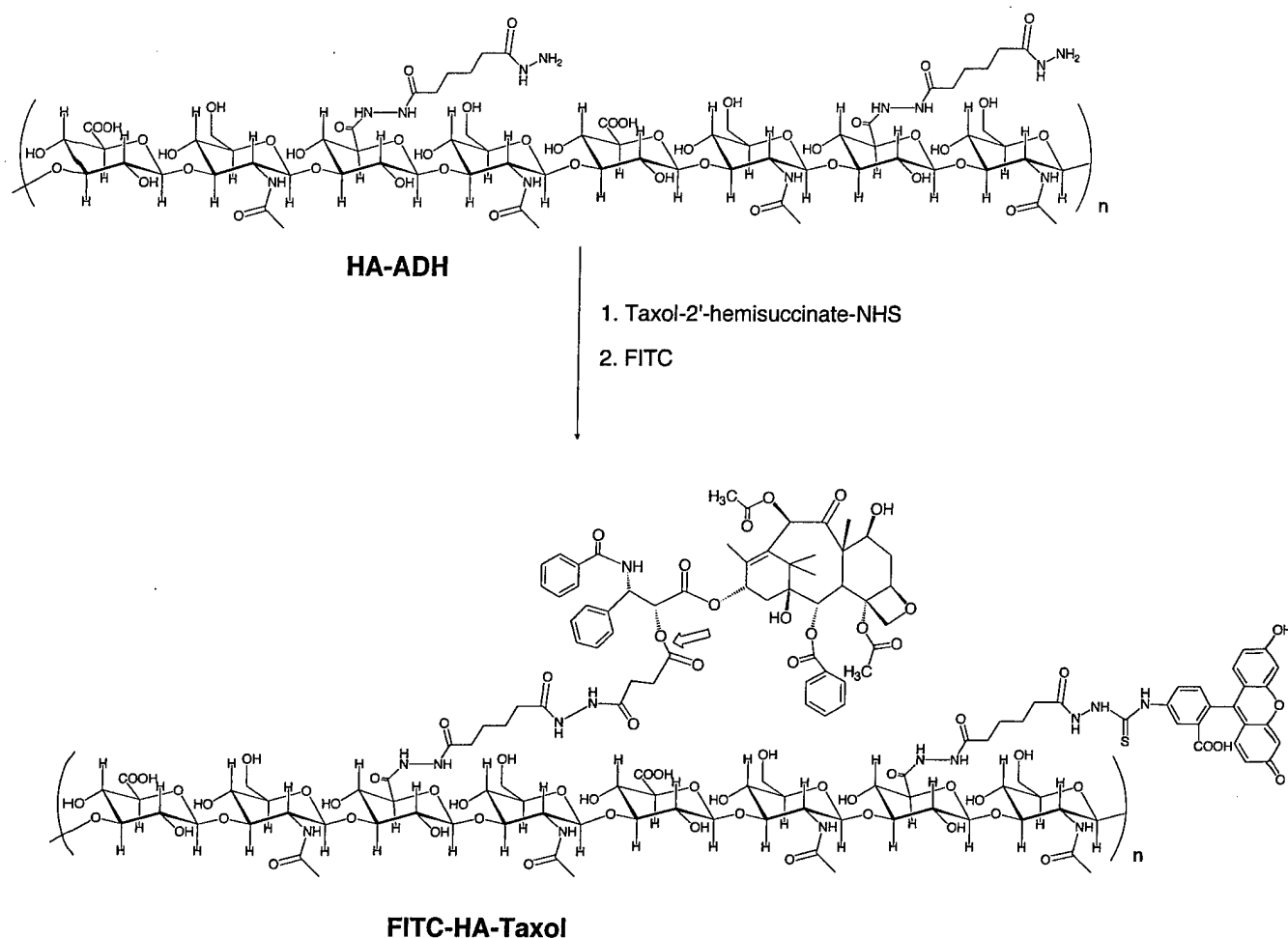


Figure 1. Synthesis of FITC-HA-Taxol.

sodium pyruvate; SK-OV-3, a human ovarian cancer cell line was cultured in D-MEM/F12 + 10% FBS; HCT-116, a colon tumor cell line, was maintained in culture in McCoy's 5A Medium Modified + 10% FBS; NIH 3T3, a mouse fibroblast cell line was cultured in high-glucose D-MEM + 10% FBS.

Analytical Instrumentation. All ^1H NMR spectral data were obtained using an NR-200 FT-NMR spectrometer at 200 MHz (IBM Instruments Inc.). UV-vis spectra were recorded on a Hewlett-Packard 8453 UV-Vis diode array spectrophotometer (Palo Alto, CA). Gel permeation chromatography (GPC) and high-performance liquid chromatography (HPLC) were carried out on the following system: Waters 515 HPLC pump, Waters 410 differential refractometer, and Waters 486 tunable absorbance detector. Waters Ultrahydrogel 250 and 2000 columns (7.8 mm i.d. \times 30 cm) (Milford, MA) were used for GPC analysis, the eluent was 150 mM pH 6.5 phosphate buffer/MeOH = 80:20 (v/v), and the flow rate was 0.5 mL/min. The system was calibrated with HA standards supplied by Dr. O. Wik (Pharmacia). HPLC analysis of Taxol release from HA-Taxol bioconjugate was performed on Altech HYPERSIL ODS C_{18} 5U 150 mm \times 4.6 mm i.d. along with Altech HYPERSIL ODS C_{18} 5U 7.5 mm \times 4.6 mm i.d. as guard column at room temperature; the eluent was acetonitrile/ H_2O = 45:55 with flow rate of 0.8 mL/min. A 1-mL C_{18} cartridge was obtained

from Varian Inc. (Palo Alto, CA). Fluorescence-activated cell sorting (FACS) was performed on a Becton Dickinson FACScan (San José, CA) with an argon-ion laser for cell binding and uptake measurement. Confocal fluorescence images of fluorescently labeled HA binding and uptake by cells were recorded using a Zeiss Microscope (Carl Zeiss, Inc., Germany). Cell viability in cell culture was determined by thiazoyl blue (MTT) dye uptake protocols measured at 540 nm, which was recorded on a BIO-RAD M-450 microplate reader (Hercules, CA). Coulter Counter was from Coulter Electronics, Inc. (Hialeah, FL).

Preparation of Low Molecular Weight (LMW) HA and HA Hydrazide Derivative (HA-ADH). Low molecular weight HA (LMW HA) was obtained by the degradation of high molecular weight HA (1.5 MDa) in pH 6.5 phosphate-buffered saline (PBS) buffer (4 mg/mL) with Hase (10 U/mg HA) as previously described.²³ The size profile was evaluated by GPC analysis. Hydrazide-derivatized HA (HA-ADH) was prepared^{46,47} using a modified purification method that gives preparations free of small molecules.²³ In one example, LMW HA (50 mg) was modified with a 5-fold excess of ADH to obtain 37 mg of HA-ADH with an 18% ADH loading based on available carboxylates modified.

Preparation of HA-Taxol Bioconjugates. Taxol 2'-hemisuccinate, which was synthesized from Taxol and succinic anhydride and purified as described,²³ was used as

a standard for release studies. Activation to the *N*-hydroxy-succinimide ester²³ gave the reagent used for coupling to HA-ADH. Several loadings were prepared. In a representative example, HA-ADH with 18% ADH loading (10 mg, 4.4 μ mol of hydrazide) was dissolved in 3 mM pH 6.5 phosphate buffer to give 1 mg/mL. To this mixture was added Taxol-NHS ester dissolved in sufficient DMF (DMF:H₂O = 2:1, v/v) to give a homogeneous solution, and the reaction mixture was stirred at room temperature for 24 h. The reaction mixture was dialyzed successively against 50% acetone/H₂O and water (membrane tubing, *M_r* cutoff 3500). The solution was then filtered through a 0.2 μ m membrane and then lyophilized. The purity of HA-Taxol conjugate was measured by GPC analysis. Taxol loading was determined by UV absorbance ($\lambda_{\text{max}} = 227$ nm, $\epsilon = 2.8 \times 10^4$) in 80:20 CH₃CN:H₂O.

Taxol Release from HA-Taxol Bioconjugate. Solid-phase extraction (SPE) and liquid-liquid extraction (LLE) methods were introduced to recover the liberated Taxol, Taxol 2'-hemisuccinate, or other potential metabolites.

SPE Method. A 1-mL C₁₈ cartridge was first conditioned with 5 mL of ethyl acetate, 5 mL of methanol, and 5 mL of Nanopure H₂O. A small amount of H₂O remained above the top frit in the cartridge at the time the crude extract was transferred to the cartridge. Several "crude extract" model solutions were prepared for calibration: 2 μ L of Taxol in DMSO (1 mg/mL) + 2 μ L of Taxol 2'-hemisuccinate in DMSO (1 mg/mL), 1 μ L of Taxol in DMSO (1 mg/mL) + 1 μ L of Taxol 2'-hemisuccinate in DMSO (1 mg/mL), and 2 μ L of Taxol in DMSO (0.1 mg/mL) + 2 μ L of Taxol 2'-hemisuccinate in DMSO (0.1 mg/mL), each mixed with 200 μ L of cell culture media (α -MEM + 10% FBS). The final concentrations of Taxol and Taxol 2'-hemisuccinate in cell culture media were 10, 5, and 1 μ g/mL (from 1 to 12 nmol/mL). After the crude extract was transferred into the cartridge, the cartridge was washed (four 1-mL portions of H₂O, 3 \times 1 mL of 20% methanol/H₂O, 4 \times 1 mL of methanol). To the combined methanol fractions was added 1 μ g of cephalomannine (internal standard) as a methanol stock solution (100 μ L of 10 μ g/mL stock solution), and solvents were concentrated in vacuo using a centrifugal concentrator at room temperature. The residue was dissolved in 500 μ L of methanol, and a 200- μ L aliquot was analyzed by HPLC.

LLE Method. The same model extracts as above were diluted with 300 μ L of H₂O. Taxol and Taxol 2'-hemisuccinate were extracted using 4.0 mL of *tert*-butyl methyl ether and vortex-mixing the sample for 1 min. The mixture was centrifuged for 10 min at 500g at room temperature, and then 2.0 mL of the organic layer was transferred to a new tube. Internal standard (1 μ g of cephalomannine) was added as a methanol stock, the mixture was evaporated to dryness, the residue was dissolved in 500 μ L of methanol, and a 200- μ L aliquot was analyzed by HPLC.

Each experiment with either the SPE method or the LLE method was performed in triplicate. The recovery of Taxol or Taxol 2'-hemisuccinate was evaluated according to the equation:

recovery =

$$\frac{\text{mean peak area ratio, extract drug}}{\text{mean peak area ratio, direct injection drug}} \times 100\%$$

Taxol release from HA-Taxol prodrug experiments was carried out in five different media: (1) cell culture media, cell culture media with added (2) HAse (1 U/mL, 10 U/mL) or (3) esterase (0.1 U/mL, 1 U/mL), (4) cell culture media with cells, and (5) human plasma. For each system, 2 μ L of HA-Taxol bioconjugate stock solution (10 mg/mL in DMSO/H₂O = 1:1, v/v) was added into 200 μ L of media solution and then maintained at 5% CO₂, 37 °C. Samples (crude extracts) were taken out at different time intervals, and SPE was used to follow drug release.

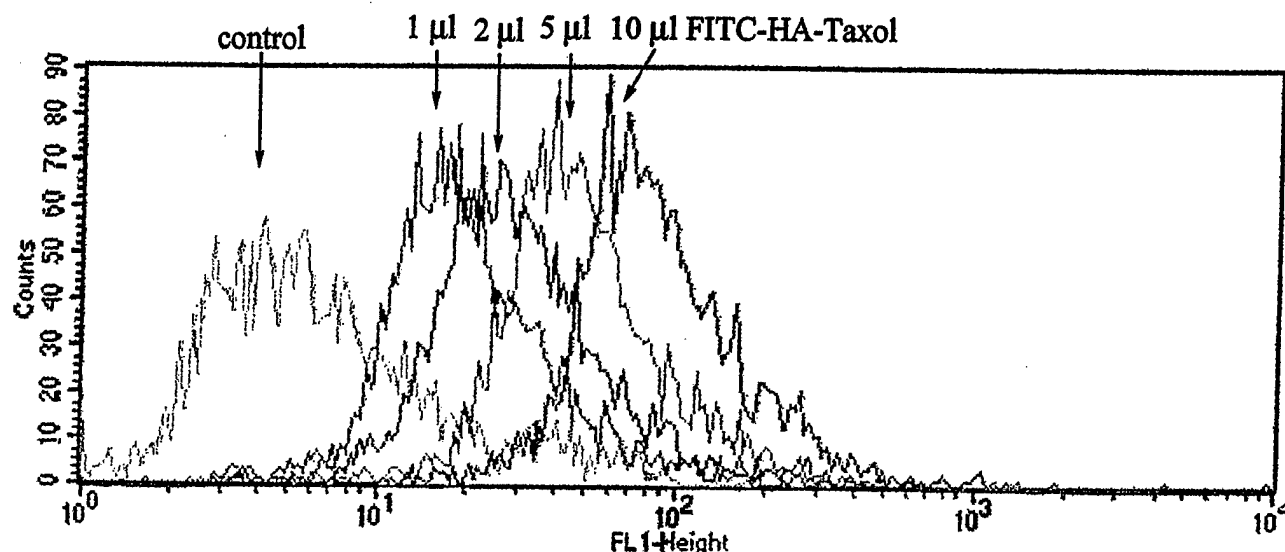
Preparation of FITC-HA-Taxol. LMW HA-ADH with 9% ADH loading (20 mg, 3.7 μ mol of hydrazide) was dissolved in 5 mL of 3 mM pH 6.5 phosphate buffer, and 10 mL of a DMF solution of Taxol NHS ester (7.8 mg, 7.4 μ mol) was added. The reaction mixture was stirred at room temperature overnight. To this mixture, FITC (1 mg, 2.6 μ mol) in 2 mL of DMF was added, and the reaction was stirred at room temperature overnight. FITC-HA-Taxol was purified by dialysis against 50% acetone/H₂O, and its purity was determined by GPC with UV detection at 210 nm (HA, Taxol), and 493 nm (FITC).

In Vitro Cell Culture Cytotoxicity. The cytotoxicity of HA-Taxol conjugates was determined using a 96-well plate format in quadruplicate with increasing doses: 0.001, 0.01, 0.1, 0.5, 1, 5, 10, 50, and 100 μ g/mL. Each well contained approximately 20 000 cells in 200 μ L of cell culture media. HA-Taxol conjugates were added as a stock solution in DMSO:H₂O = 1:1, v/v; free Taxol was added as a DMSO stock solution. Thus, a 2- μ L aliquot of the stock solution was added to each well, cells were incubated at 37 °C for 3 days with the test substance, and cell viability was determined using MTT dye uptake at 540 nm. Response was graded as percent live cells compared to untreated controls.⁴⁸

In competition experiments, 100-fold excess of either high molecular weight HA or CS (as compared to HA-Taxol) was employed; either the competitor was added at the same time as the drug or, alternatively, cells were preincubated with competitor for 4 h before the addition of HA-Taxol conjugate or free Taxol. The in vitro cytotoxicity was analyzed as described above.

Binding and Uptake Measurement by FACS. Cells were incubated in a cell culture flask, harvested by trypsinization, and transferred into clean tubes. An aliquot (1 μ L) of FITC-HA-Taxol (stock solution 1 mg/mL in PBS buffer) was added into tubes with suspension cells and analyzed by FACS. For competition or blocking studies, a 100-fold excess of either high molecular weight HA or CS (as compared to FITC-HA-Taxol) was preincubated with cells for 4 h, or an anti-CD44 mAb was preincubated with cells for 30 min, prior to addition of FITC-HA-Taxol and FACS analysis.

Uptake Measurement by Confocal Microscopy. An aliquot (2 μ L) of FITC-HA-Taxol (stock solution 1 mg/mL in PBS buffer) was added to 100 μ L of cell culture media containing cells cultured on cover slips, and confocal images



FLUORESCENCE

Figure 2. Flow cytometry measurements of FITC-HA-Taxol binding SK-OV-3 cells. Colored peaks show dose-dependent binding of the labeled polymeric prodrug to the CD44-overexpressing cells.

were recorded immediately. Competition experiments used cells preincubated with 100-fold excess HA for 4 h prior to addition of the FITC-HA-Taxol.

Results

Preparation of HA-Taxol. The hydrazide method^{46,47} allows attachment of reporter molecules, drugs, cross-linkers, and combinations of these moieties to HA.^{16,18,43} LMW HA was modified in this study for three reasons: (i) proton NMR allowed rapid quantification of the modification, (ii) LMW HA and its derivatives give injectable, nonviscous solution at concentrations up to 10 mg/mL, and (iii) LMW HA has a longer plasma half-life and is readily cleared by renal ultrafiltration. The LMW HA was generated by partial degradation of high molecular weight HA (1.5 MDa) with testicular Hase⁴⁹ in pH 6.5 PBS buffer at 37 °C. The final LMW HA product was characterized by GPC analysis: M_n = 3883, M_w = 11 199, and molecular dispersity (DP) = 2.88. Next, HA-ADH samples with different ADH loadings were prepared by carbodiimide coupling chemistry,²³ in which the extent of ADH modification was controlled through use of specific molar ratios of hydrazide, carboxylate equivalents, and carbodiimide. The purity and molecular size distribution of the HA-ADH were measured by GPC, and the loading of ADH on the polymer backbone was determined by ¹H NMR in D₂O.⁴⁶ HA-ADH with ADH loadings of 9% and 18% were obtained and used in preparing the HA-Taxol bioconjugates.

Because of the problems in administering emulsified forms of Taxol,⁵⁰ a water-soluble bioconjugate was prepared. The single symmetrical GPC peak showed that no free Taxol or other small molecular impurities remained. The loading of Taxol on polymer backbone was quantified by UV absorbance at 227 nm in 80% acetonitrile:H₂O. HA-Taxol bioconjugates [(HA)_x(HA-ADH)_y(HA-ADH-Taxol)_z] with the compositions of $x = 91\%$, $y = 4\%$, $z = 5\%$ and $x = 54$

82% , $y = 3\%$, $z = 15\%$ were used in the following experiments, based on previous loading optimization studies.²³

Cell-Based Assays for Binding and Uptake. Several different fluorescently labeled HA derivatives have been prepared in order to study receptor-mediated uptake. Most recently, RHAMM-mediated uptake and trafficking of HA by transformed fibroblasts⁵¹ was observed with Texas Red-HA, and BODIPY-labeled HA was employed to distinguish HA uptake in cancer vs untransformed cell lines.²³ Both of these derivatives were prepared with hydrazide modification chemistry. Previously, fluorescein-HA was employed to study HA uptake in a variety of systems, e.g., cells expressing CD44 variants,^{33,52–55} uptake by tumor cells for correlation with metastatic potential,^{42,56} internalization by chondrocytes,³⁸ and as a measure of liver endothelial cell function.⁵⁷

To correlate the binding and uptake by cells with toxicity, fluorescently labeled HA-Taxol (FITC-HA-Taxol) was prepared and purified by dialysis against 50% acetone/H₂O. The fluorescence loading of FITC-HA-Taxol was determined spectrophotometrically to be 0.6% (based on available glucuronates). GPC confirmed that mass, UV absorption, and fluorescence coeluted in the same symmetrical peak.

The interaction of the HA-Taxol bioconjugate with cells was initially investigated by laser flow activated cell sorting using FITC-HA-Taxol as fluorescence probe. To the suspended cells (after trypsin digestion), an aliquot of FITC-HA-Taxol (stock solution 1 mg/mL in PBS buffer) was added to give five different dosages. The measurements were immediately taken by FACS with untreated suspended cells as the control. The conjugate was strongly adsorbed to SK-OV-3 cells (Figure 2); similar results (not shown) were observed for HBL-100 and HCT-116 cells. The shift of the fluorescence peak in FACS was dose-dependent based on the amount of FITC-HA-Taxol added. Moreover, no fluorescence binding or shift was detected with mouse fibroblast NIH 3T3 cells. These results indicated that FITC-

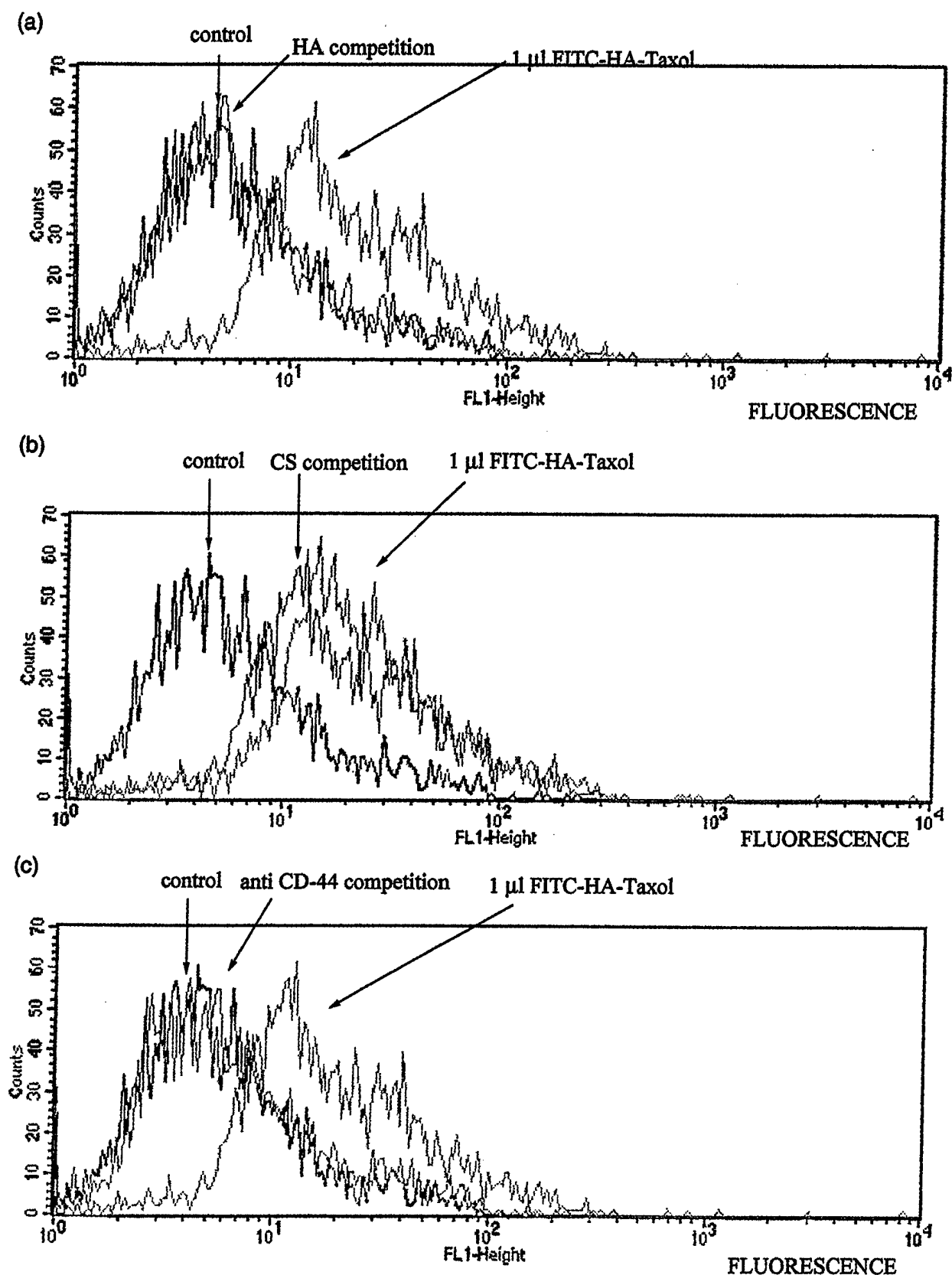


Figure 3. FACS analysis of FITC-HA-Taxol binding (red lines) to SK-OV-3 cells. Panel a shows competition by 100-fold excess HA (green) relative to controls (black) and no competitor (red); panel b shows absence of competition by excess CS (green); panel c shows blocking of uptake by anti-CD 44 mAb (green).

HA-Taxol selectively bound to, and was taken up by, the SK-OV-3, HBL-100, and HCT-116 cells. These results corroborate the previously reported selective cytotoxicity of the HA-Taxol bioconjugate to HBL-100 cells, SK-OV-3

cells, and HCT-116 cells²³ and provide an important linkage between fluorescence-visualized uptake and selective toxicity.

Since binding and uptake by cells determined the cytotoxicity of the HA-Taxol bioconjugate, experiments were

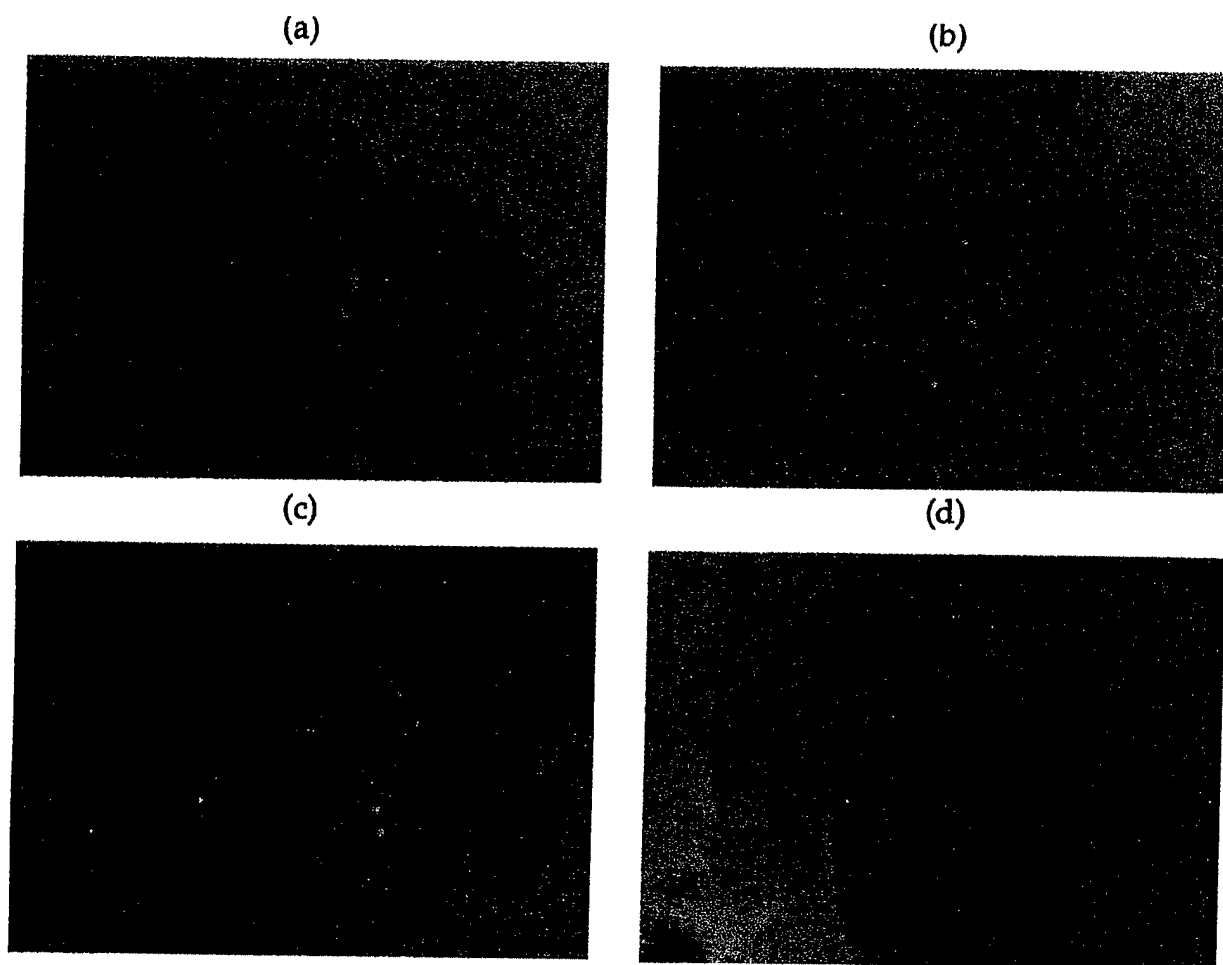


Figure 4. Binding and uptake of FITC-HA-Taxol by breast cancer HBL-100 cells. Panels a–c are confocal images indicating binding and uptake after 4 (a), 10 (b), and 20 min (c) of incubation. Panel d is a 5-fold lower magnification image that shows that preincubation with excess HA blocks the cellular uptake of FITC-HA-Taxol even at 20 min.

performed to block each of these two processes. The HA binding protein CD44 is overexpressed on the surface of HBL-100³⁹ and SK-OV-3 cells.⁴⁰ A series of competition experiments was carried out with SK-OV-3 cells using a 100-fold excess of high molecular weight HA, a 100-fold excess of CS, and an anti-CD44 mAb as potential disrupters of the cellular uptake of the FITC-HA-Taxol bioconjugate. Thus, cells were preincubated for 4 h with either HA or CS, or for 30 min with the anti-CD44 mAb. Next, FITC-HA-Taxol was added and FACS analysis was performed. Figure 3 shows that the binding and uptake of FITC-HA-Taxol into SK-OV-3 cells could be blocked by excess HA (panel a) and by the anti-CD44 mAb (panel c) but not by excess CS (panel b).

Liver endothelial cells display at least two different binding proteins for HA, including a scavenger receptor that binds to both CS and HA, and other glycosaminoglycans.⁵⁸ However, at sites in need of treatment, e.g., tumor metastases, only receptors that are HA specific appear to be expressed. We previously showed that the binding of fluorescently labeled HA alone could be blocked by excess HA in cancer cell lines.²³ The data presented herein now provide direct evidence that unambiguously correlates uptake and subsequent cytotoxicity of the bioconjugate. The ability to block uptake and toxicity with excess HA and with anti-CD44 mAb but not with excess CS confirms the receptor-mediated nature of the selective targeting and cytotoxicity. This further

substantiates the proposal that radionuclide-modified HA derivatives and HA-coupled prodrugs could be used to selectively target primary tumors and tumor metastases, provided that CS is preadministered to block "housekeeping" receptors in the liver without affecting specific HA receptors of tumor cells.^{58–61}

Confocal Microscope Images of Cellular Uptake of HA-Taxol Bioconjugate. An aliquot (1 μ L) of a 1 mg/mL aqueous stock solution in PBS buffer FITC-HA-Taxol was added to 100 μ L of cell culture media containing tumor cells grown on cover slips. Confocal images of FITC-HA-Taxol uptake by HBL-100 cells are presented in Figure 4. Initially, FITC-HA-Taxol can be seen on the cell membrane; over the course of several minutes, it is taken up into the cell and then gradually begins to accumulate in the nucleus. After 20 min, cells showed FITC-HA-Taxol in most subcellular compartments. The uptake of FITC-HA-Taxol into SK-OV-3 cells (Figure 5) and HCT-116 cells (not shown) occurred with a similar appearance and time course. Figure 5a provides a particularly dramatic illustration of the initial binding of the FITC-HA-Taxol to the cell surface prior to cellular uptake. These data confirm that HA binds readily to tumor cell surfaces and is rapidly endocytosed via HA receptor-mediated pathways. In addition, the data show that HA can act as a targeting polymer for solubilization and selective delivery of anticancer drugs to tumor cells. Importantly, nontransformed cells, such as the NIH 3T3 fibroblasts,

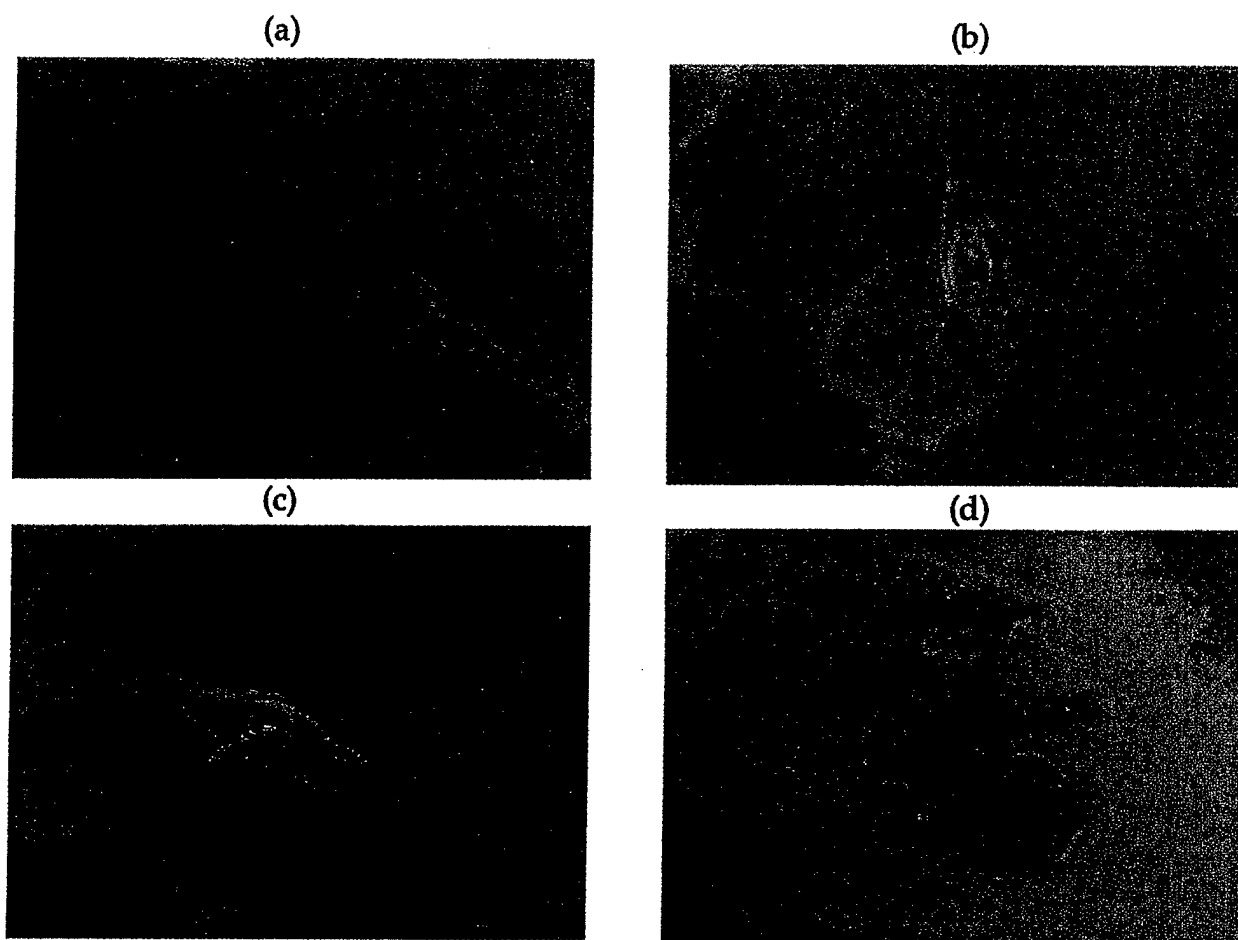


Figure 5. Binding and uptake of FITC–HA–Taxol by ovarian cancer SK-OV-3 cells. Panels a–c are confocal images indicating binding and uptake after 4 (a), 10 (b), and 20 min (c) of incubation. Panel d shows that preincubation with excess HA blocks the cellular uptake of FITC–HA–Taxol even at 20 min.

did not show this binding and rapid uptake of FITC–HA–Taxol in similar experiments (data not shown). Finally, the competition experiments show that the uptake of FITC–HA–Taxol conjugate by HBL-100 cells (Figure 4d) and SK-OV-3 cells (Figure 5d) could be blocked by preincubation of the cells with excess HA; in these images, fluorescence only accumulates outside cells. These results provide further support for the FACS experiments that the binding and cellular uptake of the HA bioconjugates are mediated through an HA-specific, receptor-mediated process.

Taxol Release from HA–Taxol Bioconjugate. Taxol release from HA–Taxol conjugate experiments was carried out in different media: cell culture media with or without cells, cell culture media with HASE (1 U/mL, 10 U/mL), esterase (0.1 U/mL, 1 U/mL), and human plasma. An HA–Taxol conjugate with composition of $(\text{HA})_{0.82}(\text{HA–ADH})_{0.03}(\text{HA–ADH–Taxol})_{0.15}$ was used for the drug release study. There are two possible cleavage sites (see Figure 1) that would result in the release of either free Taxol (ester hydrolysis) or Taxol 2'-hemisuccinate (hydrazide hydrolysis). SPE and LLE methods were introduced to extract Taxol and Taxol 2'-hemisuccinate standards from cell culture media. Table 1 shows that LLE is only suitable for the extraction of Taxol but gives poor recovery of Taxol 2'-hemisuccinate from cell culture media. In contrast, SPE showed reproducible and high recovery for both Taxol and Taxol 2'-

Table 1. Taxol and Taxol 2'-Hemisuccinate Recovery by Solid Phase Extraction (SPE) and Liquid–Liquid Extraction (LLE)

Taxol concn		Taxol 2'-hemisuccinate	
($\mu\text{g/mL}$)	recovery (%)	concn ($\mu\text{g/mL}$)	recovery (%)
Solid-Phase Extraction (SPE) Method			
10	101.4 ± 3.6	10	94.2 ± 4.5
5	95.3 ± 4.5	5	96.8 ± 3.0
1	96.4 ± 6.5	1	95.5 ± 3.2
Liquid-Liquid Extraction (LLE) Method			
10	90.2 ± 3.2	10	31.7 ± 2.0
5	102.8 ± 4.5	5	36.2 ± 1.3
1	102.0 ± 4.0	1	no detection

hemisuccinate. Thus, SPE was used as the extraction method of choice in the release study.

A 2- μL aliquot of the HA–Taxol stock solution (10 mg/mL in DMSO/H₂O = 1:1, v/v) was added to 200 μL of media and incubated at 5% CO₂ at 37 °C. Samples (crude extract) were removed at different time intervals and processed by standardized SPE protocols, and the released drug was quantified by HPLC using an internal standard. Figure 6a shows the HPLC separation of Taxol and Taxol 2'-hemisuccinate with cephalomannine as the internal standard. Figure 6b shows a typical analysis of extracted media. Figure 7a shows the time course of drug release from the bioconjugate (without added hydrolytic enzymes) in media and human plasma. HPLC analysis (Figure 6b) clearly demonstrated that

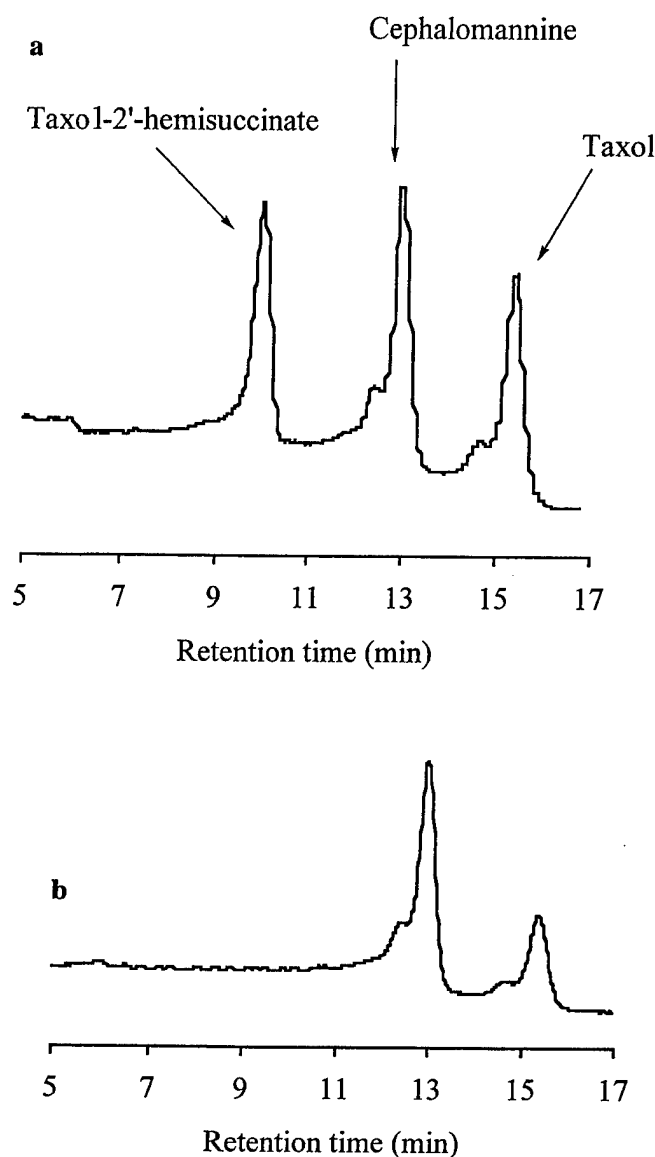


Figure 6. HPLC chromatograms of the separation of Taxol, Taxol 2'-hemisuccinate and cephalomannine. Panel a shows the separation of the standards; panel b illustrates the release of Taxol alone from HA-Taxol incubated with human plasma.

only Taxol was released from the HA-Taxol bioconjugate; no Taxol 2'-hemisuccinate was released under any of experimental conditions. This conforms with the expectation that the hydrazide linkage is much more hydrolytically stable than ester bond linkage. Moreover, the time course shows that HA-Taxol is quite long-lived in a hydrolase-free extracellular environment, with less than 20% of Taxol released from the bioconjugate during 24 h. Importantly, Taxol release rate from cell culture media with cells is similar to, or even lower than, that from cell culture media only. NIH 3T3 cells were employed for these experiments, since they did not internalize the HA-Taxol prodrug. Release from plasma was accordingly more rapid, since plasma contains a variety of endogenous hydrolytic enzymes.

Similar biphasic release rate profiles were obtained with enzyme-catalyzed drug release from HPMA-drug conjugates employing biodegradable oligopeptide spacers.⁶² In these cases, the solution behavior of polymer-drug conjugate may differ from that of the polymeric carrier when a hydrophilic

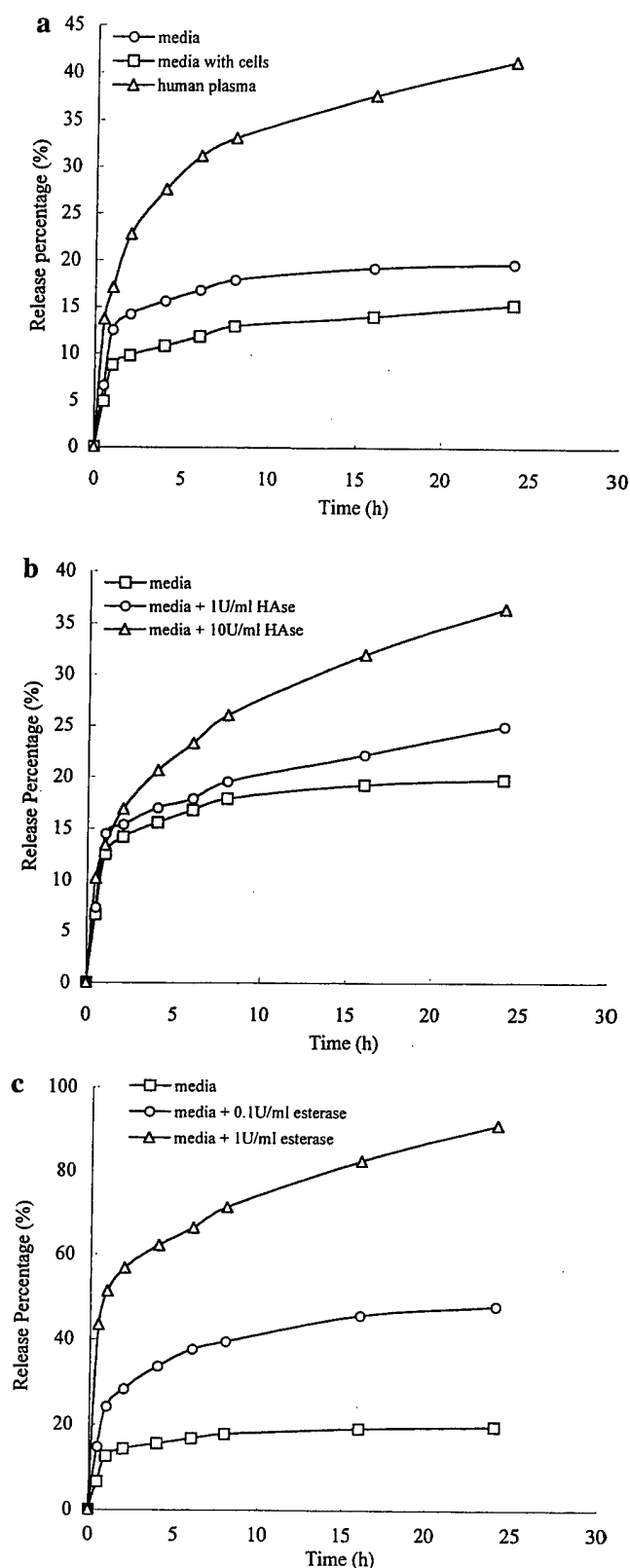


Figure 7. In vitro free Taxol release from HA-Taxol. Panel a shows release in cell culture media under cell-free conditions (○), with NIH 3T3 cells (□), and from incubation with human plasma (Δ). Panel b shows release from cell culture media in the presence of testicular Hase. Panel c shows release of drug from cell culture media with added porcine esterase.

polymeric carrier contains hydrophobic drug molecules on the side chain. Polymeric drugs containing a hydrophobic active component often aggregate due to intermolecular hydrophobic interactions. The formation of such hydrophobic

aggregates impedes formation of the enzyme–substrate complex and thus becomes an important factor in the drug release rate from the side chain of polymer–drug conjugate. Moreover, the formation of aggregates may in turn affect the accessibility of various compartments in the living organism and also the rate of release of the active drug following the entry of the polymer–drug conjugate into the target cells.

Figure 7b shows the drug release in cell culture media to which Hase (1 and 10 U/mL) was added. At the lower enzyme level, the Taxol release rate is only slightly increased over that in the Hase-free media. In contrast, the Taxol release rate increased sharply in the presence of even very modest amounts of esterase (Figure 7c). Extremely rapid release was observed in the 1 U/mL esterase experiment. Indeed, the Taxol release rate in the presence of esterase was similar to that found in human plasma. In summary, the HA–Taxol prodrug released only free Taxol, and the presence of esterase dramatically accelerated Taxol release from the bioconjugate. We conclude that following receptor-mediated cellular uptake of the HA–Taxol bioconjugate, free Taxol drug is released from the polymeric prodrug by intracellular enzymatic hydrolysis, thereby delivering the toxic agent inside the cell and disrupting mitosis leading to cell death.

In Vitro Selective Cytotoxicity. Further determinations of the cytotoxicity of HA–Taxol were performed using a 96-well plate format in quadruplicate with increasing doses ranging from 0.001 to 100 $\mu\text{g/mL}$. The cytotoxicity of HA–Taxol conjugates was studied using the MTT assay to identify cells still active in respiration.⁴⁸ In our previous experiments,²³ HA–Taxol conjugates were selective cytotoxins, killing HBL-100, SK-OV-3, and HCT-116 cells but sparing NIH 3T3 fibroblast cells at concentrations up to 10 $\mu\text{g/mL}$ of Taxol equivalents. The FITC–HA–Taxol binding and uptake results reported in this study indicate that selective cytotoxicity of HA–Taxol is due to receptor-mediated events. The in vitro cytotoxicity data confirm the selective toxicity of HA–Taxol toward different cell lines, and the known overexpression of CD44 by HBL-100³⁹ and SK-OV-3 cells⁴⁰ suggests that this selective toxicity is due to receptor-mediated binding and uptake of the HA–Taxol.

Competition experiments in which preincubation with HA protected susceptible cancer cells from the cytotoxicity of HA–Taxol strengthened this conclusion. Thus, HA–Taxol (5% loading) was employed over a 10-fold dosage range. Figure 8a summarizes the results obtained using a 100-fold excess of HA as the competitor. Simultaneous addition of HA with either Taxol or with HA–Taxol to the cells produced only modest protection against cytotoxicity of the polymeric prodrug. However, a significant reduction in cytotoxicity of the HA–Taxol was observed when cells were preincubated for 2 h with excess HA prior to the addition of HA–Taxol conjugate. Figure 8b shows that excess CS did not reduce cytotoxicity of prodrug or free Taxol under any of the conditions, thus indicating that there was no reduction in the uptake of the HA–Taxol by the HBL-100 cells. Analogous results were obtained with this prodrug conjugate with SK-OV-3 cells and HCT-116 cells (not shown). Thus,

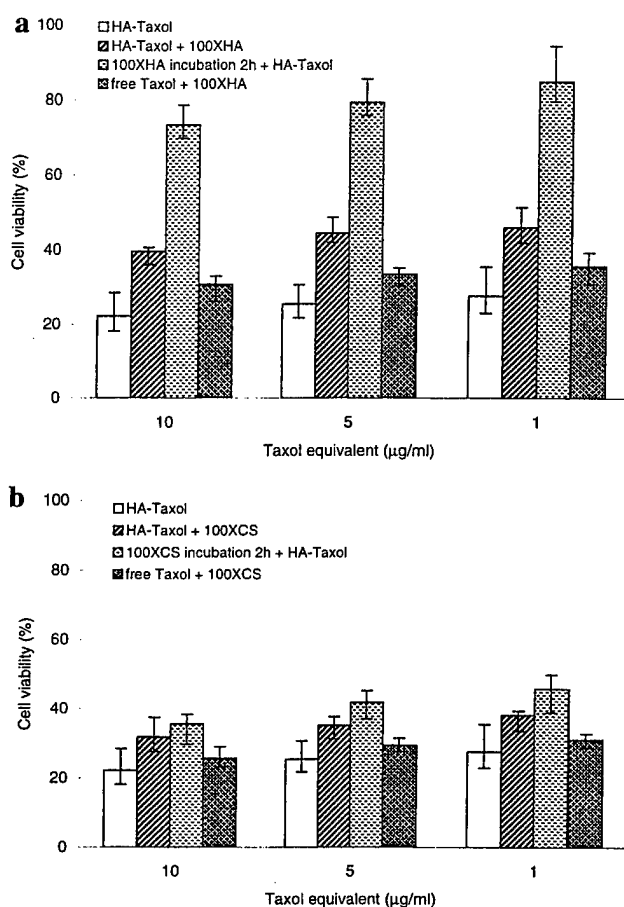


Figure 8. In vitro cytotoxicity of HA–Taxol with 5% Taxol loading against HBL-100 human breast cancer cells with excess HA (panel a) or CS (panel b) as competitors. Key: HA–Taxol only (open bars); HA–Taxol with either 100-fold excess of either HA or CS (diagonal lines); preincubation with 100-fold excess of either HA or CS, for 2 h, then additional HA–Taxol (speckled); free Taxol, plus 100-fold excess of either HA or (crosshatched).

at a 15% Taxol loading for the HA–Taxol prodrug, preincubation with HA, but not with CS, caused competitive displacement.

These data confirm the FACS and confocal microscopy results that HA–Taxol conjugate must enter the tumor cells through an HA-receptor-mediated process. Apparently, binding and uptake are not readily blocked when HA and HA–Taxol are premixed. Our previous experiments²³ showed that uptake of chemically modified HA was very rapid. Thus, effective competition and reduction of HA–Taxol uptake seem to require preincubation of the cells with HA to presaturate the receptor-mediated uptake system. This phenomenon can be rationalized in two ways. First, it is possible that the high molecular weight HA used for the competition experiments may bind with slower kinetics than the LMW HA–Taxol. Conversely, the receptor clustering that occurs in response to multivalent binding of HA to receptors provides a very effective block of the endocytotic pathway. An alternative explanation is that the attachment of multiple hydrophobic Taxol molecules to HA on flexible tethers provides the opportunity for multivalent insertion into the lipid bilayer, with receptor-mediated endocytosis occurring subsequently. In this case, HA would be ineffective in preventing this initial hydrophobic-type association. Once the HA–Taxol was immobilized on the membrane, two-

dimensional migration and receptor-mediated uptake would be entropically favored.

In conclusion, the data reported herein indicate that the cytotoxicity of HA-Taxol requires cellular uptake of the bioconjugate followed by hydrolytic release of the active Taxol by cleavage of the labile 2' ester linkage. Targeting of a variety of anticancer agents to tumor cells and tumor metastases could be achieved by receptor-mediated uptake of an HA-anticancer agent conjugate, followed by the intracellular release of the active drug and subsequent cell death. The ability to "seek and destroy" micrometastases is one of the most compelling and attractive potential outcomes for the HA-antitumor bioconjugates.

Acknowledgment. Financial support for this work was provided by Department of Army (DAMD 17-9A-1-8254) and by the Huntsman Cancer Foundation at The University of Utah (UUtah). We are grateful to D. Schmehl and Dr. L. R. Barrows (UUtah) for assistance with cell cytotoxicity experiments, Dr. W. G. Pitt (Brigham Young University, Provo, UT) for assistance with confocal microscopy, and D. Augello and Dr. W. F. Green for assistance with FACS experiments (Flow Cytometry Facility, UUtah). We thank Dr. L. Y.-W. Bourguignon (University of Miami Medical School, Miami, FL) for providing HBL-100 and SK-OV-3 cells. We are grateful to Clear Solutions Biotechnology, Inc. (Stony Brook, NY), for providing HA and the Center for Cell Signaling (UUtah) for equipment and facilities.

References and Notes

- Kim, K. H.; Hirano, T.; Ohashi, S. In *Polymeric Materials Encyclopedia*; Salamone, J. C., Ed.; CRC Press: Boca Raton, FL, 1996; pp 272-285.
- Trouet, A.; Masquelier, M.; Baurain, R.; Campeneere, D. D. *Proc. Natl. Acad. Sci. U.S.A.* **1982**, *79*, 626-629.
- Kim, S. *Drugs* **1993**, *46*, 618-638.
- Arshady, R. *J. Controlled Release* **1990**, *14*, 111-131.
- Kreuter, J. *J. Controlled Release* **1991**, *16*, 169-176.
- Waser, P. G.; Kreuter, J.; Berger, S.; Munz, K.; Kaiser, E.; Pfluger, B. *Int. J. Pharm.* **1987**, *39*, 213-227.
- Cartledge, S. A.; Duncan, R.; Lloyd, J. B.; Kopeckova, R. P.; Kopecek, J. *J. Controlled Release* **1987**, *4*, 265-278.
- Molteni, L. In *Drugs Carriers in Biology and Medicine*; Gregoriadis, G., Ed.; Academic: London, 1979; p 107.
- Molteni, L. In *Drugs Carriers in Biology and Medicine*; Gregoriadis, G., Ed.; Academic Press: London, 1979; p 43.
- Greenwald, R. B.; Gilbert, C. W.; Pendri, A.; Conover, C. D.; Xia, J.; Martinez, A. *J. Med. Chem.* **1996**, *39*, 424-431.
- Maeda, H.; Seymour, L.; Miyamoto, Y. *Bioconjugate Chem.* **1992**, *3*, 351-362.
- Minko, T.; Kopeckova, P.; Pozharov, V.; Kopecek, J. *J. Controlled Release* **1998**, *54*, 223-233.
- Hirano, T.; Ohashi, S.; Morimoto, S.; Tsuda, K. *Makromol. Chem.* **1986**, *187*, 2815-2824.
- Laurent, T. C.; Laurent, U. B. G.; Fraser, J. R. E. *Ann. Rheum. Dis.* **1995**, *54*, 429-432.
- Vercruysse, K. P.; Prestwich, G. D. *Crit. Rev. Ther. Drug Carrier Syst.* **1998**, *15*, 513-555.
- Prestwich, G. D.; Marecak, D. M.; Marecek, J. F.; Vercruysse, K. P.; Ziebell, M. R. In *The Chemistry, Biology, and Medical Applications of Hyaluronan and its Derivatives*; Laurent, T. C., Ed.; Portland Press: London, 1998; pp 43-65.
- Freed, L. E.; Vunjak-Novakovic, G.; Biron, R. J.; Eagles, D. B.; Lesnoy, D. C.; Barlow, S. K.; Langer, R. *Bio/Technology* **1994**, *12*, 689-693.
- Prestwich, G. D.; Luo, Y.; Ziebell, M. R.; Vercruysse, K. P.; Kirker, K. R.; MacMaster, J. S. In *New Frontiers in Medical Sciences: Redefining Hyaluronan*; Abatangelo, G., Ed.; Portland Press: London, 1997; p 60.
- Alam, C. A. S.; Seed, M. P.; Willoughby, D. A. *J. Pharm. Pharmacol.* **1995**, *47*, 407-411.
- Falk, R. E. PCT Int. Appl. WO 9740841, 1997.
- Ziegler, J. *J. Natl. Cancer Inst.* **1996**, *88*, 397-399.
- Akima, K.; Ito, H.; Iwata, Y.; Matsuo, K.; Watari, N.; Yanagi, M.; Hagi, H.; Oshima, K.; Yagita, A.; Atomi, Y.; Tatekawa, I. *J. Drug Targeting* **1996**, *4*, 1.
- Luo, Y.; Prestwich, G. D. *Bioconjugate Chem.* **1999**, *10*, 755-763.
- Turley, E. A.; Belch, A. J.; Poppema, S.; Pilarski, L. M. *Blood* **1993**, *81*, 446-453.
- Toole, B. P. *J. Intern. Med.* **1997**, *242*, 35-40.
- Rudzki, Z.; Jothy, S. *J. Clin. Pathol. Mol. Pathol.* **1997**, *50*, 57-71.
- Lesley, J.; Hyman, R.; English, N.; Catterall, J. B.; Turner, G. A. *Glycoconjugate J.* **1997**, *14*, 611-622.
- Underhill, C. *J. Cell Sci.* **1992**, *103*, 293-298.
- Turley, E. A. In *The Biology of Hyaluronan*; CIBA Foundation, Ed.; J. Wiley & Sons: Ltd.: Chichester, U.K., 1989; pp 121-137.
- Knudson, C. B.; Knudson, W. *FASEB J.* **1993**, *7*, 1233-1241.
- Entwistle, J.; Hall, C. L.; Turley, E. A. *J. Cell Biochem.* **1996**, *61*, 569-577.
- Day, A. *J. Biochem. Soc. Trans.* **1999**, *27*, 115-121.
- Yeo, T. K.; Nagy, J. A.; Yeo, K. T.; Dvorak, H. F.; Toole, B. P. *Am. J. Pathol.* **1996**, *148*, 1733-1740.
- Knudson, W. *Am. J. Pathol.* **1996**, *148*, 1721-1726.
- Hall, C. L.; Yang, B. H.; Yang, X. W.; Zhang, S. W.; Turley, M.; Samuel, S.; Lange, L. A.; Wang, C.; Curpen, G. D.; Savani, R. C.; Greenberg, A. H.; Turley, E. A. *Cell* **1995**, *82*, 19-28.
- Nelson, R. M.; Venot, A.; Bevilacqua, M. P.; Linhardt, R. J.; Stamenkovic, I. *Annu. Rev. Cell Dev. Biol.* **1995**, *11*, 601-631.
- Rooney, P.; Kumar, S.; Ponting, J.; Wang, M. *Int. J. Cancer* **1995**, *60*, 632-636.
- Hua, Q.; Knudson, C. B.; Knudson, W. *J. Cell Sci.* **1993**, *106*, 365-375.
- Iida, N.; Bourguignon, L. Y.-W. *J. Cell. Physiol.* **1997**, *171*, 152-160.
- Bourguignon, L. Y.-W.; Zhu, H. B.; Chu, A.; Iida, N.; Zhang, L.; Hung, M. C. *J. Biol. Chem.* **1997**, *272*, 27913-27918.
- Culty, M.; Nguyen, H. A.; Underhill, C. B. *J. Cell Biol.* **1992**, *116*, 1055-1062.
- Culty, M.; Shizari, M.; Thompson, E. W.; Underhill, C. B. *J. Cell. Physiol.* **1994**, *160*, 275-286.
- Prestwich, G. D.; Marecak, D. M.; Marecek, J. F.; Vercruysse, K. P.; Ziebell, M. R. *J. Controlled Release* **1998**, *54*, 93-103.
- Lesley, J.; Kincade, P. W.; Hyman, R. *Eur. J. Immunol.* **1993**, *23*, 1902-1909.
- Li, C.; Yu, D.; Newman, R. A.; Cabral, F.; Stephens, L. C.; Hunter, N.; Milas, L.; Wallace, S. *Cancer Res.* **1998**, *58*, 2404-2409.
- Pouyani, T.; Prestwich, G. D. *Bioconjugate Chem.* **1994**, *5*, 339-347.
- Pouyani, T.; Prestwich, G. D. US Patent 5,616,568; Research Foundation of SUNY, USA, 1997.
- Kokoshka, J. M.; Ireland, C. M.; Barrows, L. R. *J. Natl. Prod.* **1996**, *59*, 1179-1182.
- Kreil, G. *Protein Sci.* **1995**, *4*, 1666-1669.
- Li, C.; Newman, R. A.; Wallace, S. *Sci. Med.* **1999**, *38*-47.
- Collis, L.; Hall, C.; Lange, L.; Ziebell, M.; Prestwich, G.; Turley, E. *FEBS Lett.* **1998**, *440*, 444-449.
- Chow, G.; Knudson, C. B.; Homandberg, G.; Knudson, W. *J. Biol. Chem.* **1995**, *270*, 27734-27741.
- Lesley, J.; Hyman, R. *Eur. J. Immunol.* **1992**, *22*, 2719-2723.
- Lesley, J.; English, N.; Perschl, A.; Gregoroff, J.; Hyman, R. *J. Exp. Med.* **1995**, *182*, 431-437.
- Perschl, A.; Lesley, J.; English, N.; Trowbridge, I.; Hyman, R. *Eur. J. Immunol.* **1995**, *25*, 495-501.
- Asplund, T.; Heldin, P. *Cancer Res.* **1994**, *54*, 4516-4523.
- Nakabayashi, H.; Tsujii, H.; Okamoto, Y.; Nakano, H. *Int. Hepatol. Commun.* **1996**, *5*, 345-353.
- Gustafson, S.; Bjorkman, T. *Glycoconjugate J.* **1997**, *14*, 561-568.
- Samuelsson, C.; Gustafson, S. *Glycoconjugate J.* **1998**, *15*, 169-175.
- Gustafson, S.; Bjorkman, T.; Westlin, J. E. *Glycoconjugate J.* **1994**, *11*, 608-613.
- Gustafson, S. In *The Chemistry, Biology, and Medical Applications of Hyaluronan and its Derivatives*; Laurent, T. C.; Balazs, E. A. Eds.; Portland Press: London, U.K., 1997.
- Ulbrich, K.; Konak, C.; Tuzar, Z.; Kopecek, J. *Makromol. Chem.* **1987**, *188*, 1261-1272.

MODIFICATION OF NATURAL POLYMERS: HYALURONIC ACID

Yi Luo, Kelly R. Kirker, and Glenn D. Prestwich

Hyaluronic acid (HA) is an abundant nonsulfated glycosaminoglycan component of synovial fluid and the extracellular matrix. A combination of unique physicochemical properties and biological functions suggest HA as an attractive building block for new biocompatible and biointeractive materials with applications in drug delivery, tissue engineering, and viscosupplementation. This chapter highlights the chemical modification of HA and medical applications of these HA-based biomaterials. Important new products have already reached the marketplace, the approval and introduction of an increasing number of medical devices and new drugs using HA-derived biomaterials can be anticipated in the next decade.

INTRODUCTION

Hyaluronic acid (hyaluronan, HA) is a naturally occurring polysaccharide consisting of 200–10,000 repeating disaccharide units. It is composed of (β -1,4)-linked D-glucuronic acid and (β -1,3)-N-acetyl-D-glucosamine (Fig. 45.1) and has a molecular weight ranging from 1×10^5 to 5×10^6 Da. HA is an abundant glycosaminoglycan (GAG) found in the extracellular matrix (ECM) of all higher animals, and it is the only nonsulfated GAG. HA forms highly viscous aqueous solutions and takes on an expanded random coil structure as a result of strong hydrogen bonding. The coiled structure of HA can trap approximately 1000 times its weight in water. These characteristics give it unique physicochemical properties as well as distinctive biological functions [1]. HA has been implicated in the water homeostasis of tissues, in the regulation of permeability of other substances by steric exclusion phenomena, and in the lubrication of joints [2]. HA plays an important role in the structure and organization of the ECM, including the maintenance of extracellular space, the transport of ion solutes and nutrients, and the preservation of tissue hydration. HA concentrations increase whenever rapid tissue proliferation regeneration and repair occur.

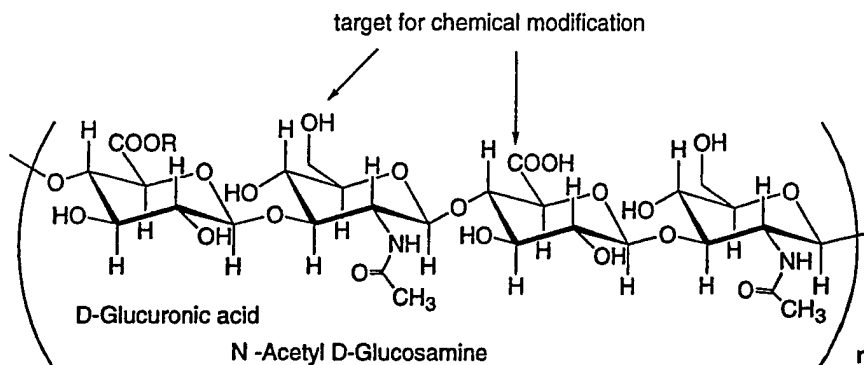
HA also binds specifically to proteins in the ECM, on cell surface receptors, and within the cell cytosol. These protein–ligand interactions are important in stabilizing the cartilage ECM [2,3], regulating cell adhesion and motility [4,5], mediating proliferation and differentiation [6], and in the action of growth factors [7]. HA has also been implicated in morphogenesis and embryonic development [8], in cancer [9–15], in modulating inflammation [13], in stimulating angiogenesis and healing [16], and as a protective coating [17]. In most situations, HA signaling occurs via cell surface receptors, such as CD44 and RHAMM, but cytosolic and nuclear proteins are also implicated in signaling.

The actions of HA appear to be related to molecular size. For example, high molecular weight HA inhibits angiogenesis, while low molecular weight HA stimulates angiogenesis [18]. At a molecular level, HA can act as a scavenger molecule for oxygen-derived toxic free radical species [18]. This unique suite of properties makes HA an attractive building

(Note - change also
header and
Kirker Table of
Contents)

present
aw. present?
(i.e. 2000-2010)

Fig. 45.1. Tetrasaccharide fragment of HA showing the disaccharide repeat units ($R = H$).



block for new biocompatible and biointeractive materials that have medical applications in drug delivery, tissue engineering, and viscosupplementation [19]. This chapter highlights the chemistry and medical applications of these HA-based biomaterials.

→ Approved uses for highly purified HA greatly increased in the ~~1990s~~ surgery, drug delivery, and cosmetics [20]. The unique rheological properties of high molecular weight HA ($>1 \times 10^6$ Da) are exploited in clinical treatment of osteoarthritis [21,22] and in ophthalmic surgery. HA has shown beneficial properties in corneal transplantation, intraocular lens implantation, and the treatment of cataracts, vitreoretinal diseases, and tympanic membrane perforations. In addition, HA solutions have been investigated as space-filling substances in laryngeal augmentation, such as vocal fold injection, and are in clinical use for urinary incontinence in women and in pediatric urology for the treatment of vesicourethral reflux [23]. HA injections also facilitate nerve growth [24], and topical HA can improve wound healing. High levels of high molecular weight HA or of an HA-sucrose formulation can enhance the healing of wounds in collagen-containing tissues, including skin, bone, and mucosa, with limited scarring [16,25]. In addition, HA is used as an adjuvant for ophthalmic drug delivery [26] and can enhance the absorption of drugs and proteins via mucosal tissues [27–29]. The rapid skin permeability and epidermal retention of HA prolongs the pharmacokinetic half-life of topically delivered drugs and growth factors [30].

However, the poor biomechanical properties of this soluble, natural polymer currently preclude many direct applications in medicine. Thus, to obtain more mechanically and chemically robust materials, it has become necessary to chemically modify natural HA. The resulting HA derivatives have physicochemical properties that are significantly different from those of the native polymer but maintain the biocompatibility and biodegradability, as well as the potential pharmacological and therapeutic properties, of HA itself. This chapter explores the chemical modification of HA (several architectures are shown in Fig. 45.2) and the potential uses of these biomaterials in tissue engineering and drug delivery.

CHEMICAL MODIFICATIONS

MODIFICATION OF THE HA CARBOXYL GROUP

Modification of HA by Esterification

Fidia Advanced Biopolymers (Abano Terme, Padua, Italy) manufactures a number of HA-derivatized materials collectively called HYAFF ($R = \text{alkyl group}$, Fig. 45.1). The HYAFF materials [31] are prepared by alkylation of the tetrabutylammonium salt of HA with an alkyl halide in dimethyl formamide (DMF) solution. At higher percentages of esterification, solubility in water is reduced. HYAFF materials can be extruded to produce membranes and fibers, lyophilized to obtain sponges, or treated by spray-drying, extraction, and evaporation to produce microspheres. These polymers show good mechanical strength when dry, but the hydrated materials are less robust [32].

The biocompatibility and biodegradability of the HYAFF materials have been studied extensively. The degree of esterification influences the size of hydrophobic patches, which produces a polymer chain network that is more rigid and stable, and less susceptible to enzymatic degradation [33,34]. Drug release from HYAFF-based devices was examined for entrapped or covalently attached molecules. For example, release of the steroids hydrocort-

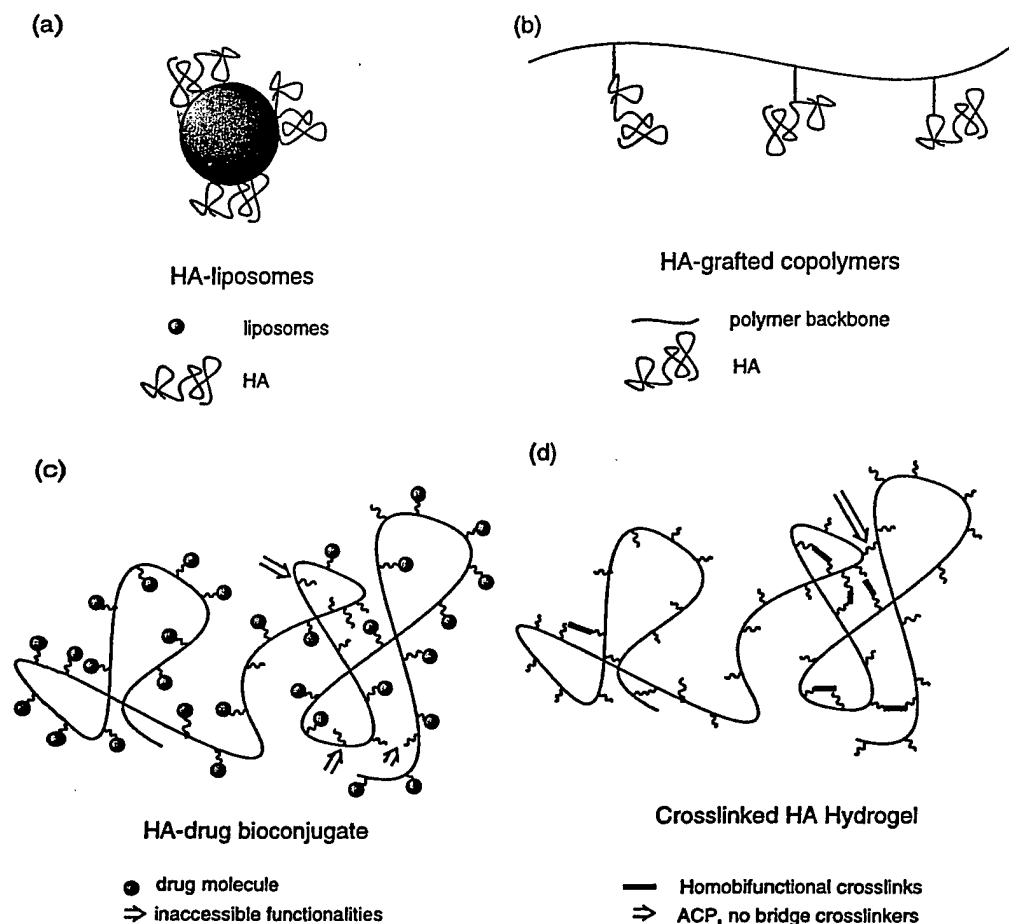


Fig. 45.2. Schematic structure of HA derivatives: (a) HA-liposome composite, (b) HA-grafted copolymer, (c) HA-drug bioconjugate, and (d) cross-linked HA.

tisone and α -methylprednisolone from microspheres fabricated from different HYAFF materials was examined with the drug either dispersed or bound to the polymer. While the hydrocortisone diffused out of the microspheres in 10 min, the release rate of the covalently bound drug was found to show zero-order release, requiring more than 100 h, consistent with ester bond hydrolysis [31,35]. Preclinical *in vivo* evaluations in a rabbit animal model demonstrated that an α -methylprednisolone carried by a HYAFF 11 formulation could maintain its anti-inflammatory and chondroprotective properties [36] and increase the residence time of the drug in the tear fluid [37,38]. Microspheres and thin films of HYAFF 11 have been found to be the most suitable physical forms for drug delivery systems.

Studies of macromolecule diffusion and release suggested a possible use of HYAFF 11 microspheres for peptide delivery. Furthermore, the mucoadhesive properties of HYAFF materials make realistic drug delivery via nasal, oral, and vaginal mucosal routes—for examples intranasal delivery of insulin in sheep [39] and vaginal delivery of calcitonin in rats [40,41] and flu vaccine in rodents [42]. Microspheres could also deliver recombinant human granulocyte-macrophage colony-stimulating factor (huGM-CSF) [43].

HA plays fundamental roles during embryonic development [44–46] and wound healing [47,48], suggesting a use for HA derivatives to create a suitable environment for the growth of cells derived from organ biopsy samples. In particular, stem elements or adults cells can be stimulated to divide and differentiate in this embryo-like environment [49,50]. HYAFF products also have water and vapor transport properties similar to those of commercial products for wound coverage, such as Bioprocess, Biobrane II [a composite of poly(dimethylsiloxane) on nylon fabric], and OpSite (polyurethane dressing with an adhesive layer of vinyl ether applied to one side).

The cultivation of fibroblasts in ECM-like structures is receiving widespread attention not only because of the need to provide a dermal substitute to epithelial sheets, but also because these living constructs may be applied in other pathologies such as ligament/tendon

aw: OK?
 (OK) → tests

repair, vascular prosthesis, and dermal augmentation. As expected, cultured human fibroblasts actively proliferated in 30 days until the degradation of HYAFF 11 nonwoven mesh commenced, and morphological ~~test~~ on paraffin-embedded specimens demonstrated that cells migrated through the nonwoven mesh and populated both sides of the biomaterial. Furthermore, immunohistochemical analysis revealed the presence of collagen I, III, and fibronectin fibers, which were evident after only 15 days of culture in the HYAFF 11 scaffold, and allowed preparation of a living dermal equivalent [51]. *In vitro* studies of Laserskin membranes, which are produced with regular laser-made microperforations from HYAFF 11, showed that keratinocytes grew on these membranes and expressed a proliferative phenotype within the microperforations. The epithelial cells cultured on the membranes were able to differentiate, and after 15 days of standard culture, the investigators observed the formation of several distinct layers—starting from a basal proliferative through an upper keratinized zone [52–54]. A three-dimensional (3D) artificial skin [55] was developed for the treatment of second- and third-degree burns, chronic wounds such as larger phlebotrophic ulcers [52,56], and diabetic foot ulcers [57]. In clinical trials on extensive burns of humans, the underlying wound bed of this 3D scaffold-treated area showed evidence of new collagen synthesis and organization into dermislike structure. The wounds were completely healed 7 weeks after burn excision, with no unusual scarring [58].

In vitro culture of chondrocytes on a HYAFF 11 nonwoven mesh was investigated in tissue engineering procedures for cartilage reconstruction. One month after subcutaneous implantation of the scaffold seeded with human chondrocytes in an athymic nude mouse model, the development of tissue similar to hyaline cartilage was observed [59]. Moreover, pluripotent mesenchymal stem cells, which are capable of giving rise to differentiated elements of several kinds (myoblasts, chondroblasts, osteoblasts, adipocytes, fibroblasts), could be cultured within a HYAFF scaffold. The mesenchymal cells within the scaffold could be induced toward a chondrocyte phenotype with the addition of basic fibroblast growth factor (bFGF) [60–62]. Similarly, culture-expanded bone marrow derived mesenchymal progenitor cells differentiate into chondrocytes or osteoblasts implanted subcutaneously *in vivo* in combination with a HYAFF 11 sponge as well as when porous calcium phosphate ceramic is used as the delivery vehicle. When coated with fibronectin, HYAFF 11 sponge bound 130% more cells than coated ceramics, which indicates the HA-based delivery vehicles are superior to porous calcium ceramic. Additionally, the HA-based vehicles have the advantage of degradation/resorption characteristics that allow complete replacement of the implant with newly formed tissue [63].

Modification of HA with Hydrazides, Amines, and Carbodiimides

The chemical modification of HA by means of its carboxylic functions, hydrazides, and carbodiimide compounds has been studied in great detail [64,65]. The modification of HA with hydrazides is performed in water at pH 4.75, with continuous addition of aqueous HCl to maintain the mild acidic pH. Although the carbodiimide reaction fails to give efficient coupling to amines, the high levels of O- to N-acyl migration gave N-acylureas with potentially important medical uses, as discussed later [66–68]. Alternatively, carbodiimide-mediated coupling to dihydrazide compounds such as adipic dihydrazide (ADH) provided an efficient and mild route for the introduction of multiple pendant hydrazide groups for further derivatization with drugs [69], for making biochemical probes [70], or for cross-linking [67,71]. For example, HA–Taxol bioconjugates were synthesized by the conjugation of HA–ADH and ester-activated Taxol. The conjugate showed selective binding and uptake by human breast cancer cells, human ovarian cancer cells, and human colon tumor cells. Increased cytotoxicity required cellular uptake of the conjugate followed by hydrolytic release of the active free Taxol [72,73]. Targeting can be accomplished by receptor-mediated uptake of the HA–drug bioconjugate that releases the drug only inside the target cell, thereby enhancing selectivity for cancerous cells [72].

As indicated earlier, attempted carbodiimide-mediated coupling of primary amines to HA, to generate polymeric amides, resulted in negligible coupling because of the protonation of the required nucleophilic nitrogen at the reaction pH. In 1999 a modified

method was developed for the coupling of polyfunctional amines to HA through mediation of carbodiimide-active ester [74]. HA ($M_w > 1$ MDa) was reacted with 30-fold excess of the amine component at pH 6.8 in the presence of a soluble carbodiimide and 1-hydroxybenzotriazole (HOBt) with DMSO/H₂O (1:1) as solvent.

Many HA-drug bioconjugates have been prepared by using the method of carbodiimide activation. HA-mitomycin C and HA-epirubicin conjugates were synthesized and found to enhance the selective delivery of the parent antitumor drugs into regional lymph nodes and cancerous tissues through HA receptor CD44 [75]. Mitomycin C was coupled to HA (1200 kDa) through an amide bond in a DMF-water cosolvent with a water-soluble carbodiimide (EDCI) as the coupling agent. The HA-mitomycin C conjugate exhibited potent antimetastatic effects against Lewis lung carcinoma xenograft at an extremely low dose (0.01 mg/kg), whereas free mitomycin C had no effect. Similarly, adriamycin was reported to couple to HA through an amide bond linkage [76]. Epirubicin was coupled to HA after the synthesis of acetylated HA to increase its solubility in organic solvents. Similarly, daunomycin, 5-fluorouracil, and cytosine arabinoside have been coupled to HA. The same carbodiimide technology was applied to prepare HA-superoxide dismutase (HA-SOD) conjugate, which was synthesized by a water-soluble carbodiimide coupling of HA and bovine Cu/Zn-SOD or bacterial Mn-SOD at pH 4.8 and 4°C for 20 h. Some 20% of the amino groups on SOD were conjugated to HA, and the HA-SOD conjugate exhibited a more pronounced anti-inflammatory effect than SOD or HA alone [77].

MODIFICATION OF THE HA HYDROXYL GROUPS

Modification of HA by Sulfation

HA is an ideal hydrophilic coating for a variety of medical devices, including catheters, guide wires, and sensors. Various *in vitro* and *in vivo* tests have been conducted over the years by Biocoat Inc. (Fort Washington, PA) to demonstrate biocompatibility of the HA coating Hydak. However, to obtain the optimum blood-compatible material for use in the body, approaches were devised for sulfating the OH group present in the HA molecule.

The sulfation of HA (M_w 150–200 kDa) with sulfur trioxide pyridine complex in DMF produced different degrees of sulfation, HyalS_x, $x = 1-4$ [78]. The sulfated hyaluronic acid HyalS_{3,5} was then immobilized onto plasma-processed polyethylene (PE) by using a diamine poly(ethylene glycol) derivative and a water-soluble carbodiimide. The thrombin time test and platelet adhesion behavior indicated that this procedure was promising for the preparation of blood-compatible, antithrombotic PE surface [79,80]. In addition, the anticoagulant polysaccharide was photoimmobilized on a poly(ethylene terephthalate) (PET) film [81]. Sulfated HA (HyalS_x) was conjugated with azidoaniline in the presence of a water-soluble carbodiimide to prepare azidophenylamino-derivatized HyalS_x. The derivative was dried on a PET surface before UV irradiation. A micropatterning profile of the anticoagulant polysaccharides was achieved with photolithography, and platelet adhesion was reduced on the sulfated hyaluronic acid areas. Surfaces coated with sulfated HA exhibited a marked reduction of cellular attachment, fouling, and bacterial growth compared with uncoated surfaces [82]. The coating was stable to degradation by chondroitinase and hyaluronidase and acquired new antithrombogenic properties [83].

Other Chemistries

Several other modifications have been accomplished with the hydroxyl groups in the HA molecule. Butyric acid, which is known to induce cell differentiation and to inhibit the growth of a variety of human tumors, was conjugated to HA [84] via the reaction between butyric anhydride and HA (M_w 85 kDa) *sym*-collidinium salt, in the presence of pyridine or dimethylaminopyridine, with DMF as solvent, at room temperature for 24 h. The results of cell culture on a human breast cancer cell line (MCF-7) suggested that the conjugation of butyrate residue to HA led to an increased half-life of the active component. In addition, HA butyrate offered a novel drug delivery system targeted specifically at tumor cells.

The anthracycline antibiotics adriamycin and daunomycin were coupled to HA via cyanogen bromide (CNBr) activation [76]. This reaction scheme is purported to lead to

the attachment of the drug via a urethane bond to one of the hydroxylic functions of the polysaccharide, but no spectroscopic verification was provided.

A wider utilization of HA biomaterials can be envisaged if two obstacles can be overcome: enzymatic degradation and poor mechanical properties. Approaches to solving the first problem are based on the formation of chemically modified HA sols and hydrogels. Approaches to the second problem include the preparation of HA composite materials by grafting of other polymers or by formation of interpenetrating networks.

MODIFICATION OF HA HYDROGEL FORMATION

HA can be readily degraded by tissue hyaluronidases and free radicals, which commonly occur during inflammation. A small number of breaks in the molecular structure can result in a profound decrease in its molecular size, resulting in drastic alterations in viscosity. Currently, several cross-linking chemistries are being investigated to improve the stability of HA toward biodegradation.

Auto-Cross-Linked Polymer

Auto-cross-linked polymer (ACP, Fidia) consists of inter- and intramolecularly esterified HA (200 kDa) in which both the carboxyl groups and hydroxyl groups belong to HA molecules. ACP is a white powder and, upon hydration with water, gives rise to a transparent gel [85]. This novel biomaterial has shown promising results for several applications. For example, it can be used as a barrier between organs to reduce postoperative adhesions after abdominal and gynecological surgery [86–88]. In addition, the biocompatible, biodegradable, porous ACP behaves as a scaffolding for reparative cells to regenerate and to integrate when it is placed in natural reparative tissue defects, such as osteochondral defects in a rabbit knee model [89]. Subcutaneous implantation of ACP porous sponges seeded with chondrocytes or osteoblasts were found to regenerate bone and cartilage [63,90].

HA Cross-Linked with Diepoxide Cross-Linkers

Laurent and colleagues [91] cross-linked high concentration HA (average molecular mass 1.5 MDa, 50–175 mg/ml) in an alkaline environment with 1,2,3,4-diepoxibutane and sodium borohydride (50°C, 2 h). Using similar chemistry, HA (average molecular mass 870 kDa) at high concentration was allowed to react with either ethylene glycol diglycidyl ether [92] or polyglycerol poly(glycidyl ether) [93] in 0.1 N NaOH at 60°C with ethanol as a cosolvent. The gels obtained had a high water content (95%) even though high concentrations of cross-linker had been used. This HA gel was specifically degraded *in vitro* and *in vivo* by hydroxyl radicals, and the inflammatory responsive degradation proceeded via surface erosion [94,95]. This HA gel has been investigated for use as inflammation (stimulus)-responsive degradable matrices and as an electrically responsive and pulsatile release system [92] for implantable drug delivery. Hydrogels prepared by reaction of HA with 1,4-butanediol diglycidyl ether in the presence of 0.5% NaOH gave a porous material that was activated with periodate [96] and then modified with an 18 amino acid peptide containing the cell attachment domain sequence Arg-Gly-Asp (RGD). The presence of this peptide markedly enhanced cell attachment to the HA gels. Following cell attachment [MG63 cells (human osteosarcoma)], cells actively proliferated and colonized the pores of the matrix. This material may prove useful for the maintenance of cells as a scaffold for enhancing tissue repair and could have clinical implications for wound healing therapies [97].

Photo-Cross-Linking of HA

A methacrylate anhydride modified HA (14% modification) was synthesized by the reaction between HA and excess methacrylate anhydride; this derivative was photo-cross-linked to form a stable hydrogel by using ethyl eosin 0.5% w/v in 1-vinyl-2-pyrrolidone and triethanolamine as an initiator under argon ion laser with wavelength of 514 nm. The use of *in situ* photopolymerization of an HA derivative resulting in the formation of a cohesive gel enveloping the injured tissue may provide isolation from surrounding organs and thus prevent the formation of adhesions [98]. A preliminary cell encapsulation study was also successfully performed with islet of Langerhans.

HA Cross-Linked by Glutaraldehyde

HA strands fabricated from the cation-exchanged sodium hyaluronate (M_w 1.6 MDa) were cross-linked in glutaraldehyde aqueous solution [99]. Afterward, the strand surfaces were remodeled by the absorption of poly(D-lysine) and poly(L-lysine). The polypeptide-resurfaced HA strands have good biocompatibility and positive advantages for cellular adhesion.

HA Cross-Linked by Trivalent Iron

Intergel (FeHA, formerly Lubriccoat) is a formulation of HA electrostatically cross-linked with trivalent iron. This gel is intended for postsurgical applications to prevent adhesions [100].

HA Cross-Linked with Carbodiimide Chemistry

Incert, under development by Anika Therapeutics, Inc. (Woburn, MA), is a bioresorbable sponge derived from cross-linked HA with a biscarbodiimide coupling agent in the presence of 2-propanol- H_2O as cosolvent [19]. It adheres to tissues without the need for sutures and retains its efficacy even in the presence of blood. Recently, it was found to be effective at preventing postoperative adhesions in a rabbit cecal abrasion study. In addition, Ossigel, which incorporates ~~with~~ bFGF, was examined for acceleration of fracture healing.

Building on the hydrazide modification already described, hydrogels have been prepared using bishydrazide, trishydrazide, or polyvalent hydrazide compounds as cross-linkers [71]. HA (average molecular weight 1.5–2.0 MDa) would react with the hydrazide cross-linkers in the presence of a water-soluble carbodiimide at pH 3.5–4.7. Depending on the reaction conditions and the molar ratios of the reagents involved, gels with physicochemical properties ranging from soft-pourable gels to more mechanically rigid and brittle gels could be obtained. Applications of this chemistry are in development by Clear Solutions Biotech, Inc. (Stony Brook, NY).

HA-ADH can be cross-linked using commercially available homobifunctional cross-linkers [67]. HA-ADH was dissolved in 0.1 M $NaHCO_3$ to give a concentration of 15 mg/ml, and the cross-linker was added in solid form. Gelation was observed within 30–90 s. The gels appeared clear and colorless after washing with water.

Recently, an *in situ* polymerization technique was developed by cross-linking HA-ADH with a macromolecular cross-linker, PEG-dialdehyde, under physiological conditions [Y. Luo, K. R. Kirker, and G. D. Prestwich, unpublished results]. Biocompatible and biodegradable HA hydrogel films with well-defined mechanical strength were obtained after the evaporation of solvent. Drug release from these HA hydrogel films was investigated, and preliminary data with the HA films showed accelerated reepithelialization during wound healing.

A low water content HA hydrogel film [101] was made by cross-linking HA (1.6 MDa) film with a water-soluble carbodiimide as a coupling agent in H_2O containing a water-miscible nonsolvent of HA (e.g., ethanol or acetone). The highest degree of cross-linking that gave a low water content hydrogel was achieved in 80% ethanol. This film, having 60% water content, remained stable for 2 weeks after immersion in buffered solution. The cross-linking of HA films with a water-soluble carbodiimide in the presence of L-lysine methyl ester prolonged the *in vivo* degradation of HA film. The higher resistance to hydrolytic degradation might be attributable to amide bonds, in contrast to those cross-linked through ester bonds.

Hylans

Hylan is a hydrogel formed by cross-linking HA containing residual protein with formaldehyde (soluble gel) or divinyl sulfone [102]. In an alkaline environment at 20°C (10–15 min), the divinyl sulfone reagent is believed to react with hydroxyl groups of HA, forming cross-links. Similar cross-linking was obtained by using dimethylolurea, ethylene oxide, and polyisocyanate reagents. Soluble hylan is a high weight-average molecular weight form (8–23 MDa) of HA (5–6 MDa) that exhibits enhanced rheological properties compared, composites to these of HA. Hylan gel is an insoluble form that has greater elasticity

to HA alone.

newly published

aw: OK? No

(at all frequencies) and viscosity (at low shear rates) than soluble hylan and retains the high biocompatibility of the native macromolecule (nonimmunogenic, noninflammatory, and nontoxic). The hylans are produced by Biomatrix, now owned by Genzyme (Cambridge, MA).

Hylan exhibits biocompatibility identical to that of native HA and has been investigated in a number of medical applications. In the treatment of degenerative joint disease and rheumatoid arthritis, hylan was found to protect cartilage and prevent further chondrocyte injury. However, the effect was found to be reversible and viscosity dependent [103]. The hylan product Synvisc was developed specifically as a device for viscosupplementation therapy in osteoarthritis of the knee. It can increase the viscoelastic properties of the synovial fluid and the intercellular matrix of the synovial tissue and capsule [104,105].

Results from the clinical trials of hylan B gel slurry injections (Hylaform gel) suggested that it provides a safe, effective alternative for soft tissue augmentation [106–108]. Additionally, the injection of viscoelastic hylan B gel gave a durable augmentation of the soft tissues in the vocal fold in a rabbit model [109]. The gel can remain in place for 12 months, allowing the ingrowth of newly formed connective tissue after only a month. The new soft tissue contained collagen, HA, fibroblasts, and a few new vessels, without causing inflammation and adverse reactions. Finally, hylan has been used in plastic surgery for intradermal implantations and cosmetic injection [110]. Similarly, Restylane (Q-Med Inc., Sweden), a partially cross-linked HA derivative, has been available for soft tissue augmentation in Europe for more than 4 years [108]. However, neither Restylane nor hylan gel is currently approved by the FDA.

Hylagel is an engineered hylan gel being investigated as an adjuvant to prevent post-surgical adhesions. Finally, hylans can be used as drug carriers by the incorporation of therapeutic agents. For example, the *in vitro* biological activity of cytokine α -interferon was enhanced by approximately 40% as a result of its covalent attachment to hylan matrix [111].

Multiple-Component Cross-Linking of HA

Another way to prepare hyaluronan-based networks is based on the Passerini reaction and the Ugi reaction [112]. In the Passerini reaction, an aqueous solution of hyaluronan is mixed with aqueous glutaraldehyde (or other water-soluble dialdehyde) and added to a known amount of cyclohexylisocyanide. In the Ugi four-component reactions, the same mixture contains a diamine, as well. The degree of cross-linking is controlled by the amount of dialdehyde and diamine. Passerini reactions are kinetically faster and give good yields of a single condensation product. The ensuing hydrogels are transparent and mechanically stable; they swell in aqueous salt solutions depending on ion strength, and exhibit values of the compression modulus markedly dependent on the degree of cross-linking.

COMPOSITES

Synthetic polymers have been prepared as biomedical devices, and different physicochemical and mechanical properties are required for a given application. Synthetic polymers often have optimized mechanical properties but suffer from insufficient biocompatibility. In contrast, biocompatible biopolymers often have suboptimal mechanical properties. Blending synthetic polymers with biological macromolecules can yield composite materials that feature the desired properties of the individual polymers. Specifically, HA has been blended with other materials to produce novel biomaterials with the desired physicochemical, mechanical, and biocompatible properties. Two different synthetic polymers, poly(vinyl alcohol) (PVA) and poly(acrylic acid) (PAA), were blended with either collagen or HA [113]. HA-PAA sponges were prepared by dissolving both polymers in water at different ratios, lyophilizing, and cross-linking them by thermal treatment at 130°C under vacuum for 24 h. HA-PVA hydrogels were prepared by dissolving both polymers in water at different ratios and subjecting these mixtures to eight cycles of freeze-thawing.

HA-Liposome Composites

HA has been incorporated into liposomes. For example, HA was combined with cyclosporin A (CsA) and encapsulated within phospholipid liposomes [114]. HA (M_w 10 and 1000 kDa) powder was added into and hydrated with CsA-liposome composites to provide a final solution concentration of 2.5 wt% HA. Developed as a topically administered pharmaceutical agent, the solution was found to effectively treat skin disorders while minimizing systemic circulation. These compositions can also be administered orally, parenterally, and intrarectally.

Bioadhesive liposomes, in which HA is the surface-anchored bioadhesive ligand on a liposome surface, were prepared by the preactivation of HA with a carbodiimide and then added to a suspension of multilamellar liposomes consisting of phosphatidylcholine, phosphatidylethanolamine, and cholesterol [115]. In principle, an HA-coated liposome functionally resembles the PEG-coated "stealth" liposomes. These were investigated for their ability to act as site-adherent and sustained-release carriers of epidermal growth factor for the topical therapy of wounds and burns [116].

HA-Gelatin Composites

A porous matrix composed of gelatin and HA was prepared by dipping a gelatin-HA water-soluble sponge into 90% w/v acetone-water mixture with a small amount of a carbodiimide (EDCI) as cross-linking agent [117]. This sponge-type biomaterial was constructed for either wound dressings or scaffolds for tissue engineering. The sponge, impregnated with silver sulfadiazine, was found to facilitate the epidermal healing rate in a rat model.

HA-Alginate Composites

The association of alginate with another polysaccharide has been proposed to combine alginate's gel-forming effects with the properties of the partner macromolecule. Alginate-HA gels were prepared through the diffusion of calcium into alginate-HA mixtures. The resulting gels with a weight ratio of alginate to HA up to 0.50, had satisfactory mechanical properties. This composite matrix might be suitable as a biopolymeric carrier, or for articular surgery applications, because of its stability in synovial fluid [118,119].

HA-Collagen Composites

Composite materials consisting of HA and collagen have been prepared by complexing both components into a coagulate followed by cross-linking, with either glyoxal or starch dialdehyde as the cross-linking agent [120]. Atelocollagen was suspended in 0.5 M acetic acid, and the addition of an HA solution resulted in formation of coagulated material. The fabricated membrane was then chemically cross-linked with starch dialdehyde and glyoxal by immersing the membrane into a solution of this cross-linker. This membrane was quite resistant to collagenase and permitted fibroblast growth. Other composite materials consisting of HA and collagen were prepared by cross-linking the dried HA-collagen coagulates with polyethylene oxide and hexamethylene diisocyanate [121].

In addition, a hydroxyapatite-collagen-HA composite material was prepared by adding hydroxyapatite particles to an HA solution followed by blending with an aqueous dispersion of collagen fibers [122]. The final material, consisting of 90% hydroxyapatite, 9.2% collagen, and 0.8% w/w HA, is biocompatible and mechanically robust; it can be used as a bone defect filler. In 1999 a porous collagen-HA matrix was prepared by cross-linking collagen with HA-aldehyde made from the periodate oxidation of HA [123]. The presence of HA within the collagen matrix supported new bone formation, and this collagen-HA matrix has potential uses for the delivery of growth factors or as an implantable-cell-seeded matrix.

High concentrations of HA (1 mg/ml) in cell culture medium not only inhibit fibroblast contraction of a floating collagen fibrillar matrix (CFM) but also stimulate fibroblast migration on the CFM [52]. HA incorporation into an artificial skin material (collagen-gelatin sponge) accelerates the ingrowth of granulation tissue, thus providing a more suitable graft

bed to support a skin graft [124]. Further investigation of HA covalently bound to a collagen matrix found significantly reduced collagen contraction in fibroblast cultures. Such results warrant consideration of HA as an alternative biomaterial for building a dermal substitute and tissue engineering scaffold [125].

HA-Carboxymethylcellulose Composites

A bioabsorbable membrane, Seprafilm, has been developed as a physical barrier for prevention of postsurgical adhesions. Genzyme scientists prepared this material by blending two anionic polymers, HA and carboxymethylcellulose (CMC) [126], followed by carbodiimide-mediated modification. An anionic-cationic cross-linked network produces a rather fragile biomaterial. Seprafilm was approved by the FDA in 1996 for use in patients undergoing abdominal or pelvic laparotomy, to reduce the incidence, extent, and severity of postoperative adhesion [127]. The use of Seprafilm is limited to accessible areas that can be fully covered. Since for many adhesions the location is unpredictable or inaccessible, the general clinical utility of Seprafilm is compromised. In addition, Seprafilm is reported to suffer from handling difficulties, hampering its acceptance by surgeons. The same technology has been expanded to reduce the development of adhesions to synthetic nonabsorbable mesh, such as hernia repair products. Sepramesh is a composite of polypropylene mesh and a foam form of the Seprafilm membrane. This composite reduces the development of adhesions to the surface of the hernia repair mesh without compromising the long-term abdominal wall incorporation into the mesh [128]. Similar technology has also been used in presurgical coating, which would theoretically limit tissue trauma and prevent desiccation during surgery. However, a Genzyme-conducted clinical trial of Sepracoat, an HA-CMC solution applied in presurgical manipulation, failed to meet efficacy end points.

HA-Grafted Copolymers

A variety of HA-grafted copolymers have been prepared in recent years. In one example, several polyampholyte comb-type copolymers consisting of poly(L-lysine) (PLL) main chains, a DNA binding site, and an HA side chain with cell-specific ligands were prepared to target sinusoidal endothelial cells of liver [129]. The reducing end of HA and ϵ -amino groups of PLL were covalently coupled by reductive amination, using sodium cyanoborohydride to obtain the resulting comb-type copolymers (PLL-graft-HA). The PLL backbone selectively formed the polyion complex with DNA even in the presence of the HA side chain. In addition, the PLL-graft-HA-DNA complex may form a multiphase structure in which the hydrophobic PLL-DNA complex was surrounded by a hydrated shell of free HA. Complex formation with free HA chains was considered to be essential for directing the complex to target cells.

A PEG-grafted-HA copolymer was prepared by coupling HA with methoxy-PEG-hydrazide in the presence of EDCI as a coupling agent at acidic pH [130]. The copolymer is expected to be used for the delivery of water-soluble peptides. For example, when loaded with insulin, the loaded insulin appeared to partition into PEG moieties and intermolecular interactions, preventing the conformational changes of insulin. This appears to be a reasonable method to prevent drug leakage and to achieve degradation-controlled insulin release. Moreover, such a heterogeneously structured polymeric solution may be useful as an injectable therapeutic formulation for ophthalmic or arthritis treatment with a suitable drug.

CONCLUSION

HA is an important starting material for preparation of new biocompatible and biodegradable polymers that have applications in drug delivery, tissue engineering, and viscosupplementation. HA derivatives containing a variety of versatile functional groups can be produced with varying chemical structures and morphology. In this way, the rate of degradation, the degree of hydration, the cellular responses, and the overall tissue response can be manipulated. Approval and introduction of an increasing number of medical devices and new drugs using HA-derived biomaterials can be anticipated in the next decade.

ACKNOWLEDGMENT

We thank the University of Utah, Clear Solutions Biotech, Inc. (Stony Brook, NY), the U.S. Department of Defense, and the Center for Biopolymers at Interfaces (University of Utah) for financial support of research developed in our laboratories.

REFERENCES

1. Laurent, T. C., Laurent, U. B. G., and Fraser, J. R. E. (1995). Functions of hyaluronan. *Ann. Rheum. Dis.* 54, 429-432.
2. Fraser, J. R. E., Laurent, T. C., and Laurent, U. B. G. (1997). Hyaluronan: Its nature, distribution, functions and turnover. *J. Intern. Med.* 242, 27-33.
3. Dowthwaite, G. P., Edwards, J. C. W., and Pitsillides, A. A. (1998). An essential role for the interaction between hyaluronan and hyaluronan binding proteins during joint development. *J. Histochem. Cytochem.* 46, 641-651.
4. Hardwick, C., Hoare, K., Owens, R., Hohn, H. P., Hook, M., Moore, D., Cripps, V., Austen, L., Nance, D. M., and Turley, E. A. (1992). Molecular cloning of a novel hyaluronan receptor that mediates tumor cell motility. *J. Cell Biol.* 117, 1343-1350.
5. Collis, L., Hall, C., Lange, L., Ziebell, M. R., Prestwich, G. D., and Turley, E. A. (1998). Rapid hyaluronan uptake is associated with enhanced motility: Implications for an intracellular mode of action. *FEBS Lett.* 440, 444-449.
6. Entwistle, J., Hall, C. L., and Turley, E. A. (1996). Receptors: Regulators of signalling to the cytoskeleton. *J. Cell. Biochem.* 61, 569-577.
7. Cheung, W. F., Cruz, T. F., and Turley, E. A. (1999). Receptor for hyaluronan-mediated motility (RHAMM), a hyal-adherin that regulates cell responses to growth factors. *Biochem. Soc. Trans.* 27, 135-142.
8. Toole, B. P. (1997). Hyaluronan in morphogenesis. *J. Intern. Med.* 242, 35-40.
9. Gotoda, T., Matsumura, Y., Kondo, H., Saitoh, D., Shimada, Y., Kosuge, T., Kanai, Y., and Kakizoe, T. (1998). Expression of CD44 variants and its association with survival in pancreatic cancer. *Jpn. J. Cancer Res.* 89, 1033-1040.
10. Herrlich, P., Sleeman, J., Wainwright, D., Konig, H., Sharman, L., Hilberg, F., and Ponta, H. (1998). How tumor cells make use of CD44. *Cell Adhes. Commun.* 6, 141-147.
11. Baumgartner, G., Boltzman, L., and Hamilton, G. (1998). The impact of extracellular matrix on chemoresistance of solid tumors—experimental and clinical results of hyaluronidase as additive to cytostatic chemotherapy—Symposium on novel aspects in chemoresistance, Vienna, 20th March 1998—Editorial. *Cancer Lett.* 131, 1-2.
12. Baumgartner, G., Gomar-Hoss, C., Sakt, L., Ulsperger, E., and Wogritsch, C. (1998). The impact of extracellular matrix on the chemoresistance of solid tumors—experimental and clinical results of hyaluronidase as additive to cytostatic chemotherapy. *Cancer Lett.* 131, 85-99.
13. Gerdin, B., and Hallgren, R. (1997). Dynamic role of hyaluronan (HYA) in connective tissue activation and inflammation. *J. Intern. Med.* 242, 49-55.
14. Delpech, B., Girard, N., Bertrand, P., Courel, M. N., Chauzy, C., and Delpech, A. (1997). Hyaluronan: Fundamental principles and applications in cancer. *J. Intern. Med.* 242, 41-48.
15. Hall, C. L., Yang, B. H., Yang, X. W., Zhang, S. W., Turley, M., Samuel, S., Lange, L. A., Wang, C., Curpen, G. D., Savani, R. C., Greenberg, A. H., and Turley, E. A. (1995). Overexpression of the hyaluronan receptor RHAMM is transforming and is also required for H-ras transformation. *Cell (Cambridge, Mass.)* 82, 19-28.
16. Boyce, D. E., Thomas, J. H., Moore, K., and Harding, K. (1997). Hyaluronic acid induces tumour necrosis factor- α production by human macrophages *in vitro*. *Br. J. Plast. Surg.* 50, 362-368.
17. Patsch, G., Ch., S., Neumuller, J., Dunky, A., Petera, P., Broll, H., Ittner, G., and Jantsch, S. (1989). Modulation of the migration and chemotaxis of PMN cells by hyaluronic acid. *Z. Rheum.* 48, 123-128.
18. Chen, W. Y. J., and Abatangelo, G. (1999). Functions of hyaluronan in wound repair. *Wound Repair Regeneration* 7, 79-89.
19. Vercruysse, K. P., and Prestwich, G. D. (1998). Hyaluronate derivatives in drug delivery. *Crit. Rev. Ther. Drug Carrier Syst.* 15, 513-555.
20. Sutherland, I. W. (1998). Novel established applications of microbial polysaccharides. *Trends Biotechnol.* 16, 41-46.
21. Pasquali, R. I., Guerra, D., Taparelli, F., Georgountoz, A., and Frizziero, L. (1999). In "New Frontiers in Medical Sciences: Redefining Hyaluronan," p. N28. Abbazia di Praglia, Padua, Italy.
22. Punzi, L., Pianon, M., Schiavon, F., and Todesco, S. (1999). In "New Frontiers in Medical Sciences: Redefining Hyaluronan," p. N32. Abbazia di Praglia, Padua, Italy.
23. Hallen, L., Johansson, C., Dahlqvist, A., and Laurent, C. (1999). In "New Frontiers in Medical Sciences: Redefining Hyaluronan," p. N22. Abbazia di Praglia, Padua, Italy.
24. Seckel, B. R., Jones, D., Hekimian, K. J., Wang, K. K., Chakalis, D. P., and Costas, P. D. (1995). Hyaluronic acid through a new injectable nerve guide delivery system enhances peripheral nerve regeneration in the rat. *J. Neurosci. Res.* 40, 318-324.
25. Jorgensen, T., Moss, J., Nicolajsen, H. V., and L. S. N. (1998). PCT Int. Appl. WO 9822114A1.
26. Saettone, M. F., Monti, D., Torracca, M. T., and Chetoni, P. (1994). Mucoadhesive ophthalmic vehicles: Evaluation of polymeric low-viscosity formulations. *J. Ocul. Pharmacol.* 10, 83-92.
27. Morimoto, K., Yamaguchi, H., Iwakura, Y., Morisaka, K., Ohashi, Y., and Nakai, Y. (1991). Effects of viscous hyaluronate-sodium solutions on the nasal absorption of vasopressin and an analogue. *Pharm. Res.* 8, 471-474.
28. Miller, J. A., Ferguson, R. L., Powers, D. L., Burns, J. W., and Shalaby, S. W. (1997). Efficacy of hyaluronic acid/nonsteroidal anti-inflammatory drug systems in preventing postsurgical tendon adhesions. *J. Biomed. Mater. Res. (Appl. Biomater.)* 38, 25-33.

Schwarzer, CH.
aw: last name.

aw: OK? OK

the mechanism?
aw: ch. title?
editors? see attached page

aw: descr. title?
aw: last name. ditto

29. Gowland, G., Moore, A. R., Willis, D., and Willoughby, D. A. (1996). Marked enhanced efficacy of cyclosporin when combined with hyaluronic acid. Evidence from two T cell-mediated models. *Clin. Drug Invest.* 11, 245-250.
30. Brown, T. J., Alcorn, D., and Fraser, J. R. E. (1999). Absorption of hyaluronan applied to the surface of intact skin. *J. Invest. Dermatol.* 113, 740-746.
31. Benedetti, L. M., Topp, E. M., and Stella, V. J. (1990). Microspheres of hyaluronic acid esters—fabrication methods and *in vitro* hydrocortisone release. *J. Controlled Release* 13, 33-41.
32. Iannace, S., Ambrosio, L., Nicolais, L., Rastrelli, A., and Pastorello, A. (1992). Thermomechanical properties of hyaluronic acid-derived products. *J. Mater. Sci.: Mater. Med.* 3, 59-64.
33. Campoccia, D., Hunt, J. A., Doherty, P. J., Zhong, S. P., Oregan, M., Benedetti, L., and Williams, D. F. (1996). Quantitative assessment of the tissue response to films of hyaluronan derivatives. *Biomaterials* 17, 963-975.
34. Benedetti, L., Cortivo, R., Berti, T., Berti, A., Pea, F., Mazzo, M., Moras, M., and Abatangelo, G. (1993). Biocompatibility and biodegradation of different hyaluronan derivatives (HYAFF) implanted in rats. *Biomaterials* 14, 1154-1160.
35. Benedetti, L. M., Joshi, H. N., Goei, L., Hunt, J. A., Callegaro, L., Stella, V. J., and Topp, E. M. (1991). Dosage forms from polymeric prodrugs: Hydrocortisone esters of hyaluronic acid. *New Polym. Mater.* 3, 41-48.
36. Drobnik, J. (1991). Hyaluronan in drug delivery. *Adv. Drug Delivery Res.* 7, 295-308.
37. Hume, L. R., Lee, H. K., Benedetti, L. M., Sanzgiri, Y. D., Topp, E. M., and Stella, V. J. (1994). Ocular sustained delivery of prednisolone using hyaluronic acid benzyl ester films. *Int. J. Pharm.* 111, 295-298.
38. Kyyronen, K., Hume, L., Benedetti, L. M., Urtti, A., Topp, E., and Stella, V. (1992). Methyl-prednisolone esters of hyaluronic acid in ophthalmic drug delivery. *Int. J. Pharm.* 80, 161-169.
39. Ilium, L., Farraj, N. F., Fisher, A. N., Gill, I., Miglietta, M., and Benedetti, L. M. (1994). Hyaluronic acid ester microspheres as a nasal delivery system for insulin. *J. Controlled Release* 29, 133-141.
40. Richardson, J. L., Ramires, P. A., Miglietta, M. R., Rochira, M., Bacelle, L., Callegaro, L., and Benedetti, L. M. (1995). Novel vaginal delivery systems for calcitonin. 1. Evaluation of HYAFF calcitonin microspheres in rats. *Int. J. Pharm.* 115, 9-15.
41. Bonucci, E., Ballanti, P., Ramires, P. A., Richardson, J. L., and ^{Benedetti} ~~Bacelle~~, L. (1995). Prevention of ovariectomy osteopenia to rats after vaginal administration of HYAFF 11 microspheres containing calcitonin. *Calcif. Tissue Int.* 56, 274-279.
42. Singh, M., Briones, M., and O'Hagan, D. (1999). In "New Frontiers in Medical Sciences: Redefining Hyaluronan," p. N34. Abbazia di Praglia, Padua, Italy.
43. Nightlinger, N. S., Benedetti, L., Soranzo, C., Pettit, D. K., Pankey, S. C., and Gombotz, W. R. (1995). *Proc. Int. Symp. Controlled Release Bioact. Mater.*, Seattle, WA, pp. 738-739.
44. Rooney, P., and Kumar, S. (1993). Inverse relationship between hyaluronan and collagens in development and angiogenesis. *Differentiation (Berlin)* 54, 1-9.
45. Wheatley, S. C., Isacke, C. M., and Crossley, P. H. (1993). Restricted expression of the hyaluronan receptor, CD44, during postimplantation mouse embryogenesis suggests key roles in tissue formation and patterning. *Development (Cambridge, UK)* 119, 295-306.
46. Peterson, P. E., Pow, C. S. T., Wilson, D. B., and Hendrickx, A. G. (1993). Distribution of extracellular matrix components during early embryonic development in the macaque. *Acta Anat.* 146, 3-13.
47. Knudson, C. B., and Knudson, W. (1993). Hyaluronan-binding proteins in development, tissue homeostasis, and disease. *FASEB J.* 7, 1233-1241.
48. Siebert, J. W., Burd, A. R., McCarthy, J. G., Weinzwieg, J., and Ehrlich, H. P. (1990). Fetal wound healing: A biochemical study of scarless healing. *Plast. Reconstr. Surg.* 85, 495-502.
49. Cortivo, R., De Galateo, A., Castellani, I., Brun, P., Giro, M. G., and Abatangelo, G. (1990). Hyaluronic acid promotes chick embryo fibroblast and chondroblast expression. *Cell Biol. Int. Rep.* 14, 111-122.
50. Shepard, S., Becker, H., and Hartmann, J. X. (1996). Using hyaluronic acid to create a fetal-like environment *in vitro*. *Ann. Plast. Surg.* 36, 65-69.
51. Denizot, F., and Lang, R. (1986). Rapid colorimetric assay for cell growth and survival. *J. Immunol. Methods* 89, 271-277.
52. Pianigiani, E., Andreassi, A., Taddeucci, P., Alessandrini, C., Fimiani, M., and Andreassi, L. (1999). A new model for studying differentiation and growth of epidermal cultures on hyaluronan-based carrier. *Biomaterials* 20, 1689-1694.
53. Burn, P., Cortivo, R., Zavan, B., Vecchiato, N., and Abatangelo, G. (1999). *In vitro* reconstructed tissues on hyaluronan-based temporary scaffolding. *J. Mater. Sci., Mater. Med.* 10, 683-688.
54. Andreassi, L., Casini, L., Trabucchi, E., Diamantini, S., Rastrelli, A., and Donati, L. (1991). Human keratinocytes cultured on membranes composed of benzyl ester of hyaluronic acid suitable for grafting. *Wounds* 3, 116-126.
55. Soranzo, C., Abatangelo, G., and Callegaro, L. (1996). PCT Int. Appl. WO 9633750.
56. Zacchi, V., Soranzo, C., Cortivo, R., Radice, M., Brun, P., and Abatangelo, G. (1998). *In vitro* engineering of human skin-like tissue. *J. Biomed. Mater. Res.* 40, 187-194.
57. Caravaggi, C., Faglia, E., L.D., P., De Giglio, R., Cavaiani, P., Mantero, M., Gino, M., Quarantiello, A., Sommariva, E., and Pritelli, C. (1999). In "New Frontiers in Medical Sciences: Redefining Hyaluronan," p. N9. Abbazia di Praglia, Padua, Italy.
58. Harris, P. A., Francesco, F., Barisono, D., Leigh, I. M., and Navsaria, H. A. (1999). Use of hyaluronic acid and cultured autologous keratinocytes and fibroblasts in extensive burns. *Lancet* 353, 35-36.
59. Aigner, J., Tegeler, J. A., Hutzler, P., Campoccia, D., Pavesio, A., ^{Benedetti} ~~C., H., E., K.~~, and Naumann, A. (1998). Cartilage tissue engineering with novel nonwoven structured biomaterial based on hyaluronic acid benzyl ester. *J. Biomed. Mater. Res.* 42, 172-181.
60. Radice, M., Burn, P., Cortivo, R., Scapinelli, R., Battalardi, C., and Abatangelo, G. (2000). Hyaluronan-based biopolymers as delivery vehicles for bone-marrow-derived mesenchymal progenitors. *J. Biomed. Mater. Res.* 50, 101-109.

Benedetti aw: OK?

see aw: ch
sheet
tittle
editor

see aw: give
sheet desc.
tittle?

see aw: ch
tittle
editor
initials
last name(s)

Hammer,
C.,
Kastenbauer, E.

61. Wakitani, S., Goto, T., Pineda, S. J., Young, R. G., Mansour, J. M., Caplan, A. I., and Goldeberg, V. M. (1994). Mesenchymal cell-based repair of large, full-thickness defects of articular cartilage. *J. Bone Jt. Surg. (Am. Vol.)* 76-A(4), 579-592.
62. Butnariu-Ephrat, M., Robinson, D., Mendes, D. G., Halperin, N., and Nevo, Z. (1996). Resurfacing of goat articular cartilage by chondrocytes derived from bone marrow. *Clin. Orthop. Relat. Res.* 330, 234-243.
63. Solchaga, L. A., Goldberg, V. M., and Caplan, A. I. (1999). In "New Frontiers in Medical Sciences: Redefining Hyaluronan," p. N55. Abbazia di Praglia, Padua, Italy.
64. Prestwich, G. D., ~~P. M., M.~~ Marecek, J. F., Vercruysse, K. P., and Ziebell, M. R. (1997). Controlled chemical modification of hyaluronic acid: Synthesis, applications and biodegradation of hydrazide derivatives. *J. Controlled Release* 53, 99.
65. Kuo, J.-W., Swann, D. A., and Prestwich, G. D. (1994). U.S. Pat. 5,356,883.
66. Kuo, J.-W., Swann, D. A., and Prestwich, G. D. (1991). Chemical modification of hyaluronic acid by carbodiimides. *Bioconjugate Chem.* 2, 232-241.
67. Pouyani, T., Harbison, G. S., and Prestwich, G. D. (1994). Novel hydrogels of hyaluronic acid: Synthesis, surface morphology, and solid-state NMR. *J. Am. Chem. Soc.* 116, 7515-7522.
68. Pouyani, T., Kuo, J.-W., Harbison, G. S., and Prestwich, G. D. (1992). Solid-state NMR of N-acylureas derived from the reaction of hyaluronic acid with isotopically-labeled carbodiimides. *J. Am. Chem. Soc.* 114, 5972-5976.
69. Pouyani, T., and Prestwich, G. D. (1994). Functionalized derivatives of hyaluronic acid oligosaccharides: Drug carriers and novel biomaterials. *Bioconjugate Chem.* 5, 339-347.
70. Pouyani, T., and Prestwich, G. D. (1994). Biotinylated hyaluronic acid: A new tool for probing hyaluronate-receptor interactions. *Bioconjugate Chem.* 5, 370-372.
71. Vercruysse, K. P., ~~Marecek, D. M., Marecek, J. F., and Prestwich, G. D.~~ (1997). Synthesis and *in vitro* degradation of new polyvalent hydrazide cross-linked hydrogels of hyaluronic acid. *Bioconjugate Chem.* 8, 686-694.
72. Luo, Y., and Prestwich, G. D. (1999). Synthesis and selective cytotoxicity of a hyaluronic acid-antitumor bioconjugate. *Bioconjugate Chem.* 10, 755-763.
73. Luo, Y., Ziebell, M. R., and Prestwich, G. D. (2001). A hyaluronic acid-Taxol antitumor bioconjugate targeted to cancer cells. *Biomacromolecules (in press)* 1, 208-218.
74. Bulpitt, P., and Aeschlimann, D. (1999). New strategy for chemical modification of hyaluronic acid: Preparation of functionalized derivatives and their use in the formation of novel biocompatible hydrogels. *J. Biomed. Mater. Res.* 47, 152-169.
75. Akima, K., Ito, H., Iwata, Y., Matsuo, K., Watari, N., Yanagi, M., Hagi, H., Oshima, K., Yagita, A., Atomi, Y., and Tatekawa, I. (1996). Evaluation of antitumor activities of hyaluronate binding antitumor drugs: Synthesis, characterization and antitumor activity. *J. Drug Target.* 4, 1.
76. Cera, C., Terbojevich, M., Cosani, A., and Palumbo, M. (1988). Anthracycline antibiotics supported on water-soluble polysaccharides: Synthesis and physicochemical characterization. *Int. J. Biol. Macromol.* 10, 66-74.
77. Sakurai, K., Miyazaki, K., Koder, Y., Nishimura, H., Shingu, M., and Inada, Y. (1997). Anti-inflammatory activity of superoxide dismutase conjugated with sodium hyaluronate. *Glycoconjugate J.* 14, 723-728.
78. Magnani, A., Albanese, A., Lamponi, S., and Barbucci, R. (1996). Blood-interaction performance of different sulfated hyaluronic acids. *Thromb. Res.* 81, 383-395.
79. Favia, P., Palumbo, F., and D'Agostino, R. (1997). Grafting of functional groups onto polyethylene by means of RE glow discharges as first step to the immobilization of biomolecules. *Polym. Prepr.* 38, 1039-1040.
80. Favia, P., Palumbo, F., D'Agostino, R., Lamponi, S., Magnani, A., and Barbucci, R. (1998). Immobilization of heparin and highly-sulfated hyaluronic acid onto plasma-treated polyethylene. *Plasma Polym.* 3, 77-96.
81. Chen, G. P., Ito, Y., Imanishi, Y., Magnani, A., Lamponi, S., and Barbucci, R. (1997). Photoimmobilization of sulfated hyaluronic acid for antithrombogenicity. *Bioconjugate Chem.* 8, 730-734.
82. Hoekstra, D. (1999). Hyaluronan-modified surfaces for medical devices. *Med. Devices Diagn. Ind.* 48-58.
83. Barbucci, R. (1999). In "New Frontiers in Medical Sciences: Redefining Hyaluronan," p. N4. Abbazia di Praglia, Padua, Italy.
84. Coradini, D., Pellizzaro, C., Miglierini, G., Daidone, M. G., and Perbellini, A. (1999). Hyaluronic acid as drug delivery for sodium butyrate: Improvement of the anti-proliferative activity on a breast-cancer cell line. *Int. J. Cancer* 81, 411-416.
85. Mensitieri, M., Ambrosio, L., and Nicolais, L. (1996). Viscoelastic properties modulation of a novel autocrosslinked hyaluronic acid polymer. *J. Mater. Sci.: Mater. Med.* 7, 695-698.
86. De Iaco, P. A., Stefanetti, M., Pressato, D., Piana, S., Dona, M., Pavesio, A., and Bovicelli, L. (1998). A novel hyaluronan-based gel in laparoscopic adhesion prevention: Preclinical evaluation in an animal model. *Fertil. Steril.* 69, 318-323.
87. De Iaco, P. (1999). In "New Frontiers in Medical Sciences: Redefining Hyaluronan," p. N12. Abbazia di Praglia, Padua, Italy.
88. Lise, M. (1999). In "New Frontiers in Medical Sciences: Redefining Hyaluronan," p. N24. Abbazia di Praglia, Padua, Italy.
89. Caplan, A. I., Solchaga, A. I., and Goldberg, V. M. (1999). In "New Frontiers in Medical Sciences: Redefining Hyaluronan," p. N8. Abbazia di Praglia, Padua, Italy.
90. Solchaga, L. A., Dennis, J. E., Goldberg, V. M., and Caplan, A. I. (1999). Hyaluronic acid-based polymers as cell carriers for tissue-engineered repair of bone and cartilage. *J. Orthop. Res.* 17, 205-213.
91. Laurent, T. C., Hellsing, K., and Gelotte, B. (1964). Cross-linked gels of hyaluronic acid. *Acta Chem. Scand.* 18, 274-275.

92. Tomer, R., Dimitrijevic, D., and Florence, A. T. (1995). Electrically controlled release of macromolecules from cross-linked hyaluronic acid hydrogels. *J. Controlled Release* 33, 405-413.
93. Yui, N., Okano, T., and Sakurai, Y. (1993). Photo-responsive degradation of heterogeneous hydrogels comprising crosslinked hyaluronic acid and lipid microspheres for temporal drug delivery. *J. Controlled Release* 26, 141-145.
94. Yui, N., Okano, T., and Sakurai, Y. (1992). Inflammation responsive degradation of crosslinked hyaluronic acid gels. *J. Controlled Release* 22, 105-116.
95. Yui, N., Nihira, J., Okano, T., and Sakurai, Y. (1993). Regulated release of drug microspheres from inflammation responsive degradable matrices of crosslinked hyaluronic acid. *J. Controlled Release* 25, 133-143.
96. Glass, J. R., Dickerson, K. T., Stecker, K., and Polarek, J. W. (1996). Characterization of a hyaluronic acid-Arg-Gly-Asp peptide cell attachment matrix. *Biomaterials* 17, 1101-1108.
97. Cooper, M. L., Hansbrough, J. F., and Polarek, J. W. (1996). The effect of an arginine-glycine-aspartic acid peptide and hyaluronate synthetic matrix on epithelialization of meshed skin graft interstices. *J. Burn Care Rehabil.* 17, 108-116.
98. Burns, J. M., Skinner, K., Colt, J., Sheidlin, A., Bronson, R., Yaacobi, Y., and Goldberg, E. P. (1995). Prevention of tissue injury and postsurgical adhesions by precoating tissues with hyaluronic acid solutions. *J. Surg. Res.* 59, 644-652.
99. Hu, M., Sabelman, E. E., Lai, S., Timek, E. K., Zhang, F., Hentz, V. R., and Lineaweaver, W. C. (1999). Polypeptide resurfacing method improves fibroblast's adhesion to hyaluronan strands. *J. Biomed. Mater. Res.* 47, 79-84.
100. diZerega, G. S. (1999). In "New Frontiers in Medical Sciences: Redefining Hyaluronan," p. N13. Abbazia di Praglia, Padua, Italy.
101. Tomihata, K., and Ikada, Y. (1997). Crosslinking of hyaluronic acid with water-soluble carbodiimide. *J. Biomed. Mater. Res.* 37, 243-251.
102. Larsen, N. E., and Balazs, E. A. (1991). Drug delivery systems using hyaluronan and its derivatives. *Adv. Drug Delivery Rev.* 7, 279-293.
103. Larsen, N. E., Lombard, K. M., Parent, E. G., and Balazs, E. A. (1992). Effects of hylan on cartilage and chondrocyte cultures. *J. Orthop. Res.* 10, 23-32.
104. Pozo, M. A., Balazs, E. A., and Belmonte, C. (1997). Reduction of sensory responses to passive movements of inflamed knee joints by hylan, a hyaluronan derivative. *Exp. Brain Res.* 116, 3-9.
105. Adams, M. E. (1993). An analysis of clinical studies of the use of crosslinked hyaluronan, hylan, in the treatment of osteoarthritis. *J. Rheumatol.* 20, 16-18.
106. Larsen, N. E., Pollak, C. T., Reiner, K., Leshchiner, E., and Balazs, E. A. (1993). Hylan gel biomaterial: Dermal and immunologic compatibility. *J. Biomed. Mater. Res.* 27, 1129-1134.
107. Larsen, N. E., Pollak, C. T., Reiner, K., Leshchiner, E., and Balazs, E. A. (1994). Hylan gel for soft tissue augmentation. In "Biotechnology and Bioactive Polymers" (C. Gebelein and C. Carrahar, eds.), pp. 25-33. Plenum, New York.
108. Krauss, M. C. (1999). Recent advances in soft tissue augmentation. *Semin. Cutaneous Med. Surg.* 18, 119-128.
109. Hallen, L., Johansson, C., and Laurent, C. (1999). Cross-linked hyaluronan (hylan B gel): A new injectable remedy for treatment of vocal folds insufficiency-an animal study. *Acta OtoLaryngol.* 119, 107-111.
110. Piaquadio, D., Jarcho, M., and Glotz, R. (1997). Evaluation of hylan B gels as a soft tissue augmentation implant material. *J. Am. Acad. Dermatol.* 36, 544-549.
111. Larsen, N. E., Parent, E., and Balazs, E. (1999). In "New Frontiers in Medical Sciences: Redefining Hyaluronan," p. N21. Abbazia di Praglia, Padua, Italy.
112. Crescenzi, V., Tomasi, M., and Francescangeli, A. (1999). In "New Frontiers in Medical Sciences: Redefining Hyaluronan," p. N11. Abbazia di Praglia, Padua, Italy.
113. Cascone, M. G., Sim, B., and Downes, S. (1995). Blends of synthetic and natural polymers as drug delivery systems for growth hormone. *Biomaterials* 16, 569-574.
114. Marriott, C., Martin, G. P., and Brown, M. (1998). PCT Int. Appl. WO 9812024.
115. Yerushalmi, N., and Margalit, R. (1998). Hyaluronic acid-modified bioadhesive liposomes as local drug depots: Effects of cellular and fluid dynamics on liposome retention at target sites. *Arch. Biochem. Biophys.* 349, 21-26.
116. Yerushalmi, N., Arad, A., and Margalit, R. (1994). Molecular and cellular studies of hyaluronic acid-modified liposomes as bioadhesive carriers for topical drug delivery in wound healing. *Arch. Biochem. Biophys.* 313, 267-273.
117. Chio, Y. S., Hong, S. R., Lee, Y. M., Song, K. W., Park, M. H., and Nam, Y. S. (1999). Studies on gelatin-containing artificial skin: II. Preparation and characterization of cross-linked gelatin-hyaluronate sponge. *J. Biomed. Mater. Res.* 48, 631-639.
118. Oerther, S., Gall, H. L., Payan, E., Lapique, F., Presle, N., Hubert, P., Dexheimer, J., Netter, P., and Lapique, F. (1999). Hyaluronate-alginate gel as a novel biomaterial: Mechanical properties and formation mechanism. *Biotechnol. Bioeng.* 63, 206-215.
119. Oerther, S., Payan, E., Lapique, F., Presle, N., Hubert, P., Muller, S., Netter, P., and Lapique, F. (1999). Hyaluronate-alginate combination for the preparation of new biomaterials: Investigation of the behavior in aqueous solutions. *Biochim. Biophys. Acta* 1426, 185-194.
120. Rehakova, M., Bakos, D., Vizarova, K., Soldan, M., and Jurickova, M. (1996). Properties of collagen and hyaluronic acid composite materials and their modification by chemical crosslinking. *J. Biomed. Mater. Res.* 30, 369-372.
121. Soldan, M., and Bakos, D. (1997). In "Advances in Medical Physics, Biophysics and Biomaterials," pp. 58-61. Stara Lesna, Slovak Republic.
122. Bakos, D., Soldan, M., and Vanis, M. (1997). In "Advances in Medical Physics, Biophysics and Biomaterials," pp. 54-56. Stara Lesna, Slovak Republic.
123. Liu, L., Thompson, A. Y., Heidaran, M. A., Poser, J. W., and Spiro, R. C. (1999). An osteoconductive collagen/hyaluronate matrix for bone regeneration. *Biomaterials* 20, 1097-1108.

OK - sheet
 aw. Ch. title editor?

OK sheet
 aw. Ch. title editor?
 aw. give title

OK aw. 2 authors
 Yes, two people

See sheet
 aw. Ch. title editor?

124. Murashit, T., Nakayama, Y., Hirano, T., and Ohashi, S. (1996). Acceleration of granulation tissue ingrowth by hyaluronic acid in artificial skin. *Br. J. Plast. Surg.* 49, 58-63.
125. Huang-Lee, L. L. H., and Nimni, M. E. (1994). Crosslinked CNBr-activated hyaluronan-collagen matrices: Effects on fibroblast contraction. *Matrix Biol.* 14, 147-157.
126. Burns, J. W., Burgess, L., Skinner, K., Rose, R., Colt, M. J., and Diamond, M. P. (1996). A hyaluronate based gel for the prevention of postsurgical adhesions: Evaluation in two animal species. *Fertil. Steril.* 66, 814-821.
127. Bowers, D., Raybon, B., and Wheelless, C. R. (1999). Hyaluronic acid-carboxymethyl-cellulose film and perianastomotic adhesions in previously irradiated rats. *Am. J. Obstet. Gynecol.* 181, 1335-1338.
128. Hooker, G. D., Taylor, B. M., and Driman, D. K. (1999). Prevention of adhesion formation with use of sodium hyaluronate-based bioresorbable membrane in a rat model of ventral hernia repair with polypropylene mesh—A randomized, controlled study. *Surgery* 125, 211-216.
129. Asayama, S., Nogawa, M., Takei, Y., Akaike, T., and Maruyama, A. (1998). Synthesis of novel polyampholyte comb-type copolymers consisting of a poly(L-lysine) backbone and hyaluronic acid side chains for a DNA carrier. *Bioconjugate Chem.* 9, 476-481.
130. Moriyama, K., Ooya, T., and Yui, N. (1999). Hyaluronic acid grafted poly(ethylene glycol) as a novel peptide formulation. *J. Controlled Release* 59, 77-86.

See attached
sheet →

HYALURONAN BIOMATERIALS FOR TARGETED DRUG DELIVERY AND WOUND HEALING

Glenn D. Prestwich^{*1,2}, Yi Luo¹, Kelly R. Kirker²,
Michael R. Ziebell³, & Jane Shelby⁴

¹Department of Medicinal Chemistry, The University of Utah,
30 South 2000 East, Room 201, Salt Lake City, Utah 84112-5820 USA

²Department of Bioengineering, The University of Utah,
20 South 2030 East, Room 506, Salt Lake City, Utah 84112-9458 USA

³Department of Neurobiology, Harvard Medical School,
220 Longwood Avenue, Boston, Massachusetts 02115 USA

⁴Department of Surgery, The University of Utah, 50 North Medical Drive,
Salt Lake City, Utah 84132 USA

*Address for correspondence: Professor Glenn D. Prestwich
Tel: +1-801-585-9051; Fax: +1-801-585-9053; E-mail: gprestwich@deans.pharm.utah.edu

ABSTRACT

A mild chemical modification of hyaluronic acid (HA) provides functionalized derivatives for fabrication of targeted drug delivery systems, wound dressings, tissue engineering scaffolds, and probes for cellular binding and transport of HA. First, we describe the use of covalent HA-anti-cancer agents for use as potential therapeutics. Data from cell culture, flow cytometry, and *in vivo* mouse models support this targeted anti-tumor strategy. Second, we describe new flexible hydrogel films composed of crosslinked chondroitin sulfate (CS) and HA, which have potential as wound dressings capable of biointegration and drug release.* Lyophilization and rehydration of these flexible films also provide porous materials for cell growth and tissue engineering. Third, we describe progress on the elucidation of the structure determination of the HA-binding domain (HABD) of RHAMM and the use of this domain to identify peptides that mimic HA.

KEYWORDS

Hyaluronic acid, biocompatible, anti-cancer, targeting, bioconjugate, crosslinking, hydrogel, biodegradable, drug release, wound healing

INTRODUCTION

Hyaluronan (hyaluronic acid, HA) has an important duality *in vivo*. As a bulk material, it is implicated in water homeostasis, joint lubrication, and as the key viscoelastic component of the extracellular matrix (ECM). As a signaling molecule, HA binds specifically to proteins in the ECM, on the cell surface, and within the cell cytosol, thereby having a role in cartilage matrix stabilization^{1,2}, cell motility^{3,4}, growth factor action⁵, morphogenesis and embryonic development⁶, and inflammation⁷. Our research captures both functions. First, we present two examples of the use of chemically-modified HA⁸ as a building block for biocompatible and biodegradable polymers with applications in drug delivery, tissue engineering, and viscosupplementation^{9,10}. Second, we present approaches to studying the structure and function of HA-protein complexes^{11,12}.

HA also has an important role in wound healing. An HA-rich matrix favors the infiltration of migratory cells into the injured tissue¹³, and provides an environment that promotes cell mobility and proliferation¹⁴. Degradation products of HA modulate the inflammatory response¹⁵ and stimulate angiogenesis¹⁶. Additionally, HA acts as a signaling molecule in cell

mobility, inflammation, and wound healing¹⁷. Thus, a wound dressing that has these characteristics would be an important tool in rapid stabilization of burn patients.

Composite materials containing HA, using HA and chemically-modified HA in drug delivery¹⁸, and covalently attaching HA to plastic surfaces have been described¹⁹. Herein we present uses of adipic dihydrazide (ADH)-modified HA^{20,21} on targeted delivery of anti-cancer drugs^{22,23}, and for the preparation of cell-compatible crosslinked hydrogels²⁴.

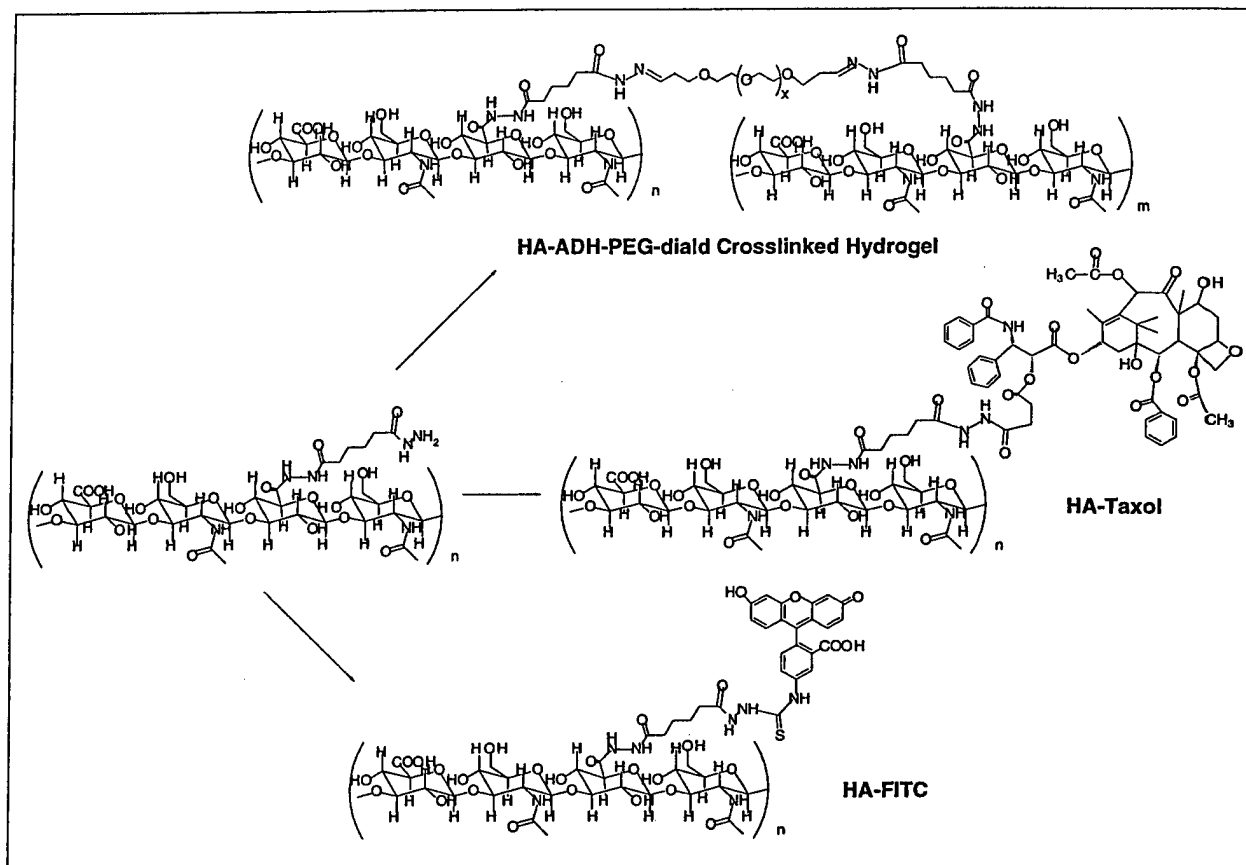


Figure 1. Conversion of HA-ADH into biomaterials and bioprobes

MATERIALS & METHODS

Preparation and characterization of HA-Taxol and HA-PEG hydrogel films

We modified published methods²¹ to better control degree of modification and to obtain homogeneous HA-ADH²². After dialysis, HA-ADH purity was determined by gel permeation chromatography (GPC) and the degree of glucuronate modification (from 2% to over 55%) was determined by ¹H-NMR. HA-Taxol was obtained by coupling the activated ester of Taxol 2-hemisuccinate, and HA-FITC-Taxol was obtained by reaction of HA-ADH with 5 mol% of FITC and then coupling with the activated Taxol derivative. Products were again purified by dialysis and purity established by GPC, NMR, and UV.

Crosslinking of HA-ADH²⁵ was also modified by poly(ethylene glycol)-propiondialdehyde (PEG-diald) to give a bis-hydrazone hydrogel with epidermis-like biomechanical properties²⁴. The hydrogel formed within 60 sec after mixing HA-ADH and PEG-diald solutions; after solvent evaporation, a flexible, hydratable HA hydrogel film was obtained.

HA-Taxol uptake and cell toxicity assays

Four human cancer cell-lines (SK-OV-3, HBL-100, HCT-116, and MDA-231) and control cells (NIH 3T3 murine fibroblasts) were employed for fluorescently-labeled HA uptake and

toxicology studies^{22,23}. Cytotoxicity was determined using a 96-well plate format in quadruplicate with increasing doses of 20,000 cells in 200 μ L cell culture media per well. HA-Taxol conjugates were added from a stock solution of DMSO:H₂O = 1:1, v/v; free Taxol was added as a DMSO stock solution. Cells were incubated at 37 °C for 3 days with the test substance, and cell viability was determined using MTT dye uptake at 540 nm. Response was graded as percent live cells compared to untreated.

Wound healing using HA hydrogel film on a mouse model

In the experimental mouse model, a 1-cm diameter wound was created on the dorsal side of a Balb/c mouse. Both the skin epidermal and dermal layers were removed. The wounds were then dressed with either Biobrane® or Tegaderm® (controls), or ethylene oxide sterilized HA hydrogel films followed by either Biobrane® or Tegaderm®. Wounds were bandaged and allowed to heal. After 5 days, the mice were sacrificed, the wound sites were excised, and the tissue samples were analyzed histologically. Time courses for wound healing were established from biopsies at 3, 5, 7, and 10 days.

Sub-cloning, expression, and purification of a RHAMM HA-binding domain

The cDNA for the HA-binding domain (HABD) RHAMMv4 (Receptor for HA-Mediated cell Motility) in a pCRII vector²⁶ was used to construct RHAMM(518-580)-GST in pGEX-2T (Pharmacia) using *Eco*R1 and *Bam*H1 unique restriction sites. GST-RHAMM(518-580) (RDSYAQLLGHQNLKQKIKHVVKLKDENSQ LKSEVS KLRSQLVKRKQNELRLQGELDKALGIR) containing two BX₂B motifs (underlined) was expressed in BL21 *E. coli* cells in ampicillin-containing media by induction with IPTG^{27,28}. Cells were harvested, lysed, and GST fusion protein was purified on a GSH-Sepharose column at 4 °C by elution with 50 mM glutathione, 10 mM Tris, pH 8.0.

RESULTS & DISCUSSION

Selective cell uptake and cytotoxicity of HA-Taxol

A cell-targeted polymeric prodrug prepared from Taxol and chemically-modified HA was evaluated *in vitro*. We have obtained six lines of evidence in support of the selective uptake and targeted toxicity of HA-linked prodrugs. First, fluorescently-labeled HA was prepared with three different fluors (Texas Red, FITC, and BODIPY) with two sizes of HA (12 kDa, 200 kDa). Both laser confocal microscopy and fluorescence-activated cell sorting confirmed the uptake of HA-fluors into cells expressing HA receptors. Cells lacking such surface HA receptors failed to internalize HA-fluors. Moreover, the rate of uptake was dependent on the size of HA, with 12 kDa HA completely taken up in 30 min and 200 kDa HA requiring 8 to 24 h for complete uptake.

Second, fluorescently-modified HA-Taxol (FITC-HA-Taxol) was synthesized and used to demonstrate cell-specific binding and uptake using flow cytometry and confocal microscopy²³. Third, the selective cytotoxicity of FITC-HA-Taxol allowed direct correlation of uptake with selective cytotoxicity. Fourth, the rapid uptake and selective cytotoxicity of HA-Taxol bioconjugates could be blocked by either excess HA or by an anti-CD44 antibody, but not by CS²². Fifth, the release of free Taxol from HA-Taxol in human plasma or in cell culture media revealed that the free drug was hydrolytically released from the bioconjugate by cleavage of the labile 2' ester linkage²⁵. Taken together, these data support the notion that the targeted cytotoxicity of HA-Taxol bioconjugates requires receptor-mediated cellular uptake of the bioconjugate followed by hydrolytic release of free Taxol. Finally, the addition of 12 kDa HA fragments to a lysosome-targeted poly(HPMA)-adriamycin adduct²⁹ (currently in Phase II clinical trials) increased the selective cytotoxicity of this polymeric prodrug to cancer cells by 10- to 20-fold (Y. Luo, J. Kopecek, G. D. Prestwich, unpublished results). Extension of the cell-based results to efficacy in human tumor xenograft mouse models are in progress.

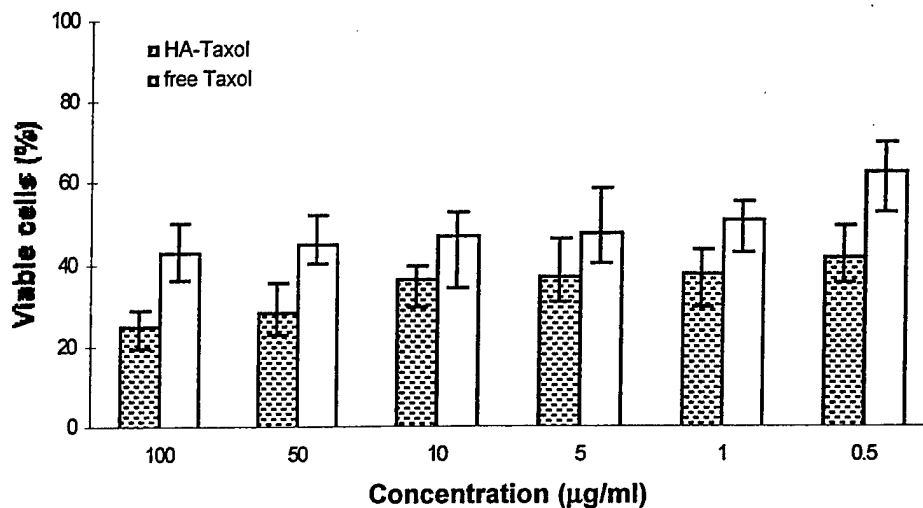


Figure 2. Toxicity of HA-Taxol to HCT-116 cells

Preparation of a flexible, biocompatible HA hydrogel for wound healing and drug release

A new HA hydrogel was prepared under neutral aqueous conditions using a macromolecular crosslinker. This new biocompatible material gels in minutes and, after solvent evaporation, swells from a flexible dry film to a flexible porous hydrogel in seconds. This novel fast-gelling and fast-swelling hydrogel film may prove to be a more acceptable biomaterial than the previously reported HA hydrogels. The chemistry of the crosslinking reaction involves hydrazone formation, which is rapid and occurs at neutral to acidic pH. The hydrogel thus formed can be used directly in virtually any biological system, as both the hydrogel and its two macromonomer components are biocompatible and biodegradable³⁰. It has significant advantages for drug loading in comparison to previously reported HA hydrogels, since alkaline conditions, high temperatures, and small, potentially toxic crosslinkers are not employed during the preparation. The use of this material for drug delivery is summarized elsewhere^{24,31}. Importantly, the same ADH-modification and PEG diald crosslinking techniques are applicable to polyacrylic acid, alginic acid, pectin, and sulfated glycosaminoglycans; thus, a wide spectrum of mechanical and chemical properties may be explored to obtain optimal hydrogels for specific medical applications.

The literature demonstrates that tissue-compatible hydrogels can provide a natural, hydrophilic environment for controlled drug delivery³², and the rate of drug release can be regulated by controlling gel-swelling and crosslinking density. A variety of crosslinked HA hydrogels³³ have been prepared with bisepoxides such as diepoxybutane and ethyleneglycol diglycidylether under strongly alkaline conditions with ethanol as a co-solvent^{34,35}. These crosslinking methods produce HA hydrogel films with water content as low as 60 wt%. Hylan hydrogels are made by treatment of HA containing traces of proteins (partially-purified rooster-comb extract) with formaldehyde to give a soluble gel. Other crosslinkers, e.g., divinyl sulfone, afforded infinite molecular networks^{36,37}. A variety of bis-carbo-diimides³⁸ were employed to crosslink HA and thus produce hydrogels containing bis-*N*-acylurea linkages. Modification with bifunctional hydrazides²⁵ or polyhydrazide crosslinkers also gave crosslinked hydrogels³⁹.

Obtaining HA-derived biomaterials with sufficient strength to withstand biomechanically stressful applications has been problematic. HA derivatives with the best mechanical properties have generally been prepared with highly alkaline crosslinking conditions and at elevated temperatures^{34,35}, conditions that preclude inclusion of sensitive molecules or living cells during preparation of the polymer network hydrogel. Additionally, such reactions employed small molecular crosslinking reagents, often in large excess, which required considerable purification in order to obtain materials for physiological use. The results with our new crosslinked HA and

CS hydrogel films provide impetus to proceed with applications in topical wound healing and prevention of post-surgical adhesions.

Assessing re-epithelialization in a mouse model

Increased wound healing by re-epithelialization was observed in the wound sites covered with HA hydrogel films in comparison to wound sites covered with the commercially available wound dressing material, Biobrane®. Histological examination of tissue biopsies in the control group indicates a large, unhealed wound area (Figure 3a), with little or no epidermal coverage at the surface of the wound site. Magnification (10×) shows the healing edge of the wound site. Covering the wound site with HA (or CS) hydrogel films, followed by protection with Biobrane®, resulted in improved re-epithelialization. The unhealed wound area is significantly smaller than that of the control group (Figure 3b). The magnified image shows new, thick, several cell-layered, epidermal growth covering the wound site. Additionally, neo-dermal tissue has filled in underneath the new epidermis.

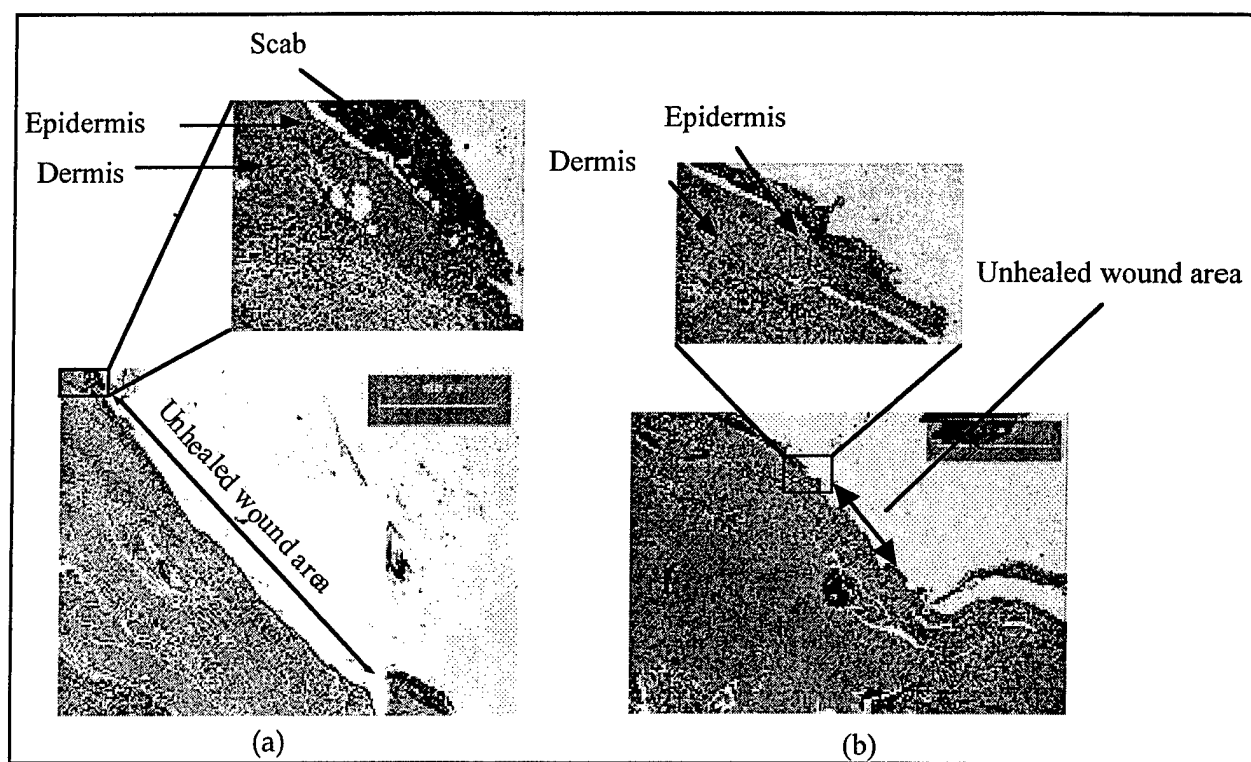


Figure 3. Histological analysis of tissue samples from wound sites covered with Biobrane® (**panel a**) and HA hydrogel film (**panel b**) [scale bar = 1 mm]

Structure of the RHAMM HABD and identification of peptides that bind RHAMM

The secondary structure of RHAMM, an important mediator of cell transformation and signaling¹⁷ and of cell motility⁵, is predicted to be predominantly helical. Indeed, the structure of HABD was recently determined using multidimensional NMR and was found at 3 Å resolution to be a helix-loop-helix with a coiled coil tertiary structure²⁸. This contrasts with the link module of the protein TSG-6⁴⁰ and CD44⁴¹ in which β -sheet secondary structure is predominant. Using murine RHAMM numbering⁴², the N-terminal of the HABD is completely

contained within a loop (residues 531-539), while the second half of the domain (residues 553-562) spans a loop and a helical region. The interaction of HA with HA binding proteins requires both electrostatic interactions between the glucuronate carboxylates and HABD basic residues, as well as hydrophobic interactions involving C-H-rich patches on HA¹¹.

We screened two one-bead, one-peptide libraries⁴³ of 8-mers and a library of phage-displayed 15-mers with the RHAMM-HABD to identify high-affinity peptides that bind to the HABD²⁷. One peptide library was a biased library with alternating acidic amino acids, designed to mimic the natural pattern of alternating glucuronic acid carboxylates found in HA. This is the first reported rational drug design approach for identification of a non-GAG ligand for an HA binding site. Successful identification of such peptide ligands would permit selective targeting of different HA receptors. In addition, the biased library included both natural and unnatural configurations of the acidic residues to further explore possible oligosaccharide conformations that could be important in ligand recognition.

We obtained four principal results. First, recurring peptide motifs that bind to HABDs were identified in both biased and random libraries. These dipeptide and tripeptide motifs could be recognized in both random phage and biased bead-based libraries. Second, two assays were developed to quantify the relative affinity and selectivity of peptide-RHAMM interactions. Selectivity of the peptide ligands for the HABDs was established by (i) detection of binding of biotin- or fluorescein-labeled peptides to immobilized proteins, and (ii) fluorescence polarization of FITC-labeled peptides with HABDs in solution. High-affinity peptides bound only the RHAMM-HABD employed as the bait for screening, and failed to bind with high affinity to link-module-type HABDs. HA competitively displaced peptide-HABD binding, while other glycosaminoglycans were less effective competitors. Third, the importance of including acidic amino acids with unnatural configurations was demonstrated. The absolute stereochemistry of the three highest affinity-biased octapeptides was established by synthesis and binding assays with the 16 stereoisomers of each peptide. A strong preference for alternating D- and L-configurations for the acidic residues was observed, consistent with the predicted orientation of glucuronic acid moieties of HA. Finally, MDA-MB-231 breast cancer cells that overexpress RHAMM bind and internalize fluorescent HA-mimicking peptides, and this uptake was prevented by pre-incubation of cells with HA. This suggests that non-glycosaminoglycan ligands specific for a given HA receptor could be designed to permit targeted drug delivery to a chosen cell population. These results suggest important new uses of HA-mimicking peptides in basic cell biology and in the development of new therapeutic drugs.

CONCLUSIONS

HA covalently modified with hydrazides can be linked to therapeutic agents to provide targeted drug delivery systems. Tumor-specific toxicity was demonstrated with an HA-Taxol adduct. Moreover, HA can be crosslinked to furnish hydrogel films well-suited for drug delivery, cell culture or tissue engineering. The use of a macromolecular bisaldehyde crosslinker resulted in film that accelerated re-epithelialization during wound healing. *In vitro* drug release from this novel biomaterial showed potential for releasing anti-infective or analgesic drugs at wound sites. Finally, the structure of the HABD of RHAMM was determined, illustrating an α -helical HA recognition element quite different from the β -sheet in link protein. The RHAMM HABD was employed to select peptides from random and biased libraries with nanomolar binding affinity specific for this HABD.

ACKNOWLEDGEMENTS

We thank the Center for Biopolymers at Interfaces, The University of Utah, and the U.S. Department of Defense (DAMD17-98-1-8254) for financial support, and Clear Solutions Biotech, Inc. (Stony Brook, NY) for providing HA. New technologies described herein may be licensed from The University of Utah and from Clear Solutions.

REFERENCES

1. Fraser, J. R. E., Laurent, T. C. & Laurent, U. B. G. Hyaluronan: Its nature, distribution, functions and turnover. *J. Intern. Med.* **242**, 27-33 (1997).

2. Dowthwaite, G. P., Edwards, J. C. W. & Pitsillides, A. A. An essential role for the interaction between hyaluronan and hyaluronan binding proteins during joint development. *J. Histochem. Cytochem.* **46**, 641-651 (1998).
3. Collis, L. et al. Rapid hyaluronan uptake is associated with enhanced motility: implications for an intracellular mode of action. *FEBS Lett.* **440**, 444-449 (1998).
4. Hardwick, C. et al. Molecular cloning of a novel hyaluronan receptor that mediates tumor cell motility. *J. Cell Biol.* **117**, 1343-1350 (1992).
5. Cheung, W. F., Cruz, T. F. & Turley, E. A. Receptor for hyaluronan-mediated motility (RHAMM), a hyaladherin that regulates cell responses to growth factors. *Biochem. Soc. Trans.* **27**, 135-142 (1999).
6. Toole, B. P. Hyaluronan in morphogenesis. *J. Intern. Med.* **242**, 35-40 (1997).
7. Gerdin, B. & Hallgren, R. Dynamic role of hyaluronan (HYA) in connective tissue activation and inflammation. *J. Intern. Med.* **242**, 49-55 (1997).
8. Prestwich, G. D., Marecak, D. M., Marecek, J. F., Vercruysse, K. P. & Ziebell, M. R. in *The Chemistry, Biology, and Medical Applications of Hyaluronan and its Derivatives* (ed. T. C. Laurent) pp. 43-65 (Portland Press, London, 1998).
9. Prestwich, G. D. & Vercruysse, K. P. Therapeutic applications of hyaluronic acid and hyaluronan derivatives. *Pharmaceut. Sci. & Technol. Today* **1**, 42-43 (1998).
10. Vercruysse, K. P. & Prestwich, G. D. Hyaluronate derivatives in drug delivery. *Crit. Rev. Therapeut. Carrier Syst.* **15**, 513-555 (1998).
11. Day, A. & Prestwich, G. D. Hyaluronan binding proteins: structure and regulation. *J. Biol. Chem.*, in press (2000).
12. Day, A. J. The structure and regulation of hyaluronan-binding proteins. *Biochem. Soc. Trans* **27**, 115-121 (1999).
13. Mignatti, P., Welgus, H. G. & Rifkin, D. B. in *The molecular and cellular biology of wound healing* (eds. Clark, R. A. F. & Henson, P. M.) (Plenum Press, New York, 1988).
14. Turley, E. A. in *The Biology of Hyaluronan* (ed. Foundation, C.) 121-137 (J. Wiley & Sons, Ltd., Chichester, UK, 1989).
15. Weigel, P. H., Fuller, G. M. & LeBoeuf, R. D. A model for the role of hyaluronic acid and fibrin in the early events during the inflammation response and wound healing. *J. Theor. Biol.* **119**, 219-234 (1986).
16. West, D. C., Hampson, I. N., Arnold, F. & Kumar, S. Angiogenesis induced by degradation products of hyaluronic acid. *Science* **228**, 1324-1326 (1991).
17. Entwistle, J., Hall, C. L. & Turley, E. A. Receptors: regulators of signalling to the cytoskeleton. *J. Cell Biochem.* **61**, 569-577 (1996).
18. Gustafson, S. in *The Chemistry, Biology, and Medical Applications of Hyaluronan and its Derivatives* (eds. Laurent, T. C. & Balazs, E. A.) 291-304 (Portland Press, UK, 1997).
19. Mason, M. et al. Attachment of hyaluronic acid to polypropylene, polystyrene, and polytetrafluoroethylene. *Biomaterials* **21**, 31-36 (2000).
20. Prestwich, G. D., Marecak, D. M., Marecek, J. F., Vercruysse, K. P. & Ziebell, M. R. Controlled chemical modification of hyaluronic acid: Synthesis, applications, and biodegradation of hydrazide derivatives. *J. Controlled Rel.* **53**, 93-103 (1998).
21. Pouyani, T. & Prestwich, G. Functionalized derivatives of hyaluronic acid oligosaccharides: drug carriers and novel biomaterials. *Bioconjugate Chem.* **5**, 339-347 (1994).
22. Luo, Y. & Prestwich, G. D. Synthesis and selective cytotoxicity of a hyaluronic acid-antitumor bioconjugate. *Bioconjugate Chem.* **10**, 755-763 (1999).
23. Luo, Y., Ziebell, M. R. & Prestwich, G. D. A hyaluronic acid-Taxol antitumor bioconjugate targeted to cancer cells. *Biomacromolecules* **1**, 208-218 (2000).
24. Luo, Y., Kirker, K. R. & Prestwich, G. D. Crosslinked hyaluronic acid hydrogel films: New biomaterials for drug delivery. *J. Controlled Rel.*, in press (2000).
25. Pouyani, T., Harbison, G. & Prestwich, G. Novel hydrogels of hyaluronic acid: Synthesis, surface morphology, and solid-state NMR. *J. Am. Chem. Soc.* **116**, 7515-7522 (1994).
26. Hall, C. L. et al. Overexpression of the hyaluronan receptor RHAMM is transforming and is also required for H-ras transformation. *Cell* **82**, 19-28 (1995).
27. Ziebell, M. R. et al. Peptides that mimic glycosaminoglycans: high affinity ligands for a hyaluronic acid binding domain. *Chem. & Biol.*, submitted (2001).
28. Ziebell, M. R. Ph.D. Dissertation, Ligand Binding and Structural Characterization of a Recombinant Hyaluronic Acid, The University at Stony Brook, 2000.

29. Minko, T., Kopecekova, P. & Kopecek, J. Comparison of the anti-cancer effect of free and HPMA copolymer bound adriamycin in human ovarian carcinoma cells. *Pharm. Res.* **16**, 986-996 (1999).
30. Zhong, S. P. et al. Biodegradation of hyaluronic acid derivatives by hyaluronidase. *Biomaterials* **15**, 359-365 (1994).
31. Luo, Y., Kirker, K. R. & Prestwich, G. D. in *HA2000* in press (Woodhead Publishing Ltd., Abington, UK, 2000).
32. Kim, S.-W., Bae, Y. H. & Okano, T. Hydrogel: Swelling, drug loading and release. *Pharm. Res.* **9**, 283-290 (1992).
33. Laurent, T. C., Hellsing, K. & Gelotte, B. Cross-linked gels of hyaluronic acid. *Acta Chem. Scand.* **18**, 274-275 (1964).
34. Yui, N., Okano, T. & Sakurai, Y. Inflammation responsive degradation of crosslinked hyaluronic acid gels. *J. Controlled Rel.* **22**, 105-116 (1992).
35. Tomihata, K. & Ikada, Y. Preparation of cross-linked hyaluronic acid films of low water content. *Biomaterials* **18**, 189-195 (1997).
36. Larsen, N. E., Leshchiner, E. A., Parent, E. G. & Balazs, E. A. in *Cosmetic and Pharmaceutical Applications of Polymers* (ed. Gebelein, C. G.) 147-157 (Plenum Press, New York, 1991).
37. Shah, C. B. & Barnett, S. M. Hyaluronic acid gels. *ACS Symposium Series* **480**, 116-308 (1991).
38. Kuo, J.-w., Swann, D. A. & Prestwich, G. D. Chemical modification of hyaluronic acid by carbodiimides. *Bioconjugate Chem.* **2**, 232-241 (1991).
39. Vercruysse, K. P., Marecak, D. M., Marecek, J. F. & Prestwich, G. D. Synthesis and *in vitro* degradation of new polyvalent hydrazide cross-linked hydrogels of hyaluronic acid. *Bioconjugate Chem.* **8**, 686-694 (1997).
40. Kohda, D. et al. Solution structure of the link module: a hyaluronan-binding domain involved in extracellular matrix stability and cell migration. *Cell.* **86**, 767-775 (1996).
41. Bajorath, J., Greenfield, B., Munro, S. B., Day, A. J. & Aruffo, A. Identification of CD44 residues important for hyaluronan binding and delineation of the binding site. *J. Biol. Chem.* **273**, 338-343 (1998).
42. Entwistle, J. et al. Characterization of the murine gene encoding the hyaluronan receptor RHAMM. *Gene.* **163**, 233-238 (1995).
43. Lam, K. S. Application of combinatorial library methods in cancer research and drug discovery. *Anticancer Drug Des.* **12**, 145-167 (1997).

Peptides that Mimic Glycosaminoglycans:
High Affinity Ligands for A Hyaluronan Binding Domain

Michael R. Ziebell^{‡,†,*}, Zhan-Gong Zhao[‡], Bai Luo[∞],
Yi Luo[‡], Eva A. Turley[§], and Glenn D. Prestwich^{‡,@,¶}

[†]Department of Physiology and Biophysics, The University at Stony Brook,
Stony Brook, New York 11794-8661

[‡]Department of Medicinal Chemistry, The University of Utah,
30 South 2000 East, Room 201, Salt Lake City, Utah 84112-5820

[§]London Regional Cancer Centre, Cancer Research Laboratories, Department of Oncology
790 Commissioners Road East, London, Ontario N6A 4L6 Canada

[∞]Huntsman Cancer Institute, 2000 Circle of Hope, Room LL376,
The University of Utah, Salt Lake City, Utah 84112-5550

[@]Center for Cell Signaling, 421 Wakara Way, Suite 360,
Salt Lake City, Utah 84108

Running Title: Peptide Mimics of Hyaluronan

* Current address: Department of Neurobiology, Harvard Medical School, 220 Longwood Avenue,
Boston, Massachusetts 02115

¶ To whom all correspondence should be addressed:
Department of Medicinal Chemistry
The University of Utah
30 South 2000 East, Room 201
Salt Lake City, Utah 84112-5820
Phone: 801 585 9051; **fax:** 801 585-9053
E-mail: gprestwich@deans.pharm.utah.edu

Background: Hyaluronan (HA) is a non-sulfated glycosaminoglycan (GAG) that promotes motility, adhesion, and proliferation in mammalian cells, as mediated by cell-surface HA receptors. We sought to identify non-carbohydrate ligands that would bind to and activate cell-surface HA receptors. Such analogs could have important therapeutic uses in the treatment of cancer, wound healing, and arthritis, since such ligands would be resistant to degradation by hyaluronidase (Hase).

Results: Peptide ligands that bind specifically to the recombinant HA binding domain (BD) of the **R**eceptor for **H**yAluronan **M**ediated **M**otility (RHAMM) were obtained by screening two peptide libraries: (i) random 8-mers and (ii) biased 8-mers with alternating acidic side chains, i.e., XZXXZXXZ (X = all L-amino acids except Cys, Lys, or Arg; Z = D-Asp, L-Asp, D-Glu, or L-Glu). Selectivity of the peptide ligands for the HABD was established by (i) detection of binding of biotin- or fluorescein-labeled peptides to immobilized proteins and (ii) fluorescence polarization of FITC-labeled peptides with the HABD in solution. HA competitively displaced binding of peptides to the HABD, while other GAGs were less effective competitors. The stereochemistry of four biased octapeptides was established by synthesis of the 16 stereoisomers of each peptide. Binding assays demonstrated a strong preference for alternating D and L configurations for the acidic residues, consistent with the calculated orientation of glucuronic acid moieties of HA.

Conclusions: Two classes of Hase-resistant peptide mimetics of HA were identified with high affinity, HA-competable binding to the RHAMM HABD. This demonstrated that non-HA ligands specific to a given HA binding protein could be engineered, permitting receptor-specific targeting.

Abbreviations Footnote

¹The abbreviations used are:

bHA, biotinylated hyaluronic acid; **BCIP**, 5-bromo-4-chloro-3-indolyl phosphate; **BD**, binding domain; **CS**, chondroitin sulfate; **EDCI**, 1-[3-(dimethylamino)propyl]-3-ethylcarbodiimide hydrochloride; **Erk1**, extracellular signal-regulated protein kinase; **FAK**, focal adhesion kinase; **Fmoc**, 9-fluorenylmethoxycarbonyl; **FP**, fluorescence polarization; **GAG**, glycosaminoglycan; **GnHCl**, guanidinium hydrochloride; **GPI**, glycosyl phosphatidyl inositol; **GST**, glutathione-S transferase; **HA**, hyaluronic acid or hyaluronan; **HABD**, hyaluronic acid binding domain; **Hase**, hyaluronidase; **HBTU**, (*o*-benzotriazol-1-yl-*N,N,N',N'*-tetramethyluronium hexafluorophosphate); **HOBt**, 1-hydroxybenzotriazole; **PBS**, phosphate-buffered saline; **PEG**, polyethylene glycol; **mP**, millipolarization units; **PVP-40**, polyvinyl pyrrolidone; **RHAMM**, receptor for hyaluronan mediated motility; **SA-HRP**, streptavidin-horseradish peroxidase; **TBS**, Tris-buffered saline; **TMB**, 3,3',5,5'-tetramethylbenzidine.

INTRODUCTION

The extracellular matrix polysaccharide hyaluronan [β -1,4-GlcUA- β -1,3-GlcNAc] $_n$ (hyaluronic acid, or simply HA¹) is a non-sulfated glycosaminoglycan (GAG) that promotes cell motility, adhesion, and proliferation in mammalian cells [1], thereby playing roles in morphogenesis [2], wound healing [3] and metastasis [4]. These functions are mediated by cell-surface HA receptors, which initiate key cell signaling cascades when activated by HA, leading to physiological changes [4]. Non-carbohydrate ligands that would bind to and activate cell-surface HA receptors could have important therapeutic uses in the treatment of cancer, wound healing, and arthritis, since such ligands would be resistant to degradation by hyaluronidase (HAse). To this end, two peptide libraries were prepared and screened to identify high-affinity ligands for the HA receptor RHAMM (Receptor for HyAluronan Mediated Motility).

RHAMM mediates cell migration and proliferation in many normal cells and in tumor cell-lines [5]. Isoforms of RHAMM are functionally active both in the cytoplasm and on the cell surface [4]. The extracellular forms of RHAMM appear to act as co-receptors, which modulate signaling through integral receptors, such as the PDGF receptor [6-8]. RHAMM requires the small GTPase p21 ras and pp60 src to promote motility [8,9]. A target of src-regulated phosphorylation is focal adhesion kinase (FAK) (pp125^{FAK}), which is an important integrin binding protein. Phosphorylation of FAK leads to focal adhesion turnover, a critical step in cell locomotion [10].

RHAMM occurs naturally as a functional HA receptor in primary human endothelial cells [11] and is overexpressed as several isoforms in human tumors and tumor cell-lines including colorectal [12], breast [13,14], pancreatic [15], and multiple myeloma [16]. A dominant negative mutant of RHAMM, possessing a non-functional HABD, can block cell transformation by mutant active ras. Furthermore, overexpression of one RHAMM isoform constitutively activates the kinase erk1 [7] and is transforming in fibroblasts [10]. RHAMM occurs as an intracellular protein but can be expressed on the cell surface, a condition observed most often in single cells such as

leukocytes [17,18] and in subconfluent fibroblasts [7]. Cell-surface RHAMM binds to extracellular HA and the HA-RHAMM complex undergoes receptor-mediated endocytosis [19]. Intracellular RHAMM binds to cytoskeletal proteins [20] and associates with proteins in the erk kinase cascade [7].

Mutational analysis of RHAMM identified two regions near the C-terminus that are required for full HA binding [21]. These regions have clusters of basic residues and have a so-called BX₇B motif (B = basic residue, X = any non-acidic residue) present in several HA binding proteins [22]. Synthetic peptides representing the RHAMM domains inhibit HA binding to full length RHAMM, while peptides representing other parts of the primary sequence fail to inhibit binding [21]. RHAMM has one of the highest density of basic residues of any HA receptor. CD44 and other link module-containing proteins may have the BX₇B motif, but these HABDs are architecturally and functionally distinct [23]. Although RHAMM is known to bind heparin at the same binding site as HA [24], no other GAGs have been reported to bind to RHAMM with high affinity.

The secondary structure of RHAMM is predicted to be predominantly helical. The structure of the HABD was recently studied using multi-dimensional NMR and was observed at 3 Å resolution to be a helix-loop-helix with a coiled-coil tertiary structure [25]. This contrasts with the beta-sheet containing link module of the protein TSG-6 [26,27]. Using RHAMM numbering [28], the N-terminal of the HABD is completely contained within a loop (residues 531-539), while the second half of the domain (residues 553-562) spans a loop and a helical region. The interaction of HA with HABDs requires both electrostatic interactions between the glucuronate carboxylates and basic residues of the protein, as well as potential hydrophobic interactions involving methine patches on HA [27].

In this study, two synthetic peptide libraries, one composed of random octapeptides and one containing alternating acidic and non-acidic residues, were examined for potential non-GAG ligands for the HABD. These one-bead, one-peptide libraries [29] were screened with the RHAMM-HABD in order to identify high-affinity peptides for the HABD. The biased acidic

library was designed to mimic the natural pattern of alternating glucuronic acid carboxylates present in HA; this represents the first rational approach to identification of a non-GAG ligand for an HA binding site. Importantly, this library included both natural and unnatural configurations of the acidic residues to further explore possible oligosaccharide conformations that could be important in ligand recognition.

This paper will present three major results. First, recurring peptide motifs that bind to HABDs were identified in both biased and random libraries. Second, solid-phase binding and fluorescence polarization (FP) assays were developed to quantify the relative affinity and selectivity of peptide-RHAMM interactions. Third, the importance of including acidic amino acids with unnatural configurations was demonstrated. A molecular model based on minimized structures of the active enantiomeric peptides suggested that the staggered carboxylate orientation relative to the peptide backbone is similar to the carboxylate orientation in HA.

RESULTS

Initial Library Screening

A solid-phase method was employed to confirm that RHAMM HABD-containing proteins would bind to biotinylated HA (bHA), based on earlier methods used for bHA-HABD studies [30,31]. To this end, a dot blot of purified glutathione-S transferase (GST)-RHAMM(518-580), GST, and RHAMM(518-580) on PVDF membrane was employed, since the highly-basic, small RHAMM(518-580) polypeptide itself failed to electrotransfer to PVDF. GST-RHAMM(518-580) and RHAMM(518-580) bound bHA, but neither GST alone nor BSA bound bHA (data not shown). Comparison of electrotransferred proteins on PVDF with electrophoretically separated GST-RHAMM(518-580) and thrombin-cleaved GST-RHAMM(518-580) (only GST remained) showed that the fusion protein could be detected with bHA (data not shown) while GST alone could not. Similarly, thrombin cleavage of GST-RHAMM(518-580) in a 96-well plate released the HABD, which was detected using a dot blot. These control experiments validated the use of thrombin digestion for the early rounds of phage screening in which positive phage bound to RHAMM(518-580) were eluted by cleavage of the linker to the immobilized GST domain.

Two eight-amino acid libraries were synthesized on 100- μ m Tentagel beads and screened using GST-RHAMM(518-580) as the HABD. Library **R** contained completely random sequences of 19 L-amino acids (excluding Cys), while Library **B** consisted of alternating acidic residues in an *XXZZXXZZ* pattern. For Library **B**, the acidic (Z) residues were allowed to have either the natural L or unnatural D absolute configuration. The synthesis generated three million beads for each library; typically, an aliquot of ca. 100,000 beads was used for each screen. The number of beads was determined by the practical limits of the experimental approach, and by the calculation that this number should adequately represent the dipeptide or tripeptide motifs that were anticipated in an octapeptide population. Thus, starting with 100,000 beads, approximately 30 positive "blue" beads were identified after three rounds of screening. The final round of screening included a competition step with HA to block peptide binding to the HABD; positive beads in this step were "white."

Table 1 also summarizes the peptides directly sequenced following screening of Libraries **R** and **B** with GST-RHAMM(518-580). Approximately half of the positive beads were sequenced, and of these, 20% of the sequencing attempts failed for technical reasons. A single "white" bead from the first screening was selected as a negative control; peptide **NB** had the sequence IDSDWEGE.

Deconvolution of Library B Hits

Since Library **B** was synthesized with either the D- or L-isomers at the alternating acidic residues, it was necessary to deconvolve the particular combination of natural and unnatural amino acids in each positive hit. Solid-phase synthesis on each bead created one of 16 possible diastereoisomers of a given "letter" sequence, corresponding to a total of two enantiomers at each of four positions. Using automated Edman degradation for peptide sequencing, the chirality of the PTH amino acid sequenced at any given cycle could be determined. Prior to micromole-scale synthesis of peptides to determine binding affinities, the diastereomeric ambiguity was first resolved by construction of a mini-library of the 16 individual diastereomers of the Library **B** peptides. This peptide mini-library was constructed as an array of spots on cellulose membrane (Pepspots®), in which each spot contained a single diastereomer of the Library **B** peptide letter-sequence (3-5 nmol/spot). The membrane mini-library was prepared commercially, and consisted of an array of 72 spots: 16 diastereomers of peptides **B-1**, **B-2**, **B-3**, and **B-4**, four negative control spots (using the sequence of a non-binding negative control, IDSDWEGE), and four spaces between each set of 16 diastereomers.

GST-RHAMM(518-580) binding to the Pepspots® mini-library was carried out by semi-dry transfer in order to permit use of the original membrane for multiple protein-stripping and reprobing experiments. Thus, GST-RHAMM(518-580) was incubated with the blocked Pepspots® membrane and specifically-bound protein was transferred to a PVDF membrane. Bound GST-RHAMM(518-580) was detected using goat anti-GST, followed by anti-goat-IgG horseradish peroxidase (HRP) conjugated antibodies. Binding was visualized and quantified (Figure 1) with a chemiluminescent HRP substrate. These data allowed selection of specific

diastereomers of Library **B** peptides to analyze binding of a single homogeneous species rather than a diastereomeric mixture. Four pairs of diastereomers with ca. 100-fold binding differences were synthesized and used as described below to measure binding affinities for the RHAMM HABD (see Table 2).

The data in Figure 1 illustrate that peptide diastereomers containing only L-Glu and L-Asp do not exhibit the optimal affinity. This most likely reflects the importance of the orientation of the carboxylate-containing side chains. With a combination of D- and L-amino acids in a single peptide, the structures with carboxylates on alternating "sides" of the peptide more closely imitate the orientation of the glucuronate carboxylates in HA. The B1, B3 and B4 series demonstrate this clearly, in that the all-L-peptide exhibits no observable binding. The all-L peptide in B2 bound with lower affinity than diastereomers containing a single D-Asp or D-Glu residue. This suggests that one component of binding is derived from the hydrophobic repeats as well as charge orientation. Similarly, the aromatic residue-rich B3 peptides showed robust binding to the HABD, as favored by the "opposite side" carboxylate orientation. Hydrophobic and aromatic-rich patches on HA have been implicated in HA structure [32,33] and in HA-HABD interactions [23,34].

Affinities of Peptides for RHAMM HABD

Three microplate binding assays were employed to measure the affinity of synthetic peptides for RHAMM(518-580): ELISA, a fluorescence-based analog of the ELISA, and FP. The ELISA required a biotinylated peptide, while both the fluorescence-based solid-phase and the FP assays required a fluorophore-modified peptide. Thus, two thiol-reactive maleimide reporter groups were used, requiring an N-terminal cysteine for probe attachment. For competition assays with probe-modified peptides or bHA, peptides lacking the Cys residue were also required. These were conveniently prepared by removal of half of the synthetic peptide from the synthesizer prior to addition of the final Cys residue. Synthetic peptides from each sub-group of similar peptides of Library **R** were prepared (see Table 1). For Library **B**, each of the four positive peptides containing both D- and L-acidic residues, as identified by the Pepspots® deconvolution experiment, were synthesized.

The binding affinities of the synthetic peptides were measured with the ELISA method as described in the experimental methods, and K_D values were determined mathematically [35]. In a typical experiment, the K_D for a given biotinylated peptide was determined using successive fivefold dilutions of probe and using a fixed amount of immobilized protein. Experiments were performed in triplicate with background (no protein) subtraction prior to calculations. The stoichiometry of binding was determined using a standard curve of streptavidin (SA)-HRP serial dilutions. For example, **R-3**, one of the highest affinity random peptides, had a K_D value of 48 nM with a 1:1 binding ratio; biased peptide **B-2A** had a K_D value of 8 nM. The binding affinities are summarized in Table 2.

Domain Selectivity and Competitive Displacement of Peptide Binding by GAGs

The ELISA was modified to address selectivity of binding. Thus, a domain selectivity and a GAG competition assay were each conducted using a modification of the solid-phase ELISA that allowed use of fluorescein-labeled peptides. Although the data from this modification are less accurate for absolute quantitation, a lower background could be achieved as compared to the SA-HRP ELISA method. First, we demonstrated that RHAMM HABD, not the GST fusion partner, was responsible for peptide binding. Peptides from the two libraries were evaluated. Figure 2 illustrates that the majority of peptides show negligible binding to the GST domain. It is possible that the fluorophore modification could increase the nonspecific binding beyond that detected in the original library screening protocols.

Second, we evaluated the effectiveness of several GAGs to inhibit binding of synthetic peptides to the HABD of RHAMM. HA was used as a competitor for all synthetic peptides, and other GAGs were evaluated with a subset of peptides. Fluorescein-labeled peptides representing each of the libraries were added to ELISA plates containing immobilized GST-RHAMM(518-580) that had been pre-incubated with 4 - 40 kDa HA, and washed to remove excess ligand. Figure 3a shows the competitive displacement of peptide binding to GST-RHAMM(518-580) by HA for six selected peptides. In all but one instance, 0.1 mg/ml of the 4 - 40 kDa HA provided optimal competition of the peptide. For the highest-affinity peptide **B-2A**, 1 mg/ml of 4 - 40 kDa HA was necessary to

compete for peptide binding. Figure 3b illustrates the relative competitive displacement by HA and three sulfated GAGs for four selected peptides; in this ELISA assay, the biotinylated peptides were employed in conjunction with the SA-HRP reporter system. The data in Figure 3b show an overall higher background than those in Figure 3a as a result of additional nonspecific interactions from the secondary ELISA detection system. The nonspecific interactions of both HA and CS with bovine serum albumin are well known [36] [37]. The colorimetric detection system was used for experiments in Figure 3b rather than fluorescence to be consistent with the binding assay used for the majority of the peptide binding. The differences in competition between CS-A and CS-C are noteworthy, since these 4-sulfate (CS-A) and 6-sulfate (CS-C) regioisomers of CS interact differently with different HA binding proteins [14,38-40]. Preliminary data from our laboratories indicated that CS-A showed modest, but higher affinity to RHAMM than CS-C.

FP Assays to Verify Solid-Phase Binding Results

The data from the solid-phase binding assays were supplemented by a second methodology. FP measures the change in anisotropy of a fluorescent probe in free and bound states [41-43]. An increase in anisotropy is proportional to the ligand-protein complex formation; this assay is independent of fluorescence intensity. Using a fixed concentration of each fluorescein-labeled peptide, increasing concentrations of the RHAMM-HABD were added to a 96-well plate optimized for low-background fluorescence measurements. The concentrations were chosen so that the measurements span the range from $0.01 \times K_D$ to $100 \times K_D$. Figure 4 illustrates the primary data for peptides **B-1A** (17 ± 5 nM), and **B-4B** (220 ± 58 nM), which showed affinities of 49 nM and 499 nM, respectively, in the ELISA assay. This correlation validated the FP assay for use in measuring peptide-protein interactions for HA-mimicking peptides. However, due to the multivalent nature and viscosity-altering properties of HA, it was not practical to use the FP assay for competitive displacement experiments.

DISCUSSION

The importance of RHAMM in cell motility and metastatic progression [12,13] provided the impetus to identify potential non-GAG ligands that could serve as HAse-resistant HA surrogates in basic research and as leads for drug design. We sought ligands that could specifically target the HABD of RHAMM but would not be recognized by other hyaladerins such as CD44 and link protein. We reasoned that peptide mimics can explore conformations and chemical functionalities unavailable to natural GAG ligands. Consequently, peptide mimics could achieve novel selectivities for binding to, and activation of, different HA receptors. To this end, two peptide libraries were screened using the HABD of RHAMM as bait for octapeptides with high affinity and selectivity. Both libraries afforded high-affinity ligands that acted as HA surrogates, as determined by three *in vitro* binding assays. Library **B**, which contained alternating acidic residues, was inspired by the alternating pattern of glucuronic acid and N-acetylglucosamine that characterizes the linear HA structure. Moreover, we anticipated that nucleophile-rich residues would be commonly found in the HA-mimetic peptides identified by this screen. In contrast, we identified common motifs in which hydrophobic residues predominated in Library **R**, a bead-based library of random octamers. This unexpected result was nonetheless consistent with the observation that HA can interact with aromatic-rich patches on another HA binding protein, the link module of human TSG-6 [34]. Thus, the two different peptide libraries provided both rational and unbiased approaches to ligand identification.

The Random Bead Library Has Tripeptide Motifs

Three recurring dipeptide or tripeptide motifs were noted in library **R**: (i) the PV Ψ motif, where Ψ is F or Y, was present in **R-7** and **R-3**; (ii) the QAM motif was present in **R-5** and in retrograde form in **R-10**; and (iii), the P Ψ /YP dipeptide sequence was found in **R-1**, **R-11**, and **R-12** (Table 3). Of these random library-derived ligands, the peptide with the highest affinity for

RHAMM(518-580) was **R-3** (EGEWPVYP) with an apparent K_D value of 48 nM. Interestingly, the negative control peptide **NB** (IDSDWEGE) shared the EGE tripeptide, which thus appeared not to participate in binding; this provided additional support for the importance of the PVY motif in binding to RHAMM. Moreover, **R-3** contained a PYYP motif, which could further enhance the affinity of this peptide.

Since the structure of the RHAMM(518-580) showed the HABD to be a surface-exposed domain [25], peptide binding could be governed by a short motif; this would account for the sequence diversity within the peptide ligands identified. In addition, differences in solubility and elements of secondary structure could affect relative binding affinities. It is surprising that few peptides were represented in both libraries. Only one Library **R** peptide showed the acidic-X-acidic motif imposed synthetically on the Library **B**, and in that example, the EGE may not even be important for binding. The results from the Library **B** peptides and the importance of alternating absolute configurations of the acidic side chains can account for this apparent paradox, as described below.

The PYYP motif also occurred in peptides screened with the link module-containing HA-binding protein TSG-6 [26]. TSG-6 is a 275-amino acid secretory protein involved in cell-cell and cell-matrix interactions during inflammation [44], and a three-dimensional solution structure of the HA-binding link module has been determined by NMR [26]. None of the peptides obtained with this structurally different "bait" protein bound to GST-RHAMM(518-580), and these data will be presented in due course (M.R. Ziebell, A.J. Day, and G.D. Prestwich, unpublished results).

Precedent for Alternating Charged D- and L-Amino Acids in the Biased Library

The rationale for synthesizing Library **B** with alternating acidic amino acids was to mimic the alternation of glucuronic acids of HA, in both the linear and three-dimensional distribution of charge. The glucuronic acid moieties of HA are separated by approximately 10 Å [45], with a dihedral angle between -110° and -167°, indicating that they protrude from opposite faces of a plane that approximates the linear sequence of sugars. Since these charge repeats appear to be

important in HA – protein interactions, Library **B** was designed to detect peptides with alternating carboxylates with high affinity for RHAMM-HABD. To this end, Library **B** was prepared with either D- or L-enantiomers of Glu or Asp in the acidic residue position.

A non-optimized model of a random coil peptide suggested that alternating acidic residues should give a pattern of negative charges separated by approximately 10 Å. A model was thus constructed based on diastereomers discovered from the library screen. The peptides **B-2** (YDSEYESE) and **B-2B** (YDSEYeSE) were modeled using InsightII (Molecular Simulations, Inc.). From a family of ten conformers, each minimized and subjected to a routine molecular dynamics protocol, a marked difference in the orientation of the acidic side chains was apparent (Figure 5). The average distance between Glu4 HE2 and Glu6 OE1 for **B-2** was 6.11 ± 1.72 Å, while for **B-2B** this distance was 12.56 ± 1.47 Å. The averages of the absolute value of the dihedral angles between Glu4 and Glu6 side chains was $41.9 \pm 29.6^\circ$ for **B-2** and $129.5 \pm 44.2^\circ$ for **B-2B**. These parameters suggest that a peptide with alternating acidic residues, one with D configuration and one with L configuration, should most closely mimic HA. The results of this series of minimizations is graphically represented in Figure 5, where each point represents the minimized distance between the two protons. Figure 6 illustrates three structures obtained from the molecular modeling experiments. Coordinates for HA (Figure 6, top) were obtained from the Protein Databank (accession no. 4HYA) [45] with the glucuronic acid sugar residues highlighted. The calculated structures for the all L-configuration octapeptide **B-2** (center) and the peptide with a single D-configuration side chain **B-2B** (bottom) showed the distance and angular relationships between acidic side chains. In the minimum energy conformer for **B-2**, these constants poorly imitated HA; in contrast, the minimum energy conformer for **B-2B** more adequately approximated the spatial and angular measurements of an HA oligosaccharide.

The Biased Library Favors Unnatural Acidic Residues

A number of high-affinity "hits" were sequenced from beads in Library **B**. However, even though each hit was a unique molecular species, the Edman degradation could not provide

information on the absolute configuration of the particular linear sequence obtained. Thus, each sequence represented sixteen possible molecular structures. Deconvolution was accomplished by synthesis of each of the sixteen diastereomers of three Library **B** peptides using the commercial Pepspots® technology. The strongest binding peptides from the biased library were specific diastereomers of peptide **B-1** (MdYEPeQe, peptide **B-1A**) and **B-2** (YDSeYeSe, peptide **B-2A**); D-amino acids are indicated with lower case letters. Peptides with alternating D- and L-acidic residues showed the highest affinity. The "anti" relationship appeared to most closely reflect the angular orientation of carboxylates on HA, consistent with the model used to design these HA mimetic peptides. In Library **B**, we deliberately created a pattern of charges within each octapeptide. While many octapeptides bound with high affinity to the RHAMM HABD, charge distribution was not the only factor dictating binding affinity, as previously observed for Library **R** peptides.

Small aromatic residues (Tyr or Phe) and Ser residues were abundant in Library **B**, e.g., **B-2** (YDSEYESE) and **B-3** (FDFDSEYE). The aromatic residues may mimic the putative hydrophobic patches of HA. In peptides with alternating D- and L-acidic side chains as well as Tyr, Phe, or Ser (e.g., peptide **B-3A**, FDFdSEYe), the random coil conformation predicts that the polar and nonpolar side chains would be oriented at a 180° dihedral angle. The formation of a hydrophobic surface consisting of two phenyl rings could reflect the conformation of HA in which the eight methines on the hydrophobic face span three sugar residues. Modeling of these peptides into a three-dimensional model of RHAMM is in progress [25].

In summary, a fusion protein was generated that contains a 62-amino acid polypeptide comprising the HABD of RHAMM [46]. This RHAMM construct was shown to have HA binding activity and the purified protein had defined secondary and tertiary structures [25]. Using this HABD as "bait," two peptide libraries were screened for molecules that specifically target the HABD of RHAMM. Several of the peptide hits that were identified and sequenced were then synthesized and evaluated to determine their affinity and specificity in binding to RHAMM. Many of these peptides bound to RHAMM with high affinity, and competition by HA or other GAGs suggested that the peptides were directed to the HABD.

SIGNIFICANCE

We have identified two classes of HAse-resistant peptide mimetics of HA that exhibit high affinity, HA-competable binding to RHAMM, a receptor important in cell motility, adhesion, and proliferation and implicated in the pathology of cancer. These peptides may serve as antagonists that could block the transforming potential of RHAMM. In related work, we also identified a number of 15-mer peptides by phage display that bind with high affinity to RHAMM(518-580) and affect cell physiology and erk1-RHAMM interactions [47]. Analogously, phage-derived peptides that bound the CTLA4 receptor were found to activate T-cells [48].

Peptides that mimic HA could also be useful for drug targeting. The problem of directing anti-cancer agents to tumors remains one of the technological barriers to developing effective therapies for cancer treatment [49]. The overexpression of RHAMM on cancer cells relative to normal epithelial cells provides an opportunity for tumor-specific drug targeting. HA-conjugated anti-tumor agents [50] and other drugs [51] often lack specificity for a particular class of HA receptors.

Either as therapeutics or targeting moieties, HA-mimetic peptides offer several unique properties. First, the peptides are resistant to HAse degradation. Second, peptides can act as antagonists rather than agonists. Third, peptides can be selected that would not be recognized by liver endothelial cell receptors involved in HA clearance from circulation [52]. Fourth, peptides could be selected to be specific for RHAMM isoforms or CD44 isoforms present in pathological situations.

MATERIALS AND METHODS

Sub-cloning of RHAMM(518-580) into PGEX-2T -- The RHAMMv4 cDNA in a pCRII vector [10] was used as a template for PCR production of the RHAMM constructs.

Sequence-specific primers encoded restriction sites to permit ligation of PCR products into the appropriate vectors. Thus, the RHAMM(518-580) PCR product was digested, purified, and ligated directly into PGEX-2T (Pharmacia) using unique *Eco*R1 and *Bam*H1 restriction sites. Initial ligation of PCR products into a PGEM-T vector (Novagen) improved the ligation efficiency. Plasmid and PCR insert purification followed standard protocols, and DNA was purified by either phenol chloroform extraction [53] or with Qiagen columns.

Purification of GST Fusion Protein -- GST-RHAMM(518-580) (R D S Y A Q L L G H Q N L K Q K I K H V V K L K D E N S Q L K S E V S K L R S Q L V K R K Q N E L R L Q G E L D K A L G I R) [28,46], with BX₇B motifs underlined, was expressed in BL21 *E. coli* cells in ampicillin-containing media by induction with IPTG (2 mM). Cells were harvested by centrifugation at $2,000 \times g$ for 30 min, resuspended in phosphate-buffered saline (PBS) with 30 μ g/ml leupeptin and 1 mM PMSF, and lysed using a French press at 20,000 psi. TX-100 (1% final concentration) was added to the lysate, incubated on ice for 30 min, and centrifuged at $12,000 \times g$ for 30 min. The brown supernatant was applied to 10 ml of glutathione Sepharose equilibrated in PBS at 4 °C, the column was washed with 15-20 ml of PBS at 1 ml/min, and the GST-RHAMM(518-580) was eluted with 50 mM glutathione, 10 mM Tris, pH 8.0. Glycerol was added to 10% final concentration, and 1.5-ml aliquots of purified protein were flash frozen on dry ice and stored at -30 °C. Then, a sample was thawed in ice water and diluted to the required concentration in Tris-buffered saline (TBS). Unused protein from a thawed aliquot was discarded; no loss of activity was noted for a single freeze-thaw cycle.

Synthesis of Biotinylated HA -- bHA was prepared using the hydrazide method [54,55]. Bacterially-expressed HA (100 mg, 0.25 mmol disaccharide equivalents, MW 700,000) (Clear Solutions Biotech, Inc., Stony Brook, NY) was dissolved in 20 ml of water by stirring vigorously

overnight. To obtain ca. 5% modification of carboxyl groups (0.0125 mmol), 18.6 mg of biotin-LC-hydrazide (Pierce, Rockford, IL) dissolved in 180 μ l DMSO was added, followed by 24 mg (0.125 mmol) of 1-[3-(dimethylamino)propyl]-3-ethylcarbodiimide hydrochloride (EDCI). The bHA was purified by extensive dialysis over several days, alternating between 500 mM NaCl and water [56].

bHA Blot Method -- PVDF membranes (BioRad) were pre-wetted in MeOH and then 3-5 μ l of the protein was added dropwise as the MeOH evaporated. After the membrane absorbed the protein solution, it was immediately immersed in blocking buffer (TBS + 1% polyvinyl pyrrolidone (PVP-40) and 1% casein) for 2 h. The membrane was then incubated with 10 μ g/ml of bHA in blocking solution for 2 h, washed three times with TBS-T, incubated with 1:4,000 dilution of SA-HRP for 40 min, washed, and visualized after a 60 sec incubation with BM chemiluminescent enzyme linked immunosorbent assay (ELISA) substrate (Boehringer Mannheim). The membrane was covered with plastic wrap and immediately exposed to X-ray film (X-Omat-AR film, Kodak). The signal was quantified with a computer-controlled scanner (UMAX 1200S), and the digitized signal was analyzed using NIH Image.

Construction of the Peptide Libraries -- Two eight-amino acid one-bead, one-peptide libraries were constructed [57]. Library **R** was a completely random library in which only cysteine was omitted during synthesis. Library **B** had an alternating acidic pattern, XZXZXZXZ, with X = any residue except Cys, Arg, or Lys, and Z = D-Asp, L-Asp, D-Glu, or L-Glu. Thus, Tentagel S NH₂ beads (Rappe Polymere GmbH, Tübingen, Germany) are 80-100 μ m in diameter with 0.3 mmol reactive amine/ gram dry weight [57,58]. A typical starting sample size was six million beads, which were incubated with 9-fluorenylmethoxycarbonyl (Fmoc)-protected amino acids whose free carboxyls were activated with 1-hydroxybenzotriazole (HOBt) and (*o*-benzotriazol-1-yl-*N,N,N',N'*-tetramethyluronium hexafluorophosphate (HBTU) (Advanced Chemtech, Louisville, KY). The reaction proceeded in dimethylformamide (DMF) and the beads were purified at each step by washing with DMF. The Fmoc-protected amine was deprotected using 20% piperidine in DMF and quantitative analysis determined the amount of available amine. To ensure a completely random library for Library **R**, the following strategy was used. The entire

batch of beads was split into 19 equal pools, each in a separate plastic column. Each batch was allowed to react with a single variety of Fmoc amino acid followed by a DMF wash. All beads were then combined, mixed, and then separated again into 19 new pools, and the process was repeated eight times. This method ensures the presence of a random population of peptides, while only one species is attached per bead. An analogous split-pool-split procedure was performed for Library **B**, alternating between a four-pool split and a 17-pool split.

Bead Screening -- Beads (2 ml, approximately 2×10^5 beads) from Library **B** or Library **R** were placed in a 5-ml plastic column (Biorad) and pretreated by washing with decreasing concentrations of DMF in TBS and finally with TBS containing 0.1% PVP-40. Next, 1 ng/ml of GST-RHAMM(518-580) was incubated with the beads for 1 h at room temperature on an orbital shaker. The beads were washed with 20 column volumes of buffer, and incubated with a 1:5,000 dilution of anti-GST. This washing was repeated, followed by incubation with a 1:10,000 dilution anti-goat IgG-alkaline phosphatase. After extensive washing, the beads were then incubated with 0.27 mM 5-bromo-4-chloro-3-indolyl phosphate (BCIP) in detection buffer (TBS + 2 mM $MgCl_2$). The positive beads turned blue within 10-30 min, and were then sorted under $100\times$ magnification using a syringe fitted with a 10- μ l pipette tip. The beads were stripped of bound protein and color by washing with 6 M guanidinium hydrochloride (GnHCl), pH 2.5, followed by three washes with DMF. This screening process was repeated three times, with the total number of beads decreasing after each successive screen. The final screen included a pre-incubation step with 1 mg/ml digested HA as competitor, such that beads that did not turn blue in the final screen were candidates for binding to the HABD of RHAMM.

Peptides on beads were sequenced by placing a single bead on a filter in the same manner that a polypeptide in solution would be immobilized. Sequencing was accomplished using Edman degradation chemistry on an Applied Biosystems Model 477A Gas Phase Peptide Sequencer. A single "white" bead from the first screening was selected as a negative control, designated peptide **NB**, and its sequence was determined to be IDSDWEGE.

Pepspots® Analysis of Biased Library Results to Determine Chirality of Peptides -- Each of the sixteen possible diastereomers for four positive Library **B** peptides were synthesized in spots immobilized on cellulose (Pepspots®, Jerini Biotools, Wilmington, NC). Four diastereomers of the negative control peptide **NB** (IDSDWEGE) were also synthesized. The amount of immobilized peptide is reported to be 3-5 nmol on the membrane as a 2-mm dot.

Binding to the Pepspots® was detected by incubation of the blocked (TBS + 0.1% casein) membrane with 50 µg/ml GST-RHAMM(518-580) in blocking buffer. After washing, the bound protein was semi-dry electrotransferred from the cellulose membrane onto a PVDF membrane using the Phast (Pharmacia) system. A system of three buffers recommended by Jerini Biotools was used in this transfer: cathode buffer (25 mM Tris, 40 mM 6-aminohexanoic acid, 0.01% SDS and 20% methanol); anode buffer I (30 mM Tris base, 20% methanol); and anode buffer II (300 mM Tris base, 20% methanol). Filter paper squares were soaked in these buffers, three sets for each membrane to be transferred. First, the anode buffer I-soaked filter papers were placed on the anode, followed by the anode buffer II-soaked membranes; the two membranes were arranged with the PVDF membrane on the anode side of the cellulose membrane. The sandwich was completed with the cathode buffer-soaked filter papers. The cathode was placed on top of the sandwich and the transfer was performed at 0.8 mA/cm² of membrane for 40 min at 4 °C.

The PVDF membrane with the blotted GST-RHAMM(518-580) was blocked and incubated with a 1:5,000 dilution of anti-GST, followed by a 1:10,000 dilution of anti-goat antibody-HRP. To detect bound material, a chemiluminescence detection kit (Boehringer Mannheim) was used followed by exposure to film. The developed film was scanned and quantified as above. Each experiment was repeated several times with different GST-RHAMM(518-580) concentrations; increased GST-RHAMM(518-580) concentrations resulted in increased background and non-specific binding.

Synthesis of Labeled Peptides for Binding Assays -- Peptides were synthesized using conventional Fmoc chemistry on an Applied Biosystems Model 431A Peptide Synthesizer. The synthesized peptides were split into two batches. The first batch remained unlabeled, while a

second batch was carried through an additional synthetic cycle to add an N-terminal Cys. All cleaved peptides were characterized by MALDI-TOF and purified on high performance liquid chromatography (HPLC) prior to use.

Either *N*^α-(3-maleimidylpropionyl)biocytin or fluorescein-5-maleimide (Molecular Probes, Eugene, OR) was linked to the free thiol of the N-terminal Cys, using a 3 × molar excess of maleimide and ca. 1 mg of peptide. The maleimide probe was dissolved in DMSO to 10 mg/ml and the peptide was dissolved in 20 mM Tris, pH 7.0 to 1 mg/ml concentration in a microfuge tube. The Cys-containing peptides were handled in degassed reaction buffers and lyophilized from trifluoroacetic acid solutions to maintain the free thiol. After mixing the peptide and maleimide reagents, precipitation occurred in some cases; for those mixtures, the reaction was centrifuged at 16,000 × g for 2 min, and the reaction supernatant was removed and recombined with the DMSO-redissolved precipitate. After shaking for 12 h at room temperature, the conjugated peptides were purified by HPLC.

Preparation of Low Molecular Weight HA -- Bacterially-expressed HA (700 - 1,200 kDa) was dissolved overnight in 50 mM sodium acetate buffer (pH 6.0) to give a 4 mg/ml solution. Ten units of testicular Hase (Sigma) per mg HA were added to the solution and the reaction was shaken for 12 h at 37 °C. An additional aliquot of Hase was added and the solution was again incubated at 37 °C for 12 h. This material was boiled for 5 min to inactivate any remaining Hase, and particulate matter was removed by centrifugation. The molecular weight was analyzed using gel permeation chromatography (Waters), which showed a distribution of molecular sizes from 4 - 40 kDa. This material was employed in the binding assays.

Solid-Phase Binding Assay -- GST-RHAMM(518-580) was immobilized in a 96-well plate (Greiner GmbH) and either bHA or biotinylated peptides were added. Bound probes were detected using SA-HRP and the colorimetric HRP substrate 3,3',5',5'-tetramethylbenzidine (TMB). Thus, 50 µl of 0.5 mg/ml GST-RHAMM(518-580) in 50 mM Tris (pH 8.0) was incubated in each well for 1 h at 4°C with shaking. The wells were washed with TBS-T (20 mM Tris, 130 mM NaCl, pH 7.6, 0.1% Tween) three times, and then blocked with TBS-T-PVP-40 (TBS-T + 0.1% PVP-40) for

2 h at 4 °C. Dilutions of biotinylated probe (either HA or peptide) were added to each well in 50 µl TBS-T-PVP-40. After incubation for 45 min, wells were washed with TBS-T and bound biotinylated probes were detected using 50 µl 0.5 µg/ml SA-HRP (40 min, room temperature). After three washes, 50 µl TMB was added and color was detected after 10 min using a Perkin Elmer HTS-7000 Microplate Reader with the absorbance filter set at 360 nm. Experiments were performed in triplicate, and background was measured using a biotinylated probe that was added to blocked wells lacking GST-RHAMM(518-580). Control experiments included measuring binding with the negative control peptide **NB**.

Alternatively, this experiment was performed using fluorescein-labeled peptides rather than biotinylated peptides. In this case, after the incubation step with fluorescein-labeled probes, the plate was washed three times with TBS-T and then 50 µl TBS was added to each well. The plate was then read on the microplate reader using 485 nm excitation and 535 nm emission filters. The gain was set to optimal and 50 flashes were used to improve sensitivity.

FP Binding Assay -- Purified GST-RHAMM(518-580) was prepared at a stock concentration of 1.3 mg/ml (40 µM), and the initial concentration of fluorescent peptide was 0.1 µM. Thus, 200 µl of each dilution of GST-RHAMM(518-580) was added to the wells of a low-bind 96-well plate with black sides and a clear bottom (Corning Costar). For each set of experiments, the fluorescein-labeled probe concentration was kept constant, while the concentration of protein was incremented. Data was collected using a Polarion (Tecan Inc.) microplate spectrofluorimeter equipped with a 485 nm excitation filter and a 585 nm emission filter. Fifty flashes were used to achieve optimal sensitivity, and free fluorescein was used as a standard at a value of 20 mP (millipolarization units). To generate a binding isotherm, a plate was prepared with triplicates of each concentration, serial dilutions of GST-RHAMM(518-580) optimally covering the range from 20-fold below the K_D to approximately 100-fold above the K_D . Identical aliquots of fluorescein-peptide were added to each well, the solutions were thoroughly mixed, the plate was incubated until equilibration was reached, and then the fluorescence anisotropy was measured. The binding data, mP values, and receptor concentrations were used to calculate the binding constants.

This assay is most useful for probes that bind with K_D values $< 1 \mu\text{M}$, which constitutes a practical limit of protein concentrations needed to generate the isotherm.

FP data was analyzed as described [43,59] to measure the amount of ligand bound by measurement of the anisotropy of the complex. The total change in polarization is calculated as $\Delta mP = mP_{\text{max}} - mP_{\text{min}}$. The bound ligand at each concentration is calculated as $B_T = [(mP - mP_{\text{min}})(\text{total tracer concentration})]/\Delta mP$. Assuming 1:1 stoichiometry, $B_T = R_{\text{bound}}$, and free [HABD] can be calculated as $R_{\text{free}} = R_{\text{tot}} - R_{\text{bound}}$. Scatchard analysis by plotting $R_{\text{bound}}/R_{\text{free}}$ vs. R_{bound} led to a best-fit line with a slope equal to the negative reciprocal of the K_D [43].

Competition Experiments Using a Fluorescence-Based Solid-Phase Binding Assay --

Competition experiments were performed as outlined above except the blocking buffer included 1 mg/ml competitor. The wells were pre-incubated with competitor, and the biotinylated or fluorescein-labeled probe was added together with competitor. Digested HA was used for competition. Heparin, CS-A, and CS-C were dissolved in H_2O to 10 mg/ml, and were diluted to 1 mg/ml in TBS-T-PVP-40 in the competition experiments.

ACKNOWLEDGMENTS

This work was supported by grants to G.D.P. from the U.S. Department of Defense, the State of Utah Centers of Excellence Program, and The University of Utah (UUtah), and by a grant to E.A.T. from the National Cancer Institute of Canada. We thank Dr. J.T. Elliott (The University at Stony Brook, USB) and Professor R. El Magrahbi (USB) for biophysical advice, Mr. R. Gerhart (UUtah) for bead-picking, and Dr. R.W. Schackmann (UUtah) for peptide sequencing and synthesis.

FIGURE LEGENDS

- Figure 1.** Deconvolution of Library **B** diastereoisomers. Uppercase letters represent the natural L-configurations and lowercase letters represent the D-configurations of Glu (E, e) and Asp (D, d). Peptides were synthesized as 5 nmol "Pepspots®" and transferred to PVDF as described in the text. A chemiluminescence assay with an HRP-labeled secondary antibody was used to detect GST-RHAMM(518-580) bound to each peptide spot. The intensity of each spot was quantified with NIH Image software. Data shown is from a single film, but the results were validated from three blots..
- Figure 2.** Binding of nine fluorescein-labeled peptides to GST-RHAMM(518-580) and GST alone using the solid-phase fluorescence binding assay.
- Figure 3.** **Panel a:** competitive displacement of six selected fluorescein-labeled peptides (**B-2A**, **B-2B**, **B-3A**, **B-3B**, **R-5**, and **R-12**) by HA using the solid-phase fluorescence binding assay. The concentration of 4 - 40 kDa HA was 0.1 mg/ml, except for **B-2A**, for which 1 mg/ml of 4 - 40 kDa HA was used. **Panel b:** Competitive displacement of biotinylated peptide binding to GST-RHAMM(518-580) by HA and three sulfated GAGs using the solid-phase colorimetric ELISA for four selected biotinylated peptides (**B-1A**, **B-2A**, **R-5**, and **R-12**). **Key:** **HA**, hyaluronan ; **HEP**, heparin; **CS-A**, chondroitin 4-sulfate; **CS-C**, chondroitin 6-sulfate.

Figure 4. Binding curves and Scatchard analyses of FP measurements of GST-RHAMM(518-580) with peptides **B-1A** and **B-4B**.

Figure 5. Summary of ten molecular dynamics and minimization routines on peptides **B-2** and **B-2B**. The distance is measured between Glu4 HE2 and Glu6 OE1 on either peptide. The modeling was performed using Discover and included 1,000 iterations of minimization runs using an Amber force field. The dynamics routine had 10,000 steps including charge and Morse terms.

Figure 6. Molecular model showing calculated minimum energy structures for HA (top), peptide **B-2**, YDSEYESE (middle, all L-amino acids), and peptide **B-2B**, YDSEYeSE (bottom), which contains a single D-Glu residue. The carboxylate-to-carboxylate distances are indicated by double-headed arrows in each energy-minimized structure.

REFERENCES

1. Fraser, J. R. E., Laurent, T. C., & Laurent, U. B. G. (1997). Hyaluronan: Its nature, distribution, functions and turnover. *J. Intern. Med.* **242**, 27-33.
2. Toole, B. P. (1997). Hyaluronan in morphogenesis. *J. Intern. Med.* **242**, 35-40.
3. Oksala, O., Salo, T., Tammi, R., Hakkinen, L., Jalkanen, M., Inki, P., & Larjava, H. (1995). Expression of proteoglycans and hyaluronan during wound healing. *J. Histochem. Cytochem.* **43**, 125-135.
4. Entwistle, J., Hall, C. L., & Turley, E. A. (1996). HA receptors: regulators of signalling to the cytoskeleton. *J. Cell. Biochem.* **61**, 569-577.
5. Sherman, L., Sleeman, J., Herrlich, P., & Ponta, H. (1994). Hyaluronate receptors: key players in growth, differentiation, migration and tumor progression. *Curr. Opin. Cell. Biol.* **6**, 726-733.
6. Turley, E. A., & Harrison, R. In www.glycoforum.gr.jp: 1999; pp.
7. Zhang, S., Chang, M. C., Zylka, D., Turley, S., Harrison, R., & Turley, E. A. (1998). The hyaluronan receptor RHAMM regulates extracellular-regulated kinase. *J. Biol. Chem.* **273**, 11342-11348.
8. Hall, C. L., Wang, C., Lange, L. A., & Turley, E. A. (1994). Hyaluronan and the hyaluronan receptor RHAMM promote focal adhesion turnover and transient tyrosine kinase activity. *J. Cell Biol.* **126**, 575-588.
9. Hall, C. L., Lange, L. A., Prober, D. A., Zhang, S., & Turley, E. A. (1996). pp60(c-src) is required for cell locomotion regulated by the hyaluronan receptor RHAMM. *Oncogene* **13**, 2213-2224.
10. Hall, C. L., Yang, B., Yang, X., Zhang, S., Turley, M., Samuel, S., Lange, L. A., Wang, C., Curpen, G. D., Savani, R. C., & Turley, E. A. (1995). Overexpression of the hyaluronan receptor RHAMM is transforming and is also required for H-ras transformation. *Cell* **82**, 19-26.

11. Lokeshwar, V., & Selzer, M. (2000). Differences in hyaluronic acid-mediated functions and signaling in arterial, microvessel, and vein-derived human endothelial cells. *J. Biol. Chem.* **274**, 27641-27649.
12. Yamada, Y., Itano, N., Narimatsu, H., Kudo, T., Hirohashi, S., Ochiai, A., Niimi, A., Ueda, M., & Kimata, K. (1999). Receptor for hyaluronan-mediated motility and CD44 expressions in colon cancer assessed by quantitative analysis using real-time reverse transcriptase-polymerase chain reaction. *Jpn. J. Cancer Res.* **90**, 987-992.
13. Wang, C., Thor, A. D., Moore, D. H., 2nd, Zhao, Y., Kerschmann, R., Stern, R., Watson, P. H., & Turley, E. A. (1998). The overexpression of RHAMM, a hyaluronan-binding protein that regulates ras signaling, correlates with overexpression of mitogen-activated protein kinase and is a significant parameter in breast cancer progression. *Clin. Cancer Res.* **4**, 567-576.
14. Assmann, V., Marshall, J. F., Fieber, C., Hofmann, M., & Hart, I. R. (1998). The human hyaluronan receptor RHAMM is expressed as an intracellular protein in breast cancer cells. *J. Cell. Sci.* **111**, 1685-1694.
15. Abetamann, V., Kern, H. F., & Elsasser, H. P. (1996). Differential expression of the hyaluronan receptors CD44 and RHAMM in human pancreatic cancer cells. *Clin. Cancer Res.* **2**, 1607-1618.
16. Crainie, M., Belch, A. R., Mant, M. J., & Pilarski, L. M. (1999). Overexpression of the receptor for hyaluronan-mediated motility (RHAMM) characterizes the malignant clone in multiple myeloma: identification of three distinct RHAMM variants. *Blood* **93**, 1684-1696.
17. Till, K. J., Zuzel, M., & Cawley, J. C. (1999). The role of hyaluronan and interleukin 8 in the migration of chronic lymphocytic leukemia cells within lymphoreticular tissues [In Process Citation]. *Cancer Res.* **59**, 4419-4426.
18. Pilarski, L. M., Pruski, E., Wizniak, J., Paine, D., Seeberger, K., Mant, M. J., Brown, C. B., & Belch, A. R. (1999). Potential role for hyaluronan and the hyaluronan

receptor RHAMM in mobilization and trafficking of hematopoietic progenitor cells. *Blood* **93**, 2918-2927.

19. Collis, L., Hall, C., Lange, L., Ziebell, M., Prestwich, R., & Turley, E. A. (1998). Rapid hyaluronan uptake is associated with enhanced motility: implications for an intracellular mode of action. *FEBS Lett.* **440**, 444-449.

20. Assmann, V., Jenkinson, D., Marshall, J. F., & Hart, I. R. (1999). The intracellular hyaluronan receptor RHAMM/THABP interacts with microtubules and actin filaments. *J. Cell Sci.* **112**, 3943-3954.

21. Yang, B., Zhang, L., & Turley, E. A. (1993). Identification of two hyaluronan-binding domains in the hyaluronan receptor RHAMM. *J. Biol. Chem.* **268**, 8617-8623.

22. Yang, B. H., Yang, B. L., Savani, R. C., & Turley, E. A. (1994). Identification of a common hyaluronan binding motif in the hyaluronan binding proteins RHAMM, CD44 and link protein. *EMBO J.* **13**, 286-296.

23. Day, A. J. (1999). The structure and regulation of hyaluronan-binding proteins. *Biochem. Soc Trans* **27**, 115-121.

24. Yang, B., Hall, C. L., Yang, B. L., Savani, R. C., & Turley, E. A. (1994). Identification of a novel heparin binding domain in RHAMM and evidence that it modifies HA mediated locomotion of ras-transformed cells. *J. Cell. Biochem.* **56**, 455-468.

25. Ziebell, M. Ph. D. Thesis, The University at Stony Brook, 2000.

26. Kohda, D., Morton, C. J., Parker, A. A., Hatanaka, H., Inagaki, F. M., Campbell, I. D., & Day, A. J. (1996). Solution structure of the link module: a hyaluronan-binding domain involved in extracellular matrix stability and cell migration. *Cell* **86**, 767-775.

27. Bajorath, J., Greenfield, B., Munro, S. B., Day, A. J., & Aruffo, A. (1998). Identification of CD44 residues important for hyaluronan binding and delineation of the binding site. *J. Biol. Chem.* **273**, 338-343.

28. Entwistle, J., Zhang, S. W., Yang, B. H., Wong, C., Li, Q., Hall, C. L., JA, Mowat, M., Greenberg, A. H., & Turley, E. A. (1995). Characterization of the murine gene encoding the hyaluronan receptor RHAMM. *Gene* **163**, 233-238.
29. Lam, K. S. (1997). Application of combinatorial library methods in cancer research and drug discovery. *Anticancer Drug Des.* **12**, 145-167.
30. Yang, B. H., Yang, B. L., & Goetinck, P. F. (1995). Biotinylated hyaluronic acid as a probe for identifying hyaluronic acid-binding proteins. *Analyt. Biochem.* **228**, 299-306.
31. Hoare, K., Savani, R. C., Wang, C., Yang, B., & Turley, E. A. (1993). Identification of hyaluronan binding proteins using a biotinylated hyaluronan probe. *Connect. Tissue Res.* **30**, 117-126.
32. Scott, J. E., & Heatley, F. (1999). Hyaluronan forms specific stable tertiary structures in aqueous solution: a ^{13}C NMR study. *Proc. Natl. Acad. Sci. USA.* **96**, 4850-5.
33. Scott, J. E. (1989). Secondary structures in hyaluronan solutions: chemical and biological implications. In *The Biology of Hyaluronan*; (Foundation, C., Ed.), pp 6-20 J. Wiley & Sons, Ltd., Chichester, UK.
34. Kahmann, J., O'Brien, R., Werner, J., Heinegard, D., Ladbury, J., Campbell, I., & Day, A. (2000). Localization and characterization of the hyaluronan-binding site on the Link module from human TSG-6. *Structure* **8**, 763-774.
35. Friguet, B., Chaffotte, A. F., Djavadi-Ohanian, L., & Goldberg, M. E. (1985). Measurements of the true affinity constant in solution of antigen-antibody complexes by enzyme-linked immunosorbent assay. *J. Immun. Meth.* **77**, 305-319.
36. Gold, E. (1982). An interaction of albumin with hyaluronic acid and chondroitin sulfate. *Biopolymers* **19**, 1407-1414.
37. Xu, S., Yamanaka, J., Sato, S., Miyama, I., & Yonese, M. (2000). Characteristics of complexes composed of sodium hyaluronate and bovine serum albumin. *Chem. Pharm. Bull.* **48**, 779-783.

38. Fujimoto, T., Kawashima, H., Tanaka, T., Hirose, M., Toyama-Sorimachi, N., Matsuzawa, Y., & Miyasaka, M. (2001). CD44 binds a chondroitin sulfate proteoglycan, aggrecan. *Int. Immunol.* **13**, 359-366.
39. Kawashima, H., Hirose, M., Hirose, J., Nagakubo, D., Plaas, A., & Miyasaka, M. (2000). Binding of a large chondroitin sulfate/dermatan sulfate proteoglycan, versican, to L-selectin, P-selectin, and CD44. *J. Biol. Chem.* **275**, 35448-35456.
40. Termeer, C., Hennies, J., Voith, U., Ahren, T., Weiss, J., Prehm, P., & Simon, J. (2000). Oligosaccharides of hyaluronan are potent activators of dendritic cells. *J. Immunol* **165**, 1863-1870.
41. Checovich, W. J., Bolger, R. E., & Burke, T. (1995). Fluorescence polarization: a new tool for cell and molecular biology. *Nature* **375**, 254-256.
42. Wei, A., & Herron, J. (1993). Detection of HCG-anti-HCG interactions by fluorescence polarization. *Analyt. Chem.* **65**, 3372-3377.
43. Lynch, B. A., Loiacono, K. A., Tiong, C. L., Adams, S. E., & MacNeil, I. A. (1997). A fluorescence polarization based Src-SH2 binding assay. *Analyt. Biochem.* **247**, 77-82.
44. Lee, T. H., Wisniewski, H. G., & Vilcek, J. (1992). A novel secretory tumor necrosis factor-inducible protein (TSG-6) is a member of the family of hyaluronate binding proteins, closely related to the adhesion receptor CD44. *J. Cell Biol.* **116**, 545-57.
45. Winter, W. T., & Arnott, S. (1977). Hyaluronic acid: The role of divalent cations in conformation and packing. *J. Mol. Biol.* **117**, 761-84.
46. Wang, C., Entwistle, J., Hou, G. P., Li, Q. A., & Turley, E. A. (1996). The characterization of a human RHAMM cDNA: conservation of the hyaluronan-binding domains. *Gene* **174**, 299-306.
47. Zhang, S., Ziebell, M., Cheung, W.-F., Lu, J., Haddad, A., Litchfield, D., Ahn, N., Cruz, T., Prestwich, G., & Turley, E. (2000). Intracellular RHAMM is an erk1 binding protein and removal of its N-terminal sequence is required for activation of erk1. *Molec. Biol. Cell* in revision.

48. Fukumoto, T., Torigoe, N., Kawabata, S., Murakami, M., Uede, T., Nishi, T., Ito, Y., & Sugimura, K. (1998). Peptide mimics of the CTLA4-binding domain stimulate T-cell proliferation. *Nat. Biotechnol.* **16**, 267-270.
49. Dubowchik, G. M., & Walker, M. A. (1999). Receptor-mediated and enzyme-dependent targeting of cytotoxic anticancer drugs. *Pharmacol. Ther.* **83**, 67-123.
50. Luo, Y., Ziebell, M. R., & Prestwich, G. D. (2000). A hyaluronic acid-Taxol anti-tumor bioconjugate targeted to cancer cells. *Biomacromolecules* **1**, 208-218.
51. Vercruysse, K. P., & Prestwich, G. D. (1998). Hyaluronate derivatives in drug delivery. *Crit. Rev. Therapeut. Drug Carr. Syst.* **15**, 513-555.
52. McCourt, P. A. G., Smedsrod, B. H., Melkko, J., & Johansson, S. (1999). Characterization of a hyaluronan receptor on rat sinusoidal liver endothelial cells and its functional relationship to scavenger receptors. *Hepatology* **30**, 1276-1286.
53. Sambrook, J., Fritsch, E. F., & Maniatis, T. (1989). Molecular Cloning, A laboratory manual. In; 2 ed. Cold Spring Harbor Laboratory Press, Plainview, NY.
54. Pouyani, T., & Prestwich, G. D. (1994). Biotinylated hyaluronic acid: a new tool for probing hyaluronate-receptor interactions. *Bioconjugate Chem.* **5**, 370-372.
55. Yu, Q., & Toole, B. P. (1995). Biotinylated hyaluronan as a probe for detection of binding proteins in cells and tissues. *Biotechniques* **19**, 122-125.
56. Luo, Y., & Prestwich, G. D. (1999). Synthesis and selective cytotoxicity of a hyaluronic acid-antitumor bioconjugate. *Bioconjugate Chem.* **10**, 755-763.
57. Lam, K. S., & Lebl, M. (1994). Selectide technology: bead-binding screening. *Methods: A Companion to Meth. Enz.* **6**, 372-380.
58. Wu, J., Ma, Q. N., & Lam, K. S. (1994). Identifying substrate motifs of protein kinases by a random library approach. *Biochemistry* **33**, 14825-14833.
59. Dandliker, W., Hsu, M., Levin, J., & Rao, B. (1981). Equilibrium and kinetic inhibition assays based upon fluorescence polarization. *Methods Enzymol.* **74**, 3-28.

Table 1. Sequences of HA-mimetic peptides. Peptide sequences were obtained by direct Edman degradation using positive library beads screened with RHAMM(518-580). Peptide **NB** sequence was obtained from a negative control (non-binding) bead selected from the first round of screening of Library **B**.

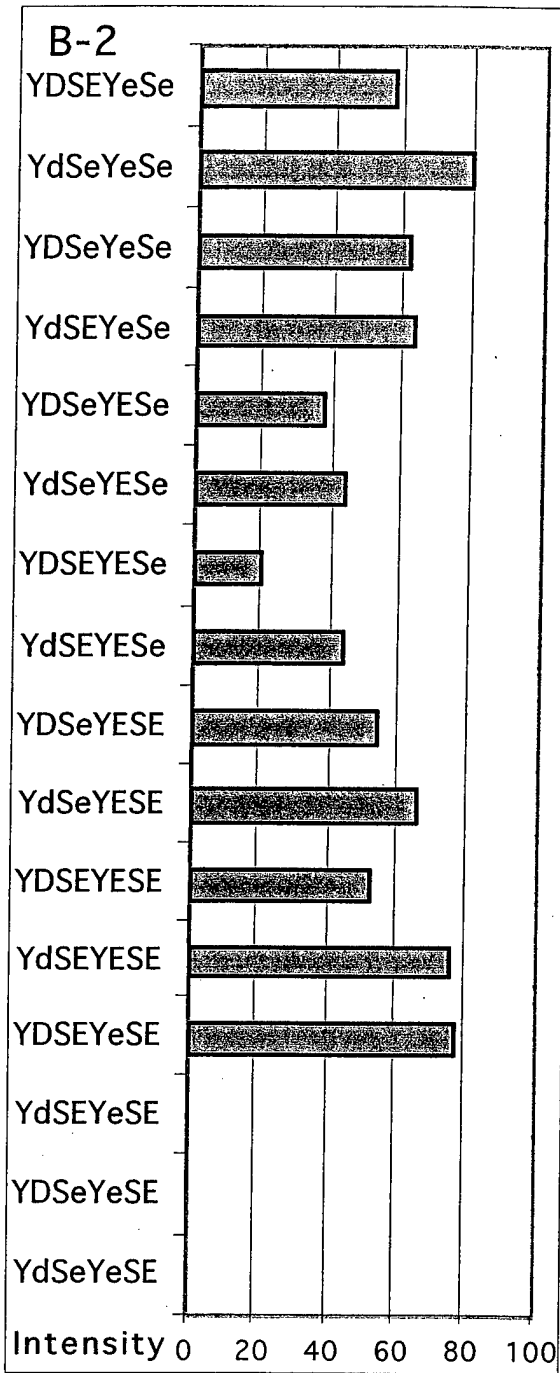
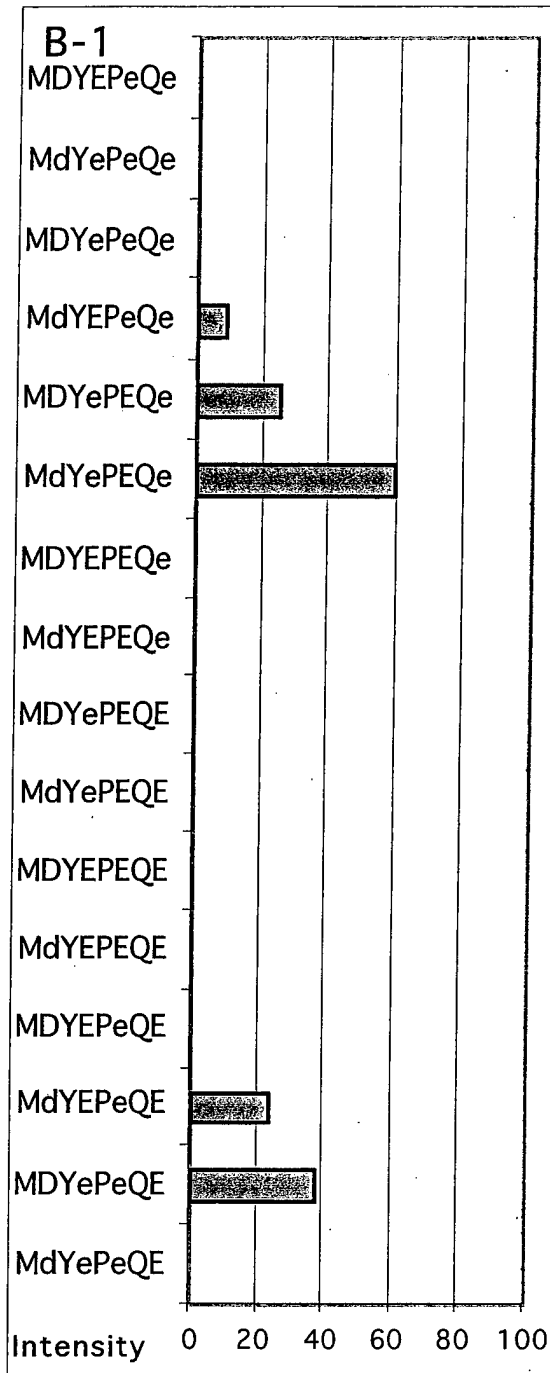
Random		Biased	
R-1	SGRPYKPP	B-1	MDYEPEQE
R-2	YXSSNKPG	B-2	YDSEYESE
R-3	EGEWPVYP	B-3	FDFDSEYE
R-4	WNYTEAKG	B-4	EDAENDEE
R-5	QAMNKFTF		
R-6	NTDSNKNM	NB	IDSDWEGE
R-7	NPVFNDGY		
R-9	FLRWFIMI		
R-10	EMAQMLLE		
R-11	PFLMKFPI		
R-12	IYIYPQPQ		

Table 2. Binding affinities for synthetic HA-mimetic peptides. An N-terminal Cys was added to each bead-derived sequence to permit attachment of reporter groups. The K_D values from the plate assay were obtained using the solid-phase ELISA using N-terminally-biotinylated peptides as described in the text. Competitive displacement was determined by preincubation of RHAMM-HABD with 1 mg/ml of 4-40 kDa HA. In the amino acid sequences, uppercase letters represent the natural L-configurations and lowercase letters represent the D-configurations of Glu (E, e) and Asp (D, d). **Key:** nd = not determined.

Name	Sequence	% Binding Displaced by HA	K_D from Plate Assay (nM)	K_D from FP (nM)
Library B				
B-1A	CMdYEPeQe	33 \pm 5%	49 \pm 3	17 \pm 5
B-1B	CMDYePEQe	61 \pm 8%	73 \pm 5	nd
B-2A	CYDSeYeSe	76 \pm 5%	8 \pm 1	nd
B-2B	CYDSEYeSE	78 \pm 8%	74 \pm 8	nd
B-3A	CFDFdSEYe	86 \pm 7%	730 \pm 25	nd
B-3B	CFdFdSEYE	67 \pm 10%	1400 \pm 200	nd
B-4A	CEDAeNdEe	37 \pm 8%	110 \pm 13	nd
B-4B	CEdAENdEe	53 \pm 5%	499 \pm 75	220 \pm 58
Library R				
R-3	CEGEWPVYP	67 \pm 5%	48 \pm 2	nd
R-5	CQAMNKFTF	58 \pm 5%	270 \pm 45	nd
R-12	CIYIYPQPQ	75 \pm 9%	5300 \pm 85	nd

Table 3. Alignment of random peptide sequences showing tri- and dipeptide motifs

NPV <u>EN</u> DGY EGEW <u>PV</u> YP	<u>R-7</u> <u>R-3</u>
ELLMO <u>AE</u> <u>QA</u> MNKFTF	R-10 retrograde <u>R-5</u>
PPKY <u>PR</u> GS EGEW <u>PV</u> YP PFLMK <u>FP</u> I IYI <u>Y</u> PQPQ	R-1 retrograde <u>R-3</u> <u>R-11</u> <u>R-12</u>



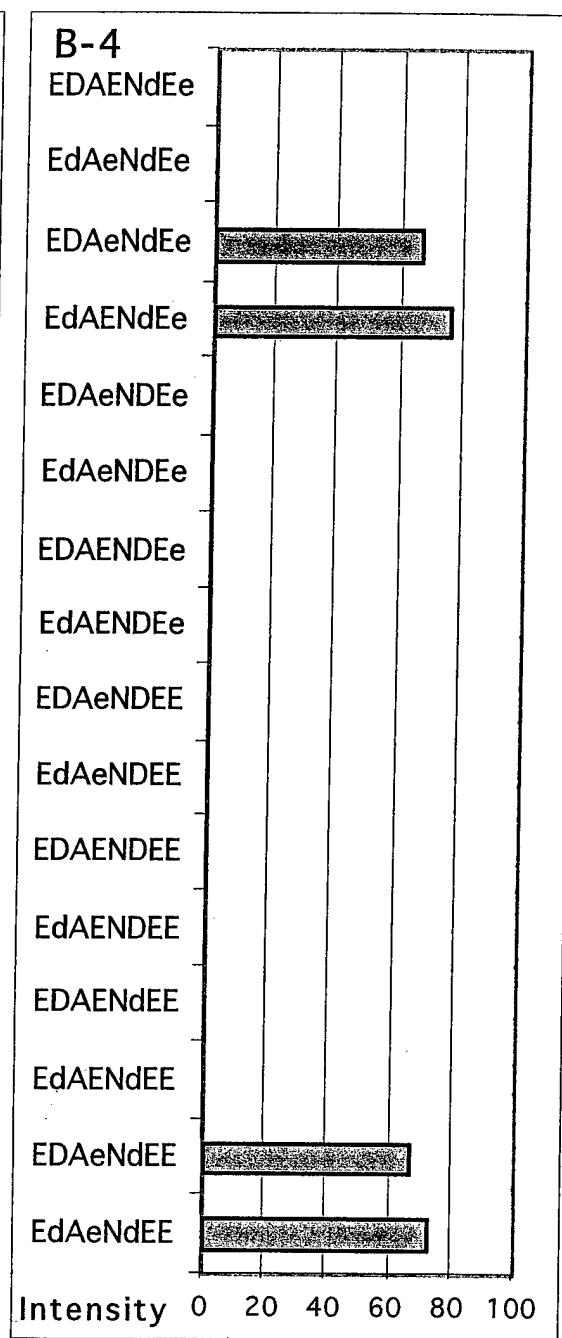
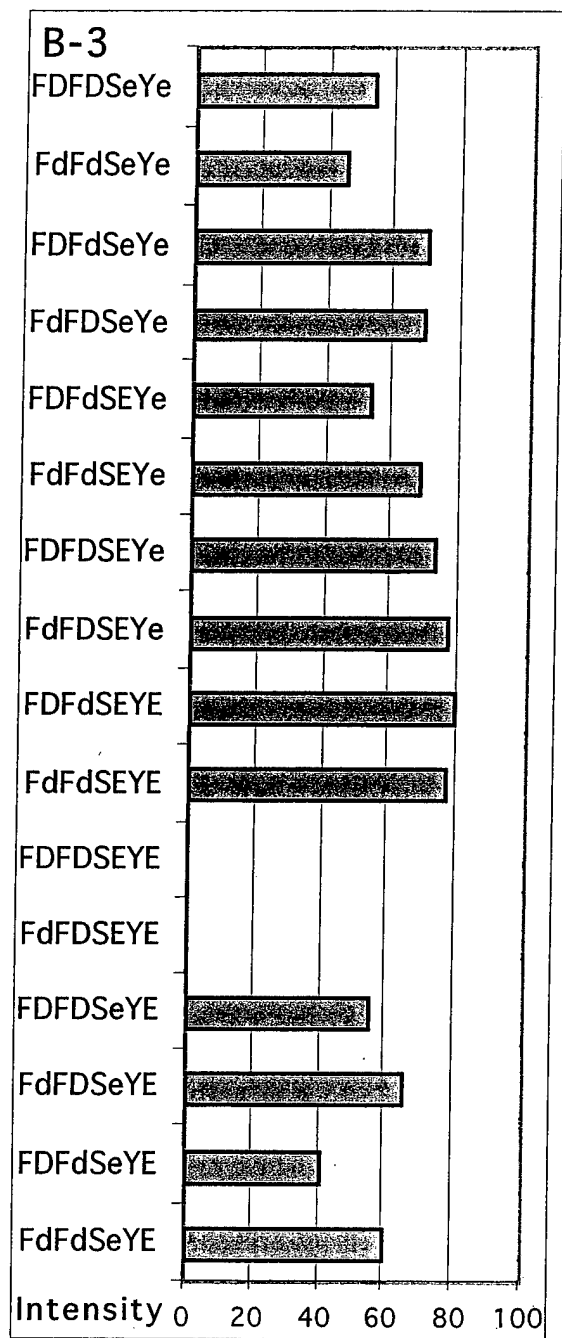
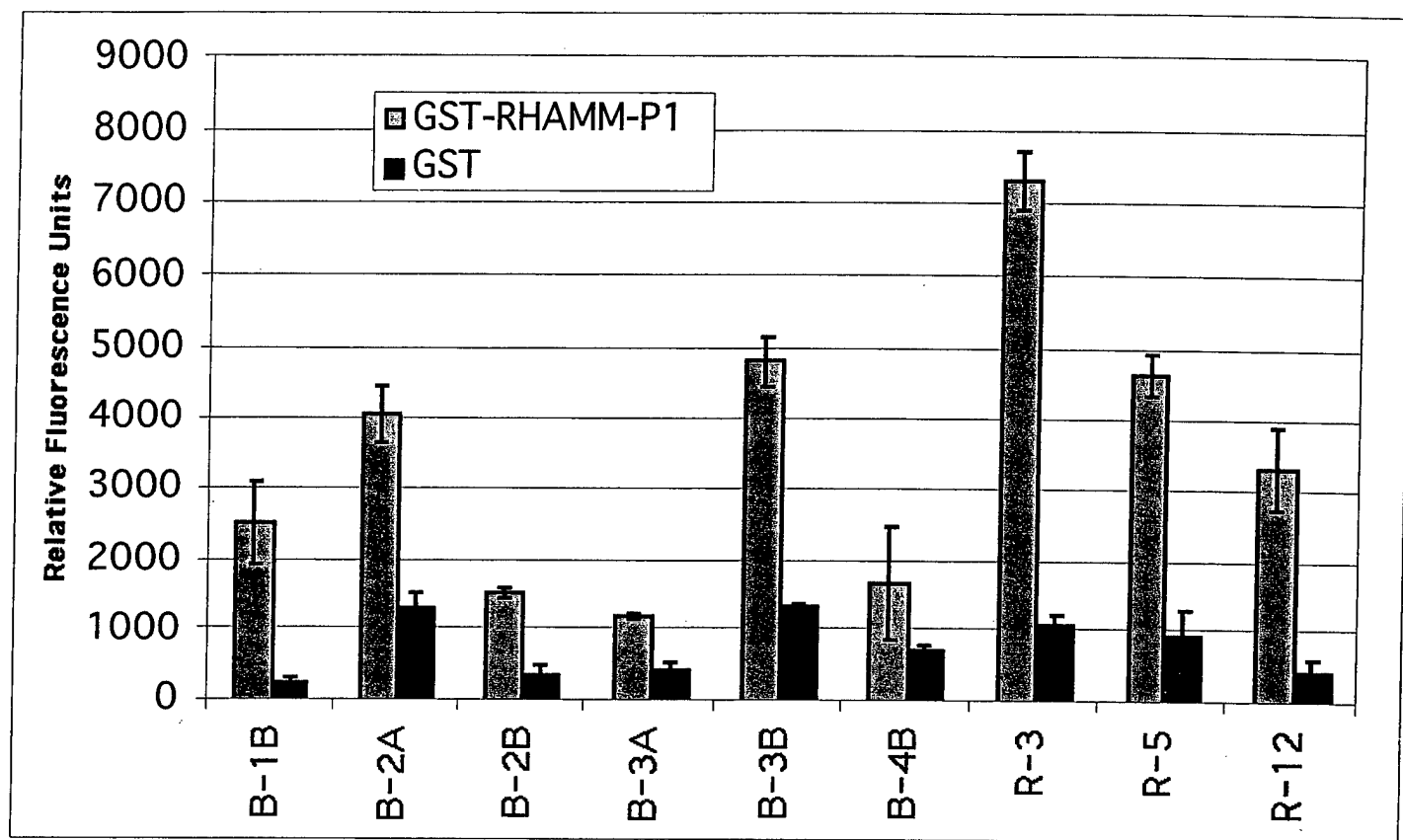


Figure 1
(continued)



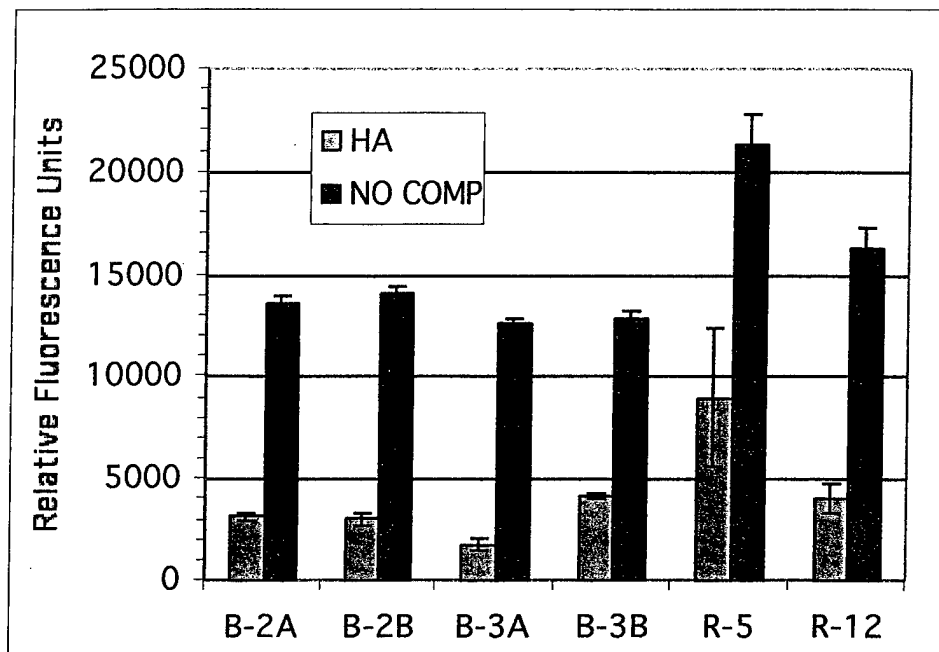


Figure 3a

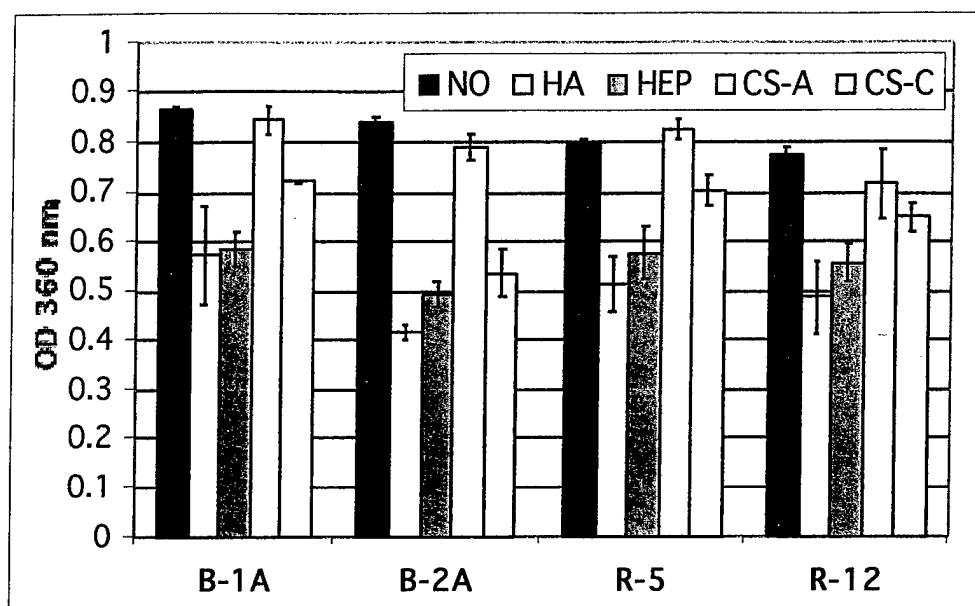


Figure 3b

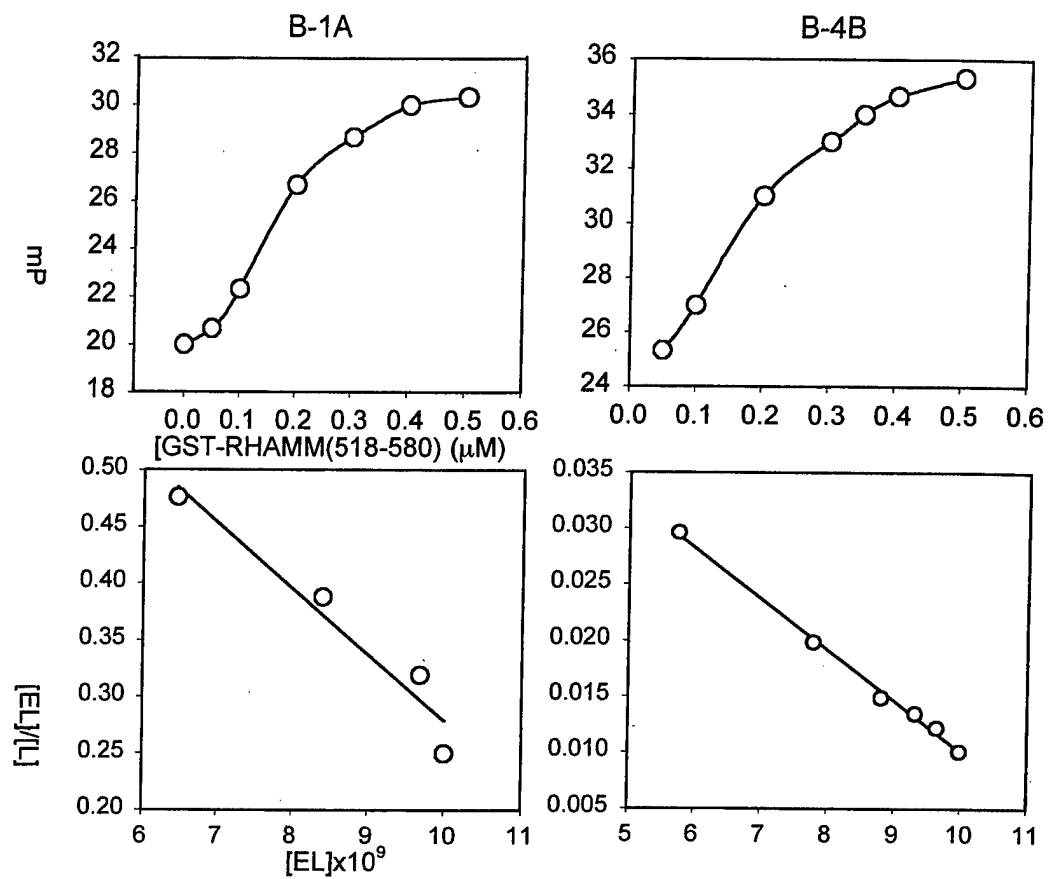


Figure 4

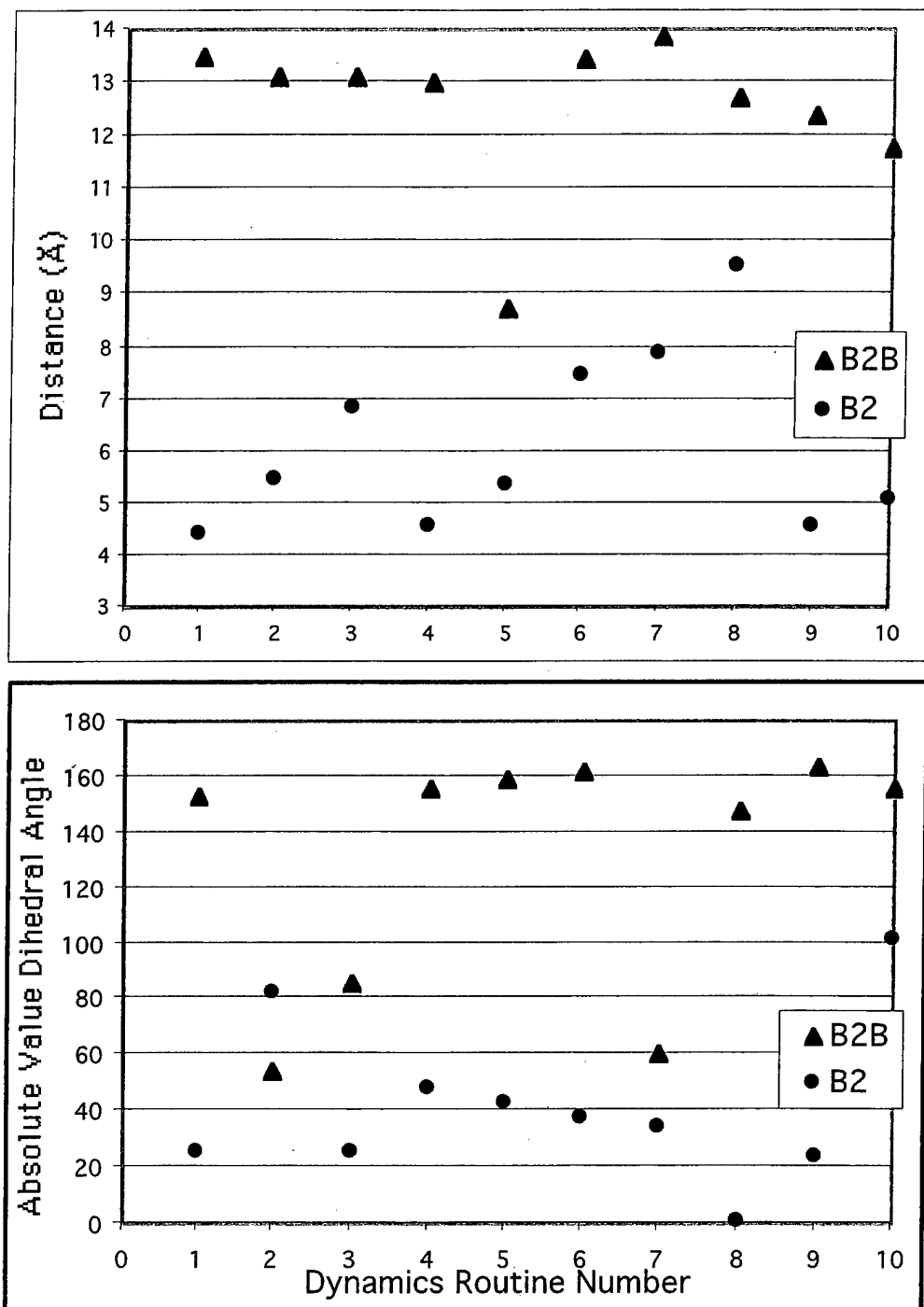


Figure 5

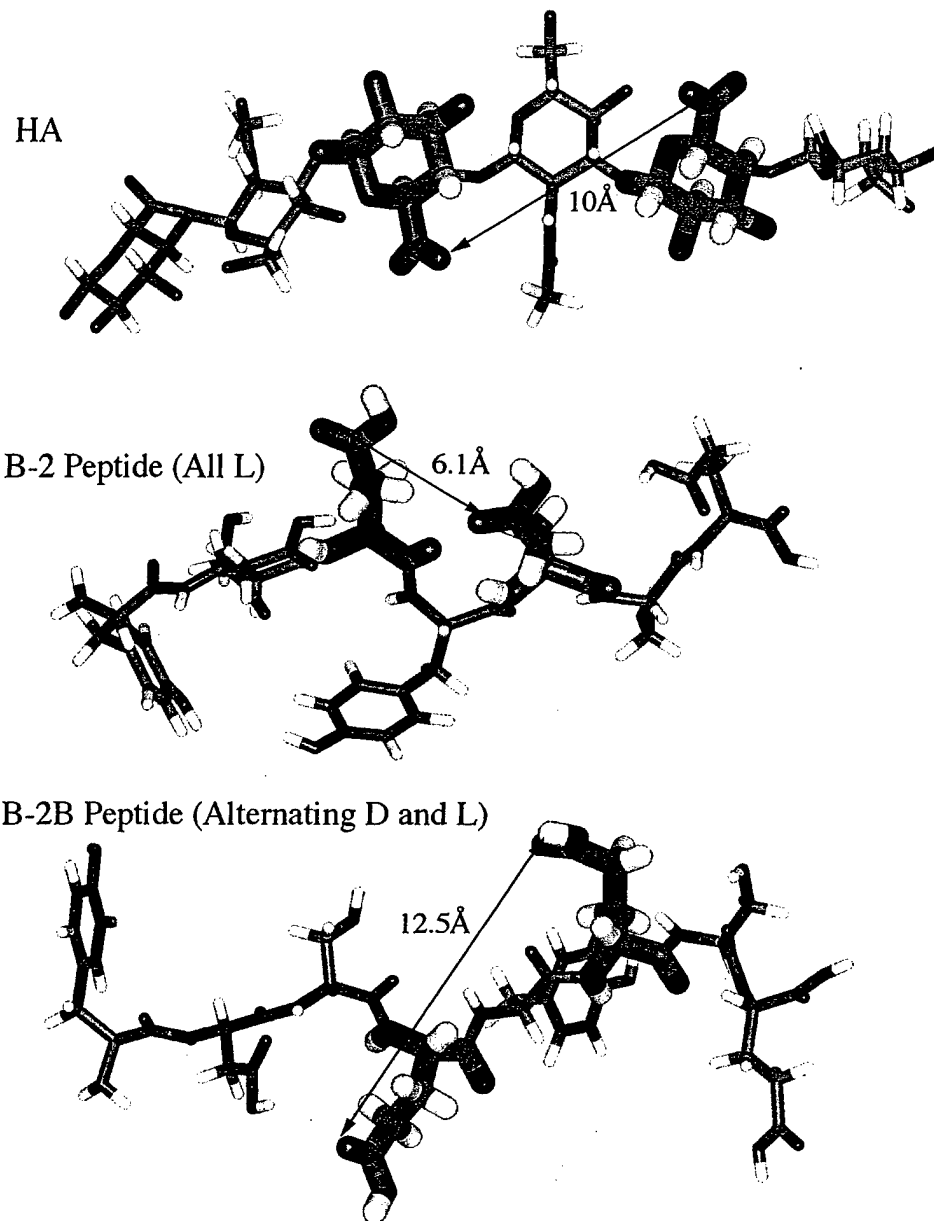


Figure 6

Expert Opinion

1. Introduction
2. Biomaterials in drug delivery systems
3. Conclusions
4. Expert opinion

Monthly Focus: Biologicals, Immunologicals & Drug Delivery

Novel biomaterials for drug delivery

Yi Luo & Glenn D. Prestwich

Department of Medicinal Chemistry, The University of Utah, 30 South 2000 East, Room 201, Salt Lake City, Utah 84112-5820, USA

Safety and efficacy of pharmaceutical agents can be greatly improved by encapsulation within, or covalent attachment to, a biomaterial carrier. Such drug delivery systems differ from conventional drug dosage forms (pills, tablets, ointments, creams, injectables and 'tiny time capsules') in that a localised depot of drug provides patterned release of the active agent with a pre-determined time course. The pattern of drug release may be constant, oscillating, declining continuously, or even pulsatile. The need to engineer different release patterns for drugs of different molecular sizes, potency, stability and hydrophobicity provides the impetus for active study of the design of new biomaterials, intelligent delivery systems and approaches for delivery through different portals in the body. The field of controlled drug delivery provides a driving force for current innovations in biomaterials. For most drug delivery systems, polymers function simply as inert, biocompatible carriers. In other systems, polymers can be designed with targeting or pathology-responsive functions. This review summarises some of the recently developed intellectual property in the field of biomaterials applied to drug delivery systems. Included are implantable ceramics and other inorganic materials, non-degradable and degradable synthetic polymers, natural polymers and hybrid biomaterials derived from synthetic and natural polymers.

Keywords: biodegradable, biomaterials, drug delivery, hybrid, inorganic, natural, polymer, synthetic

Expert Opin. Ther. Patents (2001) 11(9):

1. Introduction

Drugs are generally administered by six conventional routes: oral, iv. bolus (i.v.), iv. infusion (i.v. inf.), im. injection (i.m.), ip. (i.p.) and sc. injection (s.c.). Each drug has a therapeutic range above which it is toxic and below which it is ineffective. Conventional administration of drugs results in the peaks and valleys of plasma drug concentration; oscillations may result in periods of toxicity or ineffectiveness. Drug delivery systems have been developed to overcome these principal disadvantages of conventional drug therapy. In a short time, new drug delivery systems have had a significant impact on nearly every branch of medicine, including cardiology, ophthalmology, endocrinology, oncology, pulmonology, immunology and pain management.

A controlled-release preparation maintains the drug in the desired therapeutic range with a single administration. In addition, controlled-release systems allow:

- localised delivery of the drug to a particular body compartment, thereby lowering the systemic drug level
- stabilisation of medications that are rapidly metabolised, e.g., polypeptides
- reduced need for follow-up care
- increased patient comfort
- improved patient compliance [1].

Ashley Publications
www.ashley-pub.com



Drug delivery systems can be manipulated, in a number of ways, to achieve the desired therapeutic levels in the body. The design of the delivery system takes into account the route of administration; the duration of drug action and the need for removal after the drug has been released. During the last two decades, significant advances have been made in the field of controlled release technology. Early efforts were focused on the development of zero-order release devices. The premise of zero-order release was to maintain steady-state drug concentrations through a constant rate of drug release. However, initial studies had shown that zero-order release does not necessarily translate into constant drug levels in the blood. Recent advances in controlled release technology have resulted from the design of novel biomaterials with different charge density, side chain functionality, phase transformations, crystallinity and degradability. As a result, sustained drug levels can be achieved in the body while minimising side effects and improving patient compliance.

2. Biomaterials in drug delivery systems

Biomaterials have an enormous impact on human healthcare. The design of materials for specific biomedical applications has rapidly expanded during the last 20 years [2]. Biocompatible materials are the key components for tissue engineering scaffolds and drug delivery systems [3,4]. Biomaterials can be composed of various components, e.g., polymeric materials, ceramics and metals.

A specific field of interest is the use of biomaterials for pharmaceutical applications [5]. Controlled delivery devices are generally diffusion-based release systems applicable to release of drugs intended for systemic circulation or for a localised site. The classic polymeric drug delivery system is the implantable contraceptive NorplantTM, which comprises a silicone rubber (polydimethylsiloxane) tube filled with a steroid dispersion. Drug release is controlled by the permeability of the steroid in the tube wall and remains fairly constant over several years after initial transient. Few drugs, though, are amenable to release by a Norplant-like system, which has driven the development of new polymers and release modes.

Drug delivery systems have challenging material requirements, since the therapeutic effect must be produced over prolonged periods of time at rates that are independent of patient-to-patient variables. Moreover, the chemical nature of the materials or surfaces of such devices may initiate biorejection processes that are enhanced or suppressed by the presence of the drug being administered. Selection of materials for such systems is further complicated by the need for compatibility with the drug contained within the system. This review summarises recent advances in the development of biomaterials for drug delivery.

2.1 Inorganic materials in drug delivery systems

The selection and application of synthetic materials for surgical implants has been directly dependent upon the biocom-

patibility profiles of specific prosthetic devices. The early rationale for bioceramics was based on the relative chemical and biochemical inertness of compounds that constituted these structural materials. Subsequently, mildly biointeractive, as well as partially and fully degradable ceramics, were identified for clinical use. Application of ceramic biomaterials range from bulk ceramic structures, such as joint and bone replacements, to fully or partially-biodegradable substrates for the controlled delivery of pharmaceutical drugs, growth factors and morphogenetically inductive substances [6].

Calcium phosphate (CaP) is the principal inorganic constituent of bone, which can be characterised as a composite material of CaP and collagen. Development of new bone replacement biomaterials requires prevention of microbial infections following osteoarticular trauma or prosthesis implantation. As an alternative to parenteral administration of an antibiotic, an antibiotic-loaded biomaterial would allow a high concentration to be generated *in situ* with minimal systemic toxicity. CaP ceramics have recently been proposed as a potential matrix for a bioactive drug delivery system in which the *in situ* effect of a released therapeutic agent is favoured by the biocompatibility, osteocondition and bioresorption of the ceramic material. A dynamic compaction allows use of polymyxin B (PMB), a polypeptide antibiotic with CaP ceramics, without any loss in its integrity and biological effects [7]. The PMB was released from the CaP matrix, retained its antibacterial activity and inhibited lipopolysaccharide effects on monocyte/macrophage CaP degradation. The formulation of biphasic calcium phosphate (BCP)-vancomycin granules by isostatic compression has recently been used to produce drug delivery devices [8]. Local administration of human growth hormone (hGH) by macroporous biphasic CaP (MBCP) implants appears to be effective for local delivery of hGH, resulting in improved bone substitution [9]. Further studies indicate that hGH not only stimulates bone cells implicated in the synthesis of the extracellular matrix (ECM), but also those involved in the early degradation of CaP biomaterial [10]. An hGH formulation with apatite powder was prepared by an adsorption method [11] and the biological activity of the hGH was retained.

Macroporous β -tricalcium phosphate ceramic beads were elaborated to be a resorbable bone substitute and a drug delivery system carrying an antibiotic, e.g., gentamicin or vancomycin [12]. Antibiotic release was early and complete (before the third day), except that gentamicin remained in the bone for ten days.

CaP shows a similar chemical composition to hydroxylapatite (HAP). Many devices with HAP have been developed for medical use because of its excellent biocompatibility. The hardness of HAP is adequate for supportive and protective functions in the skeleton and HAP also participates in regulation of calcium and phosphate levels in the blood and other bodily fluids. The pore size was controlled by applying HAP powder of nanometer dimensions and nylon and acrylic monofilaments [13]. The HAP processed with nylon monofila-

ment showed similar micro-pores to those of the Haversian canal in natural bone. This porous HAP could be applied to either a biofilter or a drug delivery system.

Composite biomaterials, [14] based on ceramic material with good mechanical response and a partially biodegradable character, were prepared by the free radical polymerisation of mixtures of α - Al_2O_3 , low-molecular weight but crystalline poly(L-lactic acid) (PLLA) and methyl methacrylate (MMA). Formation of a relatively porous structure with good cohesion after the biodegradative treatment was observed. These systems can be considered as candidates for applications in orthopaedic surgery as filling biomaterials and even as control drug delivery systems.

Other inorganic biomaterials can be used for the encapsulation of biologically active molecules. For example, a silica-based glass containing antibiotics, growth factors, anti-inflammatory agents and analgesics (specifically, vancomycin and TGF- β) was claimed to be useful as a substitute for autologous bone grafts [20]. Controlled release of vancomycin for 1 month could be achieved *in vitro*, providing an effective method for inhibiting growth of *Staphylococcus aureus*.

2.2 Polymeric materials in drug delivery systems

Since the appearance of synthetic polymers 60 years ago, the medical profession has rapidly adapted these materials for therapeutic applications. Many types of polymers, both synthetic and natural, including homopolymers and co-polymers, have been evaluated as potential biomaterials. The wide variety of chemical compositions, structures and properties is needed by the medical industry to address an even wider range of applications [15]. Homopolymers include poly(methacrylate), poly(ethylene), poly(propylene), poly(tetrafluoroethylene), poly(vinyl chloride), poly(dimethyl siloxane), poly(carbonate) and nylon; co-polymers include poly(glycolide-co-lactide) (PLGA), poly(urethanes) and many others. Nylon, poly(methacrylate), poly(vinyl chloride), TeflonTM, high density polyethylene and polypropylene, DacronTM polyester and polyurethane etc., remain important in clinical medicine. They are employed in fabrication of permanent prosthetic devices, including limb and hip implants, artificial lenses, artificial heart, dialysis membrane, large diameter vascular grafts and catheters. Research continues to optimise the stability and performance of these materials *in vivo*.

Polymeric biomaterials can be divided into two groups. The first group is suited for permanent aids such as prostheses. The second group is used for temporary aids and is based on the capacity of living systems to self-repair. Degradable polymers are of great interest for temporary therapeutic applications such as wound closure, tissue repair and regeneration and drug delivery. Degradable polymers have the advantage that they perform their functions and are then metabolised, thus obviating the need for surgical removal. A degradable system also minimises the risk of long-term toxicity or immune rejection of the polymeric device, as compared with non-degradable systems. Applications of degradable polymers

include resorbable surgical sutures, matrices for the controlled time-release of drugs, scaffolds for tissue engineering and resorbable orthopaedic devices such as bone pins [16].

In most drug delivery systems, polymers serve as carriers. Polymers with a variety of properties can be designed for special functions. In drug delivery applications, the main requirement is that the polymer carriers are degradable; however, many polymers such as TeflonTM and polyethylene are essentially indestructible *in vivo*. Most degradable polymers contain labile linkages in their backbone, e.g., esters, orthoesters, anhydrides, carbonates, amides, urethanes, or ureas. The currently available degradable polymers include: poly(glycolic acid) (PGA), poly(lactic acid) (PLA), poly(ϵ -caprolactone) (PCL), polydioxane, poly(γ -ethyl glutamate), poly(ortho esters), polyiminocarbonates, polyphosphates, polyanhydrides, as well as polyalkanoates (PHA).

The hydrophilicity, crystallinity and lability to metabolism of the polymer matrix is key in determining the drug release profile. PGA, PLA and PCL are all hydrolysed by bulk erosion, while polyanhydride and poly(ortho ester) materials are hydrolysed by surface erosion mechanism. The latter gives zero-order drug release kinetics under controlled conditions, since the release rate is governed by water penetration into the polymer matrix followed by degradation, rather than by diffusion of the drug out of the polymer matrix.

2.3 Synthetic polymers in drug delivery systems

2.3.1 Non-biodegradable synthetic polymers

Non-biodegradable synthetic polymers frequently contain a C-C backbone that is stable in the physiological environment. The molecular weight and molecular weight distribution are important factors in determining biocompatibility. The molecular weight of a synthetic carrier must be below the renal threshold to ensure its elimination after injection. The biocompatibility of the non-biodegradable polymers should be extensively evaluated for therapeutic drug delivery.

Biomaterials, which release locally high concentrations of antithrombotic agents, should lessen the thrombogenicity of the materials. To evaluate this approach, novel polyurethane matrices loaded with hirudin and then coated with 2-hydroxyethyl methacrylate (HEMA) by glow discharge plasma deposition (GDPD) to reduce the release rate, were prepared [17]. HEMA plasma treatment of matrices produced a thin, highly cross-linked film on the surface as a diffusional barrier. The initial burst and subsequent release of hirudin was significantly reduced and the release kinetics of hirudin could be controlled by changing the various plasma coating conditions. Delivery of hirudin using these biomaterials at the site of cardiovascular diseases can have the advantage of locally raising drug levels, as well as lowering systemic hirudin exposure, thereby minimising the possibility of side effects.

A poly(vinylamine)-grafted polystyrene nanosphere was prepared by free radical polymerisation of poly(*N*-vinylacetamide) macromonomer and styrene and subsequent acid hydrolysis [18]. Lactose was conjugated to the nanosphere by

an amide linkage and the lactose was recognised by a galactose-specific lectin, RCA120. The carbohydrate-conjugated nanosphere was proposed as a useful biomaterial for site-specific drug delivery.

Macromolecular complexes were formulated by the electrostatic forces comprising a drug with at least one quaternary ammonium nitrogen atom, e.g., insulin and a natural (e.g., heparin) or synthetic (e.g., polyvinylphosphonic acid (PVPA)) polymer and polyacrylic acid (PAA). The reduction of glucose levels of the macromolecular complexes in rabbit models by iv. injection was significantly better than for free insulin [202].

Polymers of N-vinylpyrrolidinone (NVP) are known to have excellent biocompatibility when implanted in the vitreous body or used as a vitreous substitute. Although poly(NVP) is capable of absorbing relatively large amounts of water, it is not readily hydrolysed. To design a biomaterial that combines the excellent intraocular biocompatibility with and controlled kinetics of degradation, a series of three-dimensional networks of poly(NVP), which were crosslinked by a dimethacrylate crosslinker, was synthesised [19]. This approach offers several advantages. First, the hydrolysis of the carbonate groups in the crosslinks leads to liberation of poly(NVP) and/or oligo(NVP) chains that are then cleared from the eye *via* phagocytosis. Second, hydrolysis generates two alcohols and CO₂ (i.e., there is no catalytic burst effect). Third, when these materials are implanted in dry form, swelling and degradation will progress from the exterior of the material toward its interior. Therefore, these materials can be designed such that surface degradation rather than bulk degradation occurs; the hydrolysis rate can be controlled *via* the degree of crosslinking or through synthesis of crosslinkers that are more or less labile. The poly(NVP) materials may be useful for a number of applications in ophthalmology, e.g., as biodegradable matrix materials for controlled drug delivery of ganciclovir in the vitreous body.

Thermosensitive polyoxamers (polyoxyethylene-polyoxypropylene block co-polymers) [203] have a sol-gel transition dependent on the concentration of the polymer and has the ability to transform into a solid, clear gel having excellent optical properties at 25 °C. The polyoxamers thus become more viscous in the eye and could be used as a long-lasting formulation for treating dry eye syndrome.

The polyoxyethylene-polyoxypropylene-polyoxyethylene triblock co-polymers have linear polymeric segments of alternating hydrophilic and hydrophobic blocks. These so-called ABA block co-polymers form micelles that can contain a biologically-active agent, such as an antimicrobial compound, an anticancer agent, an enzyme, tissue plasminogen activator, a cytokine, clotting factors, hormones, or erythropoietin [204]. One method for delivering an antineoplastic drug (e.g., adriamycin) to a selected site uses a polyoxyethylene-polyoxypropylene-polyoxyethylene ABA triblock co-polymer (e.g., Pluronic 105) as the micellar drug carrier; the hydrophobic drug is encapsulated in the interior of the micelles [205]. Ultra-

sonic energy can be applied to the selected site to release the drug, thereby reducing side effects and multiple drug resistance.

The use of hydrogels in biomedical and pharmaceutical applications is growing rapidly. The non-toxicity and biocompatibility of these materials makes them very attractive as biomaterials and drug carriers in the body. Cationic hydrogels of poly(diethylaminoethyl methacrylate-ethylene glycol) were prepared for controlled release of proteins and other macromolecules [20]. Glucose-sensitive hydrogels, comprised of the same materials, were also studied for applications in insulin release.

Mucoadhesive poly(ethylene glycol) (PEG) star polymer hydrogels were synthesised by γ irradiation for use in protein delivery [21]. Grafted poly (methacrylic acid-*graft*-ethylene glycol) (P(MMA-g-EG)) co-polymers were investigated for their pH sensitivity [22] and interpolymer complexation was found to occur by hydrogen bonding. P(MMA-g-EG) membranes showed pH-sensitivity due to complex formation and dissociation. These gels show great promise for a number of biomedical applications for which rapid biomaterial response is necessary.

PEG and pluronic F-127 were silylated with 3-isocyanatopropyltriethoxysilane to synthesise PEG-based hydrogels by sol-gel transition of silane [23]. Silanes on different PEG molecules formed covalent bonds by acid-catalysed hydrolysis and condensation. PEG hydrogels in microspheres were prepared by emulsifying aqueous silylated PEG solution in oil followed by curing. Crosslinked pluronic F-127 hydrogels displayed inverse thermosensitivity. The ability to obtain hydrogels by simple sol-gel transition of silylated PEG can be used to prepare new drug delivery systems and biomaterials.

The incorporation of a model protein, bovine serum albumin (BSA), into poly(vinyl alcohol) (PVA) hydrogel film during the freezing and thawing process and the subsequent zero-order release behaviour could be achieved [24]. Covalent attachment of biologically-active macromolecules (e.g., serum proteins) to a photopolymerisable PVA macromer was investigated [25]. The abundant pendant hydroxyl groups on PVA could be modified to attach drugs, adhesion peptides, growth factors and other macromolecules to the polymer backbone. Depending upon the chemistry of the polymer-macromolecule attachment, a variety of unique responses could occur in a wide range of biomedical applications, including tissue engineering and drug delivery.

2.3.2 Degradable synthetic polymers

Permanent implants elicit a chronic inflammation known as a foreign body response. This response is characterised by formation of a poorly-vascularised fibrous layer, analogous to a scar at the material-tissue interface. The foreign body response is typically benign and it is sometimes desirable to anchor devices into host tissue. However, it often leads to clinical complications (e.g., infection, tissue contraction) thus is considered a risk to be avoided. Biodegradable polymers

have been developed for applications that include sutures and temporary replacement of soft tissues. Most recently, these polymers have been used in drug delivery systems, where it is particularly undesirable to leave an expired polymer device in the patient permanently. Thus, a wide variety of both solid and hydrogel-type degradable polymers have been developed for drug delivery and tissue engineering [26], including aliphatic polyesters, polyanhydrides, poly(ortho esters), poly(phosphoesters), poly(iminocarbonates), poly(carbonates), poly(depsipeptides), poly(phosphazenes), poly(dioxanones) and poly(alkyl α -cyano acrylates). Each of these polymers has a hydrolysable functional group in the polymer backbone.

The basic concept of introducing the biodegradable polymers to a drug delivery system involves two aspects. First, nontoxic degradation products must be produced and must be eliminated from the body, alleviating the need for post-surgical procedures for removal of expired drug carrier. Second, the degradation itself can be used to modulate the drug release profile. A typical mechanism of elimination of the biodegradable polymers from the body is glomerular clearance. Drugs are released initially from the biodegradable polymer devices by diffusion and later by a combination of diffusion and matrix degradation.

The most investigated system in regard to clinical and toxicological data are polyesters based on lactide/glycolide. PGA, PLA and PLGA materials are biocompatible, have predictable degradation kinetics, show good solubility in common solvents and are FDA-approved for commercial suture applications [27]. Most of the applications using lactide/glycolide polymers employ microspheres as delivery systems for steroid hormones, antibiotics, anticancer drugs and narcotic antagonists [28-31].

2.3.3 Polyanhydrides

Polyanhydrides are comprised of monomers joined by hydrolytically-labile anhydride bonds that yield two carboxylic acids upon hydrolysis. The surface erosion mechanism makes it possible to obtain zero-order release profiles, as well as allowing control of the rate and duration of drug release. Polyanhydrides show excellent *in vivo* biocompatibility. A variety of drugs and proteins, including insulin, bovine growth factors, angiogenesis inhibitors, such as heparin and cortisone and enzymes, such as alkaline phosphatase and β -galactosidase, have been incorporated within polyanhydride matrices [32]. Once in the polymer, the drug is protected from degradation and will last as long as the polymer matrix persists. The prototype hydrophobic polyanhydride, for medical applications, is a co-polymer of 1,3-bis-(*p*-carboxyphenoxy)propane and sebacic acid, developed in the 1960s by the Langer group at Massachusetts Institute of Technology. In the clinical treatment of brain tumours, a polymer disk containing a formulation of the anticancer agent BCNU is used to deliver this short half-life (12 min) drug [2]. Polyanhydride microspheres can be used orally to deliver pharmaceuticals to bloodstream;

for example, the absorption of dicumarol, insulin and plasmid DNA was increased [32, 33].

A new family of polyanhydride co-polymers, the poly(anhydride-co-imides) (poly[trimellitylimido-L-tyrosine-co-sebacic acid-co-1,3-bis(carboxyphenoxy)propane]) microspheres, were studied in protein release with BSA as a model protein [16]. BSA was released at approximately the same rate as the polymer eroded. This erosion mechanism leads to predictable drug release rates that may be appropriate for the delivery of many protein therapeutics, including vaccine antigens. The anhydride-imide co-polymers were well-tolerated in acute toxicity studies in rats and therefore show promise as biomaterials.

2.3.4 Polyesters

Synthetic degradable polyesters were adopted in surgery 30 years ago as materials for sutures and bone fixation devices and remain among the most widely used synthetic degradable polymers. No significant new materials have been described during the period covered by this review.

2.3.5 Polyalkanoate (PHA)

PHAs are aliphatic polyesters that are produced by a number of species of bacteria as a carbon reserve material. The hydrophobic PHA is biosynthesised within the cytoplasm and deposited as inclusion bodies. Along with polyisoprenoids, polypeptides, polysaccharides and polynucleotides, PHAs have been suggested as being a fifth class of physiologically-important organic biopolymers [34].

Due to the versatility of possible structures of PHA, a wide range of drug delivery systems could be developed, including thin films (patches), microspheres and tubings. Poly(3-hydroxybutyrate) (PHB), the most commonly occurring member of the PHA family, has been proposed for use as a degradable biomaterial for drug delivery systems, sutures, bone plates and short-term implants [35]. It has been reported as a microencapsulation carrier for several anticancer agents [32], such as 1-(2-chloroethyl)-3-cyclohexaylnitrosourea (CCNU), latet, alcarubicin, 2',3'-diacyl-5-fluoro-2'-deoxyuridine and the contraceptive drug progesterone. PHB microspheres show low toxicity and good biocompatibility. Typically, as a result of its high crystallinity, PHB does not form perfectly spherical particles.

A novel composite, in the form of interpenetrating polymer networks was prepared by photopolymerisation of poly(hydroxybutyrate-co-hydroxyvalerate) and 2-hydroxyethyl methacrylate [36]. The products exhibited interesting and novel properties, such as partial hydrophilicity and hydrophobicity on the same membrane, as well as significantly altered mechanical properties. The material has potential applications as a drug carrier and an intestinal patch.

Partially-degraded and trans-esterified poly(3-hydroxybutyrate) and its co-polymer with hydroxyvalerate (22 mol%) were synthesised and microencapsulation by double emulsion (water-oil-water) of peptide hormones (follicle stimulating

hormone and luteinizing hormone) in these modified polymers was prepared [37]. Drug release profiles obeyed the Fickian-type $T_{1/2}$ dependence, indicating that diffusion was the controlling step.

2.3.6 Poly(lactides) and poly(glycolides)

Interest has increasingly focused on the applications of biodegradable polymers to advanced devices in the fields of tissue engineering and drug delivery. For devices used in the human body, polymers must have high biocompatibility as well as modulated biodegradability. At present, only a limited number of synthetic polymers meet these strict requirements. The group of polymers studied most extensively so far in this regard is PLA and its derivatives, some of which have already been commercialised as surgical sutures and microspheres for controlled drug delivery. These polymers are degraded by bulk hydrolysis of ester bonds to give the constituent monomers, lactic and glycolic acids, which are excreted. The clearance and biocompatibility [38,39] of these polymers has enabled use as resorbable sutures since 1970s, under the trade names of DexonTM (PGA) and as VicrylTM or Polyglactin 910TM (PLGA).

PLGAs are used extensively as implants and as injectable microparticulate systems for controlled release of therapeutic agents, including narcotic antagonists, contraceptive steroids, vaccines, LHRH analogues, anticancer agents, local anesthetics, antibiotics and antimalarial agents [40]. For drug delivery applications, racemic PLA is commonly used, since it is important to have a homogeneous matrix for drug dispersion [41].

PLGA implants were compressed from microcapsules, prepared by nonsolvent-induced phase-separation using two solvent-nonsolvent systems, such as methylene chloride-hexane (non-polar) and acetone-phosphate buffer (polar), to develop a biodegradable, implantable delivery system containing ciprofloxacin hydrochloride (HCl) for the localised treatment of osteomyelitis and to study the extent of drug penetration from the site of implantation into the bone [42,43]. Osteomyelitis is an inflammatory bone disease caused by pyrogenic bacteria and involves the medullary cavity, cortex and periosteum. The advantages of localised biodegradable therapy include high, local antibiotic concentration at the site of infection and obviation of the need for removal of the implant after treatment. Sustained drug levels above the minimum inhibitory concentration (MIC) of ciprofloxacin were detected for a period of six weeks at a distance of 70 mm from the site of implantation. Recently, delivery of protein and growth factors was studied extensively with PLGA microspheres, such as bovine superoxide dismutase (bSOD) [44], L-asparaginase [45], insulin [46], IL-12 [47], IFN- γ [48], human growth hormone (rhGH) [49], transforming growth factor β 1 [50], basic fibroblast growth factor (bFGF) [51], nerve growth factor (NGF) [52] and granulocyte-macrophage colony-stimulating factor (GM-CSF) [53].

Thermoplastic biodegradable hydrogels based on PEG-block-poly(D,L-lactide) block co-polymers (PEG-b-PLA) were prepared through successive ring-opening polymerisations [54,55]. Aqueous solutions of these co-polymers, with the proper combination of molecular weights, exhibit temperature-dependent reversible sol (at low temperature)-gel (at body temperature) transition. The use of these thermosensitive polymers demonstrated advantages for sustained injectable drug delivery systems. The formulation is free of organic solvents. In sol or aqueous solution state, this polymer solubilised hydrophobic drugs prior to forming a hydrogel matrix.

PEG was attached to PLA in a variety of combinations, to obtain biodegradable block co-polymers with variable surface properties [56]. The resulting PLA-PEG-monomethyl ether (MePEG-PLA) diblock co-polymers were subject to comprehensive investigations concerning their bulk microstructure and surface properties, in order to evaluate their suitability for drug delivery applications, as well as for the manufacture of scaffolds in tissue engineering. The polymer bulk microstructure contains MePEG domains segregated from racemic PLA domains by varying the composition of the diblock co-polymers. The presence of the MePEG chains in the polymer surface suppressed the adsorption of two model peptides (salmon calcitonin and human atrial natriuretic peptide). Modification of the polymer bulk microstructure, as well as surface properties by varying the co-polymer composition, is a prerequisite for its efficient use in the fields of drug delivery and tissue engineering.

PLA-PEG block co-polymers with a range of PLA and PEG molecular weights were tested in implantation pellets as bone morphogenetic protein (BMP) carrier materials [57]. In combination with biomaterials, BMPs can be used in a clinical setting as bone graft substitutes to promote bone repair. The PLA 6,500-PEG 3,000 polymer with plastic properties was found to function well as a BMP carrier.

Hydrogels from PLA/PEG/PLA triblock co-polymers were prepared by a phase-separation method [58], consisting of introducing a small amount of water over solutions of the co-polymer in a biocompatible organic solvent, tetraglycol. The phase separation-derived hydrogels were soft enough to be injected through a trocar. A linear release profile of fibrinogen was observed from the hydrogel, which acted as a reservoir drug delivery system.

The triblock co-polymers of PEG-PLGA-PEG, with a low molecular weight of 2-4 kDa, possess reverse thermal gelation properties. These biodegradable polymers can be used to deliver poorly water-soluble and/or labile drugs [206]. Specifically, delivery of cytotoxic drugs (e.g., paclitaxel, methotrexate) and peptide hormones (e.g., insulin, calcitonin) was demonstrated.

2.3.7 Poly(ϵ -caprolactone)

PCL is a hydrophobic and crystalline polymer, whose crystallinity increases with decreasing molecular weight. PCL

degrades more slowly than PLA and is regarded as nontoxic and tissue-compatible. The co-polymer of caprolactone and lactide was also investigated to control degradation and the drug release profile. PCL polymers are often used to deliver therapeutic drugs and growth factors in the form of microspheres and porous membranes [59]. Capronor® is an implantable reservoir system, using a PCL matrix that provides sustained release of the contraceptive drug levonorgestrel for one year. PCL-PEG co-polymers were obtained from ring opening polymerisation of ϵ -caprolactone in the presence of ethylene oxide. The presence of PEG domains considerably enhanced the hydrophilicity of the co-polymers, as compared with PCL homopolymer. Nevertheless, the degradability of PCL chains was not enhanced due to the phase separation between the two components. These materials, which have both hydrophilic and hydrophobic microdomains, should be of great biomedical utility as matrices for sustained drug delivery [60]. Finally, porous PCL disks were prepared by the solvent-casting particulate leaching method and these disks were employed as a delivery system for recombinant hGH [59].

2.3.8 Other polyesters

ABA-type polyester block co-polymers with poly[3(*S*)-isobutyl-morpholine-2,5-dione] (PIBMD, A) and poly(ethylene oxide) (PEO) ($M_n = 6000$, PEO, B) blocks, PIBMD-*b*-PEO-*b*-PIBMD, were synthesised *via* ring-opening polymerisation of 3(*S*)-isobutyl-morpholine-2,5-dione in the presence of hydroxytelechelic PEO with stannous octanoate as a catalyst [61]. These block co-polymers may find applications in cell encapsulation and in drug delivery.

New lactide-based polydepsipeptide polymer networks and crosslinked beads have been prepared by UV photopolymerisation of acrylated poly(L-lactic acid-co-glycolic acid-co-L-serine) [PLA(Glc-Ser)] [62]. These materials have been developed for use as polymer scaffolds in tissue engineering, cell encapsulation and injectable drug delivery, which have ligand-immobilisable and biodegradable characteristics. The acrylated PLA(Glc-Ser) crosslinked polymer networks that were obtained were glassy and transparent and the gel content was approximately 90%. The networks showed relatively low swelling in water, due to their crosslinked nature, but readily swelled in chloroform and in DMSO. The acrylate polymers, on co-polymerisation with HEMA, resulted in crosslinked networks (PLA(Glc-Ser)/HEMA), which swelled in water and in DMSO, showing the potential of the polymer in hydrogel applications.

A novel biodegradable polyester with pendent amine functional groups was synthesised from *N*-(benzyloxycarbonyl)-L-aspartic anhydride and 1,4-cyclohexanedimethanol by polycondensation reaction using *p*-toluenesulfonic acid as a catalyst [63]. This new polymer has potential as a drug delivery biomaterial. Microsphere formulations of biodegradable terephthalate polyester-poly(phosphonate) and polyester-poly(phosphite) co-polymers was developed to deliver anti-

oplastic agents (e.g., paclitaxel), antiviral, antifungals, anti-inflammatories and anticoagulants [207].

2.3.9 Dendrimers

Recent advances in dendrimer syntheses have made available arborised cascade molecules with a wide range of sizes, functionalities and properties. Of the many possible monomer structures, those that contain natural or unnatural amino acids are particularly appealing because of their chirality and potential to produce dendrimers with enhanced biocompatibility and diversity. Dendrimers based on L-polylysine, L-valine and L-leucine were developed [64] and have potential applications as drug delivery carriers, asymmetric catalysts, peptido- and protein mimetics and new biomaterials. Poly(amidoamine) (PAMAM) dendrimers are also used as a polymeric drug carrier to increase the drug microvascular transport [65] based on their extravasation across microvascular network endothelium.

2.3.10 Poly (amino acids) and genetic designed polypeptides

Poly(L-lysine) [66,67], poly(L-glutamic acid) [68-70] and poly(L-aspartic acid) have been studied extensively as water-soluble drug carriers for the delivery of anticancer drugs, e.g., 5-FU, methotrexate, adriamycin etc. Currently, poly-L-lysine and its ester analogues are among the most widely used non-viral polymeric carriers for gene delivery.

Loosely crosslinked poly(acryloyl-L-proline methyl ester) gels exhibit a lower critical solution temperature (LCST) of approximately 14°C, which allows thermo-responsive functions such as swelling below the LCST and contraction above the LCST. This gel forms a rigid membrane barrier at the surface immediately after immersion in water at temperatures above 14°C. Such a barrier markedly blocks the diffusion of water from the interior side of the gel, suggesting that this feature is applicable to drug delivery systems as external stimulus-responsive biomaterials [71]. However, poly(amino acids) are difficult to process and polymers containing three or more amino acids often promote immune responses, thus limiting their medical use.

Many natural polymeric materials (particularly structural proteins) display a hierarchy of structures as sizes increase. Block co-polymers are able to self-assemble into ordered nanostructures, but the random coiled nature of their polymer chains usually suppresses any further levels of organisation. The use of components with regular structures, such as rigid-rod polymers, can increase the extent of spatial organisation in self-assembling materials. However, the synthesis of such polymeric components typically involves a complex series of reactions, which are difficult to adapt to large-scale production. Proteins form hierarchically organised structures in which the fundamental motifs are generally α -helical coils and β -sheets. Attempts to synthesise polypeptides with well defined amino acid sequences, which might adopt similar

organised structures, have been plagued by unwanted side reactions results in products with a wide range of molecular weights. Well defined peptide block co-polymers could provide new peptide based biomaterials with potential applications in tissue engineering, drug delivery and biomimetic composite formation.

Amphiphilic peptides with alternating hydrophobic and hydrophilic residues, for example, (AEAEAKAK)₂ and (ARARADAD)₂, self-assembled into macroscopic membranes [208,209]. These membrane forming peptides were between 12 and 16 amino acids in length. The macroscopic membrane was stable in aqueous solution, serum and ethanol, were highly resistant to heat, alkaline and acid pH, chemical denaturants and proteolytic digestion and non-cytotoxic. The membrane was potentially useful in biomaterial applications such as slow-diffusion drug delivery, artificial skin and as a separation matrix.

Proteinoid microspheres [210] were disclosed as oral drug delivery systems for the administration of drugs required for growth disorders and diabetes, using labile agents such as monoclonal antibodies, erythropoietin, human growth factor, α -IFN, calcitonin, insulin, heparin and IL-2. The proteinoid microspheres were soluble within selected pH ranges within the gastrointestinal tract and displayed enhanced stability. The proteinoid microspheres were prepared from proteinoids of 2 - 8 amino acids and with molecular weights ~ 1 kDa.

Silk-elastin-like block co-polymers, a family of closely related protein polymers, are composed of tandemly repeated sequential amino acid blocks of silk (Gly-Ala-Gly-Ala-Gly-Ser) and elastin (Gly-Val-Gly-Val-Pro). These nature inspired co-polymers show promise for the development of novel biomaterials for controlled drug delivery where slight changes in temperature or pH can cause rapid self-assembly of the polymers [72].

Genetically engineered, thermally-responsive, elastin-like polypeptides (ELPs) [73] are biopolymers with the pentapeptide repeat Val-Pro-Gly-Xaa-Gly (residue Xaa can be any of natural amino acids, except Pro). ELPs undergo an inverse temperature phase transition; that is, soluble in aqueous solution below the transition temperature but hydrophobically collapse and aggregate at higher temperatures. A 60-kDa ELP had a phase transition temperature at ~ 41 °C, such that targeting ELP to solid tumours by local hyperthermia could be achieved. In nude mice xenografts bearing human tumours (SK OV-3 ovarian carcinoma and D-54 MG glioma), hyperthermic targeting of thermally-responsive ELP for 1 h provides a ~ 2-fold increase in tumour localisation compared to the same polypeptide without hyperthermia. In addition, thermally responsive ELP was found to aggregate within the heated tumour microvasculature, which demonstrates that the phase transition of the thermally responsive ELP carrier can be engineered to occur *in vivo* at a specific temperature. By exploiting the phase transition induced aggregation of those polypeptides, this method provides a new way to thermally target polymer-drug conjugates to solid tumours.

Peptide-amphiphiles with collagen-model head groups and monoalkyl or dialkyl chain tails are able to self-assemble into highly ordered polyPro II-like triple-helical structures when dissolved in aqueous sub-phases [74]. The assembly process was driven by the hydrophobic tail, and may provide a general method for creating well-defined protein molecular architectures. Peptide-amphiphile structures, possessing these alkyl moieties, have the potential to be used for biomaterial surface modification to improve biocompatibility or, by mimicking fusion of viral envelopes with cellular membranes, as drug delivery vehicles.

Full length fusion proteins can be generated containing an N-terminal 11-amino acid protein transduction domain (PTD) (Tyr-Gly-Arg-Lys-Lys-Arg-Arg-Gln-Arg-Arg-Arg), from the HIV tat protein [75]. Protein transduction occurs in a rapid, concentration-dependent fashion that appears to be independent of receptors and transporters and is thought instead to target the lipid bilayer component of the cell membrane. Thus, in principle, all mammalian cell types should be susceptible to protein transduction and, indeed, this protein has been applied to transfer proteins ranging in size from 15 - 120 kDa into a wide variety of human and murine cell types. This technology has potential in future for macromolecular drug (protein) delivery and gene delivery.

2.3.11 Pseudo-poly(amino acids)

Pseudo-poly(amino acids), a class of polymers based on natural amino acids linked by nonamide bonds, including ester, iminocarbonate, urethane and carbonate, offer improved mechanical properties, processing, stability and ease of synthesis over traditional amide-linked polypeptides. The range of monomers and bonds has enabled development of a combinatorial approach to obtaining polymers with desired properties, such as glass transition temperature (T_g), crystallinity and hydrophobicity.

Non-cytotoxic tyrosine-PEG-derived poly(ether carbonates) were prepared by condensation co-polymerisation of PEG and desaminotyrosyltyrosine alkyl esters with phosgene [76]. Microspheres could be prepared by solvent evaporation techniques from co-polymers with low PEG content. The rate of release of *p*-nitroaniline and fluorescein isothiocyanate-dextran from the microspheres increased with increasing PEG content.

Biodegradable poly(iminocarbonates), based on diphenols such as hydroquinone, bisphenol A, or tyrosine were synthesised [77,78]. Near zero-order sustained drug release from the poly(bisphenol A-iminocarbonate) transparent films and strong fibers could be achieved.

2.3.12 Other biodegradable polymers

A class of bisphenol-A based biodegradable poly(phosphoesters) was studied for its potential as a matrix for controlled drug delivery [79]. The degradability of the phosphorus ester linkage and the versatility of phosphorus containing polymers makes poly(phosphoesters) attractive candidates for develop-

ment as a degradable biomaterial. The mechanism of drug release was found to be a combination of diffusion, swelling and degradation. The structure of the side chain influenced the release behavior in all instances.

Poly(orthoesters) are hydrophobic polymers that are labile in an acidic environment, which can be formulated to allow surface erosion of devices. The drug imbedded in the device is released at a constant rate. Poly(orthoesters) have been used for the controlled release of 5-FU, mytomycin C, cyclobenzaprine, steroids, bupivacaine [80], as well as other pharmaceutical compounds [81,82].

Poly(alkyl cyanoacrylate) nanoparticles and nanospheres have been used to prolong ophthalmic delivery of pilocarpine and betaxolol [83]. Polyphosphazenes have the advantage of versatility of reactions with other nucleophiles, making it easy to manipulate their properties by changing substituent groups. They are good candidates for biodegradable materials for drug-polymer conjugates, due to ease of nucleophilic reaction for conjugation [84].

2.4 Natural polymers in drug delivery systems

Natural polymers are often more suitable than synthetic polymers because of their intrinsic biocompatibility and biodegradability. However, natural biopolymers often possess poor biomechanical properties and are too readily degraded; these drawbacks preclude use in many medical applications. To obtain more mechanically and chemically robust materials, it has been necessary to chemically modify natural biopolymers.

Phosphatidylethanolamine (PE) is one of the most common naturally occurring phospholipids. The primary amino group of PE is readily derivatised. Unfortunately, PE tends to form micelles and hexagonal clusters instead of forming lamellar sheets and vesicles (liposomes). A dimeric PE molecule was synthesised [85] in which the acyl chains at the 2-position of glycerol are joined at their fatty acyl methyl termini by a carbon-carbon bond, thus resulting in a transmembrane-type fatty acyl linkage. Such tail-to-tail bipolar transmembrane lipids are found in the membranes of thermophilic and other extremophilic bacteria. The dimeric PE readily forms very uniform, flat, self-assembled lamellar supramolecular arrays and liposomes that are stable at temperatures up to 80°C. This extremely stable and readily functionalisable dimeric phospholipid has potential use in the fabrication of biomaterials, stable membrane models and liposomal drug-delivery systems.

2.4.1 Polysaccharides.

Polysaccharide derivatives, used for the preparation of biocompatible and biodegradable biomaterials with absorbent properties for body fluids and physical haemostatic activity, are used in both venous and arterial vascular anastomoses and to prevent the formation of post-surgical adherence of the vessels with scar formation in the surrounding tissue. A formulation for the delivery of a pharmacological agent to the respiratory tract, using hydroxyethyl starch microspheres, was

prepared. Specifically, insulin, calcitonin, PTH, IFN, oligonucleotides and DNA were used as the active components [211].

Chitin and chitin-derived hydrogels [212] that contain growth factors, drugs promoting wound healing, or plasma proteins may have potential for wound healing and drug delivery (e.g., an antibiotic). Chitosan is a very interesting biomaterial for drug delivery; however, oral administration is restricted by its rapid dissolution in the stomach and limited capacity for controlling the release of drugs. To address this limitation, a new microparticulate chitosan controlled release system, consisting of hydrophilic chitosan microcores entrapped in a hydrophobic cellulosic polymer, such as cellulose acetate butyrate, was proposed [86]. The microparticles were stable at low pH and thus, suitable for oral delivery without requiring any harmful cross-linkage treatment.

Alginate hydrogels have found extensive use in various biomedical applications including tissue engineering and controlled drug delivery applications. Alginate hydrogels are poorly biodegradable and have a limited range of mechanical properties. Alginate was partially oxidised with sodium periodate and crosslinked with a homobifunctional crosslinker to form biodegradable hydrogels [87,88]. These hydrogels exhibited a range of physical properties that were dependent on the concentration of the polymer, crosslinker and concentration of calcium ions. In addition, cell adhesion peptides can be readily coupled to these materials to allow for specific cell adhesion. These biomaterials show promise as vehicles for controlled drug delivery and cell transplantation applications. Calcium crosslinked alginate hydrogels have been evaluated as a simple mimic of natural ECM for the controlled release of VEGF in response to the external mechanical stress [89]. It may also be possible to develop delivery systems of small drug molecules using the similar concept of mechanical stimuli-mediated controlled release.

Pectin and pectin derivatives, plus galactomannan, can be formulated with biologically active molecules for drug delivery to the colon [213]. The polysaccharides provide an elastic gel, which prevents early drug release in the upper gastrointestinal (GI) tract.

In research from our laboratories, hyaluronic acid (HA), a naturally occurring polysaccharide in ECM, was extensively studied in biomedical applications [90,301]. A mild, controllable modification of HA was developed in which monovalent, divalent, or polyvalent hydrazides can be covalently attached to HA to give functionalised derivatives with a high degree of synthetic versatility [214]. HA can be covalently modified to produce drug delivery systems and novel hydrogel biomaterials with a variety of desired physical and chemical properties [91]. Specific applications include, localisable delivery of anti-inflammatory agents at wound site by HA-derived hydrogel carrier [92], materials for tissue engineering and prevention of post-surgical adhesions, novel grafted co-polymers for drug delivery, tumour-targeted anticancer drugs [93,94] and techniques for coating surfaces of polymeric and metal medical

devices. Recently, an HA-benzyl ester polymer was fabricated into a three-dimensional scaffold for the delivery of chondrocytes and mesenchymal cells in tissue engineering [95,96].

Hyaluronic acid amides or derivatives of specified structure, e.g., total or partial esters or salts with heavy metals or pharmacologically-active substances, useful for the preparation of pharmaceutical compositions, biomaterials, surgical and healthcare articles, slow-release systems and systems for the coating of biomedical objects, are prepared and claimed [215]. These derivatives are prepared by:

- deacetylation of HA
- preparation of a quaternary ammonium compound of deacetylated acid
- preparation of an acylating agent in the form of an active ester
- N-acylation

However, the use of hydrazine sulfate/hydrazine as the deacetylation agent will result in the degradation of the HA polymer. An option is the activation of the carboxyl groups of HA with 1,1-carbonyldiimidazole, followed by amidation.

2.4.2 Carriers from biological sources.

Collagen is the most abundant mammalian protein accounting for ~ 30% of all body proteins. It is a major structural component of many tissues such as skin, bone, cartilage, tendon and basement membrane. The use of collagen as a biomaterial is currently undergoing a renaissance in the field of tissue engineering. The biotechnological application focuses on the aspects of cellular growth or delivery of proteins capable of stimulating cellular response. The attractiveness of collagen rests largely on the view that it is a natural material of low immunogenicity, and is therefore seen by the body as a normal constituent rather than foreign matter. Collagen can be processed into a number of forms, such as sheets, tubes, sponges, powders, fleeces, injectable solutions and dispersions, all of which have found use in medical practice. Furthermore, attempts have been made to apply these systems for drug delivery to ophthalmology, wound and burn dressing, tumour treatment and tissue engineering. The most successful and stimulating applications are shields in ophthalmology, injectable dispersions for local tumour treatment, sponges carrying antibiotics and mini-pellets loaded with protein drugs [97,98].

Gelatin is a natural polymer that can be extracted from collagen by alkaline or acid pretreatment and thermal denaturation [99]. Cross-linked gelatin gels are used as biomaterials in living tissues, either as bioadhesives or as devices for sustained drug release. An injectable and flowable material for tissue repair, reconstruction and bulking is comprised of gelatin microspheres incorporated with active components, such as drugs or growth factors, to elicit a specific tissue response or to provide local delivery of a therapeutic agent [216]. The close packing of the microspheres at the site of application and the biodegradation of the materials allow for retention of the par-

ticles at the target site to permit tissue repair and in-growth into the implant.

Fibres of the biocompatible and biodegradable poly- β -1,4-N-glucosamine (p-GlcNAc) [217] were produced by and purified from, microalgae, especially diatoms of the genus *Thalassiosira*. The pure, fully acetylated polyGlcNAc can be derivatised chemically to produce a large range of different compounds with modified biological activities. Small molecules and proteins can be linked to the polyGlcNAc fibres. A polyGlcNAc gel was shown to prevent post-surgical adhesions and to control bleeding. It can also be used as a 3-D matrix with controlled pore size for cell encapsulation, tissue engineering and targeted drug delivery systems.

Proteins and antibodies can also be used as drug carriers. Albumin, antiGP60 antibodies, GP60 peptide fragments (e.g., CGMC motif) can serve as transcytosis vehicles and enhancers capable of transporting physiologically active agents across epithelia, endothelia and mesothelia, that contain the GP60 receptor. The therapeutic agent can be co-administered with the transcytosis factor or can be conjugated to it to facilitate the transcytosis process [218].

A novel IgM-type mAb [219], 105A5, is described, which binds specifically to the native, unmodified peanut agglutinin (PNA)-binding glycoprotein MGC-24 on the cell-surface. The antibody inhibits the hematopoietic development *in vitro* of CD34+ cells. The coupling of therapeutics to the antibody for cell-targeted delivery was contemplated, with applications for the diagnosis and treatment of tumours.

Using isolated or integrated membrane vesicles of a micro-organism [220] to carry therapeutic agents, including antimicrobial and antiviral agents and nucleic acids, could be useful for the treatment of infectious diseases. Impermeable drugs such as gentamycin could be delivered into eukaryotic cells using the membrane vesicle system. Surface antigens, such as lipopolysaccharides, could be transferred from bacteria using membrane vesicles, which in turn could be used to directly target a drug to a specific tissue.

A novel two plasmid system was claimed for creating modified adenoviral particles with fibre proteins having affinity to different tissues [221]. This presents a novel system for delivery of a therapeutic DNA sequence to a tissue or cell-type of choice. The chimeric fibre protein can have protein sequences that give the adenovirus novel cell tropism.

The use of novel neurotoxins, or fragments thereof, to transport nucleic acids into the nervous system was proposed for treating diseases of the nervous system that require gene therapy [222]. The use of neurotoxins from bacteria, including tetanus or botulinum toxin, or from snake, including crotoxin or dendrotoxin, were specifically claimed, although the preferred fragments would be non-toxic binding domains.

2.5 Hybrid materials in drug delivery systems

Both natural polymers and their derivatives are finding applications in the biomedical field. While many natural polymers are better for *in vivo* application because of their facile absorp-

tion, important advances have been made with synthetic polymers, which sometimes offer properties not otherwise accessible with natural biomacromolecules. However, neither natural nor synthetic polymers can meet all the complex demands of biomaterials by themselves. Hence, much attention has been focused on the composites of natural and synthetic polymers that combine the advantageous properties of both constituents. In order to achieve the desired biocompatibility and biodegradability and the appropriate physical and chemical properties, hybrid materials have been prepared from synthetic polymers and natural biopolymers such as proteins and polysaccharides.

A blend hydrogel of hyaluronate-hydroxyethyl acrylate [100] was developed as a controlled release device for cationic drugs, e.g., chlorpromazine. The cationic drug was incorporated in the matrix through electrostatic interaction. The drug release profile corresponded to polymer swelling, which was responsive to ionic strength and pH.

A hybrid hydrogel system [101] was assembled from a water-soluble synthetic polymer (poly(*N*-hydroxypropylmethacrylamide), HPMA) and a well defined protein folding motif, the coiled coil. The hydrogel underwent a temperature-induced collapse due to the co-operative conformational transition of the coiled-coil protein domain. This system showed that well characterised water-soluble synthetic polymers, can be combined with well defined folding motifs of proteins in hydrogels with engineered volume-change properties. This stimulus-sensitive smart hydrogel will be pursued in drug delivery systems.

A biodegradable interpenetrating network (IPN)-structured hydrogels were synthesised by sequential crosslinking reaction of *N*-methacryloyl-glycyl-glycylglycyl-terminated PEG (by γ -irradiation) and dextran (by hexamethylene diisocyanate at 60°C) [102]. The IPN-structured hydrogels contain physical chain entanglements between networks, as well as chemically-crosslinked networks. The hydrogel was not degraded by either papain or dextranase alone, but was degraded in the presence of both enzymes. Such degradation properties of the IPN-structured hydrogel can be useful as a fail-safe system for guaranteed drug delivery and/or medical micromachines.

The conjugates of cholera toxin B subunit protein, coupled to poly-L-lysine, possess the ability to localise functional polynucleotides to mucosal tissues, neural tissues and to other tissues that display the GM1 receptor. This system was claimed to be potentially useful for gene delivery and/or vaccination [223].

Immunoliposomes [224] comprising a Fab' domain, which binds to the cell-surface marker and an amphipathetic vesicle-forming lipid, can be used in target drug delivery of anticancer agents (e.g., adriamycin) and in the treatment of carcinoma. The immunoliposomes were internalised efficiently into the cytoplasm of the target breast cancer cells. The Fab' fragments were also conjugated to distal ends of liposome-grafted PEG chains *via* sulfhydryl-reactive maleimide groups

and this modification improved specific targeting and internalisation.

Fibrin was grafted with poly (glycidyl methacrylate) (PGMA) [103]. This biomaterial could be used as a drug delivery system after coupling to a suitable antibiotic through the epoxy functional groups that were introduced by PGMA.

Biodegradable polyrotaxanes exhibit unique supramolecular architectures. Many α cyclodextrins (α -CDs) can be threaded onto a single PEG chain capped with biodegradable bulky end-groups. Furthermore, a stimuli-responsive polyrotaxane, in which many β -CDs are threaded onto a triblock-copolymer of PEG and poly(propylene glycol) (PPG) capped with fluorescein-4-isothiocyanate, was designed as a novel 'smart' material. Polyrotaxanes, as supramolecule-structured polymers, were characterised aiming at a drug carrier, a drug permeation enhancer, an implantable material and a stimuli-responsive material [104].

3. Conclusions

Drug delivery systems can overcome the problems of conventional dosage forms, which include cyclical fluctuations of drug concentration in blood, patient compliance, targeting of the drug to a specific site and control of the kinetics of drug concentration in blood. Despite the number of controlled-release systems that have been researched and/or employed in recent years, the area of controlled-release technology is still under development. The proper evaluation of existing biomaterials, as well as the creation of new biomaterials, will play an important role in the future drug development efforts.

4. Expert opinion

Both synthetic and natural polymers have made important contributions to the biomedical field. In drug delivery systems, polymers can function as therapeutic drug carriers. The properties of matrix polymers, such as hydrophilicity, crystallinity, lability and the degradation mechanism, play important roles in determining stability of the delivery devices and the drug release profile. Many natural polymers are better for *in vivo* application because of their biological functions, good biocompatibility, biodegradability, facile absorption and lack of immunogenicity. Important advances have also been made with synthetic polymers, to improve mechanical properties, balance of hydrophilicity and hydrophobicity and ease of processing. However, neither natural nor synthetic polymers alone can meet all the complex demands of biomaterials. The meaningful interaction within the areas of synthetic and natural polymers has been well recognised in recent years. Hence, much attention has been focused on the composites of natural and synthetic polymers that combine the advantageous properties of both constituents.

To achieve the desired drug delivery devices, hybrid materials from synthetic polymers and natural biopolymers will be the future of biomaterials. Importantly, the optimised drug

delivery system should have a biomaterial matrix with good mechanical property, balance of hydrophilicity and hydrophobicity, good biocompatibility and controllable biodegradability where minimal bioerosion occurs during the time that drug is being released; the empty system then slowly erodes. 'Smart' biomaterials that respond to external stimuli will provide further advantages for the controlled delivery of therapeutic drugs.

Bibliography

Papers of special note have been highlighted as either of interest (*) or of considerable interest (**) to readers.

- 1 LANGER R: Biomaterials and biomedical engineering. *Chem. Eng. Sci.* (1995) 50(24):4109-4121.
- 2 LANGER R: Biomaterials: new polymers and novel applications. *MRS Bull.* (1995) 20(8):18-22.
- 3 LANGER R: Drug delivery and targeting. *Nature* (1998) 392 (Suppl.):5S-10S.
- ** Polymeric materials in drug delivery systems.
- 4 LANGER R: Biomaterial in drug delivery and tissue engineering: one laboratory's experience. *Acc. Chem. Res.* (2000) 33:94-101.
- 5 FEIJEN J: The impact of biomaterials on pharmaceutical sciences. *Euro. J. Pharm. Sci.* (1994) 2:7-9.
- 6 LEMONS JE: Ceramics: past, present, and future. *Bone* (1996) 19(1 Suppl.):121S-128S.
- Recent paper describing the development of ceramics as implants and its application in drug delivery.
- 7 KIMAKHE S, BOHIC S, LARROSE C *et al.*: Biological activities of sustained Polymyxin B release from calcium phosphate biomaterial prepared by dynamic compaction: an *in vitro* study. *J. Biomed. Mater. Res.* (1999) 47(1):18-27.
- 8 GAUTIER H, CAILLON J, LE RAY AM, DACULSI G, MERLE C: Influence of isostatic compression on the stability of vancomycin loaded with a calcium phosphate-implantable drug delivery device. *J. Biomed. Mater. Res.* (2000) 52(2):308-314.
- 9 GUICHEUX J, GAUTHIER O, AGUADO E *et al.*: Human growth hormone locally released in bone sites by calcium-phosphate biomaterial stimulates ceramic bone substitution without systemic effects: a rabbit study. *J. Bone Miner. Res.* (1998) 13(4):739-748.
- 10 GUICHEUX J, KIMAKHE S, HEYMANN D, DACULSI G: Growth hormone stimulates the degradation of calcium phosphate biomaterial by human monocytes/macrophages *in vitro*. *J. Biomed. Mater. Res.* (1998) 40(1):79-85.
- 11 GAUTIER H, GUICHEUX J, GRIMANDI G, FAIVRE-CHAUVEY A, DACULSI G, MERLE C: *In vitro* influence of apatite-granule-specific area on human growth hormone loading and release. *J. Biomed. Mater. Res.* (1998) 40(4):606-613.
- 12 LAMBOTTE JC, THOMAZEAU H, CATHELIN G, LANCIEN G, MINET J, LANGLAIS F: Tricalcium phosphate, an antibiotic carrier: a study focused on experimental osteomyelitis in rabbits. *Chirurgie* (1998) 123(6):572-9.
- 13 TAGAI T, HOSHI T, YAMADA T: Development of the porous apatitic materials. *Kobun Kagaku Zasshi* (1997) 26(2):59-62.
- 14 RODRIGUEZ-LORENZO LM, SALINAS AJ, VALLET-REGI M, SAN ROMAN J: Composite biomaterials based on ceramic polymers. I. Reinforced systems based on Al₂O₃/PMMA/PLLA. *J. Biomed. Mater. Res.* (1996) 30(4):515-522.
- 15 HOFFMAN AS: Synthetic polymeric biomaterials. In: *Polymeric materials and artificial organs*. Gebelein Cg (Ed.). American Chemical Society, Washington DC, USA (1984):13-19.
- 16 HANES J, CHIBA M, LANGER R: Degradation of porous poly(anhydride-co-imide) microspheres and implications for controlled macromolecule delivery. *Biomaterials* (1998) 19(1-3):163-172.
- 17 KIM D-D, TAKENO MM, RATNER, HORBETT TA: Glow discharge plasma deposition (GDPD) technique for the local controlled delivery of hirudin from biomaterials. *Pharm. Res.* (1998) 15(5):783-786.
- 18 SERIZAWA T, UCHIDA T, AKASHI M: Synthesis of polystyrene nanospheres having lactose-conjugated hydrophilic polymers on their surfaces and carbohydrate recognition by proteins. *J. Biomater. Sci., Polym. Ed.* (1999) 10(3):391-401.
- ** Site-specific drug carrier of lactose conjugated polystyrene nanosphere.
- 19 BRUINING MJ, EDELBROEK-HOOGENDOORN PS, BLAAUWGEERS HGT, MOOY CM, HENDRIKSE FH, KOOLE LH: New biodegradable networks of poly(N-vinylpyrrolidone) designed for controlled nonburst degradation in the vitreous body. *J. Biomed. Mater. Res.* (1999) 47(2):189-197.
- 20 SCHWARTE LM, PODUAL K, PEPPAS NA: Cationic hydrogels for controlled release of proteins and other macromolecules. *ACS Symp. Ser.* (1998) 709:56-66.
- Tailored polymeric materials for controlled delivery systems.
- 21 PEPPAS NA, KEYS KB, TORRES LM, LOWMAN AM: Poly (ethylene glycol)-containing hydrogels in drug delivery. *J. Controlled Release* (1999) 62(1-2):81-87.
- Mucoadhesive PEG star polymer hydrogels for protein delivery.
- 22 BELL CL, PEPPAS NA: Swelling/syneresis phenomena in gel-forming interpolymer complexes. *J. Biomater. Sci. Polym. Ed.* (1996) 7(8):671-683.
- 23 JO S, PARK K: Novel poly(ethylene glycol) hydrogels from silylated PEGs. *J. Bioact. Compat. Polym.* (1999) 14(6):457-473.
- 24 HASSAN CM, STEWART JE, PEPPAS NA: Diffusional characteristics of freeze/thawed poly(vinyl alcohol) hydrogels: Application to protein controlled release from multilaminate devices. *Euro. J. Pharm. Biopharm.* (2000) 49(2):161-165.
- 25 NUTTELMAN CR, ANSETH KS: Attachment of proteins to poly(vinyl alcohol) for biomedical applications. *Polym. Prepr. (Am. Chem. Soc., Div. Polym. Chem.)* (2000) 41(2):1685-1686.
- 26 GRIFFITH LG: Polymeric biomaterials. *Acta Mater.* (2000) 48:263-277.

Acknowledgements

The authors acknowledge the financial support from US Department of Defence (DAMD 17-9A-1-8254), the Center for Biopolymers at Interfaces and the Huntsman Cancer Foundation at The University of Utah.

- Recent review on the polymeric biomaterial development and applications.
- 27 LI S: Hydrolytic degradation characteristics of aliphatic polyesters derived from lactic and glycolic acids. *J. Biomed. Mater. Res.* (1999) 48:342-353.
- Recent review on the degradation mechanism of PLGA polymers.
- 28 SUH H, JEONG B, RATHI R, KIM SW: Regulation of smooth muscle cell proliferation using paclitaxel-loaded poly(ethyleneoxide)-poly-(lactide/glycolide) nanospheres. *J. Biomed. Mater. Res.* (1998) 42(2):331-338.
- 29 KREITZ MR, DOMM JA, MATHIOWITZ E: Controlled delivery of therapeutics from microporous membranes. II. *In vitro* degradation and release of heparin-loaded poly(D,L-lactide-co-glycolide). *Biomaterials* (1997) 18(24):1645-1651.
- 30 BEMOIT MA, MOUSSET B, DELLOYE C, BOUILLET R, GILLARD J: Antibiotic-loaded plaster of Paris implants coated with poly lactide-co-glycolide as a controlled release delivery system for the treatment of bone infections. *Int. Orthop.* (1997) 21(6):403-408.
- 31 SANCHEZ A, GUPTA RK, ALONSO MJ, SIBER GR, LANGER R: Pulsed controlled-release system for potential use in vaccine delivery. *J. Pharm. Sci.* (1996) 85(6):547-552.
- 32 NOBES GAR, MARCHESSAULT RH, MAYSINGER D: Polyhydroxyalkanoates: Materials for delivery systems. *Drug Delivery* (1998) 5:161-177.
- Recent review on polyhydroxyalkanoates in drug delivery.
- 33 MATHIOWITZ E, JACOB JS, JONG YS *et al.*: Biologically erodable microspheres as potential oral drug delivery systems. *Nature* (1997) 386:410-414.
- Bioerodable polyanhydride microspheres in oral drug delivery.
- 34 MULLER H-M, SEEBACH D: Poly(hydroxyalkanoates): a fifth class of physiologically important organic biopolymer? *Angew. Chim. Intl. Ed. Engl.* (1993) 32:477-502.
- 35 CHAPUT C, YAHIA LH, SELMANI A, RIVARD C-H: Natural poly(hydroxybutyrate-hydroxyvalerate) polymers as degradable biomaterials. *Mater. Res. Soc. Symp. Proc.* (1995) 385(Polymer/Inorganic Interfaces 2):49-54.
- 36 GURSEL I, BALCIK C, ARICA Y, AKKUS O, AKKAS N, HASIRCI V: Synthesis and characterization of PHBV and PHEMA interpenetrating networks. *Proc. Int. Symp. Controlled Release Bioact. Mater.* (1997) 24th:1045-1046.
- Hydrophilicity and hydrophobicity balanced PHBV and PHEMA interpenetrating networks.
- 37 ELIGIO T, RIEUMONT J, SANCHEZ R, SILVA JFS: Characterization of chemically modified poly(3-hydroxyalkanoates) and their performance as matrix for hormone release. *Angew. Makromol. Chem.* (1999) 270:69-75.
- 38 KOBAYASHI H, SHIRAKI K, KADA Y: Toxicity test of biodegradable polymers by implantation in rabbit cornea. *J. Biomed. Mater. Res.* (1992) 26:1463-1476.
- 39 WADE CWR, HEGYELI AF, KULKARNI RK: Standards for *in-vitro* and *in-vivo* comparison and qualification of bioabsorbable polymers. *J. Test. Eval.* (1977) 5:397-400.
- 40 JALIL R-U: Biodegradable poly(lactic acid) and poly(lactide-co-glycolide) polymers in sustained drug delivery. *Drug Dev. Ind. Pharm.* (1990) 16:2353-2367.
- 41 ENGELBERG I, KOHN J: Physico-mechanical properties of degradable polymers used in medical applications: a comparative study. *Biomaterials* (1991) 12:290-304.
- 42 RAMCHANDANI M, PANKASKIE M, ROBINSON D: The influence of manufacturing procedure on the degradation of poly(lactide-co-glycolide) 85:15 and 50:50 implants. *J. Controlled Release* (1997) 43(2,3):161-173.
- 43 RAMCHANDANIA M, ROBINSON D: *In vitro* and *in vivo* release of ciprofloxacin from PLGA 50:50 implants. *J. Controlled Release* (1998) 54(2):167-175.
- 44 MORITA T, SAKAMURA Y, HORIKIRI Y, SUZUKI T, YOSHINO H: Protein encapsulation into biodegradable microspheres by a novel S/O/W emulsion method using poly(ethylene glycol) as a protein micronization adjuvant. *J. Controlled Release* (2000) 69(3):435-444.
- 45 GASPAR MM, BLANCO D, CRUZ MEM, ALONSO MJ: Formulation of L-asparaginase-loaded poly(lactide-co-glycolide) nanoparticles: influences of polymer properties on enzyme loading, activity and *in vitro* release. *J. Controlled Release* (1998) 52:53-62.
- 46 ROSA GD, IOMMELI R, LA ROTONDA MI, MIRO A, QUAGLIA F: Influence of the co-encapsulation of different non-ionic surfactants on the properties of PLGA insulin-loaded microspheres. *J. Controlled Release* (2000) 69(2):283-295.
- 47 EGILMEZ NK, JONG YS, SABEL MS, JACOB JS, MATHIOWITZ E, BANKERT RB: *In situ* tumor vaccination with interleukin-12-encapsulated biodegradable microspheres: induction of tumor regression and potent antitumor immunity. *Cancer Res.* (2000) 60(14):3832-3837.
- 48 CLELAND JL, JONES AJS: Stable formulation of recombinant human growth factor hormone and interferon- γ for microencapsulation in biodegradable microspheres. *Pharm. Res.* (1996) 13(10):1464-1475.
- 49 CLELAND JL, MAC A, BOYD B *et al.*: The stability of recombinant human growth hormone in poly(lactic-co-glycolic acid) (PLGA) microspheres. *Pharm. Res.* (1997) 14(4):420-425.
- 50 LU L, STAMATAS GN, MIKOS AG: Controlled release of transforming growth factor β 1 from biodegradable polymer microparticles. *J. Biomed. Mater. Res.* (2000) 50:440-451.
- 51 ZHU G, MALLERY SR, SCHWENDEMAN SP: Stabilization of proteins encapsulated in injectable poly(lactide-co-glycolide). *Nature Biotech.* (2000) 18:52-57.
- 52 PEAN J-M, BOURY F, VENIER-JULIENNE M-C, MENEI P, PROUST J-E, BENOIT J-P: Why does PEG 400 co-encapsulation improve NGF stability and release from PLGA biodegradable microspheres? *Pharm. Res.* (1999) 16(8):1294-1299.
- 53 PETTIT DK, LAWTER JR, HUANG WJ *et al.*: Characterization of poly(glycolide-co-D,L-lactide)/poly(D,L-lactide) microspheres for controlled release of GM-CSF. *Pharm. Res.* (1997) 14(10):1422-1430.
- 54 JEONG B, CHOI K, BAE YH, ZENTNER G, KIM SW: New biodegradable polymers for injectable drug delivery systems. *J. Controlled Release* (1999) 62:109-114.
- 55 JEONG B, BAE YH, KIM SW: Biodegradable block copolymers as injectable drug-delivery systems. *Nature* (1997) 388:860-862.
- Temperature sensitive PEO-PLA copolymer as injectable drug carrier.

- 56 LUCKE A, TESSMAR J, SCHNELL E, SCHMEER G, GOPFERICH A: Biodegradable poly(D,L-lactic acid)-poly(ethylene glycol)-monomethyl ether diblock copolymers: structures and surface properties relevant to their use as biomaterials. *Biomaterials* (2000) 21(23):2371-2370.
- 57 SAITO N, OKADA T, TOBA S, MIYAMOTO S, TAKAOKA K: New synthetic absorbable polymers as BMP carriers: Plastic properties of poly-D,L-lactic acid-polyethylene glycol block copolymers. *J. Biomed. Mater. Res.* (1999) 47(1):104-110.
- 58 MOLINA I, LI S, MARTINEZ MB, VERT M: Protein release from physically crosslinked hydrogels of the PLA/PEO/PLA triblock copolymer-type. *Biomaterials* (2001) 22:363-369.
- Physically crosslinked PLA/PEO/PLA hydrogel in protein delivery.
- 59 GOODWIN CJ, BRADEN M, DOWNES S, MARSHALL NJ: Release of bioactive human growth hormone from a biodegradable material: poly(ϵ -caprolactone). *J. Biomed. Mater. Res.* (1998) 40(2):204-213.
- 60 LI SM, CHEN XH, GROSS RA, MCCARTHY SP: Hydrolytic degradation of PCL/PEO copolymers in alkaline media. *J. Mater. Sci. Mater. Med.* (2000) 11(4):227-233.
- 61 FENG Y, KLEE D, HOCKER H: New biomaterial. Triblock copolymers of poly[3(5)-isobutyl-morpholine-2,5-dione]-poly(ethylene oxide). *Materialwiss. Werkstofftech.* (1999) 30(12):862-868.
- 62 JOHN G, MORITA M: Synthesis and characterization of photo-crosslinked networks based on L-lactide/serine copolymers. *Macromolecules* (1999) 32(6):1853-1858.
- Photocrosslinking of acrylated poly(L-lactide/serine) to form polymer networks and beads in drug delivery, copolymerisation with HEMA to be a degradable hydrogel.
- 63 WON CY, CHU CC, YU TJ: Novel amine-containing biodegradable polyester via copolymerisation of aspartic anhydride and 1,4-cyclohexanedimethanol. *Macromol. Rapid Commun.* (1996) 17(9):653-659.
- 64 KIM Y, ZENG F, ZIMMERMAN SC: Peptide dendrimers from natural amino acids. *Chem. Euro. J.* (1999) 5(7):2133-2138.
- Biodegradable dendrimers from natural amino acids.
- 65 EL-SAYED M, NAIMARK M, KIANI MF, GHANDEHARI H: Transport of macromolecular drug carriers across microvascular beds. *Polym. Prepr. (Am. Chem. Soc. Div. Polym. Chem.)* (2000) 41(2):1726-1727.
- 66 CAMPBELL P, GLOVER GL, GUNN JM: Inhibition of intracellular protein degradation by pepstatin, poly(L-lysine) and pepstatinyl-poly(L-lysine). *Arch. Biochem. Biophys.* (1980) 203:676-680.
- 67 JEONG SY, KIM SW: Biodegradable polymeric drug delivery systems. *Arch. Pharm. Res.* (1986) 9(2):63-73.
- 68 LI C, YU D, NEWMAN RA *et al.*: Complete regression of well-established tumors using a novel water-soluble poly(L-glutamic acid)-paclitaxel conjugate. *Cancer Res.* (1998) 58:2404-2409.
- 69 KISHIDA A, GOTO H, MURAKAMI K, KAKINOKI K, AKASHI M: Polymer drugs and polymeric drugs. IX: synthesis and 5-fluorouracil release profiles of biodegradable polymeric prodrugs γ -poly(α -hydroxy-methyl-5-fluoro-uracil-glutamate). *J. Bioact. Compat. Polym.* (1998) 13:222-233.
- 70 KISHIDA A, MURAKAMI K, GOTO H, AKASHI M: Polymer drugs and polymeric drugs. X: slow release of 5-fluorouracil from biodegradable poly(γ -glutamic acid) and its benzyl ester matrices. *J. Bioact. Compat. Polym.* (1998) 13:270-278.
- 71 YOSHIDA M, ASANO M, OMICHI H, KATAKAI R: Environmental responsive polymers based on pendant α -amino acid groups. *Hoshasen* (1993) 19(3):27-37.
- Temperature sensitive loosely crosslinked poly(acryloyl-L-proline methyl ester).
- 72 NAGARSEKAR A, CRISSMAN J, CRISSMAN M, FERRARI F, CAPPELLO J, GHANDEHARI H: Synthesis and characterization of pH and temperature sensitive silk-elastin-like block copolymers for controlled drug delivery. *Abstr. Pap. Am. Chem. Soc.* (2000) 220th: OLY-317.
- The development of a protein-based block copolymer biomaterials for stimuli-sensitive drug delivery systems using genetic engineering techniques.
- 73 MEYER DE, KONG GA, DEWHIRST MW, ZALUTSKY MR, CHILKOTI A: Targeting a genetically engineered elastin-like polypeptide to solid tumors by local hyperthermia. *Cancer Res.* (2001) 61:1548-1554.
- Targeting a genetically engineered elastin-like polypeptide to solid tumors by local hyperthermia.
- 74 YU Y-C, TIRRELL M, FIELDS GB: Minimal lipidation stabilizes protein-like molecular architecture. *J. Am. Chem. Soc.* (1998) 120(39):9979-9987.
- 75 SCHWARZE SR, HO A, VOCERO-AKBANI A, DOWDY SF: *In vivo* protein transduction: Delivery of biologically active protein into the mouse. *Science* (1999) 285:1569-1572.
- Protein transduction by TAT peptide sequence.
- 76 YU C, KOHN J: Tyrosine-PEG-derived poly(ether carbonate)s as new biomaterials part. I: synthesis and evaluation. *Biomaterials* (1999) 20(3):253-264.
- 77 KOHN J, LANGER R: Poly(liminocarbonates) as potential biomaterials. *Biomaterials* (1986) 7(3):176-182.
- 78 KOHN J: Optimization of biocompatibility and materials properties in the design of degradable biomaterials. *Polym. Prepr. (Am. Chem. Soc. Div. Polym. Chem.)* (1991) 32(2):223-224.
- Design of biodegradable polymers with defined physical, chemical, biological properties.
- 79 DAHIYAT BI, RICHARDS M, LEONG KW: Controlled release from poly(phosphoester) matrices. *J. Controlled Release* (1995) 33(1):13-21.
- 80 HELLER J, BARR J, NG S *et al.*: Development of a new family of poly(ortho esters) and their application in protein and bupivacaine delivery. *Tenth International Symposium on Recent Advances in Drug Delivery Systems*, Salt Lake City, Utah, USA, (2001) 49-52.
- 81 HELLER J, NG SY, PENHALE DW, FRITZINGER BK: Use of poly(ortho esters) for the controlled release of 5-fluorouracil and a LHRH analogue. *J. Controlled Release* (1987) 6:217-224.
- 82 HELLER J: Development of poly(ortho esters): A histological review. *Biomaterials* (1990) 11:659-665.
- A review on the development and biomedical application of poly(ortho ester).
- 83 MERKLI A, TABATABAY C, GURNY R: Use of insoluble biodegradable polymers in ophthalmic systems for the sustained release of drugs. *Euro. J. Biopharm.* (1995) 41(5):271-283.
- 84 ALLCOCK HR, HYMER WC, AUSTIN PE: Diazocoupling of catecholamines with poly(organophosphazenes). *Macromolecules* (1983) 16:1401-1408.

- 85 WANG G, HOLLINGSWORTH RI: Synthesis and properties of a bipolar, bisphosphatidyl ethanolamine that forms stable 2-dimensional self-assembled bilayer systems and liposomes. *J. Org. Chem.* (1999) 64(11):4140-4147.
- 86 REMUNAN-LOPEZ C, LORENZO-LAMOSA ML, VILA-JATO JL, ALONSO MJ: Development of new chitosan-cellulose multicore microparticles for controlled drug delivery. *Euro. J. Pharm. Biopharm.* (1998) 45(1):49-56.
- 87 BOUHADIR KH, YUE I, CHEN L, HAUSMAN D, MOONEY DJ: Synthesis and crosslinking of partially oxidized alginate for tissue engineering applications. *Book of Abstracts, 216th ACS National Meeting, Boston, USA August 23-27 (1998)*: BTEC-078.
- 88 BOUHADIR KH, ROWLEY JA, KRUGER GM, LEE KY, MOONEY DJ: Biodegradable hydrogels for controlled cell and drug delivery. *Book of Abstracts, 217th ACS National Meeting, Anaheim, California, USA March 21-25 (1999)*: OLY-175.
- 89 LEE KY, PETERS MC, ANDERSON KW, MOONEY DJ: Controlled growth factor release from synthetic extracellular matrices. *Nature* (2000) 408:998-1000.
- Mechanical-stimuli controlled growth factor release from alginate hydrogel.
- 90 PRESTWICH GD, LUO Y, ZIEBELL MR, VERCRUYSE KP, KIRKER KR, MACMASTER JS: Chemically-modified hyaluronan: new biomaterials and probes for cell biology. *Int. Congr. Ser.* (2000) 1196:181-194 New Frontiers in Medical Sciences: Redefining Hyaluronan.
- Hyaluronan derivatives in drug delivery, wound healing and cell biology study.
- 91 VERCRUYSE KP, PRESTWICH GD: Hyaluronate derivatives in drug delivery. *Crit. Rev. Therap. Drug Carr. Syst.* (1998) 15:513-555.
- Hyaluronan derived biomaterials in drug delivery application.
- 92 LUO Y, KIRKER KR, PRESTWICH GD: Cross-linked hyaluronic acid hydrogel films: New biomaterials for drug delivery. *J. Controlled Release* (2000) 69:169-184.
- 93 LUO Y, PRESTWICH GD: Synthesis and selective cytotoxicity of a hyaluronic acid-antitumor bioconjugate. *Bioconjugate Chem.* (1999) 10:755-763.
- 94 LUO Y, ZIEBELL MR, PRESTWICH GD: A hyaluronic acid-taxol antitumor bioconjugate targeted to cancer cells. *Biomacromolecules* (2000) 1:208-218.
- 95 RADICE M, BURN P, CORTIVO R, SCAPINELLI R, BATTALIARD C, ABARTANGELO G: Hyaluronan-based biopolymers as delivery vehicles for bone-marrow-derived mesenchymal progenitors. *J. Biomed. Mater. Res.* (2000) 50:101-109.
- Benzyl ester derived hyaluronan scaffold in tissue engineering.
- 96 CAMPOCCIA D, DOHERTY P, RADICE M, BRUN P, ABATANGELO G, WILLIAM DF: Semisynthetic resorbable materials from hyaluronan esterification. *Biomaterials* (1998) 19:2101-2127.
- 97 FRIESS W: Collagen. Biomaterial for drug delivery. *Euro. J. Pharm. Biopharm.* (1998) 45(2):113-136.
- Recent review on collagen in drug delivery.
- 98 RAO KP: Recent developments of collagen-based materials for medical applications and drug delivery systems. *J. Biomater. Sci. Polym. Ed.* (1995) 7(7):623-45.
- 99 KUIJPERS AJ, ENGBERS GHM, KRIJGSVELD J, ZAAAT SAJ, DANKERT J, FEIJEN J: Crosslinking and characterization of gelatin matrices for biomedical applications. *J. Biomater. Sci., Polym. Ed.* (2000) 11(3):225-243.
- 100 INUKAI M, JIN Y, YOMOTA C, YONESE M: Preparation and characterization of hyaluronate-hydroxyethyl acrylate blend hydrogel for controlled release device. *Chem. Pharm. Bull.* (2000) 48(6):850-854.
- 101 WANG C, STEWART RJ, KOPECEK J: Hybrid hydrogels assembled from synthetic polymers and coiled-coil protein domains. *Nature* (1999) 397(6718):417-20.
- Temperature sensitive hybrid hydrogels from synthetic polymers and coiled-coil protein domains.
- 102 KURISAWA M, TERANO M, YUI N: Double-stimuli-responsive degradation of hydrogels consisting of oligopeptide-terminated poly(ethylene glycol) and dextran with an interpenetrating polymer network. *J. Biomater. Sci., Polym. Ed.* (1997) 8(9):691-708.
- The biodegradability of IPN structured hydrogel based on oligopeptide-terminated PEG and dextran exhibiting a double-stimuli-response function.
- 103 SASTRY TP, MADHAVAN V, NAZER MN, GOMATHINAYAGAM S, ROSE C, RAO NM: Graft copolymerization of glycidyl methacrylate onto fibrin prepared from slaughter-house waste. *J. Macromol. Sci., Pure Appl. Chem.* (1997) A34(5):915-925.
- 104 OOOYA T, YUI N: Supramolecular-structured polymers for drug delivery. *ACS Symp. Ser.* (2000) 752:375-384 Controlled Drug Delivery.
- A stimuli-responsive polyrotaxane with supermolecular architecture assembled by cyclodextrins threaded onto a PEG chain.

Patents

Patents of special note have been highlighted as either of interest (*) or of considerable interest (**) to readers.

201. UNIVERSITY OF PENNSYLVANIA: US5591453 (1997).
- Controlled release of antibiotics, growth factors, anti-inflammatory agents and analgesics from within the matrix of a silica-based glass is claimed to be applicable as a substitute for autologous bone grafts.
202. BOARD OF TRUSTEES OF THE UNIVERSITY OF ILLINOIS: WO9737680 (1997).
- Macromolecular complexes comprising insulin and polyacrylic acid were formulated by the electrostatic forces for the use of reduction of glucose level.
203. DV TECH., INC.: WO9721441 (1997).
- Long-lasting ocular drug delivery by thermosensitive polyoxamers (polyoxyethylene-polyoxypropylene block co-polymers).
204. SUPRATEK PHARM INC: WO9943343 (1999).
- Polyoxyethylene-polyoxypropylene-polyoxyethylene ABA triblock co-polymers micelles for drug delivery.
205. UNIV. OF UTAH RES FDN: WO9915151 (1999).
- Polyoxyethylene-polyoxypropylene-polyoxyethylene ABA triblock co-polymers (pluronic 105) micelles for anticancer drug delivery.
206. MACROMED, INC.: WO9918142 (1999).
- Low molecular weight triblock co-polymers of PEG-PLGA-PEG possess reverse thermal gelation properties to deliver poorly water soluble and/or labile drugs.
207. GUILFORD PHARM., INC.: WO0019976 (2000).
- Microsphere formulations of biodegradable terephthalate polyester-poly(phosphonate) and polyester-poly(phosphite) co-polymers were developed to deliver antineoplastic

Novel biomaterials for drug delivery

- agents, antivirals, antifungals, anti-inflammatory and anticoagulants.
208. MASSACHUSETTS INSTITUTE OF TECHNOLOGY: US5670483 (1997).
 209. MASSACHUSETTS INSTITUTE OF TECHNOLOGY: US5955343 (1999).
 - Amphiphilic peptides with alternating hydrophobic and hydrophilic residues self-assembled into macroscopic membranes for slow-diffusion drug delivery.
 210. EMISPHERE TECH., INC.: US5601846 (1997).
 - Proteinoid microspheres as oral drug delivery systems.
 211. DANBIOSYST UK LTD: WO9735562 (1997).
 - Hydroxyethyl starch microspheres for protein drug delivery.
 212. DROHAN WN: WO9641818 (1996).
 - Chitin and chitin derived hydrogel for drug delivery and wound healing.
 213. SAMYANG CORP: WO0004924 (2000).
 - Elastic Pectin or a pectin derivative and galactomannan gel for colonic drug delivery.
 214. RESEARCH FOUNDATION OF SUNY: US5616568 (1997).
 - Hyaluronic acid derivatives and hydrogel for drug delivery.
 215. FIDIA ADVANCED BIOPOLYMERS: WO0001733 (2000).
 - Hyaluronic acid amides for the preparation of pharmaceutical compositions, biomaterials, surgical and healthcare articles, slow-release systems and systems for the coating of biomedical objects.
 216. POINT BIOMEDICAL CORPORATION: WO9911196 (1999).
 - An injectable and flowable gelatin microspheres for local delivery of growth factors in tissue repair, reconstruction and bulking.
 217. MARINE POLYMER TECH., INC.: US5624679 (1997).
 - 3-D poly- β -1,4-*N*-glucosamine in tissue engineering and targeted drug delivery.
 218. ANDARIS LTD.: WO9710850 (1997).
 - GP60 peptide fragments to facilitate transcytosis process in drug delivery.
 219. EBERHARD-KARLS-UNIV. TUBINGEN: WO9707204 (1997).
 - The conjugates of drug and mAb antibody for cell-targeted delivery for the diagnosis and treatment of tumours.
 220. UNIV. OF GUELPH: WO9705899 (1997).
 - Membrane vesicles of microorganism targeted delivery of a drug to a specific tissue.
 221. UNIV. OF ALABAMA AT BIRMINGHAM RES FDN: WO9720575 (1997).
 - A novel two plasmid system for creating modified adenoviral particles with fibre proteins having affinity to different tissues in gene delivery.
 222. SMITHKLINE BEECHAM PLC: WO9720579 (1997).
 - The use of novel neurotoxins or fragments to transport nucleic acids into the nervous system was proposed for treating diseases of the nervous system that require gene therapy.
 223. MAXIM PHARM: WO9705267 (1997).
 - GM1 receptor targeted conjugates of cholera toxin B subunit protein and poly-L-lysine possess the ability to localise functional polynucleotides to mucosal tissues, neural tissues and to other tissues.
 224. UNIV. OF CALIFORNIA: WO9738731 (1997).
 - Immunoliposome for targeted anticancer drug delivery.

Websites

301. PRESTWICH GD: Biomaterials from chemically-modified hyaluronan. *Glycoforum* (2001): <http://glycoforum.gr.jp/science/hyaluronan/HA18/HA18E.html>
- Recent review on the chemical modification of hyaluronan.

Affiliation

Yi Luo and Glenn D. Prestwich[†]

[†]Author for correspondence

Professor Glenn D. Prestwich, The University of Utah, Department of Medicinal Chemistry, 30 South 2000 East, Room 201, Salt Lake City, Utah 84112-5820, U.S.A. Tel.: 801 585-9051; Fax.: 801 585-9053, E-mail: gprestwich@deans.pharm.utah.edu

Manuscript for:
Current Cancer Drug Targets
Submitted: July, 2001

Professor Glenn D. Prestwich
The University of Utah
Department of Medicinal Chemistry
30 South 2000 East, Room 201
Salt Lake City, Utah 84112-5820
Phone: 801 585-9051; **fax:** 801 585-9053
E-mail: gprestwich@deans.pharm.utah.edu

Cancer-Targeted Macromolecular Chemotherapeutics

Yi Luo and Glenn D. Prestwich*

Department of Medicinal Chemistry,
The University of Utah, Salt Lake City, Utah 84112

Key words: macromolecule, polymer-drug conjugate, targeting, cancer, chemotherapy

Running title: Cancer targeted macromolecular chemotherapeutics

*Address correspondence to this author:

Professor Glenn D. Prestwich
The University of Utah
Department of Medicinal Chemistry
30 South 2000 East, Room 201
Salt Lake City, Utah 84112-5820
Phone: 801 585-9051; **fax:** 801 585-9053
E-mail: gprestwich@deans.pharm.utah.edu

Table of Contents

1. Introduction
2. Passive targeting
 - 2.1 SMANCS
 - 2.2 PEGylation
 - 2.3 Polymeric micelles
 - 2.4 *N*-(2-hydroxypropyl) methacrylamide (HPMA) copolymers
 - 2.4.1 HPMA copolymer-DOX conjugate, PK1
 - 2.4.2 HPMA-platinite conjugate
 - 2.4.3 HPMA-chlorin e_6 conjugate for photodynamic therapy
 - 2.5 Poly(divinyl ether-*co*-maleic anhydride) (DIVEMA)
 - 2.6 Polysaccharides
 - 2.7 Polyamino acids
 - 2.8 Other polymer carriers
3. Active targeting
 - 3.1 Immunoconjugates
 - 3.1.1 Chemoimmunotherapeutics
 - 3.1.2 Photoimmunoconjugates
 - 3.1.3 Immunotoxins
 - 3.1.4 Future development
 - 3.2 *N*-(2-hydroxypropyl) methacrylamide copolymers
 - 3.2.1 HPMA copolymer-carbohydrate conjugate, PK2
 - 3.2.2 HPMA copolymer-antibody conjugates
 - 3.2.3 HPMA copolymer-protein conjugates
 - 3.2.4 Other HPMA copolymer cancer targeting conjugates
 - 3.3 Protein carriers for cancer targeting
 - 3.3.1 Growth factor carriers
 - 3.3.2 Transferrin carrier
 - 3.3.3 Other protein carriers
 - 3.4 Polysaccharides carriers for cancer targeting
 - 3.5 Other polymer-drug targeting conjugate system
4. Conclusion and future perspectives

Abstract

A major challenge in cancer chemotherapy is the selective delivery of small molecule anticancer agents to tumor cells. Water-soluble polymer-drug conjugates have great potential, because they traverse compartmental barriers in the body, thereby gaining access to a greater variety of cell types. Such polymer-drug conjugates have exhibited good water solubility, increased half-life in the body, and potent antitumor effects. Moreover, by localizing the drug at the desired site of action, macromolecular therapeutics have improved efficacy and enhanced safety at lower doses. Since small molecule drugs and macromolecular drugs enter cells by different pathways, multi-drug resistance can be minimized.

Anticancer polymer-drug conjugates can be divided into two targeting modalities: passive and active. Tumor tissues have anatomical characteristics different from normal tissues. Macromolecules penetrate and accumulate preferentially in tumors relative to normal tissues, leading to extended pharmacological effects. This “enhanced permeability and retention” (EPR) effect is the principal reason for current successes with macromolecular anti-cancer drugs. A variety of natural and synthetic polymers have been used as drug carriers, including proteins, polysaccharides, poly(amino acids), polyethylene glycol, and *N*-(2-hydroxypropyl)methacrylamide. Several bioconjugates have been clinically approved or are in human clinical trials.

Although clinically useful antitumor activity has been achieved using passive macromolecular drug delivery systems, the goal of targeted delivery of the active drug to the cancer cells has not been fully satisfied. Actively-targeted drug delivery can be achieved by exploiting ligand-receptor interactions by attaching targeting moieties to the polymer backbone. This would augment the EPR effect with a strategy that targets the therapeutic

agents to the tumor cells, thus further improving the therapeutic index of the parent drug. Antibodies, sugars, proteins, growth factors, hormones, glycolipids and other ligands have been used as targeting moieties for specific interactions with targeted cancer cells. In this review, the basic principles for design of soluble polymeric drug delivery systems are explained and illustrated.

1. Introduction

Several modalities including radiation, chemotherapy, and surgery, either alone or in combination, are used for the treatment of cancer. Among them, chemotherapy has played an important role and has been effective in treating both hematological malignancies and solid tumors. Despite successes in cancer management, unacceptable damage to normal tissue at doses required to eradicate cancer cells is still a significant clinical cause of patient morbidity and mortality. Hence, improved delivery of anticancer drugs to tumor tissues remains an important challenge. Therapeutic efficacy could be markedly enhanced and toxicity could be greatly diminished if high concentrations of anticancer agents could be selectively administered only to malignant cells.

The majority of current cancer chemotherapeutic drugs are low molecular weight (Mw) chemicals that possess a high pharmacokinetic volume of distribution, leading to the ubiquitous presence of cytotoxic compounds in the patient. Low Mw anti-cancer drugs are rapidly removed by renal excretion, are not protected from enzymatic degradation. Consequently, normal tissues are exposed to the cytotoxic effects of the drug, leading to the many well-known side effects to rapidly dividing cells, such as the bone marrow and the gut mucosa. Chemotherapeutic drugs invariably have a very narrow therapeutic index that separates the toxic dose from the clinically effective dose. Furthermore, the development of multi-drug resistance (MDR) in tumor cells exacerbates the problem of achieving selective toxicity.

Many attempts have been made to improve cancer chemotherapy over the few decades. The goal is to increase the therapeutic index by improving the specificity and efficacy of the drug while simultaneously reducing the nonselective cytotoxicity. One of the most promising methods involves the combination, either by admixture or covalent attachment, of the cytotoxic agent within a macromolecular carrier [1]. Many macromolecular carriers,

including soluble synthetic and natural polymers [2], implants [3], liposomes [4], microspheres [5], and nanospheres [6] have been employed to increase drug concentration in target cells. By altering the pharmacokinetic distribution of drugs, and a sustained therapeutic concentration can be maintained at tolerable doses.

Paul Ehrlich [7] first described “the magic bullet” concept in 1906 to describe drugs which might be selectively directed to their site of action. Ringsdorf presented the first clear concept of targetable polymeric drugs [8] (Figure 1), in which he combined the notion of site-specific drug release with site-specific recognition and predicted some important beneficial properties of polymer-drug conjugates as compared with their low Mw analogs. He envisioned that chemotherapy could be improved by tailoring polymers that could incorporate not only cancer drugs but also molecules that guide the drugs to tumor cells.

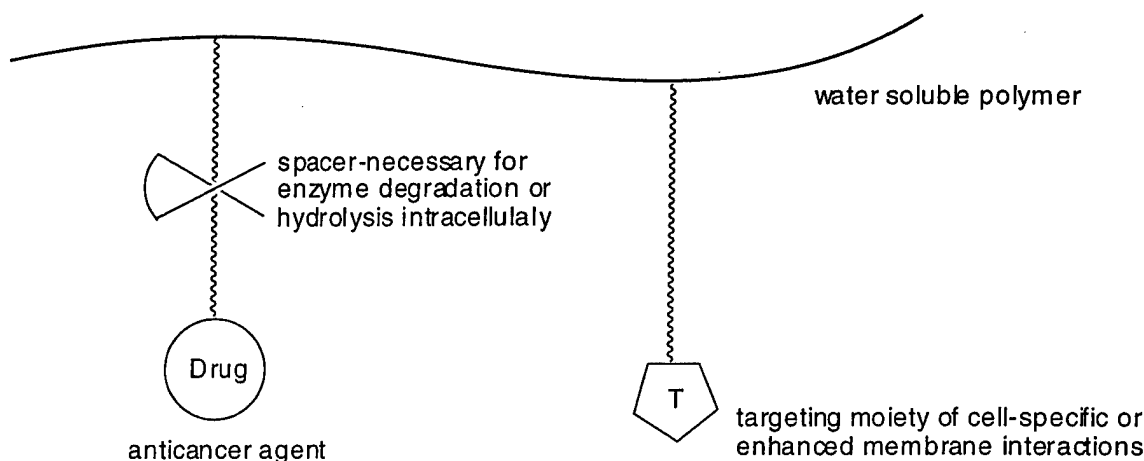


Figure 1. Schematic diagram showing the composition of typical polymer-drug conjugates

A variety of water-soluble polymers, such as human serum albumin (HSA) [2], dextran [1], lectins [9], poly(amino acids) [10], poly(ethylene glycol) (PEG) [11], poly(styrene-*co*-maleic anhydride) (SMA) [12], poly(*N*-hydroxypropylmethacrylamide) (HPMA) [13], and poly(divinylether-*co*-maleic anhydride) (DIVEMA) [14] have been developed polymeric-anticancer drug conjugates for cancer treatment. Poly (styrene-*co*-maleic acid)-

neocarzinostatin conjugate (SMANCS) has been approved for the treatment of liver cancer in Japan. PEG-L-asparaginase (ONCASPARG) has been approved by FDA to be used in chemotherapy for acute lymphoblastic leukemia (ALL). The linking of doxorubicin (DOX) to HPMA copolymer (HPMA-DOX, PK1) gave a new conjugate which showed improved tumor retention, a higher therapeutic ratio and negligible multi-drug resistance. This system has passed the Phase I safety trial and is currently in Phase II clinical trials for treatment of ovarian cancer.

Soluble macromolecular carriers are useful drug delivery vehicles with several important features. They can (i) increase the plasma half-life of low Mw drugs, (ii) to increase the solubility of hydrophobic drugs, (iii) permit controlled release of the drug at lower drug doses, (iv) provide passive targeting to tumors by the EPR effect, and (v) provide site-specific targeting to increase the concentration of drugs at the tumor site [15]. The potential use of macromolecular drugs as a means of achieving targeted drug delivery has rapidly become an important approach for improvement of cancer chemotherapy. Conjugates obtained by a bioreversible attachment of drugs to a wide range of macromolecules, with or without attachment to a targeting system, have been evaluated *in vitro* and *in vivo*. The theory and practical use of macromolecular drugs for site-specific delivery has been extensively reviewed [16-18].

Polymer-drug conjugates manifest their anticancer activity through a several mechanisms. The macromolecules themselves may have intrinsic anticancer activities [16]. More typically, the biocompatible polymers serve as solubilizing carriers for low Mw anticancer agents. This article will review the recent literature in water-soluble targeting polymer-drug conjugates used for both passive and active targeting in cancer chemotherapy. The rationale of design, polymeric drug carriers, and efficacy of these diverse antitumor conjugates will be discussed, along with the future prospects for improving anticancer drug delivery.

Rational design of macromolecular chemotherapeutics

. The overall macromolecular chemotherapeutic system consists of a carrier macromolecule, a degradable spacer, and pendant targeting moieties. Polymer-conjugated drugs have been developed to provide increased plasma half-life, increased tumor targeting efficacy, and decreased nonspecific toxicity of the chemotherapeutic agent. To be efficient, the polymer-drug conjugate should fulfill several criteria. First, the polymeric conjugate must have low intrinsic activity and protect the drug from inactivation during transit from site of delivery to target tissues. Second, the drug must be released in its pharmacologically active form following endocytosis of the conjugate by target cells. Third, the linkage between the drug and the carrier must be stable in the plasma and the extracellular spaces must be cleaved within lysosomes after endocytosis of the conjugate. Fourth, the conjugate must be permeable to anatomic barriers in order to localize the drug at the desired site of action. Fifth, the conjugate must be recognized specifically by receptors or antigens present on the plasma membrane of target cells. Sixth, the bioconjugate should be non-toxic, non-immunogenic and be ideally biodegradable to avoid accumulation in the body. Finally production of the bioconjugates in the amounts and conditions (sterility, apyrogenicity, storage stability) required for clinical use should be technically and economically practicable

Internalization mechanism

The intracellular uptake of low Mw drugs is limited primarily by diffusion. The uptake of macromolecules, on the other hand, is limited by physical and biochemical parameters. Macromolecules that are taken up by endocytosis are channeled to the lysosomal compartment of the cell through the endosomal pathway by vesicular transport [19]. Incorporation of targeting moieties in the macromolecular structure that are complementary to cell surface receptors or antigens allows the macromolecule to be biologically recognized

[3-16]. The macromolecule is internalized specifically by a select subset of cells; both the rate of uptake and the distribution of uptake in the body is substantially altered. Receptor-mediated endocytosis thus provides the vehicle for delivery of targeted macromolecular chemotherapeutics.

Biodistribution

There are four main compartments involved in the entry of a water-soluble macromolecule [16]: (i) blood and lymphatic system, (ii) interstitium, (iii) intestinal lumen, and (iv) intracellular lysosomes. The nonspecific capture of soluble macromolecules by the specialized cells of the reticuloendothelial system (RES) is generally an order of magnitude lower than that by other vesicular carriers. The biodistribution of soluble macromolecules depends on their structure, charge, Mw distribution [20], conformation (and changes in conformation when crossing compartmental barriers), and biodegradability. For example, cationic polymers are rapidly cleared, whereas anionic polymers have increased blood residence time, resulting in better accumulation in tumors [21].

The antitumor activity of a polymer-drug conjugate depends on the distribution of active drug, which is in turn affected by the physicochemical properties of the polymer and the biological recognition and processing of pendant molecular cargo. For example, the attachment of targeting moieties may alter both the solubility and the biodistribution due to the biorecognition of the conjugate at an organ or subset of tumor cells.

Macromolecular carriers

Many natural or synthetic polymers for targeted drug delivery to improve sustained drug release in the body and to increase drug concentration in tumor cells. Such polymers must meet certain requirements in order to maximize their potential as polymeric drug carriers. They must be biocompatible, hemocompatible [22], non-toxic, and non-

immunogenic; in addition, they should be water-soluble, and either biodegradable or simply readily eliminated after fulfilling their drug delivery function. Biodegradable polymeric drug carriers are traditionally derived from natural products, e.g. polysaccharides, poly(amino acids), with the expectation that the body's natural catabolic mechanisms will digest the macromolecular structure into small, easily eliminated fragments. However, drug substitution on polymer carriers may reduce normal biodegradation of the macromolecules, due to changes in hydrophobicity conformation, or enzymatic recognition.

In contrast, synthetic polymers can be engineered to possess physical and biochemical properties that match the biological situation. However, to minimize the accumulation in human body, their entire Mw distribution must be under the renal threshold. The absence of nonspecific interactions with plasma membranes will minimize the probability of accumulation of the carrier in non-target cells and thus increase its biocompatibility. It is important to note that the substitution of a hydrophilic polymer with a hydrophobic drug to make a macromolecular drug can result in the formation of aggregates [23]. Such aggregates may be expected to behave quite differently to unmodified polymer.

Spacer between drug and polymer carrier

Due to the low permeability of lysosomal membrane to macromolecules, only the free drug can penetrate into the cytoplasm and produce a biological result. Drugs that must access the cell nucleus, but are bound to a macromolecular carrier via a non-degradable covalent bond (e.g., GlyGly) are inactive because they are retained in the lysosomal compartment [24]. On the other hand, the stability of polymer-drug conjugate in the blood circulation is a prerequisite for the limited systemic toxicity of the delivery system. Therefore, the polymer-drug linkage should be designed to be stable in the peripheral circulation, yet still allow for site-specific enzymatic or hydrolytic cleavage to release the free active drug within the target cells [25].

The susceptibility of oligopeptide sequences to cleavage by proteolytic enzymes and lysosomal thiol proteinase such as cathepsin B, H, and L [26] suggested the GlyPheLeuGly (GFLG) tetrapeptide linkage as a front-line candidate for a lysosomal degradable sequence. Other linkages that can be either hydrolyzed or reduced in the pre-lysosomal or lysosomal compartments of acidic pH environment have also been developed [16]. Hydrazone bonds can be hydrolyzed at pH 4.5-5.5. Binding DOX to a lectin carrier through a *cis*-acotinyl spacer results in an acid sensitive linkage [27]. The reduction of disulfide bonds occurs at an intracellular level, and the Golgi apparatus was suggested as the most probable major site of cleavage for the disulfide bonds.

In this review, we describe two categories of anticancer polymer-drug conjugates. First, we describe those that are passively targeted based on the anatomical characteristics of tumor tissue for macromolecules. Second, we summarize current information on those that are actively targeted based on specific interactions between receptors on cell surface and targeting moieties conjugated to the polymer backbone.

2. Passive targeting

Tumor tissues have several characteristics that differentiate them from normal tissues. For drug uptake, the most noteworthy are the enhanced permeability of neovasculature to macromolecules, hypervascularization of the surrounding tissues, and the limited recovery of macromolecules through either blood vessels or lymphatic vessels. The combination of poor tissue drainage with increased tumor vascular permeability and lack of lymphatic capillaries results in a phenomenon known as the “enhanced permeability and retention effect”, or EPR. The accumulation of macromolecules in tumor tissues provides a convenient means by which to deliver chemotherapeutic agents to a tumor using a soluble polymer-drug conjugate. The degree of accumulation depends on Mw, charge, and the

overall hydrophobic-hydrophilic character of the conjugate. After accumulation in the tumor tissues, the macromolecular drugs can act as a depots, slowly releasing the low Mw active drugs.

The advantages of attaching drugs to polymeric carriers are numerous. Macromolecular conjugates of drugs will have altered distribution in the body, with prolonged activity by slowed drug release or delayed drug action. The conjugates retain the majority of the original drug activity, but have lower systemic toxicity. In this section, we describe antitumor activities of several kinds of polymeric drugs and we summarize the clinical results using polymer carriers.

DNA was one of the first macromolecular carriers investigated for daunorubicin (DNR) [28], DOX [29]. DNA as a carrier was limited because of the instructional nature of DNA that may become incorporated in a random manner into genomic DNA, leading to unwanted side effects. The limitation of DNA as a carrier led to the use of albumin. A conjugate of DNR, attached via degradable spacers such as GlyPheAlaLeu or AlaLeuAlaLeu, to human serum albumin (HSA), led to a 200% increase in life-span in mice inoculated with L1210 leukemia [2]. Methotrexate-albumin conjugate (MTX-HSA) with a low MTX loading provided optimal tumor targeting and therapeutic efficacy during preclinical testing. A Phase I study of the conjugate showed no signs of toxicity or drug accumulation [30]. Altered pharmacological properties of MTX-HSA such as plasma half-life, tumor targeting, or intracellular metabolism might have contributed to these responses.

2.1 Poly(styrene-*co*-maleic acid) conjugated neocarcinostatin (SMANCS)

Neocarcinostatin (NCS) is a 12 kDa protein antineoplastic agent that acts by inhibiting DNA synthesis in tumor cells. NCS demonstrates immunosuppressive activity but has a very short half-life due to rapid renal clearance. NCS itself also causes severe bone marrow

suppression. Conjugation with a synthetic copolymer of styrene-maleic acid (SMA, Mw 2,500) led to the conjugate SMANCS. This conjugate had an estimated Mw of 15-18 kDa showed improved tumor targeting, prolonged half-life, and improved antitumor activity [31] when compared with its parent NCS compound or mitomycin C (MMC). The tumor accumulation of SMANCS was explained by the EPR effect [12-32].

A marked clinical advantage of SMANCS was attained by formulating it in a lipid contrast medium (Lipidol), which makes the drug have an extremely slow release in tumor tissue [33]. Stability and tumor targeting activity of SMANCS are much improved. Lipiodol specifically targets the lymphatic system and is also selectively retained in primary and secondary hepatic tumors when injected into the hepatic artery [34]. In clinical trials, arterial administration of SMANCS in Lipidol shrunk tumor size and prolonged survival of patients in targeting chemotherapy for hepatoma. When injected via a catheter in an artery to patients with renal cell carcinoma (RCC) [33], a pronounced anticancer effect was recognized without severe site effects.

2.2 PEGylation

Various enzyme or cytokine-poly(ethylene glycol) (PEG) conjugates have been developed as new cancer therapeutics taking advantages of their decreased immunogenicity, resistance to proteolytic degradation, and persistence in the blood stream [9]. These conjugates include such as PEG-L-asparaginases, PEG-arginine deiminase, and PEG-lymphokines e.g. recombinant interleukin 2 (IL-2).

L-asparaginase, an enzyme which converts L-asparagine to L-aspartic acid, exerts its anticancer activity by depriving tumor cells of an essential amino acid. As a protein of non-human origin, it has a short intravascular half-life and is immunogenic. Conjugation with PEG dramatically improves its biological functions, most likely by reducing proteolytic

biodegradation. PEG-L-asparaginase (ONCASPAR) has been approved by FDA to be used in chemotherapy for acute lymphoblastic leukemia (ALL), as a leading form of childhood cancer [35].

Arginine deiminase is an antitumor enzyme used to treat hepatoma (MH134), colon carcinoma (colon 26), sarcoma (S180), and melanoma (B16). PEG modification of the enzyme reduced the enzyme antigenicity and increased plasma half-life [36].

Human IL-2 is a lymphokine that is able to promote the long-term proliferation of activated T-cells. IL-2 also has an immunoregulatory effect on other antigen-specific cytotoxic T lymphocytes, natural killer cells, and on lymphokine-activated killer cells. Recombinant IL-2 has demonstrated antitumor activity in patients against renal cell carcinoma (RCC) and metastatic melanoma. However, the application of IL-2 as an antitumor protein is restricted by its poor solubility, short plasma half-life due to proteolysis in the body, and significant toxicity in the form of chills, rigors, fevers, malaise. The PEG-IL-2 conjugates [37] were found to have a 25× longer half-life, and an antitumor effect similar to that obtained with multiple repeated bolus doses of free IL-2 against L10 hepatocarcinoma and the regional lymph-node metastases. A Phase I study of PEG-IL-2 in patients with a variety of tumor types resulted in extended duration of action and reduced antigenicity, whilst maintaining its antitumor activity.

Xanthine oxidase (XO) mediates anticancer activity because of its ability to generate cytotoxic reactive oxygen species, including superoxide anion radicals and hydrogen peroxide. However, the high binding affinity of XO to blood vessels can cause systemic vascular damage and hence limits the use of native XO in clinical settings. Chemical conjugation of XO with PEG significantly enhanced the tumor-targeting efficacy and the antitumor activity of XO [38].

Using the PEGylation strategy other compounds are currently under development. These include including humanized A33 antibody (huA33) against colon cancers [39], interferon- α (IFN- α), paclitaxel (Taxol) [40], DOX [41], camptothecin [42], arabinoside (ara-C) [43], and a photosensitizer of porphyrin analogs [44] for targeted photodynamic therapy (PDT) against advanced ovarian cancer.

2.3 Polymer-drug conjugate micelles

The behavior of macromolecules will change when a drug and/or a targeting moiety is attached to the polymer backbone. In case a hydrophobic drug was conjugated to the side chain of a hydrophilic polymer carrier, such conjugates may associate in aqueous phase forming micelle-like structures. Micelle shells were shown to hinder the penetration of enzymes into the micelle core, thus reducing the rate of drug release. On the other hand, the micelle forming properties of DOX conjugated to PEG-poly(aspartic acid) were exploited using block copolymers(PEG-P[Asp(DOX)]). By “hiding “ the hydrophobic DOX drug in the core of the micelle, higher concentrations of the toxic can be achieved.

The biodistribution of the PEG-P[Asp(DOX)] conjugates was dependent on micelle stability [45]. Long circulation time in blood is prerequisite for enhanced uptake at target tumor sites. The *in vitro* and *in vivo* activity of the micelle-forming conjugate were highly dependent on the composition with varying chain lengths of the constituting segments of the block copolymer. This micelle-forming system was demonstrated to be a highly effective and selective drug delivery system for solid tumors [46]. Injection of this conjugate into tail vein of murine colon adenocarcinoma 26-bearing mice showed a high antitumor activity, attributable to effective and preferential delivery of the conjugate to the tumor [47].

2.4 *N*-(2-hydroxypropyl)methacrylamide copolymer-drug conjugates

The *N*-(2-hydroxypropyl)methacrylamide (HPMA) copolymers and their drug conjugates [16] have been extensively studied [1]. The Mw of synthetic non-degradable HPMA carrier has to be below the renal threshold to ensure its elimination. The biocompatibility of HPMA homopolymers and HPMA copolymers have been extensively evaluated [48]. Numerous drugs, including DNR [49], DOX [26], sarcolysin (SE) [50] and melphalan (ME) (L-phenylalanine mustard) [51], have been attached to HPMA copolymer through an oligopeptide spacer (GFLG). HPMA copolymer-drug conjugates are stable in blood plasma and serum [52] but release drugs intracellularly in lysosome compartment due to the degradability of GFLG by intralysosomal enzymes.

HPMA copolymer conjugates have shown activity toward various tumor models [18]. HPMA copolymer-DNR conjugate was active in the treatment of experimental Walker sarcoma [49] and L1210 leukemia [53]. HPMA copolymer-DOX conjugates were active against L1210 leukemia [53], B16F10 melanoma [54], LS174T human colorectal carcinoma xenografts [55] and sensitive/resistant human ovarian carcinoma models [13]. HPMA copolymer-platinates showed biological activity *in vivo* against B16F10 melanoma [56]. HPMA copolymer-SE and ME conjugates demonstrated efficacy against Walker sarcoma in rats [51]. The prolonged plasma residence time of the HPMA copolymer-anticancer drug conjugates correlated with their increased tumor accumulation by EPR. Preclinical observations suggested that these covalent polymer-cytotoxics could be safely administered to humans. HPMA-DOX conjugate (PK1) is currently under Phase II clinical evaluation against ovarian cancer. The conjugates HPMA-camptothecin [57], HPMA-platinate [56] and HPMA-Taxol conjugate [58] were also preclinically evaluated and are now in Phase I clinical trials.

2.4.1 HPMA copolymer-DOX conjugate, PK1

The anthracycline cytotoxic antibiotic agent DOX has been widely used in the treatment of many solid and hematological tumors with a high degree of efficacy. However, it has a significant toxicity profile, and its utility is strictly limited by its cumulative cardiotoxicity. Covalent conjugation of DOX dramatically changes its pharmacokinetics and as a result significantly increases the tumor drug concentration relative to free drug when administered at equivalent doses. PK1 consists of the HPMA copolymer carrier covalently linked via the GFLG oligopeptide spacer to DOX. PK1 has a Mw of 28,000, Mw/Mn=1.3 and DOX approximately 10 wt%, and must enter the intracellular compartment by endocytosis. PK1 is able to accumulate preferentially within solid tumor sites, by way of the putative EPR effect [59]. Once in the intracellular compartment, the linker is cleaved by lysosomal cysteine proteases to release DOX intratumorally. There is also evidence to suggest that PK1 may partially overcome the multi-drug resistance phenotype *in vitro* [13-60].

Phase I clinical trial [61] demonstrated several principles behind the strategy of polymeric drugs development. PK1 exhibited altered pharmacokinetics with increased half-life in blood circulation (distribution $t_{1/2}$ of 1.8 h and an elimination $t_{1/2}$ of 93 h) compared to free DOX (distribution $t_{1/2}$ of 5 min and an elimination $t_{1/2}$ of 20-50 h). No polymer-related toxicities were experienced, and a reduced toxicity profile compared with native DOX was observed. In addition, PK1 demonstrated antitumor activity in refractory tumors. Given this very encouraging result, PK1 is under further clinical assessment in the Phase II setting.

A long-circulating high Mw, branched, water-soluble HPMA copolymer conjugate featured PK1 crosslinked with a biodegradable crosslinker, N², N⁵-bis(N-methacryloyl-GFLG-ornithine). The half-life of conjugate in blood was up to 5× longer and the elimination rate from the tumor was up to 25× slower, and properties improved as the Mw of conjugates increased from 22 to 1230 kDa. The treatment of nude mice bearing s.c.

human ovarian OVCAR-3 carcinoma xenograft with the conjugates possessing a Mw higher than 160 kDa inhibited the tumor growth more efficiently than that of 22 kDa or free DOX. The data clearly indicated that higher Mw conjugates were more effective for treating human ovarian xenografts in nude mice [62].

2.4.2 HPMA copolymer-platinate conjugate

Cisplatin and its analog carboplatin, are currently the mainstay of treatment in a number of solid tumors, including ovarian, lung, testicular, upper gastrointestinal, head and neck cancer. The cytotoxicity of cisplatin is due to direct DNA binding to form inter- and intra-strand adducts followed inhibition of DNA synthesis. Cisplatin is poorly soluble in water and has significant toxic effects, especially irreversible renal dysfunction. A polymer conjugate of platinum may offer an attractive means of reducing toxicity, increasing solubility and passive tumor targeting via the EPR effect [18].

Using the same principles employed to design PK1, HPMA copolymer-platinates containing the GFLF tetrapeptidyl spacer with Mw of 25-31 kDa and a platinum content of 3-7%, showed significant *in vivo* antitumor activity against B16F10 melanoma, with a distribution $t_{1/2}$ of 10 h vs. < 5 min for free cisplatin. Phase I clinical trial of the HPMA copolymer-platinates is now underway.

2.4.3 HPMA copolymer-chlorin e₆ for photodynamic therapy

Photodynamic therapy (PDT) is an experimental approach to the treatment of neoplasms in which photosensitizers accumulated in malignant tissues are photoactivated with appropriate wavelengths of light. Side effects of current PDT treatment, e.g., light ultrasensitivity in skin may be reduced by improving localization [63]. Improved efficiency of the delivery of photosensitizers to tumors may be obtained by binding them to water-

soluble polymeric carriers, i.e., *via* the attachment to macromolecule carriers that may alter their spectral and photosensitizing properties [64].

Combination therapy with the HPMA copolymer-anticancer drug conjugate (DOX *via* GFLG linker and chlorin e_6 , *via* GG linker) showed tumor cures which could not be obtained by chemotherapy or PDT alone. They were administered simultaneously to mice bearing C1300 neuroblastoma tumors followed two days later by laser irradiation. The treatment resulted in sharp decrease of the tumor volume [65]. It is hypothesized that the cytotoxicity of anticancer drug might be enhanced by PDT.

2.5 Poly(divinyl ether-*co*-maleic anhydride) (DIVEMA)

DIVEMA, an alternating copolymer of divinyl ether and maleic anhydride, has been extensively studied as an antitumor or antiviral agent itself. Synergy might be expected in the treatment of tumor owing to the antitumor activities of both polymer carrier itself and the drug conjugated to DIVEMA backbone. DIVEMA bioconjugates containing DNR, DOX [14], MTX [66], NCS [67], cyclophosphamide [68], and 5-fluorouridine have demonstrated improved antitumor effects. The slow release of anticancer agents from the polymer carriers made these materials more efficacious than the unconjugated drugs.

2.6 Polysaccharides

Polysaccharides such as dextran, chitosan and pullulan have been used as polymeric drug carriers in cancer chemotherapy. Two such examples are a chitosan-cisplatin conjugate [69] and carboxymethyl-pullulan-DOX conjugate [70].

Dextrans are colloidal, hydrophilic, and water-soluble polysaccharides, inert but biodegradable in biological systems, and do not affect cell viability. Owing to the slow clearance of dextrans from the body, they have been developed as drug carriers to improve therapeutic efficacy.

Both the acute and subacute toxicities of dextran-DNR conjugate were lower than that of free drug [71]. Dextran-MMC conjugates with ϵ -aminocaproic acid as a spacer [1] showed significant antitumor activity against P388 leukemia, L1210 leukemia and B16 melanoma in mouse model only after i.p. injection. This group of polymeric drugs differs from the lysosomotropic agents, and the contact of drug with tumor cells in the peritoneal cavity was important for this compound to exhibit its antitumor effect. Different length spacers between dextran carrier and MMC were also developed, such as γ -aminobutyric acid (C4), ϵ -aminocaproic acid (C6), and ω -aminocaprylic acid (C8). Dextran-C6-MMC conjugate showed superior antitumor effects against P388 leukemia, comparing with free MMC and other conjugates, suggesting that the spacer length is the main determination of the release of MMC and subsequent antitumor activity.

Complexes of cisplatin with carboxymethyldextran exhibited excellent antitumor activity, substantially matching that of cisplatin, against HeLa and human osteogenic sarcoma, human ovarian cancer OVCAR-3 cells in athymic mice [72]. The complexes were also effective against F9 embryonal carcinoma in Balb/c mice and showed sustained release of the platinum complex. Higher drug loading resulted in loss of solubility.

A carboxymethyl dextran-camptothecin analogue conjugate (T-0128) was prepared using a triglycine spacer [73]. This Mw of 130,000 conjugate was developed to improve the pharmacological profiles of the clinically available camptothecins (CPTs), such as irinotecan (CPT-11) and topotecan, representatives of a promising class of antitumor agents. Pharmacokinetic studies in Walker-256 tumor-bearing rats showed that after i.v. administration, the conjugate continued to circulate at a high concentration for an extended period, resulting in tumor accumulation. In the tumor, sustained release of free drug occurred. In contrast, free drug disappeared rapidly from the body. T-0128 below its maximal tolerated doses (MTD) consistently cured or regressed MX-1 mammary

carcinoma, LX-1 lung carcinoma, St-4 gastric and HT-29 colorectal tumor xenografts that are highly refractory to CPTs.

7. Poly(amino acids)

The use of poly(amino acids) as carriers has been explored for many years. The degradability of poly(amino acids) is a highly attractive feature as is the ease of chemical modification. Polymers of most amino acids have been prepared and evaluated (Table 1). The most popular systems are poly (glutamic acid), poly(lysine), poly(hydroxyethylglutamine) and poly(hydroxyethylaspartamide). However, the use of poly(amino acids) as macromolecular drug carriers is restricted due to their general cytotoxicity.

Studies using a poly(L-glutamic acid)-Taxol conjugate (PG-TXL) [10], which is currently in Phase I clinical trial, demonstrated that the polymer carrier enhanced aqueous solubility of Taxol, prolonged plasma residence time, and greatly increased the distribution of Taxol to tumor tissue in a murine model. PG-TXL demonstrated significant inhibition of tumor growth in ovarian and breast cancer animal models [74], which compared with similar doses of Taxol. Radiation followed by PG-TXL, will produce a supra-additive antitumor effect in the treatment of murine ovarian OCA-1 tumor [75]. The enhancement of EPR effect of macromolecules by radiation may cause enhanced tumor uptake of macromolecular drugs, leading to improved antitumor efficacy, thus the synergistic effect of combined radiation and PG-TXL therapy was observed.

Table 1 : Poly(amino acids) as polymeric carrier for cancer chemotherapy

Polymer carrier	Drug conjugated	Cancer targeted
poly(L-glutamic acid)	MMC cisplatin	[76] human ovarian carcinoma (OVCAR-3 cells) [72]
	DOX	L1210 leukemia and B16 melanoma [77]

	camptothecin (CPT)	mice bearing syngeneic OCA-1 ovarian carcinoma [10]
	Taxol	ovarian cancer and breast cancer [10-74]
poly(γ -glutamic acid)	5-FU	[78]
poly[N-(2-hydroxyethyl)-L-glutamine] (PHEG)	MMC	P388 leukemia, solid C26 colorectal carcinoma xenografts in mice [79]
	mustard (N,N-bis(2-chloroethyl)-4-phenylenediamine)	C26 colorectal carcinoma [80]
poly(aspartic acid)	MMC	[76]
poly(L-lysine)	MTX	[81]
	DNR	[82]
poly(D-lysine)	Bowman-Birk inhibitor (BBI)	lung cancer [83]
PEG-grafted poly(L-lysine)	cis-diamminedichloroplatinum (II)	mouse embryonal F9 carcinoma [84]
PEG-poly(L-lysine)	DOX	mice colorectal C26 carcinoma, EL-4 lymphoma [85]
block copolymer		
poly(L-cysteine)	5-FU	Ehrlich ascites carcinoma [86]

On the other hand, some polymer-drug conjugates have been designed to be biodegradable only by chemical hydrolysis. The antitumor activities of such conjugates depend primarily on the rate of drug release from the conjugate and extent of cellular interaction of the conjugate. For example, the conjugates of poly(α -malic acid) with 5-FU [87] exhibited significant survival effects against P388 lymphocytic leukemia in mice by i.p. transplantation/i.p. injection. These conjugates did not display an acute toxicity in the high dose ranges. A nanoparticle formulation of poly(DL-lactic-co-glycolic acid)-DOX (PLGA-DOX) conjugate with DOX chemically conjugated to a terminal end OH group of PLGA through an ester linkage [88], exhibited sustained DOX release profiles over a 1-month period, and DOX release patterns could be controlled by conjugating DOX to PLGA having different Mw. The nanoparticles had comparable antitumor activity to that of free DOX administered by daily injection.

Other polymer-drug conjugate systems have been investigated including polyamines-platinum (II) conjugates [89], polyethyleneimine-cisplatin conjugates [90], acrylic polymer-antitumor drug conjugates [91], polyphosphamide-5-FU conjugates [92]. Polyamideamine (PAMAM) dendrimers, like other carriers, have the advantage to accumulate passively in solid tumor due to the EPR effect. The optimum synthetic control over dendritic architecture

encourages the exploration of using these non-toxic macromolecules as “smart”, or stimulus-responsive, delivery mechanisms to targeting cisplatin to tumor cells [93].

3. Active targeting

Tumor invasion, metastasis, and resistance to chemotherapeutic drugs or radiation are major obstacles for the successful treatment of cancer. To overcome some of these limitations, therapeutic strategies that increase the specificity and efficacy and reduce the toxicity of the anticancer drugs or toxins are being explored. A variety of features unique to malignant human tumor cells can be exploited in the development of targeting therapeutic agents. For example, cancer cells often overexpress specific tumor-associated antigens, carbohydrate structures, or growth factor receptors on their cell surface. Incorporation of a biorecognizable moiety into the polymer carrier structure (Figure 1) leads to active targeting drug delivery systems. Potential targeting moieties include monoclonal, polyclonal antibodies and their fragments, carbohydrates (galactose, mannose), peptides/proteins (melanocyte stimulating hormone, transferrin, growth factors), glycolipids, vitamins and other ligands. Using the targeting moieties, active polymer-drug conjugates can be selectively transported to tumor tissues.

3.1 Immunoconjugates

The development of hybridoma technology and the advances in monoclonal antibody (McAb) production have revitalized the concept of creating cancer cell-targeted, specific “magic bullets”. A now conventional targeting strategy is the use of a McAb that binds to a tumor-specific antigen, either alone or as a bioconjugate with a toxin or radionuclide [94]. Targeted cancer therapy using McAb or their conjugates has been reported by many investigators, and the results are quite promising to lead to several clinical trials. Strategies

for the employment of McAb for cancer immunotherapy include: (i) immune reaction directed destruction of cancer cells; (ii) interference with the growth and differentiation of malignant cells; (iii) antigen epitope directed transport of anticancer agents to malignant cells; (iv) anti-idiotypic vaccines. The therapeutic efficacy for an immunoconjugate is dependent on its binding affinity and avidity to the target tumor cells, the distribution of target antigen on tumor vs. normal tissue, the density of tumor antigens on the cell surface as well as on the heterogeneity of the antigen distribution within the tumor tissue. Radioimmunoconjugates, antibody directed enzyme prodrug therapy (ADEPT) and macromolecular directed enzyme prodrug therapy (MDEPT), in which the tumor located enzyme converts a non-toxic prodrug into a cytotoxic drug at tumor sites, are considered to be beyond the scope of this review.

3.1.1 Chemoimmunoconjugates

The prototypical targeting vehicles are McAbs, which are used frequently for site-specific delivery of chemotherapeutic agents. Two design strategies have emerged for chemoimmunoconjugates: (i) attachment of modified drug directly at functional groups available at McAb, or (ii) attachment through a macromolecule carrier, previously loaded with the modified drug to McAb. A number of synthetic and natural polymeric carriers have been investigated as discussed below.

Most studies have employed drugs that have a proven clinical efficacy in conventional chemotherapy, e.g. anthracyclines DOX and DNR, peptide antibiotics NCS, the vinca alkaloids vinblastine and vincristine, MTX and MMC [95]. The McAbs are sensitive to tumor-specific antigens, e.g., prostate specific antigen (PSA) [96], or overexpressed growth factor receptors on tumor cell surface [97]. For example, murine McAb A7 is an IgG1 antibody reactive with a human colon cancer-associated cell surface antigen. Clinical trials of A7-NCS conjugate in patients with colon and rectum carcinoma showed significant

suppression of tumor growth when compared with free NCS [98]. Furthermore, the acute toxicity of the conjugate was lower than that of free NCS. In another example, McAb BR96 conjugated to DOX (BR96-DOX, now called SGN15) for treatment of intracerebral and subcutaneous human LX-1 small cell lung carcinoma xenografts in rats [99], resulted in significant regression of subcutaneous tumors, in contrast to control groups receiving DOX alone, saline, or a non-binding DOX immunoconjugate.

TES-23, an antitumor tissue endothelium-specific McAb which strongly and selectively recognizes tumor tissue endothelial cells, was covalently conjugated with NCS [100]. The TES-23-NCS conjugate induced tumor hemorrhagic necrosis, and showed marked antitumor effects against rat/mice KMT-17 fibrosarcoma. Mice treated with the immunoconjugate showed improved survival with no side effects. From a clinical view, TES-23 would be a novel drug carrier because of its high specificity to tumor vascular endothelium and its application to many different types of cancer.

Aminophospholipids, such as phosphatidylserine and phosphatidylethanolamine, are specific, accessible and stable markers of the luminal surface of tumor blood vessels. Aminophospholipid-targeted antibody-therapeutic agent conjugates that bind to aminophospholipids target the stably-expressed aminophospholipids of tumor blood vessels, thereby inducing thrombosis, necrosis and tumor regression. This has been useful in the the treatment of solid tumors [101].

A "dual-warhead missile" made of ^{131}I -AFP McAb conjugated with MMC was tested in patients with moderately advanced and advanced primary liver cancer (PLC) by i.v. injection [102]. It was suggested that antibody targeted radiochemotherapy could be the treatment of choice for advanced PLC.

3.1.2 Photoimmunoconjugates

In photodynamic therapy (PDT), nontoxic photosensitizers are preferentially accumulated in malignant tissues. Activation with light produces a phototoxic effect by the production of active molecule species. The only photosensitizer approved for experimental clinical application is photofrin, a mixture of porphyrins. The therapeutic efficacy of photofrin is limited due to a significant nonspecific accumulation in the skin, leading to prolonged cutaneous phototoxicity for up to 8-10 weeks. Tumor specificity could be improved by linking photosensitizers with McAb [103].

OC125 is a murine McAb that recognizes the antigen CA 125, which is expressed on 80% of nonmucinous ovarian tumors. Chlorin e_6 conjugated to OC125 was shown to be selectively phototoxic to human ovarian cancer and other CA 125-positive tumors [104]. The conjugate was more effective than free photosensitizer against tumor cells. The antitumor specificity of the conjugate had been greatly improved and demonstrated that undesired side effects could be minimized by reducing the therapeutic dose required.

3.1.3 Immunotoxins

Immunotoxins are chimeric proteins consisting of a toxin coupled to an antibody against tumor associated antigens by either chemical conjugation or genetic engineering. Toxins of bacterial or plant origin [17], e.g., ricin, abrin, gelonin, *Pseudomonas* exotoxin, diphtheria toxin, staphylococcal enterotoxin A (SEA), are characterized by extremely potent cytotoxins. They are only useful in a therapeutic setting if they can be targeted to cancer cells.

An immunocytokine is an antibody-cytokine fusion protein and represents a novel approach in cancer immunotherapy. Targeted IL-2 was developed using a ganglioside GD2-specific antibody-IL-2 fusion protein (ch14.18-IL-2) for the treatment of established melanoma metastases. This approach could provide an effective tool in cancer immunotherapy and could establish a link between T cell-mediated vaccination and objective

clinical responses [105]. A McAb against fibronectin in the endothelial subcellular matrix, when conjugated with IL-2, was also very effective against LS174T colon carcinoma model which has highly vascularized tumors [106].

Unfortunately, most immunotoxins are effective only *in vitro* [17]. *In vivo*, they exhibit a loss of biological activity (instability, rapid clearance, and catabolism), nonspecific toxicity, binding of the Fc region to normal cells, cross-reactivity of the antibody with normal tissues, and occurrence of a relatively high concentration in a non-tumor tissue. Moreover, many tumor cells escape the therapy due to the lack of access of immunotoxins to the systemic circulation and to large tumor burdens. Immunotoxin therapy can also fail due to the emergence of resistance clones of cells that do not express the surface target antigen. Other cells become resistant to killing by immunotoxins because they fail to take up the conjugate or because of alternation in the cell enzymes essential for cleaving the targeted conjugate and release of active free drug. Finally, the generation of anti-immunotoxins antibodies *in vivo* and the presence of tumor antigens in circulation can also compromise the success of immunotoxin therapy.

3.1.4 Future developments

The development of McAb against antigens associated preferentially with human tumors has reawakened interest in the use of antibodies as site-specific targeting agents for cancer therapy. However, limitations to the *in vivo* therapeutic application of these conjugates have been realized biologically and chemically [17]. These limitations include: (i) low drug-antibody ratio, (ii) loss of the antibody activity due to the chemical modification [107], (iii) phenotypic heterogeneity of many human carcinomas, (iv) antigenic modulation, (v) poor penetration of conjugate within tumor masses, especially solid tumors [108], and (vi) immune response against murine immunoglobulin, and (vii) toxicity to normal cells [109].

Additional strategies will probably have to be employed to make immunotoxin therapy of more practical value in the next decades. For instance, improvements could include the use of intermediate carriers to increase drug to antibody ratios in conjugates or the production of conjugates without extreme overall charge or conformation changes. Other techniques would be to increase antibody affinity and specificity for tumor localization, or to use PEGylated antibody and antibody fragments to limit immunogenicity.

Bispecific antibodies combine the specificity of two different antibodies within one molecule and can thus cross-link an effector or killer cells with the target cell to be destroyed [110]. A bispecific single chain antibody that can bind both the epidermal-growth-factor (EGF) and ErbB-2 receptor and linked to pseudomonas exotoxin was developed, and its efficacy was demonstrated *in vitro* and in animal model [111]. Bispecific F(ab')₂ antibodies (BsAb) with specificity for CD19, CD22, and CD37, were used for delivering the ribosome-inactivating protein saporin to human B cell lymphoma [112]. Selected combinations of BsAb which bind cooperatively to a toxin and the cell surface may provide an efficient way of toxin delivery to unwanted cells in the patient body.

3.2 Targeted N-(2-hydroxypropyl)methacrylamide copolymer-drug conjugates

By targeting cell specific receptors, active and selective uptake into tumors can be achieved. In addition to tumor-associated antigens, several other important candidates for targeted cytostatic therapy have emerged. Targetable cell surface carbohydrate receptors include the asialoglycoprotein receptor for galactose on hepatocytes and lung metastasis, the fucosylamine receptor on mouse leukemia L1210 cells, and the mannose receptor on macrophages. Other targetable cell surface molecules include transferrin receptors, low-density-lipoprotein (LDL) receptors, and a variety of growth factor receptors. The photodynamic activity of HPMA copolymer bound photosensitizer chlorin e₆ and its

targeted or non-targeted conjugates were evaluated on the human hepatocarcinoma cell line PLC/PRF/5 using galactosamine as the targeting ligand. A similar HPMA-chlorin e_6 conjugate was delivered to mouse T splenocytes using anti-Thy 1.2 antibodies [113]. In both cases, the targeted conjugate was as much as 500 hundred times more phototoxic than its non-targeted counterpart.

3.2.1 HPMA copolymer-carbohydrate conjugate, PK2

PK2 represents a further development in macromolecular chemotherapeutics. Galactosamine-bearing polymer conjugates can selectively target the hepatocyte galactose-receptor, promoting liver specific receptor mediated uptake of conjugate. PK2 is a HPMA copolymer-DOX-galactosamine conjugate with GFLG tetrapeptide spacer, that targets the asialoglycoprotein receptors selectively expressed by hepatocytes [60]. A preclinical study indicated that 80% of PK2 administrated was taken up by the liver and provided antitumor activity [114]. The Phase I study of PK2 in human hepatoma patients with is underway. *In vivo* test of HPMA copolymer-DNR bearing galactosamine also indicated no significant hepatotoxicity [114].

Inclusion of fucosylamine-or glucosamine-terminating side chains into HPMA copolymer-5-FU conjugates greatly increased the endocytosis of the conjugates into colon cancer cells, and demonstrated anticancer activity both *in vitro* and *in vivo* with a protective effect on the bone marrow stem cells. The anticancer activity of these conjugates was dependent upon the targeting carbohydrate [115].

The protein synthesis inhibitor puromycin was bound to HPMA copolymer for delivery to cancer tissue using either galatosamine or fucosylamine [116] as to confer specificity for hepatoma or mouse L1210 leukemia cells, respectively. Such carbohydrate-targeted polymer-drug conjugates were cytotoxic both *in vitro* and *in vivo* and they prolonged the

life of experimental animals and produced an increase in the number of long-term survivors [51-116].

Most recently, a cell-targeted polymeric drug delivery system was designed based on the specific interaction between hyaluronic acid (HA) and its cell surface receptors overexpressed on cancer cell surface [117]. HPMA copolymer-DOX conjugates containing HA as a side chain (HPMA-HA-DOX) exhibited higher cytotoxicity against human breast cancer HBL-100 cells, human ovarian cancer SKOV-3 cells and human colon cancer HCT-116 cells than non-targeted PK1 conjugate. Fluorescence confocal microscopy revealed that the targeted HPMA-HA-DOX conjugates were internalized more efficiently by cancer cells through a receptor-mediated pathway. Cell culture of the conjugates against mouse fibroblast NIH 3T3 cells showed lower cytotoxicity against non-cancerous cells, which indicated that it is possible to apply the HPMA-HA-DOX conjugates in a therapeutic dose against cancer cells only with few side effects to normal cells.

3.2.2 HPMA copolymer-antibody conjugates

Binding of an antibody (Ab) targeted polymer conjugate to antigens expressed on cancer cell surface would theoretically promote specific receptor-mediated intracellular uptake. In addition, this strategy could be more effective for micrometastases, in which the tumor has not yet developed an extensive blood supply and therefore EPR effect is not so pronounced. Specifically, antibody-targeted HPMA copolymer-drug conjugates represent a promising system for cancer chemotherapy [118]. A new generation of antibody-targeted cytostatics (DNR, DOX) drugs and photosensitizers (chlorin e_6) were effective *in vitro* and *in vivo*. Antibody-targeted polymer-bound drugs showed considerably decreased toxicity [24], and significantly decrease of Ab immunogenicity has been achieved by conjugation to HPMA copolymer [85].

HPMA-DNR conjugates were prepared containing anti-Thy 1.2 Ab, which recognizes the surface Thy 1.2 alloantigen of T-lymphocyte [119]. This antigen is important for all types of immune reactions. These targeted macromolecular drugs were 70 times more cytotoxic against T-lymphocytes than HPMA copolymers with a non-specific immunoglobulin. HPMA copolymer conjugates having a biodegradable spacer of GFLG were effective at concentrations 100 times lower than those having a non-degradable GG spacer. In another study, anti-CD3 antibody against TCR/CD3 complex was used to target the DOX bound HPMA copolymers conjugates to T-cells [120].

In order to further investigate this strategy, HPMA copolymer-DOX-OV-TL 16 Ab has been developed and tested in epithelial ovarian carcinoma cell line OVCAR-3 *in vitro* [121]. The Ab targeted polymer conjugate was internalized into the lysosomal compartment, where DOX was released. The Ab targeted polymer conjugates were twice as cytotoxic as the non-targeted HPMA copolymer-DOX. Preliminary research also indicated that the Ab-targeted polymer conjugates could overcome multi-drug resistance [60]. Polymerizable antibody Fab' fragments (from OV-TL 16 Ab) was copolymerized with HPMA and mesochlorin e_6 (Mce $_6$)-containing monomers with a GFLG spacer [122]. The targeted copolymer exhibited a higher cytotoxicity toward OVCAR-3 human ovarian carcinoma cells with more efficient internalization. HPMA copolymers conjugated to the McAb of P glycoprotein (PGP) were biorecognizable and localized on the extracellular side of the cell [123]. The binding of the conjugate specifically to PGP reduced the IC $_{50}$ for the McAb and Fab' targeted copolymers, which showed that the photosensitizers could kill resistant cancer cells by destabilizing the plasma membrane.

Recently, a new star-like HPMA-copolymer-drug-antibody conjugates was developed to narrow the Mw distribution. In this new construct, semitelechelic poly HPMA chains were linked to the Ab via the terminal carboxylate of the HPMA polymer [124]. The release of DOX by lysosomal enzymes was unchanged. Both *in vitro* and *in vivo* effects of targeted

star-like polymeric drugs were superior to the effects of the classical HPMA copolymer conjugate system against mouse T-cell lymphoma EL4 or human colorectal carcinoma SW 620 [125].

3.2.3 HPMA copolymer-protein conjugate

A further consideration is the use of hormone receptor interactions to promote internalization and drug targeting. The melanocyte-stimulating hormone (α -MSH) receptor is expressed by the majority of melanocytes in malignant melanoma [25]. Malignant melanoma is a cancer difficult to treat, often leading to hepatic and brain metastases. Effective targeting of the DOX bearing HPMA copolymer via a degradable GFLG spacer was demonstrated both *in vitro* in B16F10 cells, and *in vivo* in mice inoculated with B16F10. In experimental animals bearing established s.c. B16F10 tumors, conjugates containing MSH administered i.p. were significantly more effective than those without MSH, with the maximum T/C being approximately 324 and 148 respectively. Preliminary pharmacokinetic experiments showed evidence of selective MSH targeting of polymer conjugates to s.c. B16F10. Although these results were promising, it has been reported that other receptors for MSH are expressed in other tissues, particularly in the brain, which may limit the therapeutic opportunities for these macromolecular conjugates.

The area of lectin-mediated drug delivery has been widely explored [126]. Lectins bind complex oligosaccharides *in vivo*. Two plant lectins (peanut agglutinin (PNA) and wheat germ agglutinin (WGA)) as targeting moieties and DOX were conjugated to HPMA copolymer [127]. The anti-proliferative effect of conjugates targeted with WGA was comparable to that with the conjugates targeted with the anti-Thy-1.2 monoclonal antibody or their F(ab')₂ fragments against primary (SW 480, HT 29) and metastatic (SW 620) human colorectal cancer cell lines. The magnitude of the cytotoxic effect of HPMA-DOX

targeted with PNA was lower in all tested cell lines. While the conjugates with WGA were more cytotoxic, the conjugates with PNA were more specific as their binding is limited to cancer cells and to the sites of inflammation.

Because the transferrin receptor is expressed in high density on rapidly proliferating cells, including malignant cells, this has been proposed for targeted drug delivery. HPMA-DNR conjugates containing transferrin as a targeting moiety [17] were tested in DBA2 mice bearing L1210 leukemia, and an increase in life span and long-term survivors were observed. However, the transferrin containing conjugates did not show improved activities, which might be due to the rapid exit of conjugate from the peritoneal compartment or could relate to the known endosomal recycling of the transferrin receptor.

3.2.4 Other HPMA copolymer cancer targeting conjugate

The therapeutic macromolecules can be targeted to tumor cells by covalently attached a vitamin (e.g. folic acid, cobalamin) to the polymer carrier. Many tumors of epithelial origin express the high-affinity folate receptor (hFR), e.g. ovarian tumors [128]. HPMA copolymer bound DNR via GFLG spacer with folate on the side chain as targeting moiety was also studied [129].

A synthetic peptide, GFLFEDPGFFNVE, when conjugated to HPMA copolymer, is an effective targeting molecule which can specifically deliver DOX to human T-cell lymphomas [130].

3.3 Protein carriers for cancer targeting

3.3.1 Growth factors

Certain tumor cells, such as squamous carcinomas, gliomas and breast carcinoma, expressed high levels of epidermal-growth-factor (EGF) receptors (R). The EGF receptors

can in these cases be targets for toxic conjugates with specific binding. EGF-based toxic conjugates are potential targeting agents to achieve the tumor selectivity.

Recombinant human EGF was conjugated to the soybean-derived PTK inhibitor genistein (Gen) to construct an EGFR-directed cytotoxic agent with PTK inhibitory activity. The EGF-Gen conjugate triggered rapid apoptotic cell death in human breast cancer cells and abrogated their *in vitro* clonogenic growth. The conjugate significantly improved tumor-free survival in a severe combined immune deficiency (SCID) mouse xenograft model of human breast cancer [131], and was more effective than cyclophosphamide, DOX or MTX.

Compared to free disulfochloride cobalt phthalocyanine [Pc(Co)], i.v. injections of EGF-Pc(Co) conjugate inhibited tumor development and increased mean life span and mean survival time of experimental animals with murine melanoma B16 [132].

Transforming growth factor (TGF- α) is a protein that specifically binds and stimulates phosphorylation of cell surface EGFR and, subsequently, triggers cell proliferation. TGF- α as a ligand for EGFR is internalized upon binding and decomposed within lysosome. Conjugates of TGF- α and ricin A showed significant inhibitory effect of human epidermoid cancer cells A431 [133], but no inhibitory effect human non-small cell lung cancer (NSCLC) cells and normal human lung cells because of the fewer available EGF binding sites on the surface of these cells. The amount of the available EGF receptors will contribute to the cytotoxic effect on human cancer cells, thereby demonstrating involvement of the receptor-mediated endocytosis of the conjugate.

Many cancer cell lines express basic fibroblast growth factor (bFGF) receptors, making them potential targets for the delivery of bFGF-based cytotoxic compounds. A novel mitotoxin of bFGF-saporin (FGF-SAP) [134], a conjugate of bFGF and a ribosome-inactivating protein, is cytotoxic to human melanoma, teratocarcinoma, and neuroblastoma cells expressing bFGF-receptors. Mice treated with the conjugate by i.v., showed dramatic

tumor growth inhibition with minimal toxicity. The bFGF-SAP conjugate was also highly toxic to Kaposi's sarcoma-derived cell line IST-KS2 and the permanent endothelium-derived EAhy926 cell line which are highly vascularized. Conjugate of FGF 2 and saporin was developed to targetedly eliminate breast cancer in clinical settings.

Inhibition of tumor neovascularization has profound effects on the growth of solid tumors. Conjugates of vascular endothelial growth factor (VEGF) were linked directly or via a linker to a cytotoxic ribosome-inactivating protein. This construct was achieved targeted delivery to vascular endothelial cells [135]. The conjugates were particularly useful for treating solid tumors, such as Kaposi's sarcoma, and ophthalmic disorders with underlying vascular proliferation. The treatment of subconfluent cultures of human umbilical vein endothelial cells and human microvascular endothelial cells with a recombinant VEGF165-truncated diphtheria toxin molecule (DT385) conjugate [136] resulted in a selective, dose-dependent inhibition of growth. In an *in vivo* model of angiogenesis, the VEGF-toxin conjugate blocked bFGF-induced neovascularization of the chick chorioallantoic membrane. These studies demonstrated the successful targeting of a cytotoxic polypeptide to proliferating vascular endothelial cells (normal and tumorigenic) and the potential utility of such conjugates in blocking tumor neovascularization.

3.3.2 Transferrin

Transferrin is a serum glycoprotein involved in iron transport. Transferrin acts in cell growth regulation through membrane receptors. The number of transferrin receptors is increased in tumor and other rapidly dividing cells. This makes transferrin suitable for use in cytotoxic drugs targeting tumor cells by transferrin receptor-mediated endocytosis.

Macromolecular conjugates of human holo-transferrin (TF)-MMC [137] were able to bind specifically to the TF receptor on Sarcoma 180 cells, and the amount of conjugate specifically bound to the TF receptor decreased as the MMC content of the conjugate

increased. A cancer-targeted transferrin-DNR conjugate was less toxic and more active on malignant cells than the free drug, while being less toxic for normal cells [138]. Taxol was derivatized on 2' carbon and coupled with transferrin using glutaraldehyde [139]. The cytotoxicity of the conjugate was evaluated on small cell carcinoma of the lung cell line (H69). As compared to Taxol, the conjugate exhibited a slight decrease in cytotoxicity.

The conjugate of human diferric transferrin and the anticancer polypeptide, NCS, is capable of binding to the transferrin receptor and is internalized by endocytosis. The inhibitory effect of the conjugate on cell growth was significant towards human colorectal cancer cell line, M7609 and human leukemia K562 cells [140] *in vitro*. A significant inhibition of growth was observed in M7609 transplanted into nude mice. The half-life of elimination of the conjugate was 55 min, while that of the free NCS was 7 min. No serious side effects with regard to liver or kidney function were detected.

3.3.3 Other protein carriers

DNR can be targeted to the liver by linking it to galactosylated human serum albumin [141]. The linkage was stable in the blood stream and allowed the release of active DNR after endocytosis of the conjugate by the target cells. When tested against human hepatoma xenografts in mice, the conjugate induced tumor regression whereas neither free DNR nor the mixture of protein and drug were active.

The class A Type-I scavenger receptor of macrophages, which recognizes maleylated serum albumin is a good candidate for improving the selectivity of photodynamic therapy. Chlorin e_6 was covalently attached to bovine serum albumin (BSA) to give conjugates with molar substitution ratios of 1:1 and 3:1 (dye to protein), and these conjugates could then be further modified by maleylation [142]. The scavenger receptor-targeted PDT gives a high degree of specificity toward macrophages and may have applications in the treatment of tumors and atherosclerosis.

Wheat germ agglutinin (WGA) as a targeting lectin carrier for an acid-labile chemotherapeutic prodrug of DOX directed against colon carcinoma cells was evaluated [27]. The *cis*-aconityl-linked DOX-WGA conjugate-binding capacity of colon carcinoma cells exceeded that of human colonocytes and lymphoblastic MOLT-4 cells 4.5-fold, and yielded 160% of the cytostatic activity (IC_{50}) of free DOX against Caco-2 cells.

Active targeting of a muramyl dipeptide (MDP) to macrophages could be achieved by conjugation with gelatin [143]. The MDP-gelatin conjugate strongly suppressed the *in vivo* growth of mouse Meth A fibrosarcoma cells (R1) cells compared with free MDP at a 1000 times larger MDP dose.

DOX was conjugated to human chorionic gonadotropin (hCG) via glutaraldehyde in order to specifically target ovarian cancer OVCAR 3 cells [144]. The conjugate demonstrate a more than 8-fold increase in cytotoxicity compared to free DOX. It was also shown that this targeting effect was not restricted to an acute toxic event but resulted in a prolonged anti-proliferative activity.

MTX-neoglycoprotein conjugates against 7721 hepatoma cells were investigated [145]. The inhibitory effects on the growth of the tumor cells were higher than that of MTX-BSA though the effects were lower than that of free MTX. It was suggested that the effects of MTX-neoglycoprotein conjugates on tumor cells were mediated by endogenous lectins on cellular membranes. In another example, an oncofetal protein, human α -fetoprotein, was selected as a vector molecule for targeted delivery of antitumor agents (e.g. diphtheria toxin, MTX) [146], which are highly selective to tumor cells owing to receptor-mediated endocytosis.

The cytotoxicity of the conjugate of long-acting somatostatin (SST) analog, octreotide with Taxol, was mainly mediated by the binding of SST to endogenous G-protein-coupled receptors (SST receptors or SSTRs) which have been reported that a high density of SSTRs

is present on most hormone-secreting tissue tumors [147]. The conjugate exerted the same antitumor effect as free Taxol on stabilizing microtubule formation and inducing cell death against human breast cancer MCF-7 cells. This conjugate triggered tumor cell apoptosis mediated by SSTRs and was exclusively toxic to SSTR-expressing cells, but less toxic to low-SSTR-expressing cells compared with free Taxol.

3.4 Polysaccharides carriers for cancer targeting

A cancer cell-targeted conjugate with Taxol attached to hyaluronic acid (HA) was evaluated [148]. HA-Taxol conjugates showed selective toxicity toward the human cancer cell lines (breast, colon, and ovarian) that are known to overexpress HA receptors, while no toxicity was observed toward a mouse fibroblast cell line at the same concentrations used with the cancer cells. The targeted cytotoxicity of HA-Taxol bioconjugates required receptor-mediated cellular uptake of the bioconjugate followed by hydrolytic release of free Taxol [149].

Heparin-steroids conjugates were able to targeted vascular endothelial cells [150], and the steroids exerted a specific effect on the target cells following release from the carrier. Conjugates comprising heparin and the anti-angiogenic steroid, cortisol, suppressed DNA synthesis and cell migration in human umbilical vein endothelial cells. In addition, these conjugates retarded or abolished the vascularization of sponges *in vivo* and retarded lung tumor growth in mice by 65%. No adverse effects of the conjugate were detected, and equivalent treatments with a mixture of heparin plus cortisol were significantly less effective in all cases.

Carboxymethyl-*N*-acetylpolygalactosamine/DOX conjugates via GlyPheLeuGly spacer [151] were prepared for targeting to hepatoma cells and lysosomal release of drug. The conjugates were able to bind hepatoma *in vitro*, and the survival effect against mice bearing MH 134Y hepatoma was investigated.

The use of various drug antibody conjugates using dextran bridge for targeting of DNR, DOX, MTX, MMC, 5-fluorouridine, cisplatin, cyclophosphamide, ricin A and ara-C has been reviewed [1-152]. The conjugates of McAb and anticancer agents through dextran bridge exhibited specific cytotoxicity to antibody-targeted cells and the conjugate was highly effective against tumor xenografts in nude mice with more marked tumor inhibition than the mixture of McAb and free chemotherapeutic agents at comparable dose levels. Multi-drug resistance (MDR) has been reported to be partially overcome by specifically targeting DOX to resistant cells using this antibody-mediated drug targeting system [153]. Dextran conjugates with growth factors TGF- α , or EGF, were candidates for targeted therapy against EGF-receptor rich tumors such as gliomas or squamous carcinomas [154]. A conjugate in which fibronectin is connected through oxidized dextran with DOX was also designed for targeting morbid cells (sarcoma) [155]. Some of these conjugates are now in clinical trials, but the details will not be discussed herein.

3.5 Other polymer-drug targeting conjugate system

Poly(amino acids) have been studied as carriers for immunoconjugates to selectively deliver the anticancer agents to desired tumors through antibody-mediated targeting. Photoimmunoconjugates were prepared between the anti-colon McAb 17.1A and the photosensitizer chlorin e_6 with polylysine, to develop a strategy for the selective destruction of colorectal cancer cells [156]. Chlorin e_6 was conjugated via polyglutamic acid to OC125, an antibody directed against CA125 antigen on human ovarian cancer cells [157]. Photochemical destruction with high levels of antigen selectivity were achieved with photoimmunotargeting. A polymeric (poly[N⁵-(2-hydroxyethyl)-L-glutamine]) immunoconjugates of DOX and a targeting antibody such as human IgM antibody directly against tumor associated antigen. These immunoconjugates were designed to allow selective

release of DOX in the acidic environment of the tumor through a new acid-labile maleamic acid linker [158]. 5-fluoro-2'-deoxyuridine (FUDR) was conjugated to lactosaminated poly-L-lysine [159]. The conjugate entered human hepatocarcinoma Hep G2 cells through the asialoglycoprotein receptor and, after intracellular penetration, released the drug in a pharmacologically active form. When administered to mice, the conjugate led to enhanced accumulation of the drug in liver when compared with intestine and heart tissues.

Poly(α -malic acid) is of interest as a biodegradable and bioadsorbable polylactide type drug carrier that can be covalently attached to both drug and targeting moiety. The design of poly(α -malic acid)/5FU/saccharide and poly(α -malic acid)/DOX/saccharide conjugates were investigated [160]. Monosaccharides such as galactosamine, glucosamine and mannosamine were used as targeting moieties. Poly(α -malic acid)/5FU/galactosamine and poly(α -malic acid)/DOX/galactosamine conjugates showed stronger growth-inhibitory effects than conjugates without targeting sugars against human hepatoma cells *in vitro*. These results could be explained by galactose receptor-mediated specific uptake into hepatocyte cells. The survival of mice bearing tumor cells *in vivo* was also tested.

Targeting polymeric antitumor agents, poly[(2-acetoxy-3,4-dihydro-2H-pyran)-alt-(maleic anhydride)] as polymer backbone, chlorophyll derivatives (CpD) extracted from silkworm excreta as targeting moiety, 5-FU and 6-mercaptopurine as drugs were selected [161]. The polymer exhibited an antitumor activity comparable to that of cyclophosphamide *in vivo*. CpD targeted polymer conjugates were localized on tumor cells *in vitro* and delivered to tumor tissues *in vivo* specifically. CpD has UV at 670 nm comparing with hematoporphyrin (HpD) at 615 nm, which provided not only more tissue penetration but also less reflection of light by tissue on its application in photodynamic therapy. In another study, a liver targeting polymeric anticancer drug was developed with polyphosphazene

linked via L-glutamate spacers with (cyclohexanediamine)Pt(II), and a liver-targeting carbohydrate moiety glucose [162].

Conjugates of hematoporphyrin, meso-chlorine₆ with human low-density lipoprotein (LDL), human high-density lipoprotein (HDL) and bovine HDL have been investigated [163]. Targeted photodynamic therapy could be achieved because photosensitizer-lipoprotein conjugates were taken up in large amount by cells possessing scavenger receptors and/or phagocytic activity (e.g. macrophages). Targeting tumor cells by low density lipoprotein (LDL) receptor has been reviewed [164],

4. Conclusion and future perspectives

The varied designs of polymer-drug conjugates illustrate the diversity and potential of macromolecular chemotherapeutics for the treatment of cancer. A further systematic study of their advantages and limitations will be necessary to fully evaluate their clinical applications. This review has attempted to demonstrate high potential of hydrophilic polymers in the development of new site-specific drug delivery systems designed for human therapy.

In the case of passive targeting, polymer-drug conjugates preferentially accumulate in tumor tissues due to the EPR effect, and slow release of active drugs in the tumor tissues and low levels in the circulation confer improved therapeutic activity at lower doses. Some conjugates exhibiting promising antitumor effects in clinical tests have recently received market approval for clinical use, e.g., PEG-asparaginase, SMANCS, and others about to be approved.

With respect to the active targeting systems, various kinds of targeting moieties that recognize tumor-specific surface antigens or antigens have attached to polymer backbones, with the aim of obtaining more efficient delivery of active drugs to the target cells. In some cases, this approach produced almost the same, or less antitumor activity in clinical

evaluations as that obtained from polymer-drug conjugate without specific targeting moiety. When an antibody is used as a targeting moiety, it is difficult to isolate antigen specific only to the tumor. Moreover, when an Ab is conjugated to a polymer, a decrease in antibody activity is generally observed and a reduction in the selectivity of the conjugate toward the tumor may also occur. Additionally, a hormone immune response to polymer-drug-Ab conjugates may be elicited, resulting in serious side effects such as anaphylaxis. Other ligands like carbohydrates, peptides/proteins, glycolipids, vitamins have also been used as targeting moieties. But, so far, most of them have not resulted in increased antitumor activity. Though a receptor for a given ligand is present mostly on the tumor cells surface, it may also be present on normal cells. Another problem in the use of some ligands as targeting moieties is control of receptor saturation by ligands. To date, there are no polymer-drug conjugates containing a targeting moiety that have been approved for clinical use.

The drawback of macromolecules is their limited penetration into tissues and the relatively slow rates of internalization by endocytosis. However, targeted polymer-drug conjugates have growing importance as an effective strategy in cancer therapy. The successful design of targeted macromolecular chemotherapeutics can only be achieved with prior consideration of the pathology and stage of the disease, tumor accessibility, biochemistry and cell biology of the molecular targets and effectors influencing tumor growth. In addition, the choice of appropriate therapeutic agent(s) and understanding of its fundamental mode of action is essential. With these design criteria incorporated, exciting and potentially more selective antitumor chemotherapeutics based on polymer technologies will emerge. Close collaboration between biologists, chemists, pharmacists, and clinicians will be crucial in designing and testing polymeric drugs.

Finally, marketable macromolecular conjugates depend on the dosage formulation. The combined use of the conjugates and some physical device and well-designed formulation would certainly offer additional advantages and open up new aspects of drug therapy.

ACKNOWLEDGMENTS

The authors wish to acknowledge the financial support from Department of Army (DAMD 17-9A-1-8254) and the Huntsman Cancer Foundation at The University of Utah.

References

- [1] Kim, K. H.; Hirano, T.; Ohashi, S. In *Polymeric Materials Encyclopedia*; Salamone, J. C., Ed.; CRC Press: Boca Raton, FL, 1996, pp. 272-285
- [2] Trouet, A.; Masquelier, M.; Baurain, R.; Campeneere, D. D. A covalent linkage between daunorubicin and proteins that is stable in serum and reversible by lysosomal hydrolases, as required for a lysosomotropic drug-carrier conjugate: *in vitro* and *in vivo* studies. *Proc. Natl. Acad. Sci. USA* 1982, 79, 626-629
- [3] Langer, R. Drug delivery and targeting. *Nature (London)* 1998, 392 (suppl.), 5-10
- [4] Kim, S. Liposomes as carriers of cancer chemotherapy. *Drugs* 1993, 46, 618-638
- [5] Arshady, R. Albumin microspheres and microcapsules: methodology of manufacturing techniques. *J. Controlled Release* 1990, 14, 111-131
- [6] Kreuter, J. Nanoparticle-based drug delivery systems. *J. Controlled Release* 1991, 16, 169-176
- [7] Ehrlich, P. Eds. *Studies in Immunity*; Jon Wiley & Sons: New York, 1906
- [8] Ringsdorf, H. Structure and properties of pharmacologically active polymers. *J. Polym. Sci. Polym. Symp.* 1975, 51, 135-153
- [9] Burnham, N. L. Polymers for delivering peptides and proteins. *Am. J. Hosp. Pharm.* 1994, 51, 210-218

- [10] Singer, J. W.; De Vries, P.; Bhatt, R.; Tulinsky, J.; Klein, P.; Li, C.; Milas, L.; Lewis, R. A.; Wallace, S. Conjugation of camptothecins to poly-(L-glutamic acid). *Ann. N. Y. Acad. Sci.* 2000, 922, 136-150
- [11] Greenwald, R. B.; Gilbert, C. W.; Pendri, A.; Conover, C. D.; Xia, J.; Martinez, A. Drug delivery systems: water soluble taxol 2'-poly(ethylene glycol) ester prodrugs -- design and in vivo effectiveness. *J. Med. Chem.* 1996, 39, 424-431
- [12] Maeda, H. The tumor blood vessel as an ideal target for macromolecular anticancer agents. *J. Controlled Release* 1992, 19, 315-324
- [13] Minko, T.; Kopeckova, P.; Pozharov, V.; Kopecek, J. HPMA copolymer bound adriamycin overcomes MDR1 gene encoded resistance in a human ovarian carcinoma cell line. *J. Controlled Release* 1998, 54, 223-233
- [14] Hirano, T.; Ohashi, S.; Morimoto, S.; Tsuda, K. Synthesis of antitumor-active conjugates of adriamycin or daunomycin with the copolymer of divinyl ether and maleic anhydride. *Makromol. Chem.* 1986, 187, 2815-2824
- [15] Stastny, M.; Strohalm, J.; Plocova, D.; Ulbrich, K.; Rihova, B. A possibility to overcome P-glycoprotein (PGP)-mediated multidrug resistance by antibody-targeted drugs conjugated to N-(2-hydroxypropyl)methacrylamide (HPMA) copolymer carrier. *Eur. J. Cancer* 1999, 35, 459-466
- [16] Putnam, D.; Kopecek, J. Polymer conjugates with anticancer activity. *Adv. Polym. Sci.* 1995, 122, 55-123
- [17] Rihova, B. Targeting of drugs to cell surface receptors. *Crit. Rev. Biotechnol.* 1997, 17, 149-169
- [18] Kopecek, J.; Kopeckova, P.; Minko, T.; Lu, Z. R. HPMA copolymer-anticancer drug conjugates: design, activity, and mechanism of action. *Eur. J. Pharm. Biopharm.* 2000, 50, 61-81

- [19] Seymour, L. W. Passive tumor targeting of soluble macromolecules and drug conjugates. *Critical Reviews in Therapeutic Drug Carrier Systems* 1992, 9, 135-187
- [20] Seymour, L. W.; Duncan, R. Effect of molecular weight of *N*-(2-hydroxypropyl)methacrylamide copolymers on body distribution and rate of excretion after subcutaneous, intraperitoneal, and intravenous administration to rats. *J. Biomed. Mater. Res.* 1987, 21, 1341-1358
- [21] Takakura, Y.; Fujita, T.; Hashida, M.; Sezaki, H. Disposition characteristics of macromolecules in tumor-bearing mice. *Pharm. Res.* 1990, 7, 339-346
- [22] O'Mullane, J.; Daw, A. Macromolecular prodrugs: blood interactions and targeting. *J. Controlled Release* 1991, 16, 113-120
- [23] Ulbrich, K.; Konak, C.; Tuzar, Z.; Kopecek, J. Solution properties of drug carriers based on [poly(*N*-2-hydroxypropyl)methacrylamide] containing biodegradable bonds. *Makromol. Chem.* 1987, 188, 1261-1272
- [24] Rihova, B.; Kopeckova, P.; Strohalm, J.; Rossmann, P.; Vetvicka, V.; Kopecek, J. Antibody directed affinity therapy applied to the immune system: in vivo effectiveness and limited toxicity of daunomycin conjugates to HPMA copolymers and targeting antibody. *Clin. Immunol. Immunopathol.* 1988, 46, 100-114
- [25] O'Hare, K. B.; Duncan, R.; Strohalm, J.; Ulbrich, K.; Kopeckova, P. Polymeric drug-carriers containing doxorubicin and melanocyte-stimulating hormone: in vitro and in vivo evaluation against murine melanoma. *J. Drug Targeting* 1993, 1, 217-229
- [26] Subr, V.; Strohalm, J.; Ulbrich, K.; Duncan, R.; Hume, I. C. Polymers containing enzymically degradable bonds, XII. Effect of spacer structure on the rate of release of daunomycin and adriamycin from poly[*N*-(2-hydroxypropyl)methacrylamide] copolymer drug carriers in vitro and antitumor activity measured in vivo. *J. Controlled Release* 1992, 18, 123-132

- [27] Wirth, M.; Fuchs, A.; Wolf, M.; Ertl, B.; Gabor, F. Lectin-mediated drug targeting: preparation, binding characteristics, and antiproliferative activity of wheat germ agglutinin conjugated doxorubicin on Caco-2 cells. *Pharm. Res.* 1998, 15, 1031-1037
- [28] Trouet, A.; Deprez-De Campeneere, D.; De Duve, C. Chemotherapy through lysosome with a DNA-daunomycin complex. *Nat. New Biol.* 1972, 239, 110-112
- [29] De Duve, C.; De Barse, T.; Poole, B.; Trouet, A.; Tulkens, P.; van Hoof, F. Lysosomotropic agents. *Biochem. Pharmacol.* 1974, 23, 2495-2531
- [30] Hartung, G.; Stehle, G.; Sinn, H.; Wunder, A.; Schrenk, H. H.; Heeger, S.; Kranzle, M.; Edler, L.; Frei, E.; Fiebig, H. H.; Heene, D. L.; Maier-Borst, W.; Queisser, W. Phase I trial of methotrexate-albumin in a weekly intravenous bolus regimen in cancer patients. Phase I Study Group of the Association for Medical Oncology of the German Cancer Society. *Clin. Cancer Res.* 1999, 5, 753-759
- [31] Maeda, H. SMANCS and polymer-conjugated macromolecular drugs: advantages in cancer chemotherapy. *Adv. Drug Delivery Rev.* 2001, 46, 169-185
- [32] Maeda, H.; Wu, J.; Sawa, T.; Matsumura, Y.; Hori, K. Tumor vascular permeability and the EPR effect in macromolecular therapeutics. A review. *J. Controlled Release* 2000, 65, 271-284
- [33] Kobayashi, M.; Imai, K.; Sugihara, S.; Maeda, H.; Konno, T.; Yamanaka, H. Tumor-targeted chemotherapy with lipid contrast medium and macromolecular anticancer drug (SMANCS) for renal cell carcinoma. *Urology* 1991, 37, 288-294
- [34] Iwai, K.; Maeda, H.; Konno, T. Use of oily contrast medium for selective drug targeting to tumor: enhanced therapeutic effect and x-rays image. *Cancer Res.* 1984, 44, 2115-2121
- [35] Keating, M. J.; Holmes, R.; Lerner, S.; Ho, D. H. L-Asparaginase and PEG asparaginase-past, present and future. *Leuk. Lymphoma* 1993, 10, 153-157

- [36] Duncan, R.; Spreafico, F. Polymer conjugates. Pharmacokinetic considerations for design and development. *Clinical Pharmacokinetics* 1994, 27, 290-306
- [37] Prakash, R. K.; Clemens, C. M. Conjugates targeted to target receptors and/or interleukin-2 receptors. *PCT Int. Appl.* 2000, WO 0007543
- [38] Sawa, T.; Wu, J.; Akaike, T.; Maeda, H. Tumor-targeting chemotherapy by a xanthine oxidase-polymer conjugate that generates oxygen-free radicals in tumor tissue. *Cancer Res.* 2000, 60, 666-671
- [39] Deckert, P. M.; Jungbluth, A.; Montalto, N.; Clark, M. A.; Finn, R. D.; Williams, C., Jr.; Richards, E. C.; Panageas, K. S.; Old, L. J.; Welt, S. Pharmacokinetics and microdistribution of polyethylene glycol-modified humanized A33 antibody targeting colon cancer xenografts. *Int. J. Cancer* 2000, 87, 382-390
- [40] Safavy, A. Taxane derivatives for targeted therapy of cancer. *PCT Int. Appl.* 2000, WO 0050059
- [41] Rodrigues, P. C.; Beyer, U.; Schumacher, P.; Roth, T.; Fiebig, H. H.; Unger, C.; Messori, L.; Orioli, P.; Paper, D. H.; Mulhaupt, R.; Kratz, F. Acid-sensitive polyethylene glycol conjugates of doxorubicin: preparation, in vitro efficacy and intracellular distribution. *Bioorganic and Medicinal Chemistry* 1999, 7, 2517-2524
- [42] Conover, C. D.; Greenwald, R. B.; Pendri, A. Camptothecin delivery systems: enhanced efficacy and tumor accumulation of camptothecin following its conjugation to polyethylene glycol via a glycine linker. *Cancer Chemother. Pharmacol.* 1998, 42, 407-414
- [43] Conover, C. D.; Borowski, V.; Hsu, J.; Shum, K. L. PEG-prodrugs of cytosine arabinoside II: *in vivo* anti-tumor activity. *AACR meeting, USA, 2000.*, 3330
- [44] Hornung, R.; Fehr, M. K.; Monti-Frayne, J.; Krasieva, T. B.; Tromberg, B. J.; Berns, M. W.; Tadir, Y. Highly selective targeting of ovarian cancer with the photosensitizer PEG-m-THPC in a rat model. *Photochem. Photobiol.* 1999, 70, 624-629

- [45] Kwon, G. S.; Yokoyama, M.; Okano, T.; Sakurai, Y.; Kataoka, K. Biodistribution of micelle-forming polymer-drug conjugates. *Pharm. Res.* 1993, 10, 970-974
- [46] Yokoyama, M.; Okano, T.; Sakurai, Y.; Okamoto, K.; Fukushima, S.; Kataoka, K. Strategy and requirements of selective anticancer drug delivery to solid tumors with polymeric micelle. *Polym. Prepr. (Am. Chem. Soc., Div. Polym. Chem.)* 1996, 37, 121-122
- [47] Yokoyama, M.; Kwon, G. S.; Okano, T.; Sakurai, Y.; Ekimoto, H.; Kataoka, K. In vivo antitumor activity of polymeric micelle anticancer drug against murein C 26 tumor. *J. Controlled Release* 1994, 28, 336-337
- [48] Rihova, B.; Kopecek, J.; Ulbrich, K.; Pospisil, J.; Mancal, P. Effect of the chemical structure of N-(2-hydroxylpropyl)methacrylamide copolymers on their stability to induce antibody formation in inbred strains of mice. *Biomaterials* 1984, 5, 143-148
- [49] Cassidy, J.; Newell, D. R.; Wedge, S. R.; Cummings, J. Pharmacokinetics of high molecular weight agents. *Cancer Surv.* 1993, 17, 315-341
- [50] Ulbrich, K.; Zacharieva, E. I.; Kopecek, J.; Hume, I. C.; Duncan, R. Polymer-bound derivatives of sarcolysin and their antitumor activity against mouse and human leukemia in vitro. *Makromol. Chem.* 1987, 188, 2497-2509
- [51] Duncan, R.; Hume, I. C.; Yardley, H. J.; Flanagan, P. A.; Ulbrich, K.; Subr, V.; Strohm, J. Macromolecular prodrugs for use in targeted cancer chemotherapy: melphalan covalently coupled to N-(2-hydroxypropyl)methacrylamide copolymers. *J. Controlled Release* 1991, 16, 121-136
- [52] Rejmanova, P.; Kopecek, J.; Duncan, R.; Lloyd, J. B. Stability in rat plasma and serum of lysosomally degradable oligopeptide sequences in N-(2-hydroxypropyl)methacrylamide copolymers. *Biomaterials* 1985, 6, 45-48
- [53] Duncan, R.; Seymour, L. W.; Ulbrich, K.; Kopecek, J. Soluble synthetic polymers for targeting and controlled release of anticancer agents, particularly anthracycline antibiotics. *J. Bioact. Compat. Polym.* 1988, 3, 4-15

- [54] Seymour, L. W.; Ulbrich, K.; Steyger, P. S.; Brereton, M.; Subr, V.; Strohalm, J.; Duncan, R. Tumor tropism and anti-cancer efficacy of polymer-based doxorubicin prodrugs in the treatment of subcutaneous murine B16F10 melanoma. *Br. J. Cancer* 1994, 70, 636-641
- [55] Duncan, R.; Seymour, L. W.; O'Hare, K. B.; Flanagan, P. A.; Wedge, S.; Hume, I. C.; Ulbrich, K.; Strohalm, J.; Subr, V.; et al. Preclinical evaluation of polymer-bound doxorubicin. *J. Controlled Release* 1992, 19, 331-346
- [56] Nannan, P. V. R.; Meerum, T. J. M.; Tenbokkel, H. W. W. Phase I and pharmacological study of water soluble polymer-conjugated paclitaxel (PNU 166945) administrated as a 1-hour infusion in patients with advanced solid tumors. 34th ASCO meeting, Los Angeles, USA, 1998,, 742
- [57] Ciaolfa, V. R.; Zama, M.; Fiorino, A.; Frigerio, E.; Pellizzoni, C.; d'Argy, R.; Ghiglieri, A.; Castelli, M. G.; Farao, M.; Pesenti, M.; Gigli, F.; Angelucci, F.; Suarato, A. Polymer-bound camptothecin: initial biodistribution and antitumor activity studies. *J. Controlled Release* 2000, 65, 105-119
- [58] Mongelli, N.; Pesenti, E.; Suarato, A.; Biasoli, G. Polymer-bound paclitaxel derivatives. U.S. 1994, US 5362831
- [59] Duncan, R. Polymer conjugates for tumor targeting and intracytoplasmic delivery. The EPR effect as a common gateway? *Pharm. Sci. Technol. Today* 1999, 2, 441-449
- [60] Omelyanenko, V.; Kopeckova, P.; Gentry, C.; Kopecek, J. Targetable HEMA copolymer-adriamycin conjugates. Recognition, internalization, and subcellular fate. *J. Controlled Release* 1998, 53, 25-37
- [61] Vasey, P. A.; Kaye, S. B.; Morrison, R.; Twelves, C.; Wilson, P.; Duncan, R.; Thomson, A. H.; Murray, L. S.; Hilditch, T. E.; Murray, T.; Burtles, S.; Fraier, D.; Frigerio, E.; Cassidy, J. Phase I clinical and pharmacokinetic study of PK1 [N-(2-

- hydroxypropyl)methacrylamide copolymer doxorubicin]: First member of a new class of chemotherapeutic agents-drug-polymer conjugates. *Clin. Cancer Res.* 1999, 5, 83-94
- [62] Shiah, J.-G.; Dvorak, M.; Sun, Y.; Peterson, C. M.; Kopecekova, P.; Kopecek, J. Long-circulating HPMA copolymer-adriamycin conjugates. 14th Annual Meeting of the American Association of Pharmaceutical Scientists, New Orleans, LA, 1999, 1, S432
- [63] Krinick, N. L.; Sun, Y.; Joyner, D. A.; Reed, R.; Spikes, J. D.; Straight, R. C.; Kopecek, J. A polymeric drug delivery system for the simultaneous delivery of drugs activable by enzymes and/or light. *J. Biomater. Sci., Polym. Ed.* 1994, 5, 303-324
- [64] Gu, Z. W.; Spikes, J. D.; Kopeckova, P.; Kopecek, J. Synthesis and photoproperties of a substituted zinc(II) phthalocyanine - N-(2-hydroxypropyl)methacrylamide copolymer conjugate. *Collect. Czech. Chem. Commun.* 1993, 58, 2321-2336
- [65] Kopecek, J.; Krinick, N. Polymer conjugates for the simultaneous delivery of neoplasm inhibitor activatable by enzymes and light. *PCT Int. Appl.* 1993, WO 9314142
- [66] Hirano, T.; Todoroki, T.; Ohashi, S.; Kokubu, T.; Tanaka, H. Polymeric conjugate of methotrexate compound and pyran copolymer and method for the preparation thereof. U.S. 1995, US 5401742
- [67] Yamamoto, H.; Miki, T.; Oda, T. Reduced bone marrow toxicity of neocarzinostatin by conjugation with divinylether-maleic acid copolymer. *Eur. J. Cancer* 1990, 26, 253-260
- [68] Hirano, T.; Ringsdorf, H.; Zaharko, D. Antitumor activity of monomeric and polymeric cyclophosphamide derivative compound with in vitro hydrolysis. *Cancer Res.* 1980, 40, 2263-2267
- [69] Carraher, C. E., Jr.; Francis, A.-M.; Siegmann-Louda, D. W. Synthesis of chelation products between chitosan and tetrachloroplatinate toward the synthesis of water soluble cancer drugs. *Abstr. Pap. - Am. Chem. Soc.* 2001, 221st, MSE-364
- [70] Nogusa, H.; Yamamoto, K.; Yano, T.; Kajiki, M.; Hamana, H.; Okuno, S. Distribution characteristics of carboxymethyl pullulan-peptide-doxorubicin conjugates in

- tumor-bearing rats: different sequence of peptide spacers and doxorubicin contents. *Biol. Pharm. Bull.* 2000, 23, 621-626
- [71] Levi-Schaffer, F.; Bernstein, M.; Meshorer, A.; Arnon, R. Reduced toxicity of daunorubicin by conjugation to dextran. *Cancer Treatment Reports* 1982, 66, 107-114
- [72] Avichezer, D.; Schechter, B.; Arnon, R. Functional polymers in drug delivery: carrier-supported CDDP (cis-platin) complexes of polycarboxylates - effect on human ovarian carcinoma. *React. Funct. Polym.* 1998, 36, 59-69
- [73] Okuno, S.; Harada, M.; Yano, T.; Yano, S.; Kiuchi, S.; Tsuda, N.; Sakamura, Y.; Imai, J.; Kawaguchi, T.; Tsujihara, K. Complete regression of xenografted human carcinomas by camptothecin analogue-carboxymethyl dextran conjugate (T-0128). *Cancer Res.* 2000, 60, 2988-2995
- [74] Li, C.; Yu, D.; Newman, R. A.; Cabral, F.; Stephens, L. C.; Hunter, N.; Milas, L.; Wallace, S. Complete regression of well-established tumors using a novel water-soluble poly(L-glutamic acid)-paclitaxel conjugate. *Cancer Res.* 1998, 58, 2404-2409
- [75] Li, C.; Ke, S.; Milas, L.; Charnsangavej, C.; Wallace, S. Sensitization of macromolecular chemotherapy: modulation of EPR effect by radiation. *Proc. Int. Symp. Controlled Release Bioact. Mater.* 2000, 27th, 207-208
- [76] Roos, C. F.; Matsumoto, S.; Takakura, Y.; Hashida, M.; Sezaki, H. Physicochemical and antitumor characteristics of some polyamino acid prodrugs of mitomycin C. *Int. J. Pharm.* 1984, 22, 75-87
- [77] Hoes, C. J. T.; Potman, W.; Van Heeswijk, W. A. R. Optimization of macromolecular prodrugs of the antitumor antibiotics adriamycin. *J. Controlled Release* 1985, 2, 205-218
- [78] Kishida, A.; Goto, H.; Murakami, K.; Kakinoki, K.; Akashi, M.; Endo, T. Polymer drugs and polymeric drugs IX. Synthesis and 5-fluorouracil release profiles of

- biodegradable polymeric prodrugs γ -poly(α -hydroxymethyl-5-fluorouracil-glutamate). *J. Bioact. Compat. Polym.* 1998, 13, 222-233
- [79] Seymour, L. W.; Soyez, H.; De Marre, A.; Shoaibi, M. A.; Schact, E. H. Polymeric prodrugs of mitomycin C designed for tumor tropism and sustained activation. *Anti-Cancer Drug Des.* 1996, 11, 351-365
- [80] Soyez, H.; Seymour, L. W.; Schacht, E. Macromolecular derivatives of N,N-di-(2-chloroethyl)-4-phenylene diamine mustard. 2. In vitro cytotoxicity and in vivo anticancer efficacy. *J. Controlled Release* 1999, 57, 187-196
- [81] Chu, B. C. F.; Howell, S. B. Pharmacological and therapeutic properties of carrier bound methotrexate against tumor confined to a third space body compartment. *J. Pharmacol. Exp. Ther.* 1981, 219, 389-393
- [82] Zunino, F.; Savi, G.; Giulliani, F. Comparison of antitumor effects of daunorubicin linked covalently to poly-L-amino acid carriers. *Eur. J. Cancer Clin. Oncol.* 1984, 20, 421-424
- [83] Ekrami, H.; Kennedy, A. R.; Witschi, H.; Shen, W. C. Cationized Bowman-Birk protease inhibitor as a targeted cancer chemopreventive agent. *J. Drug Targeting* 1993, 1, 41-49
- [84] Bogdanov, A., Jr.; Wright, S. C.; Marecos, E. M.; Bogdanova, A.; Martin, C.; Petherick, P.; Weissleder, R. A long-circulating co-polymer in "passive targeting" to solid tumors. *J. Drug Targeting* 1997, 4, 321-330
- [85] Ulbrich, K.; Subr, V.; Pechar, M.; Strohalm, J.; Jelinkova, M.; Rihova, B. Hydrophilic polymers for drug delivery. *Macromol. Symp.* 2000, 152, 151-162
- [86] Yang, F.; Zhuo, R. Synthesis and antitumor activity of poly(L-cysteine) bonded covalently 5-fluorouracil. *Polym. J. (Tokyo)* 1990, 22, 572-577

- [87] Ouchi, T.; Kobayashi, H.; Banba, T. Design of poly(α -malic acid)-5FU conjugate exhibiting antitumor activity. *Br. Polym. J.* 1990, 23, 221-228
- [88] Yoo, H. S.; Lee, K. H.; Oh, J. E.; Park, T. G. In vitro and in vivo antitumor activities of nanoparticles based on doxorubicin-PLGA conjugates. *J. Controlled Release* 2000, 68, 419-431
- [89] Siegmann, D. W.; Brenner, D.; Colvin, A.; Polner, B. S.; Strother, R. E.; Carraher, C. E., Jr. Platinum (II) polyamines: determination of size, degradation and biological activity. *Inorg. Met.-Containing Polym. Mater.*, (Proc. Am. Chem. Soc. Int. Symp.) 1990, 335-361
- [90] Carraher, C. E., Jr.; Ademu-John, C.; Fortman, J. J.; Giron, D. J.; Linville, R. Platinum(II) derivatives of polyethylenimine as model carriers for natural drug carriers in the treatment of cancers and viruses. *Polym. Mater. Sci. Eng.* 1983, 49, 210-214
- [91] Duncan, R. Design of polymeric drug delivery systems for controlled release of antitumor agents. *Spec. Publ. - R. Soc. Chem.* 1993, 138, 13-17
- [92] Luo, Y.; Zhuo, R. X.; Fan, C. L. Synthesis and antitumor activity of biodegradable polyphosphamides containing 5-fluorouracil. *Chemical Journal of Chinese Universities* 1994, 15, 767-769
- [93] Esfand, R.; Tomalia, D. A.; Duncan, R.; Malik, N. Efficient delivery of platinum-containing compounds to malignant tumors. *Book of Abstracts, 218th ACS National Meeting*, New Orleans, USA, 1999, COLL-129
- [94] Ram, B. P.; Tyle, P. Immunoconjugates: applications in targeted drug delivery for cancer therapy. *Pharm. Res.* 1987, 4, 181-188
- [95] Bos, E. S.; Boon, P. J.; Kaspersen, F.; McCabe, R. Passive immunotherapy of cancer: perspectives and problems. *J. Controlled Release* 1991, 16, 101-112

- [96] Sinha, A. A.; Quast, B. J.; Reddy, P. K.; Elson, M. K.; Wilson, M. J. Intravenous injection of an immunoconjugate (anti-PSA-IgG conjugated to 5-fluoro-2'-deoxyuridine) selectively inhibits cell proliferation and induces cell death in human prostate cancer cell tumors grown in nude mice. *Anticancer Res.* 1999, 19, 893-902
- [97] Osaku, M.; Ueda, M.; Ando, N.; Shinozawa, Y.; Hirota, N.; Shimizu, N.; Abe, O. Targeted killing of squamous carcinoma cells by a monoclonal antibody-peplomycin conjugate which recognizes the EGF receptor. *Anticancer Res.* 1991, 11, 1951-1956
- [98] Okamoto, K.; Yamaguchi, T.; Otsuji, E.; Yamaoka, N.; Yata, Y.; Tsuruta, H.; Kitamura, K.; Takahashi, T. Targeted chemotherapy in mice with peritoneally disseminated gastric cancer using monoclonal antibody-drug conjugate. *Cancer Lett. (Shannon, Irel.)* 1998, 122, 231-236
- [99] Remsen, L. G.; Trail, P. A.; Hellstrom, I.; Hellstrom, K. E.; Neuwelt, E. A. Enhanced delivery improves the efficacy of a tumor-specific doxorubicin immunoconjugate in a human brain tumor xenograft model. *Neurosurgery* 2000, 46, 704-709.
- [100] Wakai, Y.; Matsui, J.; Koizumi, K.; Tsunoda, S.-I.; Makimoto, H.; Ohizumi, I.; Taniguchi, K.; Kaiho, S.-I.; Saito, H.; Utoguchi, N.; Tsutsumi, Y.; Nakagawa, S.; Ohsugi, Y.; Mayumi, T. Effective cancer targeting using an anti-tumor tissue vascular endothelium-specific monoclonal antibody (TES-23). *Jpn. J. Cancer Res.* 2000, 91, 1319-1325
- [101] Thorpe, P. E.; Ran, S. Cancer treatment methods using antibodies to aminophospholipids. *PCT Int. Appl.* 2000, WO 0002584
- [102] Li, Z.; Wu, Y.; Zhou, D.; Gan, X.; Huang, B.; He, H.; Song, X.; Hu, X. Antibody-targeted radiochemotherapy of human primary liver cancer with radioiodinated AFP monoclonal antibodies conjugated with mitomycin C: A preliminary clinical observation. *Zhonghua Zhongliu Zazhi* 1996, 18, 368-371

- [103] Hamblin, M. R.; Del Governatore, M.; Rizvi, I.; Hasan, T. Biodistribution of charged 17.1A photoimmunoconjugates in a murine model of hepatic metastasis of colorectal cancer. *Br. J. Cancer* 2000, 83, 1544-1551
- [104] Goff, B.; Blake, J.; Bamberg, M.; Hasan, T. Treatment of ovarian cancer with photodynamic therapy and immunoconjugates in a murine ovarian cancer model. *Br. J. Cancer* 1996, 74, 1194-1198
- [105] Lode, H. N.; Reisfeld, R. A. Targeted cytokines for cancer immunotherapy. *Immunol. Res.* 2000, 21, 279-288
- [106] Epstein, A. L.; Khawli, L. A.; Hornick, J. L.; Taylor, C. R. Identification of a monoclonal antibody, TV-1, directed against the basement membrane of tumor vessels, and its use to enhance the delivery of macromolecules to tumors after conjugation with interleukin 2. *Cancer Res.* 1995, 55, 2673-2680
- [107] Seymour, L. W.; Flanagan, P. A.; al-Shamkhani, A.; Subr, V.; Ulbrich, K.; Cassidy, J.; Duncan, R. Synthetic polymers conjugated to monoclonal antibodies: vehicles for tumour-targeted drug delivery. *Selective Cancer Therapeutics* 1991, 7, 59-73
- [108] Jain, R. K. Delivery of molecular medicine to solid tumors. *Science* 1996, 271, 1079-1080
- [109] Jain, R. K. Physiological barriers to delivery of monoclonal antibodies and other macromolecules in tumors. *Cancer Res.* 1990, 50, 814s-819s
- [110] Fanger, M. W.; Guyre, P. M. Bispecific antibodies for targeted cellular cytotoxicity. *Trends Biotechnol.* 1991, 9, 375-380
- [111] Schmidt, M.; Hynes, N. E.; Groner, B.; Wels, W. A bivalent single-chain antibody-toxin specific for ErbB-2 and the EGF receptor. *Int. J. Cancer* 1996, 65, 538-546
- [112] Bonardi, M. A.; French, R. R.; Gromo, G.; Modena, D.; Glennie, M. J. Delivery of saporin to human B-cell lymphoma using bispecific antibody: Targeting via CD22 but not

CD19, CD37, or immunoglobulin results in efficient killing. *Cancer Res.* 1993, 53, 3015-3021

[113] Rihova, B.; Krinick, N. L.; Kopecek, J. Targetable photoactivatable drugs. 3. In vitro efficacy of polymer bound chlorin e6 toward human hepatocarcinoma cell line (PLC/PRF/5) targeted with galactosamine and to mouse splenocytes targeted with anti-Thy 1.2 antibodies. *J. Controlled Release* 1993, 25, 71-87

[114] Seymour, L. W.; Ulbrich, K.; Wedge, S. R.; Hume, I. C.; Strohalm, J.; Duncan, R. N-(2-hydroxypropyl)methacrylamide copolymers targeted to the hepatocyte galactose-receptor: pharmacokinetics in DBA2 mice. *Br. J. Cancer* 1991, 63, 859-866

[115] Putnam, D.; Rihova, B.; Jelinkova, M.; Kopecek, J. Biorecognition and biological activity of synthetic polymer glycoconjugates containing 5-fluorouracil. *Proc. Int. Symp. Controlled Release Bioact. Mater.* 1996, 23rd, 75-76

[116] Duncan, R.; Kopeckova, P.; Strohalm, J.; Hume, I. C.; Lloyd, J. B.; Kopecek, J. Anticancer agents coupled to N-(2-hydroxypropyl) methacrylamide copolymers. 2. Evaluation of daunomycin conjugates *in vivo* against L1210 leukemia. *Br. J. Cancer* 1988, 57, 147-156

[117] Luo, Y.; Benshaw, N.; Lu, Z.-R.; Kopecek, J.; Prestwich, G. D. HPMa copolymer-hyaluronic acid-doxorubicin bioconjugates: targeted delivery of anticancer drug to cancer cells. *in press*,

[118] St'astny, M.; Strohalm, J.; Ulbrich, K.; Rihova, B. Specificity of antibody-targeted drugs. *Proc. Int. Symp. Controlled Release Bioact. Mater.* 1997, 24th, 105-106

[119] Rihova, B.; Kopecek, J.; Kopeckova-Rejmanova, P.; Strohalm, J.; Plocova, D.; Semoradova, H. Bioaffinity therapy with antibodies and drugs bound to soluble synthetic polymers. *J. Chromatogr.* 1986, 376, 221-233

- [120] Ulbrich, K.; Strohalm, J.; Subr, V.; Plocova, D.; Duncan, R.; Rihova, B. Polymeric conjugates of drugs and antibodies for site-specific drug delivery. *Macromol. Symp.* 1996, 103, 177-192
- [121] Omelyanenko, V.; Gentry, C.; Kopeckova, P.; Kopecek, J. HPMa copolymer-anticancer drug-OV-TL16 antibody conjugates. II. Processing in epithelial ovarian carcinoma cells in vitro. *Int. J. Cancer* 1998, 75, 600-608
- [122] Lu, Z.-R.; Kopeckova, P.; Kopecek, J. Polymerizable Fab' antibody fragments for targeting of anticancer drugs. *Nature Biotechnol.* 1999, 17, 1101-1104
- [123] Fowers, K.; Kopeckova, P.; Kopecek, J. Targeting of HPMa copolymer-drug conjugates to A2780/AD ovarian cancer cells using anti-P-glycoprotein antibodies or fragments. *Proc. Int. Symp. Controlled Release Bioact. Mater.* 1999, 26th, 527-528
- [124] Ulbrich, K.; Subr, V.; Strohalm, J.; Plocova, D.; Jelinkova, M.; Rihova, B. Polymeric drugs based on conjugates of synthetic and natural macromolecules I. Synthesis and physico-chemical characterization. *J. Controlled Release* 2000, 64, 63-79
- [125] Rihova, B.; Jelinkova, M.; Strohalm, J.; Subr, V.; Plocova, D.; Hovorka, O.; Novak, M.; Plundrova, D.; Germano, Y.; Ulbrich, K. Polymeric drugs based on conjugates of synthetic and natural macromolecules. II. Anti-cancer activity of antibody or (Fab')₂-targeted conjugates and combined therapy with immunomodulators. *J. Controlled Release* 2000, 64, 241-261
- [126] Seymour, L. W. Soluble polymers for lectin-mediated drug targeting. *Adv. Drug Delivery Rev.* 1994, 14, 89-111
- [127] Rihova, B.; Jelinkova, M.; Strohalm, J.; St'astny, M.; Hovorka, O.; Plocova, D.; Kovar, M.; Draberova, L.; Ulbrich, K. Antiproliferative Effect of a Lectin- and Anti-Thy-1.2 Antibody-Targeted HPMa Copolymer-Bound Doxorubicin on Primary and Metastatic Human Colorectal Carcinoma and on Human Colorectal Carcinoma Transfected with the Mouse Thy-1.2 Gene. *Bioconjugate Chem.* 2000, 11, 664-673

- [128] Ward, C. M.; Acheson, N.; Seymour, L. W. Folic acid targeting of protein conjugates into ascites tumor cells from ovarian cancer patients. *J. Drug Targeting* 2000, 8, 119-123
- [129] Russell-jones, G. J.; McEwan, J. F. Amplification of folate-mediated targeting to tumor cells using polymers. *PCT Int. Appl.* 2000, WO 0066091
- [130] Prakash, R. K.; Clemens, C. M.; Ebert, C. D.; Omelyanenko, V.; Kopeckova, P.; Kopecek, J. Targeting of macromolecular prodrug to T-lymphocytes. *Proc. Int. Symp. Controlled Release Bioact. Mater.* 1997, 24th, 859-860
- [131] Uckun, F. M.; Narla, R. K.; Zeren, T.; Yanishevski, Y.; Myers, D. E.; Waurzyniak, B.; Ek, O.; Schneider, E.; Messinger, Y.; Chelstrom, L. M.; Gunther, R.; Evans, W. In vivo toxicity, pharmacokinetics, and anticancer activity of genistein linked to recombinant human epidermal growth factor. *Clin. Cancer Res.* 1998, 4, 1125-1134
- [132] Lutsenko, S. V.; Feldman, N. B.; Finakova, G. V.; Posypanova, G. A.; Severin, S. E.; Skryabin, K. G.; Kirpichnikov, M. P.; Lukyanets, E. A.; Vorozhtsov, G. N. Targeting phthalocyanines to tumor cells using epidermal growth factor conjugates. *Tumor Biol.* 1999, 20, 218-224
- [133] Fang, K. A toxin conjugate containing transforming growth factor-alpha and ricin A specifically inhibits growth of A431 human epidermoid cancer cells. *Proceedings of the National Science Council, Republic of China. Part B, Life Sciences* 1998, 22, 76-82
- [134] Beitz, J. G.; Davol, P.; Clark, J. W.; Kato, J.; Medina, M.; Frackelton, A. R., Jr.; Lappi, D. A.; Baird, A.; Calabresi, P. Antitumor activity of basic fibroblast growth factor-saporin mitotoxin in vitro and in vivo. *Cancer Res.* 1992, 52, 227-230
- [135] Sosnowski, B. A.; Victor, K. D.; Houston, L. L.; Nova, M. P.; Freund, E.; Fleurbaaij, G. A. Conjugates of vascular endothelial growth factor (VEGF) with targeted agents. *PCT Int. Appl.* 1996, WO 9606641

- [136] Ramakrishnan, S.; Olson, T. A.; Bautch, V. L.; Mohanraj, D. Vascular endothelial growth factor-toxin conjugate specifically inhibits KDR/flk-1-positive endothelial cell proliferation in vitro and angiogenesis in vivo. *Cancer Res.* 1996, 56, 1324-1330
- [137] Tanaka, T.; Kaneo, Y.; Miyashita, M. Synthesis of transferrin-mitomycin C conjugate as a receptor-mediated drug targeting system. *Biol. Pharm. Bull.* 1996, 19, 774-777
- [138] Lemieux, P.; Page, M.; Noel, C. In vivo cytotoxicity and antineoplastic activity of a transferrin-daunorubicin conjugate. *In Vivo* 1992, 6, 621-627
- [139] Bicamumpaka, C.; Page, M. In vitro cytotoxicity of paclitaxel-transferrin conjugate on H69 cells. *Oncology Reports* 1998, 5, 1381-1383
- [140] Tsushima, N.; Kohgo, Y.; Sasaki, K. Preparation of transferrin-neocarzinostatin conjugate and its antitumor effect. *Sapporo Igaku Zasshi* 1991, 60, 379-389
- [141] Ceulemans, F.; Baurain, R.; Geubel, A.; Lesur, B.; Rolin-Van Swieten, D.; Trouet, A. Anthracycline targeting and hepatomas. *Pathol. Biol.* 1987, 35, 61-68
- [142] Hamblin, M. R.; Miller, J. L.; Ortel, B. Scavenger-receptor targeted photodynamic therapy. *Photochemistry and Photobiology* 2000, 72, 533-540
- [143] Tabata, Y.; Ikada, Y. Targeting of muramyl dipeptide to macrophages by gelatin conjugation to enhance their in vivo antitumor activity. *J. Controlled Release* 1993, 27, 79-88
- [144] Beck, E. P.; Vincenti, D.; Licht, P.; Berkholz, A.; Jager, W.; Lang, N.; Merkle, E. In vitro activity of human chorionic gonadotropin (hCG) - doxorubicin conjugates against ovarian cancer cells. *Anticancer Res.* 2000, 20, 3001-3006
- [145] Zhang, S.; Cui, Z.; Wu, M.; Chen, H.; Tu, Z. Endogenous lectin-mediated-targeting killing of hepatoma cells by MTX-neoglycoproteins. *Shengwu Huaxue Yu Shengwu Wuli Xuebao* 1991, 23, 543-546

- [146] Severin, S. E.; Moskaleva, E. Y.; Shmyrev, I. I.; Posypanova, G. A.; Belousova, Y. V.; Sologub, V. K.; Luzhkov, Y. M.; Nakachian, R.; Andreani, J.; Severin, E. S. Alpha-fetoprotein-mediated targeting of anticancer drugs to tumor cells in vitro. *Biochem. Mol. Biol. Int.* 1995, 37, 385-392
- [147] Huang, C.-M.; Wu, Y.-T.; Chen, S.-T. Targeting delivery of paclitaxel into tumor cells via somatostatin receptor endocytosis. *Chem. Biol.* 2000, 7, 453-461
- [148] Luo, Y.; Prestwich, G. D. Synthesis and Selective Cytotoxicity of a Hyaluronic Acid-Antitumor Bioconjugate. *Bioconjugate Chem.* 1999, 10, 755-763
- [149] Luo, Y.; Ziebell, M. R.; Prestwich, G. D. A Hyaluronic Acid-Taxol Antitumor Bioconjugate Targeted to Cancer Cells. *Biomacromolecules* 2000, 1, 208-218
- [150] Thorpe, P. E. Methods of using steroid-polyanionic polymer-based conjugated targeted to vascular endothelial cells. U.S. 1998, US 5762918
- [151] Ouchi, T.; Tada, M.; Ohya, Y.; Matsumoto, T.; Suzuki, S.; Suzuki, M. A lysosomal release type of macromolecular prodrug of doxorubicin using N-acetylpolygalactosamine as a targeting carrier to hepatoma. *Polym. Prepr. (Am. Chem. Soc., Div. Polym. Chem.)* 1996, 37, 141-142
- [152] Larsen, C. Eds. dextran prodrugs; Villadsen & Christesen: Copenhagen, **1990**
- [153] Sheldon, K.; Marks, A.; Bauml, R. Sensitivity of multidrug resistant KB-C1 cells to an antibody-dextran-adriamycin conjugate. *Anticancer Res.* 1989, 9, 637-641
- [154] Loeqvist, A.; Lindstroem, A.; Carlsson, J. Binding, internalization and excretion of TGF α -dextran associated radioactivity in cultured human glioma cells. *Cancer Biother.* 1993, 8, 345-356
- [155] Kagitani, Y.; Ueda, Y.; Munechika, K.; Morimoto, S.; Komeda, S.; Tanaka, K.; Yokoyama, K. Fibronectin-dextran-drug complex. *Eur. Pat. Appl.* 1985, EP 160521

- [156] Del Governatore, M.; Hamblin, M. R.; Piccinini, E. E.; Ugolini, G.; Hasan, T. Targeted photodestruction of human colon cancer cells using charged 17.1A chlorine6 immunoconjugates. *Br. J. Cancer* 2000, 82, 56-64
- [157] Goff, B. A.; Bamberg, M.; Hasan, T. Experimental photodynamic treatment of ovarian carcinoma cells with immunoconjugates. *Antibody, Immunoconjugates, Radiopharm.* 1992, 5, 191-199
- [158] Hoes, C. J. T.; Ankone, M.; Grooten, J.; Feijen, J.; van der Strijk, E.; van Doormalen, A.; Pham, D.; A., d. M.; van Ettehoven, A.; Schlachter, I.; Boon, P. J.; Kaspersen, F.; Bos, E. S. Synthesis and biological evaluation of immunoconjugates of adriamycin and a human IgM linked by poly[N⁵-(2-hydroxyethyl)-L-glutamine]. *J. Controlled Release* 1996, 38, 245-266
- [159] Di Stefano, G.; Busi, C.; Derenzini, M.; Trere, D.; Fiume, L. Conjugation of 5-fluoro-2'-deoxyuridine with lactosaminated poly-L-lysine to reduce extrahepatic toxicity in the treatment of hepatocarcinomas. *Ital. J. Gastroenterol. Hepatol.* 1998, 30, 173-177
- [160] Ouchi, T.; Kobayashi, H.; Hirai, K.; Ohya, Y. Design of poly(α -malic acid)-antitumor drug-saccharide conjugate exhibiting cell-specific antitumor activity. *ACS Symp. Ser.* 1993, 520, 382-394
- [161] Han, M. J.; Choi, K. B.; Kim, K. H.; Hahn, B. S.; Lee, W. Y. Biologically active polymer - targeting polymeric antitumor agents. *Makromol. Chem., Macromol. Symp.* 1990, 33, 301-309
- [162] Song, S. C.; Sohn, Y. S. Synthesis of polyphosphazene/(diamine)-platinum(II)/carbohydrate conjugates. *Proc. Int. Symp. Controlled Release Bioact. Mater.* 1997, 24th, 551-552

- [163] Hamblin, M. R.; Luke Newman, E. Photosensitizer targeting in photodynamic therapy. II. Conjugates of hematoporphyrin with serum lipoproteins. *J. Photochem. Photobiol., B* 1994, 26, 147-157
- [164] Favre, G.; Samain, D. Targeting of tumor cells via the LDL receptor. Concept and synthesis of supramolecular biovectors which mimic LDL. *Actual. Chim. Ther.* 1993, 20, 215-228

Manuscript for: *Pharmaceutical Research*
Draft: July 7, 2001
Submitted:

HPMA Copolymer-Hyaluronan-Doxorubicin Bioconjugates:

Targeted Delivery of an Anti-cancer Agent

Yi Luo,^a Nicole J. Bernshaw,^b Zheng-Rong Lu,^c Jindrich Kopecek,^c
and Glenn D. Prestwich^{a,b,*}

^aDepartment of Medicinal Chemistry

^bCenter for Cell Signaling

^cDepartment of Pharmaceutics and Pharmaceutical Chemistry
The University of Utah, Salt Lake City, Utah

Running title: HPMA-HA-Doxorubicin

*Address correspondence to this author:

Professor Glenn D. Prestwich
The University of Utah
Department of Medicinal Chemistry
30 South 2000 East, Room 201
Salt Lake City, Utah 84112-5820
Phone: 801 585-9051; **Fax:** 801 585-9053
E-mail: gprestwich@deans.pharm.utah.edu

ABSTRACT

A cell-targeted polymeric drug delivery system was developed to exploit the specific uptake of hyaluronan (HA) by receptors overexpressed on cancer cells. HA-doxorubicin (DOX) bioconjugates (HA-DOX), and *N*-(2-hydroxypropyl)methacrylamide (HPMA) copolymer-DOX conjugates containing HA as a side chain (HPMA-HA-DOX) were synthesized. Cytotoxicity of this targeted bioconjugate *in vitro* was higher against human breast cancer (HBL-100), human ovarian cancer (SKOV-3), and human colon cancer (HCT-116) cells when compared to the non-targeted HPMA-DOX conjugate. Fluorescence confocal microscopy revealed that the targeted HPMA-HA-DOX conjugates were internalized more efficiently by cancer cells relative to the non-targeted HPMA-DOX conjugate. . Both HPMA-DOX and HPMA-HA-DOX showed minimal cytotoxicity towards mouse fibroblast NIH 3T3 cells. Thus, cytotoxic drugs coupled to an HA-modified HPMA copolymer should have a significantly improved therapeutic ratios *in vivo*, as they combine biochemical targeting with enhanced permeability and retention characteristic of macromolecular anticancer drugs.

Key words: polymer-drug conjugates, HPMA copolymer, hyaluronan, receptor-mediated targeting, doxorubicin, cancer

INTRODUCTION

A major challenge in cancer therapy is to selectively deliver small molecule anti-cancer agents to tumor cells. One promising approach uses the covalent attachment of the cytotoxin to a macromolecular carrier (1). Many kinds of drug carriers, including soluble synthetic and natural polymers (2), liposomes (3), microspheres (4), and nanospheres (5,6), have been employed to increase drug concentration in target cells; by altering the pharmacokinetic distribution of drugs, a sustained therapeutic concentration can be maintained at tolerable doses. Water-soluble polymer-anti-cancer drug conjugates seem to offer great potential because they can traverse compartmental barriers in the body (7), and thus gain access to a greater number of cell-types. A variety of water-soluble polymers, such as human serum albumin (HSA) (2), dextran (8), lectins (9), poly(ethylene glycol) (PEG) (10), poly(styrene-co-maleic anhydride) (SMA) (11), poly(*N*-hydroxypropylmethacrylamide) (HPMA) (12), and poly(divinylether-co-maleic anhydride) (DIVEMA) (13) have been used to prepare polymeric anti-cancer prodrugs for cancer treatment. Such drug-polymer conjugates have demonstrated good solubility in water, increased half-life in the body, and high anti-tumor effects. For example, poly(styrene-co-maleic acid)-neocarzinostatin conjugate (SMANCS) was approved for the treatment of liver cancer in Japan (11,14). Similarly, linking of doxorubicin to HPMA (HPMA-DOX) produced a prodrug with improved *in vitro* tumor retention, a higher therapeutic ratio and avoidance of multi-drug resistance (12). This system has passed the Phase I clinical trial and is currently in Phase II trials against ovarian cancer (15). A conjugate of

HPMA copolymer with camptothecin was also pre-clinically evaluated and is now in Phase I trials (16,17).

Anti-cancer polymer-drug conjugates can be divided into two targeting modalities: passive and active. The biological activity of the passive targeting drug delivery systems is based on the anatomical characteristics of tumor tissue, and allows polymeric prodrugs to more easily permeate tumor tissues and accumulate over time. This is one of the principal reasons for the success of polymeric drugs, and it is often referred to as the enhanced permeability and retention (EPR) effect. Macromolecules can accumulate more efficiently than free drugs in solid tumors (11). Active targeting in drug delivery systems can be achieved by exploiting specific interactions between receptors on the cell surface and targeting moieties conjugated to the polymer backbone. In this way, active therapeutic agents conjugated to polymers can be selectively transported to tumor tissues. The active approach therefore takes advantage of the EPR effect, but further increases the therapeutic index through receptor-mediated uptake by target cancer cells. Previous studies showed that *N*-acylated galactosamine (18) and monoclonal antibody fragments (19) were valuable targeting moieties for HPMA-DOX conjugates, selectively increasing the cytotoxicity of the polymer-drug conjugates to tumor cells.

HA (Figure 1), a linear polysaccharide of alternating D-glucuronic acid (GlcUA) and *N*-acetyl-D-glucosamine (GlcNAc) units, is present in the extracellular matrix (ECM), the synovial fluid of joints, and the scaffolding that comprises cartilage (20,21). It is an immunoneutral building block for preparing biocompatible and biodegradable biomaterials (22-26), and has been employed as both a vehicle and as an angiostatic agent in cancer therapy (27-29). Mitomycin C and epirubicin

were coupled to HA by carbodiimide chemistry, and the HA-mitomycin adduct was selectively toxic to a lung carcinoma xenograft (30). Recently, we described the use of mild dihydrazide chemistry to prepare an HA-Taxol® bioconjugate (31,32), which showed good selectivity in cell culture studies. Moreover, uptake and cytotoxicity were directly correlated using a fluorescently-labeled HA-Taxol® derivative, and the parent drug was released intracellularly by hydrolysis *in vitro*.

HA serves a variety of functions within the ECM, including direct receptor-mediated effects on cell behavior. These effects occur *via* intracellular signaling pathways in which HA binds to, and is internalized by, cell-surface receptors. Several cell membrane-localized receptors (HA binding proteins) have been identified, including: CD44, RHAMM, IVd4, and the liver endothelial cell clearance receptor (33-39). HA-protein interactions (40,41) play crucial roles in cell adhesion, growth (42) and migration (43-45), and HA acts as a signaling molecule in cell motility, inflammation, wound healing, and cancer metastasis (46,47). The structure and regulation of HA receptors (41,48) is a growing research that is critical to understanding how HA-protein interactions promote metastasis.

Most malignant solid tumors and their surrounding stromal tissue contain elevated levels of HA (49,50), and these high levels of HA production provide a matrix that facilitates invasion (51). Clinically, high HA levels correlate with poor differentiation and decreased survival rate in some human carcinomas. HA is an important signal for activating kinase pathways (52,53) and regulating angiogenesis in tumors (54). HA internalization is mediated *via* matrix receptors, including CD44, which is a transmembrane receptor that can communicate cell-matrix interactions into cells and can alter the matrix in response to intracellular

signals. The pathological enrichment of HA in tumor tissues suggests that manipulation of the interactions between HA and its receptors could lead to dramatic inhibition of growth or metastasis of several types of tumor.

Antibodies to CD44, soluble forms of CD44 or RHAMM, hyaluronidase (HAse), and oligomers of HA have all been used effectively to inhibit tumor growth or metastasis in animal models.

In addition to elevated HA in the environment surrounding tumors, most malignant cell-types overexpress CD44 and RHAMM. As a result, malignant cells with the highest metastatic potential often show enhanced binding and internalization of HA (55). Apparently, such cells can effectively breach the tumor-associated HA barrier by binding, internalizing, and degrading this glycosaminoglycan. Cell culture experiments suggest that CD44-HA interactions occur *in vivo* and are likely to be responsible for retention of HA-enriched matrices. Thus, HA can bind to the cell surface *via* interactions with CD44, and a portion subsequently undergoes endocytosis. In addition, internalization of [³H]-labeled HA revealed that intracellular degradation of HA occurs within a low pH environment, such as that of lysosome. Targeting of anti-cancer agents to tumor cells and tumor metastases can be accomplished by receptor-mediated uptake of bioconjugates of anti-cancer agents conjugated to HA (30-32), followed by the release of free drugs through the degradation of HA in cell compartments. Isoforms of HA receptors, CD44 and RHAMM are overexpressed in transformed human breast epithelial cells (56-59), human ovarian tumor cells (60,61), human colon cancer (62), lung cancer (63), stomach cancer (64), acute leukemia (65), and other cancers (66,67). Thus, we tested the

hypothesis that the selective delivery of a polymeric-anti-tumor agent conjugate to cancer cells could be markedly enhanced, and overall doses could be reduced. In this study, cell-targeted HA-DOX bioconjugates and HPMA copolymer-DOX conjugates containing HA as a side chain (HPMA-HA-DOX) were synthesized based on the specific interaction between HA and its receptors overexpressed on the cancer cell-surface. Selective *in vitro* cell cytotoxicity was studied using three human cancer cell-lines (HCT-116 colon tumor, HBL-100 breast cancer, and SK-OV-3 ovarian cancer), and a non-cancerous cell-line-mouse fibroblast NIH 3T3. In addition, enhanced uptake of HPMA-HA-DOX conjugate into cancer cells was observed in comparison to the non-targeted HPMA-DOX, as visualized using the intrinsic fluorescence of the DOX. This provides additional evidence for the uptake of the targeted conjugates through a receptor-mediated pathway.

MATERIALS AND METHODS

Reagents. Fermentation-derived HA (sodium salt, M_r 1.5 MDa) was provided by Clear Solutions Biotech, Inc. (Stony Brook, NY). 1-Ethyl-3-(3-(dimethylamino)-propyl)carbodiimide (EDCI), Adipic dihydrazide (ADH), succinic anhydride, anhydrous DMF, and triethylamine were purchased from Aldrich Chemical Co. (Milwaukee, WI). Testicular Hase, Dulbecco's phosphate-buffered saline (DPBS) and cell culture media were purchased from Sigma (St. Louis, MO). DOX was a kind of gift from Dr. A. Suarato, Pharmacia-Upjohn, Milano, Italy. Fluorescence images were recorded on a Bio-Rad (Hercules, CA) MRC 1024 laser scanning confocal imaging system based on a Zeiss (Oberkochen, Germany) Axioplan microscope and a krypton/argon laser.

Cell Lines. HBL-100, a human breast cancer cell-line, was maintained in culture in high glucose D-MEM (Dulbecco's Modified Eagle Medium), which was supplemented with 10% γ -irradiated fetal bovine serum (FBS) and 1% sodium pyruvate; SK-OV-3, a human ovarian cancer cell-line was cultured in D-MEM/F12 + 10% FBS; HCT-116, a colon tumor cell-line, was maintained in culture in α -MEM (Minimal Essential Medium, Eagle) + 10% FBS; NIH 3T3, a mouse fibroblast non-cancerous cell-line, was maintained in high glucose D-MEM + 10% FBS.

Analytical Instrumentation. All ^1H NMR spectral data were obtained using an NR-200 FT-NMR spectrometer at 200 MHz (IBM Instruments Inc.). UV-Vis spectra were recorded on a Hewlett Packard 8453 UV-Vis diode array spectrophotometer (Palo Alto, CA). HA was characterized by gel permeation chromatography (GPC) using the following system: Waters 515 HPLC pump,

Waters 410 differential refractometer, and Waters™ 486 tunable absorbance detector. Waters Ultrahydrogel 250 and 2000 columns (7.8 mm ID × 30 cm) (Milford, MA) were used for GPC analysis, the eluent was 150 mM pH 6.5 phosphate buffer/MeOH = 80:20 (v/v), and the flow rate was 0.5 ml/min. The system was calibrated with HA standards supplied by Dr. O. Wik (Pharmacia). HPMa copolymer conjugates were characterized by GPC on a Pharmacia FPLC with Superose analytical column, pH 7.4 phosphate-buffered saline (PBS) buffer was used as eluent with a flow rate of 0.4 ml/min. Cell viability in cell culture was determined by thiazoyl blue (MTT) dye uptake protocols measured at 540 nm, which was recorded on a BIO-RAD M-450 microplate reader (Hercules, CA). Laser scanning confocal microscopy was carried out on a Keller type Bio-Rad MRC 1024 with LASERSHARP acquisition software. Fluorescence images were taken using FITC settings with the 488 nm excitation line and a 522 nm 32 bandpass filter was used to collect the images.

Preparation of low molecular weight (LMW) HA and HA adipic dihydrazide derivative (HA-ADH). LMW HA was obtained by the degradation of high molecular weight HA (1.5 MDa) in pH 6.5 PBS buffer (4 mg/ml) with HAse (10 U/mg HA) as previously described, and purified by dialysis against H₂O (31). HA-ADH was prepared (31,68) using a modified purification method that gives preparations free of small molecules (31). In a representative example, LMW HA (50 mg) was dissolved in water to give a concentration of 4 mg/mL, and then a fivefold excess of ADH was added into the solution. The pH of the reaction mixture was adjusted to 4.75 by addition of 0.1 N HCl. Next, 2 equiv. of EDCI was added in solid form. The pH of the reaction mixture was maintained at 4.75 by

addition of 0.1 N HCl. The reaction was quenched by addition of 0.1 N NaOH to adjust the pH of reaction mixture to 7.0 for different reaction time. The reaction mixture was then transferred to pretreated dialysis tubing (Mw cutoff 3,500) and dialyzed exhaustively against 100 mM NaCl, then 25% EtOH/H₂O, and finally H₂O. The purity of HA-ADH was monitored by GPC. The purified polymer solution was then filtered through 0.2 µm cellulose acetate membrane, flash frozen, and lyophilized. The loading of ADH on the polymer backbone was determined by ¹H NMR in D₂O (68). HA-ADH (37 mg) was obtained with 9 mol% and 18 mol% loading, based on available carboxylates modified, by using reaction times of 12 min and 20 min, respectively.

Preparation of HA-DOX conjugates (Figure 2). First, DOX was converted to an active ester form (DOX-NHS) (69). Thus 20 mg DOX (34 µmol) was dissolved in 1.2 ml of anhydrous DMF, followed by addition of 15 µl triethylamine and 3.8 mg succinic anhydride. The reaction was stirred at room temperature (rt) in the dark for 24 h. DOX-hemisuccinate was purified by C₁₈ cartridge (Varian, Harbor City, CA), with methanol as the eluent.

Next, *N*-hydroxysuccinimido diphenyl phosphate (SDPP) was prepared from 10 mmol of diphenylphosphoryl chloride, 10 mmol of *N*-hydroxysuccinimide, and 10 mmol triethylamine in 6 mL of CH₂Cl₂ as previously described (31,70). Crude SDPP was triturated with ether, dissolved in ethyl acetate, washed (2 × 10 mL H₂O), dried (MgSO₄), and concentrated *in vacuo* to give SDPP with m.p. 89-90 °C (85%). To the solution of DOX-hemisuccinate and 18.5 mg (1.5 equiv.) of SDPP in 2 ml DMF, was added with 60 µL (10 equiv.) triethylamine. The reaction was stirred for

6 h at rt, and then concentrated *in vacuo*. The DOX-NHS ester was purified on an LH-20 column with methanol as the eluent.

HA-DOX conjugates were prepared by the conjugation of LMW HA-ADH and DOX-NHS. HA-ADH (50 mg, 9 mol% and 18 mol%) was dissolved in 7 ml 3 mM pH 6.0 phosphate buffer, 2 mg DOX-NHS in 15 ml DMF was added to this solution in an ice-water bath. The reaction was stirred at rt for 3 days. The HA-DOX conjugates were purified on a Sephadex G-25 column using PBS buffer as the eluent, followed by dialysis against H₂O to remove the buffer salt. The DOX loading was determined by the absorption of UV spectrum at $\lambda = 484$ nm.

Preparation of HPMA-HA-DOX conjugates (Figure 3). The HPMA copolymer-bound DOX (HPMA-DOX) was synthesized as described (71,72). A lysosomally degradable glycyphenylalanylleucylglycine (GFLG) spacer was used as the oligopeptide side chain. The conjugate was synthesized using a two-step procedure (73). In the first step, the polymer precursor HPMA-(GFLG)-ONp was prepared by radical precipitation copolymerization of HPMA and *N*-methacryloylglycyphenyl-alanylleucylglycine *p*-nitrophenyl ester (72). The polymer precursor contained 7.1 mol% active ester groups ($M_w = 17,800$, $M_n = 14,500$). DOX was bound to the polymer precursor by aminolysis (74). HPMA-(GFLG)-ONp (200 mg) and DOX (21.9 mg) hydrochloride were dissolved in 1.0 ml DMSO, and 50 μ l of Et₃N was added. The mixture was stirred at rt for 1 h, and precipitated in acetone/ether (3:1) mixture solvent. The red polymer solid was collected and washed with acetone/ ether, and dried under vacuum to give 210 mg of product. The HPMA-(GFLG)-DOX-ONp conjugate contained 1.1 mol% of DOX.

HPMA-HA-DOX conjugates were prepared by the conjugation of HA-ADH (9 mol% and 18 mol% hydrazide modification) to the drug-polymer conjugate precursor HPMA-(GFLG)-DOX-ONp. For example, 90 mg HPMA-(GFLG)-DOX-ONp copolymer-drug conjugate prepared previously was dissolved in 2.0 ml DMSO, and 90 mg HA-ADH (18 mol% hydrazide modification) was dissolved in 1.0 ml water and 2.0 ml DMSO. The two solutions were mixed together and stirred overnight at rt. Aminoethanol (100 μ l) was added to destroy unreacted ONp active ester. The HPMA-HA-DOX conjugate was isolated and purified by gel filtration on a Sephadex LH-20 column twice, with methanol as eluent. The solvent was removed under vacuum, and the residue was dissolved in distilled water and lyophilized. The DOX loading was determined by the absorption of UV spectrum at $\lambda = 484$ nm. HA composition was calculated by mass balance.

In Vitro Cell Culture. The cytotoxicity of HA-DOX and HPMA-HA-DOX conjugates against HBL-100, SKOV-3, and HCT-116 cells was determined using a 96-well plate format in quadruplicate with increasing doses ranging from 0.001-10 mg/ml of DOX equivalent. Each well contained approximately 20,000 cells in 200 μ l cell culture media. Thus, a 2- μ l aliquot of the stock solution was added to each well, and cells were continuously incubated at 37 °C, 5% CO₂ for 3 days with the test substance, and cell viability was determined using MTT dye uptake at 540 nm. Response was graded as percent live cells compared to untreated controls (75). Dose-response curves were constructed, and the concentration necessary to inhibit the growth of the cells by 50% relative to the non-treated control cells (IC₅₀ dose) was determined.

Internalization of HPMA-HA-DOX and HPMA-DOX conjugates by cancer cells. SKOV-3 cells were incubated in a cell culture flask, harvested by trypsinization, and transferred into an eight-well cell culture slide. Then, 20,000 cells were seeded in each well of the slide and cultured for 48 h. The cultured medium was replaced with medium containing HPMA-HA-DOX conjugates, the concentration was adjusted to 50 µg/ml of HA equivalent. Meanwhile, the HPMA-DOX conjugate with an equal amount of DOX drug to HPMA-HA-DOX was used as a control. Cells were cultured with the conjugates at various time intervals. Unbound conjugate was removed by washing the cell layer 3 × with DPBS. Cells were fixed with 3% paraformaldehyde for 10 min at rt and washed again with DPBS. The internalized HPMA-HA-DOX conjugate was visualized by fluorescence images obtained by confocal microscopy.

In the cell-surface binding experiment, cells were incubated with the HPMA-HA-DOX conjugate at 0 °C for 2 h (a condition under which no internalization occurs), followed by the DPBS washing and paraformaldehyde fixing described above. The cell surface binding conjugate was determined by the fluorescence images.

Fluorescence microscopy. Cells were examined using an inverted microscope (Nikon) and a Bio-Rad (Hercules, CA) MRC 1024 laser scanning confocal microscope. Cell images were collected by a x 60 oil immersion objective; no post-acquisition enhancement of images was performed. DOX fluorescence image acquisition was accumulated *via* the BHS block of filters (excitation 488 nm and emission through a 522 nm 32 bandpass filter). A coverslip was mounted on a

slide containing fixed cells with ProLong Antifade Kit (Molecular Probes, Eugene, OR) as the mounting medium. Fluorescence images were scaled to 256 gray levels.

RESULTS & DISCUSSION

Preparation of HA-DOX conjugates. The hydrazide method for the preparation of HA-ADH derivatives (31,68,76) allows attachment of reporter molecules, drugs, crosslinkers, and combinations of these moieties to HA (24,25). LMW HA was employed in this study for three reasons: (i) proton NMR allowed rapid quantification of the modification, (ii) LMW HA and its derivatives give injectable, non-viscous solution at concentrations up to 10 mg/ml, and (iii) LMW HA has a longer plasma half-life and is readily cleared by renal ultrafiltration. The LMW HA was prepared by partial degradation of high molecular weight HA (1.5 MDa) with testicular Hase (77) in pH 6.5 PBS buffer at 37 °C. The final size of LMW HA was characterized by GPC analysis: $M_n = 3,883$, $M_w = 11,199$, and molecular dispersity (DP) = 2.88. Next, HA-ADH with different ADH loadings were prepared by carbodiimide coupling chemistry (31,32), in which the extent of ADH modification was controlled through use of specific molar ratios of hydrazide, carboxylate equivalents, and carbodiimide. The purity and molecular size distribution of the HA-ADH were measured by GPC, and the substitution degree of ADH was determined by the ratio of methylene hydrogens to acetyl methyl protons, as measured by ^1H NMR (68). HA-ADH with ADH loadings of 9 mol% and 18 mol% were obtained and used in the preparation of the HA-DOX and HPMA-HA-DOX conjugates.

Furthermore, HA-DOX conjugates were synthesized by the conjugation of HA-ADH to DOX-NHS with an activated ester (NHS) group attached to DOX, to give a non-cleavable hydrazide linkage between the DOX drug and the HA polymer carrier. The HA-DOX conjugates were purified by gel filtration on a Sephadex G-25 column using PBS buffer as the eluent, following by dialysis against H₂O. The DOX loading was determined by the UV spectrum at $\lambda = 484$ nm. The DOX composition of the HA-DOX conjugates used in the *in vitro* cytotoxicity test were 2.3 wt% and 3.5 wt%, which were made from 9 mol% and 18 mol% ADH loading of HA-ADH, respectively.

Preparation of HPMA-HA-DOX conjugates. The cell-targeted delivery system was designed with HA on the side chain of the HPMA copolymer serving as a targeting moiety to the cancer cell-surface, and DOX linked to the polymer carrier through a lysosomal enzyme degradable peptide linkage (12). Thus, the designed conjugates will increase their specificity and selectivity against cancer cells by internalization through receptor-mediated endocytosis, release the free active DOX drug in the lysosomal compartment following the endocytosis, diffuse into nucleus through cytoplasm, and kill the cancer cells. HPMA-HA-DOX conjugates were synthesized by the conjugation of HA-ADH with HPMA-DOX copolymer containing an active ester (drug-polymer precursor, HPMA-(GFLG)-DOX-ONp). Two levels of modification by HA-ADH, 9 mol% and 18 mol%, were used in the conjugation. The HPMA-HA-DOX conjugates were purified by gel filtration on a Sephadex LH-20 column. HA loading was determined by mass balance, while the DOX loading was determined by the UV absorbance at $\lambda=484$ nm. HPMA-HA-DOX conjugates made from 18 mol% HA-ADH gave 36 wt% HA and 3.3 wt%

DOX with molecular weight of $M_w = 35,000$ and $M_n = 19,000$. HPMA-HA-DOX conjugates made from 9 mol% HA-ADH gave 17 wt% HA and 3.2 wt% DOX with molecular weight of $M_w = 18,000$ and $M_n = 14,000$.

Cytotoxicity assay of HA-DOX and HPMA-HA-DOX conjugates.

Free DOX drug, non-targeted HPMA-DOX and targeted HA-DOX, and HPMA-HA-DOX conjugates were assessed for their dose-dependent growth inhibitory effect on human breast cancer HBL-100 cells, human ovarian cancer SKOV-3 cells and human colon cancer HCT-116 cells. Each of these cell types has been reported to overexpress HA receptors on the tumor cell-surface. The non-cancerous mouse fibroblast cell-line NIH3T3 was used as a negative control. Cells were exposed to various DOX concentrations (DOX equivalent for polymer-drug conjugates) to determine the concentration necessary to inhibit the tumor cell growth by 50% relative to non-treated control cells (IC_{50} dose). Figure 4 illustrates dose-dependence of cell viability on the concentration of DOX equivalents covalently bound to the polymer conjugates. The IC_{50} doses for the free DOX drug and the conjugates are summarized in Table 1. From these results, it is evident that covalent attachment of DOX to a non-targeted polymer carrier (HPMA-DOX) markedly decreases the cytotoxicity of the parent drug. For SKOV-3 cells, the IC_{50} dose increases from $0.92 \mu M$ for free DOX drug to $58.2 \mu M$ for HPMA-DOX. These increases, in each the three cancer cell-lines tested, probably reflect the different mechanisms of cell uptake, e.g., free diffusion for free DOX drug vs. endocytosis for DOX-polymer conjugates, resulting in different intracellular drug concentration. Importantly, the targeted HPMA-HA-DOX conjugates that can enter cells by receptor-mediated endocytosis have dramatically lower IC_{50} values based on

equivalent amounts of the DOX drug. The IC_{50} values against HBL-100 cells were at doses of 0.52 μ M and 1.67 μ M for the targeted HPMA-HA-DOX conjugates with 36 wt% and 17 wt% HA loading, respectively, in comparison to 18.7 μ M for the non-targeted HPMA-DOX conjugate and 0.15 μ M for free DOX drug. The cytotoxicity of targeted HPMA-HA-DOX conjugates to cancer cells showed an order of magnitude greater potency relative to HPMA-DOX. Most likely, the receptor-mediated endocytosis contributed to the increase of the cytotoxicity of the targeted conjugates. Despite the increased cytotoxicity to cancer cells, the HPMA-DOX showed minimal toxicity to normal fibroblasts.

Interestingly, the cytotoxicity of the HA-DOX conjugates were even slightly lower than the non-targeted HPMA-DOX conjugate. The higher IC_{50} values against HBL-100 cells were 100 μ M and 75.5 μ M for HA-DOX conjugates, compared to 18.7 μ M for non-targeted HPMA-DOX conjugate, and 0.52 μ M for targeted HPMA-HA-DOX conjugate (36 wt%). The reduction in cytotoxicity is best explained by the poorly hydrolyzed hydrazide linkage between DOX and the HA polymer carrier. In earlier work, we showed that the cytotoxicity of HA-Taxol conjugates required an esterase-cleavable linkage between Taxol drug and HA polymer carrier, giving a comparable value to free Taxol drug in cell culture against HBL-100 cells (31). In the present example, the effectively non-cleavable linkage between DOX drug and HA carrier prevents the drug from exerting its effect, either by retarding entry to the nucleus or reducing intercalation, or both.

With a non-cancerous cell-line, a mouse-fibroblast NIH3T3 as the negative control, the IC_{50} values of the targeted conjugates, HA-DOX and HPMA-HA-DOX were significantly higher, indicating much lower cytotoxicity (Table 1). For example,

the IC_{50} value of HA-DOX (3.5 wt% DOX) against HBL-100 cells was a dose of 75.5 μ M, however, it was >883 μ M against NIH 3T3 cells; for HPMA-HA-DOX conjugates (36 wt% HA), the IC_{50} was 0.52 μ M against HBL-100 cells, but 21.2 μ M against NIH 3T3 cells. The decreased cytotoxicity of the targeted conjugates against non-cancerous cells was over an order of magnitude in comparison to cancer cells, which further support the role of receptor targeting in determining the selectivity of the HA conjugates against cancer cells. .

Cell binding and uptake of HPMA-HA-DOX conjugates. Several fluorescently-labeled HA derivatives have been prepared in order to study receptor-mediated cellular uptake. Previously, fluorescein-HA was employed to study HA uptake in a variety of systems, e.g., cells expressing CD44 variants (41,49,78-81), uptake by tumor cells for correlation with metastatic potential (67,82), internalization by chondrocytes (55), and as a measure of liver endothelial cell function (83). Most recently, RHAMM-mediated uptake and trafficking of HA by transformed fibroblasts (84) was observed with Texas Red-HA, and BODIPY-labeled HA was employed to distinguish HA uptake in cancer vs. untransformed cell-lines (31,32).

In order to correlate the receptor-mediated endocytosis of conjugates by cells with their cytotoxicity, the cell binding and uptake of the targeted HPMA-HA-DOX conjugates were followed by fluorescence microscopy using the intrinsic fluorescence of DOX. Cells were cultured in the presence of HPMA-HA-DOX conjugates of 50 μ g/ml HA equivalent for various time intervals, afterwards the amount of material internalized and bound to cell surface was visualized by confocal fluorescence microscopy.

SKOV-3 cells were chilled to 0 °C and then incubated with HPMA-HA-DOX for 2 h. After fixing and washing, a well-developed cluster of cells was chosen for the fluorescence microscope analysis. Cells were sectioned optically using confocal microscopy, fluorescence images were taken *via* the BHS block of filters of excitation 488 nm and emission 522 nm, along with the transmission images. Figure 5 provides a particularly dramatic illustration of the initial binding of the HPMA-HA-DOX conjugate on the SKOV-3 cells surface by the HA receptor CD44. The anchoring of the targeted HPMA-HA-DOX on the cell-surface prior to the cellular uptake through the a ligand-receptor complex followed by receptor-mediated endocytosis of the drug-containing macromolecular complex.

In addition, the internalization of polymer conjugates directly determined the cytotoxicity of conjugate system. Thus, with the intrinsic fluorescence of DOX, the cellular uptake of the targeted HPMA-HA-DOX conjugates could be directly observed by fluorescence microscopy. SKOV-3 cells were incubated with the HPMA-HA-DOX conjugates (36 wt% and 17 wt% HA loading) of 50 µg/ml HA equivalent for various time intervals, before the fluorescence images were taken. The non-targeted HPMA-DOX of an equal amount of DOX equivalent was used as a control. Confocal fluorescence images of HPMA-HA-DOX uptake by SKOV-3 cells were presented in Figure 6. Initially, the 2 h images of HPMA-HA-DOX polymer conjugates showed membrane localization. Over the course of 8 h, the HPMA-HA-DOX was gradually taken up into the cells; in 24 h, cells showed the polymer conjugates in most subcellular compartments. The uptake of HPMA-HA-DOX conjugate with 36 wt% HA loading was faster than the conjugate with 17 wt% HA loading; however, no significant difference was observed. In non-targeted

HPMA-DOX controls, the fluorescence uptake slowly increased with incubation time; however, very weak fluorescence (polymer conjugate) was observed even after 24 h incubation, in comparison to the targeted HPMA-HA-DOX system. The uptake of HPMA-HA-DOX into HBL-100 cells and HCT-116 cells occurred with a similar appearance and time course. These images provided a particularly dramatic illustration of the initial binding of the targeted HPMA-HA-DOX conjugates onto the tumor cell surface, following by rapid endocytosis *via* HA receptor-mediated pathways. HA, which has been incorporated into HPMA-DOX conjugates significantly increases the efficiency of the endocytosis process by cancer cells. The trafficking of cellular binding and uptake of HPMA-HA-DOX conjugates by confocal fluorescence images is consistent with the cytotoxicity results, and provided further support for the increased cytotoxicity of targeted HPMA-HA-DOX conjugates.

In summary, the data reported herein indicate that the cytotoxicity of targeted HPMA-HA-DOX polymer conjugates requires cellular uptake of the bioconjugate followed by the release of the active free DOX drug by the lysosomal enzymatic cleavage of the GFLG tetrapeptide spacer. Targeting of a variety of anti-cancer agents to tumor cells and tumor metastases could be achieved by receptor-mediated uptake of an HA containing-anti-cancer agent conjugate, followed by the intracellular release of the active drug and subsequent cell death. The ability to "seek and destroy" micrometastases is one of the most compelling and attractive potential outcomes for the HA containing-anti-tumor bioconjugates.

ACKNOWLEDGMENTS

Financial support for this work was provided by Department of Army (DAMD 17-9A-1-8254) and by the Huntsman Cancer Foundation at The University of Utah (UUtah). We are grateful to Joseph C. Shope and Dr. Daryll B. DeWald of Department of Biology of Utah State University for assistance with confocal microscopy. We thank Dr. L. Y.-W. Bourguignon of University of Miami Medical School for providing HBL-100 and SK-OV-3 cells. We are grateful to Clear Solutions Biotechnology, Inc. (Stony Brook, NY) for providing HA and the Center for Cell Signaling (UUtah) for access to its equipment and facilities.

Table 1. Cytotoxicity of free DOX drug, HA-DOX conjugates and HPMA-HA-DOX conjugates against cancer cells (HBL-100, SKOV-3 and HCT-116) and a fibroblast NIH 3T3 cells *in vitro* (n.t. = not tested).

Drugs	IC ₅₀ (μM) of DOX equivalent			
	HBL-100	SK-OV-3	HCT-116	NIH 3T3
DOX	0.15	0.92	0.35	>0.68
HA-DOX (2.3 wt% DOX)	100	157	140	n.t.
HA-DOX (3.5 wt% DOX)	75.5	141	62.0	>883
HPMA-DOX	18.7	58.2	56.6	>70
HPMA-HA-DOX (36 wt% HA)	0.52	9.2	4.32	21.2
HPMA-HA-DOX (17 wt% HA)	1.67	10.3	5.66	26.6

FIGURE LEGENDS

- Figure 1.** Tetrasaccharide fragment of HA showing the disaccharide units.
- Figure 2.** Synthesis of HA-DOX conjugates.
- Figure 3.** Structure of HPMA-HA-DOX conjugates.
- Figure 4.** *In vitro* cytotoxicity of HPMA-HA-DOX conjugates against HBL-100 human breast cancer cells, (Δ), free DOX drug; (\diamond), non-targeted HPMA-DOX conjugate; (O), targeted HPMA-HA-DOX conjugate (36 wt% HA); (), targeted HPMA-HA-DOX conjugate (17 wt% HA). Cell viability of HBL-100 cells as function of DOX equivalent concentration. The cytotoxicity of polymer conjugates (targeted and non-targeted) were determined using MTT assay.
- Figure 5.** Binding of targeted HPMA-HA-DOX conjugate (36 wt% HA) on human ovarian cancer SK-OV-3 cells surface, (a) transmission image, (b) fluorescence image (50 μ g/ml HA equivalent) of HPMA-HA-DOX incubated with cells at 0°C for 2hrs.
- Figure 6.** Time course of internalization of targeted HPMA-HA-DOX conjugates ((a) 36 wt% HA, (b) 17 wt% HA) on human ovarian cancer SK-OV-3 cells in comparison with non-targeted HPMA-

DOX conjugate (c). Cells were incubated with bioconjugates with 50 $\mu\text{g/ml}$ HA equivalent for 2, 8, and 24 hrs respectively.

REFERENCES

1. K. H. Kim, T. Hirano, and S. Ohashi Anticancer Polymeric Prodrugs, targetable. In *Polymeric Materials Encyclopedia*; J. C. Salamone, Ed.; CRC Press: Boca Raton, FL, 1996; pp 272-285.
2. A. Trouet, M. Masquelier, R. Baurain, and D. D. Campeneere. A covalent linkage between daunorubicin and proteins that is stable in serum and reversible by lysosomal hydrolases, as required for a lysosomotropic drug-carrier conjugate: *in vitro* and *in vivo* studies. *Proc. Natl. Acad. Sci. USA* **79**, 626-629 (1982).
3. S. Kim. Liposomes as carriers of cancer chemotherapy. *Drugs* **46**, 618-638 (1993).
4. R. Arshady. Albumin microspheres and microcapsules: methodology of manufacturing techniques. *J. Controlled Release* **14**, 111-131 (1990).
5. J. Kreuter. Nanoparticle-based drug delivery systems. *J. Controlled Release* **16**, 169-176 (1991).
6. P. G. Waser, J. Kreuter, S. Berger, K. Munz, E. Kaiser, and B. Pfluger. Localization of colloidal particles (liposomes, hexylcyanoacrylate nanoparticles and albumin nanoparticles) by histology and autoradiography in mice. *Int. J. Pharm.* **39**, 213-227 (1987).
7. S. A. Cartlidge, R. Duncan, J. B. Lloyd, R. P. Kopeckova, and J. Kopecek. Soluble, crosslinked *N*-(2-hydroxypropyl) methacrylamide copolymers as potential drug carrier 3. Targeting by incorporation of galactosamine residue. Effect of route of administration. *J. Controlled Release* **4**, 265-278 (1987).
8. L. Molteni Dextran as drug carriers. In *Drugs Carriers in Biology and Medicine*; G. Gregoriadis, Ed.; Academic: London, 1979; pp 107.

9. L. Molteni Lectins as drug carriers. In *Drugs Carriers in Biology and Medicine*; G. Gregoriadis, Ed.; Academic Press: London, 1979; pp 43.
10. R. B. Greenwald, C. W. Gilbert, A. Pendri, C. D. Conover, J. Xia, and A. Martinez. Drug delivery systems: water soluble taxol 2'-poly(ethylene glycol) ester prodrugs -- design and *in vivo* effectiveness. *J. Med. Chem.* **39**, 424-431 (1996).
11. H. Maeda, L. W. Seymour, and Y. Miyamoto. Conjugates of anticancer agents and polymers: advantages of macromolecular therapeutics *in vivo*. *Bioconjugate Chem.* **3**, 351-362 (1992).
12. T. Minko, P. Kopeckova, V. Pozharov, and J. Kopecek. HPMa copolymer bound adriamycin overcomes MDR1 gene encoded resistance in a human ovarian carcinoma cell line. *J. Controlled Release* **54**, 223-233 (1998).
13. T. Hirano, S. Ohashi, S. Morimoto, and K. Tsuda. Synthesis of antitumor-active conjugates of adriamycin or daunomycin with the copolymer of divinyl ether and maleic anhydride. *Makromol. Chem.* **187**, 2815-2824 (1986).
14. H. Maeda, M. Ueda, T. Morinaga, and T. Matsumoto. Conjugation of poly(styrene-co-maleic acid) derivatives to the antitumor protein neocarzinostatin: pronounced improvements in pharmacological properties. *J. Med. Chem.* **28**, 455-461 (1985).
15. P. A. e. a. Vasey. Phase I clinical and pharmacokinetics study of PK1 [N-(2-hydroxypropyl)methacrylamide copolymer doxorubicin]: first member of a new class of chemotherapeutic agents-drug-polymer conjugates. *Clin. Cancer Res.* **5**, 83-94 (1999).

16. V. R. Ciaolfa, M. Zamai, A. Fiorino, E. Frigerio, R. d'Argy, A. Ghiglieri, M. Farao, F. Angelucci, and A. Suarato In *Ninth international symposium on recent advances in drug delivery systems*; Salt lake City, Utah, USA, 1999; pp 46.
17. V. R. Ciaolfa, M. Zamai, A. Fiorino, E. Frigerio, C. Pellizzoni, R. d'Argy, A. Ghiglieri, M. G. Castelli, M. Farao, M. Pesenti, F. Gigli, F. Angelucci, and A. Suarato. Polymer-bound camptothecin: initial biodistribution and antitumor activity studies. *J. Controlled Release* **65**, 105-119 (2000).
18. L. W. Seymour, D. R. Ferry, C. Boivin, P. Julyan, J. Doran, M. David, D. Anderson, C. Christodoulou, A. M. Young, D. J. Kerr, and S. Hesslewood In *Eighth international symposium on recent advances in drug delivery systems*; Salt lake City, Utah, USA, 1997; pp 132-135.
19. Z.-R. Lu, P. Kopecekova, and J. Kopecek. Polymerizable Fab' antibody fragments for targeting of anticancer drugs. *Nature Biotechnology* **17**, 1101-1104 (1999).
20. T. C. Laurent, U. B. G. Laurent, and J. R. E. Fraser. Functions of hyaluronan. *Ann. Rheum. Dis.* **54**, 429-432 (1995).
21. G. D. Prestwich. Biomaterials from Chemically-Modified Hyaluronan. *Glycoforum* <http://glycoforum.gr.jp> (2001).
22. Y. Luo, K. R. Kirker, and G. D. Prestwich. Cross-linked hyaluronan hydrogel films: new biomaterials for drug delivery. *J. Controlled Release* **69**, 169-184 (2000).
23. K. P. Vercruysse, and G. D. Prestwich. Hyaluronate derivatives in drug delivery. *Crit. Rev. Ther. Drug Carr. Syst.* **15**, 513-555 (1998).

24. G. D. Prestwich, D. M. Marecak, J. F. Marecek, K. P. Vercruysse, and M. R. Ziebell Chemical modification of hyaluronan for drug delivery, biomaterials, and biochemical probes. In *The Chemistry, Biology, and Medical Applications of Hyaluronan and its Derivatives*; T.C. Laurent, Ed.; Portland Press: London, 1998; pp 43-65.
25. G. D. Prestwich, Y. Luo, M. R. Ziebell, K. P. Vercruysse, K. R. Kirker, and J. S. MacMaster Chemically-modified hyaluronan: New biomaterials and probes for cell biology. In *New Frontiers in Medical Sciences: Redefining Hyaluronan*; G. Abatangelo, Ed.; Portland Press: London, 2000; pp 181-194.
26. L. E. Freed, G. Vunjak-Novakovic, R. J. Biron, D. B. Eagles, D. C. Lesnoy, S. K. Barlow, and R. Langer. Biodegradable polymer scaffolds for tissue engineering. *Bio/Technology* **12**, 689-693 (1994).
27. C. A. S. Alam, M. P. Seed, and D. A. Willoughby. Angiostasis and vascular regression in chronic granulomatous inflammation induced by diclofenac in combination with hyaluronan in mice. *J. Pharm. Pharmacol.* **47**, 407-411 (1995).
28. R. E. Falk In *PCT Int. Appl. WO 9740841*; 1997; pp.
29. J. Ziegler. Hyaluronan seeps into cancer treatment trials. *J. Nat. Cancer Inst.* **88**, 397-399 (1996).
30. K. Akima, H. Ito, Y. Iwata, K. Matsuo, N. Watari, M. Yanagi, H. Hagi, K. Oshima, A. Yagita, Y. Atomi, and I. Tatekawa. Evaluation of antitumor activities of hyaluronate binding antitumor drugs: synthesis, characterization and antitumor activity. *J. Drug Targeting* **4**, 1 (1996).
31. Y. Luo, and G. D. Prestwich. Synthesis and selective cytotoxicity of a hyaluronan-antitumor bioconjugate. *Bioconjugate Chem.* **10**, 755-763 (1999).

32. Y. Luo, M. R. Ziebell, and G. D. Prestwich. A hyaluronan-taxol antitumor bioconjugate targeted to cancer cells. *Biomacromolecules* **1**, 208-218 (2000).
33. E. A. Turley, A. J. Belch, S. Poppema, and L. M. Pilarski. Expression and function of a receptor for hyaluronan-mediated motility on normal and malignant lymphocytes-B. *Blood* **81**, 446-453 (1993).
34. B. P. Toole. Hyaluronan in morphogenesis. *J. Intern. Med.* **242**, 35-40 (1997).
35. Z. Rudzki, and S. Jothy. CD44 and the adhesion of neoplastic cells. *J. Clin. Pathol. Mol. Pathol.* **50**, 57-71 (1997).
36. J. Lesley, R. Hyman, N. English, J. B. Catterall, and G. A. Turner. CD44 in inflammation and metastasis. *Glycoconjugate J.* **14**, 611-622 (1997).
37. L. Collis, C. Hall, L. Lange, M. Ziebell, R. Prestwich, and E. A. Turley. Rapid hyaluronan uptake is associated with enhanced motility: implications for an intracellular mode of action. *Febs Lett* **440**, 444-449 (1998).
38. W. F. Cheung, T. F. Cruz, and E. A. Turley. Receptor for hyaluronan-mediated motility (RHAMM), a hyaladherin that regulates cell responses to growth factors. *Biochem Soc Trans* **27**, 135-142 (1999).
39. L. Huang, N. Grammatikakis, M. Yoneda, S. D. Banerjee, and B. P. Toole. Molecular characterization of a novel intracellular hyaluronan-binding protein. *J Biol Chem* **275**, 29829-29839 (2000).
40. B. P. Toole. Hyaluronan is not just a goo! *J Clin Invest* **106**, 335-336 (2000).
41. A. J. Day. The structure and regulation of hyaluronan-binding proteins. *Biochem. Soc. Trans.* **27**, 115-121 (1999).

42. R. M. Peterson, Q. Yu, I. Stamenkovic, and B. P. Toole. Perturbation of hyaluronan interactions by soluble CD44 inhibits growth of murine mammary carcinoma cells in ascites. *Amer J Pathol* **156**, 2159-2167 (2000).
43. C. Underhill. CD44 - The Hyaluronan Receptor. *J. Cell Sci.* **103**, 293-298 (1992).
44. E. A. Turley The role of a cell-associated hyaluronan binding protein in fibroblast behavior. In *The Biology of Hyaluronan*; C. Foundation, Ed.; J. Wiley & Sons, Ltd.: Chichester, UK, 1989; pp 121-137.
45. C. B. Knudson, and W. Knudson. Hyaluronan-Binding proteins in development, tissue homeostasis, and disease. *FASEB J* **7**, 1233-1241 (1993).
46. J. Entwistle, C. L. Hall, and E. A. Turley. Hyaluronan receptors: regulators of signalling to the cytoskeleton. *J. Cell Biochem.* **61**, 569-577 (1996).
47. C. X. Zeng, B. P. Toole, S. D. Kinney, J. W. Kuo, and I. Stamenkovic. Inhibition of tumor growth in vivo by hyaluronan oligomers. *Int J Cancer* **77**, 396-401 (1998).
48. J. D. Kahmann, R. OBrien, J. M. Werner, D. Heinegard, J. E. Ladbury, I. D. Campbell, and A. J. Day. Localization and characterization of the hyaluronan-binding site on the Link module from human TSG-6. *Structure Fold Des* **8**, 763-774 (2000).
49. T. K. Yeo, J. A. Nagy, K. T. Yeo, H. F. Dvorak, and B. P. Toole. Increased hyaluronan at sites of attachment to mesentery by CD44-positive mouse ovarian and breast tumor cells. *Am. J. Pathol.* **148**, 1733-1740 (1996).
50. V. B. Lokeshwar, C. Obek, H. T. Pham, D. Wei, M. J. Young, R. C. Duncan, M. S. Soloway, and N. L. Block. Urinary hyaluronan and hyaluronidase:

- Markers for bladder cancer detection and evaluation of grade. *J Urol* **163**, 348-356 (2000).
51. W. Knudson. Tumor-associated hyaluronan: providing an extracellular matrix that facilitates invasion. *Am. J. Pathol.* **148**, 1721-1726 (1996).
 52. C. L. Hall, B. H. Yang, X. W. Yang, S. W. Zhang, M. Turley, S. Samuel, L. A. Lange, C. Wang, G. D. Curpen, R. C. Savani, A. H. Greenberg, and E. A. Turley. Overexpression of the hyaluronan receptor RHAMM is transforming and is also required for H-ras transformation. *Cell* **82**, 19-28 (1995).
 53. R. M. Nelson, A. Venot, M. P. Bevilacqua, R. J. Linhardt, and I. Stamenkovic. Carbohydrate-protein interactions in vascular biology. *Annu. Rev. Cell Dev. Biol.* **11**, 601-631 (1995).
 54. P. Rooney, S. Kumar, J. Ponting, and M. Wang. The role of hyaluronan in tumour neovascularization (review). *Int. J. Cancer* **60**, 632-636 (1995).
 55. Q. Hua, C. B. Knudson, and W. Knudson. Internalization of hyaluronan by chondrocytes occurs via Receptor-Mediated endocytosis. *J. Cell Sci.* **106**, 365-375 (1993).
 56. N. Iida, and L. Y.-W. Bourguignon. Coexpression of CD44 variant (v10/ex14) and CD44S in human mammary epithelial cells promotes tumorigenesis. *J. Cell. Physiol.* **171**, 152-160 (1997).
 57. G. Egger, R. Pfragner, V. Siegl, K. Zatloukal, A. Glasner, A. Bader, and P. Steindorfer. The affinity of MCF7 breast cancer cells to hyaluronan substrates of different molecular weight and concentrations in an <IT>in vitro</IT> model. *Int J Oncol* **17**, 1019-1023 (2000).

58. L. Y. W. Bourguignon, H. B. Zhu, L. J. Shao, and Y. W. Chen. CD44 interaction with Tiam1 promotes Rac1 signaling and hyaluronan-mediated breast tumor cell migration. *J Biol Chem* **275**, 1829-1838 (2000).
59. J. A. Foekens, P. Dall, J. G. M. Klijn, P. SkrochAngel, C. J. C. Claassen, M. P. Look, H. Ponta, W. L. J. VanPutten, P. Herrlich, and S. C. HenzenLogmans. Prognostic value of CD44 variant expression in primary breast cancer. *Int J Cancer* **84**, 209-215 (1999).
60. L. Y.-W. Bourguignon, H. B. Zhu, A. Chu, N. Iida, L. Zhang, and M. C. Hung. Interaction between the adhesion receptor, CD44, and the oncogene product, p185(HER2), promotes human ovarian tumor cell activation. *J. Biol. Chem.* **272**, 27913-27918 (1997).
61. J. B. Catterall, L. M. H. Jones, and G. A. Turner. Membrane protein glycosylation and CD44 content in the adhesion of human ovarian cancer cells to hyaluronan. *Clin Exp Metastas* **17**, 583-591 (1999).
62. Y. Yamada, N. Itano, H. Narimatsu, T. Kudo, S. Hirohashi, A. Ochiai, A. Niimi, M. Ueda, and K. Kimata. Receptor for hyaluronan-mediated motility and CD44 expressions in colon cancer assessed by quantitative analysis using real-time reverse transcriptase-polymerase chain reaction. *Jpn J Cancer Res* **90**, 987-992 (1999).
63. Y. Matsubara, S. Katoh, H. Taniguchi, M. Oka, J. Kadota, and S. Kohno. Expression of CD44 variants in lung cancer and its relationship to hyaluronan binding. *J Int Med Res* **28**, 78-90 (2000).

64. H. Li, L. Guo, J. W. Li, N. Liu, R. Qi, and J. Liu. Expression of hyaluronan receptors CD44 and RHAMM in stomach cancers: relevance with tumor progression. *Int J Oncol* **17**, 927-932 (2000).
65. A. Yokota, G. Ishii, Y. Sugaya, M. Nishimura, Y. Saito, and K. Harigaya. Potential use of serum CD44 as an indicator of tumour progression in acute leukemia. *Hematol Oncol* **17**, 161-168 (1999).
66. M. Culty, H. A. Nguyen, and C. B. Underhill. The hyaluronan receptor (CD44) participates in the uptake and degradation of hyaluronan. *J. Cell Biol.* **116**, 1055-1062 (1992).
67. M. Culty, M. Shizari, E. W. Thompson, and C. B. Underhill. Binding and degradation of hyaluronan by human breast cancer cell lines expressing different forms of CD44: correlation with invasive potential. *J. Cell. Physiol.* **160**, 275-286 (1994).
68. T. Pouyani, and G. D. Prestwich. Functionalized derivatives of hyaluronan oligosaccharides - drug carriers and novel biomaterials. *Bioconjugate Chem.* **5**, 339-347 (1994).
69. L. B. Shih, D. M. Goldenberg, H. Xuan, H. Lu, R. M. Sharkey, and T. C. Hall. Anthracycline Immunoconjugates prepared by a site-specific linkage via an amino-dextran intermediate carrier. *Cancer Res.* **51**, 4192-4198 (1991).
70. H. Ogura, S. Nagai, and K. Takeda. A novel reagent (N-succinimidyl diphenylphosphate) for synthesis of active ester and peptide. *Tetrahedron Lett.* **21**, 1467-1468 (1980).
71. J. Kopecek, P. Rejmanova, J. Strohalm, K. Ulbrich, B. Rihova, V. Chytrý, J. B. Lloyd, and R. Duncan In *U.S. Patent*, USA, 1991; pp.

72. V. G. Omelyanenko, P. Kopecekova, C. Gentry, J.-G. Shiah, and J. Kopecek. HPMa copolymer-anticancer drug-OV-TL16 antibody conjugates. 1. Influence of the methods of synthesis on the binding affinity to OVCAR-3 ovarian carcinoma cells in vitro. *J. Drug Target.* **3**, 357-373 (1996).
73. D. Puttnam, and J. Kopecek. Polymer conjugates with anticancer activity. *Adv. Polym. Sci.* **122**, 55-123 (1995).
74. P. Rejmanova, J. Labsky, and J. Kopecek. Aminolyses of monomeric and polymeric p-nitrophenyl esters of methacryloylated amino acids. *Makromol. Chem.* **178**, 2159-2168 (1977).
75. J. M. Kokoshka, C. M. Ireland, and L. R. Barrows. Cell-based screen for identification of inhibitors of tubulin polymerization. *J. Nat. Prod.* **59**, 1179-1182 (1996).
76. T. Pouyani, and G. D. Prestwich In *US Patent 5,616,568*; Research Foundation of SUNY: USA, 1997; pp.
77. G. Kreil. Hyaluronidases - a group of neglected enzymes. *Protein Sci.* **4**, 1666-1669 (1995).
78. G. Chow, C. B. Knudson, G. Homandberg, and W. Knudson. Increased expression of CD44 in bovine articular chondrocytes by catabolic cellular mediators. *J. Biol. Chem.* **270**, 27734-27741 (1995).
79. J. Lesley, and R. Hyman. CD44 can be activated to function as an hyaluronan receptor in normal murine T-cells. *Eur. J. Immunol.* **22**, 2719-2723 (1992).

80. J. Lesley, N. English, A. Perschl, J. Gregoroff, and R. Hyman. Variant cell lines selected for alterations in the function of the hyaluronan receptor CD44 show differences in glycosylation. *J. Exp. Med.* **182**, 431-437 (1995).
81. A. Perschl, J. Lesley, N. English, I. Trowbridge, and R. Hyman. Role of CD44 cytoplasmic domain in hyaluronan binding. *Eur. J. Immunol.* **25**, 495-501 (1995).
82. T. Asplund, and P. Heldin. Hyaluronan receptors are expressed on human malignant mesothelioma cells but not on normal mesothelial cells. *Cancer Res.* **54**, 4516-4523 (1994).
83. H. Nakabayashi, H. Tsujii, Y. Okamoto, and H. Nakano. Fluorescence-labeled-hyaluronan loading test as an index of hepatic sinusoidal endothelial cell function in the rat. *Int. Hepatol. Commun.* **5**, 345-353 (1996).
84. L. Collis, C. Hall, L. Lange, M. Ziebell, G. Prestwich, and E. Turley. Rapid hyaluronan uptake is associated with enhanced motility: implications for an intracellular mode of action. *FEBS Lett.* **440**, 444-449 (1998).

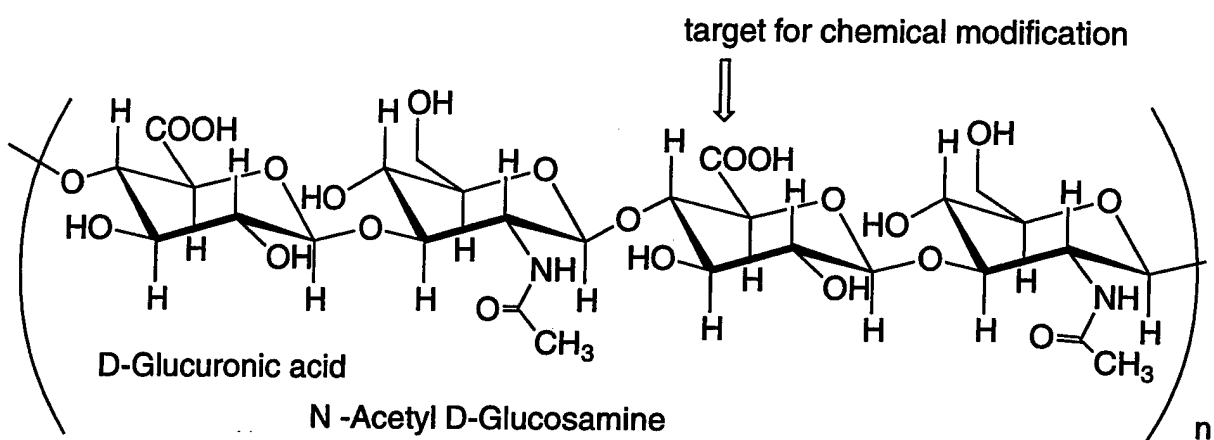


Fig 1

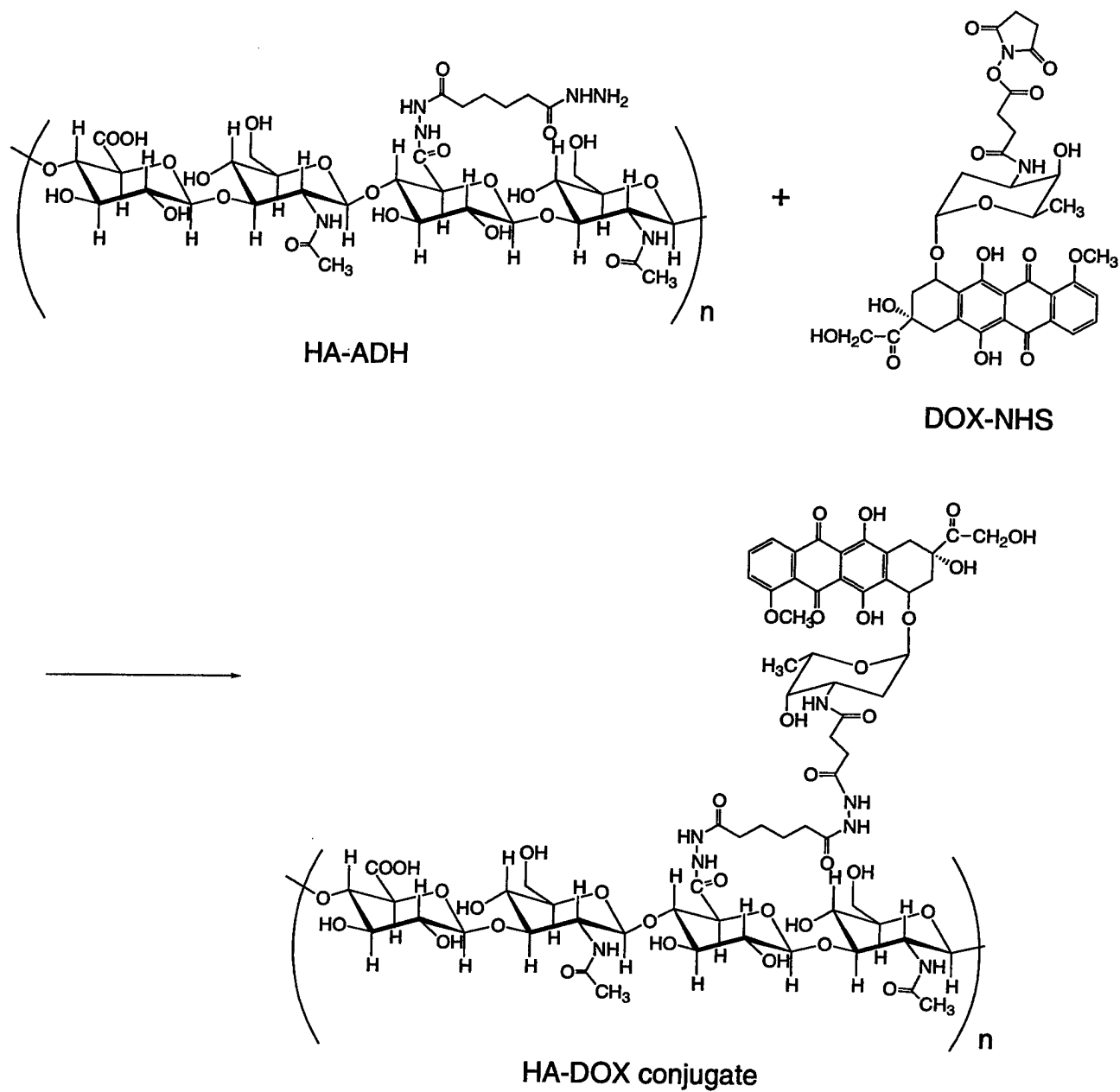


Fig 2

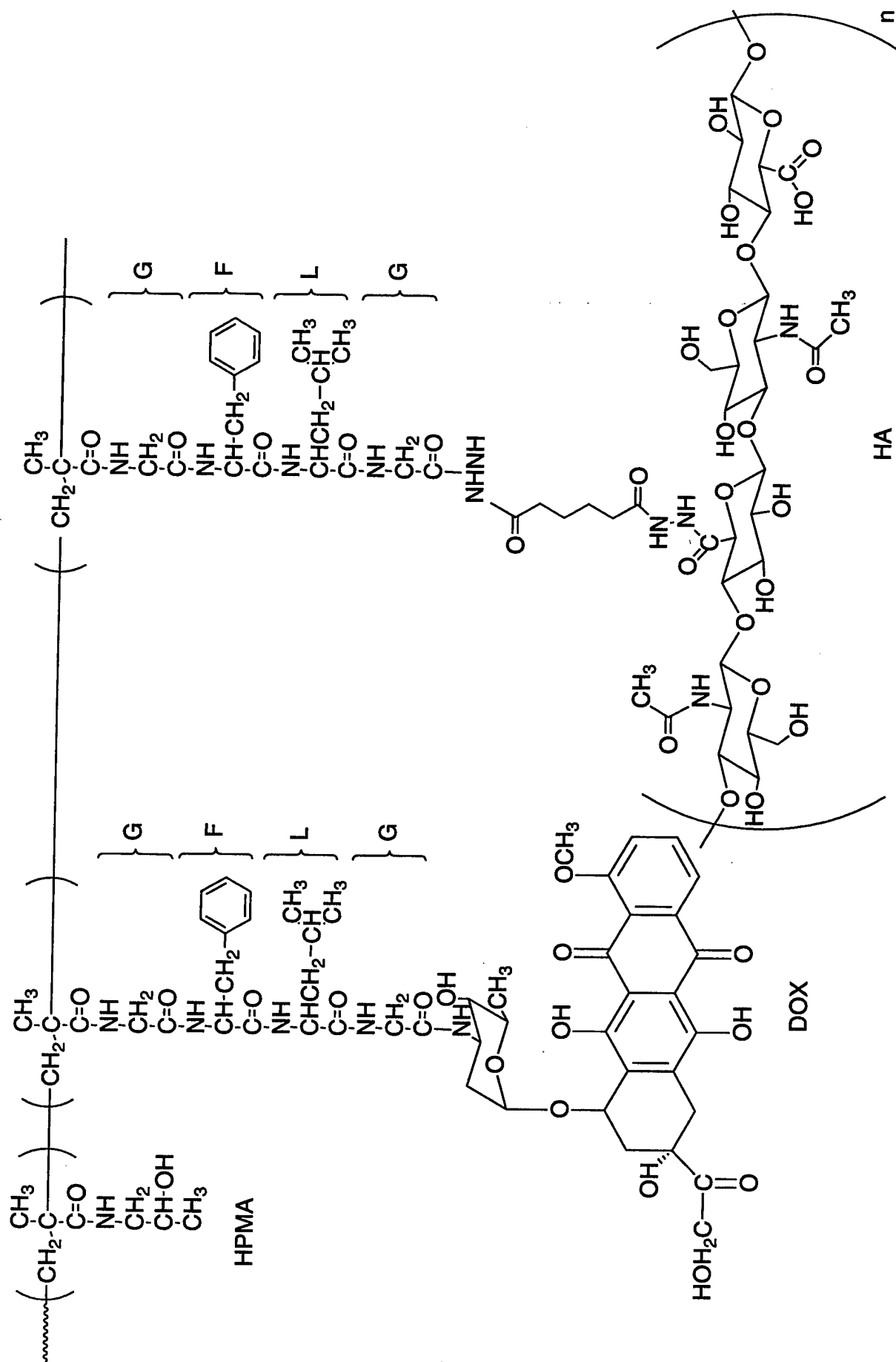


Fig 3

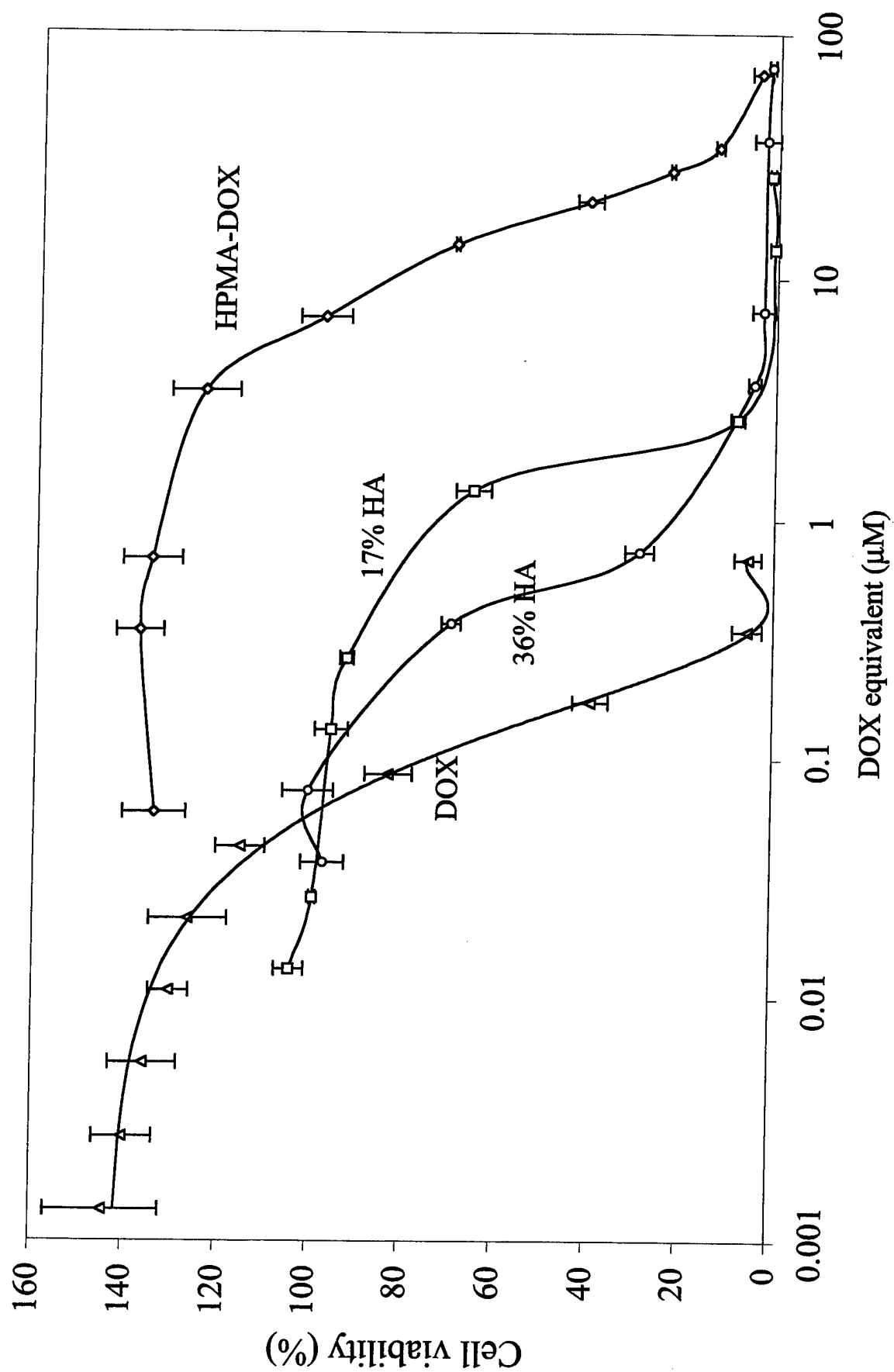


Fig 4

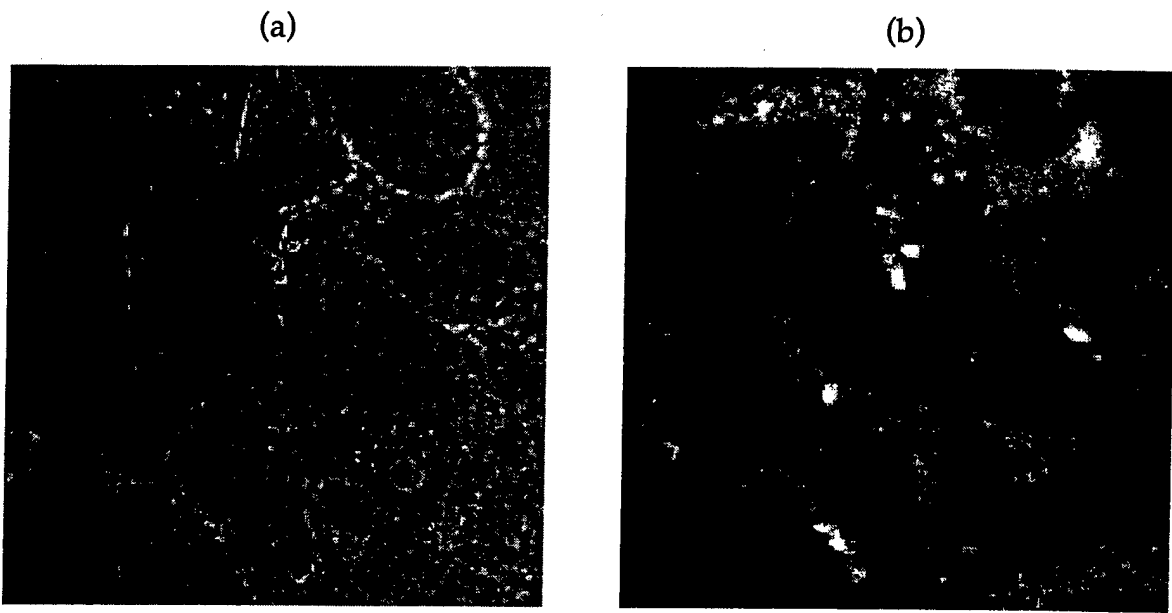
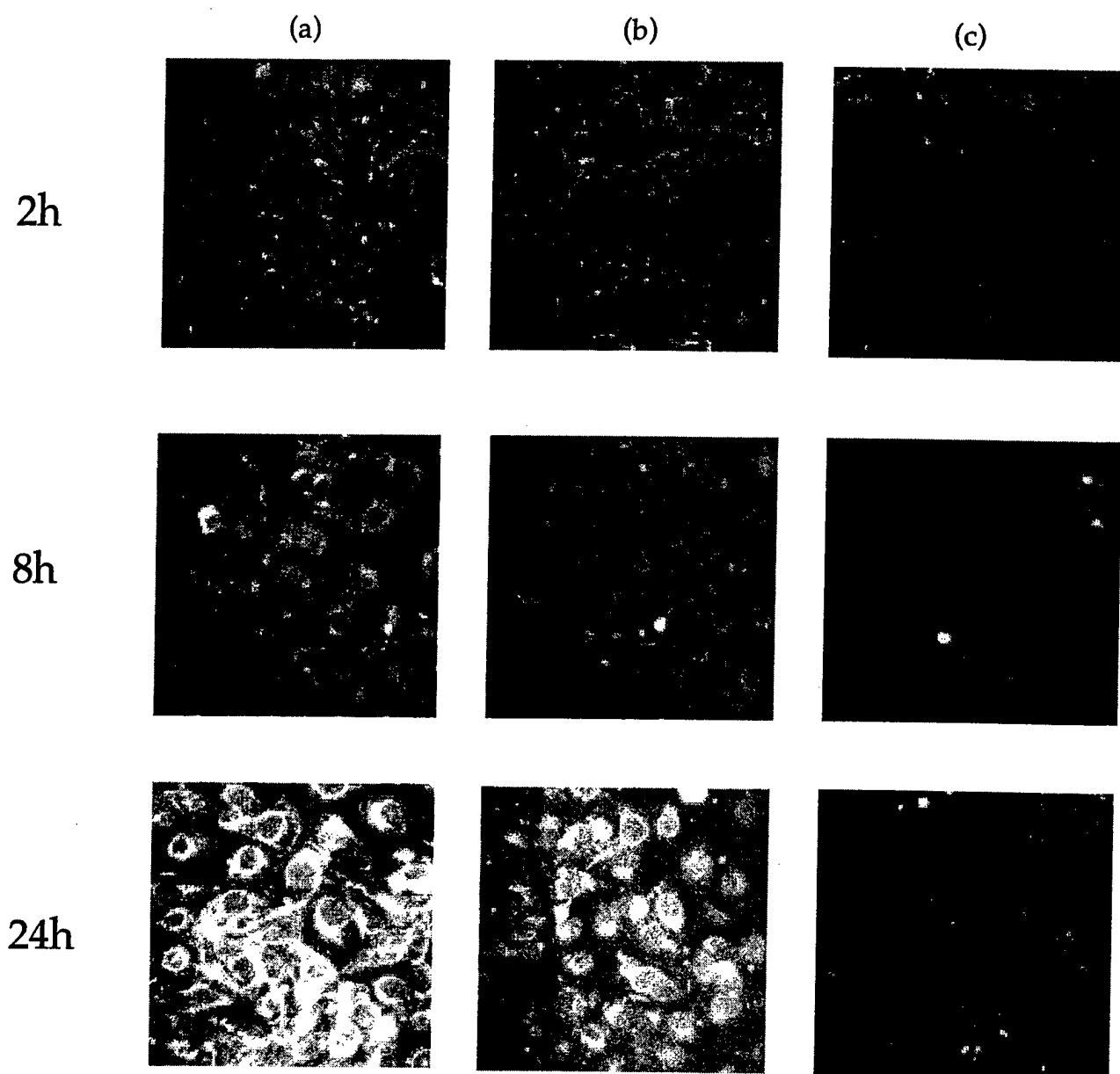


Fig 5



Intracellular RHAMM is an erk1 Binding Protein and Removal of its N-Terminal Sequence is Required for Activation of erk1

SHIWEN ZHANG,¹ M. ZIEBELL,² WING-FAI CHEUNG,³ JIE LU,¹
ABRAHAM HADDAD,¹ DAVID LITCHFIELD,⁴ NATALIE G. AHN,⁵ TONY T. CRUZ,³
GLENN D. PRESTWICH,² AND EVA A. TURLEY^{1*}

¹*Division of Cardiovascular Research, The Hospital for Sick Children, and the Departments of Anatomy/Cell Biology, Laboratory Medicine and Pathology, University of Toronto, Toronto, ON M5G 1X8; [*²*University of Utah, Department of Medicinal Chemistry, Salt Lake City, UT 84112-5820;* ³*Samuel Lunenfeld Research Institute, Mount Sinai Hospital, Toronto, ON M5G 1X5,*

⁴*Department of Biochemistry, University of Western Ontario, London, ON N6A 5C1;*

⁵*Department of Chemistry and Biochemistry, University of Colorado, Boulder, CO 80309-0215*

*Corresponding author. The Hospital for Sick Children, Div'n of Cardiovascular Research,
555 University Avenue, Toronto, ON Canada M5G 1X8
Telephone: (416) 813 5918. FAX: (416) 813 7480. e-mail: eturley@sickkids.on.ca

Running title: RHAMM binds to erk1

ABSTRACT

Several molecular weight forms of intracellular RHAMM have been reported to be expressed, a common 95 kDa protein (termed v5) and lesser amounts of 60-73 kDa forms. The latter represent N-terminal truncations of the 95 kDa protein. We show here that ras transformed fibroblasts express 95 and 73 kDa RHAMM forms. The 73 kDa protein corresponds to a RHAMM isoform termed v4, that has previously been shown to be transforming when overexpressed, to co-immunoprecipitate with erk 1 and to be required for activation of erk through ras. *In vitro* binding and competition analyses, as well as *in vivo* analyses of mutant proteins show that both v4 and v5 RHAMM proteins bind directly to erk 1 by two non-contiguous sequences near their COOH-terminus. Both RHAMM proteins associate with MEK1 *in vivo* but do not bind directly to this kinase. This association requires the presence of 20 amino acids present in both proteins and previously shown to be required for the transforming function of RHAMMv4. Overexpression of a cDNA, representing v4, activates erk 1, activates AP-1, enhances expression and release of MMP-9, and transforms fibroblasts. Furthermore, v4 synergizes with mutant active MEK1 to promote activation of erk1 and to strongly enhance transformation of fibroblasts. Deletion of the erk1 binding domains or the domain required for association of MEK1 block the ability of v4 to synergize with mutant active MEK1 and to enhance the expression and release of MMP-9. In contrast, overexpression of v5, which contains additional 163 N terminal amino acids not present in v4, does not affect erk activity and does not transform fibroblasts. Further, v5 only weakly synergizes with mutant active MEK1 to promote activation of erk, and does not enhance the transforming function of the mutant active kinase. These results indicate that intracellular RHAMM forms are erk1 binding proteins that regulate the activation of erk1 at the level of erk1/MEK1 interactions. V5, which is the most common form of intracellular RHAMM, is negatively regulated in this function by its unique N-terminal sequence, while the shorter forms of RHAMM, such as v4, appear to be biologically active. Possible physiological roles for active RHAMM forms are discussed.

Key words: RHAMM, erk1, MEK1, MMP-9, cell transformation

INTRODUCTION

Activating mutations or overexpression of the small GTPase ras are amongst the most common events in human tumors (50). Ras regulates multiple signaling pathways, many of which can lead to tumorigenesis when constitutively activated (5,19,53). Recently, studies using transgenic animal models suggest that amplification of ras and constitutive activation of the erk kinase cascade is a late event associated with tumor progression (23,33,44) consistent with many studies showing activation of this map kinase cascade is required for cell motility, tumor invasion (16,21,22,48,56), the production of several classes of proteases involved in cell motility/invasion (20) and with an ability of transformed cells to metastasize (20,23,53). Delineating the molecular mechanisms controlling erk activation will therefore be highly relevant to understanding the nature of tumor invasion and metastasis.

Identification of yeast Ste-5, a scaffold protein that complexes a map kinase cascade (7,27,38), first suggested that accessory proteins may play key roles in the regulation and compartmentalization of map kinase cascades, a phenomenon that had previously been noted for other signaling cascades (35). The recent identification of a mammalian map kinase accessory protein, MP-1, that enhances activation and association of MEK1 with erk1 (42), as well as of Jip-1 (55), a scaffold protein linking components of the jnk map kinase cascade, and IkAP, a scaffold protein of the Ikappa B lamin complex (8), predict that diverse accessory proteins regulate activation, insulation and targeting of map kinase cascades.

We previously identified a hyaluronan binding protein, RHAMM, as a regulator of ras-controlled cell motility and proliferation (14). This protein occurs both on the cell surface (9,12,14,36,60), despite an apparent lack of signal sequence and transmembrane domain, and intracellularly (3,9,14,17,51). Antibody/peptide mimetic blocking and use of intracellular dominant negative RHAMM mutants, suggest a functional role for both cell surface and intracellular forms of RHAMM in ras-regulated pathways, in particular the erk 1 kinase cascade (9,12,14,36,52,60). We (51) and others (3,17) have noted that the most common murine RHAMM RNA transcript encodes a 95 kDa protein. We have also reported a rare RHAMM

mRNA transcript (v4) that encodes a 73 kDa protein, which lacks 163 N-terminal amino acids found in the longer RHAMM form (10). This shortened RHAMM form associates with erk 1 *in vivo*, is transforming when overexpressed and regulates activation of the erk kinase cascade through ras as determined by use of dominant negative v4 mutants and overexpression of v4 (14,60). Although others (17,24,28) have also noted the presence of both the 95 kDa and 73 kDa proteins in cultured cells, the functional significance of these two RHAMM forms has not previously been determined.

Here, we demonstrate that ras-transformed fibroblasts express both the 95 kDa (termed RHAMMv5) and 73 kDa (termed RHAMMv4) (10) proteins. We note that the v5 mRNA transcript is highly expressed in these cells but a minor v4 transcript, detectable by RT-PCR, is expressed early after cell plating. We confirm that this transcript represents a full length RHAMM mRNA corresponding to the 73 kDa RHAMM protein. Both the v4 and v5 RHAMM proteins directly bind to erk1 and indirectly associate with MEK1. Evidence is presented that the RHAMMv4 protein represents an activated form, resulting from lack of an inhibitory N-terminal domain unique to the longer v5 protein. Thus, only RHAMMv4 is able to activate erk 1, enhance MMP-9 expression and transform fibroblasts. These properties of RHAMMv4 require its erk 1 binding domains and a domain that mediates an indirect association with MEK1. V4 appears to act by enhancing the ability of MEK1 to activate erk1.

MATERIALS AND METHODS

Cell Lines and Cell Culture. The cell lines used were derived from parental murine 10T1/2 or NIH3T3 mutant active fibroblasts. H-*ras*-transfected 10T1/2, CIRAS-3 (C3), RHAMMv4 transfected, RHAMMv5 transfected, 10T1/2 cells expressing RHAMM anti-sense (U21 cells) and parental 10T1/2 cells were grown as described (14). Briefly, cells were maintained at 37°F in 5% CO₂ in DMEM growth medium (GIBCO, Gaithersburg, MD) supplemented with 10% fetal calf serum (Invitrogen). Cells were grown to 70-80% confluence prior to passage. Cell cultures used for analysis were always plated at 50% confluence.

Plasmid Constructs and Protein Purification. For transfection, the RHAMMv4 and v5 cDNA and mutant forms of RHAMM were subcloned into the expression vector ph β Apr-1-neo as described (14,60). A mutant active MEK1(Δ N3/S218E/S222D) construct was obtained from N. Ahn (Howard Hughes Institute, University of Colorado, Boulder, CO). For transient co-transfection of RHAMMv4 dominant negative with erk1, RHAMMv4 cDNA hyaluronan binding domains were mutated as described (14) and a triple HA tag was placed close to the C-terminus of RHAMMv4 as described (60). A myc-tagged RHAMMv5 was constructed by PCR using primers, 5'-GCCCTCGAGTTGTTGTCTGA GTTGATTTTTC-3' and 5'-GCCCTC GAGCAGAAGCTAATAAGCGAAGAAGACCTCAAC GATGGAAGACTTTAGGAAGCAG. The myc tag sequence (underlined) was inserted between RHAMM #631 and #632 amino acids. Myc-tagged RHAMMv5 cDNA was subcloned into pCDNA3.1 (Invitrogen) with an EcoR I site. A myc-tagged erk1 was generated by polymerase chain reaction using the 5' primer GCGGGATCCATGGGCGGGGGCGGGGAGCCCAGG and a 3' primer containing myc tag sequence (underlined) ACGGAATTCGTTTAGGTCCTCTTCGCTGATTAGCTTTTGTTCATGGC CCCTG GCTGGAAGCGGGCTGT. The resulting cDNA was subcloned into expression vector, pCDNA3.1 (Invitrogen) and sequenced.

For recombinant protein purification, the cDNAs of ERK1 and MEK1 were subcloned into the pQE-30 vector (Qiagen). His6-tagged erk1 and MEK1 were expressed and purified on Ni₂ ±NTA agarose and MonoQ (26). To construct fusion protein expression vectors, RHAMMv4 cDNA and mutant cDNAs were subcloned into pGEX-2T plasmids. RHAMMv4 D5⁻ (mutant hyaluronan binding domains) plasmids were constructed as described (14,57). For the construction of v4 D4⁻ (repeat sequence) mutant, PCR was used to produce 2 fragments which were inserted into an XhoI site, using four primers. For the N-terminal fragment, two primers, 5'-GCGGGATCCATGAGAGCTCTAAGCCTG-3' and 5'-GCGCTCGAGTGCAATCAAGATG GCTTG-3', were used. For the C-terminal fragment, two primers, 5'-GCCGAATTCTCAGC AGCAGTTTGGGTT and 5'-GCCCTGGAGTATAAGTCATCAACACTTAA-3', were used. The two fragments were ligated with an XhoI site and then subcloned into the pGEX-2T vector with

BamHI and EcoRI sites. To Construct RHAMM4v-D4⁻ / D5⁻ mutants, pGEX-v4-D4⁻ plasmids were digested with BamHI and Bgl II and then ligated with the released fragment (750 bp) into pGEX-v4-D5⁻ plasmids, which were digested with BamHI and Bgl II. Expressed proteins were purified on glutathione beads and cleaved with thrombin (32). All purified proteins were dialyzed against 4 x buffer (15 mM HEPES, 100 mM KCL, 6.25% glycerol, pH 7.3) and concentrated to 1-5 mg/ml with a Microcon 30 concentrator (Amicon, Beverly, MA). Protein was snap frozen in liquid nitrogen and stored, aliquated, at -80°C.

Northern Analysis. mRNA was isolated and analyzed with Northern blots as described by Sambrook et al. (40). Briefly, RNA was prepared from cells harvested at 50-70% confluence, 12-24 hr after cell plating. Cells were lysed in buffer (4m guanidinium thiocyanate, 25 mM EDTA, 0.1 μ M21-mercaptoethanol, pH 7.0), and total RNA was extracted using the Guanidine/CsCl method. Poly(A)⁺ mRNA was purified using an mRNA purification kit (Pharmacia). 10 μ g of mRNA were separated by electrophoresis (50% formaldehyde/1.2% agarose), transferred onto nylon nitrocellulose (Amersham) and fixed by U.V. crosslinking, using a U.V. Stratalinker (Stratagene, La Jolla, CA). Membranes were pre-hybridized for 4 hours at 42°C in a solution consisting of 50% formamide, 6X SSPE, 5X Denhardt's solution, 0.5% SDS and denatured salmon sperm DNA. RNA was detected by hybridization with anti-sense ³²P-end labeled RHAMM nucleotides (GCTATTTCTTGGATGTATTCTAAGAGTTTTCTGTTTCACA TTTTTCATCGATCTTTCTTTCTCTATTGAAAC). After hybridization, the membranes were washed with 1X SSPE/0.1% SDS, 0.1X SSPE/0.1% SDS at 42-60°C, and bound label was detected by autoradiography. Equal loading of RNA was confirmed by stripping the filters, then reprobing them with a ³²P-labeled GAPDH cDNA. For detecting MMP-9 mRNA expression, 20 μ g of denatured RNA was electrophoresed, transferred and hybridized with ³²P-labeled cDNAs of mouse MMP-9 (47). The hybridization and washing conditions were the same for detecting mRNA.

RT-PCR. C3 fibroblasts were harvested 8 hr after plating at 50% confluence. Total RNA and mRNA were prepared as described above under Northern analysis. cDNA's were synthesized

using a Clontech Marathon™ cDNA amplification kit, following manual instructions. For amplification of mouse RHAMMv5 and RHAMMv4, PCR was performed with Advantage Taq polymerase (Clontech) and conditions were as follows: 45 s at 94°C, 40 s at 60°C and 3 minutes at 72°C for 25 cycles. Primer sets for RT-PCR as follows:

- Primer 1, 5'-TCAGCAGCAGTTTGGGTTGC-3'
Primer 2, 5'-GAATAGATATCTGAGTTCTTATG-3'
Primer 3, 5'-ATGTCCTTTCCTAAGGCGCC-3'
Primer 4, 5'-CAGGATCTGCATCTCAGCAC-3'
Primer 5, 5'-GAAGCAAAGCTCAATGCAGCA-3'.

Genomic clone. To obtain genomic RHAMM sequence, a portion of a RHAMM cDNA (10) was used to screen a 3T3 mouse fibroblast genomic library. Several clones were isolated, analyzed by restriction mapping and partially sequenced. Clone #1 contained the v4 initiation codon and open reading frame. This clone was completely sequenced to determine whether or not the 5'UTR previously identified by 5'RACE and primer extension of 3T3 cell RNA populations (10) was present in the RHAMM gene.

Stable transfection of fibroblasts. 10T1/2 or NIH 3T3 fibroblast lines were plated at 50% confluence then transfected 12-24 hr after cell plating with 2 µg of the various cDNAs using 25 µg of Lipofectin (GIBCO/BRL). Cells were exposed to these reagents in serum-free medium for 12-16 hours. Serum-free medium was then replaced with DMEM + 10% FBS alone and cells were allowed to recover for an additional 24 hours. Transfected cells were trypsinized and plated onto two 10 mm dishes containing selection medium (DMEM + 10% FBS + 800 µg/ml Geneticin) (Sigma). G418 resistant colonies were cloned by limiting dilution. Clones that overexpressed RHAMM were selected for 2-3 fold enhancement of RHAMM relative to empty-vector transfected cells, using western analyses to detect protein expression (see below).

Transient transfection of 10T1/2 and U21 fibroblasts. 10T1/2 and U21 cells were cultured to 40-50% confluence and transfected with 10 µg of RHAMM wild type or mutant cDNAs in 60 µl superFect reagent. After five hours of incubation, monolayers were washed twice with

PBS and the transfected cells were cultured an additional 48 hours with growth medium supplemental with 10% FBS. The cells were harvested with RIPA buffer and RHAMM expression was detected by western analysis. Only the transfectants which expressed similar level (2-3 fold higher than parental cells) were used for immunoprecipitation assays.

Focus formation. For focus formation assays, cells were grown to 70% confluence (48-72 hr after cell plating) in DMEM supplemented with 10% FBS. Transfections were performed using the Lipofectin reagent. 50 ng of pH β Apr-Neo plasmid containing RHAMMv4 and RHAMMv5 cDNA, and/or 50 ng of PEXV₃ containing MEK1AN3/S218E/S222D were used for each 100 cm dish. Post-transfected cells were maintained in DMEM supplemented with 10% FBS and 10-15 days later the number of foci were counted after cultures were fixed and stained with methylene blue.

Western Analyses. Cells were plated at 50% confluence and grown for 6-24 hr then monolayers were washed with cold PBS, lysed in RIPA buffer and subjected to SDS-PAGE as described (14). Separated protein was transferred onto nitrocellulose membranes (Bio-Rad) using a transfer buffer of 25 mM Tris-HCl, 192 mM glycine, 20% methanol, pH 8.3. Non-specific binding sites were blocked with 5% defatted milk in Tris buffer (TBST, 10 mM Tris base, 150 mM NaCl, pH 7.4, with 0.1% Tween 20) (57). The blocked membranes were incubated with rabbit anti-RHAMM antibodies (1:1500) overnight at 4°C or for 2 hours at room temperature on a gyratory shaker. RHAMM antibodies (Zymed Laboratories, Inc.) were prepared against the following sequences: antibody 1 (which detects both v4 and v5 forms of RHAMM), peptide sequence: VSIEKEKIDEK. Antibody 2 (which detects only RHAMMv5), peptide sequence: QERGTQDKRIQDME. The anti-HA tag antibody (Boehringer Mannheim) recognizes the peptide sequence, YPYDVPDYA. The anti-c-myc antibody (Santa Cruz) recognizes the peptide sequence AEEQKLISEEDLLRKRREQLKHKLEQLRNSCA. Some blots were incubated with biotinylated hyaluronan for detection of hyaluronan binding capacity of proteins as previously described (14). Membranes were washed 3 times with TBST, then incubated with horseradish peroxidase-conjugated goat anti-rabbit IgG (1:10,000) for 30 minutes at room temperature. Bound antibody

was visualized by chemiluminescence (ECL) (Amersham), according to the manufacturer's instructions. The densitometry was determined with a Multi-Analyst program (Bio-Rad). To determine antibody specificity, anti-RHAMM antibodies were incubated with beads- linked with RHAMM protein (1 μ g antibody/20 μ l beads for 1 hr at 4°C on a Rotator, then centrifuged for 5 minutes. The supernatant was used to probe membranes.

Zymogram Analysis. Cell culture supernatant medium from subconfluent monolayers was harvested and proteins therein were separated on a 10% SDS-polyacrylamide gel impregnated with 1 mg/ml of gelatin (29). After electrophoresis, SDS was removed from the gel by incubation with 2.5% Triton X-100 for 30 minutes. The gels were then incubated in a buffer containing 50 mM Tris-HCl, 5 mM CaCl₂, 0.02% NaN₃, pH8.0, at 37°C for overnight. The gels were stained with 0.25% coomassie blue R250 in acetic acid:isopropyl alcohol:water (1:3:6) and destained in water. Proteolytic activity was seen as a clear band against stained blue background. Permanent records were prepared by photography.

Immunoprecipitation and Erk Kinase Assays. Parental 10T1/2 and transfected cell lines were plated at 50% confluence for 6-24 hr and washed two times with cold PBS and lysed in a lysis buffer (25 mM Tris HCl, pH 7.2, 0.1% SDS, 1% triton-X 100, 0.5% sodium deoxycholate, 50 mM NaCl 1 mM EGTA 10 mM MgCl₂ and 1mM EDTA) (60) containing the A (1 μ g/ml), aprotinin (0.2 TIU/ml), and 3,4-dichloroisocoumarin (200 μ M). The lysates were centrifuged and equal amounts of protein (300-400 μ g) from each sample were added to 2 μ g of anti-RHAMM antibody (R3.2), anti-erk1 (K23), antibody (Santa Cruz) and anti-MEK1 (C18) antibody (Santa Cruz). After 1 hr incubation at 4°C on a Nutator rotator, 50 μ l of a 50% solution of protein G Sepharose was added and incubated at 4°C for an additional 1 hr, then washed four times with lysis buffer and once with kinase buffer (25 mM HEPES, pH 7.4, 1 mM dithiothreitol, 10 mM MgCl₂, 1 mM EGTA, 3 mM Na₃VO₄ and 0.3 mg/ml MBP). The protein G antibody-antigen complex was incubated for 20 minutes at 37°C in 15 μ l of kinase buffer supplemented with 15 μ M ATP and 10 Ci of (γ -³²p)ATP (39). 10 μ l of each sample was spotted onto P81 filter

paper, washed three times with 75 mM phosphoric acid, and once with 100% acetone. Dried samples were quantified by scintillation counting or developed for autoradiography.

***In vitro* Myelin Basic Protein Kinase Assays.** 1 μ g of mutant activate MEK1 His6-fusion protein (MEK1 S/D) (26) was incubated with 2 μ g of erk1 with or without RHAMMv4 GST-fusion protein in kinase buffer (25 mM HEPES, pH7.4, 1 mM dithiothreitol, 10 mM MgCl₂, 1mM EGTA, 15 μ M ATP) using MBP (0.3 mg/ml) as substrate, in the presence of 10 μ Ci of (γ -³²P)ATP for 15 minutes at 30°C (39). Reactions were stopped by the addition of sample loading buffer. Labeled proteins were resolved by polyacrylamide gel electrophoresis and detected by autoradiography.

***In vitro* Binding and Competition Assays.** Purified GST-RHAMM proteins were released from GST with thrombin as described (14) and RHAMM was coupled to Amino Link plus coupling gel (Pierce), following manufacturers instructions. After several washes with PBS, RHAMM-coupled beads were incubated with purified erk1, erk2 or MEK1 His-6-tagged fusion proteins in binding buffer (25 mM HEPES, pH 7.2, 50 mM NaCl 2, 10 mM MgCl₂) for 1 hr at 4°C on a Nutator rotator. After several washes with cold binding buffer, the beads were boiled for 2 minutes in loading buffer, then proteins were separated on SDS-PAGE and transferred to nitrocellulose blots for western analyses. Anti-erk1 antibody (K23, Santa Cruz, and anti-MEK1 antibody (C18, Santa Cruz) were used to detect this kinase on western blots. For competition assays, 1 μ g purified erk1 His-6 fusion protein was incubated with 10 μ g soluble RHAMM protein for 1 hr at 4°C, then incubated with beads-RHAMM for an additional 1 hr. For peptide competition assays, 1 μ g of erk1 His-6 fusion protein was incubated with 10 μ g of peptides for 1 hr and then incubated with beads-RHAMM for another 1 hr on a Rotator. Three different peptides were used in competition binding assay, D4: QEKYNDTAQSLRDVTAQLESV, D5: KQKIKHVVKLKDENSEQLKSEVSKLRSQLVKRK and phage display peptides HA2, GVCNADFCWLPAVVV and HA3, SASPSASKLSLMSTV.

Expression of the RHAMM Hyaluronan Binding Domains (P-1). A C-terminal 70 amino acid GST-RHAMM fusion protein (RHAMM-P1) was expressed which includes the two

amino acid HA binding domains plus additional sequence. This was generated using the sequence specific primers, a 5' primer GCCGGATCCAACCTAAAGCAAAAAATCAAACAT and 3' primer GCCGAATTCGCAGCAGTTTGGGTTGCCTTC and ligated into PGEX-2T. The protein was grown in luria broth to an OD 1.0, induced with 1 mM IPTG, cells harvested and lysed using standard procedures. The clarified cell lysate was passed over glutathione sepharose, and GST-RHAMM-P1 was eluted using glutathione elution buffer (10 mM Tris, pH 8.0, 50 mM glutathione). The protein was stored in 10% glycerol in -30°C at a stock concentration of 1 mg/mL. To test the above constructs for HA binding, several standard binding assays were used. First a dot blot was performed in which dilutions of the stock protein were placed on PVDF membrane and probed with biotinylated HA (14). After a series of washes, the membranes were incubated with streptavidin horseradish peroxidase (HRP), and binding was detected using TMB (3,3',5,5'-Tetramethylbenzidine) substrate.

A low level of HA modification was obtained by using a ratio of EDCI to carboxylic function of 1:10 and a biotin hydrazide ratio of 1:15. The reaction was carried out at pH 4.75 using 50 mM MES, and the product purified using extensive dialysis. The dialysis buffers alternated between 300 mM NaCl, de-ionized water, 20% ethanol, and this cycle was repeated once. Gel permeation chromatography was used to confirm the biotinylated HA was intact and to separate unreacted biotin.

Phage Screening. GST-RHAMM-P1 was either nonspecifically adsorbed onto a 30 mm polystyrene dish, or immobilized on 20 μ L of glutathione sepharose in a 1.5 mL microfuge tube. The methods are equivalent but it was noted that more non-specific phage were present using glutathione sepharose. A starting titer of 10^{11} colony forming units (cfu) of fUSE-5 phage hosting random 15 amino acid peptides was diluted 1:1000 in tris buffered saline (20 mM Tris, 130 mM NaCl, pH 7.5) with 0.1% w/v polyvinylpyrrolidone and 0.05% Tween 20 (TBS-T/PVP-40). This was applied to the immobilized GST-RHAMM-P1 and incubated at room temperature for one hour. Non-binding phage were washed away in a series of 10 washes, and specifically bound phage were eluted using 1 unit of thrombin incubated at 37°C for 40 minutes. It was anticipated

that RHAMM-P1 would be released using thrombin carrying with it all specifically bound phage, while GST would remain immobilized on the plate or on glutathione sepharose.

The phage were titered by infecting compromised K91-Kan cells and dropping serial dilutions onto LB plates. The phage bound to GST-RHAMM-P1 was propagated in 20 mL cultures overnight, and precipitated from the broth supernatant, after removing cells.

This procedure was repeated a total of four times, each time resulting in retention of fewer phage. In the final screen, phage were eluted with 1 mg/mL hyaluronidase digested HA (MW average 60,000) instead of thrombin. This procedure allowed isolation of phage that bound specifically to the HA binding domains of RHAMM P1. Positive colonies from LB Kan/Tet plates were propagated, the plasmid purified and sequenced.

Positive sequences were then synthesized both as unmodified 15 amino acid sequences and with an N-terminal biotin group. bHA2 and bHA5 were solubilized in 50:50 DMF:water, bHA3 and bHA4 were fully soluble in water to at least 1 mg/mL.

Phage Peptide Binding Assays. To verify that the peptides obtained from phage screening bound to the HA binding domains of RHAMM, a solid phase 96 well plate assay was employed. 50 μ L GST-P1 (0.25 mg/mL) in glutathione elution buffer was immobilized in wells of a polystyrene 96 well plate (Greiner). The plate was blocked with 250 μ L TBS-PVP-40 BSA (20 mM Tris, pH 7.5, 130 mM NaCl, 0.1% polyvinyl pyrrolidone-40, 1% bovine serum albumin) for 2 hours to overnight with shaking. The plate was washed with TBS-PVP-40 (no BSA) and then incubated with excess HA or chondroitin sulfate (CS) for 1 hr prior to the addition of the biotinylated ligand. The biotinylated ligand was incubated for 25 minutes (as determined from an initial time course), washed three times and blocked with TBS-PVP-40-BSA for 1 hr. Streptavidin HRP was added at a dilution 1:10,000 in TBS-PVP-40. HA was added to the streptavidin mix since it is known that streptavidin HRP binds nonspecifically to HA and CS which inherently causes misleading results in the competition experiments. After 40 minutes incubation, the plate was washed and the presence of biotinylated peptide was determined using TMB. Colorimetric development was detected at 590 nm (Perkin Elmer HTS 7000). All measurements are done in

quadruplicate. Eadie Hofstee analysis was performed, assuming that binding can be correlated to the color developed under each condition.

RESULTS

1. Two full length RHAMM mRNA transcripts are detected in ras-transformed

10T1/2 fibroblasts. Two murine RHAMM mRNA transcripts with distinct 5'UTR's have previously been reported (3,10), one initiating at exon 1 (11) and the other downstream at exon 6. The two transcripts encode a 95 kDa protein and a shorter, N-terminally truncated 73 kDa protein, respectively. RHAMM mRNA expression of several oncogene-transfected 10T1/2 fibroblasts was assayed, using Northern blots (Fig. 1A). The presence of a mutant active ras most strongly upregulated RHAMM mRNA, compared to other common oncogenes. The Northern blot suggested the presence of one major but broad mRNA transcript of 3.2 kb (Fig. 1A). RT-PCR analyses were conducted to determine if additional, more minor mRNA transcripts existed. mRNA was harvested 8 hr after cell plating when cells are beginning to locomote, a time previously shown to correspond to maximal expression of a 73 kDa RHAMM protein (41). We first confirmed that the 5'UTR reported to be unique to the v4 transforming mRNA transcript (10), is present in genomic RHAMM sequence upstream of the Kozak consensus sequence predicted to initiate this short transcript. The 5'UTR sequence was found in a genomic clone containing v4 sequence (Fig. 1B), and its sequence contained two in-frame stop codons upstream of the start codon initiating v4 (Fig. 1B). The presence of an intron/exon splice site suggested this putative 5'UTR is not part of exon 6 initiating the v4 open reading frame. The presence of two unique 5'UTR's permits the differential detection of each RHAMM transcript. Using two primer sets shown in Fig. 1C, mRNA inserts corresponding to v4 and v5, as determined by size and sequence, were amplified in RT-PCR (Fig. 1D). To determine whether or not the v4 insert represented partially processed RNA (11), primer sets were designed to assess whether or not a full length v4 mRNA transcript could be amplified (Fig. 1C). Full length v4 mRNA transcript was indeed amplified, as determined by size and

sequence (Fig. 1E). However, it is clearly a minor transcript and present in much smaller amounts than the v5 transcript.

To assess whether v4 can be detected in cell backgrounds other than 10T1/2 fibroblasts, mutant active ras was transiently transfected into an NIH 3T3 cell background. V4 was detected by RT-PCR, as for the ras-transformed 10T1/2 fibroblasts (Fig. 1F). These results suggest that the presence of a mutant active ras permits the expression of a full length mRNA encoding RHAMMv4. An inability to detect this RNA transcript (11) is likely related to its minor expression and the its limited expression, which occurs shortly after cell plating when cell motility is initiated.

2. Ras-transformed cells express two major RHAMM proteins. Two polyclonal antibodies were prepared against peptide sequences encoded in RHAMM cDNA (17,51) in order to differentiate between v5 and v4 proteins (see Methods). The first antibody was prepared against sequence encoded in the exon that has been reported to be required by v4 to transform fibroblasts (see Methods) (14). This sequence is encoded in both v5 and v4. The second antibody was prepared against sequence unique to v5 that is present immediately N-terminal to the initiation of a RHAMMv4 protein, as predicted from the v4 mRNA transcript (Fig. 1B) (10). As shown in Fig. 2A, antibody 1 detects both a 95 kDa RHAMM protein, predicted to correspond to v5, and a 73 kDa protein, predicted to correspond to v4. Blocking of these antibodies with either RHAMMv4-GST fusion protein or RHAMM peptide (see Methods) prevented antibody binding to these proteins on western blots (Fig. 2B), confirming the specificity of antibody 1 for RHAMM. In contrast, and as predicted, antibody 2 reacted only with 95 kDa and a minor 90 kDa protein but not with the 73 kDa protein detected with antibody 1 (Fig. 2C). These results indicate that the 73 kDa protein lacks the N-terminal sequence of the 95 kDa protein, consistent with sequence encoded in the v4 mRNA transcript. The specificity of antibody 2 was confirmed by blocking of antibody binding with recombinant RHAMMv5 (Fig. 2D). The size of v4 protein expressed in a 10T1/2 fibroblast background from a transfected, HA-tagged RHAMMv4 cDNA was compared to the RHAMM proteins

expressed in ras transformed cells (Fig. 2E,F). The protein expressed from HA-v4, detected by the HA tag, was identical in MW to the endogenous 73 kDa protein (compare Fig. 2E and 2F), and the tagged RHAMM protein also reacted with Ab 1 but not Ab 2 (Fig. 2E).

These results show that ras transformed fibroblasts express two RHAMM proteins that correspond in size and antibody reactivity to sequence predicted by the v5 and v4 RHAMM mRNA transcripts. The 73 kDa protein corresponding to v4 is most highly expressed at 8 hr after cell plating, consistent with v4 mRNA expression, while the 95 kDa protein is most highly expressed at 24-36 hr after cell plating (Fig. 2A, C). These results suggest the two RHAMM forms may perform different functions.

- 3. V4 and v5 bind directly to erk1 and indirectly to MEK1.** The ability of v4, erk1 and MEK1 to co-associate in ras-transformed cells was previously demonstrated by immunoprecipitation assays, using anti-RHAMM antibodies (60). This study had shown that only erk1, but not erk2 or other map kinases, associated with the RHAMM/erk1/MEK complex (60). Here, *in vitro* binding assays using erk1, MEK1 and RHAMM-GST or His-fusion proteins showed that both v4 and v5 RHAMM proteins (Fig. 3A) bound directly to erk1 (v4 shown here, Fig. 3B) but, under our assay conditions, did not bind to MEK1-His-fusion protein, at detectable levels (Fig. 3C). Deletion and mutation analyses of v4 revealed two sites on RHAMM that contributed to erk1 binding (Fig. 3D), a repeated sequence (D4), and D5 domains, the latter previously reported to contain hyaluronan binding motifs (14,57). Peptides mimicking either 21 amino acids of D4 or peptides mimicking D5 significantly reduced binding of erk1 to v4 whereas mixing of both peptides inhibited binding of erk1 to v4 by 90% (Fig. 3D), suggesting these domains likely co-ordinate to act as erk1 binding sites. The use of these domains for associating with erk 1 *in vivo* was then assessed by transient transfection of tagged mutant RHAMM cDNA's into cells that produce little endogenous RHAMM (Fig. 4) (14). RHAMM expressed from v4 and v5 cDNA's co-immunoprecipitated with erk1 when D6 and D5 were intact (Fig. 4A). Interestingly, approximately 3 times more erk1 associated with v4, compared with v5. When the RHAMM D4 and D5- erk1 binding domains were mutated,

erk1 binding to RHAMM was abolished (Fig. 4A). These results confirm that D4 and D5 are sites of RHAMM/erk1 interaction *in vivo*. The key contribution of D5 to erk1 binding *in vivo* provides a molecular rationale for the previously reported ability of RHAMM forms that are mutated in this domain to block both activation of erk and cell transformation by mutant active ras (14,60).

Independent verification of the ability of D5 to interact with protein sequences was confirmed by screening a 15 mer random phage display library using recombinant RHAMM (P1 peptide) containing D5, as bait. Eight peptide sequences were obtained that could be grouped according to shared sequences: A) WPVSLTVCSAVWCPL, HWCLPLLACDTFARA, GVCNADFCWLPAVVV: B) YSVYLSVVHNSVLPS, YSVYLSVAHNFLPS, IPPILPAYTLLGHP: C) PHXRPVVSASSILPV; SASPSASKLSMSTV: D) FFAGGLMYRIGFSSD and SPSLDCSWPLVKFSS. Five of these were confirmed to bind to RHAMM P-1 peptide in ELISA, and binding was quantified with Eadie Hofstee plots (Fig. 5A). Confirmation that these peptides bind to the D5 domain present in the RHAMM P-1 peptide (see Methods), was provided by the ability of hyaluronan to compete with phase peptides for binding to P-1 (Fig. 5B). More importantly, two selected peptides, GVCNADFCWLPAVVV and SASPSASKLSLMSTV, competed with erk1 for binding v4 to approximately the same extent as a RHAMM D5 peptide (Fig. 4D).

4. Interaction of v4 and v5 with MEK1 *in vivo* requires D3. Deletion of D3

(VSIEKEKIDEKCETEKLLLEYIQEIS, Fig. 4A) abolished the co-immunoprecipitation of v4 with MEK1 (Fig. 6A), although this deletion still enabled an interaction with erk1 (Fig. 4A). V5 also co-immunoprecipitated with MEK1, consistent with the presence of D3 sequence in v5 (Fig. 3A), but approximately three-fold less MEK1 associated with this RHAMM protein form (Fig. 6A). Mutation/deletion of either erk1 binding domains also prevented an association of MEK1 with RHAMMv4 (Fig. 6A). *In vitro* kinase assays showed that the presence of GST-RHAMMv4 did not promote activation of His-erk 1, by mutant active His-MEK1 (Fig. 6B)

confirming that other proteins are likely required for the ability of v4 to regulate erk1 activity via MEK1.

5. Deletion of N-terminal 163 amino acids is required for the transforming

function of RHAMM. V4 overexpression activated erk kinase and was confirmed to transform fibroblasts, as detected by focus formation (Fig. 7A,B). Interestingly, activation of erk kinase by both v4 and mutant active ras required the presence of serum in the 10T1/2 cell background (Fig. 7B). In contrast to v4, overexpression of v5 did not activate erk kinase, and was not transforming in focus forming assays (Fig. 7A). These results indicate that the N-terminal sequence unique to v5 negatively regulates the functions of downstream RHAMM sequence, and that v4, which lacks this sequence, represents the more active form of RHAMM.

The association of RHAMM with MEK1 and the ability of RHAMMv4 overexpression to activate erk 1 suggests RHAMM may modify MEK1 function. The effect of RHAMM overexpression on the ability of mutant active MEK1 to activate erk 1 and to transform fibroblasts (26) was assessed (Fig. 7C,D). V4 strongly synergized with mutant active MEK1 to both activate erk kinase and to enhance transformation of 10T1/2 fibroblasts. This ability to synergize appears to derive from an association of v4 with MEK1 since deletion of D3 blocked this affect (Fig. 7). V4 did not enhance the focus forming ability of oncogenes that it does not associate with such as rac (60, data not shown). Interestingly, v5 slightly enhanced the ability of mutant active MEK1 to activate erk kinase but did not significantly affect the transforming function of mutant active MEK1.

An additional domain, D2, shown in Fig. 3A, is required for the ability of v4 to transform (data not shown) and to enhance the transformation ability of mutant active MEK1. However, deletion of this domain did not affect the association of MEK1 or erk1 with RHAMM (data not shown).

6. Overexpression of v4 promotes MMP-9 production release and this effect

requires the v4 erk1 binding domains. The effect of v4 and v5 overexpression on gene

expression were compared to begin to address the mechanism(s) by which v4 transforms. Cells stably overexpressing v4 activated AP-1 as determined by gel shift assays, confirming a previous report (Figs. 7, 8) (6). Overexpression of v4 also strongly promoted expression of MMP-9 (Fig. 7), and release of this metalloproteinase, as detected by a zymogram (Fig. 8). Furthermore, overexpression of v4 mutated in its D5 erk1 binding domain blocked release of this metalloproteinase (Fig. 8). In contrast to v4, v5 overexpression had little effect on these parameters.

DISCUSSION

Several forms of intracellular RHAMM have been reported to be encoded by distinct full length mRNA transcripts with the most common form encodes a 95 kDa protein (v5), (10,11,14,51). We (10,28) and others (24,31) have also reported the presence of shorter protein forms, particularly a 73 kDa. The 73 kDa protein is of particular interest since overexpression of a cDNA (v4) encoding a 73 kDa protein that does not contain 163 amino N-terminal amino acids present in v5, is transforming (14), the resulting protein co-immunoprecipitates with erk1 and MEK1 kinases (60) and 73 kDa is required for signaling through mutant active ras (14). The functional properties of the more common v5 form, however, have not been previously reported and the relationship between v4 and v5 has been entirely unclear. We confirm that both v4 and v5 RHAMM forms are expressed in ras transformed cells and show that both are erk1 binding proteins that indirectly associate with MEK1 *in vivo*. Our results clearly show that v4 is a more active form of RHAMM than v5, in terms of its ability to activate erk1 kinase, and to synergize with mutant active MEK1 to enhance its downstream functions. These results indicate that the N-terminal 163 amino acids negatively regulate the ability of RHAMM to function on the erk1 kinase cascade and that RHAMM, like raf and other oncogenes (5), appears to be activated in this function by removal of a regulatory sequence.

The RHAMM N-terminal sequence (D1) that negatively regulates RHAMM-mediated erk activation is characterized by the presence of an SH3 binding site and by multiple putative erk

phosphorylation sites. As a domain, it is an entirely novel sequence (ProDom #75227) and the manner in which it regulates RHAMM-mediated erk activation is not yet clear.

Immunoprecipitation data suggest that v5 is less able to interact with erk1 and MEK1 compared to the v4 and this reduced interaction may account, in part, for the restricted ability of v5 to activate erk1. In this regard, D1 may mask key domains such as D3-D5, required for interaction with MEK1 and erk1. However, the presence of an SH3 binding domain and serine/threonine phosphorylation sites raise the possibility that v5 interacts with additional regulatory proteins and/or is targeted to subcellular compartments distinct from v4. Removal of D1 may permit RHAMM to bring erk1/MEK1 complexes close to upstream regulatory proteins and downstream erk1 substrates (5,49). Further studies are required to determine the precise molecular mechanisms by which D1 regulates RHAMM-mediated activation of erk1.

Our results suggest that both v4 and v5 are expressed in sub-confluent ras-transformed fibroblasts. Although both proteins are expressed at this time in ras-transformed cells at equivalent levels, the most common RHAMM mRNA transcript encodes the 95 kDa protein while the mRNA transcript is minor. The role of the full length v4 mRNA in generating this level of v4 protein is therefore not yet clear. It is, of course, possible that the v4 mRNA transcript is more efficiently translated than v5, as has been described for other rare messages (e.g., 61) but v4 may also be generated by other mechanisms. Possibilities include internal start codon usage of the v5 mRNA transcript and/or proteolytic processing of v5 protein. The first possibility is attractive since a number of proteins including myc, p53 and FGF isoforms (2,13,15,25) are generated in this manner. Further, there are several internal conserved consensus Kozak in sequences encoded in v5 that would generate proteins close to 73 kDa in both murine and human cells.

A recent report (11) suggested that v4 represents a partially processed RNA. The presence of the full length v4 transcript in ras-transformed cells is a consistent finding when care is taken to harvest mRNA from subconfluent cultures, to utilize mRNA rather than total RNA and to conduct RT-PCR under conditions reported in this report. The appearance of the full length v4 mRNA

transcript shortly after cell plating (8 hr) and its very minor expression likely contributed to difficulty in detecting this transcript (11).

The potent transforming/MEK1 enhancing function of v4 is related to its ability to promote complexing of MEK1/erk1 with other regulatory accessory proteins and possibly upstream components of this kinase cascade (49). It is relevant that a previously reported MEK1 accessory protein, MEK-1 activating protein (MP-1) (42) has several properties that may place it on the same regulatory pathway as v4. Both v4 (60) and MP-1 (42) specifically activate erk1 and both proteins require the presence of serum supplements in culture medium for this effect to occur *in vivo*. It is also intriguing that MP-1 encodes a six amino acid sequence, VSI/LEKE, that is identical to that present in D3 of RHAMM, which is required both for the association of v4 with MEK1 and its effect on MEK1 function. This domain may serve as a binding site for adapter proteins that link proteins such as MP-1 to v4, permitting activation of erk1 in subcellular sites that v4 is retained in, such as cell lamellae (60). In any case, a consequence of this complex formation is enhanced expression of AP-1 regulated genes such as MMP-9, that have clearly been implicated in the transformation process (37,43,54).

The D5 domains of RHAMM, which mediate binding of the extracellular polysaccharide hyaluronan to a cell surface form of RHAMM (12,14,36), contribute to the binding of erk1 to intracellular RHAMM. Several sequences have been reported to mediate the binding of erk kinases to other erk binding proteins and these include a "D" box, an FXFP motif (18) and a ribosomal 6 kinase sequence, LAQRRVRKL (45). Interestingly, the D5 domains of RHAMM contain a sequence KHVVKL, that is similar to the erk docking site present in ribosomal 6 kinase (45). The sequence in erk1 which is responsible for binding to RHAMM has not yet been defined.

We have previously reported that RHAMMv4 protein is transiently expressed in 3T3 fibroblasts (10) and show here that its maximal expression occurs at culture subconfluence and early after cell plating. However, the physiological role of such a truncated, activated form of RHAMM has not yet been clearly determined *in vivo*. Its location in cell lamellae *in vitro* (60), its ability to promote cell motility (14) and its expression shortly after wounding of cell monolayers

(41) suggest it contributes to initiation of locomotion and possibly progression through cell cycle, following tissue injury. The recent demonstration of high levels of RHAMM in sprouting olfactory nerves *in vivo* (59) and evidence that RHAMM plays a role in the extension of dynamic nor-adrenergic nerve nets such as the locus coeruleus (31) are consistent with a role for RHAMM in renewal processes that involve lamellae or axonal extension. Finally, the overexpression of several RHAMM protein forms in breast cancer, malignant pancreatic cell lines (1) and aggressive subsets of multiple myeloma cells (9) predict that it also plays a role in neoplastic progression, a process that also involves cell motility. One role for a transiently expressed v4 in these processes may be to irritate expression of AP-1 regulated genes such as MMP-9, resulting from activation of erk1. Enhanced production of metalloproteinases are required for response-to-injury processes (4,29,30,34,46,58) and for neoplastic progression (37,43,54).

In summary, we show that intracellular RHAMM forms are erk1 binding proteins and that the presence of an N-terminal 163 amino acids unique to the commonly expressed RHAMMv5 (95 kDa) suppresses the ability to downstream RHAMM sequence to participate in the activation of erk1. An activated form of RHAMM, corresponding to the previously described v4 (14), is expressed in ras-transformed fibroblasts. The physiological roles of both of these forms of RHAMM is actively under investigation.

ACKNOWLEDGMENTS

This study was funded by an MRC grant, GR-13920 (ET), NCIC grant (ET), MRC studentship (RH), NIH grant GM48521 (NA), U.S. Department of Army Breast Cancer IDEA grant (GDP), and CAN (TC).

REFERENCES

1. Abetamann, V., H.F. Kern, and H.P. Elsasser. 1996. Differential expression of the hyaluronan receptors CD44 and RHAMM in human pancreatic cancer cells. *Clin. Cancer Res.* 2:1607-1618.
2. Arnaud, E., C. Touriol, C. Boutonnet, M.C. Gensac, S. Vagner, H. Prats, and A.C. Prats. 1999. A new 34-kilodalton isoform of human fibroblast growth factor 2 is cap dependently synthesized by using a non-AUG start codon and behaves as a survival factor. *Mol. Cell Biol.* 19:505-514.
3. Assmann, V., J.F. Marshall, C. Fieber, M. Hofmann, and I.R. Hart. 1998. The human hyaluronan receptor RHAMM is expressed as an intracellular protein in breast cancer cells. *J. Cell Sci.* 111:1685-1694.
4. Bos, T.J., P. Margiotta, L. Bush, and W. Wasilenko. 1999. Enhanced cell motility and invasion of chicken embryo fibroblasts in response to Jun over-expression. *Int. J. Cancer* 81:404-410.
5. Campbell, S.L., R. Khosravi-Far, K.L. Rossman, G.J. Clark, and C.J. Der. 1998. Increasing complexity of Ras signaling. *Oncogene* 17:1395-1413.
6. Cheung, W.F., T.F. Cruz, and E.A. Turley. 1999. Receptor for hyaluronan-mediated motility (RHAMM), a hyaladherin that regulates cell responses to growth factors. *Biochem. Soc. Trans.* 27:135-142.
7. Choi, K.Y., B. Satterberg, D.M. Lyons, and E.A. Elion. 1994. Ste5 tethers multiple protein kinases in the MAP kinase cascade required for mating in *S.cerevisiae*. *Cell* 78:499-512.
8. Cohen, L., W.J. Henzel, and P.A. Baeuerle. 1998. IKAP is scaffold protein of the IkappaB kinase complex. *Nature* 395:292-296.
9. Crainie, M., A.R. Belch, M.J. Mant, and L.M. Pilarski. 1999. Overexpression of the receptor for hyaluronan-mediated motility (RHAMM) characterizes the malignant clone

- in multiple myeloma: Identification of three distinct RHAMM variants. *Blood* **93**:1684-1696.
10. Entwistle, J., S. Zhang, B. Yang, C. Wong, Q. Li, C.L. Hall, J. A. M. Mowat, A.H. Greenberg, and E.A. Turely. 1995. Characterization of the murine gene encoding the hyaluronan receptor RHAMM. *Gene* **163**:233-238.
 11. Fieber, C., R. Plug, J. Sleeman, P. Dall, H. Ponta, and M. Hofmann. 1999. Characterisation of the murine gene encoding the intracellular hyaluronan receptor IHABP (RHAMM). *Gene* **226**:41-50.
 12. Gares, S.L., N. Giannakopoulos, D. MacNeil, R.J. Faull, and L.M. Pilarski. 1998. During human thymic development, beta 1 integrins regulate adhesion, motility, and the outcome of RHAMM/hyaluronan engagement. *J. Leukoc. Biol.* **64**:781-790.
 13. Grunert, S., and R.J. Jackson. 1994. The immediate downstream codon strongly influences the efficiency of utilization of eukaryotic translation initiation codons. *EMBO J.* **13**:3618-3630.
 14. Hall, C.L., B. Yang, X. Yang, S. Zhang, M. Turley, S. Samuel, L.A. Lange, C. Wang, G.D. Curpen, and RC Savani. 1995. Overexpression of the hyaluronan receptor RHAMM is transforming and is also required for H-ras transformation. *Cell* **82**:19-26.
 15. Hann, S.R. 1994. Regulation and function of non-AUG-initiated proto-oncogenes. *Biochemie* **76**:880-886.
 16. Herrera, R. 1998. Modulation of hepatocyte growth factor-induced scattering of HT29 colon carcinoma cells. Involvement of the MAPK pathway. *J. Cell Sci.* **111**:1039-1049.
 17. Hofmann, M., C. Fieber, V. Assmann, M. Gottlicher, J. Sleeman, R. Plug, N. Howells, O. von Stein, H. Ponta, and P. Herrlich. 1998. Identification of IHABP, a 95 kDa intracellular hyaluronate binding protein. *J. Cell Sci.* **111**:1673-1684.

18. **Jacobs, D., D. Glossip, H. Xing, A.J. Muslin, and K. Kornfeld.** 1999. Multiple docking sites on substrate proteins form a modular system that mediates recognition by ERK MAP kinase. *Genes Dev.* **13**:163-175.
19. **Janes, P.W., R.J. Daly, A. deFazio, and R.L. Sutherland.** 1994. Activation of the Ras signalling pathway in human breast cancer cells overexpressing erbB-2. *Oncogene* **9**:3601-3608.
20. **Janulis, M., S. Silberman, A. Ambegaokar, J.S. Gutkind, and R.M. Schultz.** 1999. Role of mitogen-activated protein kinases and c-Jun/AP-1 trans-activating activity in the regulation of protease mRNAs and the malignant phenotype in NIH 3T3 fibroblasts. *J. Biol. Chem.* **274**:801-813.
21. **Jeffers, M., M. Fiscella, C.P. Webb, M. Anver, S. Koochekpour, and G.F. Vande Woude.** 1998. The mutationally activated Met receptor mediates motility and metastasis. *Proc. Natl. Acad. Sci. USA* **95**:14417-14422.
22. **Klemke, R.L., S. Cai, A.L. Giannini, P.J. Gallagher, P. de Lanerolle, and D.A. Cheresh.** 1997. Regulation of cell motility by mitogen-activated protein kinase. *J. Cell Biol.* **137**:481-492.
23. **Liu, M.L., F.C. Von Lintig, M. Liyanage, M.A. Shibata, C.L. Jorcyk, T. Ried, G.R. Boss, and J.E. Green.** 1998. Amplification of Ki-ras and elevation of MAP kinase activity during mammary tumor progression in C3(1)/SV40 Tag transgenic mice. *Oncogene* **17**:2403-2411.
24. **Lovvorn, H.N.III, D.L. Cass, K.G. Sylvester, E.Y. Yang, T.M. Crombleholme, N.S. Adzick, R.C. Savani.** 1998. Hyaluronan receptor expression increases in fetal excisional skin wounds and correlates with fibroplasia. *J. Pediatr. Surg.* **33**:1069-1070.
25. **Macejak, D.G., and P. Sarnow.** 1991. Internal initiation of translation mediated by the 5' leader of a cellular mRNA. *Nature* **353**:90-94.

26. **Mansour, S.J., W.T. Matten, A.S. Hermann, J.M. Candia, S. Rong, K. Fukasawa, G.F. Vande Woude, and N.G. Ahn.** 1994. Transformation of mammalian cells by constitutively active MAP kinase kinase. *Science* **265**:966-970.
27. **Marcus, S., A. Polverino, M. Barr, and M. Wigler.** 1994. Complexes between STE5 and components of the pheromone-responsive mitogen-activated protein kinase module. *Proc. Natl. Acad. Sci. USA* **91**:7762-7766.
28. **Masellis-Smith, A., A.R. Belch, M.J. Mant, E.A. Turley, L. M. Pilarski.** 1996. Hyaluronan-dependent motility of B cell and leukemic plasma cells in blood, but not of bone marrow plasma cells, in multiple myeloma: alternate use of receptor for hyaluronan-mediated motility (RHAMM) and CD44. *Blood* **87**:1891-1899.
29. **McCawley, L.J., S. Li, E.V. Wattenberg, and L.G. Hudson.** 1999. Sustained activation of the mitogen-activated protein kinase pathway. A mechanism underlying receptor tyrosine kinase specificity for matrix metalloproteinase-9 induction and cell migration. *J. Biol. Chem.* **274**:4347-4353.
30. **Mira, E., S. Manes, R.A. Lacalle, G. Marguez, and C. Martinez-A.** 1999. Insulin-like growth factor I-triggered cell migration and invasion are mediated by matrix metalloproteinase-9. *Endocrinology* **140**:1657-1664.
31. **Nagy, J.I., M.L. Price, W.A. Staines, B.D. Lynn, and A.C. Granholm.** 1998. The hyaluronan receptor RHAMM in noradrenergic fibers contributes to axon growth capacity of locus coeruleus neurons in an intraocular transplant model. *Neuroscience* **86**:241-255.
32. **Ngai, P.K., and J.Y. Chang.** 1991. A novel one-step purification of human alpha-thrombin after direct activation of crude prothrombin enriched from plasma. *Biochem. J.* **280**:805-808.
33. **Oka, H., Y. Chatani, R. Hoshino, O. Ogawa, Y. Kakehi, T. Terachi, Y. Okada, M. Kawaichi, M. Kohno, and O. Yoshida.** 1995. Constitutive activation of

mitogen-activated protein (MAP) kinases in human renal cell carcinoma. *Cancer Res.* **55**:4182-4187.

34. **Pacheco, M.M., M. Mourao, E.B. Mantovani, I.N. Nishimoto, and M.M. Brentani.** 1998. Expression of gelatinases A and B, stromelysin-3 and matrilysin genes in breast carcinomas: clinico-pathological correlations. *Clin. Exp. Metastasis* **16**:577-585.
35. **Pawson, T., and J.D. Scott.** 1997. Signaling through scaffold, anchoring, and adaptor proteins. *Science* **278**:2075-2080.
36. **Pilarski, L.M., M.J. Mant, and A.R. Belch.** 1999. Drug resistance in multiple myeloma: novel therapeutic targets within the malignant clone. *Leuk. Lymphoma* **32**:199-210.
37. **Polette, M., and P. Birembaut.** 1998. Membrane-type metalloproteinases in tumor invasion. *Int. J. Biochem. Cell Biol.* **30**:1195-1202.
38. **Printen, J.A., and G.F. Sprague, Jr.** 1994. Protein-protein interactions in the yeast pheromone response pathway: Ste5p interacts with all members of the MAP kinase cascade. *Genetics* **138**:609-619.
39. **Robbins, D.J., E. Zhen, H. Owaki, C.A. Vanderbilt, D. Ebert, T.D. Geppert, and M.H. Cobb.** 1993. Regulation and properties of extracellular signal-regulated protein kinases 1 and 2 in vitro. *J. Biol. Chem.* **268**:5097-5106.
40. **Sambrook, J., E. Fritsch, and T. Maniatis.** 1989. *Molecular Cloning: a Laboratory Manual*, Cold Spring Harbor Laboratory. In: Cold Spring Harbor, NY: 1989: Section 7.2-7.53.
41. **Savani, R.C., C. Wang, B. Yang, S. Zhang, M.G. Kinsella, T.N. Wight, R. Stern, D.M. Nance, and E.A. Turley.** 1995. Migration of bovine aortic smooth muscle cells after wounding injury. The role of hyaluronan and RHAMM. *J. Clin. Invest.* **95**:1158-1168.

42. **Schaeffer, H.J., A.D. Catling, S.T. Eblen, L.S. Collier, A. Krauss, and M.J. Weber.** 1998. MP1: a MEK binding partner that enhances enzymatic activation of the MAP kinase Cascade. *Science* **281**:1668-1671.
43. **Shapiro, S.D.** 1998. Matrix metalloproteinase degradation of extracellular matrix: biological consequences. *Curr. Opin. CellBiol.* **10**:602-608.
44. **Sivaraman, V.S., H. Wang, G.J. Nuovo, and C.C. Malbon.** 1997. Hyperexpression of mitogen-activated protein kinase in human breast cancer. *J. Clin. Invest.* **99**:1478-1483.
45. **Smith, J.A., C.E. Poteet-Smith, K. Malarkey, and T.W. Sturgill.** 1999. Identification of an extracellular signal-regulated kinase (ERK) docking site in ribosomal S6 kinase, a sequence critical for activation by ERK in vivo. *J. Biol. Chem.* **274**:2893-2898.
46. **Sympson, C.J., M.J. Bissell, and Z. Werb.** 1995. Mammary gland tumor formation in transgenic mice overexpressing stromelysin-1. *Semin. Cancer Biol.* **6**:159-163.
47. **Tanaka, H., K. Hojo, H. Yoshida, T. Yoshioka, and K. Sugita.** 1993. Molecular cloning and expression of the mouse 105-kDa gelatinase cDNA. *Biochem. Biophys. Res. Commun.* **190**:732-740.
48. **Tanimura, S., Y. Chatani, R. Hoshino, M. Sato, S. Watanabe, T. Kataoka, T. Nakamura, and M. Kohno.** 1998. Activation of the 41/43 kDa mitogen-activated protein kinase signaling pathway is required for hepatocyte growth factor-induced cell scattering. *Oncogene* **17**:57-65.
49. **Turley, E., N. Auersperg.** 1989. A hyaluronate binding protein transiently codistributes with p21k-ras in culture cell lines. *Exp. Cell Res.* **182**:340-348.
50. **Waddick, K.G., and F.M. Uckun.** 1998. Innovative treatment programs against cancer. I. Ras oncoprotein as a molecular target. *Biochem. Pharmacol.* **56**:1411-1426.

51. Wang, C., J. Entwistle, G. Hou, Q. Li, E. A. Turley. 1996. The characterization of a human RHAMM cDNA: conservation of the hyaluronan-bonding domains. *Gene* **174**:299-306.
52. Wang, C., A.C. Thor, D.H. Moore, Y. Zhao, R. Kerschmann, R. Stern, P.H. Watson, and E.A. Turley. 1998. The overexpression of RHAMM, a hyaluronan-binding protein that regulates ras signaling, correlates with overexpression of mitogen-activated protein kinase and is a significant parameter in breast cancer progression. *Clin. Cancer Res.* **4**:567-576.
53. Webb, C.P., L.Van Aelst, M.H. Wigler, and G.F. Woude. 1998. Signaling pathways in Ras-mediated tumorigenicity and metastasis. *Proc. Natl. Acad. Sci. USA* **95**:8773-8778.
54. Westermarck, J., and V.M. Kahari. 1999. Regulation of matrix metalloproteinase expression in tumor invasion. *FASEB J.* **13**:781-792.
55. Whitmarsh, A.J., J. Cavanagh, C. Tournier, J. Yasuda, and R.J. Davis. 1998. A mammalian scaffold complex that selectively mediates MAP kinase activation. *Science* **281**:1671-1674.
56. Xie, H., M.A. Pallero, K. Gupta, P. Chang, M.F. Ware, W. Witke, D.J. Kwiatkowski, D.A. Lauffenburger, J.E. Murphy-Ullrich, and A. Wells. 1998. EGF receptor regulation of cell motility: EGF induces disassembly of focal adhesions independently of the motility-associated PLCgamma signaling pathway. *J. Cell Sci.* **111**:615-624.
57. Yang, B., L. Zhang, and E.A. Turley. 1993. Identification of two hyaluronan-binding domains in the hyaluronan receptor RHAMM. *J. Biol. Chem.* **268**:8617-8623.
58. Yu, Q., and I. Stamenkovic. 1999. Localization of matrix metalloproteinase 9 to the cell surface provides a mechanism for CD44-mediated tumor invasion. *Genes Dev.* **13**:35-48.

59. **Zehntner S.P., A. Mackay-Sim, and G.R. Bushell.** 1998. Differentiation in an olfactory cell line. Analysis via differential display. *Ann. N.Y. Acad. Sci.* **855**:235-239.
60. **Zhang S., M.C. Chang, D. Zylka, S. Turley, R. Harrison, and E.A. Turley.** 1998. The hyaluronan receptor RHAMM regulates extracellular-regulated kinase. *J. Biol. Chem.* **273**:11342-11348.
61. **Zhou, B., and M. Rabinovitch.** 1998. Microtubule involvement in translational regulation of fibronectin expression by light chain 3 of microtubule-associated protein 1 in vascular smooth muscle cells. *Circ. Res.* **83**:481-489.

LEGENDS

FIG. 1. Ras-transformed cells express two RHAMM mRNA transcripts. A) Northern blot analysis of mRNA from oncogene-transfected 10T1/2 fibroblasts. Mutant active H-ras most strongly upregulated a RHAMM mRNA transcript of 3.2 kb. GAPDH was used as a control for loading RNA. B) The 5'UTR previously described for a v4 mRNA transcript (10) is confirmed to be present immediately upstream of the exon initiating the v4 open reading frame. This UTR encodes 2 in-frame stop codons upstream of the initiating ATG. C) Primers used for RT-PCR analysis of RHAMM mRNA populations. P3 +(P1 or P4) were used for detecting v5 while P2 +(P1 or P4) were used to detect v4. D) Primers used to detect partial mRNA transcripts confirm a previous study (10) showing an insert of the size expected for v4 and v5 in ras-transformed 10T1/2 fibroblasts. V5 is the major transcript, consistent with Northern Blot analysis. E) Primers used to detect full length mRNA transcript confirm the presence of a minor but full length v4 mRNA and a full length v5 transcript. Again, the v5 transcript is the major RHAMM mRNA. F) RT-PCR was used to detect v4 and v5 transcripts in ras-transformed NIH3T3 fibroblasts.

FIG. 2. Ras-transformed cells express two major RHAMM proteins. A) antibody 1, which detects sequence common to both v5 and v4 forms, reacts with two proteins of 95 and 73 kDa. B) Blocking of antibody with v4 GST-fusion protein abolishes reactivity with the 95 and 73 kDa proteins but not the non-specific protein bands C) antibody 2 was prepared against sequence immediately upstream of v4 and detects v5 and a 90 kDa RHAMM protein but not the 73 kDa protein. D) blocking of antibody with v5 GST-fusion protein abolishes reactivity with the 95 and 90 kDa proteins but not the non-specific protein bands. E) antibody 1 was used to detect v4 and v5 in ras transformed, parental 10T1/2 cells and in 10T1/2 cells transfected with an HA-tagged v4. Note that ras-transformed fibroblasts express more of both v5 and v4 protein than parental 10T1/2 cells, as predicted by Northern blot shown in Fig. 1A. F) The HA tag antibody detects only a 73 kDa RHAMM protein expressed from the v4 cDNA in transfected cells. This protein reacts with

antibody 1 and has an identical MW to the 73 kDa protein expressed in ras transformed cells. A non-specific band is also seen with the HA tag antibody.

FIG. 3. RHAMM proteins are erk1 binding proteins. A) Diagram of the v5 and v4 proteins noting the domains previously shown to be important in cell motility and transformation (14). B) Recombinant v4 and mutant v4 proteins were linked to agarose beads and incubated with His-erk1 fusion protein and bound erk1 protein was separated on SDS-PAGE then identified in western analyses. The ability of unbound v4 protein to compete with erk for v4-agarose beads confirms the specificity of binding. C) In similar assays, His-MEK1 fusion protein did not bind to v4 protein, suggesting that previously noted association of MEK1 with v4 (60) is indirect. D) Identification of D4 and D5 as sites to which erk1 binds. Mutant proteins that contained deletions/mutations of D4-D5, previously implicated in v4 signaling (14, 60) were used for *in vitro* binding assays as described in B above. V4 proteins mutated in D4 and, particularly in D5, showed reduced binding to erk1. Furthermore, peptides mimicking sequence within D4 or D5 also reduced binding of erk1 to v4 in competition assays. The presence of mutations in both D4 and D5 or, in competition assays the presence of both D4 and D5 peptides, reduced erk1 binding to v4 by 90% providing evidence that both domains are involved in this interaction.

FIG. 4. D4 and D5 mediate the association of RHAMM with erk1 *in vivo* A) Mutant v4 proteins were transfected into 10T1/2 cells that express little RHAMM (14). Transfected RHAMM was immunoprecipitated with antibody 3.2 which detects sequence between D4 and D5. Both v4 and v5 RHAMM forms associate *in vivo* with erk1 although v4 appears to bind more erk1 than v5. Deletion of D3, previously shown to be involved in activation of erk1 reduced but did not abolish the interaction of v4 with erk1. Expression of only the D4 and D5 domains (14) permitted binding of erk1 to this RHAMM fragment but binding was reduced compared to intact v4. Deletion or mutation of either D4 or D5 reduced binding of v4 to erk1 beyond detection capability of the assay. B) erk1 expression of cells used in A) to show that erk1 levels were equivalent.

FIG. 5. Confirmation that D5 interacts with peptide sequences. The D5 domain was expressed as a GST-fusion protein and used as bait to screen a random peptide phage display library. The ability of four of these peptides to bind to D5 in ELISA assays is shown in A). To confirm that phage peptides are binding to sequences within the hyaluronan binding motifs, hyaluronan was shown to compete with the phage peptides.

FIG. 6. D3 of RHAMM mediates association with MEK1 *in vivo*. A) RHAMM variants and mutants/deletions were transfected into cells and RHAMM was immunoprecipitated with antibody 3.2. MEK1 was detected in western analyses. Both v5 and v4 associated with MEK1, although more MEK1 associated with v4. Deletion of either the erk1 binding domains, D4 and D5, or D3, required for activating erk1 *in vivo* (60), abolished the association of MEK1 with RHAMM. B). *In vitro* kinase assay using mutant active MEK1 to activate erk1. The addition of v4 did not enhance the ability of erk1 to phosphorylate MBP in this *in vitro* assay.

FIG. 7. Overexpression of v5 does not enhance erk kinase activity *in vivo* or transform fibroblasts. A) focus formation assay shows that transfection of v5 (c) does not enhance focus formation above vector only controls (a) while transfection of either v4 (b) or mutant active ras (d) promote focus formation. B) Stable overexpression of v5 (or v5 protein levels 3.2 fold above vector controls) did not promote activation of erk kinase *in vivo*, as detected by erk kinase assays using immunoprecipitated erk1 and myelin basic protein as a substrate. In contrast, stable overexpression of v4 (v4 protein levels, 3.0 fold above vector controls) activated erk kinase to a similar level as mutant active ras, using identical kinase assays. As previously reported (42), the ability of ras to activate erk kinase required serum supplements in the cell growth medium, as did v4-mediated erk1 activation. C) V4 synergized with mutant active MEK1 to enhance erk kinase activity, detected by erk kinase assays described in (B) and this required the presence of D3. V5 synergized weakly with mutant active MEK1. D) V4 enhanced the ability of mutant active MEK1 to transform fibroblasts and this required D3. Both v4 and mutant active MEK1 transformed

fibroblasts, detected by focus formation, to a similar extent. Co-transfection of both v4 and mutant active MEK1 enhanced transformation by 6 fold. V5, which is not itself transforming, also did not significantly enhance transformation by mutant active MEK1.

FIG. 8. V4 activates AP-1 and enhances expression and release of metalloproteinase MMP-9: This requires the erk1 binding domains of v4. Stable overexpression of v4 enhanced AP-1 activation to a greater extent than a similar level of v5 overexpression. V4 transfected cells expressed increased levels of MMP-9, detected in a Northern blot using GAPDH as RNA loading control. Supernatant medium collected from v4-transfected cells showed a high activity of MMP-9 using a zymogram assay while v5-transfected cells did not. Overexpression of a v4 mutated in its D5 (erk1 binding) domain reduced activity of MMP-9 to the level of v5-transfected cells.

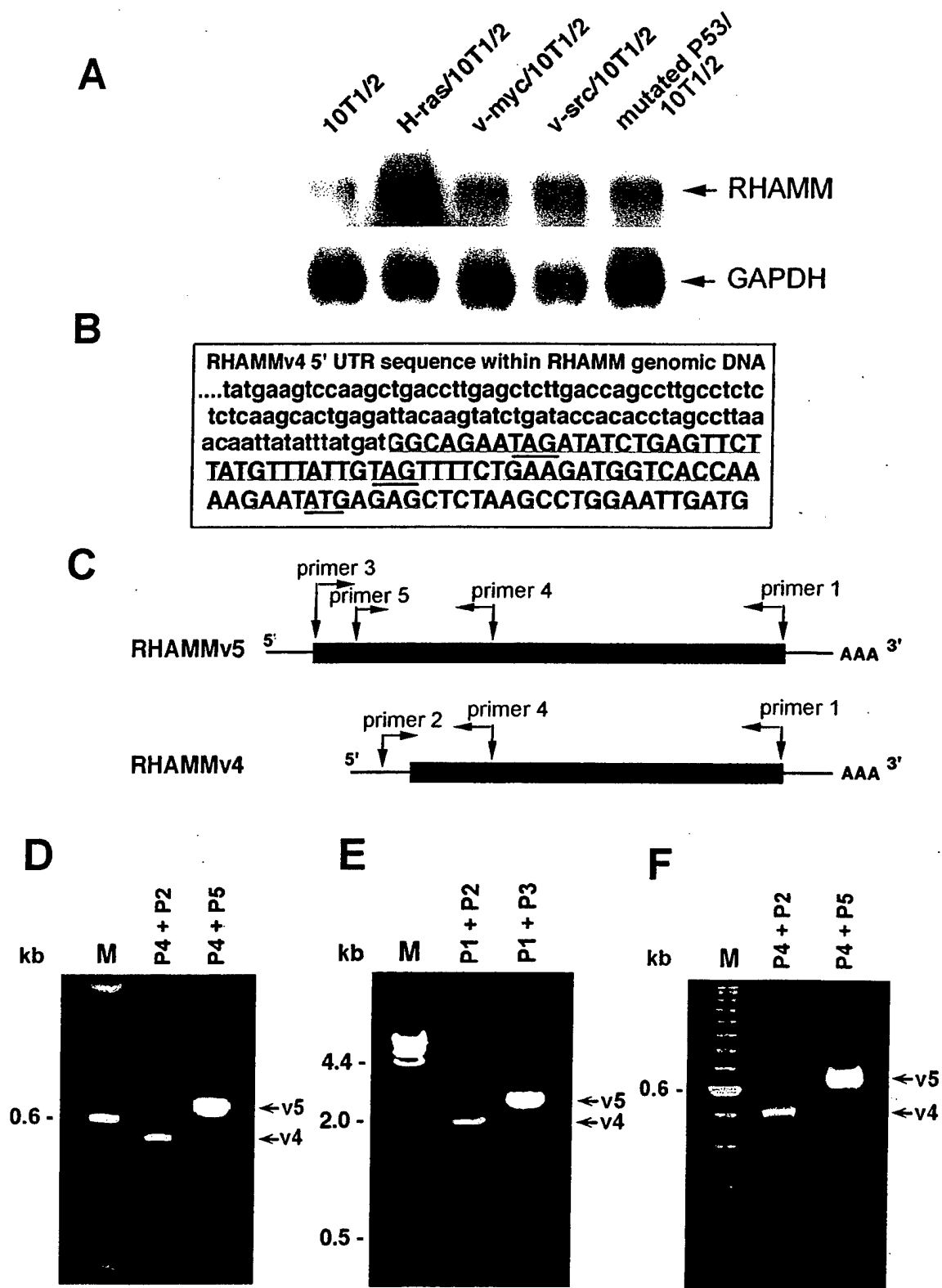


Fig 1

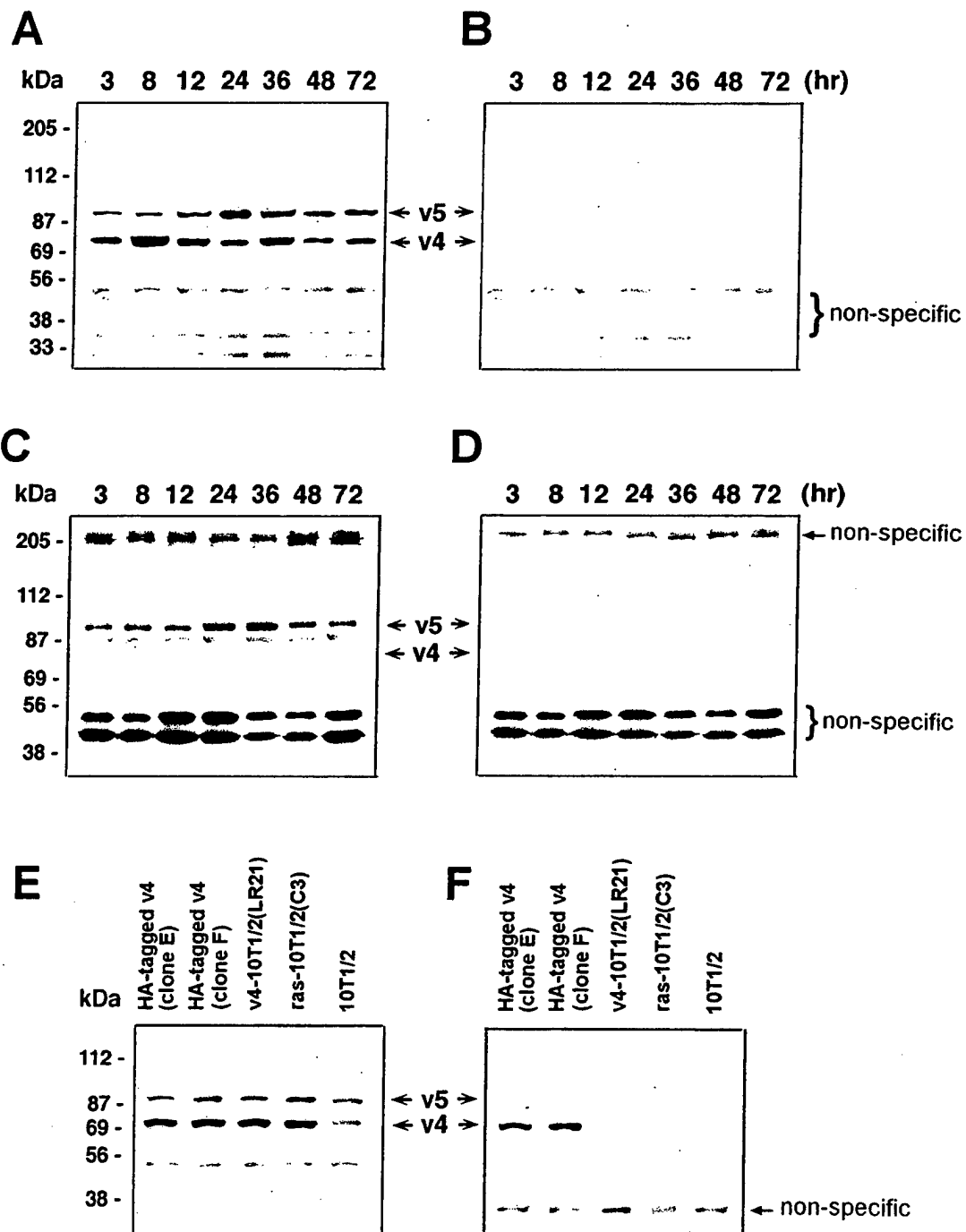
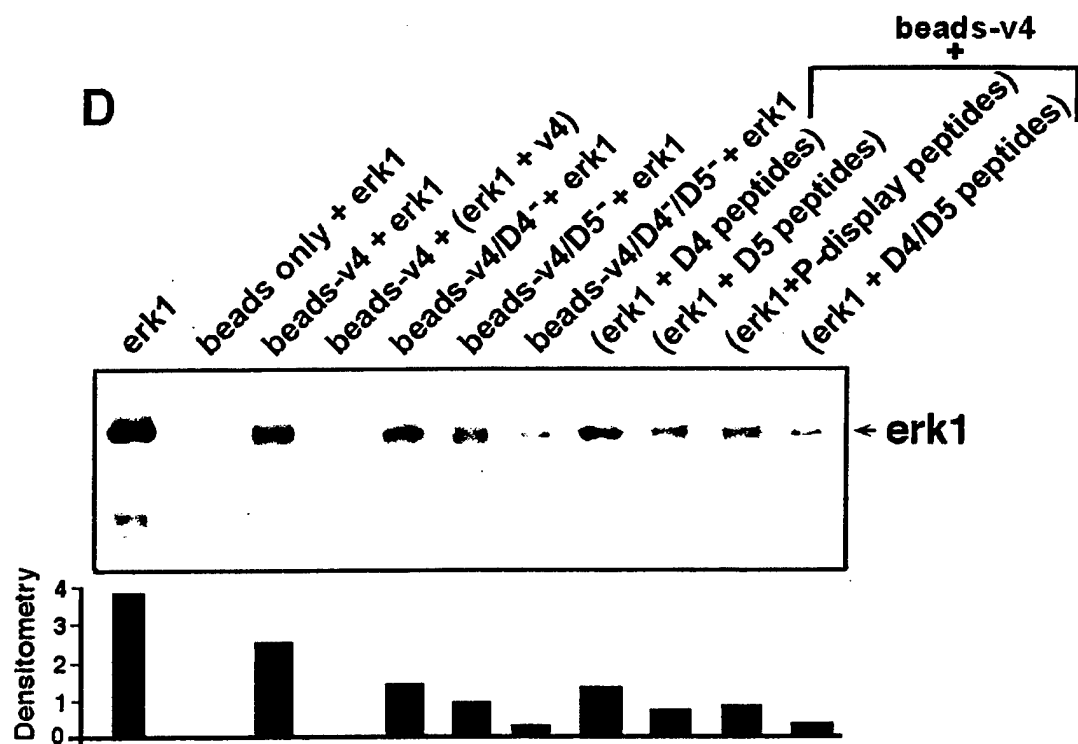
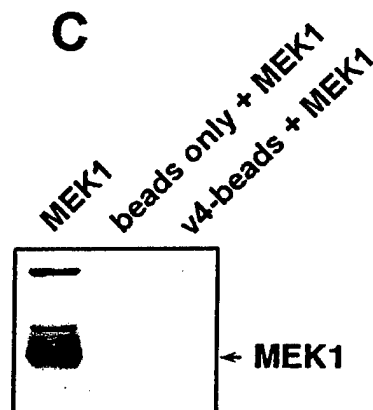
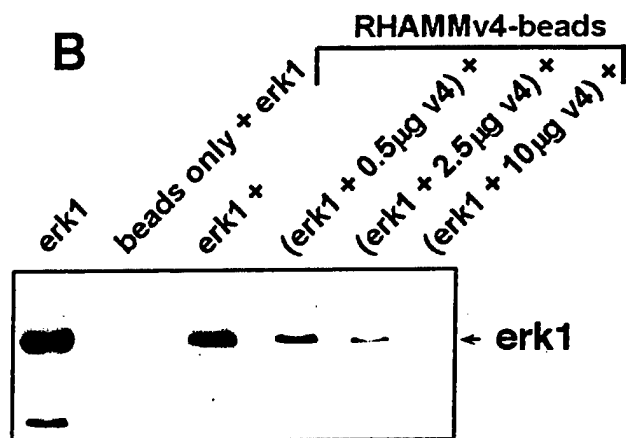
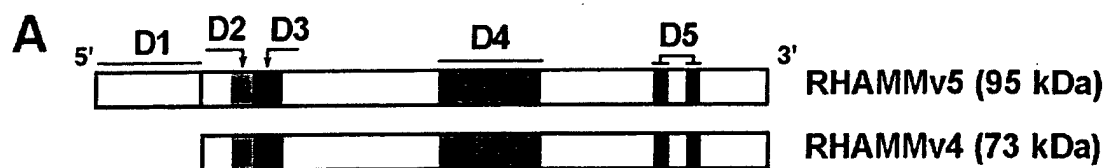
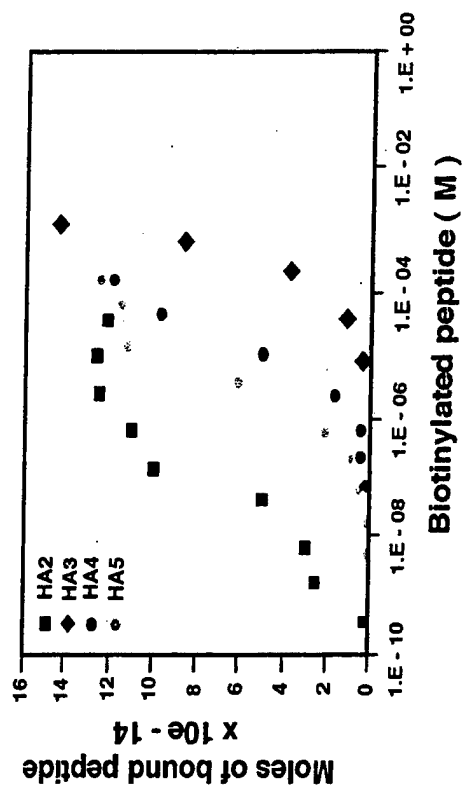


Fig 2



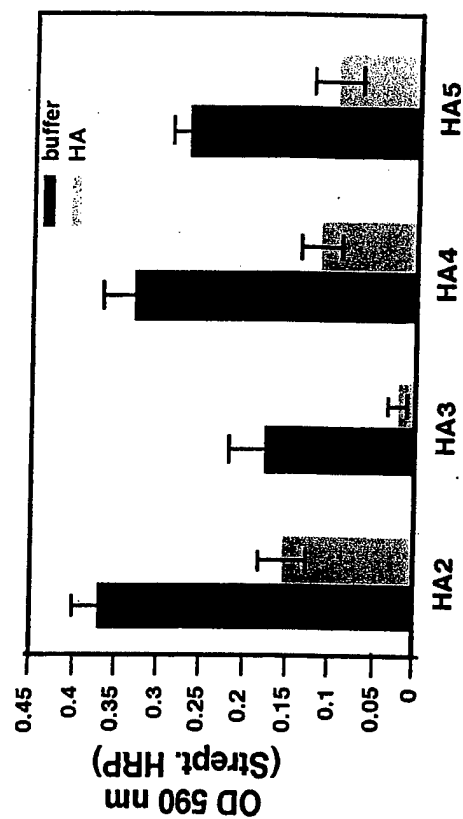
A

Overlay of HA2-5 binding data



B

Competition of phage peptides (HA2-5) bound to GST-P1



Biotinylated HA peptides

Fig 5

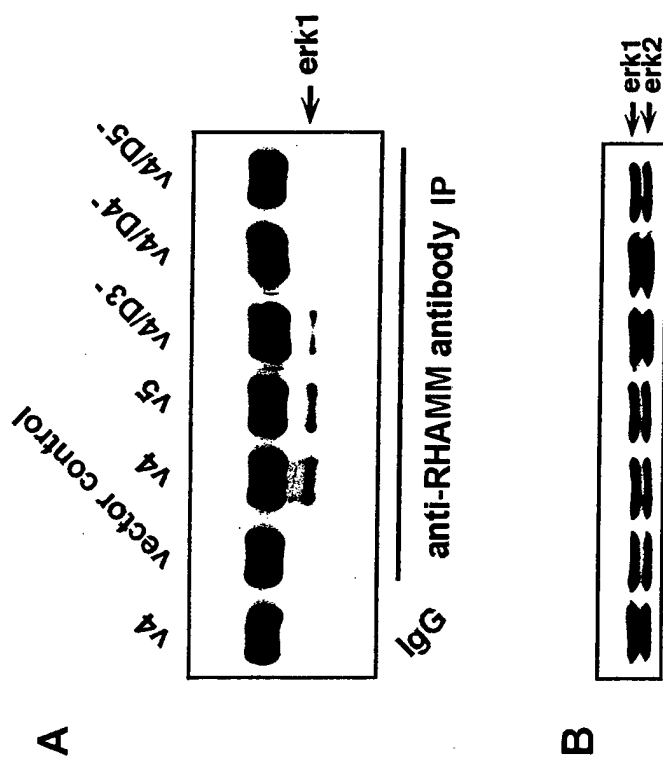


Fig 4

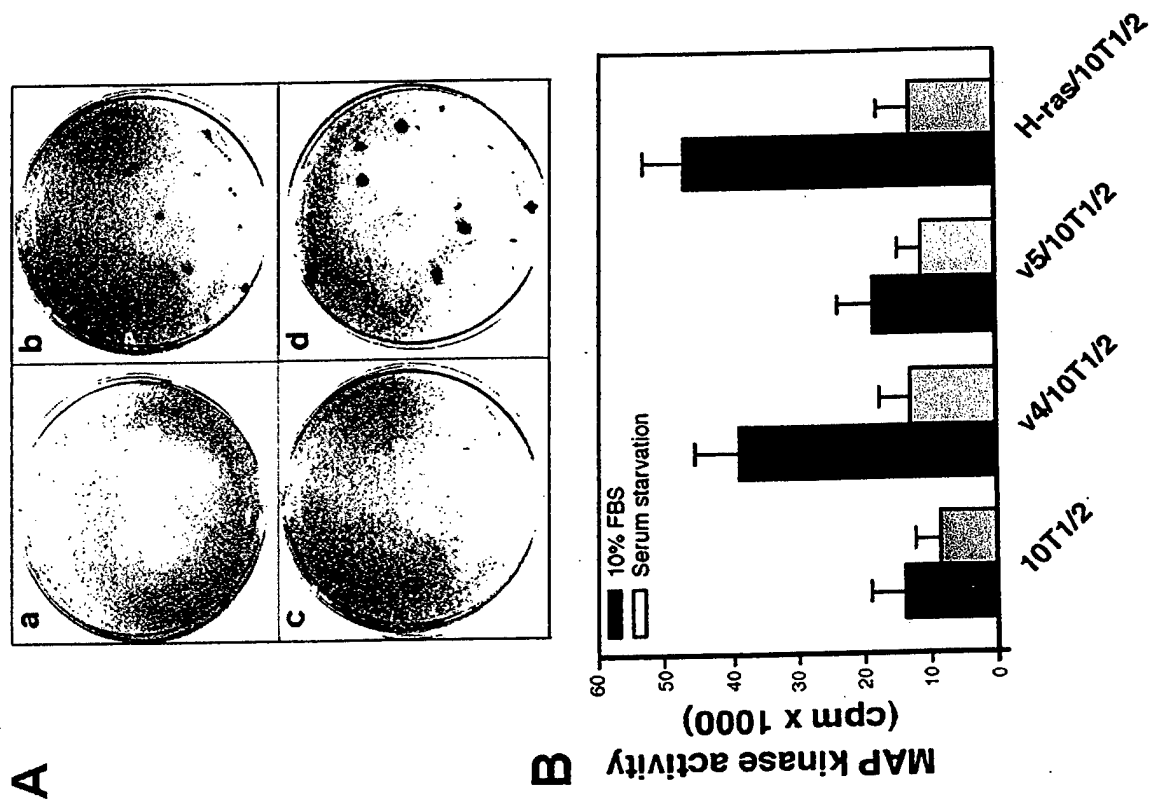


Fig 7

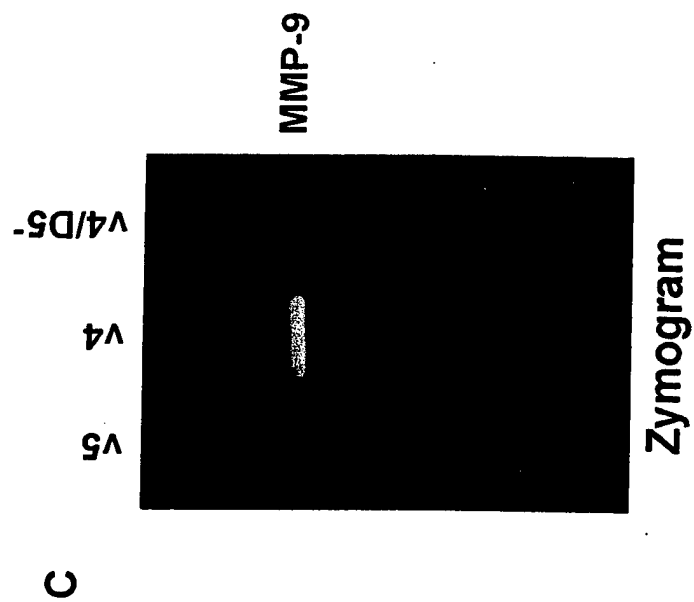
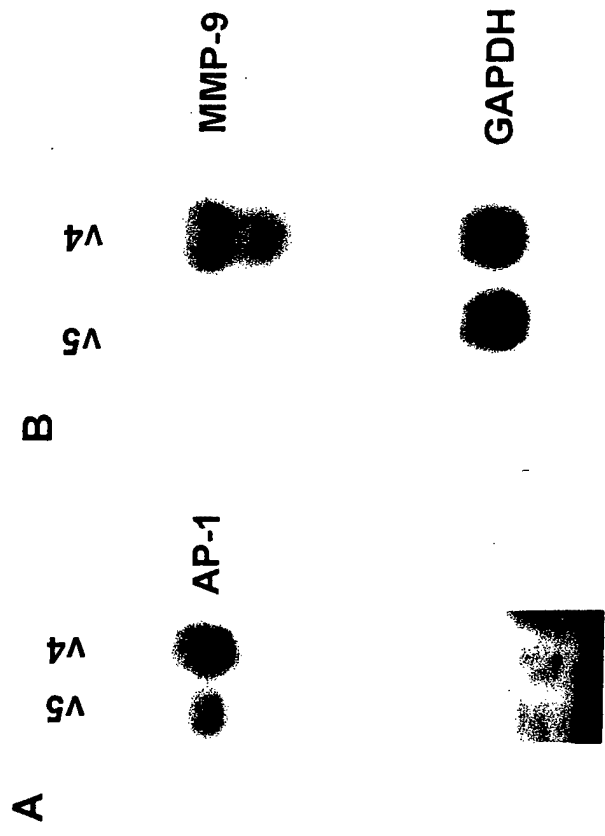


Fig 8

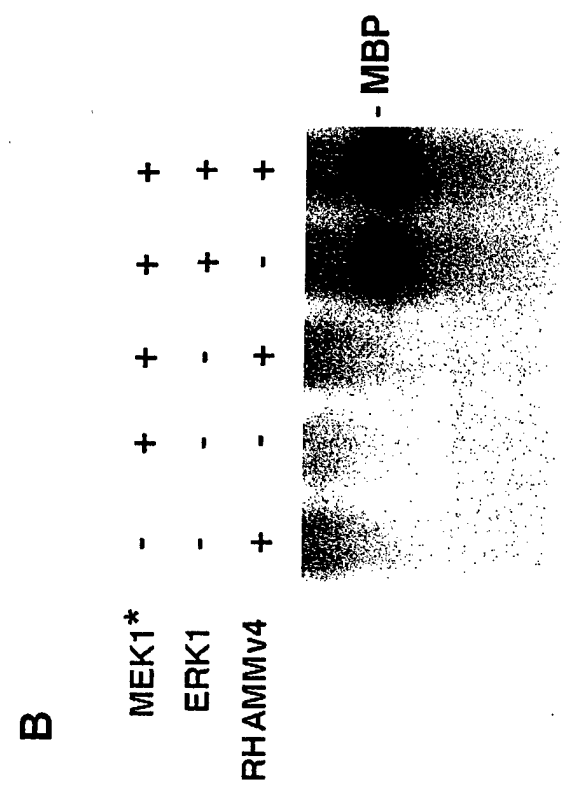
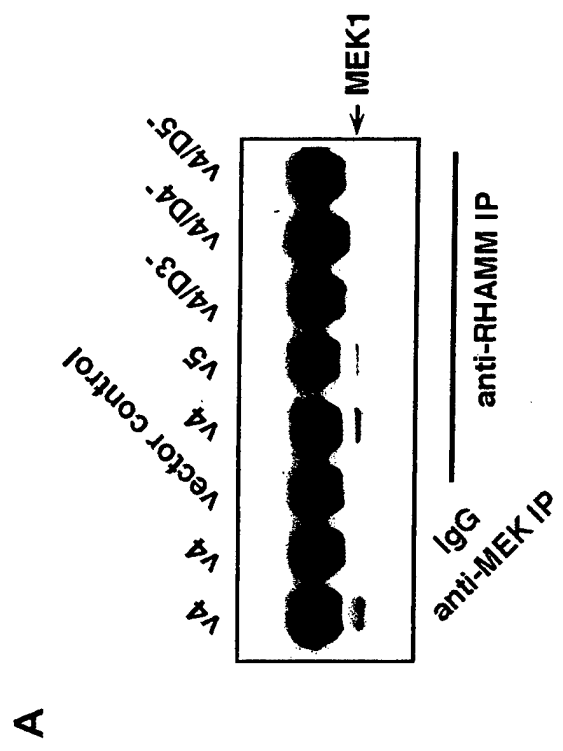
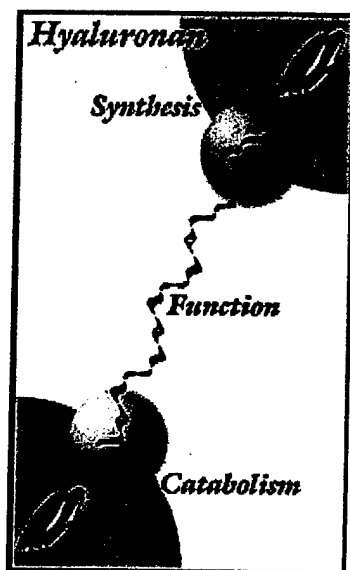


Fig 6



PDF Version(360K)

Biomaterials from Chemically-Modified Hyaluronan

I Introduction

II Chemical Modifications

III Biomaterials and Applications

IV Conclusions

V Acknowledgements

Author's Profile



Glenn D. Prestwich: Dr. Glenn D. Prestwich, Presidential Professor and Chair of Medicinal Chemistry at The University of Utah since 1996, holds concurrent appointments in the Departments of Chemistry, Biochemistry, and Bioengineering. He directs the Center for Cell Signaling, a Utah Center of Excellence, and leads the Molecular Pharmacology Program of the Huntsman Cancer Institute. His research programs comprise isoprenoid biosynthesis and signaling, antiparasitic drugs, phosphoinositide signaling, anti-cancer drugs, and biomaterials for drug delivery and tissue engineering.

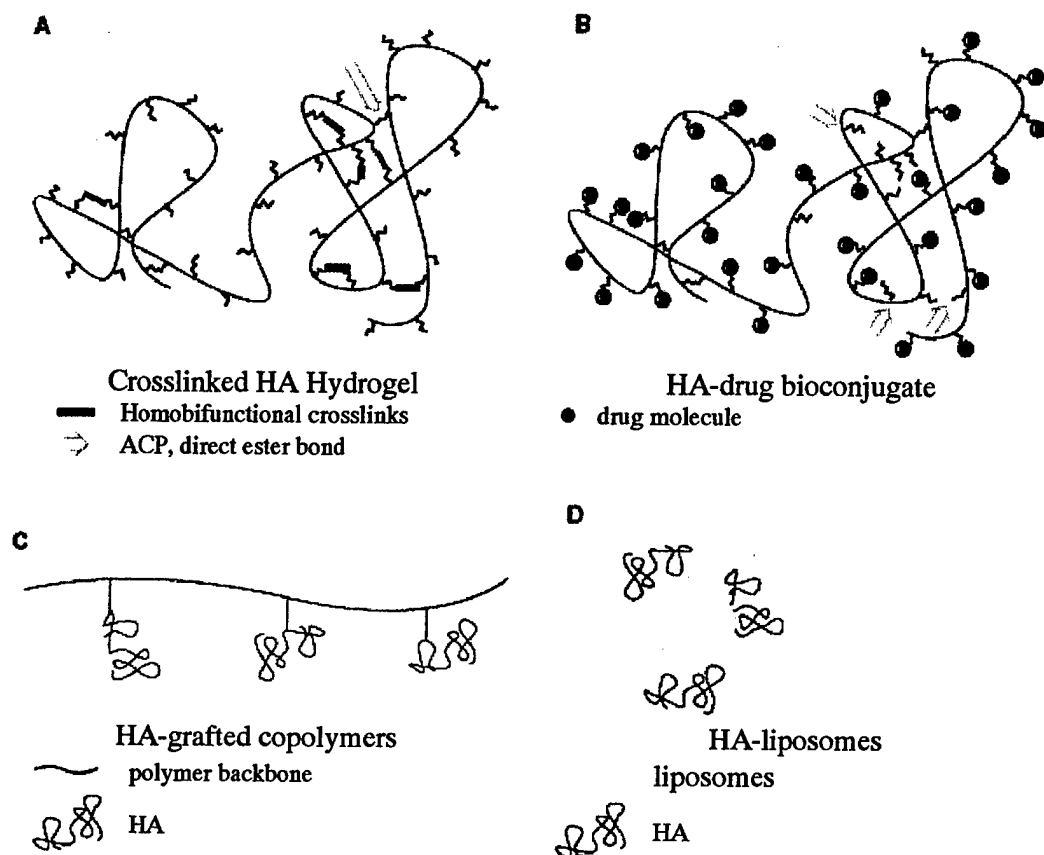
Dr. Prestwich received a B.Sc. (Honors) in Chemistry (California Institute of Technology, 1970), and a Ph.D. (Chemistry, Stanford University, 1974). He was an NIH postdoctoral fellow at Cornell University and at the International Centre for Insect Physiology and Ecology in Nairobi, Kenya (1974-77). From 1977 to 1996, he was Professor of Chemistry and of Biochemistry and Cell Biology, and Director of the Center for Biotechnology at The University

of Stony Brook, New York. Awards include an Alfred P. Sloan Research Fellowship, a Dreyfus Teacher-Scholar Award, and the 1998 Paul Dawson Biotechnology Award of the American Association of Colleges of Pharmacy.

Dr. Prestwich has published over 390 technical papers and has trained over 100 graduate and postdoctoral scientists. He is Vice President for Research for Echelon Research Laboratories, Inc. (Salt Lake City, Utah) and consultant to Clear Solutions Biotech, Inc. (Stony Brook, New York), both of which he co-founded to commercialize technologies from his laboratories.

I Introduction Hyaluronan (HA), an abundant non-sulfated glycosaminoglycan component of synovial fluid and extracellular matrices, is an attractive building block for new biocompatible and biodegradable polymers that have applications in drug delivery, tissue engineering, and viscosupplementation. However, the fabrication of new biomaterials is precluded by the poor biomechanical properties of hyaluronan. A variety of chemical modifications of native hyaluronan have been devised to provide mechanically and chemically robust materials. The resulting hyaluronan derivatives have physicochemical properties that may significantly differ from the native polymer, but most derivatives retain the biocompatibility and biodegradability, and in some cases the pharmacological properties, of native hyaluronan. This review will summarize what chemical modifications of hyaluronan have been accomplished, what kinds of novel biomaterials have been prepared, and what applications have been foreseen or developed for tissue engineering, wound healing, surgical adhesions, and drug delivery.

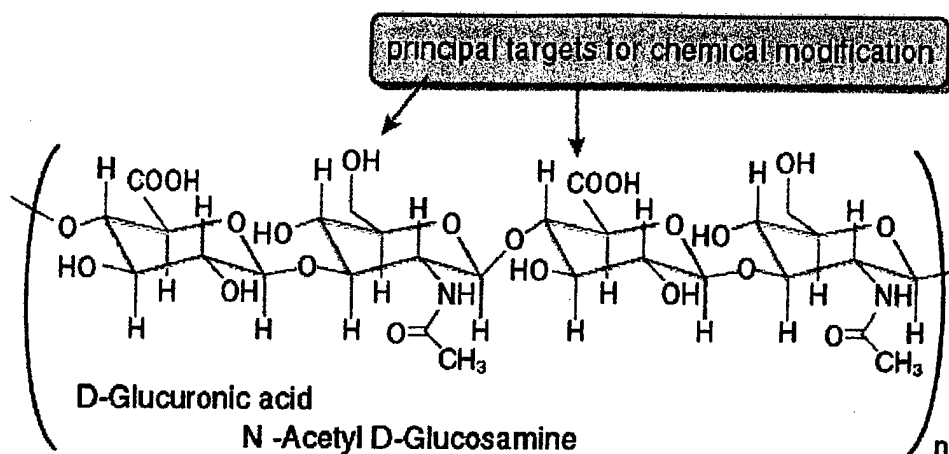
Figure 1 illustrates several molecular architectures employed in preparing hyaluronan derivatives or hyaluronan composites. The prototypical modification is conversion of the viscous sol form to a cross-linked hydrogel (Figure 1A). This modification has been accomplished under mild, neutral conditions and under alkaline conditions, and specific examples will be described. Alternatively, several methods have been devised for functionalization of hyaluronan with tethering groups that permit attachment of reporter groups (Figure 1B) in order to give new reagents for biochemical and physiological studies, or with pharmacophores to provide novel prodrugs for targeted, controlled release. The preparation of composite materials has been realized in the past decade, with hyaluronan being grafted onto natural and synthetic polymers to provide new materials with altered biomechanical and physiological properties (Figure 1C). Finally, hyaluronan can be grafted onto the surfaces of liposomes (Figure 1D), as an alternative to poly(ethyleneglycol) (PEG) coating in "stealth" liposomes, with the added benefit that hyaluronan can provide a targeting as well as a masking effect.

**Figure 1**

Schematic depiction of architectures of hyaluronan (HA) derivatives: (A) cross-linked hyaluronan; (B) hyaluronan-drug bioconjugate; (C) hyaluronan-grafted co-polymer; and (D) hyaluronan-liposome composite.



II Chemical Modifications Figure 2 shows the chemical structure of hyaluronan with the two most commonly used sites of covalent modification: the carboxylic acid and hydroxyl functionalities. Below the basic chemistry of these modifications is reviewed, and the uses of these and other reactions to produce biomedically useful hyaluronan-derived materials is explored. Figure 3 summarizes the chemical details of several of the reactions described below. Selected references to the primary literature on the chemical modifications are provided, and the remainder can best be accessed by referring to three recent reviews and a recent symposium volume.¹⁻⁴

**Figure 2**

Tetrasaccharide fragment of hyaluronan showing the disaccharide repeat units and primary sites for chemical modification.

A. Reactions of carboxyl groups

1. Esterification

Esterified hyaluronan biomaterials have been prepared by alkylation of the tetra(*n*-butyl)ammonium salt of hyaluronan with an alkyl halide in dimethylformamide (DMF) solution (Figure 3A).⁵ At higher percentages of esterification, the resulting HYAFF[®] materials (Fidia Advanced Biopolymers) became insoluble in water. These hyaluronan esters can be extruded to produce membranes and fibers, lyophilized to obtain sponges, or processed by spray-drying, extraction, and evaporation to produce microspheres. These polymers show good mechanical strength when dry, but the hydrated materials are less robust. The degree of esterification influences the size of hydrophobic patches, which produces a polymer chain network that is more rigid and stable, and less susceptible to enzymatic degradation.

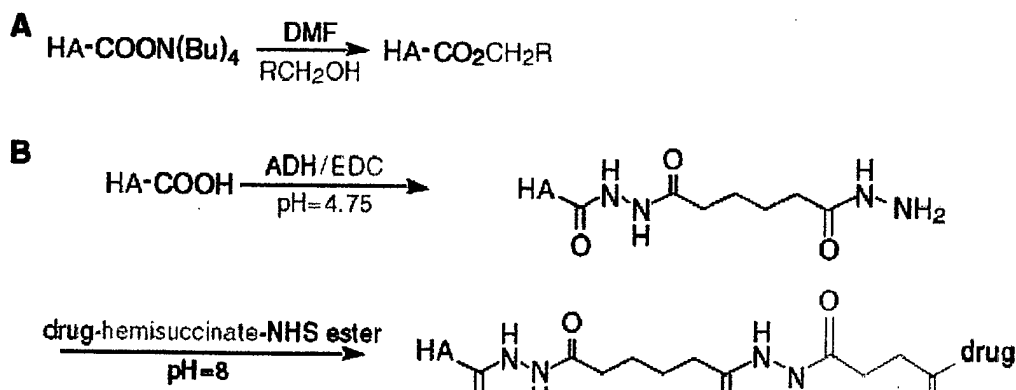
Drug release from HYAFF[®]-based devices was examined for entrapped or covalently-attached molecules. For example, release of the steroids hydrocortisone and α -methylprednisolone from microspheres fabricated from different HYAFF[®] materials was examined with the drug either dispersed or bound to the polymer. While the hydrocortisone diffused out of the microspheres in 10 min, the release rate of the covalently bound drug was found to show zero-order release ($t_{1/2} = 100$ h) by hydrolysis of the ester. Microspheres and thin films of hyaluronan benzyl esters have been found to be the most suitable physical forms for drug and peptide delivery, since the hydrophobic, mucoadhesive properties facilitated intranasal, buccal, ocular, and vaginal delivery. Finally, hyaluronan benzyl ester materials have been used as meshes and sponges for growth of cultured human fibroblasts and for culture of chondrocytes and bone-marrow derived mesenchymal cells for repair of cartilage and bone defects.

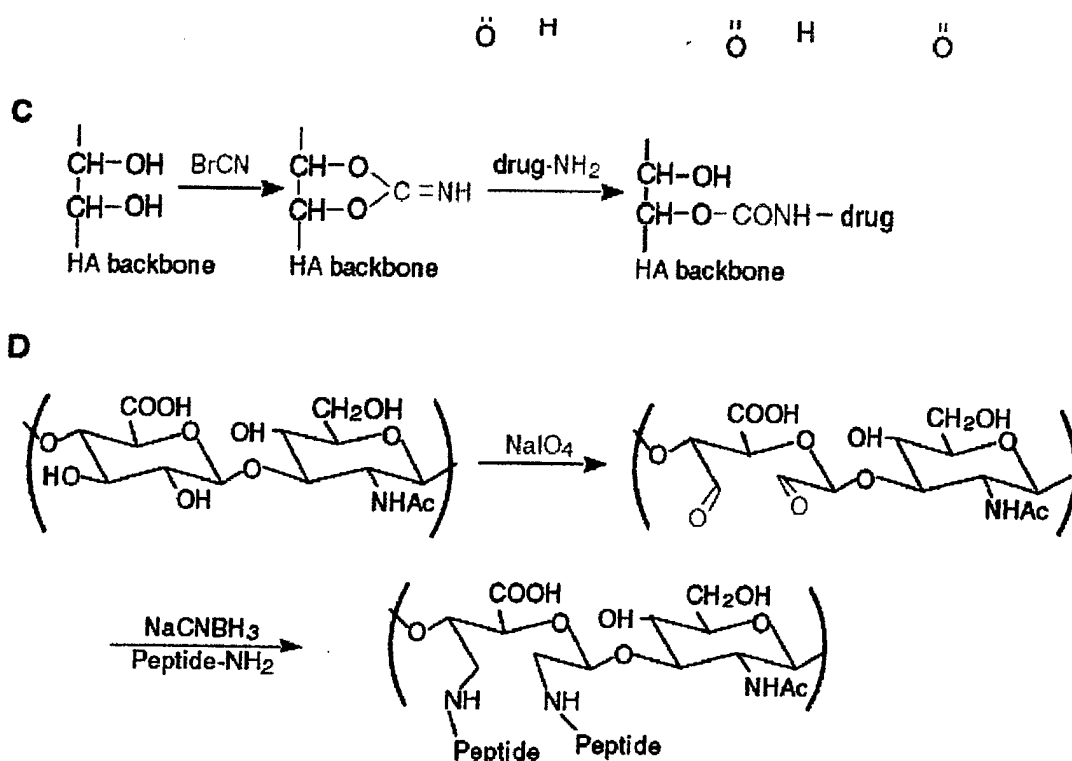
2. Carbodiimide-mediated reactions

The chemical modification of the carboxylic functions of hyaluronan by carbodiimide compounds is generally performed in water at pH 4.75. At this pH, the carboxylic acid is protonated, but a small percentage of the amine base may remain in nucleophilic form to produce a covalent adduct. However, little or no amide product was produced in attempted carbodiimide-mediated coupling of primary amines to hyaluronan. Instead, the major product was the rearranged *N*-acylurea adduct.⁶

An important milestone in hyaluronan modification chemistry was the recognition that hydrazides, which have pKa values between 2 and 4 for the corresponding conjugate acids, would retain their nucleophilicity at pH 4.75 and would couple efficiently to carbodiimideactivated glucuronic acid residues of hyaluronan (Figure 3B).⁷ The use of dihydrazide compounds, such as adipic dihydrazide (ADH), provided multiple pendant hydrazide groups for further derivatization with drugs, biochemical probes, and for cross-linking agents. Thus, the pendant hydrazide groups of ADH-modified hyaluronan can be loaded with drug molecules and then cross-linked into a hydrogel; the drug would then be present in the bulk of the hydrogel. Alternatively, a limited number of the hydrazide groups could be cross-linked and the remaining hydrazide groups on the resulting hydrogel could be loaded with a therapeutic agent. For example, HA-Taxol[®] bioconjugates were synthesized by the conjugation of HA-ADH and ester activated Taxol[®]. Labeling of the HA-ADH-Taxol conjugate with a fluorescent dye allowed monitoring uptake of the conjugate by human breast, ovarian, and colon cancer cells, and measurement of the corresponding selective toxicity of the polymeric prodrug.⁸

Other carbodiimide-mediated reactions of hyaluronan have employed hydroxylaminecontaining species to obtain hyaluronan-activated esters. For example, reaction of hyaluronan with a large excess of an amine or amino acid at pH 6.8 in the presence of a soluble carbodiimide and 1-hydroxybenzotriazole (HOBt) in aqueous dimethylsulfoxide (DMSO) gave efficient production of hyaluronan amide products.



**Figure 3**

Chemical modifications of carboxylic acid and hydroxyl groups of hyaluronan: (A) esterification; (B) bishydrazide modification; (C) cyanogen bromide activation; and (D) periodate oxidation.

B. Reactions with hydroxyl groups

1. Sulfation

In order to obtain a blood-compatible material for medical device coating, approaches involving sulfating the OH group present in the hyaluronan molecule were devised. The sulfation of hyaluronan with a sulfur trioxide-pyridine complex in DMF produced different degrees of sulfation, HyalS_x, where x = 1 - 4 per disaccharide. The sulfated hyaluronic acid HyalS_{3.5} was then immobilized onto plasma-processed polyethylene (PE) using a diamine polyethylene glycol derivative and a water-soluble carbodiimide. The thrombin time test and platelet adhesion behavior indicated that this procedure was promising for the preparation of blood-compatible, anti-thrombotic PE surfaces. In addition, HyalS_x was converted to a photolabile azidophenylamino derivative and was photoimmobilized onto a poly(ethylene terephthalate) (PET) film.⁹ Surfaces coated with sulfated hyaluronan exhibited a marked reduction of cellular attachment, fouling, and bacterial growth compared with uncoated surfaces, and the coating was stable to degradation by chondroitinase and hyaluronidase.

2. Esterification

Butyric acid, which is known to induce cell differentiation and to inhibit the growth of a variety of human tumors, was coupled to hyaluronan *via* the reaction between butyric anhydride and the *sym*-collidinium salt of low molecular weight hyaluronan in DMF containing dimethylaminopyridine. Hyaluronan butyrate

thus offered a novel drug-delivery system targeted specifically to tumor cells.

3. Isourea coupling

The anthracycline antibiotics adriamycin and daunomycin were coupled to hyaluronan *via* cyanogen bromide (CNBr) activation (Figure 3C). This reaction scheme is commonly used to activate oligosaccharides to produce affinity matrices *via* a highly-reactive isourea intermediate. The therapeutic agents appear to become attached *via* a urethane bond to one of the hydroxylic functions of the oligosaccharide or the glycosaminoglycan, but no spectroscopic verification was provided. Moreover, the harshness of the reaction conditions may compromise the integrity and biocompatibility of the hyaluronan.

4. Periodate oxidations

Reactive bisaldehyde functionalities can be generated from the vicinal secondary alcohol functions on hyaluronan (see Figure 3D) by oxidation with sodium periodate. This chemistry is a standard method for chemical activation of glycoproteins for affinity immobilization or conversion to a fluorescent probe. With periodate-activated hyaluronan, reductive coupling with primary amines can give cross-linking, attachment of peptides containing cell attachment domains, or immobilized materials. The harsh oxidative treatment also introduces chain breaks and potentially immunogenic linkages into the hyaluronan biomaterial.

C. Reducing end modification

Reductive amination of the reducing end of hyaluronan has been employed to prepare affinity matrices, fluorophore-labeled materials, and hyaluronan-phospholipids for insertion into hyaluronan-liposomes. For example, low molecular weight hyaluronan was covalently attached to phosphatidyl ethanolamine, and this conjugate has been employed for a protective "sugar decoration" on the surface of low density lipoprotein (LDL) particles.

End-labeling has not otherwise been extensively used for hyaluronan biomaterials or pro-drug applications, since there is only one attachment point per glycosaminoglycan. This severely limits loading and cross-linking possibilities for high molecular weight hyaluronan.

D. Amide modifications

Native hyaluronan has, in some preparations, an undetermined number of naturally deacylated glucosamine units that may also be derivatized. As with the reducing end modification, this provides very low modification rates. However, modification of the *N*-acetyl groups can be important if the commonly used hydrazinolysis method is employed. Limited hydrazinolysis of hyaluronan creates free glucosamine residues on hyaluronan, but can also result in base-induced backbone cleavage and reducing end modification.

E. Crosslinking strategies

The processes described below often employ the principal reactions discussed above. Nonetheless, they are discussed separately to focus on the process of converting bulk hyaluronan to a mechanically robust material, as opposed to the more selective and controlled modifications described above. Surface immobilization methods are also described in this section. Figure 4 illustrates the chemistry of selected crosslinking strategies, and Figure 5 illustrates one method of covalent surface modification with hyaluronan.

1. Bisepoxide and divinylsulfone crosslinking

Laurent prepared a cross-linked gel of hyaluronan in dilute NaOH using bisepoxybutane and sodium borohydride, a strategy first developed for cross-linking of agarose.¹⁰ Reaction of hyaluronan with ethyleneglycol diglycidyl ether in ethanolic 0.1 N NaOH at 60 °C also afforded a hydrogel (Figure 4A). The resulting gels had high water contents (>95%) and were investigated for use as an inflammation (stimulus)-responsive degradable matrix for implantable drug delivery. A hydrogel prepared from hyaluronan and alkaline 1,4-butanediol diglycidyl ether was highly porous. This material was then activated with periodate and then modified with an 18-amino acid peptide containing a cell attachment domain, ArgGly-Asp (RGD), to enhance cell attachment to the hydrogel. In alkaline medium, divinyl sulfone also crosslinks hyaluronan, most likely via reaction with hydroxyl groups (Figure 4B).

2. Internal esterification

The autocross-linked polymer (ACP™, Fidia) is an internally esterified derivative of hyaluronan, with both inter and intramolecular bonds between the hydroxyl and carboxyl groups of hyaluronan. ACP™ can be lyophilized to a white powder and hydrated to a transparent gel. This novel biomaterial has been used as a barrier to reduce post-operative adhesions as a consequence of abdominal and gynecological surgery and as a scaffolding for cell growth repair of tissue defects. Cartilage and bone regeneration occurred in subcutaneously implanted porous sponges of ACP™ that had been seeded with chondrocytes or osteoblasts.

3. Photocross-linking

A methacrylate derivative of hyaluronan was synthesized by the esterification of the hydroxyls with excess methacrylic anhydride, as described above for hyaluronan butyrate. This

derivative was photocross-linked to form a stable hydrogel using ethyl eosin in 1-vinyl-2-pyrrolidone and triethanolamine as an initiator under argon ion laser irradiation at 514 nm. The use of *in situ* photopolymerization of an hyaluronan derivative, which results in the formation of a cohesive gel enveloping the injured tissue, may provide isolation from surrounding organs and thus prevent the formation of adhesions. A preliminary cell encapsulation study was successfully performed with islets of Langerhans to develop a bioartificial source of insulin.

4. Glutaraldehyde cross-linking

Hyaluronan strands extruded from cation-exchanged sodium hyaluronate (1.6 MDa) were cross-linked in glutaraldehyde aqueous solution, although the chemical nature of this process was not identified. The strand surfaces were then remodeled by attachment of poly-D- and poly-L-lysine. The polypeptide resurfaced hyaluronan strands showed good biocompatibility and promoted cellular adhesion.

5. Metal cation-mediated cross-linking

Intergel[®] (FeHA, LifeCore) is a hydrogel formulation of hyaluronan formed by chelation with ferric hydroxide. Similar cross-linking of hyaluronan has been the basis of preparations using copper, zinc, calcium, barium, and other chelating metals. The reddish FeHA gel is in development for prevention of post surgical adhesions.

6. Carbodiimide cross-linking

Incert[®] is a bioresorbable sponge (Anika Therapeutics) prepared by cross-linking hyaluronan with a biscarbodiimide (Figure 4C) in aqueous isopropanol.¹¹ This procedure takes advantage of the otherwise undesirable propensity of carbodiimides to react with hyaluronan to form *N*-acylureas. In this application, the formation of two *N*-acylurea linkages provides a chemically stable and byproduct-free cross-link.

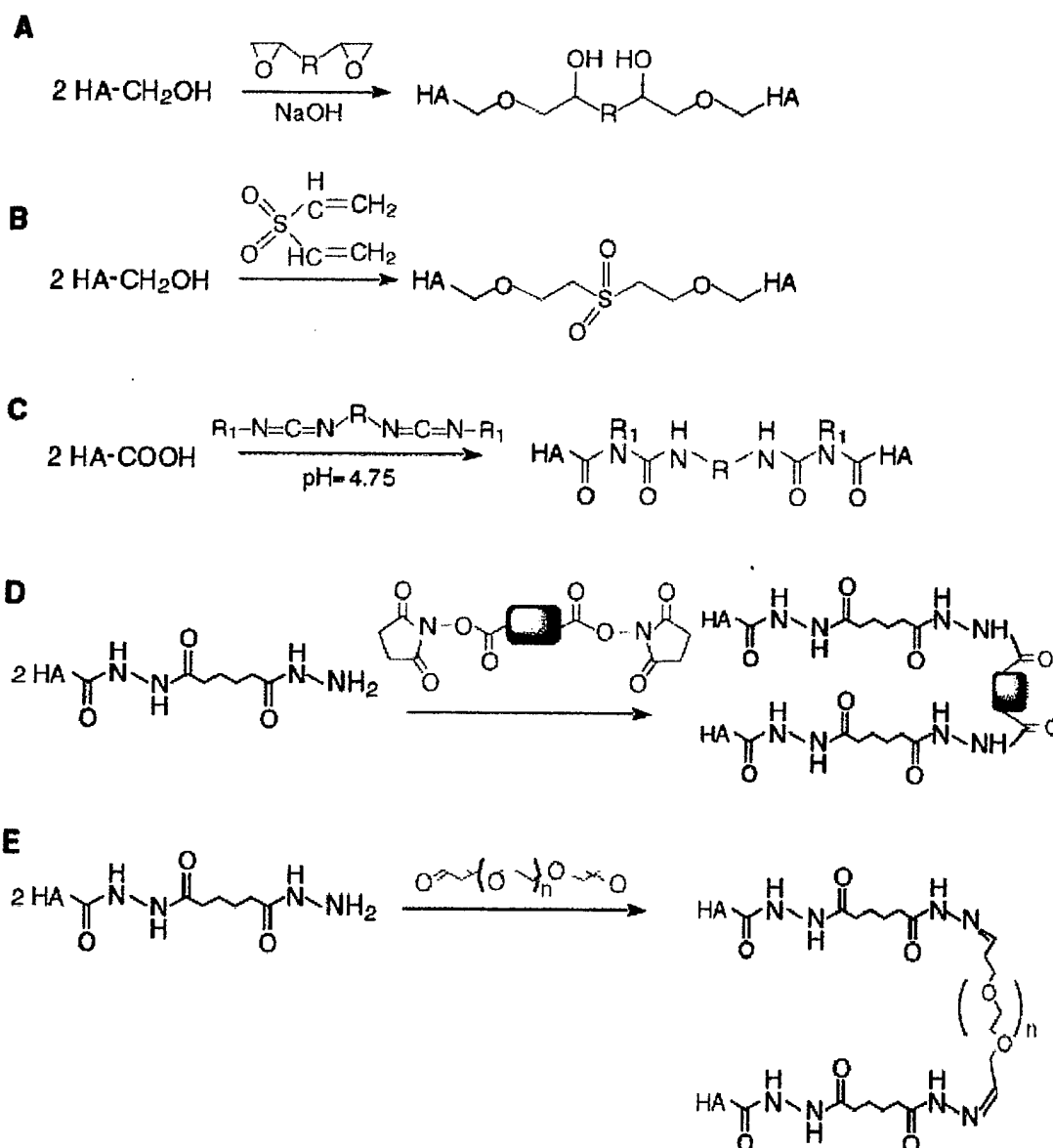
Because of the hydrophobic biscarbodiimides employed, Incert[®] adheres to tissues without the need for sutures and retains its efficacy even in the presence of blood. Recently, it was found to be effective at preventing post-operative adhesions in a rabbit cecal abrasion study.

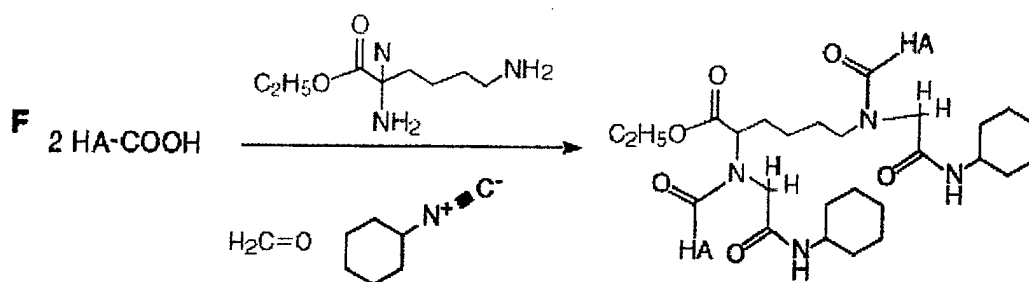
A low-water content hyaluronan hydrogel film was made by cross-linking a hyaluronan (1.6 MDa) film with a watersoluble carbodiimide as a coupling agent in an aqueous mixture containing a water-miscible non-solvent of hyaluronan. The highest degree of cross-linking that gave a low-water content hydrogel was achieved in 80% ethanol. This film, having 60% water content, remained stable for two weeks after immersion in buffered solution. The cross-linking of hyaluronan films with a water-soluble carbodiimide in the presence of Llysine methyl ester further prolonged the *in vivo* degradation of a hyaluronan film.

7. Hydrazide cross-linking

Using the hydrazide chemistry described above, hydrogels have been prepared using bishydrazide, trishydrazide, and polyvalent hydrazide compounds as cross-linkers. By adjusting the reaction conditions and the molar ratios of the reagents, gels with physicochemical properties ranging from softpourable gels to more mechanically-rigid and brittle gels could be obtained. HA-ADH can be cross-linked using commercially available small molecule homobifunctional crosslinkers (Figure 4D).

More recently, an *in situ* polymerization technique was developed by cross-linking HA-ADH with a macromolecular cross-linker, PEG-dialdehyde under physiological conditions (Figure 4E).¹² Biocompatible and biodegradable hyaluronan hydrogel films with well-defined mechanical strength were obtained after the evaporation of solvent. Macromolecular drugs were released slowly from these hyaluronan hydrogel films, and these new materials accelerated re-epithelialization during wound healing.



**Figure 4**

Chemical cross-linking strategies for hyaluronan: (A) bisepoxide cross-linking; (B) divinylsulfone cross-linking; (C) biscarbodiimide strategy; (D) use of small homobifunctional linkers with HA-ADH; (E) network formation with a macromolecular cross-linker; (F) cross-linked hydrogel formation *via* an Ugi four-component condensation of hyaluronan with formaldehyde, cyclohexyl isocyanide, and lysine ethyl ester.

8. Crosslinking with residual proteins

Hylans (Biomatrix) are hydrogels or hydrosols formed by cross linking hyaluronan-containing residual protein with formaldehyde in a basic solution.¹³ Soluble hylan is a high molecular weight form (8 - 23 MDa) of hyaluronan that exhibits enhanced rheological properties compared to hyaluronan. Hylan gels have greater elasticity and viscosity than soluble hylan materials, while still retaining the high biocompatibility of native hyaluronan. Hylans have been investigated in a number of medical applications. In the treatment of degenerative joint disease and rheumatoid arthritis, hylan was found to protect cartilage and prevent further chondrocyte injury, although the effect was reversible and viscosity-dependent. The hylan product Synvisc® has been developed specifically as a device for viscosupplementation therapy in osteoarthritis. It can increase the viscoelastic properties of the synovial fluid and the intercellular matrix of the synovial tissue and capsule.

Clinical trials of Hylan B™ gel slurry injections (Hylaform® gel) showed that it could be a safe and effective material for soft tissue augmentation, including vocal fold viscosupplementation in a rabbit model. The gel can remain in place for 12 months, allowing the in-growth of newly-formed connective tissue after only one month without causing inflammation or adverse reactions. Hylans have been used in plastic surgery for intradermal implantations and cosmetic injection, as has Restylane® (Q-Med Inc), a partially-cross-linked hyaluronan derivative for soft tissue augmentation available in Europe since 1995. Hylagel® is an engineered hylan gel being investigated as an adjuvant to prevent post-surgical adhesions. Finally, hylans can be used as drug carriers by the incorporation of therapeutic agents. For example, the *in vitro* biological activity of cytokine interferon was enhanced by approximately 40% as a result of its covalent attachment to a hylan matrix.

9. Multi-component reactions

Hyaluronan derivatives can also be prepared *via* three- and four-

component reactions known as the Passerini reaction and Ugi reactions.¹⁴ In the Passerini reaction, an aqueous solution of hyaluronan is mixed with aqueous glutaraldehyde (or another water-soluble dialdehyde) and added to a known amount of a highly reactive isocyanide, *e.g.*, cyclohexylisocyanide. In the Ugi four-component reaction (Figure 4F), a diamine is added to this three-component mixture. The degree of cross-linking is controlled by the amount of aldehyde and diamine. Figure 4F illustrates an Ugi condensation of hyaluronan (as the acid component) with cyclohexylisocyanide, formaldehyde, and lysine ethyl ester (as the diamine) to give a hydrogel. Such hydrogels are transparent, mechanically stable, swell in aqueous salt solutions, and exhibit values of the compression modulus that depend on the degree of cross-linking.

10 . Surface modification

Surfaces of polypropylene (PP) and polystyrene (PS) were activated with argon gas and ammonia gas plasmas to aminate the polymer surface. Aminated surfaces were then modified with succinic anhydride to give pendant carboxylic acid groups on the surface, which were then condensed with HA-ADH in the presence of a carbodiimide to give hydrophilic, nonadhesive, and lubricious plastic surfaces (Figure 5).¹⁵ As described above, surfaces can also be modified with sulfated hyaluronan via a plasma-etching protocol. Alternatively, cell-adhesive surfaces have been produced by surface modification with HAADH containing tethered fibronectin (RGD) peptides. Metal and glass surfaces can also be modified by surface activation followed by covalent chemical attachment of an appropriate hyaluronan derivative.

Click here

Figure 5

Plasma-etch method for activation of polypropylene with ammonia plasma, modification by succinic anhydride, and covalent modification with the hyaluronan derivative HA-ADH.



Biomaterials and Applications

A. Hyaluronan-liposomes

Unmodified hyaluronan has been incorporated into liposomes. For example, hyaluronan was combined with cyclosporin A and encapsulated within phospholipid liposomes. Hyaluronan (M_w 10 kDa and 1,000 kDa) powder was hydrated with these liposomes to provide a final concentration of 2.5 wt% HA. The solution was developed as a topically administered pharmaceutical agent, and was found to effectively treat skin disorders while minimizing systemic circulation.

Bioadhesive liposomes, in which hyaluronan is the surface-anchored

bioadhesive ligand on a liposome surface, were prepared by the pre-activation of hyaluronan with a carbodiimide.¹⁶ This activated form was then added to a suspension of multi-lamellar liposomes consisting of phosphatidylcholine, phosphatidylethanolamine, and cholesterol. The covalent nature of the hyaluronan-phospholipid adduct was not established. In principle, an hyaluronan-coated liposome functionally resembles the PEG-coated "stealth" liposomes. These latter were investigated for their ability to act as site-adherent and sustained-release carriers of epidermal growth factor for the topical therapy of wounds and burns.

B. Hyaluronan-protein

A porous matrix composed of gelatin and hyaluronan was prepared by dipping a gelatin-hyaluronan water-soluble sponge into a 90% (w/v) acetone/water mixture with a small amount of a carbodiimide (EDCI) as cross-linking agent. This sponge-type biomaterial was constructed for either wound dressings or scaffolds for tissue engineering. When impregnated with anti-bacterial silver sulfadiazine, this hyaluronan-gelatin sponge facilitated epidermal healing in a rat model.

Composite materials consisting of hyaluronan and collagen have been prepared by coagulation of the two components in aqueous acetic acid followed by cross-linking with glyoxal or a periodate-oxidized starch dialdehyde. The resulting material was resistant to collagenase and permitted fibroblast growth. Other composite materials consisting of hyaluronan and collagen have been prepared by cross-linking the dried hyaluronan/collagen coagulates with polyethylene oxide and hexamethylene diisocyanate.

In addition, a hydroxyapatite-collagen-hyaluronan composite material was prepared by adding hydroxyapatite particles to an hyaluronan solution followed by blending with an aqueous dispersion of collagen fibers. The final material, which consisted of 90% hydroxyapatite, 9.2% collagen, and 0.8% hyaluronan (w/w), was biocompatible, mechanically robust, and was used as a bone defect filler.¹⁷

Alternatively, a porous collagen-hyaluronan matrix was prepared by cross-linking collagen with periodate-oxidized hyaluronan; the resulting material supported new bone formation, and has potential uses for the delivery of growth factors or as an implantable cell-seeded matrix.

Hyaluronan incorporation into an artificial skin material (collagen-gelatin sponge) accelerated the ingrowth of granulation tissue, thus providing a more suitable graft bed to support a skin graft. Further investigation of hyaluronan covalently-bound to a collagen matrix found significantly reduced collagen contraction in fibroblast cultures suggesting an important role for hyaluronan in biomaterials for dermal substitutes and tissue engineering.

C. Hyaluronan-polycarboxylic acid polymers

A variety of other native and synthetic polymers have multiple, often regularly spaced, carboxylic acid groups. These include all glycosaminoglycans, pectin, alginate, carboxymethylcellulose (CMC), and poly(acrylic acid). Blending hyaluronan with these polymers, and

then carrying out the cross-linking chemistries described herein, offers a complex new dimension for chemically modified hyaluronan blended hydrogels.

The gel-forming properties of alginate (by metal chelation) could enhance hyaluronan hydrogel formation in a blended material. Thus, alginate-hyaluronan gels were prepared through the diffusion of calcium ions into alginate-hyaluronan mixtures. The resulting gels with an alginate:hyaluronan ratio of up to 1:1 had satisfactory mechanical properties. This composite matrix might be suitable as a biopolymeric carrier, or for articular surgery applications, due to its stability in synovial fluid.

A bioabsorbable membrane, Seprafilm[®], has been developed as the first hyaluronan product that was a bioresorbable physical barrier for prevention of post-surgical adhesions. Genzyme scientists prepared this material by blending two anionic polymers, hyaluronan and CMC, followed by carbodiimide-mediated modification.¹⁸ An anionic-cationic physically-associated network produces a rather fragile biomaterial, Seprafilm[®], that was approved in 1996 and is now approved by the FDA for a variety of surgical applications. The use of Seprafilm[®] is limited to accessible areas that can be fully covered. Since the location of many adhesions are unpredictable or inaccessible alternatives to Seprafilm[®] are being sought. Moreover, Seprafilm[®] is difficult to handle and is poorly accepted by many surgeons; a more pliable version, Seprafilm[®] II, will be available soon.

Finally, blends of hyaluronan with chondroitin sulfate (CS) have been investigated for wound-healing and drug release applications. Each polymer is first converted to its ADH derivative using the hydrazide chemistry described above, and then the HA-ADH and CS-ADH blend is cross-linked with PEG dialdehyde. These materials are strong candidates for development as materials that would decrease the time required for wound-healing.

D. Hyaluronan-grafted co-polymers

To obtain optimal properties for mechanical strength, drug delivery, or biostability, a variety of hyaluronan-grafted co-polymers have been prepared. For example, polyampholyte comb-type co-polymers consisting of poly(L-lysine) (PLL) main chains, a DNA binding site, and an hyaluronan side-chain with cell-specific ligands were prepared to target sinusoidal endothelial cells of liver. The reducing end of hyaluronan and the ϵ -amino groups of PLL were covalently-coupled by reductive amination using sodium cyanoborohydride to obtain the resulting comb-type copolymers (PLL-graft-HA).¹⁹ The polycationic PLL backbone selectively complexed the polyanionic DNA even in the presence of the hyaluronan side-chain. In addition, the PLL-graft-HA-DNA complex may form a multiphase structure in which the hydrophobic PLL-DNA complex is surrounded by a hydrated shell of free hyaluronan. Complex formation with free hyaluronan chains was considered to be essential for directing the complex to target cells.

A PEG-grafted-hyaluronan co-polymer was prepared by coupling hyaluronan with methoxy-PEG-hydrazide using a water-soluble

carbodiimide. This graft co-polymer was developed for the delivery of water-soluble peptides. For example, insulin appeared to partition into the PEG "phase," and intermolecular interactions prevented the conformational changes of insulin. This could retard drug leakage and permit degradation-controlled insulin release.

E. Hyaluronan-chitosan

Deacetylation of chitin, which is a homopolymer of the N-acetylglucosamine unit found in hyaluronan, gives the polyamine polysaccharide chitosan. A mixture of hyaluronan and chitosan glutamate was prepared as mucoadhesive microspheres containing gentamycin as a model drug. The combination of hyaluronan with chitosan glutamate appeared to combine the mucoadhesive potential of hyaluronan with the penetration enhancing effect of chitosan. When fully-deacetylated chitosan is mixed with chondroitin sulfates and hyaluronic acid, polyelectrolyte complexes are formed. These complexes are formed even in acidic media and are stable over a broad pH range. Cell-adhesion and enzymatic degradation were examined. Chitosan protected CS and hyaluronan from enzymatic hydrolysis, but pure chitosan showed the best results for cell-attachment, cell-proliferation, and wound healing.

F. Hyaluronan-DNA

A mixture of full-length cDNAs, plasmids, or simply oligonucleotides with hyaluronan, followed by carbodiimide-mediated cross-linking with ADH, affords materials that are able to transduce genetic information into cells. In initial experiments β -galactosidase was expressed in HA-DNA treated fibroblasts. Neither the identity of the complex nor the mechanism of transduction have been elucidated, but this method has the potential to become a powerful approach for targeted gene delivery.

G. Hyaluronan blends

Many synthetic polymers have excellent mechanical properties for use in biomaterials applications, but suffer from insufficient biocompatibility. In contrast, biocompatible polymers such as hyaluronan often have suboptimal mechanical properties. Blending synthetic polymers with biological macromolecules can yield composite materials that feature the desired properties of the individual polymers. Specifically, hyaluronan has been blended with other materials in order to produce interpenetrating molecular networks with good physicochemical, mechanical, and biocompatible properties. In many cases, no chemical cross-linking is required. For example, poly(vinyl alcohol) (PVA) and poly(acrylic acid) (PAA) were blended with either collagen or hyaluronan. The hyaluronan/PAA sponges were prepared by lyophilization of the blended aqueous polymers and "cross-linking" them at 130 °C *in vacuo*. The chemistry of this process remains unknown. Hyaluronan/PVA hydrogels were prepared by dissolving both polymers in water at different ratios and subjecting these mixtures to eight cycles of freezing/thawing.



IV Conclusions Hyaluronan has a combination of unique physicochemical properties and biological functions that allow it to serve as an important starting material for the preparation of new biocompatible and biodegradable polymers. This review highlights the chemistries involved in the modification of hyaluronan, and the potential medical applications of these hyaluronan-based biomaterials and hyaluronan-modified surfaces. Important new products have already reached the marketplace, and the approval and introduction of an increasing number of medical devices and new drugs using hyaluronan-derived biomaterials can be anticipated in the next decade.



V Acknowledgements

I am grateful to my co-workers in this project from 1990-2000, including Jing-wen Kuo, Tara Pouyani, Dale M. Marecak, James F. Marecek, Koen P. Vercruysse, Yi Luo, Michael R. Zeibell, and Kelly R. Kirker. I also thank my many collaborators, particularly David A. Swann, Gerard S. Harbison, Eva A. Turley, Anthony Day, and Steven D. Gray. Financial support in my laboratories has been provided by MedChem, Inc., The Center for Biotechnology at The University at Stony Brook, Clear Solutions Biotech, Inc., The University of Utah, the Center for Biopolymers at Interfaces (UUtah), the Department of Defense, and the National Institutes of Health.



References

1. Vercruysse, K. P., and Prestwich, G. D. (1998) Hyaluronate derivatives in drug delivery. *Crit. Rev. Therapeut. Carrier Syst.* 15, 513-555.
2. Prestwich, G. D., Marecak, D.M., Marecek, J. F., Vercruysse, K. P., and Ziebell, M. R. (1997) Controlled chemical modification of hyaluronic acid: synthesis, applications and biodegradation of hydrazide derivatives. *J. Controlled Release* 53, 99.
3. Luo, Y., Kirker, K., and Prestwich, G. Chemical modification of hyaluronic acid. In *Methods of Tissue Engineering*; A. Atala and R. Lanza, Ed.; Academic Press: San Diego, in press.
4. Abatangelo, G., and Weigel, P. *New Frontiers in Medical Sciences: Redefining Hyaluronan*; Elsevier: Amsterdam, 2000.

5. Benedetti, L., Cortivo, R., Berti, T., Berti, A., Pea, F., Mazzo, M., Moras, M., and Abatangelo, G. (1993) Biocompatibility and biodegradation of different hyaluronan derivatives (HYAFF) implanted in rats. *Biomaterials* 14, 1154-1160.
6. Pouyani, T., Kuo, J.-w., Harbison, G. S., and Prestwich, G. D. (1992) Solid-state NMR of *N*-acylureas derived from the reaction of hyaluronic acid with isotopically-labeled carbodiimides. *J. Am. Chem. Soc.* 114, 5972-5976.
7. Pouyani, T., Harbison, G. S., and Prestwich, G. D. (1994) Novel hydrogels of hyaluronic acid: Synthesis, surface morphology, and solid-state NMR. *J. Am. Chem. Soc.* 116, 7515-7522.
8. Luo, Y., Ziebell, M. R., and Prestwich, G. D. (2000) A hyaluronic acid-Taxol antitumor bioconjugate targeted to cancer cells. *Biomacromolecules* 1, 208-218.
9. Chen, G. P., Ito, Y., Imanishi, Y., Magnani, A., Lamponi, S., and Barbucci, R. (1997) Photoimmobilization of sulfated hyaluronic acid for antithrombogenicity. *Bioconjugate Chem.* 8, 730-734.
10. Laurent, T. C., Hellsing, K., and Gelotte, B. (1964) Cross-linked gels of hyaluronic acid. *Acta Chem. Scand.* 18, 274-275.
11. Kuo, J.-w., Swann, D. A., and Prestwich, G. D. (1991) Chemical modification of hyaluronic acid by carbodiimides. *Bioconjugate Chem.* 2, 232-241.
12. Luo, Y., Kirker, K., and Prestwich, G. (2000) Cross-linked hyaluronic acid hydrogel films: new biomaterials for drug delivery. *J. Controlled Release* 69, 169-184.
13. Larsen, N. E., Leshchiner, E. A., Parent, E. G., and Balazs, E. A. Hyaluronan and hyaluronan derivatives in drug delivery. In *Cosmetic and Pharmaceutical Applications of Polymers*; C. G. Gebelein, Ed.; Plenum Press: New York, 1991; pp 147-157.
14. Crescenzi, V., Tomasi, M., and Francescangeli, A. In *New Frontiers in Medical Sciences: Redefining Hyaluronan*; Abbazia di Praglia, Padua, Italy, 1999; pp 173-180.
15. Mason, M., Vercruysse, K., Kirker, K., Frisch, R., Marecak, D., Prestwich, G., and Pitt, W. (2000) Attachment of hyaluronic acid to polypropylene, polystyrene, and polytetrafluoroethylene. *Biomaterials* 21, 31-36.
16. Yerushalmi, N., Arad, A., and Margalit, R. (1994) Molecular and cellular studies of hyaluronic acid-modified liposomes as bioadhesive carriers for topical drug delivery in wound healing. *Arch. Biochem. Biophys.* 313, 267-273.
17. Bakos, D., Soldan, M., and Vanis, M. (1997) In *Adv. Med. Phys., Biophys. and Biomat.*; Stara Lesna, Slovak Republic, pp 54-56.
18. Burns, J. W., Burgess, L., Skinner, K., Rose, R., Colt, M. J., and Diamond, M. P. (1996) A hyaluronate based gel for the prevention of postsurgical adhesions: Evaluation in two animal species. *Fertil. Steril.* 66, 814-821.
19. Asayama, S., Nogawa, M., Takei, Y., Akaike, T., and Maruyama, A. (1998) Synthesis of novel polyampholyte comb-type copolymers consisting of a poly(L-lysine) backbone and hyaluronic acid side chain for a DNA carrier. *Bioconjugate Chem.* 9, 476-481.

Anthony J. Day‡ & Glenn D. Prestwich§

From the ‡MRC Immunochemistry Unit, Department of Biochemistry, University of Oxford, Oxford OX1 3QU, UK and §Department of Medicinal Chemistry, The University of Utah, Salt Lake City, Utah 84112-5820.

‡ To whom correspondence should be addressed: MRC Immunochemistry Unit, Department of Biochemistry, South Parks Road, University of Oxford, Oxford OX1 3QU, UK. Tel.: 44 1865 275349; Fax: 44 1865 275729; Email: ajday@bioch.ox.ac.uk.

Introduction

The ubiquitous glycosaminoglycan (GAG)¹ hyaluronan has diverse biological roles in vertebrates. These include acting as a vital structural component of connective tissues, the formation of loose hydrated matrices that allow cells to divide and migrate (e.g., during development), immune cell adhesion and activation, and a role in intracellular signaling; further details can be found in the other articles of this MiniReview series (1-3)². This wide range of activities may seem surprising for an unbranched polysaccharide comprised entirely of a repeating disaccharide, D-glucuronic acid ($\beta 1 \rightarrow 3$) *N*-acetyl-D-glucosamine ($\beta 1 \rightarrow 4$), which, unlike other GAGs, is neither attached to a protein core nor O- or N-sulfated. Such diversity results in fact from the large number of hyaluronan-binding proteins (often termed hyaladherins) that exhibit significant differences in their tissue expression, cellular localization, specificity, affinity and regulation. Therefore, characterization of the molecular basis of hyaluronan recognition by proteins, and how this is modulated *in vivo*, is an important key to understanding the biology of this GAG. In this article, we review the structural organization of vertebrate hyaladherins and how this may contribute to their different biological activities.

The hyaladherins - hyaluronan-binding proteins

Many hyaladherins contain a common structural domain of approximately 100 amino acids in length, termed a Link module, that is involved in ligand binding (4)³. However, a growing number of hyaladherins lack this domain and are unrelated to each other at the primary sequence

level. Figure 1 shows the domain organization of the Link module superfamily and other hyaluronan-binding proteins.

The Link module superfamily. The Link module (also referred to as a proteoglycan tandem repeat – see (5)) was first identified in the link protein isolated from cartilage. The link protein is comprised of an immunoglobulin domain and two contiguous Link modules, and this molecular arrangement is also found in the G1-domains of aggrecan, versican, neurocan and brevican (Fig. 1). These proteoglycans form huge, link protein-stabilized, complexes with hyaluronan that provide the load bearing function in articular cartilage, give elasticity to blood vessels and contribute to the structural integrity of many tissues, such as skin and brain (see (6,7)). A brain-specific link protein (BRAL1) has been characterized recently (8), which may be part of a larger link protein gene family (9).

The ubiquitous hyaluronan receptor CD44 has diverse functions including the attachment, organization and turnover of extracellular matrix at the cell surface, and mediates the migration of lymphocytes during inflammation (10). CD44 can exist in numerous isoforms, due to alternative splicing of 10 variant exons in different combinations. Each isoform contains a single Link module close to the N-terminus of the protein. The hyaluronan-binding properties of CD44 are determined by the isoform and the cell-type on which it is expressed (11).

Apart from CD44, the only other member of the Link module superfamily that has been clearly identified as a hyaluronan receptor is LYVE-1. This recently discovered molecule is restricted in its expression to lymph vessel endothelium and appears to be involved in hyaluronan degradation (12).

The protein product of tumor necrosis factor-stimulated gene-6 (TSG-6), that contains a single Link module, is secreted in response to inflammatory stimuli, e.g., in the articular joints of arthritis patients (13,14). TSG-6 has been implicated in the regulation of leukocyte migration, and the pattern of its expression suggests that it is likely to be involved in extracellular matrix remodelling. Although, the role of TSG-6 is, at present, poorly understood, its hyaluronan-binding properties (and their structural basis) are probably the best characterized of any hyaladherin.

Figure 1 shows several new members of the Link module superfamily (i.e., stabilin-1, CAB61358 and KIA0527), all of which contain a single Link module. Stabilin-1 (accession code AJ275213) is a transmembrane protein that was initially identified as a partial sequence (KIA0246) cloned from a myeloid cell line (15). Stabilin-1 and CAB61358 may be identical to

the proteins designated WF-HABP and BM-HABP (16), for which only the amino acid sequence for the Link modules have been reported. These both show about 50% identity with the Link module of TSG-6. However, it is unclear whether they bind hyaluronan as no functional data are yet available. The same is true for KIA0527 that was cloned from brain tissue (17).

Non-Link module hyaladherins. Inter- α -inhibitor (I α I), a serine protease inhibitor plentiful in serum, was one of the first proteins found to associate with hyaluronan (18). As shown in Figure 1 I α I is an unusual proteoglycan with a chondroitin-4-sulfate chain linked to bikunin (containing two kunitz inhibitor domains) and two heavy chains (HC1 and HC2) attached to the GAG by ester bonds via their C-terminal aspartic acid residues (19). I α I is essential during ovulation, acting to stabilise the hyaluronan-rich cumulus extracellular matrix with which it forms a covalent complex (20,21). The covalent association links the C-terminal ends of HC-1 and HC-2 to the C6-hydroxyl of an internal N-acetylglucosamine of hyaluronan via an ester bond, while the bikunin chain is released (20). It has also been reported that I α I can bind non-covalently to hyaluronan (22), as is the case for all other hyaluronan-protein interactions, but the precise regions of the molecule involved have not been determined.

CD38, a type II membrane glycoprotein, has been reported to be a hyaladherin (23). This protein is an enzyme with NADase activity, and this property has been studied much more extensively than its hyaluronan-binding function for which no biological role has yet been ascribed (24).

PHBP was purified from human plasma using hyaluronan-affinity chromatography (25). It is a serine protease that may be involved in wound healing where high levels of hyaluronan accumulate (26). It is comprised of EGF modules, a kringle domain and a serine protease domain. However, there is no information on which of these are involved in ligand binding.

Recently two related hyaladherins, IMP-150 and SPACRCAN, have been isolated from human retina. IMP-150, which may be identical to SPACR (27), is expressed by cone and rod photoreceptor cells and is present in the interphotoreceptor matrix (28). SPACRCAN (a chondroitin sulfate proteoglycan) is likely to be a receptor on photoreceptors and pinealocytes (29). SPACR and SPACRCAN both contain two SEA modules, a structural domain often associated with O-glycosylation (30). The positions of the hyaluronan-binding sites on these proteins are not yet established.

The **Receptor for Hyaluronan-Mediated Motility (RHAMM)** mediates cell migration and proliferation in normal and tumor cells (reviewed in (2)). A number of RHAMM isoforms are

present in the cytoplasm and nucleus and are also transiently expressed on the surface of activated leukocytes and subconfluent fibroblasts.

The presence of hyaladherins inside cells is not surprising given the increasing evidence for intracellular hyaluronan (1). In fact, there are three hyaluronan-binding proteins, in addition to RHAMM, which have been found in intracellular locations to date. The first is a vertebrate homologue of yeast and *Drosophila* CDC37 (31), which may be involved in cell cycle and kinase function as it associates with RAF and pp60^{v-scr} (32). The second protein, P-32 (also known as HABP-1), was originally co-purified with pre-mRNA splicing factor SF2 (33) and subsequently shown to be a hyaluronan-binding protein (34). P-32 is likely to have a role in cellular signal transduction (35), and may be involved in nucleus-mitochondrion interactions (36). As with RHAMM, P-32 can also be detected on the surface of some cells, e.g., transformed fibroblasts. The third protein, IHABP4, was identified using the same monoclonal antibody that permitted isolation of vertebrate CDC37 (37) and has been detected in the cytoplasm of IHABP4-transfected cells. Its role in hyaluronan trafficking or intracellular signalling remains to be determined.

The structures of hyaluronan-binding domains

The Link module structure (5), which has defined the 'consensus fold' for the entire Link module superfamily, consists of two α -helices and two triple-stranded anti-parallel β -sheets (Fig. 2). The single Link module from TSG-6 is sufficient for high-affinity interaction with hyaluronan (38). In contrast, CD44 has a hyaluronan-binding domain of ~160 amino acids comprised of a Link module with N- and C-terminal extensions that are essential for folding and functional activity (39,40). An even larger domain is utilized by the link protein, aggrecan and aggrecan-related proteoglycans, as these all have a pair of contiguous Link modules in their hyaluronan-binding regions. In link protein and aggrecan both Link modules are involved in binding (6,41). Therefore, hyaluronan-binding domains from Link module-containing proteins can be divided into 3 subgroups (Type A, B and C) on the basis of size (Fig. 3). The size of the binding domain appears to correlate broadly with the length of hyaluronan recognized. For instance, hexasaccharides (HA₆) and decasaccharides (HA₁₀) are the minimum sizes of hyaluronan required for high affinity interaction with Type A and Type C domains, respectively (38). Hyaluronan binding to CD44 can be displaced by either HA₆ or HA₁₀, depending on the cell background on which it is expressed (42). A recent study indicates that HA₁₀ is the smallest oligosaccharide that

binds optimally to cell-surface CD44 in a monovalent fashion, while an increase in binding avidity is seen with oligomers ($\geq \text{HA}_{20}$) that can interact with two CD44 molecules simultaneously (43).

The amino acids of CD44 involved in the interaction with hyaluronan have been determined by site-directed mutagenesis (39,44). Functionally important residues are present both on the Link module (Figure 3) and on the flanking sequences indicating that a large coherent binding site is likely to be formed (i.e., the extensions may constitute a sub-domain in intimate contact with the Link module (4)). Recently, amino acids in TSG-6 that are perturbed on interaction with hyaluronan have been identified (38), and mutagenesis has allowed residues directly involved in binding to be distinguished from those affected due to ligand-induced conformation changes (45). These studies show that in Link module-containing proteins, binding residues are brought together from different parts of the sequence and that a folded structure is necessary to generate a ligand-binding surface. It should be noted that linear sequences (so called BX₇B motifs (46) - see below) do not appear to be involved in Link module-hyaluronan interactions (38).

The hyaluronan-binding sites in TSG-6 and CD44 have similar locations on the Link module, suggesting that the position of the ligand-interaction surface may be conserved across the superfamily (45). However, there appear to be some major differences in the details of the residues (and sequence positions) involved in mediating binding in the two proteins. In fact, comparisons of the Link module sequences of CD44 and TSG-6 with all the other members of the superfamily indicate that the molecular details of hyaluronan binding (i.e., the interaction networks) are likely to be distinct in each protein. This is perhaps not surprising given the different sub-types of hyaluronan-binding domains (described above) as well as many other differences in specificity and regulation. For example TSG-6 binds to chondroitin-4-sulphate with high affinity, but this GAG is not recognized by aggrecan or link protein (47).

The structure of a P-32 homotrimer, which is likely to be its oligomeric state in physiological solutions, has been solved recently by X-ray crystallography (36). Each monomer consists of seven consecutive β -strands that form a highly twisted antiparallel β -sheet flanked by one N-terminal and two C-terminal α -helices. The position of the hyaluronan-binding site has not yet been established.

The hyaluronan-binding domain of RHAMM has been localized to a 62 amino acid segment (the P1-domain) close to the C-terminus of the protein. This domain (residues 518-580 in the murine RHAMMv4 isoform) has been expressed and shown to be functionally active, and its

solution structure has been determined (48)^{4,5}. As shown in Fig. 2, it consists of a helix-loop-helix motif. The P1-domain includes a region of 34 amino acids that has been implicated previously in hyaluronan binding by truncation mutagenesis (49). Two clusters of basic amino acids (531-KQKIKHVVKLK-541 and 553-KLRSQVLVKRK-562) have been identified within this region, and these have been reported to be involved in mediating the interaction with hyaluronan (46). This led to the suggestion (46) that linear sequences termed BX₇B motifs (where B is either lysine or arginine and X can be any amino acid apart from acidic residues) are likely to be a minimal requirement for hyaluronan binding in RHAMM and other hyaladherins. This study involved the expression of short basic peptides (and related mutants) fused onto the C-terminus of residues 1-238 of RHAMM followed by determination of hyaluronan-binding activity using a transblot assay. However, this experimental approach should be viewed with caution, since the pendant BX₇B peptides were not displayed in the normal context of the hyaluronan-binding domain and likely lacked important contributions from secondary and tertiary structure. Although Arg46 of CD44 (which is part of a BX₇B motif) was identified as important for hyaluronan binding in these experiments, subsequent work has indicated that it is not involved in the interaction (44,50). The recent determination of the structure of the P1 domain will provide the basis for a program of site-directed mutagenesis to define the position of the hyaluronan-binding surface in RHAMM.

BX₇B-like sequences are present in IoI (22), SPACR (27), SPACRCAN (29), CD38 (23), CDC37 (31), P-32 (34) and IHABP4 (37). However, there are no data to indicate that they mediate hyaluronan binding in these proteins. This spacing of basic amino acids is extremely common in protein sequences, with over 16,000 matches in the NRL-3D database alone (i.e., proteins of known tertiary structure). If X is any amino acid apart from acidic residues, there are still over 10,000 matches. Therefore, the presence of a BX₇B motif should not be interpreted as an indicator that a protein will bind hyaluronan nor should it be assumed that this is necessarily the site of hyaluronan-binding activity in a known hyaladherin.

Towards understanding the molecular basis of hyaluronan-protein interactions

Basic amino acids have long been presumed to be major determinants in hyaluronan binding by aggrecan and link protein, making ionic bonds with the carboxylic acid group of glucuronic acid (see references in (38)). This is also likely to be the case for CD44 where two arginines (Arg41 and Arg78), along with two tyrosines (Tyr42 and Tyr78) play a critical role in the interaction with hyaluronan (39,44). In addition to these four essential residues (dark blue on

Fig. 3), other, less critical, amino acids (including three lysines, four arginines, two asparagines and a tyrosine) have also been implicated (shown in light blue). The number of residues of CD44 engaged in binding indicates that there is a large network of interactions (distinct for this protein) that maintains the association with hyaluronan. The energetics are clearly finely balanced, since the loss of a single hydrogen bond or ionic interaction can be enough to diminish binding significantly (44).

The thermodynamics of hyaluronan-protein binding have been determined for the TSG-6 Link module, where the major energetic contribution driving the interaction is the enthalpy, which is large and exothermic (38). The small change in heat capacity seen on binding is consistent with an intermolecular interface comprising a significant polar or charged component rather than the burial of a large hydrophobic surface area. The interaction of the TSG-6 Link module with HA₈ is highly salt-strength dependent. However, ionic interactions may only contribute about 25% of the free energy of binding at physiological sodium ion concentrations (51). Therefore, while it is clear that ionic associations are important, non-ionic interactions (e.g., hydrogen bonding and van der Waals) also contribute significantly to the binding energy. This is consistent with data from site-directed mutagenesis showing that in addition to a lysine, 3 tyrosines and a phenylalanine have a critical role in binding (45).

Recently the crystal structure has been determined for a hyaluronan lyase (from *Streptococcus pneumoniae*) in complex with two hyaluronan disaccharides in the substrate binding cleft (52). There is an extensive network of hydrogen bonds and electrostatic interactions stabilizing the binding. In addition sugar rings are seen to stack against aromatic sidechains, which is a common feature in protein-carbohydrate complexes.

At present there are few data on the conformations adopted by hyaluronan after binding to proteins. In solution, hyaluronan is likely to be highly dynamic in nature, adopting a large number of low energy states (53,54). It is possible that different hyaladherins could capture (and stabilize) distinct transient conformations of hyaluronan, i.e., the structure of hyaluronan will be different depending on which protein it associates with. A consequence of this could be that particular hyaladherins are able to modulate the binding of other proteins by altering the conformation of hyaluronan. However, structural information on protein-hyaluronan complexes is necessary for definitive answers.

Regulation of hyaluronan-protein interactions

A unique feature of the interaction of TSG-6 with hyaluronan is that it is highly pH-dependent, which may serve to regulate the function of this protein in certain tissues (55). There is maximal binding at pH 6 and a dramatic reduction in binding as the pH is increased, but with no alteration in the Link module fold. A likely explanation is that raising the pH changes the charge-state on a histidine side chain, leading to the loss of a critical interaction (51).

CD44 is present on many cell types (e.g., lymphocytes) in a non-functional form that requires activation to acquire ligand-binding activity, unlike most hyaladherins that interact constitutively with hyaluronan. Understanding how the hyaluronan-binding function of CD44 is regulated has been a major focus of recent research. This complex issue involves the cell background on which CD44 is expressed, post-translational modifications (including N-glycosylation, GAG attachment and tyrosine sulfation), the splice isoform involved, membrane composition, phosphorylation of the intra-cytoplasmic domain, cytoskeletal attachment, molecular clustering and receptor density on the cell surface (10,43,56-58). A detailed discussion of each of these is clearly outside the scope of this review, and here we will focus just on N-glycosylation.

The hyaluronan-binding domain of human CD44 contains six potential sites for N-linked carbohydrate attachment, and expression of this region in *E. coli* indicates that glycosylation is not obligatory at any of these sites for either correct folding or functional activity (40). This conclusion is consistent with results from one study (59) but at odds with another (60). Although glycosylation is unlikely to be required for hyaluronan binding, it is clearly one of the principle mechanisms modulating the interaction between CD44 and hyaluronan (11), and there is differential glycosylation of the receptor depending on cell type and cell activation state. Removal of N-glycans by the mutation of the first or fifth glycosylation sites, which are on the N- and C-terminal extensions, respectively, can switch CD44 in an 'inducible' cell background into a constitutively active form (59). However, the presence of N-linked carbohydrate at all positions on a 'constitutive' cell-line does not inhibit binding. This may be due to particular carbohydrate structures at sites 1 and 5 causing steric interference by blocking hyaluronan binding; alternatively, certain N-glycans may prevent receptor clustering or fix the protein in a non-binding conformation.

The activation of cells to become hyaluronan binding by changes in the CD44 glycoform present on their surface (i.e., by *de novo* synthesis) would be relatively slow. Rapid induction *in vivo* (e.g., on leukocytes) may occur by the removal of sialic acid (potentially by an endogenous

sialidase) as this has been shown to be a major up-regulator of hyaluronan-binding function in CD44 (59,61,62).

The molecular basis of CD44 regulation should become clearer once the tertiary structure of the hyaluronan-binding domain is known, as this will reveal the positions of the glycosylation sites relative to the ligand interaction surface.

Summary

In recent years significant advances have been made in the identification of new hyaladherins and in our knowledge of hyaluronan-protein interactions. Determination of the three-dimensional structures of different types of hyaluronan-binding domains and their ligand complexes are clearly essential if we are to understand the molecular mechanisms underlying the diverse biology of this important glycosaminoglycan.

Acknowledgements. We thank Michael Ziebell for unpublished data and Eva Turley for informative discussions.

Figure legends

Figure 1. The modular organization of the hyaladherins. The domain structures of KIA0527, Stabilin-1, CAB61358 (a partial sequence), SPACR and SPACRCAN were determined with the assistance of the SMART programme (63) with the additional identification of OSF-2 domains (64) by databank searching.

Figure 2. Comparison of the folds of the Link module from TSG-6 (5) and the RHAMM-P1 domain⁴. Helices and β -sheets are shown in red and yellow, respectively. In the Link module, the side chains of residues involved in hyaluronan binding are depicted in blue (45).

Figure 3. The Link module superfamily can be divided into three sub-groups on the basis of the size of their hyaluronan-binding domains (4). Only the tertiary structure of Type A (i.e., a single Link module as found in TSG-6) has been determined to date. Residues in TSG-6 that mediate the interaction with hyaluronan (45) are colored in red. The Link modules illustrated for CD44 (Type B) and link protein (Type C) were modelled on the basis of the TSG-6 co-ordinates (4,45).

In the Type B domain, the structures of the N- and C-terminal extensions, represented by striped green boxes, are unknown. Amino acids of the CD44 Link module that are critical or important for hyaluronan binding are depicted in dark blue or light blue, respectively (44). In the Type C domain, the relative orientation of the two Link modules is yet to be determined, and only one possible configuration is shown. The residues of link protein predicted to be involved in the interaction with hyaluronan are colored as described in Mahoney *et al.*, (45).

Footnotes

*Financial support to A. J. D. by the Medical Research Council and Arthritis Research Campaign and to G.D.P. by the University of Utah and US Department of Defense Grant DAMD 17-98-1-8254 is gratefully acknowledged.

¹The abbreviations used are: GAG, glycosaminoglycan; RHAMM, receptor for hyaluronan-mediated motility; TSG-6, tumor necrosis factor-stimulated gene-6.

²Space limitations preclude the citation of numerous primary papers; these can be found in the review articles referenced.

³See also Day, 2001. Understanding hyaluronan-protein interactions. At <http://www.glycoforum.gr.jp/>

⁴M. R. Ziebell and G. D. Prestwich, unpublished data.

⁵M. R. Ziebell, Z. Zhao, B. Luo, L. Luo, E. A. Turley, and G. D. Prestwich, unpublished data.

References

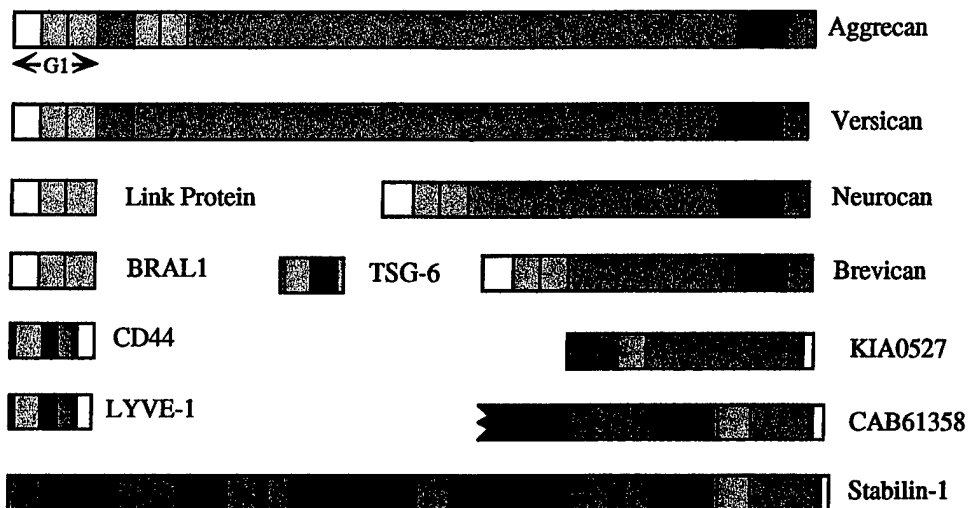
1. Tammi, M., Day, A. J., and Turley, E. A. (2001) *J. Biol. Chem.* **in press**
2. Turley, E. A., Bourguignon, L., and Noble, P. W. (2001) *J. Biol. Chem.* **in press**
3. Toole, B. P., Wight, T. N., and Tammi, M. I. (2001) *J. Biol. Chem.* **in press**
4. Day, A. J. (1999) *Biochem. Soc. Trans.* **27**, 115-121
5. Kohda, D., Morton, C. J., Parkar, A. A., Hatanaka, H., Inagaki, F. M., Campbell, I. D., and Day, A. J. (1996) *Cell* **86**, 767-775
6. Watanabe, H., Cheung, S. C., Itano, N., Kimata, K., and Yamada, Y. (1997) *J. Biol. Chem.* **272**, 28057-28065
7. Yamaguchi, Y. (2000) *Cell. Mol. Life Sci.* **57**, 276-289
8. Hirakawa, S., Oohashi, T., Su, W. D., Yoshioka, H., Murakami, T., Arata, J., and Ninomiya, Y. (2000) *Biochem Biophys Res Commun* **276**, 982-989.
9. Lee, J. Y., and Spicer, A. P. (2000) *Curr. Opin. Cell Biol.* **12**, 581-586.
10. Goodison, S., Urquidi, V., and Tarin, D. (1999) *J. Clin. Pathol.: Mol. Pathol.* **52**, 189-196
11. Lesley, J., Hyman, R., English, N., Catterall, J. B., and Turner, G. A. (1997) *Glycoconj. J.* **14**, 611-622
12. Banerji, S., Ni, J., Wang, S. X., Clasper, S., Su, J., Tammi, R., Jones, M., and Jackson, D. G. (1999) *J. Cell. Biol.* **144**, 789-801
13. Wisniewski, H. G., and Vilcek, J. (1997) *Cytokine Growth Factor Rev.* **8**, 143-156
14. Bayliss, M. T., Howat, S. L., Dudhia, J., Murphy, J. M., Barry, F. P., Edwards, J. C., and Day, A. J. (2001) *Osteoarthritis Cartilage* **9**, 42-48.
15. Nagase, T., Seki, N., Ishikawa, K., Ohira, M., Kawarabayasi, Y., Ohara, O., Tanaka, A., Kotani, H., Miyajima, N., and Nomura, N. (1996) *DNA Res.* **3**, 321-329
16. Tsifrina, E., Ananyeva, N. M., Hastings, G., and Liau, G. (1999) *Am. J. Pathol.* **155**, 1625-1633
17. Nagase, T., Ishikawa, K., Miyajima, N., Tanaka, A., Kotani, H., Nomura, N., and Ohara, O. (1998) *DNA Res.* **5**, 31-39
18. Bost, F., Diarra-Mehrpour, M., and Martin, J. P. (1998) *Eur. J. Biochem.* **252**, 339-346
19. Enghild, J. J., Thogersen, I. B., Cheng, F., Fransson, L. A., Roepstorff, P., and Rahbek-Nielsen, H. (1999) *Biochemistry* **38**, 11804-11813

20. Zhao, M., Yoneda, M., Ohashi, Y., Kurono, S., Iwata, H., Ohnuki, Y., and Kimata, K. (1995) *J. Biol. Chem.* **270**, 26657-26663
21. Hess, K. A., Chen, L., and Larsen, W. J. (1999) *Biol. Reprod.* **61**, 436-443
22. Chen, L., Mao, S. J., McLean, L. R., Powers, R. W., and Larsen, W. J. (1994) *J. Biol. Chem.* **269**, 28282-28287
23. Nishina, H., Inageda, K., Takahashi, K., Hoshino, S., Ikeda, K., and Katada, T. (1994) *Biochem. Biophys. Res. Commun.* **203**, 1318-1323
24. Ferrero, E., and Malavasi, F. (1999) *J. Leukoc. Biol.* **65**, 151-161
25. Choi-Miura, N. H., Tobe, T., Sumiya, J., Nakano, Y., Sano, Y., Mazda, T., and Tomita, M. (1996) *J. Biochem. (Tokyo)* **119**, 1157-1165
26. Vostrov, A. A., and Quitschke, W. W. (2000) *J. Biol. Chem.* **275**, 22978-22985
27. Acharya, S., Rodriguez, I. R., Moreira, E. F., Midura, R. J., Misono, K., Todres, E., and Hollyfield, J. G. (1998) *J. Biol. Chem.* **273**, 31599-31606
28. Kuehn, M. H., and Hageman, G. S. (1999) *Matrix Biol.* **18**, 509-518
29. Acharya, S., Foletta, V. C., Lee, J. W., Rayborn, M. E., Rodriguez, I. R., Young, W. S., 3rd, and Hollyfield, J. G. (2000) *J. Biol. Chem.* **275**, 6945-6955
30. Bork, P., and Patthy, L. (1995) *Protein Sci.* **4**, 1421-1425
31. Grammatikakis, N., Grammatikakis, A., Yoneda, M., Yu, Q., Banerjee, S. D., and Toole, B. P. (1995) *J. Biol. Chem.* **270**, 16198-16205
32. Perdew, G. H., Wiegand, H., Vanden Heuvel, J. P., Mitchell, C., and Singh, S. S. (1997) *Biochemistry* **36**, 3600-3607
33. Krainer, A. R., Mayeda, A., Kozak, D., and Binns, G. (1991) *Cell* **66**, 383-394
34. Deb, T. B., and Datta, K. (1996) *J. Biol. Chem.* **271**, 2206-2212
35. Rao, C. M., Deb, T. B., Gupta, S., and Datta, K. (1997) *Biochim. Biophys. Acta.* **1336**, 387-393
36. Jiang, J., Zhang, Y., Krainer, A. R., and Xu, R. M. (1999) *Proc. Natl. Acad. Sci. U.S.A.* **96**, 3572-3577
37. Huang, L., Grammatikakis, N., Yoneda, M., Banerjee, S. D., and Toole, B. P. (2000) *J. Biol. Chem.* **275**, 29829-29839
38. Kahmann, J. D., O'Brien, R., Werner, J. M., Heinegard, D., Ladbury, J. E., Campbell, I. D., and Day, A. J. (2000) *Structure Fold. Des.* **8**, 763-774

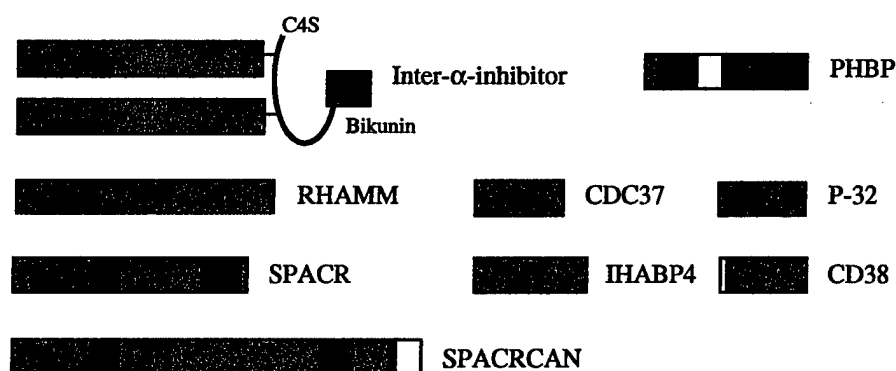
39. Peach, R. J., Hollenbaugh, D., Stamenkovic, I., and Aruffo, A. (1993) *J. Cell Biol.* **122**, 257-264
40. Banerji, S., Day, A. J., Kahmann, J. D., and Jackson, D. G. (1998) *Protein Expr. Purif.* **14**, 371-381
41. Grover, J., and Roughley, P. J. (1994) *Biochem. J.* **300**, 317-324
42. Tammi, R., MacCallum, D., Hascall, V. C., Pienimäki, J. P., Hyttinen, M., and Tammi, M. (1998) *J. Biol. Chem.* **273**, 28878-28888
43. Lesley, J., Hascall, V. C., Tammi, M., and Hyman, R. (2000) *J. Biol. Chem.* **275**, 26967-26975
44. Bajorath, J., Greenfield, B., Munro, S. B., Day, A. J., and Aruffo, A. (1998) *J. Biol. Chem.* **273**, 338-343
45. Mahoney, D. J., Blundell, C. D., and Day, A. J. (2001) *J. Biol. Chem.* **276**, in press
46. Yang, B., Yang, B. L., Savani, R. C., and Turley, E. A. (1994) *EMBO J.* **13**, 286-296
47. Parkar, A. A., and Day, A. J. (1997) *FEBS Lett.* **410**, 413-417
48. Ziebell, M. R. (2000) in *Physiology and Biophysics*, University at Stony Brook
49. Yang, B., Zhang, L., and Turley, E. A. (1993) *J. Biol. Chem.* **268**, 8617-8623
50. Telen, M. J., Udani, M., Washington, M. K., Levesque, M. C., Lloyd, E., and Rao, N. (1996) *J. Biol. Chem.* **271**, 7147-7153
51. Blundell, C. D., Kahmann, J. D., Perczel, A., Mahoney, D. J., Cordell, M. R., Teriete, P., Campbell, I. D., and Day, A. J. (2001) in *Hyaluronan 2000* (Kennedy, J. F., ed), pp. in press., Woodhead Publishing Ltd., Abington, Cambridge.
52. Ponnuraj, K., and Jedrzejewski, M. J. (2000) *J. Mol. Biol.* **299**, 885-895.
53. Almond, A., Brass, A., and Sheehan, J. K. (1998) *J. Mol. Biol.* **284**, 1425-1437
54. Almond, D., Brass, A., and Sheehan, J. K. (2000) *J. Phys. Chem. B* **104**, 5634-5640
55. Parkar, A. A., Kahmann, J. D., Howat, S. L. T., Bayliss, M. T., and Day, A. J. (1998) *FEBS Lett.* **428**, 171-176
56. Bourguignon, L. Y., Zhu, H., Shao, L., and Chen, Y. W. (2000) *J. Biol. Chem.* **275**, 1829-1838
57. Lesley, J., English, N., Charles, C., and Hyman, R. (2000) *Eur. J. Immunol.* **30**, 245-253
58. Oliferenko, S., Kaverina, I., Small, J. V., and Huber, L. A. (2000) *J. Cell. Biol.* **148**, 1159-1164
59. English, N. M., Lesley, J. F., and Hyman, R. (1998) *Cancer Res.* **58**, 3736-3742

60. Bartolazzi, A., Nocks, A., Aruffo, A., Spring, F., and Stamenkovic, I. (1996) *J. Cell Biol.* **132**, 1199-1208
61. Skelton, T. P., Zeng, C., Nocks, A., and Stamenkovic, I. (1998) *J. Cell Biol.* **140**, 431-446
62. Katoh, S., Miyagi, T., Taniguchi, H., Matsubara, Y., Kadota, J., Tominaga, A., Kincade, P. W., Matsukura, S., and Kohno, S. (1999) *J. Immunol.* **162**, 5058-5061
63. Schultz, J., Milpetz, F., Bork, P., and Ponting, C. P. (1998) *Proc. Natl. Acad. Sci. U. S. A.* **95**, 5857-5864
64. Takeshita, S., Kikuno, R., Tezuka, K., and Amann, E. (1993) *Biochem. J.* **294**, 271-278

Link module superfamily

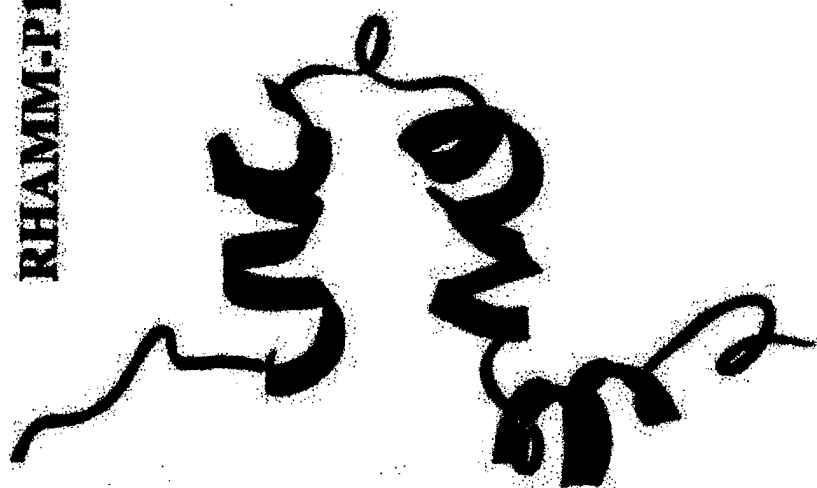


Other HA binding proteins

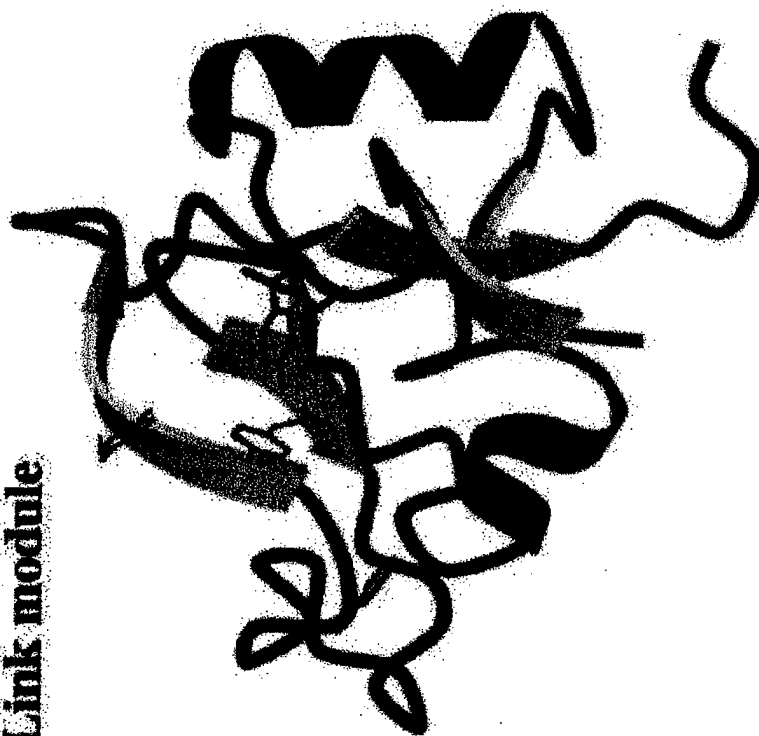


Link module	EGF module	No known module or domain
CCP module	Ig module	Transmembrane domain
C-type lectin module	SEA module	Cytoplasmic domain
CUB module	OSF-2 domain	Glycosaminoglycan attachment domain
VWFA domain	Kunitz domain	Serine protease domain
Kringle domain	BX7B motif	~100 amino acids

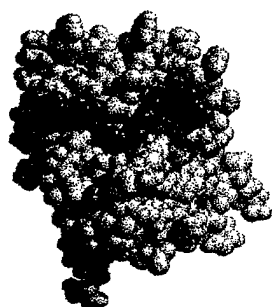
RHAMM-PI



Link module

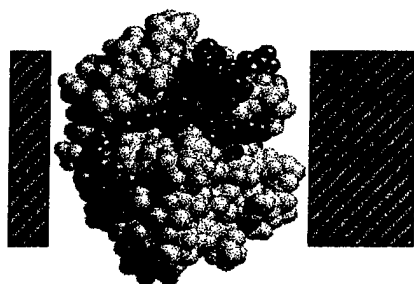


Type A



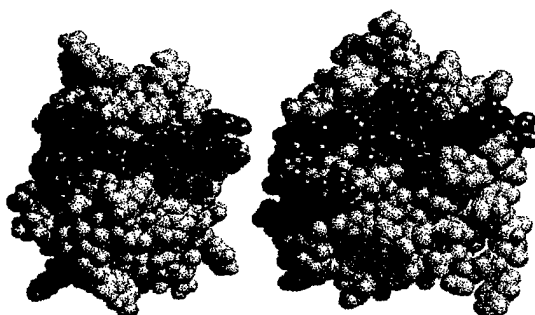
Single Link module
(~ 90 residues),
e.g., TSG-6

Type B



Link module with
N- and C-terminal
extensions (~ 160
residues),
e.g., CD44

Type C



Link module pair
(~ 200 residues),
e.g., Link protein